Structured Packing in Air Distillation

Submitted by
Paul Higginbotham

For the degree of
Doctor of Philosophy

The University of Aston in Birmingham

September 1993

The University of Aston in Birmingham

Structured Packing in Air Distillation

Paul Higginbotham

Doctor of Philosophy

1993

Summary

An economic analysis has been performed to establish when it is advantageous to use structured packing in air separation plant. A model of a low pressure cycle was developed to calculate the power saved when packing is used, and cost models were developed for the columns and cold box. The rate of return was calculated on the extra investment required for a packed plant based on the annual power saving.

Structured packing was found to be economic only in larger plants, where economies of scale mean that the increased capital cost becomes less significant compared with the power saved. It was also found that different sized plants favour different packings.

The analysis identified that the packing variable with the biggest impact on the economic balance was the efficiency and that increasing the efficiency of current packings could enhance their benefit in air distillation.

A new packing was therefore developed to have a higher efficiency than conventional ones. The vapour phase resistance was targeted for reduction, since most packing models predict this to be dominant.

The final shape was chosen as the easiest and most economic to make. It has converging and diverging channels and was manufactured in two specific areas and with two block heights by Tianjin University Packing Factory.

A 0.3 m diameter distillation column test rig was designed, built and commissioned with the standard Sulzer Mellapak 500YW. It was then used to test the new packing alongside some standard ones.

Because the packings had different specific areas, correlations of published results were developed to allow a true comparison to be made.

The test results show that, unexpectedly, the packings with 0.1 m high blocks have an efficiency about 8% greater than the standard 0.2 m blocks. The new shape as implemented in the 350Y packing shows an additional 7% greater efficiency, so it is 15% better than a standard packing with the same area. It has a better efficiency than the Mellapak 500YW and the higher capacity associated with its lower area. The new 500Y did not show a significant advantage.

A comparison of the economic advantage in air distillation of the packings tested showed that the new shaped 350Y gives the highest rate of return of all the packings except in extremely large plants. It is more economic than Mellapak 750Y and reduces the smallest viable plant size from 700 to 650 t/d oxygen.

Key Words:

Air Separation, Economic Evaluation, Packing Tests, New High Efficiency Packing, Distillation Column Internals.

To Sarah and my Parents

Acknowledgements

I am grateful to the following for all their help which has enabled me to present this thesis.

My supervisor, Professor K E Porter, for his endless ideas and encouragement.
BOC Process Plants for sponsoring my work and particularly to Mr. J T Lavin, my industrial supervisor.
The academic and technical staff in the department of Chemical Engineering and Applied Chemistry at Aston University, without whose help I could not have built the test rig.
The academic staff of the Chemical Engineering Research Centre of Tianjin University, P. R. China and particularly Professors K T Yu, S Y Wang and X J Yuan and Mr R S Lan for their advice on developing the new packing.
The staff of Tianjin University Packing Factory for manufacturing packings for the tests.
Sulzer Brothers Ltd for supplying some packing free of charge.
Norton Chemical Process Products Ltd for supplying some of their packing free of charge.
The Science and Engineering Research Council for its funding.
Mr A Gor and Miss P Wan for their help in commissioning the test rig.
Mr Z B Zhang and Mr S Robertshaw for allowing me to use some of their test results.
Measurement Technology Limited for supplying the multiplexed explosion proof barriers at half price.

Contents

List of figures

List of tables

Chapter 1- Introduction

Background

Distillation

Distillation is not new. It has been used for separating volatile mixtures over thousands of years, at least since ancient Egypt. However, most of its development has taken place in the last hundred years with the rise of the oil and chemical industries. Amongst separation processes, distillation is therefore regarded as a mature technology and any advances made are likely to be relatively minor. Since a significant proportion of man's energy consumption (a few percent) is accounted for by distillation, these minor advances are, however, of major importance; they can save a great deal of energy. Most of the recent improvements in distillation technology have been brought about by the need to reduce energy consumption as energy prices rose after the oil crisis in the early 1970's.

Trays

Contact between vapour and liquid in early continuous distillation columns was achieved by allowing the liquid to flow down the column over horizontal plates or trays. Vapour would pass up the through risers in the plates and be forced through the liquid by 'bubble caps' over the top of the risers. Each plate had a relatively low efficiency, compared to an ideal equilibrium stage, and the pressure loss of the vapour as it flowed through a plate was relatively large. Later, other types of tray were developed, for example sieve trays. These simply had holes instead of bubble caps and exhibited a lower pressure drop and higher efficiency than bubble cap trays.

Packings

Columns containing packing, such as glass beads or Raschig rings, have been used for a long time in laboratory scale distillation, and for industrial scale absorption. Packings have the advantages of higher efficiency and capacity and lower pressure drop per unit column height than trays. But until quite recently packed columns have not been used extensively for large scale distillation because of uncertainty about their performance when scaled up. Tests at Fractionation Research Incorporated during the early 1980's proved that this uncertainty could be removed by careful design of liquid distributors (Kunesh, 1987). This made

possible the revamping of trayed columns with packings to increase the number of theoretical plates, decrease the reflux ratio and reduce energy consumption, in addition to increasing throughput.

Packings are of two types, random (or dumped) and structured (or regular or ordered). Random packings can be anything from shoe eyelets or glass beads to shapes specially developed to give good performance, like Pall rings or Intalox saddles. They are generally from about 1 to 15 cm in diameter and are dumped into a column at random. Structured packings were originally developed for vacuum distillation. Here, a very low pressure drop across the column is required to avoid thermal decomposition of products at the bottom of the column. This happens if the pressure at the bottom and therefore the boiling temperature is too high. They consist of regularly arranged metal (or ceramic or plastic) or gauze sheets which are usually crimped in some way to provide channels for upward vapour flow, whilst liquid flows in a film down the surface. Because they are more efficient and the pressure drop across them is lower than random packings, they are increasingly replacing random packings in revamp work, even though they are normally considered to be more expensive.

Air separation

Air distillation was first performed on an industrial scale by Linde in 1902, in a single column process. Shortly afterwards, in 1910 the first double column system was operated (Isalski (1989)). The original purpose was to produce oxygen for use in steel making, and oxygen continued to be the most important product until the 1950's. Since then, nitrogen has become increasingly important as an inert medium in numerous industries and in the liquid state as a cheap and easy means of reaching cryogenic temperatures. Argon is also an important product, and is used particularly as an inert medium in inert gas welding, inside light bulbs and in the steel making industry. More recently, extremely pure gases are required, especially in the semiconductor industry, so ultra high purity air separation plants have been developed.

Cryogenic distillation is still the most economical process for air separation on all but the smallest scales, where the more recent membrane separation and pressure swing adsorption processes are used.

Because of the very low temperatures in an air separation plant and the high cost of refrigeration at these temperatures, air distillation plants are thermally well integrated. As much heat as possible is removed from the feed air by cooling it against the warming products, so as to reduce the refrigeration requirement. In addition, the distillation column system is enclosed in a well-insulated 'cold box' to minimise the amount of heat leaking into the plant.

To make the cold box as small as possible, to reduce the surface area through which heat may leak, the distillation columns need to be as short as possible. Traditionally, this is achieved by the use of small-holed sieve trays. These may be much more closely spaced than those with larger holes which are commonly used in the petrochemical industry.

The large power consumption of air separation plants means that a small improvement in their thermodynamic efficiency may provide a significant saving in power costs. However this usually leads to larger and more expensive plant.

The use of structured packing in an air distillation column is an example of this. Its low pressure drop provides a power saving, but the capital cost of a packed column is higher than that of a trayed one.

Aims

Because of the new confidence in the design of packed towers, the air separation industry is seriously considering a change from tray to packing technology. This will only be worthwhile if the cost of producing oxygen, nitrogen and argon can be reduced as a consequence. The important questions which must be answered are these: Is it possible to use packing for air separation? under what circumstances is it profitable to use packing instead of trays? can presently available packings be improved to increase the profitability of the changeover? The first question has already been answered by the air separation industry; various publications indicate that packings perform similarly with liquid air and organic mixtures. Some uncertainty still remains about which material the packing should be made of, but it is more appropriate that this problem should be solved by the industry. This work has set out to answer the last two questions, and has the following aims:

1. *To study the economic implications of changing from trayed to packed columns in an air separation plant.*

What are the economic, packing and process variables which affect the profitability of the change?

What conditions are required for the change to be worthwhile?

What is the relative effect of each packing variable on the profitability of the change?

What aspects of a packing should be changed to increase profit?

2. *To develop a new packing particularly suited to air separation.*

How much is understood about how packings work?

How can existing packings be improved in the ways identified by the economic analysis?

How can the new packing be manufactured?

3. *To design and build the largest practicable distillation test rig to operate with organic mixtures.*

Can we improve the understanding of how packings work?

4. *To compare experimentally the new packing with existing packings to see if it has the desired properties.*

What is the efficiency, capacity and pressure drop of the new and existing packings?

What would be the benefit of using the new packing rather than existing ones?

The remainder of this thesis describes the work undertaken to achieve these aims.

Chapter 2 - Literature review

In this chapter, the background material necessary to understand the later work will be introduced. First, we shall introduce air separation processes and the advantages to be gained by replacing distillation trays with structured packing. This will provide the context for the thesis and the background for the economic work. We shall then examine in detail the development of structured packings and survey the models and correlations used to describe them. Finally, we shall review heat and mass transfer enhancement techniques which could be used in packings.

2.1 Air Separation Plant

This work was undertaken primarily to improve the profitability of air separation by developing a new structured packing particularly suited to air separation.

In this section, we shall first consider why air separation is carried out and to what uses its products are put. We shall then survey the different processes used to separate air.

Finally, we will look in detail at cryogenic distillation; the different process cycles and design and operating considerations.

This will provide the necessary preparation for understanding the impact of structured packing on the process and the economic analysis of the plant.

2.1.1 Products of air separation - demand and use

A typical composition of dry air is: 78.08% nitrogen, 20.95% oxygen, 0.93% argon, 0.03% carbon dioxide, 0.002% neon, 0.0002% methane, 0.0001% krypton, 0.00005% Helium, 0.00005% nitrogen monoxide and 0.000009% xenon. It may also contain water vapour and other contaminants, for example hydrocarbon vapours. The first industrial separation of air was performed to provide oxygen for steel making, so the nitrogen was treated as a waste product.

The main use of oxygen is still in primary metal manufacturing, but it is also used as a raw material in the chemical industry and for welding and other minor uses, such as in medicine, pollution control and glass manufacturing. Another major use is in coal gasification; this may consume very large quantities at a single site. The market for oxygen in the developing world has declined in recent years with the decline of the steel industry, but there is potential for large expansion, in for example gasification and pollution control.

Nitrogen only began to be important as a product of air separation in the 1950's as it saw increasing use as an inert blanketing and purging medium. It had been used some time before this in ammonia synthesis, but the process changed to one

which produced its own nitrogen from air, so nitrogen ceased to be an important product of air separation. It has a number of other uses, for example liquid is used for food freezing, and gas is used to enhance oil recovery by raising the pressure in depleted oil wells. A growing important use of nitrogen is as an inert medium in semiconductor manufacture, where very high purities and low dust levels are required.

Like nitrogen, argon is used as an inert medium in steel making, inert gas welding, in light bulbs and in the semiconductor industry. Whilst the demand for oxygen fell with the decline of steel making, the demand for argon continued to rise. This made it expensive to produce by air separation, when the oxygen was not required. As a result, an alternative supply of argon was developed from the fertiliser manufacturing process, which reacted out the oxygen and nitrogen from air. Normally, crude argon, with about 2% oxygen is produced from an air separation plant. This is sufficient for most of the demand for argon, such as the argon-oxygen decarburisation (AOD) process in stainless steel production. However for some applications, particularly in the semiconductor industry, the argon must be further purified in an argon purification unit (APU).

2.1.2 Types of air separation plant

There are three types of process currently used for air separation. These are membrane separation, pressure swing adsorption and cryogenic distillation.

Of these, distillation is the oldest, having been practised since the beginning of the century. It is still the most economic process on a large scale, because although the plant is more expensive, it is more thermodynamically efficient. It also has the advantage that very pure products and liquid products may be easily produced.

Membrane separation is the most recent addition to the air separation process. It was first used extensively in the 1980's after the advent of hollow fibre membranes in about 1980, and is still being developed. It is the most economic option only in very small plants because of its high running cost to capital cost ratio. In addition, it does not permit as high a purity or recovery as cryogenic distillation.

Pressure swing adsorption was first investigated in the 1940's for the removal of water and carbon dioxide from air. But it was not until the 1970's that it was developed as a means of gas separation. Like membrane separation plants, pressure swing adsorption plants are less complex and have a lower initial cost than cryogenic plant. The product recovery is not as good, although fairly high purities can be achieved. Pressure swing adsorption is at present the most economic option for fairly small medium purity plants.

Some new hybrid processes may use combinations of these three separating methods, but these are still in the development stage.

In this work, we are concerned only with cryogenic distillation. This is likely to remain the most economic option for large and very large plants, where running costs dominate, because of its higher efficiency and product recovery than the other technologies. It also has the important advantages that liquids and ultra-pure products may be produced relatively easily and cheaply.

2.1.3 Cryogenic distillation process cycles

Because the cost of production of oxygen and nitrogen on a large scale is mostly that of the power needed to run the plant, air separation plants have become increasingly efficient since the first one built by Linde in 1902.

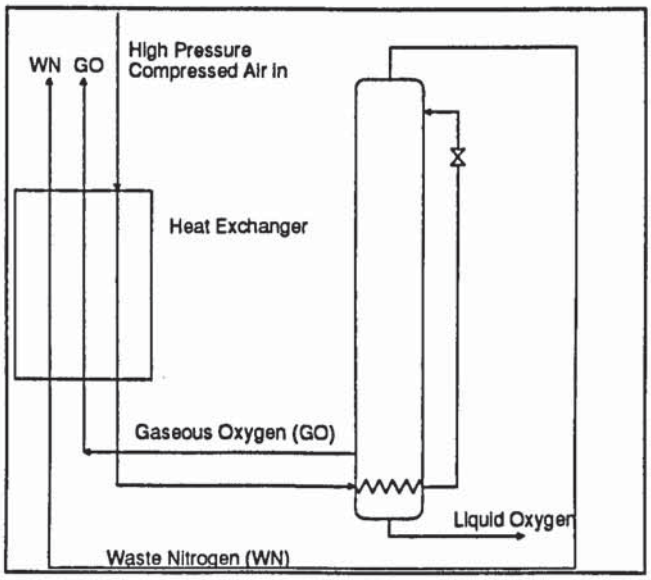

Figure 2-1 Single Column Oxygen Generator

This early plant was designed to produce oxygen and operated with the single column cycle illustrated in figure 2-1. Compressed air enters the heat exchanger and is cooled against the products as they are warmed. It is further cooled in the boiler at the bottom of the distillation column as it heats the bottom liquid. Next, it is expanded through a valve, so that it is mostly liquid. The mixture is introduced at the top of the column to provide liquid reflux. An impure nitrogen product is taken from the top of the column, whilst a pure oxygen product is withdrawn from the bottom either as liquid or vapour. The gaseous products then enter the heat exchanger to be warmed against the incoming air.

The refrigeration needed to make up for the products being cooler than the feed is provided irreversibly by the isenthalpic expansion across the valve. The air is compressed to a sufficiently high pressure that the enthalpy of the feed at the higher temperature is the same as that of the products at the lower temperature. The quantity of refrigeration needed determines the air pressure needed. If gaseous oxygen is produced, the incoming air needs to be compressed to between 30 and 60 atmospheres, but if liquid is produced, a pressure of 200 atmospheres is required.

This type of cycle is not very efficient because of the irreversibility of the refrigeration. Another disadvantage is that although a similar type of cycle may be constructed to produce pure nitrogen and impure oxygen, pure forms of both

products may not be produced together. This also means that not all the desired product in the feed is recovered.

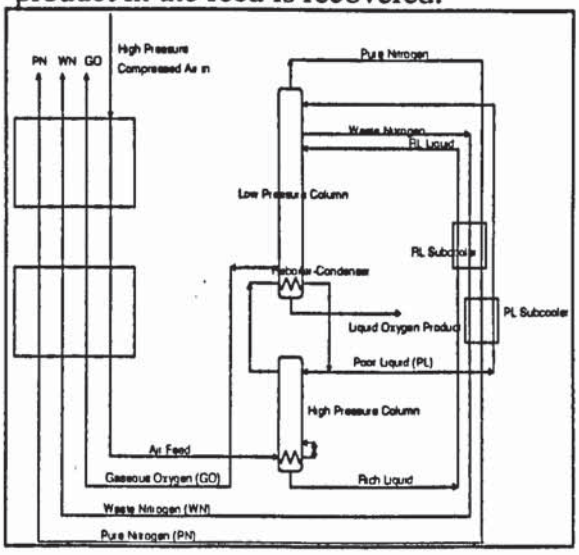

Figure 2-2 Early Two Column System

To increase product recovery and to enable pure nitrogen and oxygen to be produced together, the double column system was developed and first operated around 1910. An early version is illustrated in figure 2-2. The lower column is operated at a higher pressure so that nitrogen condensing at its top is at a higher temperature than the oxygen in the bottom of the upper column, and so will boil it. After cooling in the boiler of the high pressure column, the air feed is introduced at an intermediate point in the lower column. Pure nitrogen (known as **poor liquid**, because of its low oxygen content) is condensed at the top of the column, and some is withdrawn and expanded across a valve to provide reflux in the upper column, whilst some provides reflux in the lower column. The oxygen-rich liquid at the bottom of the high pressure column (**rich liquid**) is expanded and fed into an intermediate point in the upper column. Pure nitrogen is withdrawn from the top of this column, whilst pure oxygen is withdrawn from the bottom. This cycle is also inefficient, like the single column cycle, because refrigeration is only achieved irreversibly by the Joule-Thompson effect.

The efficiency was increased initially by separating the process and refrigeration cycles. A small amount of air compressed to a higher pressure and then expanded in a refrigeration cycle provided more efficient refrigeration than compressing all the feed air to an intermediate pressure. The remainder of the feed air only needed to be compressed to the process pressure of about 6 bar.

Because liquid production needed a large amount of refrigeration, this process was still not efficient enough in this case. A modification of the refrigeration system in the Claude and Heylandt cycles improved the efficiency by taking some compressed air from an intermediate point in the main exchanger, making it perform work in an expansion engine, thus reducing its heat content, then feeding it into the lower column. This reduced the pressure to which the air had to be compressed to provide the necessary refrigeration and reduced the power consumption of the plant.

These cycles still operated at relatively high pressures of about 150 atmospheres, as they used relatively inefficient reciprocating expansion engines. They did not need to produce large quantities of oxygen or nitrogen, and so did

not need to be particularly efficient. When oxygen became important in steel making, however, large plants became necessary and it became more important to increase their efficiency. This was achieved during the 1930's by using the more efficient turbo compressors and expanders. Use was also made of the pressure difference within the process cycle to drive an expander, thus reducing the duty of the high pressure refrigeration cycle. An example of such a plant is the Linde-Fraenkl plant, which uses the expansion of gaseous nitrogen from the high pressure column to generate refrigeration. In addition, extra heat exchangers were used to reduce heat transfer irreversibilities by matching feed and column temperatures more closely.

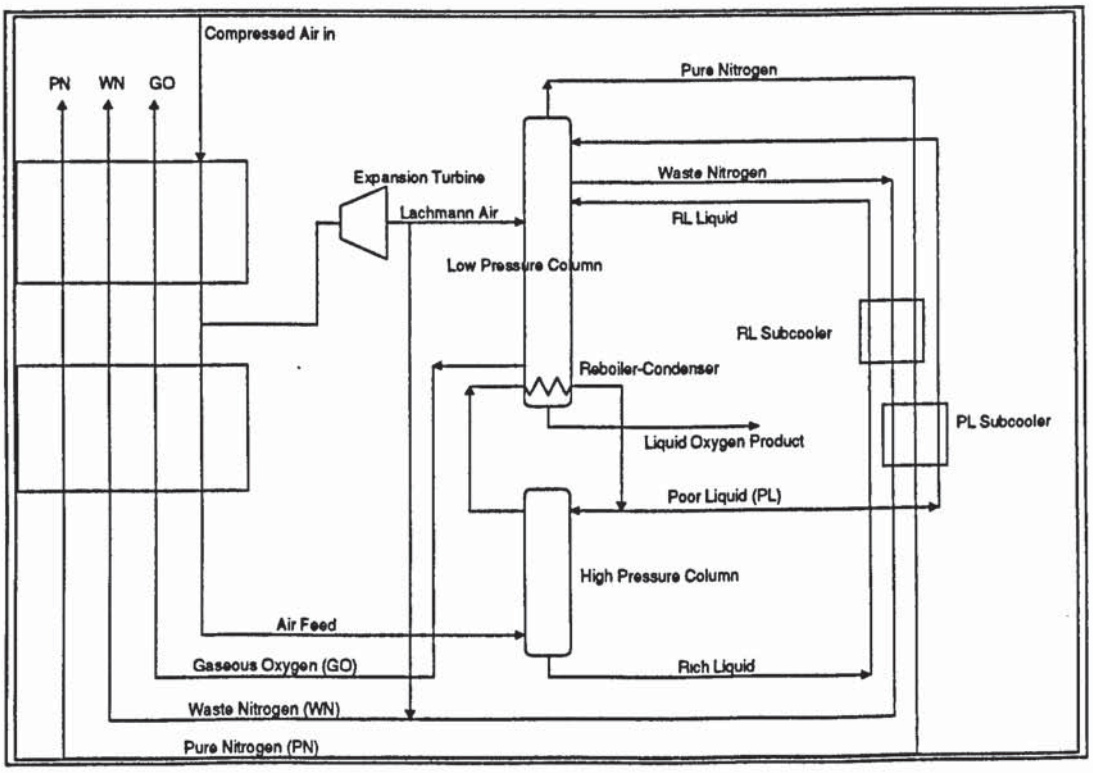

Figure 2-3, Air Expansion Cycle

The next major development was the use of the low pressure cycle, which is still the one used predominantly today. In this, the high pressure refrigeration cycle is omitted completely, and all the refrigeration is provided by expansion of part of the feed air (figure 2-3) or of nitrogen from the high pressure column (figure 2-4). The compression pressure is then only slightly higher than the high pressure column pressure.

If nitrogen expansion is used, the amount of liquid nitrogen available for reflux in the low pressure column is reduced and so it operates closer to minimum reflux. This increases the number of trays required and improves the thermodynamic efficiency of the separation. If on the other hand, air expansion is used, the turbine exhaust may either be mixed with the waste nitrogen or fed into the low pressure column as **Lachmann air.** Like the nitrogen expansion case, the Lachmann air feed reduces the reflux ratio, increases the number of trays and improves the

efficiency of the column. In fact, if the pressure drop associated with the extra trays is too great, the efficiency reaches a maximum and may be reduced if the flows are too close to minimum reflux. The use of air expansion allows a small amount of operating flexibility, because the flow of Lachmann air may be varied.

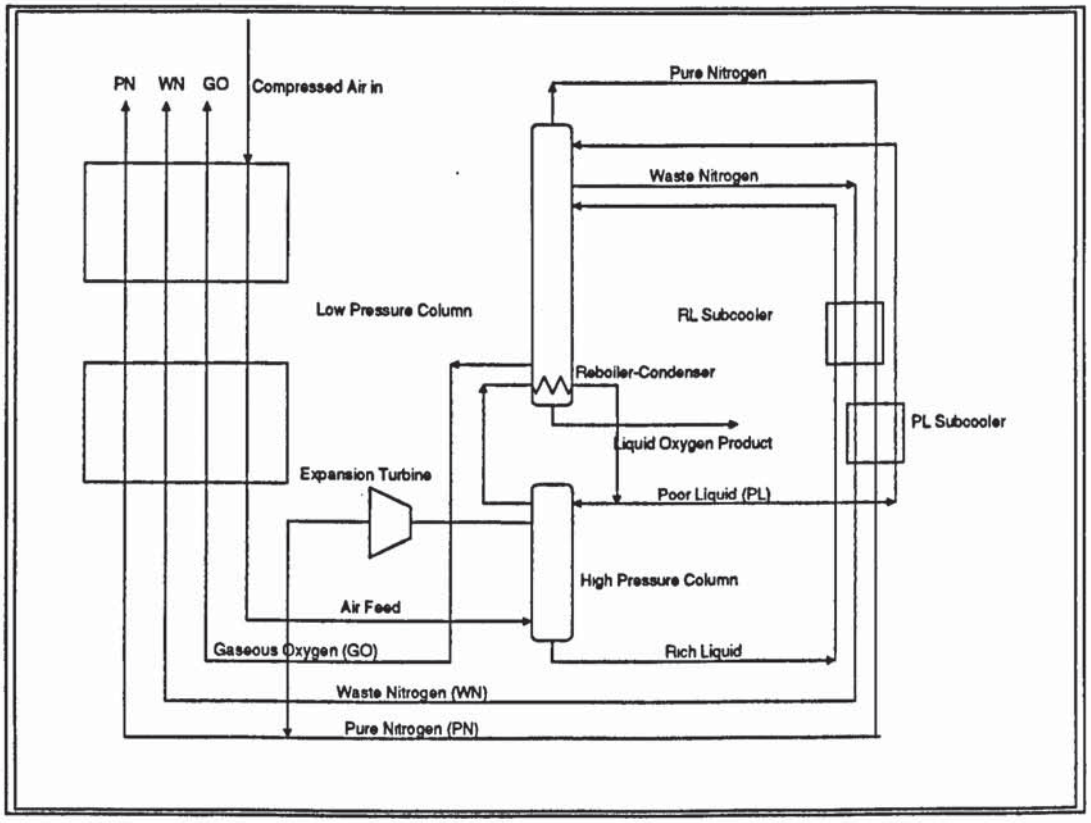

Figure 2-4, Nitrogen Expansion Cycle

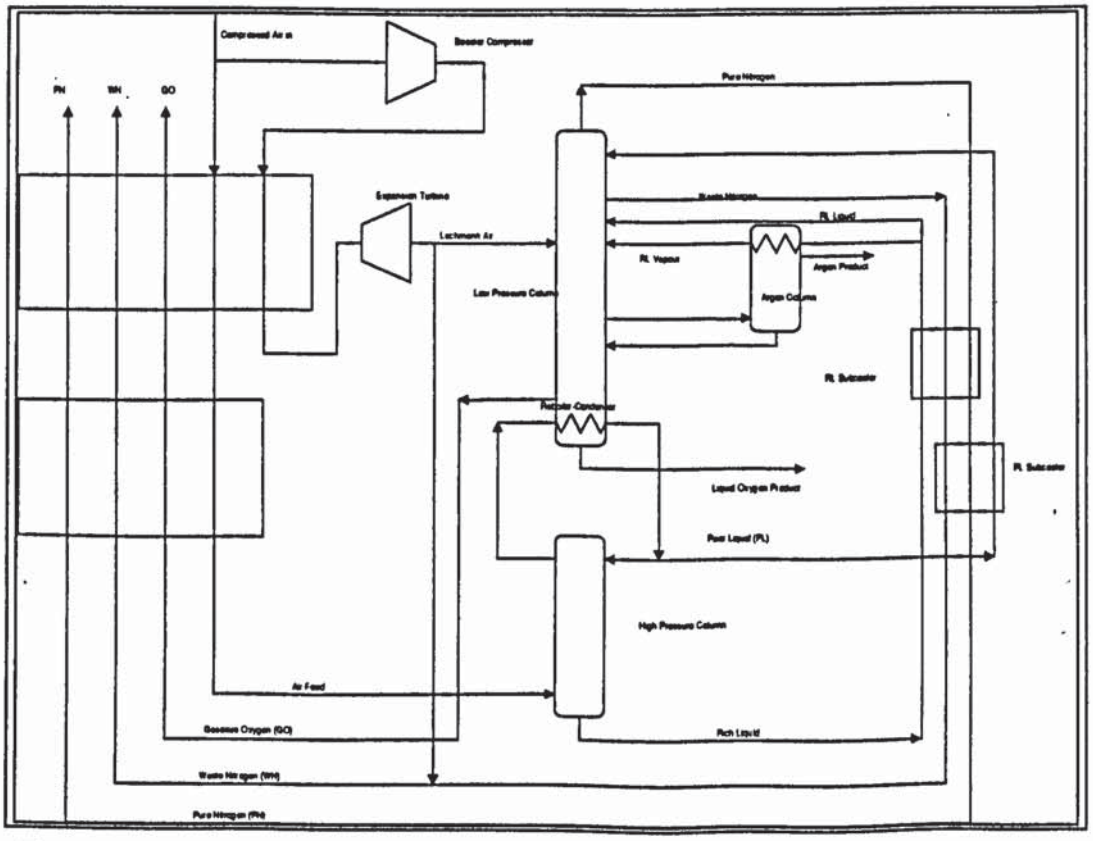

Figure 2-5, Air Boost Cycle with argon side column

A variation on the air expansion cycle is the air boost cycle, where the power recovered from the expansion turbine is used to drive a booster compressor, to compress the air before it is expanded. This leads to more efficient refrigeration, so the flow through the expander is reduced and the plant consumes less power.

If high purity oxygen and nitrogen are to be produced, or argon is required as a product, it must be separated out in a side-column (figure 2-5). Vapour is taken from the low pressure column, about half way down, where the argon concentration peaks. It passes up the argon column, is condensed by evaporating some rich liquid and fed back to the column as reflux. Liquid from the bottom of the column is returned to the tray from which the vapour is taken. The number of plates in the argon column is limited because the top must be above atmospheric pressure, to prevent contaminants leaking in and to maintain the temperature difference in the condenser. Since the argon flow, and consequently the reflux ratio is set by the mass balance, the argon purity is limited to about 98-99%.

A variety of other cycles is possible, for example using single or triple columns, extra refrigeration cycles and integrated liquefaction cycles. These will not be considered further here. More detailed information about these cycles can be found in Ruhemann (1949), Latimer (1967) and Isalski (1989).

All the cycles may be optimised for a particular mix of products depending on what is required.

2.1.4 Design and operating considerations

So far, we have looked at the basic cycles used in air separation. We will now consider the way in which these cycles are implemented.

Construction materials-cold & flammability

Many common construction materials become brittle at the low temperatures found in air separation. The most common materials of construction for air separation plant are aluminium and stainless steel, both of which can withstand these temperatures well. If a mixture of materials is used, their differential expansion must also be considered. Because the temperature of operation is so far from ambient temperatures, a plant will contract by several percent when it is started up, and any significant differential contraction could be disastrous. An additional problem is that of flammability. In parts of the plant, there is pure oxygen, and so any materials used should not be ignitable. All metals burn in oxygen, but they may be used safely if their ignition energy is high enough.

Compressors

Early air separation plants used inefficient reciprocating compressors. Most plants today use the more efficient axial turbo-compressors, driven by efficient electric motors. The compression may be done in several stages, with cooling in between, so as to increase its efficiency. Several compressors are usually operated in parallel, with some spare, so that the plant may be operated continuously during maintenance.

Air cooling

It is important that the air should enter the cold box as cold as possible, so as to reduce the refrigeration needed. It is usually cooled by direct contact with cooling water, which is itself cooled by the waste nitrogen stream. This will normally reduce its temperature to around 15 Celsius. Sometimes the air is cooled further by heat exchange with a Freon chiller system.

Air Purification

Water and Carbon dioxide are the main contaminants in atmospheric air. These freeze well above the process temperature, and so must be removed. Early plants used chemical means to remove these substances, but this was rather expensive. Later, **regenerators** were used. These were high heat capacity devices which were cyclically cooled by the products and warmed by the feed. In the warming cycle, when the feed air is cooled, carbon dioxide and ice were deposited in them, whilst they were evaporated into the feed. Regenerators have the disadvantage that the products are re-contaminated with the water and carbon dioxide at the beginning of a cycle. More recently, **reversing heat exchangers** (RHEs) were developed, in which water and carbon dioxide freeze out of the air feed. The air and waste nitrogen passages are periodically switched so that the contaminants are re-evaporated. These have the advantage that the products are not contaminated, but need a fairly high flow of waste nitrogen to clean the passages. They also have the advantage that the pressure drop through them is small. The latest, and now most commonly used method of air purification is the **pre-purification unit** (PPU). These are beds packed with an adsorbent, through which alternately feed air and heated waste nitrogen are passed. Contaminants are adsorbed in the first part of the cycle, whilst the adsorbent is regenerated in the second part. PPUs have the advantage that not so much waste nitrogen is required, but have a higher pressure drop than RHEs. They also need some power input to heat the regeneration gas. An additional advantage is that hydrocarbons are also removed. In the other types of plant, these must be removed from the liquid oxygen by adsorption, or by continuously draining a small amount.

Cold box/column arrangement

Because heat leaking into the plant must be removed by refrigeration, it is necessary to ensure that the plant is very well insulated. All the cold components are therefore enclosed within a **cold box**. This should have as small a surface area as possible for a particular volume and so should be as close to a sphere or cube as possible. It is therefore advantageous if the distillation columns are short and fat rather than tall and thin.

Heat exchanger balancing

It is important that the temperature differences in the main heat exchanger are not too large, to reduce irreversibility (second law) losses. Large temperature differences may arise from the higher heat capacity of the higher pressure feed than the products. This may be avoided by removing some of the air feed for expansion in a refrigeration turbine (in the air expansion plant) or by adding more cooling at the cold end of the exchanger (as in a nitrogen expansion plant. This is known as balancing the heat exchanger. In some circumstances, two turbines may be used to obtain even smaller temperature differences and higher thermodynamic efficiency.

Coolers

Using subcoolers and product heaters ensures that feeds enter the column at the correct temperature and that products enter the main exchanger at more closely matched temperatures, so reduces irreversibility.

Lachmann air

If an air expansion plant is used, the fraction of the expanded air which is processed in the low pressure column as Lachmann air may be varied. Less Lachmann air means a lower product recovery, but needs fewer theoretical plates. More Lachmann air increases the plant efficiency and product recovery, but more theoretical plates are needed. Increasing the Lachmann air flow too much could require so many trays that the pressure at the bottom of the low pressure column is increased, so increasing the high pressure column pressure and compressor pressure, and reducing plant efficiency.

Theoretical distillation column design

The number of theoretical plates required in each section of the distillation column must be calculated from the mass and heat balance equations and the multicomponent equilibrium relations. This will be discussed later in this chapter. If any column section operates too close to minimum reflux, a **pinch** results. This

is a region where very little change in composition occurs over many theoretical plates. It is undesirable because of the pressure drop associated with the extra plates and the extra cost of building the column.

There is only a small amount of flexibility in the design of the distillation column system, for example in changing the reflux ratio, because, unlike a normal distillation column, heat for the distillation is supplied by the components being distilled. So for a given product flow, there is only one possible rate of heat transfer and one reflux ratio; the heat transferred is not independent of product rate as it would be if it were transferred from steam or to cooling water.

The number of theoretical plates required in the high pressure column is usually between 30 and 50, and in the low pressure column between 40 and 100, depending on the product purity and efficiency of the cycle.

The pressure drop in the low pressure column should be as low as possible. This lowers the temperature at its base and at the top of the high pressure column, and so lowers the pressure in the high pressure column. This pressure reduction is several times the reduction in pressure in the low pressure column, because the boiling pressure of nitrogen changes more quickly with temperature than that of oxygen.

Reducing the pressure drop per theoretical plate also means that the maximum in efficiency is closer to minimum reflux, so that more Lachmann air can be processed efficiently, provided that extra theoretical plates are used.

Reboiler condenser temperature difference

As in the other heat exchangers, the temperature difference in the reboiler-condenser should be minimised. This minimises the pressure required in the high pressure column, and at the main compressor outlet, and so saves power.

Actual distillation column design

In designing the trays in a distillation column for air separation, several differences from the distillation of organics must be accounted for. In air distillation, more trays are needed and the column should be short and fat rather than tall and thin, to avoid heat inleak. In addition, the pressure drop should be low.

This leads to the use of sieve trays with much smaller holes than in most distillation; 1-2 mm rather than 6-12 mm. These sieve trays are operated close to the weep point, where liquid would 'weep' through the holes. As a result the vapour velocity and pressure drop are minimised, but the column diameter is larger for the same flow. The lack of spray from the small holes allows the trays to be very closely spaced - 4-6 inches as opposed to 12-24 inches in other distillation

applications. The combination of close tray spacing and minimum pressure drop means that the operating range of air separation trays is very small and the trays have little turn-up and turn-down.

The area of the tray covered by holes may be adjusted over the column to optimise the design for the different vapour and liquid rates in different sections.

A distillation column with small-holed sieve trays is therefore shorter and fatter than a traditional distillation column with the same number of theoretical plates, and has a lower pressure drop.

Start-up and shutdown

When an air separation plant is started up, it takes some time to cool down and generate enough liquid to cover all the trays. The liquid hold-up on the trays should therefore be as low as possible to speed start-up.

Turn-up/down

In some circumstances it may be necessary to alter the quantity of products produced. If the plant is capable of operating above and below its design capacity, this is easily achieved. A plant with as wide an operating range as possible is therefore desirable. Plants with sieve trays are not particularly good in this respect because the trays weep if the flow is too low and flood if it is too high, with a range of 1:2 or at best 1:3. Air separation trays have even less flexibility than conventional sieve trays.

Control

Contrary to the situation when starting up, a large liquid hold-up is better for easy control of the process because it is then less susceptible to disturbances. A column with a higher pressure drop is also easier to control for the same reason. Sieve trays have a relatively large hold-up and high pressure drop, so that control is not a problem. However, if a fast response is needed to changes in demand, the hold-up should not be too great.

2.1.5 Conclusions

There are many different cycles used in air separation plant, but most plants today use the double column system with refrigeration provided by air or nitrogen expansion. This may be optimised for different product mixes.

Because of the high degree of heat integration, there is little flexibility in design or operation of air separation plant to adjust relative product flows, purities and reflux ratios.

Air distillation columns are designed for minimum height and pressure drop, to minimise cost, heat inleak and irreversibility.

2.2 Use and economic implications of packings in Air Separation Plant

We shall now consider how packings have been used in air separation and the advantages and disadvantages of using structured packings.

Packings were first used in small-scale air separation plant during the second world war as part of the programme described by Rushton (1947). Weedman and Dodge (1947) describe tests under this programme of various random and structured packings in a two inch diameter column. Packings were used here because of their higher efficiency than small sieve trays, and their reduced susceptibility to motion (aboard ships or aircraft) during operation.

Until the late 1980's, packings were not considered for use in large scale air separation in the West, although some earlier work with structured packings was undertaken in the Soviet Union (Alekseev et al., 1973 and Zel'venskiy et al., 1978). This lack of use was mainly due to the poor scale-up performance of packings (which has only recently been understood to be due to poor liquid distribution) and to their high cost. More interest has been shown in structured packings than in random ones, because they have the higher efficiency and lower pressure drop per theoretical plate and so are closer to the ideal for air separation.

2.2.1 Advantages

Alekseev et al. (1973) first identified the possibility of saving power in a air separation plant by using structured packing. Bennett et al. (1989) explain that the main advantage of using a structured packing in air separation is the reduction in power consumption due to the reduced pressure drop in the low pressure column and the consequently reduced compression pressure. The compression pressure is reduced by 3-4 times the reduction in low pressure column pressure drop, because as the boiling pressure of oxygen is reduced, that of nitrogen in the high pressure column is reduced by 3-4 times as much. They estimate the power saving at around 8%.

Packing the high pressure column would also provide power savings, but they would not be as great as those achieved by packing the low pressure column, because in this case the compressor pressure is only reduced by the same amount as the reduction in pressure drop.

Bennett et al. (1989) also claim that the efficiency of structured packing in the distillation of mixtures of argon and oxygen containing more than 25% oxygen is unexpectedly good, based on the efficiency with mixtures of nitrogen and oxygen.

It is interesting to note that the vapour-liquid equilibrium data of Bourbo and Ischkin for argon-oxygen mixtures (given by Ruhemann, 1949) show a distinct change in character at 25% oxygen concentration. It is therefore unclear whether the advantage found by Bennett et al. is significant, given possible uncertainties in the vapour-liquid equilibrium and diffusion coefficients.

Another advantage of using structured packings in air distillation is that many more theoretical stages may be used in the argon side-column (Rohde and Corduan, 1989 and Agrawal et al., 1991). Pure argon may then be produced directly from the plant, without the need for a separate argon purification unit. The hydrogen consumed by catalytic burning of the oxygen in the argon may then be saved.

2.2.2 Disadvantages and potential problems.

Despite the high efficiency of structured packings when compared with random packings and traditional distillation trays, their efficiency compared to air separation trays is low. For example, the highest efficiency packing has an HETP of around 8 inches compared to about 6 inches for trays. In addition, at each feed or take-off a collector and distributor must be provided, which occupies a significant height of column. This means that packed air separation columns are larger than trayed ones, and more expensive, even though the opposite is true in conventional distillation. So the cost of the power saved by the use of low pressure drop structured packings must outweigh the extra construction cost of the packed plant. No-one has yet published any work on this economic balance.

If there is an argon column and the low pressure column is packed, the argon column must be at least partly packed, so that the pressure drop across it is not so high that its top pressure is below atmospheric pressure. Victor and Lockett (1989) describe a hybrid low pressure column, which is only packed below the argon column take-off, which avoids this problem but does not take advantage of the lower pressure drop possible if the whole column were packed.

The average pressure in the argon column should also be minimised so that the relative volatility of oxygen and argon is maximised. Allam and Prentice (1989) describe a way to do this by introducing a pressure-reducing valve in the argon column feed, but the liquid returned to the low pressure column must then be pumped back, or the column elevated to allow gravity feed. Victor et al. (1991) use trays in the base of the argon column to increase the pressure drop in it and lower its average pressure.

Very few published data are available on the performance of structured packings in air distillation, and so design efficiencies are uncertain. The experiments published so far (Alekseev et al., 1973, Zel'venskiy et al., 1978 and Bennett et al.,

1989) indicate that structured packings have a comparable efficiency in air distillation to that in conventional distillation.

A further problem which may affect the use of structured packings in air distillation is the uncertainty about the use of some materials. Bennett et al. (1989a) found that some materials which are commonly used in cryogenics may be unsuitable for packings in concentrations of oxygen exceeding the 21% found in air. This was because of the reduced ignition energy due to the much larger surface area per unit volume of material. They recommend the use of alloys with high copper concentrations to avoid this problem. If different materials are used for the packing and the column shell, the differential expansion should be minimised to ensure that the packing operated correctly.

2.2.3 Conclusion

The main advantage of using structured packing in air distillation is the reduced power consumption of the plant, whilst the main disadvantage is the increased capital cost. No-one has published any work on the economics of this balance. In the economic work (chapter 3), we shall perform an economic analysis to see whether it is economic to use existing packings and to identify where improvements should be made to packings to increase their advantages.

2.3 Structured packings; History, description, development and manufacture

Before developing a new packing, we must understand how packings have developed so far and where there is scope for further development. We should also examine their manufacture, so as to identify any possible cost reductions and to help identify how a new packing could be made.

2.3.1 History of packing development

Ever since the first use of stones in absorption towers, people have sought more effective packings to do the same job at a lower cost. Packing development is therefore a mature field and is as much an art as a science.

Early packings were made of ceramic (as a first development from stone) and were in the form of small rings or saddles which were dumped randomly into the column, or occasionally arranged in an ordered structure. Development of these random packings then took place so that metal sheet was used and the shapes were made more complex, so that the voidage and area available for mass transfer were increased. At the same time, wire mesh packings were developed to further

enhance the mass exchange area by encouraging complete wetting of the packing surface.

Some of the first packings with a structured design were those described by Stedman (1937). He considered the mass transfer process and identified various ways to improve the performance of packings in much the same way as this work aims to. There was particular interest in high efficiency packings around this time because of the need to separate the isotopes of water by distillation which requires several hundred stages.

Other early structured packings include the regenerator packing made from coiled corrugated strips and the Ewell gauze spiral packing tested in the programme described by Rushton (1946) and Weedman and Dodge (1947) and the double gauze corrugated packing developed by Watson (1949) and Hayter (1952). These packings were all tested in relatively small columns (up to 6 inches diameter).

One of the first structured packings used industrially (in vacuum distillation) was 'Panapak', described by Schofield (1950), which consisted of layers of corrugated metal strip assembled into a honeycomb-like structure.

The classic corrugated structured packing, from which most current structured packings are derived, is Sulzer's BX gauze packing, developed in the 1960's, again for low pressure drop in vacuum distillation (Huber and Hiltbrunner, 1966). At the same time, the less commercially successful 'Multifil' and 'Hyperfil' knitted mesh structured packings (Das, 1969) and various other packings such as that described by Ellis et al. (1969) were developed for the same purpose.

In the late 1970's, Sulzer developed a sheet metal version of their gauze packings, namely 'Mellapak', which has become the standard amongst structured packings (Meier and Stoecker, 1977).

During the 1980's, after work at FRI (Kunesh, 1987) which showed that packings could be operated reliably on a large scale provided that liquid distribution above the packed bed was good enough, confidence in and demand for structured packings increased. This led other manufacturers to develop structured packings, mostly based on the structure of Mellapak. The most notable exception to this is Kuehni's Rombopak, which has a unique expanded metal structure.

The Russian and East European patent literature shows that numerous structured packings have also been developed there in the last few decades, for example, perform grid (Hoppe and Keller, 1980) and Pyrapak (Hoppe and Kunze, 1985).

Most of the recent development of structured packings has concentrated on increasing the wetted surface area and reducing the liquid phase resistance to mass transfer by changing the texturing applied to the metal surface. We shall now go on to consider the different packings available and examine their different features.

2.3.2 Description and development of existing structured packings

Before looking at possible new packings with a performance suited to air separation, it is important to understand the presently available packings, which provide the starting point for the development. We shall first describe the geometry of structured packings, then go on to look at the differences between packings from different manufacturers and finally examine in detail the reasons why they have developed as they have.

2.3.2.1 Packing geometry

Figure 2-6 shows three types of commercially available packing; Sulzer's Mellapak 500YW, Norton's IMSP 1T and Kuehni's Rombopak. At the start of this work, Rombopak was not available in a version with a high enough surface area per unit volume to be considered worth testing, so only the geometry of the channel-type packings will be considered in detail.

These channel-type packings are made from metal sheets which have corrugations running across them at some angle θ from the horizontal (figure 2-7a and b). These sheets are arranged into blocks so that the corrugations on neighbouring sheets run in opposing directions (figure 2-7c). The depth of a corrugated sheet (i.e. the amplitude of the corrugations) is denoted by t, the wavelength of a corrugation by λ the length of metal between crimps by S and the crimp half-angle by ϕ (figure 2-7d). Considering a unit height of packing, and taking into account both sides of the metal sheet, the area per unit volume, a, is then given by:

$$a = \frac{2\,S}{S\cos\phi\; S\sin\phi} = \frac{2}{S\cos\phi\sin\phi} = \frac{2\sqrt{\left(\frac{\lambda}{2}\right)^2 + t^2}}{\frac{\lambda}{2}t} = \frac{2\sqrt{\lambda^2 + (2t)^2}}{\lambda\, t}$$

The metal sheet may be perforated or be textured so that the actual surface area available for mass transfer is different from a, however a is a good measure of the quantity of metal contained in the packing, and hence of its relative manufacturing cost.

If the thickness of the sheet is δ and the metal density ρ then the mass, μ, per unit volume is given by:

$$\mu = \frac{a}{2}\delta\rho$$

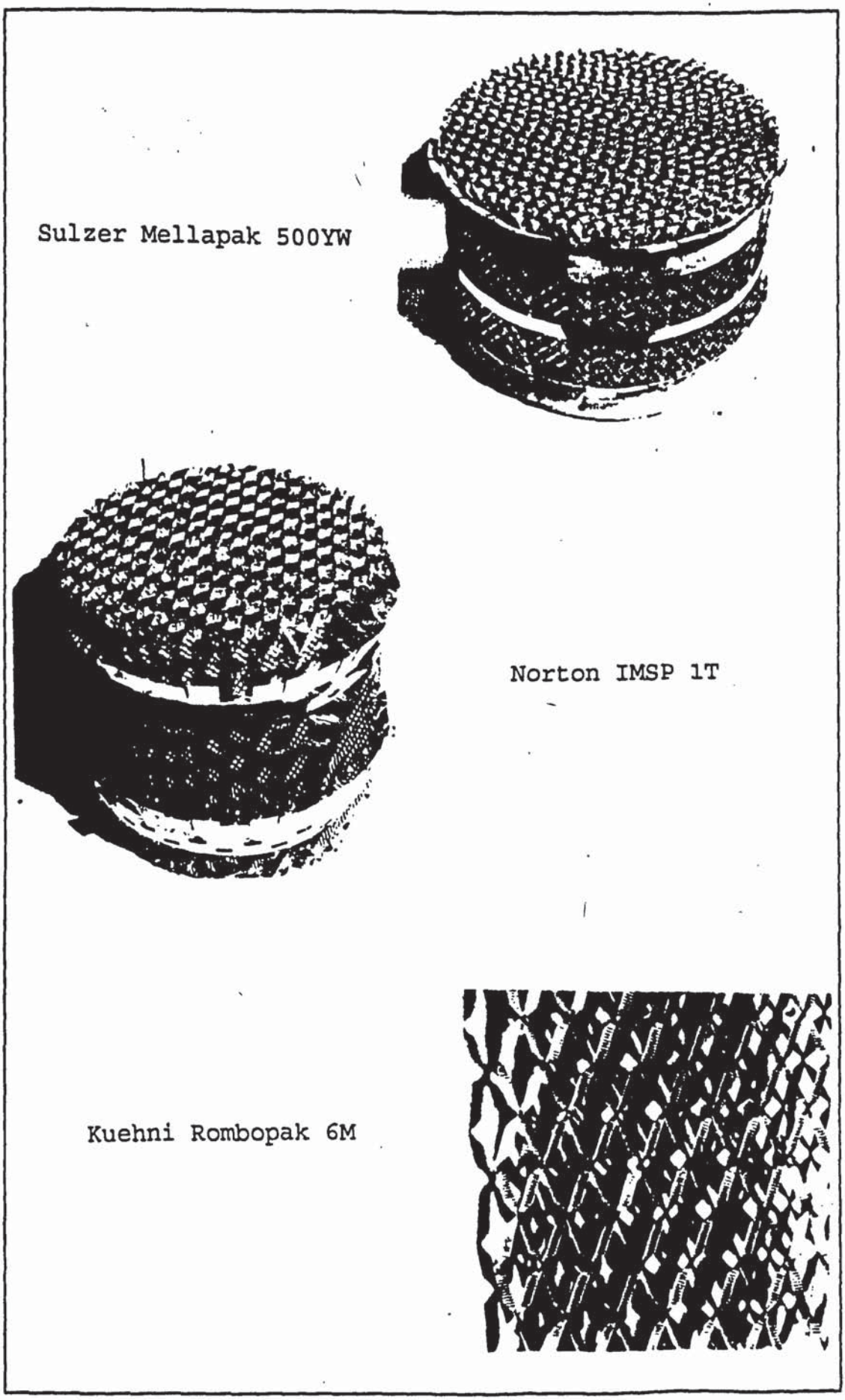

Figure 2-6 Three different types of commercially available structured packing

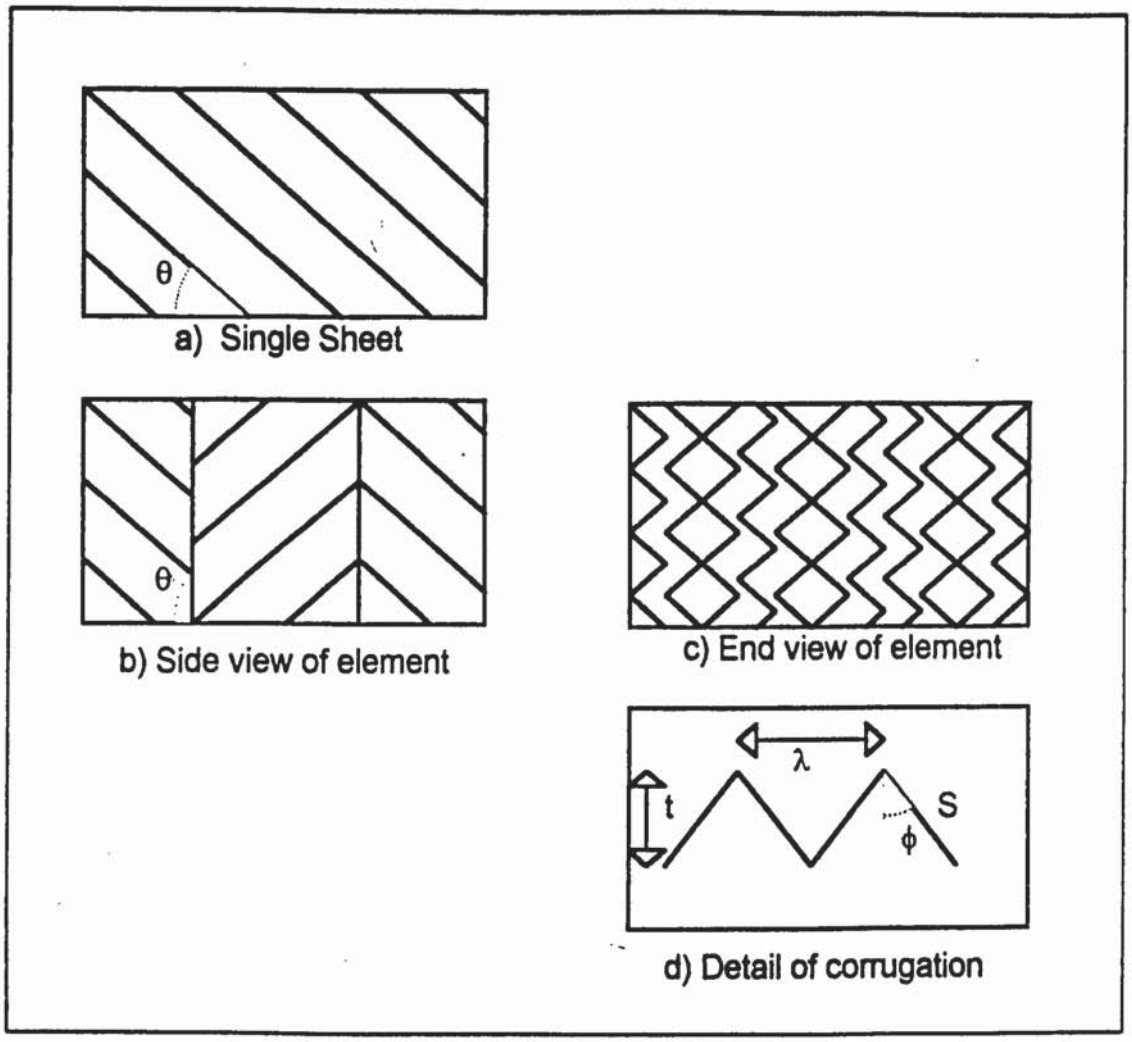

Figure 2-7 Structured packing geometry

The cost of metal in the packing will depend on μ and hence on δ as well as on a. So the thinner the metal that can be used, the cheaper the packing should be.

In addition, the void fraction, ε, is given by:

$$\varepsilon = 1 - \frac{a}{2}\delta$$

Typical void fractions are between 0.9 for gauze packings and 0.99 for low area packings made with thin metal sheet.

The hydraulic diameter for turbulent flow along a channel in the packing, d_{hyd}, defined as four times the flow area divided by the wetted perimeter, is given by:

$$d_{hyd} = \frac{4\,\varepsilon\,S\cos\phi\;S\sin\phi}{2\,S} = \frac{4\,\varepsilon\frac{\lambda}{2}t}{2\sqrt{\left(\frac{\lambda}{2}\right)^2 + t^2}} = \frac{4\,\varepsilon}{a}$$

2.3.2.2 Western commercial distillation and absorption packings

Gauze packings

Gauze packings, such as Sulzer's BX were the forerunners of modern sheet metal structured packings. Most manufacturers now offer gauze packings as well as sheet metal ones, and their performances are similar. Their particular advantage is in vacuum distillation where liquid rates are low and the pressure drop per theoretical plate must be minimised. Gauze is said to be particularly suited to low liquid rates because capillary action between the wires promotes liquid spreading and complete wetting of the surface. Packings made from gauze have a very high efficiency compared with sheet metal packings with a similar specific area (about 2-3 times more efficient), but have a lower capacity because of their smaller void fraction. Their efficiency increases much more than that of sheet metal packings as the flows of vapour and liquid are reduced. This is normally attributed to a more complete wetting of the gauze surface. Improved wetting does not however explain the increase in efficiency over a comparable sheet metal packing at high flows, where even a sheet metal surface would be completely wet.

The main disadvantage of gauze packings is their expense. Gauze costs several times as much as metal sheet, so these packings are considered too expensive for general use.

Sulzer Mellapak and Koch Flexipac

The first sheet metal packing, Mellapak, was introduced in the late 1970's (Meier, Hunkeler and Stoecker, 1979). It was subsequently licensed to Koch in the USA as Flexipac. Its surface was perforated (approximately 10% free area) and fluted, to promote liquid spreading and turbulence. Its efficiency was not as high as a gauze packing with a similar surface area, although unlike gauze packings, the efficiency was not significantly different over a wide range of flows. This is usually attributed to poor wetting at low flows reducing the efficiency more than gauze packings.

Montz Montzpak B1

An early competitor for Mellapak was Montzpak, introduced around 1983 (Bauermann and Benhamou, 1983). It was also licensed in the USA to Nutter Engineering (Nutter, 1987). Results for this packing have also been published by Billet and Mackowiak (1988). Montzpak has sinusoidally corrugated sheets, rather than sharply crimped ones, and its surface is embossed with shallow projections about 1 mm across and 1 mm deep. The sheets are not perforated. Nutter (1987) state that packing blocks are eight inches (203 mm) deep, whilst Bauermann and

Benhamou (1983) give the block height as 125 mm (4.9 inches). This increase in block height followed work by Shell, which demonstrated that there was a pressure loss at each block boundary. The results presented for vacuum distillation by Nutter (1987) and Billet and Mackowiak (1988) are in broad agreement, and show a 15% higher capacity and a 5-10% lower efficiency for type B1-300 than those presented by Bauermann and Benhamou (1983). The performance appears to be broadly similar to Mellapak, after taking into account the different surface areas.

Kuehni Rombopak

Rombopak was introduced by Kuehni in 1982 and described by Buehlmann (1983). Its structure is unique and it consists of expanded metal sheets placed next to each other. The liquid flows is confined to the metal, which promotes spreading and mixing, but the vapour flow is not as well controlled as in the channel type packings.

Despite the different structure, its performance was not significantly different from the other packings available at that time. Subsequent developments have included the addition of fluting to the metal surface (Buehlmann, 1987) and the production of packings with different areas per unit volume (Kuehni, 1992). Rombopak appears to perform better than other packings where the liquid load is low (for example in vacuum distillation and at a small percentage of the maximum capacity), but worse when the liquid load is higher (at higher pressures or towards flooding). This is similar to the behaviour of gauze packings and is probably because the surface becomes overloaded with liquid and channelling results.

Glitsch Gempak

Chen et al. (1983) described the development of Gempak, which concentrated primarily on improving the wetting of the channel type packing. They do not describe the surface, but it is described by McGlamery (1988) as lanced and perforated. Lancing describes the process of slitting the metal sheet and opening the slit by pressing the metal on one side of the slit. Again, the performance of Gempak is more or less the same as the other packings.

Raschig Ralu-Pak

In 1985, Billet and Mackowiak presented results of tests on Raschig's Ralu-Pak. This is another channel-type packing which differs from the others in that its surface is perforated with a regular arrangement of slits. Its blocks were reported to be 210mm deep, the same as Mellapak. The results show a slightly higher efficiency than Mellapak, but a slightly lower capacity, whilst the pressure gradient at flooding is smaller. The overall difference is, however insignificant.

Norton Intalox Metal Structured Packing

Norton introduced Intalox 2T and 3T in about 1988, and their brochure (Norton, 1988) gives performance data for several systems. It differs in two ways from the other channel type packings: the surface texture and the channel geometry. The surface is deeply embossed, and each dimple has a tiny perforation, whilst the channel crimp angle is larger than other packings and the channels are switched over approximately every four inches so that what was a trough becomes a peak and vice versa (see figure 2-6 and Hsia, 1987). Results indicate a higher efficiency and capacity than the other packings. In addition, the Intalox packings have a lower specific area, and so should be cheaper to manufacture. The advantage is explained by Hsia (1987) to be entirely due to the improved distribution of liquid as it is spread by and drips from the channel changeover points.

Jaeger Max-pak

The most recent structured packing on the market is Jaeger's Max-pak, introduced in 1989 (Jaeger, 1989). It has W-shaped tabs bent in the opposite direction to the corrugation. These are claimed to increase gas and liquid turbulence and to aid liquid distribution over the smooth metal surface. The packing blocks are 12 inches (305mm) deep. According to the results presented in Jaeger's brochure, (Jaeger, 1989), Max-pak does not appear to be as good as Norton's Intalox, since it has a similar efficiency to Intalox 2T and a slightly lower capacity, whilst its surface area per unit volume is higher - 250 rather than 213 m^2/m^3.

2.3.2.3 Other structured packings

In addition to the commercially available distillation and absorption packings, there is a number of cooling tower packings, made mostly from plastic, as well as other packings developed for mixing and distillation packings which are not sold for large scale use. There are also other potential shapes and variations in surface texture and channel arrangement which have been patented but have not been commercialised in the west.

Cooling tower packings

Some possible designs are illustrated in figure 2-8. Because they are normally vacuum-formed from plastic, more complex shapes are possible than if they were pressed from metal sheet. It is also easier to include spacers to separate the sheets, as in figure 2-8a. No information was found about the performance of these packings in comparison to the distillation packings. Most designs do not allow for

such good vapour mixing as the criss-crossed channels, so their performance would probably not be so good.

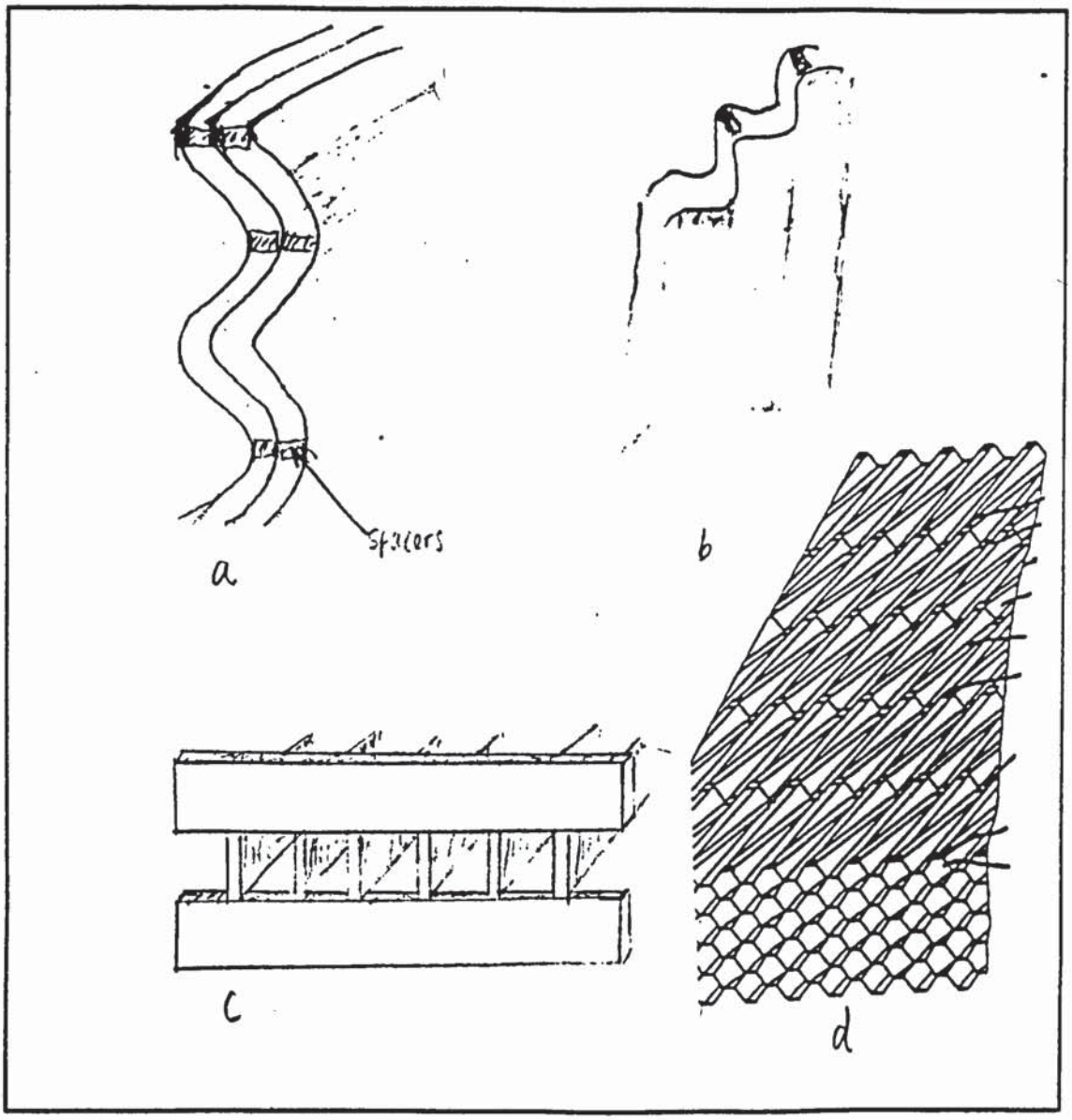

Figure 2-8 Different types of cooling tower packing

Mixing packings

The aim of mixing packings is to create as much turbulence and hence mixing as possible whilst minimising the pressure drop. They are generally only used with one phase, and so the distribution of a continuous liquid phase over the surface does not have to be considered in the same way as in distillation packings. Designs such as those of Huber (1985) Pluess (1985) and Streiff (1985) (figure 2-9) have the potential problem of inadequate control of such a liquid phase which could result in incomplete wetting or the formation of a spray, which would reduce efficiency and capacity. On the other hand, it is possible that the frequent renewal

of the liquid surface could enhance mass transfer. Again, no data was found on the performance of these packings in distillation.

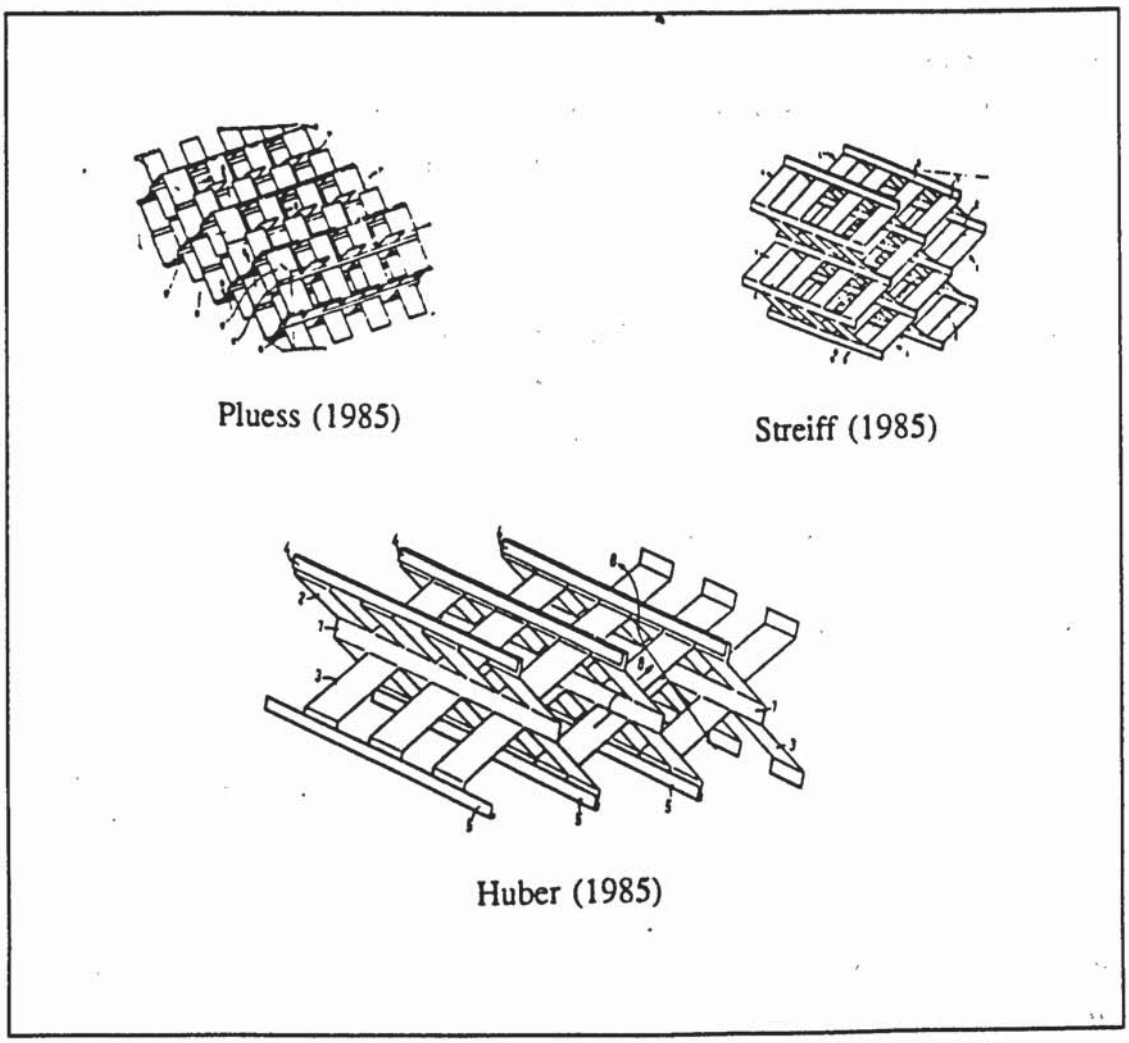

Figure 2-9 Different types of mixing packing

Small scale distillation packings

These include the gauze packings of Stedman and of Watson and Hayter, which seem to be no longer available, and the knitted wire packings sold by Knitmesh as Hyperfil and Multifil, which were originally intended for large scale use and are now very expensive. The knitted wire packings were either made with monofilament or multifilament wire. Multifilaments were used to aid wetting by capillary action. The knitted wire sheet was then crimped and either rolled up or arranged as in a channel packing. The crimps were however much smaller than in the channel-type packings. The coiled shape was found not to be as good as the one made from sheets because it caused liquid to accumulate at the centre (Das, 1969). In addition the performance was found to depend on the way in which the column was packed, and to depend critically on the initial liquid distribution.

The fact that these packings are no longer available for large-scale use probably indicates that they are uneconomic on a large scale, although their efficiency is comparable with the currently-available packings. Alternatively, they may have come too early, before the development of reliable distributors, so that they were seen as unreliable on a large scale. Some of them may be worthy of renewed investigation, particularly in specialist applications such as air separation.

Tianjin University packings

Structured packings have been produced by Tianjin University Packing factory in China since the mid 1980's. These were initially direct copies of Sulzer's Mellapak, but now some other types are also produced, in particular gauze packings and packings with a shallow embossed surface with tiny perforations, which use thinner metal sheet. The block height varies, according to the application, from 5 cm to 20 cm. Tests at Tianjin University on these packings in a 0.2 m diameter column indicate a reduction in efficiency from the peak value (near flooding) of up to 40% at lower flows. This is not apparent in Mellapak.

2.3.2.4 Reasons for development of features of structured packings

Types of structured packing

A number of structured packings are based on vertical metal or plastic sheets, rather than channels, particularly ones for use in cooling towers. Examples are those of Faigle (1972), Holmberg and Strindehag (1976), Martsenyuk (1987a and 1987b), Martsenyuk and Guseynov (1987) and Vlastimil (1989), which are illustrated in figure 2-10.

Some of these packings have corrugations on the surface of the sheets (Faigle, 1972; Holmberg and Strindehag, 1976, and Vlastimil, 1989) and some have tabs pushed out of the sheets (Martsenyuk, 1987a and 1987b, and Martsenyuk and Guseynov, 1987). Most have a number of sheets arranged parallel to each other, but in that of Martsenyuk and Guseynov (1987) the strip is coiled.

Another type of packing is that of Ukhanev et al. (1985) which consists of interlocking spirals. This is likely to be difficult to manufacture consistently.

Channel shapes

There are many variations on the channel-type structured packings. Some examples are shown in figure 2-11. These may be made from crossed corrugated sheets (like most of the commercial packings) or from alternate flat and corrugated sheets (for example Ioan et al. (1986b)) This latter type of packing, however, is less efficient than the former. Of the crossed corrugated sheet packings, most have

channels sloping alternately in opposite directions. A variant on this is to include a sheet with vertical channels in between each pair of inclined channels to reduce the pressure gradient, for example the packing of Ioan et. al. (1986a).

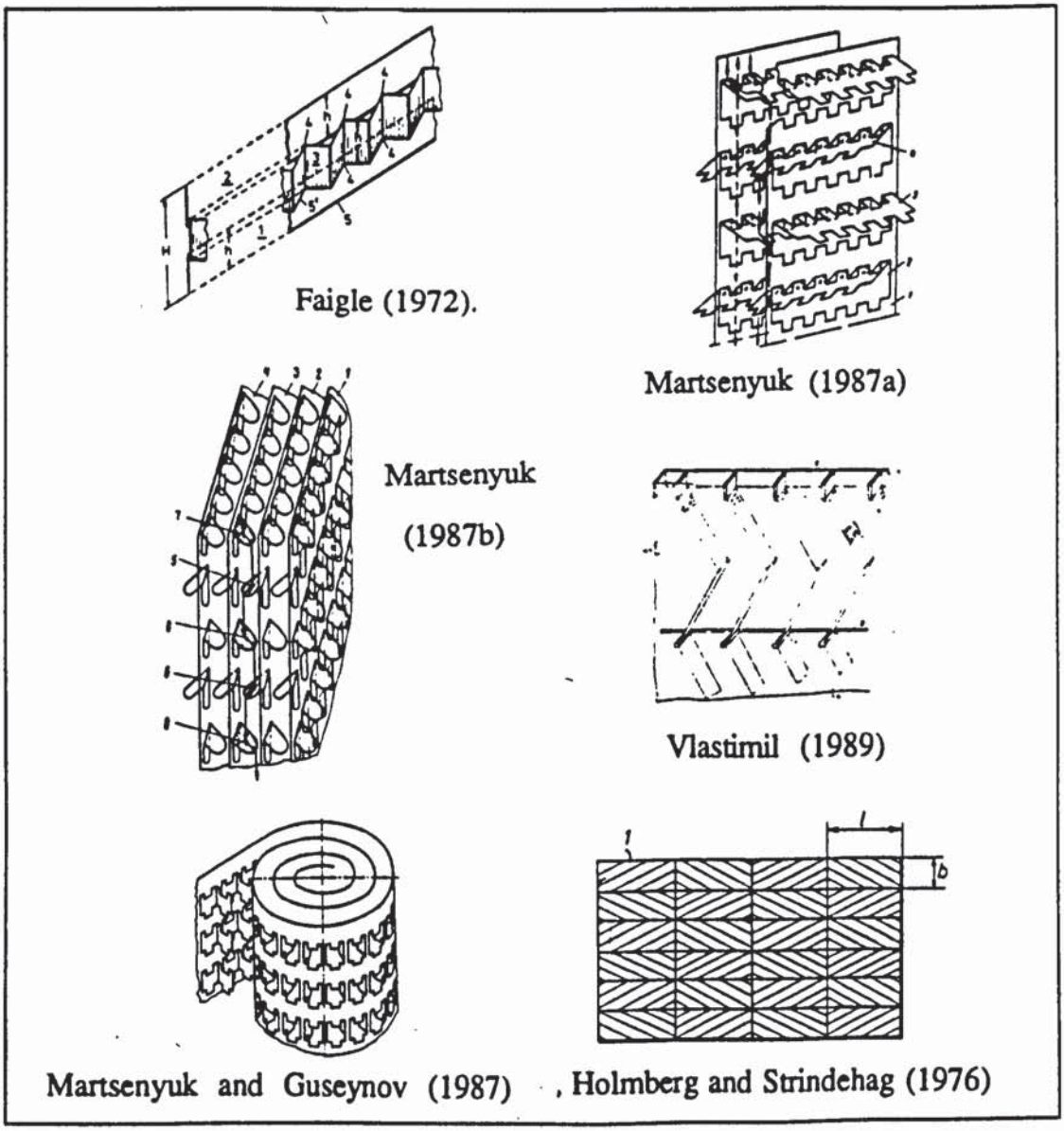

Figure 2-10 Different types of structured packing

The type of corrugations may also vary. They may be straight (as in Mellapak) or curved (as in Montz-pak A2) and the crimp may be sharp or continuous, so that the channels have triangular (Mellapak) or sinusoidal (Montz-pak) cross sections. The curved cross-section is said to reduce the liquid's tendency to flow along the peaks and troughs (Nutter, 1987).

Other variations in the channel shape are also possible. Hsia (1987) describes channels which are switched over every few centimetres so that a trough becomes a peak and vice-versa, as in the Norton packing. This arrangement is said to lead to a better distribution of liquid and to liquid dripping from the channels at the switch over points, and Hsia (1987) reports a 25% lower pressure drop per theoretical plate and 25% higher capacity than conventional packings. Another

possibility is to truncate the peaks of the channels (for example Regehr, 1973) so as to reduce the pressure gradient by allowing more vapour flow parallel to the column axis. Meier (1984) incorporates vertical surfaces between the crimps on the sheet and like Hsia describes the advantage solely in terms of better flow in the liquid phase; the steep parts allow it to accelerate and flow more vertically. Stackhouse (1987) uses a more complex three-dimensional arrangement of corrugations. He claims that this shape reduces the resistance to gas flow and improves gas and liquid distribution by reducing the number of contact points between the sheets. It does, however, require careful alignment of sheets and would be difficult to produce from sheet metal, as different parts of the sheet are stretched by different amounts.

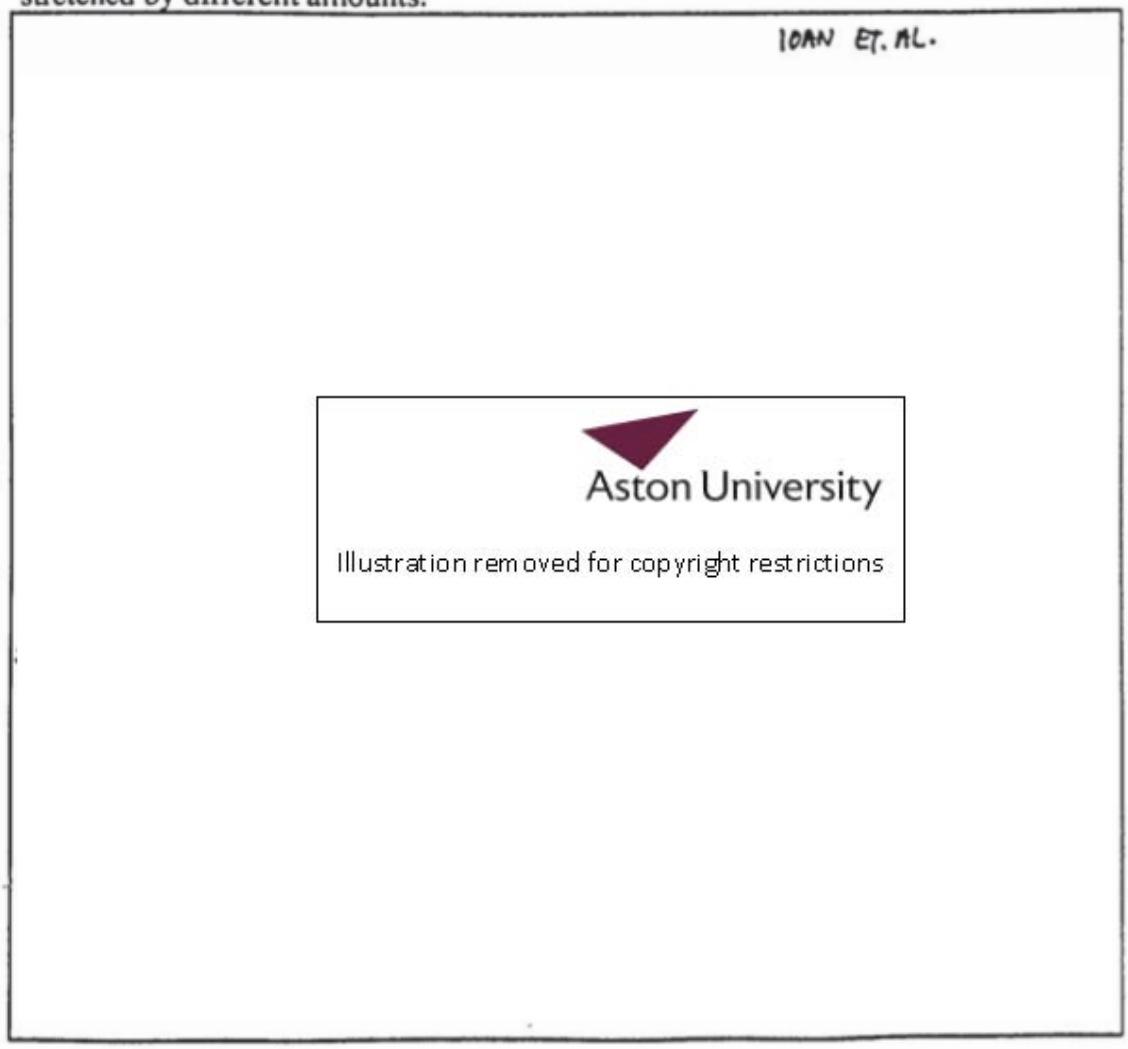

Figure 2-11 Different channel-type packings

Packing surface treatments - perforation and texture.

In addition to varying the channel shape, the nature of the surface of the packing is frequently altered. The surface may be perforated with different sizes and shapes of holes on different pitches, it may be lanced or have various shapes of tab pushed out of it and it may have small corrugations or be embossed with a three-

dimensional pattern. The aim of changing the surface texture is always described as improving liquid wetting, distribution or mass transfer. Some examples of different surfaces will now be examined.

The original Mellapak had small corrugations or fluting parallel to the axis of the packing sheet and holes of about 5 mm diameter arranged on a triangular pitch to give an open area of about 10%. The Tianjin university packings have the same surface texture and perforations. Because the fluting is parallel to the sheet axis, manufacture of this type of surface is very easy. The fluting is designed to spread the liquid across the whole surface of the sheet, and the holes allow liquid to pass from one side to the other and split the liquid stream so that mixing is promoted. Meier (1981) claims that the combination of holes and fluting provides for unexpectedly good liquid distribution. He also says that fluting is more effective if it is not horizontal, so that there is a component of gravity in the direction of the flutes and the liquid spreads along them. Huber (1981) describes a modified surface texture where a fluted surface is alternated with a smooth one going down the column. This allows for frequent renewal of the liquid surface as the flow regime and film thickness change from one section to the next. Lockett and Amory (1989) describe a modified fluting which increases the liquid hold-up. The angle of the individual flutes is chosen to form shelves on which liquid accumulates. This is claimed to increase the contact time between vapour and liquid and to increase the efficiency by about 10%. Other types of surface texture include the shallow embossing used in Montzpak, the deep embossing used by Norton and the lancing used in Ralupak and Gempak. McGlamery (1988) concluded that the deep embossed and fluted surfaces gave the best mass transfer performance, but he did not test the Ralupak surface which is lanced to a much greater extent than Gempak.

Chen and Acerra (1987) claim that holes on a square pitch are easier to punch and that they give results just as good as the triangular pitch. They also claim that smaller holes are better because the manufacturing process leaves larger burrs on them. These burrs are said to promote liquid spreading both over the sheet and from one side to the other. An improvement in efficiency of up to 30% was observed with the new hole pattern.

A further variation of the type of perforation is to punch tabs into the channels, for example Seah (1986). In this case, groups of triangular tabs project in each direction from the sheet (figure 2-11). The advantage of these is claimed to be that they promote the spreading of liquid from one side of the sheet to the other and across the sheet. They also improve the mixing of the phases by creating drops of liquid which travel through the gas and then spread out on the packing surface when they land.

The other type of surface which should be considered here is gauze rather than sheet. This has the advantage of spreading the liquid much more effectively, especially at low flow rates, by capillary action. Sulzer Brothers (1966) describe a self-wetting gauze which is especially suitable for structured packings, but conventional gauze gives similar results with organic systems. McGlamery (1988) found that mass transfer from liquid on a wetted gauze sheet was not as great as from that on textured metal sheets, which suggests that the advantage of gauze must lie in its improved wetting characteristics.

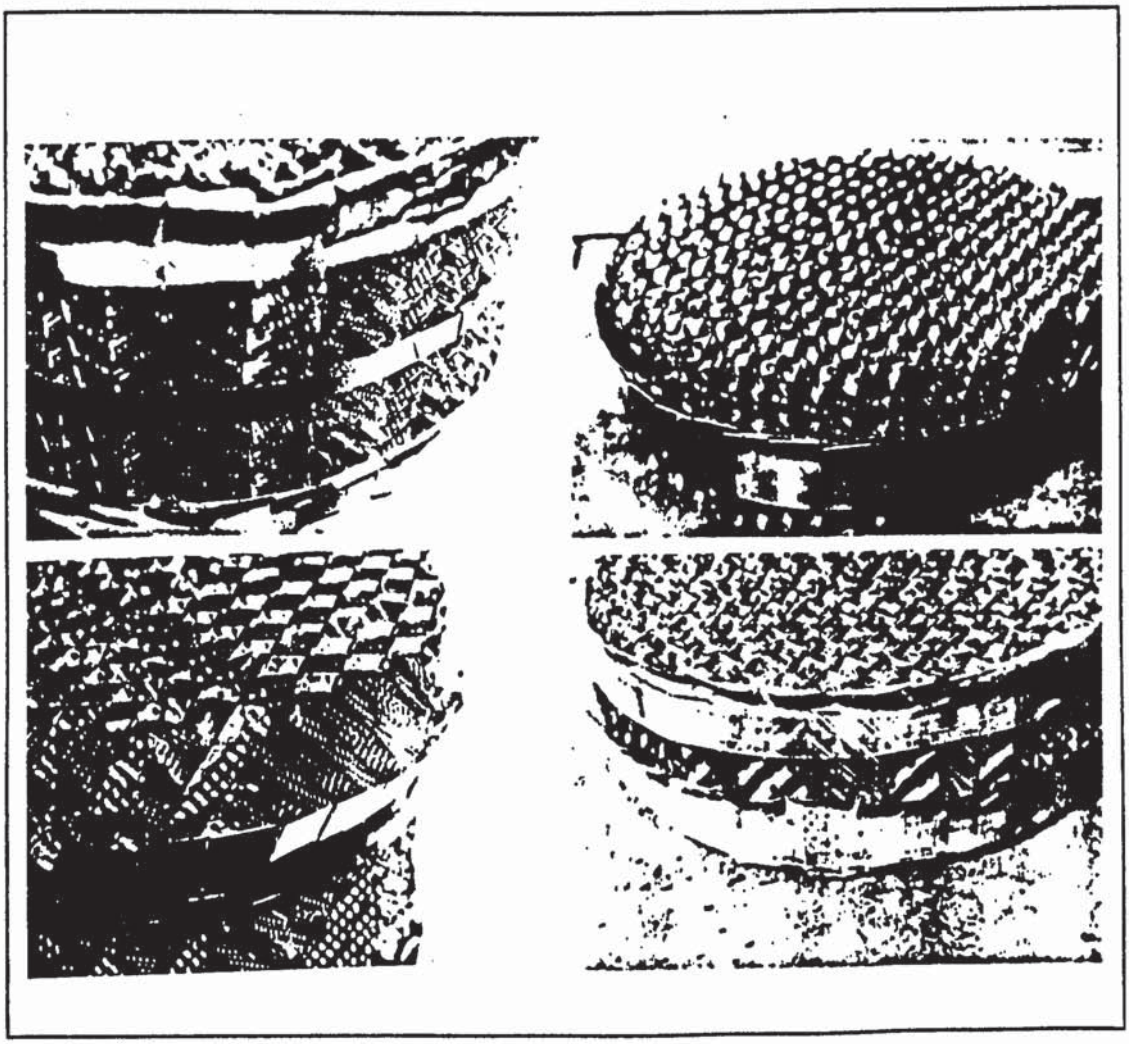

Figure 2-12 Different types of wall-wipers

Wall-wipers

Different types of wall-wipers are illustrated in figure 2-12. They are made either from gauze or sheet metal and perform three functions; they remove liquid from the wall and feed it back into the packing, they block the flow of gas up the sides of the packing and they ensure that the elements are centred in the column.

An alternative way of preventing liquid flowing down the wall is to ensure that it never reaches the wall. Bosquain et. al. (1989) show several methods of doing

this, either by cutting the sheets so as to block the ends of the channels or cutting slots into the sheets near the walls to redirect liquid into the packing.

Conclusions

We have seen that a many different ways of improving the performance of structured packings have been suggested. Most have concentrated on increasing the contact area between the phases by improving the wetting of the surface. Some have attempted to increase mass transfer in the liquid phase by promoting turbulence and surface renewal. None has set out explicitly to increase the mass transfer in the vapour phase, although some may have done so. Attempts have, however been made to reduce the pressure gradient of the vapour through the packing.

2.3.3 Manufacture of structured packings

It is important to consider how packings are made, so that when developing a new packing, we do not produce one that is much more difficult or expensive to make than existing ones.

Method

This description is based on the simple but labour intensive process used in Tianjin University Packing Factory, China. The operations would be the same in an automated process, but the machinery would be more complex to allow automatic handling of the metal sheet between the operations..

The raw material for the packing is metal strip between 0.1 and 0.3 mm thick, which is supplied in coils. The steps in the manufacturing process are illustrated in figure 2-13.

The strip is first perforated by feeding it manually under a press equipped with a perforating tool. Each press action perforates about 15 cm of strip. Next, the surface of the strip is textured by feeding it continuously between mechanically driven rollers. A photograph of the strip at this stage is shown in figure 2-14.

After this preparation, the strip is now ready to be crimped. The crimps are made one at a time by manually feeding the strip under a press. Before blocks of packing can be assembled, the continuous strip must be cut into sheets of the correct length. This is done either with a specially corrugated guillotine or by using an electric grinder.

If the blocks are to be circular, gauze strips are spot-welded into bands of the required diameter and the sheets arranged into a block onto which the band is forced. If the blocks are rectangular (for a large column), the sheets are fastened

with bolts or temporarily fastened with packaging bands which are removed after installation in the column.

Gauze packings are made in exactly the same way as sheet metal ones, except that they may be cut with tin snips rather than a guillotine.

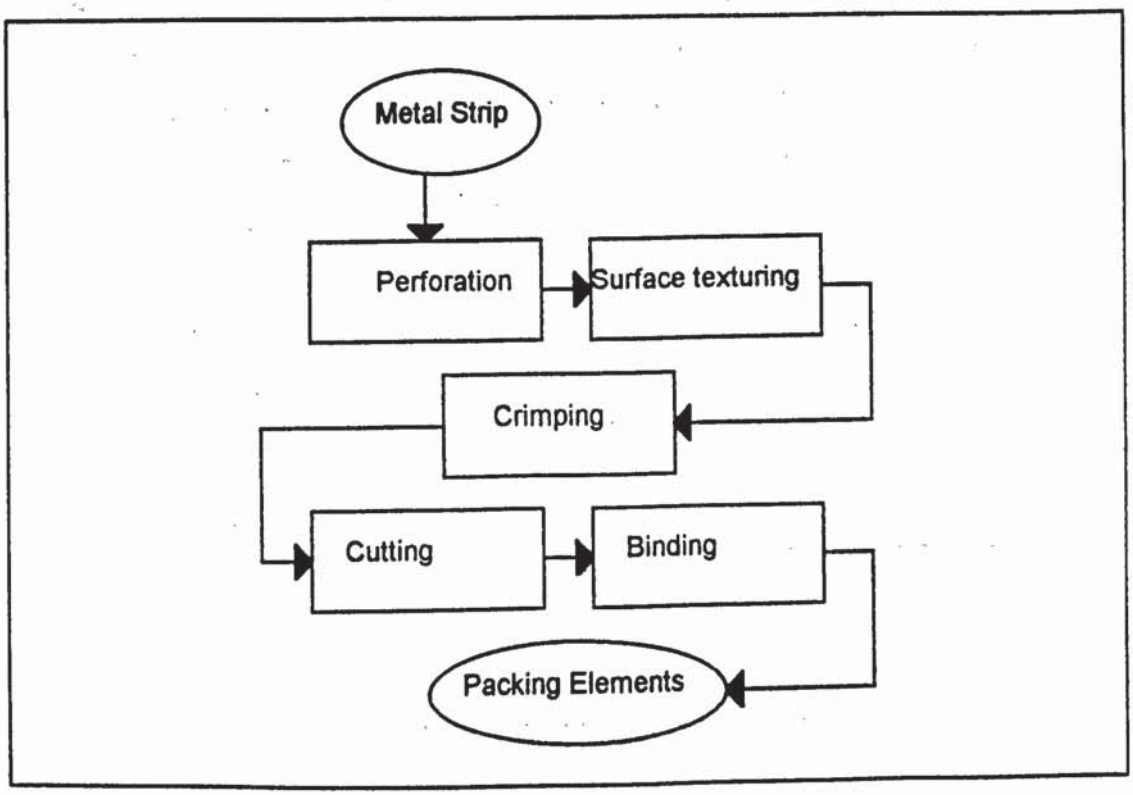

Figure 2-13 Steps in packing manufacture

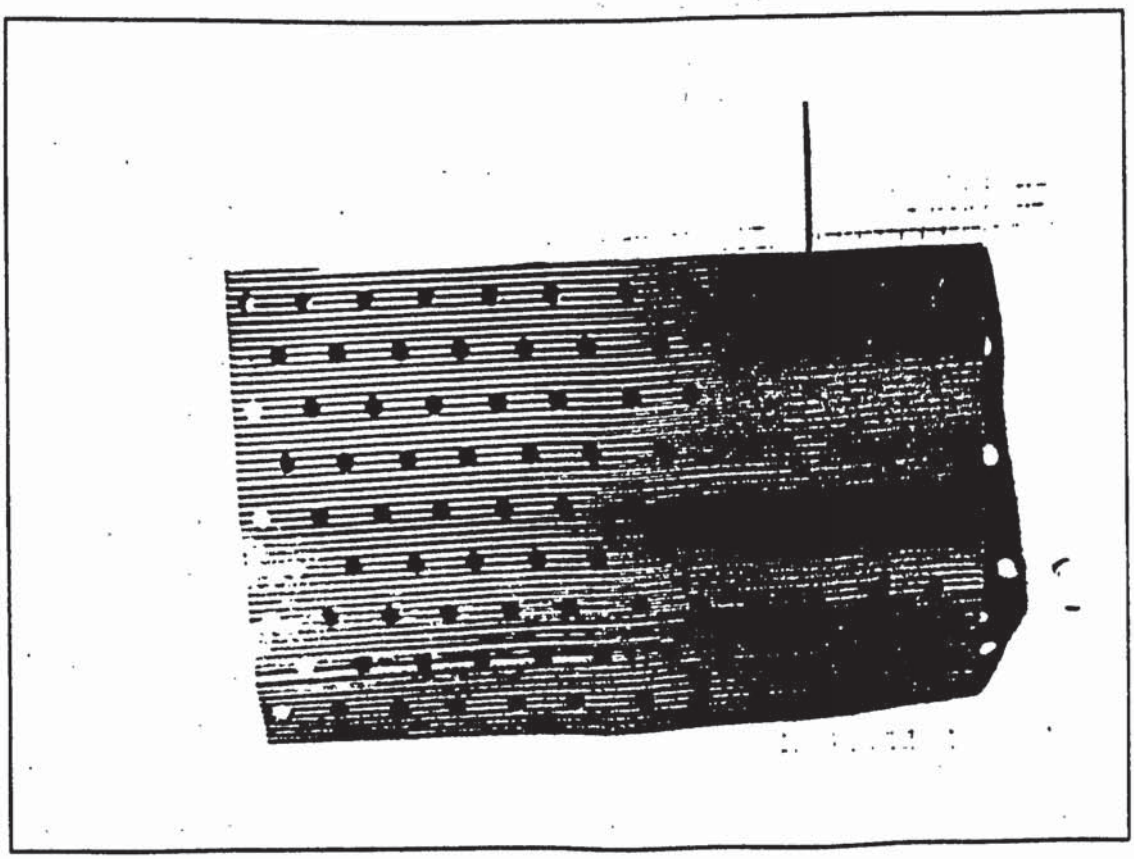

Figure 2-14 Packing sheet after perforation and surface texturing

Discussion

During the perforation process, the metal would tend to snag on the tool if were designed only to punch through the metal. In practice, a device is needed to strip the metal from the tool. The modified tool, which uses a stripping plate and a rubber block to remove the metal from the tool, is illustrated in figure 2-15. When the stripping plate hits the metal sheet, the rubber is compressed and the punches perforate it. As the tool is withdrawn, the rubber expands again and the stripping plate pushes the sheet off the tool. Other forms of perforation, such as lancing would require an even more complex tool.

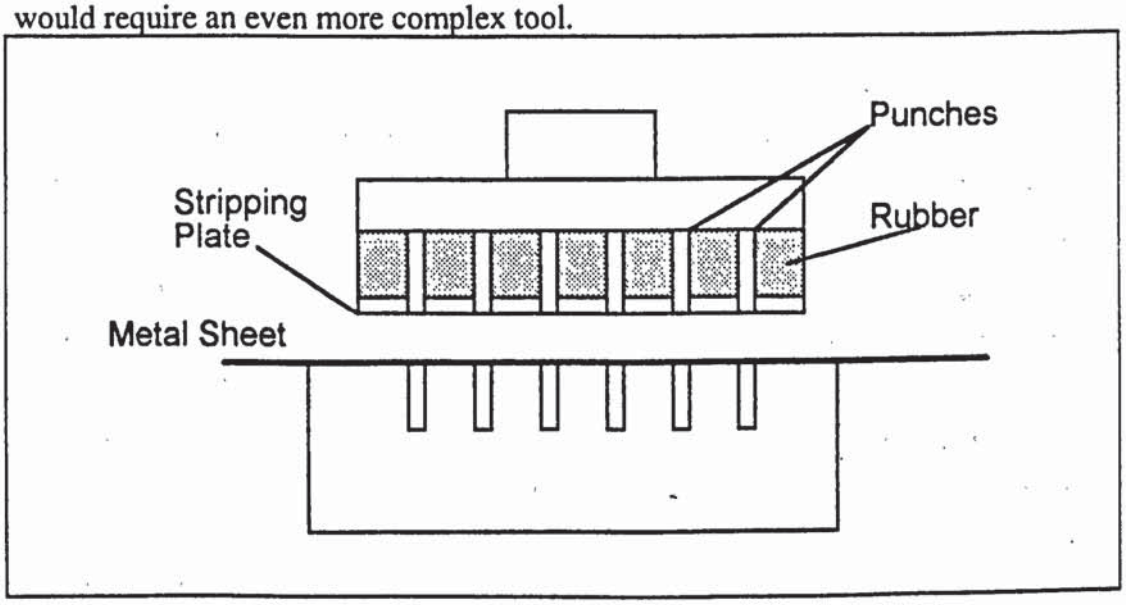

Figure 2-15 Perforation tool

The crimping tool is designed only to bend the metal sheet, not to stretch or perforate it. The metal sheet is pulled into the die as the tool descends. At the end of the cycle, the tool puts the bends into the sheet, completing the crimp. No stripping plate is needed on the crimping tool, because no part of it is likely to snag on the metal. If several crimps were to be made with one press action, the tool would need to be more complex, so that the crimps were made from the leading part of the strip towards the trailing edge. This would allow the strip to be pulled into the tool one crimp at a time and avoid any stretching of the metal.

Another possible method of forming the crimps would be similar to that described by Plegat (1969). Metal strip is passed between a pair of corrugated rollers, which give it the required shape. This method is likely to be economical only for large volume production, where the extra initial cost of the complex rollers is outweighed by the increase in production speed and reduction in cost.

When considering other shapes of packing, it is important to bear several things in mind. Any tabs would have to be pressed out either at the same time as the crimping or afterwards, or they would interfere with the crimping process. The tool to create the tabs would be fairly complex, as a stripping plate would be needed to avoid snagging. If the channels are curved, or change direction

suddenly, the metal is likely to crease. This is probably not important for the performance of the packing, but may cause weaknesses or create difficulties removing the strip from the tool. Another important point is that the length of the new shape along its surface parallel to the axis of the strip must be the same across its width, or it will tend to curve. This is equivalent to the condition that any stretching of the metal should be uniform across the whole strip.

2.4 Correlation and modelling of packing performance

To design packed distillation columns, it is necessary to predict the performance of packings with different distillation mixtures. This means that models or correlations tend to be developed for a particular packing or group of packings, with the differences between packings taken into account empirically. In this work, where the aim is to develop an improved packing, it is advantageous to have a more fundamental model of the operation of a packing so that the effect of changing the geometry may be estimated. Even these models will involve some degree of empiricism or assumption because of the complexity of the situation, for example a turbulence model may need to be used to calculate the flow or mass transfer. A further difficulty is that the more effective a packing is, the more complex and difficult it is likely to be to describe, so the usefulness of the simple models is reduced still further.

In this section, we will consider the different models proposed for structured packings and look at their suitability for packing design. We shall look in detail first at fluid flow then at mass transfer in packings. We shall also consider briefly the distribution of vapour and liquid in packed columns and the effect of maldistribution on their performance.

A selection of models which may be used to describe structured packings is summarised in table 2-1.

Author	type of packing	liquid hold-up	wetted area	pressure gradient	capacity	efficiency
Gilliland and Sherwood (1934)	Wetted-wall column	no	no	Measured friction factor with and without liquid	no	Correlation of mass transfer coefficients
Westhaver (1942)	Wetted-wall column	no	no	no	no	Solution of diffusion equation in laminar flow ignoring liquid resistance

Kaminskii and Giorgadze (1971)	Small random packings	Account for vapour flow	no	Use friction factor, calculate pressure gradient and liquid hold-up simultaneously	Flooding when friction and pressure forces equal gravity force	no
Alekseev et al. (1972)	Structured packing and wetted-wall columns	no	no	no	Empirical correlation based on dimensional analysis	no
Kaminskii and Giorgadze (1973)	Small random packings	no	no	no	no	Laminar pipe entry flow model, solution of diffusion equation in vapour and liquid
Zogg (1973)	Gauze structured packing	Laminar film thickness	no	Gives turbulent shear stress exerted on liquid film	no	Numerical solution for liquid, empirical deduction for vapour
Hughmark (1980)	Random and structured packing	Kapitsa film thickness	Random packings only: empirically. Structured packings: equal to surface area	Friction factor, constant for particular packing, effective vapour velocity based on reduced cross-section with liquid hold-up	Kraybill-type correlation, empirical constant for each packing	Vapour: Theoretical dimensionless mass transfer coefficients without viscous sublayer. Liquid: Correlation for dimensionless mass transfer coefficient
Bravo et al. (1985)	Structured packing	Empirical correlation	no	Only below loading, accounts for hold-up.	no	no
McQuillan and Whalley (1985)	Wetted-wall columns	no	no	no	Review and evaluation of various theoretical models and empirical correlations	no
Bravo et al. (1986)	Gauze structured packing	no	Assumed equal to surface area	no	no	Vapour: empirical correlation, Liquid: penetration theory.

Hughmark (1986)	Random and structured packing	Empirical correlation for dimensionless film thickness	Random packings only, empirically from absorption data and, using mass transfer model, from distillation	Friction factor, increases after loading, correlated against film thickness to equivalent diameter ratio, uses effective velocity to account for hold-up	Assumes liquid wall shear stress is zero at flooding (equivalent to no net force on film)	Vapour: Theoretical dimensionless mass transfer coefficients without viscous sublayer. Liquid: Correlation for dimensionless mass transfer coefficient
Billet (1987) and Billet and Schultes (1987)	Random and structured packing	Random: Nusselt-type film thickness with empirical exponent. Structured: Brotz equation. Both account for vapour drag.	no	Empirical friction factor in terms of superficial velocity correlated against flow parameter for a particular packing, accounts for liquid hold-up	Calculated as point where increasing hold-up would not increase allowable vapour or liquid velocities	no
Spiegel and Meier (1987)	Structured	no	Empirical correlation based on efficiency	Dry pressure drop below loading, curve fit above.	Correlation of capacity factor against flow parameter	Ignore liquid resistance, Empirical correlation for vapour resistance.
Bennett et al. (1989)	Structured packing	no	no	no	no	Correlation of results in air distillation
Stichlmair et al. (1989)	Random and structured	Correlation against liquid rate based on turbulent liquid film equation, correlation against vapour rate above loading	no	Empirical friction factor for each packing. Allow for voidage reduction due to liquid hold-up	Point where pressure gradient increases infinitely with increasing vapour load	no
Billet and Schultes (1992)	Random and structured	Laminar film below loading, correlation against vapour flow above loading	Empirically from difference between actual and calculated hold-up. Different expressions for interfacial area.	Superficial friction factor correlated against vapour and liquid rates and hold-up	Where hold-up is 2.2 times laminar film value	Liquid and Vapour penetration theory with empirical adjustment. Empirical interfacial area correlation.

Bravo et al. (1992)	Structured packing	Laminar film (Nusselt equation) with effective gravity.	Expression of Shi and Mersmann (1985) with empirical correction for packing type	Friction factor for dry pressure drop, wet pressure drop correction factor which includes hold-up	Net force on liquid (effective gravity) is zero	Liquid: penetration theory with general correction for all packings. Vapour: modified wetted wall column correlation
Kister and Gill (1992)	Structured packing	no	no	Generalised structured packing pressure drop correlation. Capacity factor against flow parameter at different pressure drops	Correlation for maximum pressure drop in terms of packing factor, then maximum capacity factor from pressure drop correlation	no
Spiegel and Meier (1992)	Structured packing	Plotted against liquid load	no	Friction factor for dry pressure gradient, correction factors for wet pressure drop below loading. Curve fit above loading	Correlation of vapour capacity factor against liquid capacity factor (Wallis diagram). Defined where pressure gradient is 12 mbar per metre	no

Table 2-1 Summary of relevant packing models

2.4.1 Fluid flow in packings

The important things to know about the fluid-dynamic performance of a packing when designing a packed column are the pressure drop of the gas per unit depth of packed bed (**pressure gradient**) and the maximum gas flow for a given liquid flow (the **maximum capacity** or **flood point**). A further variable which is less important in design for steady state operation is the liquid retained in the packing at a particular gas and liquid flow, known as the **liquid hold-up**. It is however important in dynamic calculations and in determining the available space for gas flow and hence the pressure gradient. Because of this, it is frequently measured

and correlated along with the pressure gradient and flood point. It will therefore be considered here together with the **wetted area** of the packing, which is important in calculating the liquid hold-up.

When making mass-transfer calculations, it is also important to calculate the area of the vapour-liquid interface. This depends on the wetted area, but also on the nature of the interface and will be considered in the section on mass transfer.

Gas flow and dry pressure gradient

The behaviour of a packed bed with only gas flow is relatively easy to describe, but not so easy to predict.

All the models use a friction factor, but the velocity and dimension associated with the friction factor differ between models. An overall friction factor may be used, as is usual in granular packed beds. This allows us to calculate the pressure gradient in the bed from the superficial velocity. Its dependence on voidage could be estimated from the Ergun equation, but this equation has been found not to be so accurate when the void fraction is large, as in a structured packing. Authors who have used this approach include Spiegel and Meier (1987), Kaminskii and Giorgadze (1971), Billet and Schultes (1987 and 1992) and Stichlmair et al. (1989). The alternative approach is to use a local friction factor with an effective velocity and diameter, so as to calculate the overall friction factor, in the same way as in the derivation of the Ergun equation. This method has the advantage that the change in overall friction factor with bed geometry may be taken into account; the local friction factor remains unchanged whilst the changes in effective velocity and hydraulic diameter give the effect of changing the bed geometry. Bravo et al. (1985 and 1992), and Hughmark (1980) followed this approach, but measured the pressure gradient along the axis of the bed rather than in the direction of the flow channels. As a result, the local friction factor varies with the inclination of the channels, and the model is not as useful as it could be.

Some authors (for example Bravo et al.,1985 and 1992) have assumed that the friction factor is the same for all structured packings, but others (Stichlmair, 1989) have correlated a different one for each packing. It is not surprising if the differences between friction factors are small, since most commercially available structured packings have the same channel angle, crimp angle and block height.

The only model which accounts for changes in the cross-sectional shape of the channels is that of Zogg (1973). He includes the crimp angle explicitly, but his formula includes the critical Reynolds number for the transition to turbulence, which is likely to depend on the crimp angle and must be found by experiment.

Because the channels in a structured packing are more uniform than those in a random packing or a granular bed, the transition to turbulence in a structured packing is likely to take place at a higher Reynolds number. This means that it is

possible that the laminar regime, which is relatively unimportant in gas flow through granular beds, may be observed in structured packing, especially in higher area packings and at higher pressures.

None of the models allows for changes in the packing element height and channel angle except by changing the empirical friction factor. These variables should be relatively easy to allow for; the channel angle would require only the allowance for the pressure gradient being measured along the channels rather than the bed axis, whilst changes in element height could be accounted for by splitting the friction factor into several contributions. These contributions would be due to normal skin drag in the channels, the extra skin drag caused by the entrance effect at the beginning of each block and the form drag caused by the gas changing direction when it enters a new block. The extent of the contribution of each of these factors could be found from theoretical considerations, numerical analysis or from experiments. Hughmark's (1980 and 1986) use of a fraction of the pressure gradient due to shear comes close to this approach; it could be expected that the rest of the pressure gradient is due to the gas changing direction. A splitting of the friction factor in this way should make the prediction of the properties of new packings much easier.

Liquid flow, hold-up and wetted area in the absence of gas flow.

We saw earlier that liquid film flow on smooth plates can be reasonably well described. Unfortunately, the surface of a packing is not usually smooth. Indeed, an object in developing a new packing should be to modify the surface to improve its wetting and mass transfer characteristics. This is likely to involve roughening the surface, so that the better the packing, the more it will deviate from the ideal film flow.

To calculate the liquid film thickness, hold-up and velocity profile in a packing, most authors (Kaminskii and Giorgadze, 1971, Zogg, 1973, Billet and Schultes, 1992 and Bravo et al., 1992) have used Nusselt's laminar film theory, which has been found to give a good representation of film thickness on smooth plates right up to the transition to turbulence. This predicts that, for a particular system, the film thickness is proportional to $Re^{1/3}$ and the hold-up proportional to $Fr^{1/6}$.

Davies' (1972) experiments on roughened plates indicate that in this case, the film thickness may correspond to that for turbulent flow at Reynolds numbers as low as 200; it is approximately proportional to $Re^{0.55}$. The data reported by Spiegel and Meier (1992) indicate that in Mellapak, the hold-up is proportional to the one-third power of the liquid velocity, as for laminar flow, up to a Reynolds number of about 200. Above this, it is proportional to the two-thirds power of the velocity, indicating a transition to turbulent flow. The empirical correlations of Bravo et al. (1985), Stichlmair (1989) and Hughmark (1986) indicate that hold-up

is proportional to $Fr^{1/2}$ and $Fr^{1/3}$ and approximately proportional to $Fr^{1/3}$ respectively. These results indicate a stronger dependence than that predicted by the laminar film theory and support the view that the liquid film flow is turbulent in the normal design region of a structured packing. It is still possible, however that the film flow is laminar in the higher area packings which are of interest in air separation and which have not been investigated as extensively.

None of the models allows the prediction of the static liquid hold-up, that is the hold-up with no liquid flow. This is not, however, of great importance because, in the normal region of operation of packings, it is generally much smaller than the dynamic hold-up.

An alternative explanation for the difference between the observed hold-up and that predicted from the laminar film theory is not that the film becomes turbulent, but that it wets more of the surface as the flow increases. This is the approach taken by Billet and Schultes (1992), who propose that (empirically) the wetted area is proportional to $u_l^{0.35}$ for $Re < 20$ and to $u_l^{0.45}$ for $Re > 20$. This leads to the hold-up being proportional to $u_l^{0.57}$ and $u_l^{0.63}$. Bravo et al. (1992) use Shi and Mersmann's (1985) semi-empirical expression for rivulet flow on an inclined plate. This predicts that the wetted area is proportional to $u_l^{0.1}$ and the hold-up to $u_l^{0.4}$. In addition to these results, Spiegel and Meier (1987) propose that the interfacial (rather than wetted) area is proportional to $Re^{0.2}$ i.e. to $u_l^{0.2}$.

Two-phase flow, wet pressure gradient and flooding.

When both phases flow together in a packing, the situation becomes much more complex. At low gas flows, the gas has a negligible effect on the liquid flow; the hold-up is virtually independent of gas rate until the loading point is reached, when it increases rapidly (see for example Billet, 1987). However, even a small liquid flow influences the gas flow because it reduces the available flow area and increases the local velocity. To calculate that part of the pressure gradient due to shear forces (although not that due to form drag), the gas velocity must be measured relative to the liquid velocity. So, for the same total flow, the gas velocity is higher than in a dry bed and the pressure gradient is higher.

Above the loading point, the interaction between gas and liquid at the interface increases. The liquid near the interface is slowed down by the gas flow, and so the film is thicker than it would be with no gas flow and the hold-up is greater. If the liquid rate is higher, the loading point is reached at lower gas flows. There is evidence (Hughmark, 1986) that when the liquid film becomes thicker than a certain critical value, the local friction factor for gas flow increases in proportion to the liquid film thickness, probably because the interface becomes rougher as a result of increasing turbulence. This increases the interaction between the gas and

liquid still further, and leads to the rapid increase in hold-up and pressure gradient associated with structured packings.

As the flow of gas or liquid is increased, the flooding point is eventually reached, where the gas pressure gradient and liquid hold-up increase almost infinitely with increasing flow. It is important to know the flows at flooding for the design of packed columns, which normally operate at a certain fraction of the flooding rates.

We shall now look at the models for liquid film flow and hold-up in the presence of gas, then those for gas flow in the presence of liquid and finally those to predict the flooding rates.

2.4.1.1 Liquid flow and hold-up in the presence of gas flow

The expressions used by different authors to describe liquid flow in a packing are summarised in table 2-2.

Author	liquid film flow model.
Kaminskii and Giorgadze (1971)	Laminar film equation solved, including gas interfacial shear $\frac{\Gamma}{\rho} = \frac{\rho_l g \sin\theta - dp/dz}{3 \mu_l a^3} h_{ld}^3 - \frac{\tau_0}{2 \mu_l a^2} h_{ld}^2$ with $\frac{dp}{dz} = \frac{\phi \rho_g u_{sg}^2 a}{(\varepsilon - h_{ld} - h_{ls})^2}$ and $\tau_0 = \frac{1}{a}\frac{dp}{dz}$
Zogg (1973)	Laminar film thickness with correlation for vapour interfacial shear in a triangular channel. Angle of flow is not along channels but down the steepest surface. $\delta^3 - \frac{3 \tau_{\delta z}}{2 \rho_l g \sin\alpha} \delta^2 - \frac{3 \Gamma \mu_l}{\rho_l g \sin\alpha} = 0$ with, for turbulent vapour flow: $\tau_{\delta z} = 4.73 \frac{\cos\Theta (\sin\gamma/2+1) (a\mu_g)^{0.25} \rho_g^{0.75} u_{gs}^{1.75}}{\sin\Theta (1 - a\delta_T/2)^2 Re_{gc}^{0.75}}$ where Θ is the angle between the liquid flow direction and the channel, γ is the crimp angle, α is the angle of liquid flow with the horizontal, δ_T is the thickness of the packing plus the liquid film and Re_{gc} is the critical Reynolds number for turbulent flow

Hughmark (1980)	Kapitsa film thickness equation for laminar film flow. Only valid below loading. $\delta = \left(\frac{2.4\,\Gamma\,\mu_l}{\rho_l\, g \sin\theta} \right)^{1/3}$ which is equivalent to: $\delta = (2.4)^{1/3} \left(\frac{\mu_l}{\rho_l\, g \sin\theta} \right)^{1/3} Re^{1/3}$ or $\delta = (2.4)^{2/3} \left(\frac{\mu_l}{\rho_l\, g \sin\theta} \right)^{1/3} Fr_\delta^{1/3}$ or $\delta = (2.4)^{1/3} \left(\frac{\mu_l}{\rho_l\, g \sin\theta} \right)^{1/6} Fr^{1/6} \left(\frac{4}{a} \right)^{1/2}$ Where Fr_δ is the Froude number based on film thickness and Fr that based on equivalent diameter.
Bravo et al. (1985)	Empirical correlation, only valid below loading: $h_l = C_3\, Fr^{0.5}$ Constant C_3 depends on packing and is generally larger for larger packing. Froude number defined with respect to equivalent diameter
Hughmark (1986)	Empirical correlation for dimensionless film thickness in terms of Reynolds number. For Flexipac type 2: $\delta_+ = \delta \sqrt{\frac{\tau\,\rho}{\mu^2}} = -0.3 + 0.0264\,Re$ where τ is the characteristic shear stress given by: $\tau = 2/3\,\tau_{wall} + 1/3\,\tau_{int}$ with the wall shear stress given by: $\tau_{wall} = \frac{\varepsilon}{a} \{ \rho_l\, g\, \delta\, a - \rho_g\, g\, (1-\varepsilon) - \alpha \frac{dp}{dz} \}$ and the interfacial shear stress by: $\tau_{int} = \left(\frac{\varepsilon}{a} - \frac{\delta}{2} \right) \{ \rho_g\, g\, (1-\varepsilon) - \alpha \frac{dp}{dz} \}$ with α the empirically determined fraction of pressure drop causing shear. If the interfacial shear and buoyancy effects are negligible, this leads to: $\delta_+ = \sqrt{\frac{\delta^2\,\tau\,\rho}{\mu^2}} = \sqrt{\frac{2\,\delta^3\,\rho_l^2\, g\, \varepsilon}{3\,\mu^2}}$ $= -0.3 + 0.0264\,Re$ or, approximately, $\delta \propto Re^{2/3} \propto a^{-1}\, Fr^{1/3}$

Billet (1987) and Billet and Schultes (1987)	Random: Nusselt-type film thickness with empirical exponent. Structured: Brotz equation. Both account for vapour drag. $$h_l = \left(\frac{a^2 \mu_l u_{ls}}{1/3\, \rho_l g - 1/4\, \xi \frac{a \rho_v u_{vs}^2}{h_l (\varepsilon - h_l)^2}} \right)^n$$ For $Re_l < 40$, n=1/3. For $Re_l > 40$ in structured packing, n=2/3 The resistance coefficient, $\xi = 8\phi$ and is correlated empirically by an equation of the form: $$\xi = \frac{g}{C^2 \left(\frac{L}{V} \sqrt{\frac{\rho_v}{\rho_l}} \left(\frac{\mu_l}{\mu_v} \right)^m \right)^n}$$
Stichlmair et al. (1989)	Below loading: Correlation against liquid rate based on turbulent liquid film equation. Above loading: correlation against vapour rate (measured by wet pressure gradient. Below loading: $h_l = 0.555\, Fr_{mod}^{1/3}$ where the modified Froude number is: $$Fr_{mod} = \frac{u_{ls}^2\, a}{g\, \varepsilon^{4.65}}$$ Above loading: $$h_l = h_0 \left(1 + 20 \left(\left(\frac{dp}{dz} \right)_{wet} \frac{1}{\rho_l g} \right)^2 \right)$$
Billet and Schultes (1992)	Laminar film below loading with empirical wetted area correlation, correlation against vapour flow above loading. Below loading: $$h_l = \left(\frac{a_w}{a} \right)^{2/3} \left(\frac{12 \mu_l u_{ls} a}{\rho_l g} \right)^{1/3}$$ with the wetted to total area ratio given by: $$\frac{a_w}{a} = C_h \left(\frac{Re_l}{4} \right)^{0.15} Fr_l^{0.1} \text{ for } Re_l < 20$$ $$\text{and } \frac{a_w}{a} = 0.85\, C_h \left(\frac{Re_l}{4} \right)^{0.25} Fr_l^{0.1} \text{ for } Re_l > 20$$ Above loading: $$h_l = h_{l0} + (h_{l,flood} - h_{l0}) \left(\frac{u_v}{u_{v,flood}} \right)^{13}$$ where h_{l0} is the hold-up below loading and $h_{l,flood}$, the hold-up at flooding is given by: $$h_{l,flood} = 2.2\, h_{l0} \left(\frac{\mu_l \rho_w}{\mu_w \rho_l} \right)^{0.05}$$ where w denotes water properties.

Bravo et al. (1992)	Laminar film (Nusselt equation) with effective gravity. Also correction for wetted area. $h_l = (F_t\, a)^{2/3} \left(\frac{3\, \mu_l\, u_{ls}}{\rho_l\, \varepsilon\, g_{eff} \sin\theta} \right)^{1/3}$ with the effective gravity given by: $g_{eff} = g \left(1 - \frac{\rho_g}{\rho_l} - K_1 \left(\frac{dp}{dz} \frac{1}{\rho_l\, g} \right) \right)$ $= g \left(\frac{\rho_l - \rho_g}{\rho_g} \right) \left(1 - \frac{dp/dz}{(dp/dz)_{flood}} \right)$ And the wetting factor, F_t (empirically) by: $F_t = \frac{29.12\, (We_l\, Fr_l)^{0.15}\, (4/a)^{0.359}}{Re_l^{0.2}\, \varepsilon^{0.6}\, (1\text{-}0.93 \cos\gamma)\, (\sin\theta)^{0.3}}$ where γ is the wetting angle of the liquid on the packing surface.
Spiegel and Meier (1992)	Plotted against liquid load. For small loads: $h_l \propto u_l^{1/3}$ and for higher loads (Re_l > about 200) $h_l \propto u_l^{2/3}$

Table 2-2 Models for liquid hold-up

It is possible to solve the equation for laminar film flow with an applied pressure gradient and surface shear stress. Both of these will be determined by the friction factor and the local gas velocity, which will in turn be determined by the liquid hold-up. So the equations for liquid hold-up, gas pressure gradient and friction factor must be solved simultaneously. Examples of models which use this approach are those of Kaminskii and Giorgadse (1971), Zogg (1973), Billet and Schultes (1987) and Bravo et al. (1992). The friction factor may either be determined empirically as a function of the flow rates (e.g. Billet and Schultes, 1987 and Hughmark, 1980) or assumed to be a constant and calculated from pressure gradient or flooding data (e.g. Bravo et al., 1992). The latter approach has the advantage of simplicity, but appears not to represent the data as well as the former; if the friction factor is found from flooding data, the pressure gradient at low flows is over predicted and if it is calculated from pressure gradient data, the flooding rates are over predicted.

All these models have the disadvantage that they use the equation for smooth laminar film flow on smooth surfaces, when it is probable that the flow is turbulent and the interface wavy. A different approach to determining hold-up above the flooding point is to correlate experimental hold-up results against flow rates. Stichlmair et al. (1989) expresses the hold-up above loading in terms of the hold-up with no gas flow and the irrigated pressure gradient. In contrast, Billet and Schultes (1992) correlate it against the vapour velocity as a fraction of the flooding velocity. This approach has the advantage that the hold-up may be determined

directly rather than by iteration, but it is less fundamentally-based and may not be so generally applicable to different types of packing.

Hughmark (1986) uses a correlation for liquid film thickness in Flexipac, but expresses it in terms of dimensionless film thickness and Reynolds number in the same way as Dukeler and Bergelin (1952) and Portalski (1963) give their theoretical expressions for turbulent film thickness. Hughmark (1986) takes the effect of gas flow into account by using a characteristic shear stress (after Henstock and Hanratty, 1976) to calculate the friction velocity and dimensionless film thickness. This shear stress is a weighted average of the wall and interfacial shear stresses. Hughmark's equation gives dimensionless film thicknesses of 5 and 30 at Reynolds numbers of 200 and 1200, so the film in Flexipac seems to be only as thick as the viscous sublayer and transition region, and Portalski's theoretical expressions are most appropriate. Portalski's expression for $5 < \delta_+ < 30$ is:

$$Re = 20\ \delta_+ \ln \delta_+ - 32.2\ \delta_+ + 50$$

At $\delta_+ = 5$, this gives:

$$Re = 0\ \delta_+ + 50 = 50$$

and at $\delta_+ = 30$:

$$Re = 35.8\ \delta_+ + 50 = 1124$$

This is similar to Hughmark's expression for Flexipac:

$$Re = 37.9\ \delta_+ + 11.4$$

This approach has the advantages of being fundamentally-based and allowing for liquid turbulence and interfacial shear, and should be worth investigating further.

2.4.1.2 Gas flow and pressure gradient in the presence of liquid flow

The methods used to calculate the pressure gradient of gas flowing through an irrigated packing are the same as those used to calculate the pressure gradient in a dry packing; local velocities and dimensions are used to calculate the pressure gradient in terms of superficial and dry-bed quantities. The difference between a dry bed and an irrigated one is that the void fraction is reduced by the liquid hold-up and the channel hydraulic diameter is reduced. Moreover, in contrast to a dry

bed, the gas velocity used must be relative to the liquid film and the local friction factor is likely to vary with liquid flow rate.

Bravo et al. (1985 and 1992) and Stichlmair et al. (1989) have presented their expressions for irrigated pressure gradient as a correction to the dry pressure gradient, whilst Kaminskii and Giorgadze (1971), Hughmark (1980 and 1986) and Billet and Schultes (1987 and 1992) have calculated it directly in a similar way to the dry pressure gradient. The different expressions are summarised in table 2-3.

Author	Model for vapour pressure gradient
Kaminskii and Giorgadze (1971)	Use friction factor, calculate pressure gradient simultaneously with liquid hold-up $\frac{\Gamma}{\rho} = \frac{\rho_l g \sin\theta - dp/dz}{3 \mu_l a^3} h_{ld}^3 - \frac{\tau_0}{2 \mu_l a^2} h_{ld}^2$ with $\frac{dp}{dz} = \frac{\phi \rho_g u_{sg}^2 a}{(\varepsilon - h_{ld} - h_{ls})^2}$ and $\tau_0 = \frac{1}{a}\frac{dp}{dz}$ Possible to calculate right up to flooding.
Zogg (1973)	Gives turbulent shear stress exerted on liquid film from experiments on triangular channels: $\tau_z = 4.73 \frac{(\sin\gamma/2+1)\,(a\mu_g)^{0.25}\,\rho_g^{0.75}\,u_{gs}^{1.75}}{\sin\theta\,(1 - a\delta_T/2)^2\,Re_{gc}^{0.75}}$ where γ is the crimp angle, α is the angle of liquid flow with the horizontal, δ_T is the thickness of the packing plus the liquid film and Re_{gc} is the critical Reynolds number for turbulent flow. Should be possible to get dp/dz from: $\tau_0 = \frac{1}{a}\frac{dp}{dz}$ Applicable up to flooding.
Hughmark (1980)	Restricted to turbulent flow. Calculates friction factor from pressure drop data. It is constant for particular packing, but data are restricted to below 70% flood. An effective vapour velocity is used, based on the void fraction and relative to liquid velocity.
Bravo et al. (1985)	Dry pressure gradient by correlation. All packings assumed to be the same: $\left(\frac{dp}{dz}\right)_{dry} = f \frac{\rho_g u_{ge}^2}{d_h}$ with the effective gas velocity, u_{ge}: $u_{ge} = \frac{u_{gs}}{\varepsilon \sin\theta}$ and with: $f = 4\phi = 0.171 + \frac{92.7}{Re_{ge}}$ Irrigated pressure gradient below loading is found by correcting the dry pressure drop to take account of the reduction in channel diameter by the liquid: $\left(\frac{dp}{dz}\right)_{wet} = \left(\frac{dp}{dz}\right)_{dry} \left(\frac{1}{1 - C_3 Fr^{0.5}}\right)^3$ This only applies below loading.
Hughmark (1986)	Extension of 1980 model into loading region by correlating friction factor against ratio of film thickness to hydraulic diameter. Above loading: $f = 2\phi = K \frac{\delta a}{2\varepsilon}$

Billet (1987) and Billet and Schultes (1987)	Empirical friction factor in terms of superficial velocity correlated against flow parameter for a particular packing, accounts for liquid hold-up The resistance coefficient, $\xi = 8\phi$ and is correlated empirically by an equation of the form: $$\xi = \frac{g}{C^2\left(\frac{L}{V}\sqrt{\frac{\rho_v}{\rho_l}}\left(\frac{\mu_l}{\mu_v}\right)^m\right)^n}$$
Spiegel and Meier (1987)	Empirical dry pressure drop below 50% flood. Above this a quadratic curve fit to the experimental data are used.
Stichlmair et al. (1989)	Empirical friction factor for each packing. Allow for voidage reduction due to liquid hold-up. Dry pressure gradient by correlation for each packing: $$\left(\frac{dp}{dz}\right)_{drv} = \frac{3}{4} f_0 \frac{(1-\varepsilon)}{\varepsilon^{4.65}} \frac{\rho_g u_{gs}^2}{d_p}$$ Where d_n is the characteristic particle diameter and the single particle friction factor f_0 is given by: $$f_0 = \frac{C_1}{Re} + \frac{C_2}{Re^{1/2}} + C_3$$ Wet pressure gradient by correcting friction factor and void fraction to account for liquid film: $$\left(\frac{dp}{dz}\right)_{wet} = \left(\frac{dp}{dz}\right)_{drv}\left(\frac{1}{1-h_l/\varepsilon}\right)^{4.65}\left(\frac{1-\varepsilon-h_l}{1-\varepsilon}\right)^{(2+c)/3}$$ Where c is given by: $$c = \frac{1}{f_0}\left(-\frac{C_1}{Re} - \frac{C_2}{Re^{1/2}}\right)$$ and the liquid hold-up below loading by: $h_l = 0.555\ Fr_{mod}^{1/3}$ where the modified Froude number is: $$Fr_{mod} = \frac{u_{ls}\, a}{g\, \varepsilon^{4.65}}$$ and the liquid hold-up above loading by: $$h_l = 0.555\ Fr_{mod}^{1/3}\left(1 + 20\left(\frac{dp}{dz}\frac{1}{\rho_l g}\right)^2\right)$$
Billet and Schultes (1992)	Wet pressure gradient from expression using friction factor and effective gas velocity: $$\left(\frac{dp}{dz}\right)_{wet} = \psi_l \frac{a}{(\varepsilon - h_l)^3}\frac{\rho_g u_{gs}^2}{2}\frac{1}{K}$$ Empirical friction factor $\psi_l = 2\phi$ is given by: $$\psi_l = C_p\left(\frac{64}{Re_g} + \frac{1.8}{Re_g^{0.08}}\right)\left(\frac{\varepsilon - h_l}{\varepsilon}\right)^{1.5}\exp\left(\frac{Re_l}{200}\right)\left(\frac{h_l}{h_{l0}}\right)^{0.3}$$ K is a correction factor to allow for different voidage at the wall and h_{l0} is the liquid hold-up with no gas flow.
Bravo et al. (1992)	Friction factor for dry pressure drop, wet pressure drop correction factor which includes hold-up: $$\left(\frac{dp}{dz}\right)_{wet} = \left(\frac{dp}{dz}\right)_{drv}\left(\frac{1}{1-K_2 h_l}\right)^3$$ with: $$\left(\frac{dp}{dz}\right)_{drv} = \frac{f\,\rho_g u_{gs}^2}{\varepsilon^2 \sin^2\theta\, d_h}$$ $$f = 4\phi = 0.177 + \frac{88.774}{Re_{g.eff}}$$ $K_2 = 0.614 + 71.35\, d_h$ and h_l is given with the liquid film flow models.

Kister and Gill (1992)	Generalised structured packing pressure drop correlation. Capacity Parameter, Y, against flow parameter, X, at different pressure drops $Y = c_{gs} F_p^{0.5} \nu_l^{0.05}$ $X = \frac{L}{G}\sqrt{\frac{\rho_g}{\rho_l}}$ With $c_{gs} = u_{gs}\sqrt{\frac{\rho_g}{\rho_l - \rho_g}}$ and F_p is the empirical packing factor for a particular packing.
Spiegel and Meier (1992)	Up to 45% maximum capacity use dry pressure gradient with correction factors to get wet pressure drop: $\left(\frac{dp}{dz}\right)_{wet} = f_1 f_2 f_3 \left(\frac{dp}{dz}\right)_{dry}$ Where $f_1 = (1 - h_l)^{-2.5}$ to account for space occupied by liquid, $f_2 = \left(\frac{u_g + u_l}{u_g}\right)$ to account for actual relative velocity of gas, $u_g = \frac{u_{gs}}{1-h_l}$ $u_l = \frac{u_{ls}}{h_l}$ and $f_3 = 0$ for $h_l < 0.046$ and from a curve fit to experimental data for $h_l > 0.046$ Above 45% maximum capacity, wet pressure gradient is obtained by a cubic curve fit: $\log\left(\frac{dp}{dz}\right)_{wet} = a x^3 + b x^2 + c x + d$ Where: $x = \frac{-\log\left(\frac{u_{gs}}{0.45\, u_{gs,max}}\right)}{\log 0.45}$ $a = \log 12 - m - \log\left(\frac{dp}{dz}\right)_{0.45}$ $b = 0$ $c = m$ $d = \log\left(\frac{dp}{dz}\right)_{0.45}$ $(dp/dz)_{0.45}$ is the wet pressure gradient at 45% of maximum capacity and m is the slope of the log plot of pressure gradient against vapour velocity at this point.

Table 2-3 Models for vapour pressure gradient

The general approach is as follows:

In the dry bed, the hydraulic diameter, d_h, the void fraction ε and the area per unit total packed volume, a, are related by:

$$d_h = \frac{4\varepsilon}{a}$$

and the local velocity, u_{bed}, is given by:

$$u_{bed} = \frac{1}{z}\frac{u_{sup}}{\varepsilon}$$

When liquid flows in the bed, it occupies a fraction h_l of the total bed volume, where h_l is the liquid hold-up. The void fraction then becomes $\varepsilon' = \varepsilon - h_l$ and the hydraulic diameter becomes $d_h' = 4\,\varepsilon' / a'$. In a two-dimensional channel model, where flow can occur in one direction, the liquid film occupies surfaces in two dimensions, so that the hydraulic diameter scales in proportion to the square root of the void fraction, so that $d_h'^2 = \varepsilon'/\varepsilon\, d_h^2$. If the channel model were only one dimensional, the hydraulic diameter would be proportional to the void fraction, and in a particle model, with three-dimensional channels, it would be proportional to the cube root of the void fraction. In all the models, the velocity is inversely proportional to the void fraction and the ratio of the channel length to the bed length is unchanged when liquid is present.

For the dry bed, we have:

$$\left(\frac{dp}{dz}\right)_{dry} = 8\,\phi_{bed}\,\frac{l\,\rho\,u_{bed}^2}{2\,z\,d_h}$$

In all the models so far, the factor l/z has been included in the friction factor, so that if the channel angle is changed, the friction factor must change.

For the wetted bed, if the liquid flow velocity is ignored:

$$\left(\frac{dp}{dz}\right)_{wet} = 8\,\phi'_{bed}\,\frac{l\,\rho\,u'^2_{bed}}{2\,z\,d_h'}$$

$$\text{so } \phi'_{bed} = \phi_{bed}\,\frac{u'^2_{bed}\,d_h}{d_h'\,u_{bed}^2} = \phi_{bed}\,\frac{\varepsilon^2\sqrt{\varepsilon}}{\varepsilon'^2\sqrt{\varepsilon'}} = \phi_{bed}\,\frac{1}{(1 - h_l/\varepsilon)^{2.5}}$$

This is the form of the correction factor used by Spiegel and Meier (1992) for the pressure gradient in wetted packings below loading. They also add another factor to account for the liquid velocity.

Kaminskii and Giorgadze (1971) used a similar expression, but ignored the change in hydraulic diameter in the wetted packing.

If the friction factor is a function of Reynolds number, the Reynolds number for the wetted packing must be used to calculate the friction factor in the dry bed:

$$Re'_{bed} = \frac{r\,u'_{bed}\,dh'}{m} = Re_{bed}\,\frac{u'_{bed}\,d'_h}{d_h\,u_{bed}} = Re_{bed}\,\frac{\varepsilon\sqrt{\varepsilon'}}{\varepsilon'\sqrt{\varepsilon}} = Re_{bed}\,\frac{1}{(1 - h_l/\varepsilon)^{0.5}}$$

Stichlmair et al. (1989) used a similar approach to this, but with the particle model and an empirical expression for the dependence of local velocity on void

fraction. It may be that in a structured packing, the theoretical dependence of velocity on reciprocal void fraction is a better approximation than in a random packing, because of the regular channels. If this were so, Stichlmair's model would not be so valid for structured packings as random ones.

An approximate form of the expression for friction factor may also be used, for example by Bravo et al. (1985 and 1992) following Buchanan (1969) and Bemer and Kalis (1978):

$$\phi'_{bed} = \phi_{bed} \frac{1}{(1 - h_l/2\varepsilon)^5}$$

This is derived by reducing the hydraulic diameter by twice the film thickness, which is approximated as the liquid hold-up divided by the area per unit packed volume. The error introduced is only of the order of the square of the film thickness, so it is a good approximation for the flow in packings where the film is thin compared to the hydraulic diameter. Bemer and Kalis (1978) use a constricted channel model to show that the factor 1/2 multiplying h_l/ε could vary, depending on the type of constrictions, and Bravo et al. (1992) use an empirical factor which is correlated against hydraulic diameter. Because of the approximation that $(1-x)^n \approx 1-nx$ for small x, this is equivalent to the assumption of Stichlmair et al. (1989) that the exponent is not the one predicted theoretically.

Another factor which should be taken into account when predicting the wet pressure gradient is that the dependence of the local friction factor on gas flow rate may not be the same as in a dry packing with the same void fraction and hydraulic radius as the wetted packing. This would be the case if, for example, the interface behaved as a rougher surface than the packing, because it is fluid rather than solid. The friction factor is also likely to change with the properties of the system and the relative gas and liquid flow rates.

Billet and Schultes (1987) accounted for the liquid velocity and the change in hydraulic diameter in a wetted packing by relating the friction factor to both the gas and liquid rates. They noted a sharp increase in friction factor at flooding, but this was not accounted for in their correlation. Hughmark (1986) correlated the friction factor against the ratio of liquid film thickness to hydraulic diameter and used a gas velocity relative to the mean liquid velocity, although he only used one structured packing, and it is not clear how this correlation would change with packing size.

All the models take some account of the liquid hold-up in predicting the pressure gradient in irrigated packings, but the exact expression varies. Our understanding of irrigated pressure gradient is strongly related to that of liquid

hold-up, and neither are fully understood, particularly if the physical properties of the system are different from those of commonly-used systems.

An alternative approach to finding the irrigated pressure gradient is to use a generalised correlation, such as that of Kister and Gill (1992). They correlate the capacity factor against the flow parameter at particular pressure gradients up to flooding. This approach needs an empirical packing factor for each packing, so is not very useful for estimating the effect of changing the design of the packing, but it is simple to use for preliminary design calculations. Spiegel and Meier (1987 and 1992) also use an empirical approach to determining irrigated pressure gradient at higher flows. They use a curve-fit to experimental data for each packing. This has the advantage of good accuracy for existing packings, but is of no benefit in predicting the behaviour of other types of packing.

2.4.1.3 Flooding point prediction.

The flooding point of a packing may be defined in several different ways, depending on how it is found. The hydraulic flood point may be defined as the point where the pressure gradient increases infinitely with increasing flow. It is approximately the same as the point where a pool of liquid is seen to collect on top of the packing. This is the most theoretically important definition and is the one that will be considered here. The maximum efficient capacity is where the efficiency of a packing drops to some arbitrary value - either a fraction of the maximum efficiency, or some average efficiency. This is useful in determining the maximum practical flows which will maintain the same separation and is often used for design. The maximum capacity may also be defined as the point where the pressure gradient reaches some value, for example 10 mbar/m (Spiegel and Meier, 1987) 12 mbar/m (Spiegel and Meier, 1992) or 10.25 mbar/m (Bravo et al., 1992). The advantage of this definition is its simplicity, although if the shape of the packing is altered significantly, the pressure gradient at flooding will change and this definition will not give an accurate comparison of flood points.

Two approaches have been used to predict the flooding point of packings under different circumstances. The first is to correlate experimental results and use this correlation. The second is to extend the model for flow in an irrigated packing to the point where increased flow is impossible. The second approach is more theoretically sound, but is still likely to contain empiricism, albeit at a deeper level inside the model. It could be argued that the first approach is better, because it is less confused by the variety of different factors which go into the models for pressure gradient. We shall first examine the correlations for flooding, and then look at the predictions of the pressure gradient models.

Flooding correlations

A considerable amount of work has been done on flooding in random packings and in wetted wall columns, and various forms of correlation have been used. The most common are the Wallis diagram, in which the square roots of the dimensionless gas and liquid superficial velocities at flooding are plotted against each other, and the Souders diagram, in which the superficial gas capacity factor at flooding is correlated against the flow parameter. These quantities are defined as follows:

Dimensionless superficial velocity:

$$\text{gas: } u_g^* = u_g \sqrt{\frac{\rho_g}{g\, d\, (\rho_l - \rho_g)}}$$

$$\text{liquid: } \quad u_l^* = u_l \sqrt{\frac{\rho_l}{g\, d\, (\rho_l - \rho_g)}}$$

Gas capacity factor:

$$c_s = u_g \sqrt{\frac{\rho_g}{(\rho_l - \rho_g)}}$$

Flow parameter:

$$X = \frac{L}{G} \sqrt{\frac{\rho_g}{\rho_l}} = \frac{u_l}{u_g} \sqrt{\frac{\rho_l}{\rho_g}}$$

These correlations both have the disadvantage that changes in surface tension and viscosity are not accounted for, although in distillation, Porter and Jenkins (1979) have shown that these quantities correlate against the flow parameter and so are probably taken into account indirectly. Moreover, they do not account for the shape of the channels, or for the entrance conditions, which have been found to affect the flooding rates in wetted wall columns. The Wallis diagram approach incorporates the channel diameter, but the correlation is generally different for packings with different hydraulic diameters (e.g. Spiegel and Meier, 1987).

McQuillan and Whalley (1985) reviewed a number of flooding models and correlations for wetted-wall columns, and tested them against a large data bank. They concluded that the data were best represented by a modified form of the empirical correlation of Alekseev et al. (1972)(which was derived using some data on structured packings with liquid air). This recommended correlation is given in table 2-4. It depends on the surface tension and liquid viscosity, and so should be useful for predicting the differences in flooding rates between quite different

systems. Its weighted mean error was, however, still 26%, so predictions cannot be made with great accuracy.

Spiegel and Meier (1987) and Fair et al. (1987) present Souders diagrams for various types of structured packing. These may be approximated by $c_{s,flood} \propto X^{0.3}$ for flow parameters up to those corresponding to atmospheric distillation. The dependence of the flooding rate on specific area may be approximately given by $c_{s,flood} \propto a^{-0.3}$ from these correlations.

Author	Model for maximum capacity (flooding)
Kaminskii and Giorgadze (1971)	Flooding when friction and pressure forces equal gravity force. The limiting vapour superficial velocity is given as: $u_{gs,flood} = \left(\frac{\rho_l g \sin\theta}{\frac{\psi}{(\varepsilon - h_{ls} - h_{ld})^2 h_{ld}} + \frac{\psi}{(\varepsilon - h_{ls} - h_{ld})^3}} \right)^{0.73}$ where ψ is given by: $\psi = \frac{130 \rho_g a}{8 \left(\frac{4 \rho_g}{a \mu_g} \right)^{0.64}}$ and the dynamic hold-up, h_{ld} is given in the summary of hold-up models.
Alekseev et al. (1972)	Advise against using a theoretical expression which uses friction factor and film thickness because of the difficulty in determining these at flooding. Instead use an empirical correlation based on dimensional analysis: $K = 1.13\ F^{-0.20}\ W^{-0.21}\ G^{-0.09}$ or approximately, neglecting G: $K = 0.32\ F^{-0.22}\ W^{-0.26}$ where K, F, W and G are dimensionless numbers: $K = \frac{u_{gs,flood} \rho_g^{1/2}}{g^{1/4} \sigma^{1/4} (\rho_l - \rho_g)^{1/4}} = We^{1/2} Bo^{-1/4}$ $F = \frac{\Gamma g^{1/4} (\rho_l - \rho_g)^{3/4}}{\rho_l \sigma^{3/4}} = \frac{1}{4} Fr^{1/2} Bo^{-1/4}$ $W = \frac{\sigma}{(\rho_l - \rho_g) g d_h^2} = Bo^{-1}$ $G = \frac{\sigma^{3/2}}{\nu_l^2 g^{1/2} (\rho_l - \rho_g)^{3/2}} = Re^2 Fr\ Bo^{-3/2}$ and Re, Fr, Bo and We are the Reynolds, Froude, Bond and Weber numbers.
Hughmark (1980)	Kraybill-type correlation, empirical constant for each packing - only calculated for random packings: $\frac{u_g + u_l}{(g d_h)^{1/2}} \left(\frac{\phi \rho_g \delta}{\rho_l d_h/2} \right) = C$ Where u_g and u_l are the effective velocities at flooding, the film thickness in calculated from the Kapitsa formula and the friction factor is found empirically, and is assumed constant for a particular packing.

McQuillan and Whalley (1985)	Review and evaluation of various theoretical models and empirical correlations for flooding in vertical tubes. Recommend modified form of Alekseev et al. correlation because it fits their extensive data bank the best: $K = 0.286\ Bo^{0.26}\ F^{-0.22}\left(1 + \frac{\mu}{\mu_{water}}\right)^{-0.18}$ where K, F and Bo are as before. Also comment that Wallis-type plots of vapour against liquid dimensionless velocities are not so reliable at high liquid loads.
Hughmark (1986)	Assumes liquid wall shear stress is zero at flooding (equivalent to no net force on film), that is flooding occurs when: $\rho_l \delta a + \rho_g (\varepsilon - 1) = \alpha \frac{dp}{dz}$ where α is the fraction of pressure drop due to shear. If α is known, the vapour velocity can be calculated from the pressure gradient via the equation in the pressure gradient model summary.
Billet (1987) and Billet and Schultes (1987)	The flood point is where increasing hold-up would not increase allowable vapour or liquid velocities: $\frac{du_l}{dh_l} = 0$ and $\frac{du_v}{dh_l} = 0$ This gives an expression for the hold-up at flooding: $h_{l,flood}^3 (3 h_{l,flood} - \varepsilon) = \frac{6 L \rho_v a^2 \varepsilon \mu_l u_{v,flood}}{g V \rho_l^2}$ Which is approximated numerically to: $h_{l,flood} = 0.3741\ \varepsilon \left(\frac{\rho_{water} \mu_l}{\rho_l \mu_{water}}\right)^{0.05}$ The resistance (friction) factor at flooding is correlated by: $\xi_{flood} = \frac{g}{C_{flood}^2 \left(\frac{L}{V}\sqrt{\frac{\rho_v}{\rho_l}}\left(\frac{\mu_l}{\mu_v}\right)^{0.2}\right)^{0.388}}$ Where the constant depends on the packing.
Spiegel and Meier (1987)	Correlation of gas capacity factor at maximum capacity (where pressure gradient is 10mbar/m), $c_{gs,max}$, against flow parameter, X: $c_{gs} = u_{gs}\sqrt{\frac{\rho_g}{\rho_l - \rho_g}}$ $X = \frac{L}{G}\sqrt{\frac{\rho_g}{\rho_l}}$ It is, very approximately, up to atmospheric pressure: $c_{gs} \propto X^{0.3}$ Also give correlation between maximum gas and liquid capacity factors: $c_{gs,max}^{1/2} + c_{ls,max}^{1/2} = C$ where C takes one value for low liquid rates and another for higher liquid rates.

Stichlmair et al. (1989)	Flooding is the point where pressure gradient increases infinitely with increasing vapour load. Using dry pressure drop as a measure of vapour load, this amounts to finding the point where the correction factor for wet pressure drop increases infinitely, or its reciprocal is a maximum: $\frac{\partial(dp/dz)_{wet}}{\partial(dp/dz)_{dry}} = \infty$ which is equivalent to $\frac{\partial(dp/dz)_{dry}}{\partial(dp/dz)_{wet}} = 0$ Now $(dp/dz)_{dry}$ may be written as a function of $(dp/dz)_{wet}$ and differentiated to find its maximum. $\left(\frac{dp}{dz}\right)_{dry} = \psi\left(\left(\frac{dp}{dz}\right)_{wet}\right)$ and $\psi'\left(\left(\frac{dp}{dz}\right)_{wet}\right) = 0$ where ψ' is the derivative of ψ with respect to $(dp/dz)_{wet}$. This may then be solved for $(dp/dz)_{wet}$ and then $(dp/dz)_{dry}$ and vapour velocity. It appears to over predict the flooding velocity in structured packings, although it fits well for random packings.
Billet and Schultes (1992)	Where hold-up is 2.2 times laminar film value. Given a liquid rate can calculate back to find vapour rate.
Bravo et al. (1992)	Define flooding as point where pressure gradient is 10.25 mbar/m and use this to calculate effective gravity by assuming that at flooding the net force on the liquid is zero. Calculate flooding vapour velocity as its limiting value as (dp/dz) reaches 10.25 mbar/m. Expression for pressure gradient is given in summary of pressure gradient models.
Kister and Gill (1992)	Correlation for maximum pressure drop in terms of packing factor, then maximum capacity factor from pressure drop correlation $\left(\frac{dp}{dz}\right)_{flood} = 0.115\ F_p^{0.7}$ with the pressure gradient in inches of water per foot and packing factor in ft^{-1}.
Spiegel and Meier (1992)	Maximum capacity is defined as where the pressure gradient is 12 mbar per metre. Correlation of vapour capacity factor against liquid capacity factor (Wallis diagram), as in Spiegel and Meier (1987)

Table 2-4 Models for and definitions of maximum capacity of packings

Hughmark (1980) also proposed a correlation for flooding rates, but only tested it with random packings. It was based on the work of Kraybill (1953) and is given in table 2-4. It uses the more fundamental variables of liquid film thickness and friction factor, but is consequently more difficult to use. He reports an average deviation of about 11% for Pall rings, which is more accurate than the correlation of Alekseev et al. (1972) was for wetted wall columns. The correlation still has the

problem that it does not account for differences in shape or size of packing; the constant must be found by experiment for each packing.

Kister and Gill (1992) take the slightly different approach of correlating the pressure gradient at flooding with the packing factor. The flooding rate may then be calculated by looking up this pressure gradient on their generalised pressure drop correlation chart.

Theoretical models for flood point

As we saw earlier, the theoretical models for pressure gradient all contain a degree of empiricism. The question of interest is whether it is at a sufficiently basic level to allow the effect of changing the shape of the packing to be accounted for. A problem with the theoretical approach is that the more fundamental the model, the more complex and difficult to solve the equations become.

Kaminskii and Giorgadze (1971), in their model for random packings (tables 2-3 and 2-2), obtain an expression for the limiting vapour velocity by considering that flooding occurs when there is no net force on the liquid. Their expression includes the liquid hold-up, which must be calculated from the liquid and vapour rates and friction factor, so an iterative solution is required. The exact derivation of their expression is not given in their paper.

Like Kaminskii and Giorgadze, Hughmark (1986) also uses the condition that the net force on the liquid (the wall shear stress) is zero at flooding. His expression requires a knowledge of the liquid film thickness, the pressure gradient and the fraction of the pressure gradient causing shear. These variables all depend on each other, and on the friction factor and flow rates, so again an iterative solution is required. The liquid film thickness, friction factor and shear fraction are all found empirically, so the model is specific to a particular packing, however it should be relatively easy to generalise it for packings of different areas and with different channel angles and block heights.

Another model which uses the assumption of no net force on the liquid at flooding is that of Bravo et al. (1992). In this model, an effective gravity is calculated by assuming that an effective friction factor (which accounts for the force due to the pressure gradient as well as the shear force) may be calculated from the flooding conditions and is constant over the whole range of gas flows. This model also requires the friction factor for dry flow and further constants which relate the irrigated to the dry pressure gradient and account for the surface wetting. Again, the resulting expression is complex and needs to be solved iteratively. It also has the disadvantage that the interfacial shear on the liquid is not related to the dry bed friction factor, but calculated in a completely different way; it is likely that they are in fact linked, especially at low flows, and it would reduce the degree of empiricism if this was recognised.

In contrast to these models, Billet (1987) and Stichlmair et al. (1989) do not use the condition that the net force on the liquid film should be zero at flooding. Instead, they say that flooding occurs at the point where the liquid or vapour velocity reaches a maximum as the hold-up is increased, so that du/dh=0. It is not immediately obvious how this assumption is related to that of no net force on the liquid, but it seems better theoretically. Stichlmair et al. (1989) use the irrigated pressure gradient as a measure of liquid hold-up and the dry pressure gradient as a measure of gas flow so that $d((dp/dz)_{dry})/d((dp/dz)_{wet}) = 0$. The differentiation involved in this definition of flooding leads to complex expressions, but both authors simplify them. Stichlmair et al. use an empirical correlation for liquid hold-up in terms of irrigated pressure drop, which simplifies the calculation, but it still requires iteration. Billet (1987) evaluates his expression numerically and finds that the hold-up at flooding is about 1/3 of the void fraction. He also correlates the friction factor at flooding against flow parameter and liquid viscosity, so it is then possible to calculate the flooding gas rate, given the liquid rate, although iteration is still necessary. In a later version of this model, Billet and Schultes (1992) relate the hold-up at flooding to the value if there were no gas flow, rather than to the void fraction. This complicates the calculation, but presumably leads to more accurate results.

As Alekseev et al. (1972) point out, the theoretical expressions for the flooding rates are complex. They do however have the advantage that it is in principle possible to predict the flooding rates in a packing with a different geometry, provided that the effect of the geometry on the friction factor, hold-up and so on is known.

2.4.2 Mass transfer in packings

The mass transfer efficiency is one of the most important things to know about a packing when designing a distillation column, because it determines the height of the distillation column. We have seen that it may be expressed as a mass transfer coefficient, the height of a transfer unit or the HETP. These are all closely related, so models for each will be considered, although it is most common to use the HETP for design calculations. The models for mass transfer efficiency apply only to a column in which the vapour and liquid are perfectly distributed. In larger columns (> about 1m), this is never the case, and some reduction in efficiency is usually found. Because of this, we shall look briefly in the next section at ways of calculating this reduction in efficiency from a knowledge of the gas and liquid distribution within the packing.

Several levels of approach have been used to predict the mass transfer efficiency of packings and wetted wall columns, depending on the flow regime and which phase resistances are important. Early in this century, a considerable number of

experiments were performed with wetted-wall columns to establish models and correlations for both liquid and vapour phase mass transfer coefficients. More recently, correlations have been developed for mass transfer in random packings, which are similar in form to those for wetted-wall columns. Structured packings are rather similar to wetted-wall columns, so it could be expected that the same correlations could be used for both. In the last 20 years, some correlations have been developed for mass transfer in structured packings, which are indeed similar to those for wetted-wall columns.

A problem with the prediction of mass transfer coefficients, which should be considered when assessing the accuracy of a model, is that the diffusion coefficients are often not very well known, and may sometimes be estimated to an accuracy of only about 30%. This is especially likely to be the case for systems of industrial interest, which have not been extensively studied on a fundamental level.

We shall look first at the modelling of mass transfer in the vapour or gas phase in structured packings, both in laminar and turbulent flow, and then go on to examine mass transfer in the liquid phase.

Author	Model for efficiency or mass transfer coefficients
Gilliland and Sherwood (1934)	Correlation of liquids evaporating into air in wetted wall column. Only vapour phase resistance considered. Compared with theories for laminar and turbulent flow. Turbulent correlation: $Sh = 0.023\ Re^{0.83}\ Sc^{0.44}$ Laminar - agrees with diffusion model with rod-flow
Westhaver (1942)	Solution of diffusion equation in laminar flow ignoring liquid resistance $HETP = \frac{11}{48}\frac{u_{gs}\, r^2}{D} + \frac{D}{u_{gs}}$ If back-diffusion may be ignored: $HETP = \frac{11}{48}\frac{u_{gs}\, r^2}{D}$
Kaminskii and Giorgadze (1973)	Laminar pipe entry flow model, solution of diffusion equation in vapour and liquid. Divide vapour into a core with a uniform velocity and an annulus where the velocity profile is parabolic. Liquid is in laminar flow. $\frac{HETP}{\sin\theta} = \left(\frac{1}{6}\frac{q_{ann}}{\pi D_g}\left(1-\frac{r_0^2}{R^2}\right) + \frac{1}{4}\frac{q_{core}}{\pi D_g}\left(1-\frac{r_0^2}{2R^2}\right) + \frac{11}{40}\frac{\Gamma\delta}{\rho_l D_l} + \frac{1}{80}\frac{\delta^3 \tau_0}{D_l \mu_l}\right)$ Where q is the volumetric vapour flow in the channel, r_0 the core radius, R the channel radius and τ_0 the shear stress exerted by the vapour on the liquid. The core radius is assumed to increase with Reynolds number.

Zogg (1973)	Analytic solution of diffusion equation in liquid film for liquid, empirical deduction for vapour For liquid: $Sh_l = 3.415 + 1.2496 \sqrt{\frac{Re_l\, Sc_l}{\xi}} \exp\left(\frac{-0.72054\, \xi^{0.6}}{Re_l\, Sc_l^{0.458}}\right)$ Where ξ is the dimensionless mixing-free length: $\xi = \frac{z}{\delta}$ and z is the length along the liquid flow path from the apex of the channel (of side d_h) to its edge: $z = \frac{d_h}{\sin \Theta}$ Expressions for δ and Θ are given with the liquid hold-up models. For the vapour, by subtracting the calculated liquid resistance from the experimental total resistance: $Sh_{g.loc} = 0.05144\, Re_{g.loc}^{0.8304}\, Sc_g^{1/3}$ Where the dimensionless groups are calculated with a local velocity. If superficial groups are used and liquid hold-up is negligible, this leads to: $Sh_g = 0.05144 \frac{(\sin(\gamma/2) + 1)^{0.1966}}{(\sin\theta)^{0.8034}} Re_g^{0.8304}\, Sc_g^{1/3}$
Hughmark (1980)	Vapour: Calculation for turbulent flow from addition of resistances in the transition region ($5.5<y_+<34.6$) and core ($y_+>34.6$). The viscous sublayer is assumed not to exist because of turbulence at the interface: $\frac{1}{k_{g+}} = \frac{1}{k_{t+}} + \frac{1}{k_{c+}}$ with $k_{t+} = \frac{(0.097 / Sc_g)^{1/2}}{\{\text{atan}[34.6\,(0.0094\, Sc_g)^{1/2}] - \text{atan}[5.5\,(0.0094\, Sc_g)^{1/2}]\}}$ and $k_{c+} = \frac{7.16}{Sc_g\, Re_g\, \phi^{1/2}} + 2\,\phi^{1/2}$ The friction factor used is based only on shear drag, so it is only a fraction of the total friction factor. The effective gas velocity is taken as the sum of the gas velocity and average liquid velocity. Liquid: Correlation of liquid film controlled data in packings gives: $k_{l+}\, Sc_l^{1/2} = 0.027\, Re_l^{1/3}$ where the shear velocity u_* is equal to $(g \sin\theta\, \delta)^{1/2}$ and an average value of $\sin\theta$ is found from hold-up data. For liquid film (rather than packing) data, the constant is 0.0042

Bravo et al. (1986)	Vapour: modified wetted wall column correlation: $Sh_g = 0.0338\ Re_{g.eff}^{0.8}\ Sc_g^{1/3}$ Where the velocity in $Re_{g.eff}$ is the effective gas velocity relative to the effective liquid surface velocity (1.5 times the average liquid velocity). Hydraulic diameter expression is rather complex and confused. Revised in later model (1992). Liquid: penetration theory with corrugation side (standard hydraulic diameter) as mixing length. $k_l = 2\sqrt{\frac{D_l\, u_{l.eff}}{\pi\, d_h}}$ Interfacial area assumed equal to packing area.
Hughmark (1986)	Vapour: as 1980, explained better: Effective vapour velocity, u_g, is: $u_g = \frac{u_{gs}}{\varepsilon} + u_l$ Since only a fraction α of the pressure drop is due to shear drag, the vapour shear velocity, u_{v*} is $u_g\ \alpha\ \phi^{1/2}$. The dimensionless core mass transfer coefficient is further simplified to $2\ \alpha\ \phi^{1/2}$ so the equation for the gas phase mass transfer coefficient is: $k_g = \frac{u_g\ \alpha\ \phi^{1/2}}{1/k_{t+} + 1/(2\ \alpha\ \phi^{1/2})}$ with k_{t+} as (1980) above. α is found from liquid hold-up data. Liquid: similar correlation to 1980, but use characteristic shear stress τ_c to calculate shear velocity so now: $k_{l+}\ Sc_l^{1/2} = 0.012\ Re_l^{1/3}$ with $\tau_c = 2/3\ \tau_{wall} + 1/3\ \tau_{int}$. Interfacial area assumed equal to packing area in structured packing.
Spiegel and Meier (1987)	Liquid resistance is ignored, Vapour resistance is correlated by: $Sh_{gs} \propto Re_g^{0.8}\ Sc_g^{1/3}$ with HETP given by: $HETP = \frac{d_h\, u_{gs}}{Sh_g\, D_g\, a_i}$ where a_i is the interfacial area correlated by: $a_i \propto (\rho_l\, u_{ls})^{0.2}$
Bennett et al. (1989)	Correlations based on oxygen-nitrogen distillation. Vapour: $Sh_g = 0.0295\ Re_{gs}^{0.893}\ Sc_g^{1/3}$ Liquid: $Sh_l = 0.052\ Re_{ls}^{1.19}\ Sc_l^{1/3}$

Billet and Schultes (1992)	Liquid and Vapour penetration theory with empirical adjustment. $k_l = C_l \left(\frac{g}{\nu_l}\right)^{1/6} \left(\frac{D_l}{d_h}\right)^{1/2} \left(\frac{u_{ls}}{a}\right)^{1/3}$ and $k_g = C_g \frac{1}{(\varepsilon - h_l)^{1/2}} \left(\frac{a}{d_h}\right)^{1/2} D_g \left(\frac{u_g}{a\,\nu_g}\right)^{3/4} \left(\frac{\nu_g}{D_g}\right)^{1/3}$ Empirical interfacial area correlation: $a_i = 1.5 \left(\frac{a}{d_h}\right)^{1/2} Re^{0.2} \left(\frac{Fr_l}{We_l}\right)^{0.75} Fr^{-0.45}$ In addition, for surface tension negative systems, a correction is applied to account for the Marangoni effect: $a_i = 1.5 \left(\frac{a}{d_h}\right)^{1/2} Re^{0.2} \left(\frac{Fr_l}{We_l}\right)^{0.75} Fr^{-0.45} (1 - 0.00024\, Ma^{0.5})$ Where Ma is the Marangoni number: $Ma = \frac{d\sigma}{dx} \frac{\Delta x}{D_l\, \mu_l\, a}$ The gradient $d\sigma/dx$ is along the column and Δx is the difference between the bulk and interfacial liquid concentrations.
Bravo et al. (1992)	Vapour: modified wetted wall column correlation: $Sh_g = 0.054\, Re_{g.eff}^{0.8}\, Sc_g^{1/3}$ Where the velocity in $Re_{g.eff}$ is the effective gas velocity relative to the effective average liquid velocity. Liquid: penetration theory with general correction for all packings. $k_l = 2\sqrt{\frac{D_l\, u_{l.eff}}{\pi\, d_h\, C_E}}$ with $C_E = 0.9$ for all packings. Interfacial area: from correlation shown in liquid hold-up models.

Table 2-5 Models for packing efficiency (HETP or mass transfer coefficients).

Vapour phase mass transfer, laminar flow

An early theoretical analysis of laminar gas phase mass transfer in a wetted wall column was made by Gilliland and Sherwood (1934). They concluded that their data in the laminar region were correlated better by a rod-flow model than a parabolic velocity profile model. Westhaver (1942) assumed that the flow was laminar (with a parabolic velocity profile) and that the liquid phase resistance could be neglected. He expressed the results of his analysis in terms of HETP the expression for which is given in table 2-5. If axial diffusion is ignored, it predicts that the HETP is proportional to the vapour velocity and to the square of the tube diameter, which indicates that low velocities and small tubes are advantageous. This model could be modified relatively easily for a structured packing, by using an effective vapour velocity and hydraulic diameter, but the Reynolds number in most

structured packings indicates that the flow should be turbulent, so it is only of limited use.

Kaminskii and Giorgadze (1973) used a similar approach to Westhaver to model random packings as wetted-wall sections. They included the liquid film resistance and allowed for entry effects by assuming that there was a turbulent core region with a uniform velocity. Their expression for HETP is also given in table 2-5, and is rather similar to that of Westhaver. The vapour phase terms predict the same dependence of HETP on velocity and flow area, but the constant is different from that in Westhaver's expression when there is no turbulent core. The effect of the turbulent core is to increase the mass transfer efficiency and reduce the HETP.

Vapour phase mass transfer, turbulent flow

In all the other models for mass transfer in structured packings, the vapour phase is assumed to be turbulent. Most authors have developed their own correlations, which are very similar to that of Gilliland and Sherwood (1934) for wetted wall columns. Hughmark (1980 and 1986), however, used an analogy with momentum transfer, but this still requires the empirical determination of the fraction of the pressure gradient due to shear.

Zogg (1973) was the first to develop a correlation for structured packings. He used experimental results on gauze packings and calculated the liquid film resistance theoretically. By subtracting this from the overall resistance, he derived the correlation given in table 2-5. He accounted for the geometry of the packing by correlating local dimensionless groups and writing these in terms of superficial quantities and geometric variables.

Bravo et al. (1986 and 1992) and Billet and Schultes (1992) give very similar correlations (table 2-5) to Zogg's, based on their own experimental results with sheet metal packings. Billet and Schultes' correlation was developed for both random and structured packings and shows a slightly weaker dependence on vapour velocity than the others.

In 1987, Spiegel and Meier used the form of the wetted wall column correlation to calculate the dependence of HETP on vapour rate, neglecting the liquid phase resistance. They explained the difference between the experimental results and their predictions by assuming that the wetted area depends on flow rate. This approach may be used to calculate relative HETPs for different systems, and so is of some value, but does not allow changes in packing geometry other than hydraulic diameter to be accounted for.

Bennett et al. (1989) developed a correlation for vapour phase mass transfer from experiments with the oxygen - nitrogen and oxygen - argon systems. They assumed the dependence of Sherwood number on the 1/3 power of Schmidt number and correlated its dependence on Reynolds number.

The theoretical approach taken by Hughmark (1980 and 1986) is to use dimensionless mass transfer resistances in each of the viscous sublayer, transition region and turbulent core. The resistance in the viscous sublayer is shown in an earlier paper (Hughmark, 1975) to be negligible in pipe flow for low Schmidt numbers (<1), and is expected to be even smaller in the presence of a turbulent interface. It is therefore ignored, and only the transition and core resistances are used. Molecular diffusion is included in the core resistance in the 1980 model, but omitted as negligible in the 1986 one. The core and transition region resistances are calculated by analogy with momentum transfer, but it is assumed that only a fraction of the momentum transfer occurs through shear and it is only this fraction to which the analogy may be applied. Table 2-5 gives the resulting expressions.

This approach has the advantage of being fundamentally-based, but still needs the empirical friction factor and shear fraction. These may, however be found from hydraulic tests, and so mass transfer efficiency should be predictable from these alone. It is also possible that the friction factor and shear fraction may be predicted for different packing geometries. The friction factor in Hughmark's model is calculated from the superficial relative velocity and the pressure gradient along the bed axis rather than along the channels. If the channels are inclined at an angle θ from the horizontal, this leads to a friction factor which is larger than the local one by a factor $(\sin \theta)^{-3}$. It is likely to be the local rather than superficial friction factor which determines the mass transfer coefficients, and so the shear fraction in a structured packing may in fact be close to one.

The correlation of local dimensionless groups is probably the simplest way of allowing for changes in packing geometry and distillation system, but the theoretical approach gives a better understanding of the processes within a packing. None of these models is able to allow directly for the local variations in the mass transfer coefficient within the packing. For example it is likely to be increased at the entrance to a packing block, and Gaiser and Kottke (1989) have shown that it varies according to the position in the channel. Hughmark's approach does, however, indirectly account for these effects, as they will affect the friction factor in a similar way to the mass transfer. But it is still difficult to predict the effect on the friction factor of local changes in packing geometry, and it would probably have to be found empirically. A generalised heat and mass transfer correlation for pipe flow, such as that of Stein (1992), could allow for changes in the ratio of channel length to hydraulic diameter, and may be worth using to predict the performance of structured packings with different block heights.

Liquid phase mass transfer

Kaminskii and Giorgadze (1973) and Zogg (1973) both solve different forms of the diffusion equation in the laminar liquid film. Their expressions are given in table 2-5.

Kaminskii and Giorgadze find that the HETP increases as the liquid rate, film thickness and interfacial shear stress increase, and that the liquid phase resistance is inversely proportional to the molecular diffusivity.

Zogg calculates the average Sherwood number (and hence mass transfer coefficient) over a length in which no mixing occurs. This is assumed to be the length along the liquid flow path from the apex of a channel to the edge. He ignores diffusion in the flow direction and interfacial friction. His expression is complex, but it reduces to the expression from penetration theory when the dimensionless film length is short and the product of Reynolds and Schmidt numbers is large.

The calculated liquid film mass transfer coefficients for the gauze packings show a small decrease as the flow increases, and are about five times larger in a packing with channels at 45 degrees than one with channels at 60 degrees because of the shorter mixing length. They are also bigger at higher pressures, where liquid rates are higher for a given vapour rate.

Bravo et al. (1986) use the penetration theory with the mixing length equal to the hydraulic diameter. The later (1992) version of their model incorporates an empirical correction factor of 0.9 to this mixing length, to give better agreement with experimental results. The choice of mixing length seems rather arbitrary, and it is not clear how it would change with packing geometry, but it seems to be valid in view of its agreement with experimental results. The penetration theory result is, in terms of Sherwood number (see e.g. Grossman, 1986):

$$Sh = 0.345\, Re^{1/2}\, Sc^{1/2} \sqrt{\frac{\delta}{x}}$$

where x is the contact length. If Nusselt's laminar film thickness equation is used for δ:

$$Sh = 0.329\, Re^{2/3}\, Sc^{1/2} \left(\frac{\nu^2}{g x^3}\right)^{1/6}$$

Billet and Schultes (1992) also use the penetration theory with the contact length based on the hydraulic diameter, but with an empirical correction for each type of packing. They express it, with the help of Nusselt's film thickness equation as:

$$k_l = C_l \left(\frac{g}{\nu_l}\right)^{1/6} \left(\frac{D_l}{d_h}\right)^{1/2} \left(\frac{u_{ls}}{a}\right)^{1/3}$$

This is equivalent to the other expressions with hydraulic diameter as the contact length

Hughmark (1980 and 1986) used correlations for liquid phase resistance based on liquid film controlled mass transfer data. These were developed from random packing data, but the contact length in random packings is probably similar to that in structured packings. The flow in structured packings may, however, be laminar up to higher Reynolds numbers than in random packings because the surface is continuous, and this might make a difference to the mass transfer coefficient.

Hughmark's later (1986) expression (see table 2-5) gives the dimensionless mass transfer coefficient based on the characteristic shear stress, and so allows for the effect of interfacial shear. If such shear is present, this correlation predicts an increased mass transfer coefficient, in contrast to Kaminskii and Giorgadze's prediction of increased HETP (reduced mass transfer coefficient).

In the absence of gas flow, Hughmark's dimensionless mass transfer coefficient may be written as:

$$k_{l+} = \frac{Sh}{Sc\ N_T^{3/2}}$$

so that his (1986) correlation becomes:

$$Sh = k_{l+}\ Sc\ N_T^{3/2} = 0.012\ Re^{1/3}\ Sc^{1/2}\ N_T^{3/2}$$

or, with Brauer's film thickness expression for N_T:

$$Sh = 0.00114\ Re^{1.13}\ Sc^{1/2}$$

This is similar to Yih and Chen's (1982) correlation for turbulent flow on smooth plates, but predicts Sherwood numbers about 10 times higher.

$$Sh = 6.66*10^{-5}\ Re^{1.213}\ Sc^{0.5}$$

McGlamery's (1988) expression for the structured packing surface with the best mass transfer characteristics was, in terms of numbers based on film thickness:

$$Sh = 0.00263\ Re^{1.354}\ Sc^{0.5}$$

This is again similar, but predicts Sherwood numbers 10 times higher than Hughmark's.

None of these correlations gives the same dependence on Reynolds number as the penetration theory, even if it uses a turbulent rather than laminar film thickness. This is probably because, in turbulent flow, the contact length decreases as the Reynolds number increases.

Bennett et al. (1989) correlated the liquid phase resistance as well as the vapour phase resistance from their experimental work on oxygen - nitrogen and oxygen - argon. Their correlation is given in table 2-5 and the Sherwood number shows a similar dependence on Reynolds number to the turbulent correlations of Hughmark, Yih and Chen and McGlamery. However, it is proportional to the 1/3 power of Schmidt number, as in the vapour phase correlation, rather than the 1/2 power as in the other liquid phase correlations.

The differences between these expressions illustrate the difficulty of accurate prediction of liquid phase mass transfer coefficients; they may vary over orders of magnitude, depending on the circumstances. The correlations do, however show that increasing the roughness of the surface can significantly improve mass transfer, and that it is likely that the flow over such roughened surfaces may be considered turbulent.

No-one has used a turbulence model in predicting liquid phase mass transfer coefficients in structured packings, but because of the large influence of the surface texture on the flow, such a model would involve arbitrary constants in the same way as the penetration model.

Interfacial area

Some authors have assumed that the interfacial area in structured packings, particularly gauze ones, is the same as the total area of the packing (Zogg, 1973; Bravo et al., 1986). More recently, Spiegel and Meier (1987) introduced a term to account for the difference in performance between gauze and sheet metal packings. They explained this term as the difference in interfacial area between a completely wet gauze surface and the less easily wettable sheet metal; the interfacial area was given as proportional to $Re^{0.2}$.

Bravo et al. (1992) have also allowed for changes in interfacial area. They took the more theoretically based approach of using Shi and Mersmann's (1985) semi-empirical model for flow over smooth plates. They assumed the same dependence on system properties and flows, but correlated the dependence on hydraulic diameter and corrected empirically for different surfaces. Their expressions for interfacial and wetted area are the same, as would be expected, and show only a weak dependence on liquid rate; the area is proportional to $u_l^{0.1}$.

Billet and Schultes (1992) use different expressions for wetted and interfacial area, but they give similar dependences on liquid rate and are proportional to $u_l^{0.4}$. This stronger dependence than the expressions of Bravo et al. and Spiegel and Meier may be because the correlation was developed with random as well as structured packing data; structured packings probably wet better than random ones.

A problem with all these relations is that it is difficult to separate the mass transfer coefficient from the interfacial area. As a result, it is easy to use completely wrong expressions for both, but still arrive at a reasonable result for their product. Some care should therefore be taken when comparing packings on the basis of wetted area or liquid phase mass transfer coefficients alone.

Author	Model for wetted or interfacial area
Spiegel and Meier (1987)	Empirical correlation based on efficiency: Efficiency is constant in distillation, but mass transfer coefficient should be proportional to $Re^{0.8}$, leading to an efficiency proportional to $Re^{-0.2}$. The discrepancy is assumed to be due to changes in the interfacial (wetted) area, which must be proportional to $Re^{0.2}$
Billet and Schultes (1992)	Two different expressions are used for wetted area and interfacial area for mass transfer, both empirical correlations. For wetted area, the area is obtained by calculating the difference between the actual hold-up and the hold-up calculated from the laminar film theory. It is given by: $\frac{a_w}{a} = C_h \left(\frac{Re_l}{4}\right)^{0.15} Fr_l^{0.1}$ for $Re_l < 20$ and $\frac{a_w}{a} = 0.85\, C_h \left(\frac{Re_l}{4}\right)^{0.25} Fr_l^{0.1}$ for $Re_l > 20$ A similar approach is used for interfacial area which is calculated from the difference between calculated and measured mass transfer coefficients: $\frac{a_i}{a} = 1.5\, (a\, d_h)^{-0.5}\, Re_l^{-0.2} \left(\frac{Fr_l}{We_l}\right)^{0.75} Fr_l^{-0.45}$ where the dimensionless groups are based on hydraulic diameter and superficial liquid velocity.
Bravo et al. (1992)	Expression like that of Shi and Mersmann (1985) for wetted area. Constant and exponent on hydraulic diameter from difference between experimental and calculated hold-ups: $\frac{a_w}{a} = \frac{29.12\, (We_l\, Fr_l)^{0.15}\, (4/a)^{0.359}}{Re_l^{0.2}\, \varepsilon^{0.6}\, (1-0.93 \cos\gamma)\, (\sin\theta)^{0.3}}$ Interfacial area is proportional to wetted area with an empirical correction for packing type: $\frac{a_i}{a} = F_{se} \frac{29.12\, (We_l\, Fr_l)^{0.15}\, (4/a)^{0.359}}{Re_l^{0.2}\, \varepsilon^{0.6}\, (1-0.93 \cos\gamma)\, (\sin\theta)^{0.3}}$

Table 2-6 Models for wetted and interfacial area in packings

2.4.3 Distribution and scale-up

2.4.3.1 Liquid and vapour distribution and mixing

The basic model used to find the transfer unit height or HETP for a packing from the mass transfer coefficients assumes that the flow of vapour and liquid in the column is perfectly uniform and that no back-mixing occurs. The first assumption is reasonable in small columns, where the packed height is many times the diameter, but it breaks down in larger columns. The second becomes invalid at higher pressures, where the phase densities become more similar and entrainment is more likely.

Vapour distribution is not usually a problem in packed beds except where the pressure drop is small in comparison to variations in the dynamic head of the vapour. This occurs in very large diameter, short beds or in high pressure distillation where the vapour density is high and small changes in velocity produce significant head variations. As a result it has not been studied in great detail. Liquid distribution, on the other hand, is more difficult to make uniform and has been widely studied in beds of random packings, and more recently, structured packing.

We will now look at each of these in turn, and then at the differences made when both phases are present.

Vapour distribution

Recent experimental work on gas distribution includes that of Meier et al. (1979), Ali (1984), Kouri and Sohlo (1987), Stikkelman and Wesselingh (1987) and Olujic et al. (1992). Stoter et al. (1992) describe a model which uses splitting factors to model gas and liquid distribution in structured packings.

Ali (1984) demonstrated that, in randomly packed columns, severely maldistributed gas flow becomes uniform after about half a column diameter, so that it is only a problem in shallow, large diameter beds.

Meier et al. (1979), in experiments with Mellapak 250Y, showed that a carbon dioxide tracer was almost uniformly spread over a 450 mm diameter column after only two packing elements (400 mm). They found that the Peclet number based on hydraulic diameter was constant at 0.4 for Mellapak compared to 2.8 for Raschig rings, indicating seven times more radial mixing.

Kouri and Sohlo (1987) found that the gas distribution in both random and structured packings was good and almost unaffected by packed height. Interestingly, it was slightly worse in the structured packing, which showed a slightly reduced flow in the central region.

In a 0.5m diameter column, Stikkelman and Wesselingh (1987) found that a uniform gas distribution was established after 0.3m with random packings, in agreement with Ali's (1984) results. They also examined the gas distribution after four blocks of structured packing. It was very uniform in BX gauze packing, but less so in Mellapak 250Y. In contrast to the results of Kouri and Sohlo (1987), they found a slightly higher gas velocity along one diameter. With an area gas source, they report some lateral spread of gas through the perforations in Mellapak, but none in the BX packing.

In experiments on a 0.5 by 3 m rectangular column, packed with Montz-pak B1-250, Olujic et al. (1992) find that a point source of gas is converted to a uniform distribution in a 4.2 m packed height. Unlike Meier et al. (1979), they found that a tracer was not spread uniformly over the column width after this height, but had spread out over about 1.5 m. They concluded that dispersion (mixing) in the gas phase was much less efficient than the spreading. Stoter et al. (1992) report dispersion coefficients in the same apparatus of 0.15 m^2/s in the liquid and 0.2 m^2/s in the gas. They do not comment on any variation with velocity.

In none of the work was gas maldistribution found to be a serious problem, although there seems to be conflicting evidence on the extent of radial mixing. Structured packings differ from random packings in that they consist of large blocks which only spread gas and liquid in one dimension. Several blocks are therefore needed to achieve a uniform distribution in small diameter columns, where the block height is of the order of the column diameter.

Liquid distribution

The maldistribution of liquid in a packed bed may occur on a large or small scale. Large scale maldistribution may be caused by a poor distribution at the top of the bed or by large scale non-uniformities in the bed, such as increased voidage at the wall or at boundaries between blocks of structured packing. Small scale maldistribution or liquid channelling occurs over distances of the order of the packing dimension or hydraulic diameter.

Small scale maldistribution - rivulet or channel flow

The small scale maldistribution of liquid in random packings was first demonstrated by Porter (1968) and confirmed more recently by Hoek (1983). Hoek also performed experiments with the 'Mellapak' sheet metal and BX plastic gauze structured packings. He finds that the channelling in the sheet metal packing is much greater than in the gauze one, and that the number of channels is reduced further down the bed and as the liquid rate is increased. This could provide an

explanation for the lower efficiency of sheet metal packings compared with gauze ones at lower liquid rates. Because the channelling is regarded as a feature of the packing which defines its HETP (Zuiderweg and Hoek, 1987), it is large scale maldistribution which has received more attention.

Large scale maldistribution - initial distribution

The effect of the initial distribution on the distribution of liquid in granular beds and random packings has been investigated since the end of the last century. Experimental results on large scale columns, where wall effects are negligible have been successfully simulated with the spreading equation. Liquid distribution in structured packings has been investigated by Hoek (1983), Kouri and Sohlo (1987) and Olujic et al. (1992).

Hoek (1983) found that a point source of liquid tends to flow along the channels, so that after one block of packing, two liquid streams are present. This effect is reduced at high flows in the gauze packing, where liquid flows more vertically and is spread uniformly along a line. Subsequent elements behave in the same way as the first, so that the flow is split into more and more channels and spreads radially very quickly, but does not become uniformly distributed. If there is some form of initial distribution, even if it is poor, a uniform distribution is established after only two layers of packing. Kouri and Sohlo (1987) confirmed this result with BX packing, and found no change in the distribution with liquid load. Olujic et al. (1992) found, in contrast to their results for gas distribution, that liquid spreading and dispersion were identical and independent of liquid load. The radial spreading in their packing did not appear to be as large as Hoek's (1983) results for Mellapak. This shows that in this packing, the liquid does not follow the packing channels, but flows more vertically, as in Hoek's experiments on gauze packings at higher flow rates. A result of this reduced spreading is that very severe initial maldistribution (only half the bed irrigated) is not corrected very quickly in Montz-pak. In addition, if the wall region is not well irrigated at the top of the column, it remains poorly irrigated over their 4.2 m deep bed.

The differences between the results of Hoek (1983) and Olujic et al. (1992) show that spreading factors may differ widely even in very similar structured packings. The better correction of initial liquid maldistribution found by Hoek emphasises the importance of a high liquid spread factor.

Large scale maldistribution - wall flow and block boundary flow

Wall flow has long been known as a problem in random packings. The effect of column diameter on wall flow was investigated by Porter and Templeman (1968), who concluded that the proportion of the flow on the wall was proportional to the

ratio of packing diameter to column diameter, so that it is not so important in larger columns.

In structured packings, Hoek (1983) found a slightly higher liquid load near the walls of his column, but said it did not amount to real wall flow. Kouri and Sohlo (1987) show that whilst pall rings show significant wall flow, BX gauze packing shows none; in fact the liquid flow in the outer region is less than the average flow. Olujic et al. (1992) report no wall flow in their rectangular bed, but do notice that liquid tends to flow down the small gaps between blocks of packing. They recommend that blocks should be as long as possible and installed carefully to avoid this problem.

Distribution in two-phase flow.

Most early distribution tests were carried out with a single phase, because of the difficulty of collecting or measuring one phase whilst distributing the other. There is conflicting evidence as to the effect of gas flow on liquid distribution and vice-versa.

Hoek (1983) has summarised the effects of gas flow on liquid distribution. He reports that Baker et al. (1935) and Dutkai and Ruckenstein (1970) all found that liquid distribution in random packings is unaffected below loading and made more uniform above loading. His experiments with 15 mm Pall rings, however show that liquid maldistribution increases as the gas flow is increased above loading, although he comments that this may be due to gas maldistribution at the base of the bed.

Kouri and Sohlo (1987) found similar results; BX gauze packing and 50 mm Pall rings both showed worse liquid distribution with increasing gas load, although 25 mm Pall rings did not. They observed that the liquid spreading and wall flow increased with increasing gas load and so that an initially maldistributed liquid flow was smoothed more quickly. The gas at the top of the bed with poor liquid distribution was found to be maldistributed to a greater degree at higher liquid or gas loads. The effect was pronounced in 50 mm Pall rings, but less so in 25 mm Pall rings and BX packing, and may only be restricted to the very top of the bed.

Olujic et al. (1992) reported that the gas distribution was not altered by very severe liquid maldistribution in their rectangular column, whereas in a 0.5 m column it was. They also say that gas flow will not smooth a poor liquid distribution as it does in smaller columns. Stoter et al. (1992) also found that radial spreading of liquid was reduced at high gas loads, thus reducing the transport of liquid to irregularities in the bed.

Suess (1992) examined the effect of liquid flow on gas distribution at the base of packed beds and concluded that the gas maldistribution was less with higher liquid flow rates.

2.4.3.2 Effects of maldistribution on mass transfer efficiency

Zuiderweg and Hoek (1987) state that the effect of the small-scale 'natural' flow variations on the mass transfer efficiency is small. Moreover, its effect is included in the measurement of HETP because it is present in small test columns to the same extent as large ones. It is therefore large scale distribution which needs more attention.

Mullin (1957) first showed that if a column with maldistribution is modelled as parallel columns with different internal reflux ratios, the efficiency is seriously reduced. The taller the column, the bigger was the reduction in efficiency.

Huber and Hiltbrunner (1966) extended this model to allow for mixing between the maldistributed streams. They show that the greater the mixing, the smaller the effect of the maldistribution. Also, because the cross-mixing is caused by liquid spreading, it is restricted in horizontal extent. In large diameter columns it is therefore less, and initial maldistribution can have a larger effect on efficiency than in smaller ones.

More recently, Hoek et al. (1986) have used their zone-stage model, which can account for radial liquid spreading. In this model, the column is divided into axial stages, with heights equal to a basic HETP, and annular zones. The vapour flow is assumed to be uniform and the liquid rate is calculated from a diffusion-type equation.

Zuiderweg et al. (1987) present some of the findings of this model. They conclude that redistribution in tall beds is less desirable than mixing in the liquid and vapour phases. The liquid becomes better distributed down the bed, but the concentration profile becomes less uniform, so it would be better only to even out the concentrations without disturbing the improved distribution. They also show that it is more important for a distributor to cover a larger proportion of the column area when the diameter is larger.

Other, more complex models for predicting mass transfer efficiency by solving both the spreading and mass transfer equations together have been developed, for example by Zhang et al. (1988 and 1990). They considered various combinations of liquid and vapour phase axial and radial dispersion and reached similar conclusions to those of Zuiderweg et al. (1987).

Stoter et al. (1992) modelled a large diameter column with structured packing based on the spreading coefficients found from their rectangular column. They found that under normal conditions, the effect of the wall region was negligible, but that if it were not properly irrigated, the efficiency could be reduced by around 50%. Under loading, where liquid spreading is reduced, the efficiency would be still further reduced. They also calculated that if liquid flowing in the gaps between blocks acted as a bypass flow, the efficiency could be reduced by up to 20%, or 30% under loading conditions.

Conclusions

Liquid and vapour distribution must be considered when designing packed columns. In small columns, wall flow should be reduced, whereas in larger columns the initial distribution becomes more important. The important parameter here is the cross-mixing per theoretical plate compared to the column diameter. If the fluids move only a fraction of the column diameter as they flow through one theoretical plate, then initial distribution is very important, and, in deep beds, the phases should be re-mixed at set intervals. When designing new packing geometries, the spreading of liquid and vapour should be maximised. Additionally, in large columns, attention should be given to reducing irregularities in the bed due to boundaries between packing blocks.

2.5 Heat and mass transfer enhancement techniques

The building and operation of heat and mass transfer devices always involves a balance between initial capital costs and running costs. A larger device allows more heat or mass to be exchanged and saves running costs, but costs more to build. The idea of intensifying or enhancing the rate of heat or mass transfer is to make smaller devices to do the same job and hence save on the initial expense. However, it normally leads to an increase in running cost, because of increased pumping power, for example. So, in analysing the effectiveness of enhancement techniques, the running cost saved due to the increased transfer and capital cost saved due to a smaller device must be balanced against the increased running cost due to the extra frictional resistance.

The economic analysis of an air separation plant has shown that it is important to increase the efficiency of a packing, even at the expense of some increased pressure drop per theoretical plate, because of the high cost of tall columns. Similar considerations have led to considerable intensification of heat exchanger design in air separation plants to increase the economic number of transfer units and improve the cold recovery from the products.

A variety of methods has been used to enhance mass and heat transfer. These may be divided into two groups, passive and active. Active methods involve supplying extra energy to the flow, for example by pulsing it, applying an electric field or by spinning or vibrating part of the apparatus. These need more complex apparatus than passive methods and so are considered impractical for use in large-scale distillation and will not be considered further. Static methods involve changing only the form of the flow channels and include increasing the channel roughness, promoting swirl flow, extending the transfer area, promoting turbulence and changing the shape of the channels.

To understand the methods of enhancing heat and mass transfer and which methods are best suited to which fluids, we will first consider the effect of flow regime and fluid properties on heat and mass transfer. We shall then examine ways of increasing heat and mass transfer in single phase flow, and finally discuss the applicability of these methods in two-phase flow.

2.5.1 Flow regime and fluid properties

Flow may be either laminar or turbulent. In the turbulent regime, the transfer of heat, mass and momentum is increased by the eddying in the fluid, so that the pressure gradient and heat and mass transfer coefficients are higher at the same Reynolds number. So the turbulent regime is generally best for enhanced heat and mass transfer.

Flow may also be fully-developed or developing. In the entrance region of a pipe or duct, the boundary layer grows, until it fills the whole pipe and no further change in velocity profile occurs. This region of developing flow has a higher pressure gradient than fully developed flow because of the thinner boundary layer causing more momentum transfer. It also shows higher heat and mass transfer coefficients than fully-developed flow. The extent of the improvement depends on the fluid and whether the flow is laminar or turbulent.

The important properties of a fluid in determining momentum, heat and mass transfer are its viscosity, density, and thermal or mass diffusivity. These are expressed as the Reynolds number, Prandtl number and Schmidt number. The Prandtl and Schmidt numbers are the ratio of kinematic viscosity and thermal or mass diffusivity. They determine the relative thickness of the momentum boundary layer and the thermal or concentration boundary layer.

In liquids, the Prandtl and Schmidt numbers are generally much bigger than one, whereas in gases they are of order one. The thermal and concentration boundary layers in liquids are therefore much thinner than the momentum boundary layers, but in gases they are of similar thickness.

2.5.2 Single phase heat and mass transfer enhancement

To enhance the heat or mass transfer in a flowing fluid, we must disturb this flow in some way. We shall look first at the general effects of disturbances to the flow, then in more detail at ways of achieving such disturbances.

2.5.2.1 General effects of flow disturbance

Disturbance of flow in the wall region

The flow in the region of the wall may be disrupted by several methods. These include attaching ribs to the duct walls, increasing the roughness of the walls and putting some kind of turbulence promoter, for example an expanded metal sheet, against the walls. Various methods are discussed in more detail by Chang and Park (1986) and Zukauskas (1989).

If the fluid has a high Prandtl or Schmidt number, as in a liquid, the thermal or concentration boundary layer is much thinner than the momentum boundary layer, and may lie within the viscous sublayer. In this case, eddy transport is dominant even in the viscous sublayer. Increasing the roughness, even slightly in the wall region can increase the eddying in this sublayer and give a considerable enhancement of mass transfer, without too much increase in pressure loss. As the height of roughness is increased, the enhancement reaches a maximum where the roughness elements reach the edge of the transition layer.

In gases, however, where the molecular diffusivity is higher, eddy transport is not so important in the viscous sublayer and transition layer. It is only when the roughness elements penetrate this layer that the heat and mass transfer are enhanced. The pressure drop penalty is then much higher than in liquids. The enhancement again reaches a maximum as the roughness height is increased, but is not reduced as severely as that in liquids.

In either case, as well as an optimum height, there is also an optimum spacing of roughness elements. This is approximately where eddies shed from one element re-attach to the wall just before the next one and occurs when the ratio of spacing to height is about 10.

Three-dimensional roughness is more effective than two-dimensional, because of the interaction of eddies in two dimensions over the wall.

Disturbance of main flow

The main flow may be disturbed either by putting obstructions in it, or by changing the channel shape. This has two effects; the intensity of turbulence is increased and the vorticity is increased. Disturbing the main flow will have a bigger impact on heat and mass transfer in laminar flow, by introducing eddying where it did not previously take place.

If the turbulence intensity (the mean square fluctuation velocity as a proportion of the main stream velocity) in the main flow can be increased, the eddy transport will be enhanced into the outer part of the boundary layer, and heat and mass transfer will be improved. The improvement will be greater in gases than liquids,

because the resistance to transfer is spread more evenly through the boundary layer; in liquids it is confined to the wall region, which is unaffected by increased main stream turbulence.

If, on the other hand, a large amount of vorticity is introduced to the main flow, such as by swirling it, this disturbs the flow right to the wall. As a result, the enhancement of transfer in liquids is better than in gases because in liquids the resistance is in the wall region.

Because it is the large scale eddies which are mainly responsible for the transfer of heat and mass, it is advantageous to introduce large-scale, regular disturbances into the flow. Effective transfer is then provided by these eddies before their kinetic energy is cascaded down to smaller scale eddies and dissipated. The introduction of smaller scale eddies directly does not increase the transfer so much for the same pressure loss (energy dissipation).

2.5.2.2 Methods of disturbing the flow

Wall-region obstructions and roughness

Chang and Park (1986) give a review of the enhancement of mass transfer due to near-wall turbulence promoters. These techniques only disturb the flow in the region of the boundary layer.

Roughness enhances heat and mass transfer in liquids more than gases, unless it projects into the outer boundary layer. Similarly, it will not affect laminar flow unless it protrudes well into the flow and causes eddying.

Near-surface obstructions, such as wires or net type turbulence promoters, can create wakes which enhance the mass transfer more than roughness in laminar flow and in fluids with low Prandtl or Schmidt numbers.

Swirl flow promoters

The advantages of swirl flow are explained by, amongst others, Zukauskas (1989) and Bejan (1982). Swirl flow may be achieved by putting twisted tapes or propellers in the main flow or spiral ribs on the walls. The enhanced transfer coefficient may be several times the undisturbed flow value. The enhancement is better in laminar flow and at high Prandtl or Schmidt numbers, because the increased vorticity penetrates right into the viscous sublayer.

Central obstructions

These can be grids, disks, cylinders or other shapes. An example is in the work of Dudukovic and Koncar-Djurdjevic (1979), who used disks in a turbulent flow. Turbulence is increased downstream as the boundary layer formed on the

obstruction is shed into the flow. In addition, flow in the wall boundary layer may be disturbed by the wake of the obstruction. The exact nature of the enhancement due to a particular obstacle will depend on how much it disturbs the main flow and the wall flow. Provided the obstacle sheds a wake, the improvement to transfer will be greater in laminar flow.

Changes to channel shape

Like central obstructions, changes in the channel shape can affect both the wall region and main flow. The advantages of changing the shape are therefore dependent on the exact nature of the shape.

Channels used for enhanced heat and mass transfer include zigzag or twisted channels and channels with periodic sharp constrictions or changes in cross-sectional area or shape. These channels generally promote a transition to turbulence at a lower Reynolds number and show the greatest enhancement of transfer coefficients in the transition regime. The enhancement is generally greater if the shape is more severe, for example a bigger reduction in cross section, a steeper angle of convergence or sharper changes in direction. However, above a certain degree of severity, the pressure loss becomes unacceptably large for a diminishing improvement in transfer, so some optimum should exist.

Laminar and turbulent flow and heat and mass transfer in fluids with large and small Schmidt and Prandtl numbers have been extensively investigated in wavy-walled channels by a number of authors. These include Souza Mendes and Sparrow (1984), Nashimura et al. (1986) and Narayanan and Bhattacharyya (1988).

Souza Mendes and Sparrow (1984) measured turbulent mass transfer coefficients for naphthalene subliming into air in converging-diverging tubes and found that the enhancement decreased with increasing Reynolds number and increased with taper angle from about 1.1 at 2 degrees to between 3 and 4 at 14 degrees. The enhancement at constant pumping power was a maximum of about 1.5 at around 10 degrees. They also found that with small taper angles and at low Reynolds numbers, the converging sections showed more mass transfer, but as the taper angle or Reynolds number increased, the relative mass transfer in the diverging section increased.

In laminar flow in wavy channels, Nashimura et al. (1986) found an enhancement of around 3 in mass transfer in a sinusoidally varying channel, with an approximate angle of 27 degrees. The friction factor and mass transfer in this channel had the characteristics of turbulent flow, indicating that the channel shape had resulted in an earlier transition. Narayanan and Bhattacharyya (1988) found a similar enhancement in heat transfer in laminar flow in converging-diverging tubes with taper angles of 4.75 and 9.5 degrees. The enhancement increased as the

Reynolds number increased and as the Prandtl number increased at constant Reynolds number. It was also better with shorter segments at the same angle and at steeper angles. Their friction factor was close to the value for laminar flow, but they noticed that the velocity profile was quite flat in the centre of the tube.

The better enhancement at higher Prandtl and Schmidt numbers shows that in this type of geometry the viscous sublayer is significantly disturbed, even with quite small taper angles. As the taper angle increases, the increased enhancement in liquids tails off, but in gases the enhancement continues to increase, because of the increasing impact on the outer boundary layer.

In a numerical study of laminar mass transfer in ducts which changed direction periodically, Ramadhyani (1986) showed that the enhancement was bigger as the change in direction increased and as the length between changes in direction decreased. It rose sharply at a particular corrugation length, where the transition to turbulence would take place. He also found a greater enhancement at higher Prandtl numbers.

Discontinuous surfaces

We saw earlier that the heat and mass transfer in the entrance region of a pipe or duct is higher than in fully-developed flow. The heat or mass transfer to a plate parallel to the flow is also higher nearer to the leading edge. This is because the boundary layer is thinner in these regions, so higher temperature or concentration gradients are possible, which lead to higher transfer rates. As a result, we would expect that a good way to enhance transfer would be to break the surface up (see for example Zukauskas, 1989). The disadvantage is that the momentum transfer and pressure gradient is also increased. The advantages of a discontinuous surface depend on the regime and fluid properties.

In laminar flow, higher Schmidt or Prandtl numbers, such as in liquids, mean that the thermal or concentration entrance length is quite large, and may be several thousand diameters long. Enhanced transfer is only possible when the pipe is shorter than the entrance length, so in gases, where the entrance length is less than one hundred diameters, shorter pipes are needed for the same improvement in transfer.

In transition and turbulent flow, the effect is reversed. Here, the temperature or concentration profiles build up more quickly than the velocity profile when the Prandtl or Schmidt number is large. This is because eddy transport is more important than molecular transport in these regimes. If the diffusivity is lower, eddy transport is dominant closer to the surface, and most of the concentration or temperature difference occurs over a thin film; the larger the Prandtl or Schmidt number, the thinner the film. The fully-developed profile is then more similar to

the initial one and is established more quickly, so that the enhancement possible in liquids by reducing the entrance length is small, compared to that in gases.

If the mass transfer is already enhanced by some other means, such as turbulence promotion, the thermal or diffusion sublayer in the fully-developed flow will be thinner than in a straight tube and so the entrance length will be shorter. The effect of breaking the surface will then be reduced, and it should be done more frequently for the same enhancement over a continuous surface.

Extended surface area

In a heat exchanger, it is possible, by the use of fins, to extend the area for heat transfer in the fluid which has a high resistance. This is clearly not possible in mass transfer, where two fluids must have a common interface. In both cases, heat and mass transfer may be intensified by putting more contact area into the same volume. An example of this is the use of packings with a high surface area per unit volume for higher efficiency. This has the disadvantage, however, of increasing the momentum transfer and reducing the operating Reynolds number. It requires approximately the same amount of metal for a given transfer and so does not significantly reduce the packing cost, although it may reduce the column shell cost.

2.5.3 Applicability of methods to two-phase flow

In two-phase flow in a packing, the transfer of heat and mass is not to a solid wall, but to a liquid film. Momentum may be transferred both to the liquid and to any unwetted parts of the packing, whereas heat or mass are only transferred to the film. Most of the methods which have been described to enhance heat and mass transfer are however applicable to each phase.

The shape of the gas flow channel may be altered relatively easily because the liquid will flow over it, however it is less easy to influence the surface characteristics of the interface, such as roughness. In addition, any large scale roughness may not be covered by liquid and may waste metal area. Obstructions in the main flow should be relatively easy to introduce, as should swirl flow promoters.

The liquid film has more potential for enhanced transfer because of its laminar flow and high Schmidt number. Large scale surface roughness on the packing surface will alter the shape of the liquid film in a similar way to changing the channel shape. It will also act as an obstruction in the flow, because the film is so thin, and will help to render the film turbulent. Small scale roughness is unlikely to have an effect right up to the interface. Because of the thinness of the film, it is unlikely that swirling it would be possible.

If the surface is broken, account must be taken of the liquid flow. If it drips into the gas stream, for example entrainment may result, which would reduce the capacity of the packing.

2.6 Conclusion

In this literature review, we have covered five areas: Air separation plant, the use of packings in such plant, structured packing development and manufacture, models of packings and methods of enhancing heat and mass transfer.

The introduction to air separation plant has shown where this work fits in to air separation technology and has provided the background necessary to understand the economic work in chapter 3. The later sections have enabled us to understand what scope there is to improve the performance of structured packings and how such improvement may be brought about. This will be described in chapter 4, which describes the packing development work.

Chapter 3 - Economic Work

The economic work in this chapter is divided into two sections. In the first, a simple model of an air separation plant is developed and used to predict the power saved by using structured packing. This is combined with generalised cost estimates to provide a rate of return on the extra investment in the packed plant.

The second section deals with the economics of the packing manufacturing process, to estimate the costs of existing packings and any newly developed packings.

3.1 Economic assessment of structured packing in Air Separation Plant

A new product will be produced or a change made to a process only if it will provide some advantage. Research should therefore be undertaken not only to increase knowledge, but also because its results can be applied to provide some benefit. There are different ways of assessing the advantage due to an improved process or a new product, depending on the ultimate aim of the research and on whose advantage is being considered.

For example, if the aim is to maintain our standard of living whilst reducing the impact on our surroundings, an appropriate analysis would consider the amount of energy used (or, more strictly, the entropy generated) by the construction and operation of the new process or in the production and use of the new product in comparison to the situation beforehand. A common aim is to increase the profits of a company, for which an economic analysis is most suitable. In this case, the effects on the surroundings and on others are only accounted for in economic terms, for example in the cost of complying with any environmental legislation. Ultimately the two aims will give similar results as companies are held increasingly responsible for their environmental impact and as non-renewable energy costs increase because supplies diminish.

In this work, the advantage to be gained by using structured packing rather than trays in the distillation columns of an air separation plant is examined in economic terms, because the purpose of such a change would be to reduce the production cost of oxygen, nitrogen and argon. An advantage may be realisable because, although a packed column is more expensive, the plant consumes less power than when trays are used.

In this analysis, only the differences in capital and running costs between the packed and trayed plants are considered, so it is relative rather than absolute. This means that even if this analysis shows that a packed plant is more advantageous than a trayed one, the packed plant may still be uneconomic to build. This is

especially likely to be the case for small plants, where membrane separation or pressure swing adsorption plants will still be the most economic option.

In order to carry out the analysis, we need to calculate what the differences are in capital and running costs between the two types of plant and to use some method of relating the two costs. The capital and running cost calculations both require a good understanding of the design and operation of an air separation plant and of the differences made by changing the column internals. All three stages need economic information, which may be quite different depending on the particular circumstances, and especially on plant location.

We will first consider the simulation of an air separation plant and the insights it gives us into the effects of replacing trays with packing. In the description of the analysis we shall look first at the development of a simplified plant design model to calculate the differences in power consumption between the plants. Next we shall consider the information needed to calculate the capital and running costs. Finally, we shall see how they can be related by the calculation of a rate of return on the extra investment in the packed plant. In the last part of this section, we shall see the results of a number of calculations of this rate of return for different economic conditions, in different plants and with different packings.

3.1.1 Preliminary work - air separation plant simulation

In section 2.1, we saw that the most commonly used type of air separation plant has a main double column system and may have an argon side-column. Refrigeration is provided by near isentropic expansion of air or waste medium-pressure nitrogen and the plants are well heat-integrated. We also saw in section 2.1 that the use of a structured packing instead of trays in the low pressure column can significantly reduce the outlet pressure required from the main compressor, and hence its power consumption. To calculate the power cost saving, this power consumption must be accurately determined and to find the increase in investment needed, any changes in the plant equipment must be worked out.

To understand the detailed effects of the change to structured packing, an integrated air boost cycle was simulated with BOC's CRYOSIM computer programme. The flowsheet of this cycle is illustrated in figure 3-1. The results for a packed plant are compared with those for a trayed one in the summary in table 3-1 and the heat and mass balances are shown in table 3-2. The only difference assumed between the two plants were the pressure drops across the low pressure column (28 mbar rather than 320 mbar) and argon column (20 mbar rather than 300 mbar). In each case the Lachmann air flow was the same.

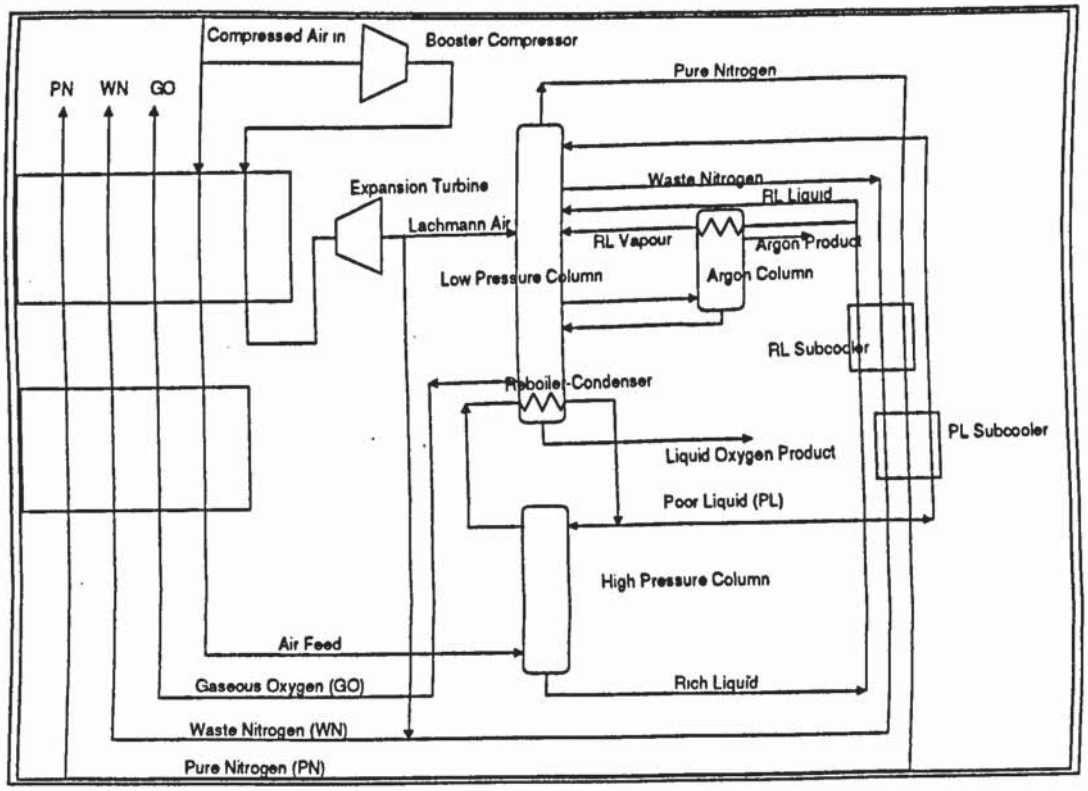

Figure 3-1 Air Boost Cycle with argon side-column

The simulation shows that in this case, the power saving actually achieved with a packing of about 1.8% is significantly lower than the 8% calculated by the analysis of Bennett et. al. (1989). Further examination of the results reveals that this is mainly due to the reduced thermodynamic efficiency of the refrigeration at the lower pressure and the increased refrigeration requirement. Although the lower pressure reduces the compressor power consumption, it reduces the temperature difference across the expansion turbine. The air flow through the turbine needed to achieve the same refrigeration is greater because heat is removed at a lower average temperature, so more air must be compressed. The reduction in power consumption is therefore smaller than if the same flow were required.

In addition to the refrigeration being less efficient in a packed plant, more is required and so the turbine flow is increased still further. The heat balance shows that this is mainly due to the increased flow through the booster meaning that more heat is generated by its inefficiency, but also to a reduced Joule-Thompson effect in the compressed air, more heat leaking into the cold box and the increased loss due to the larger flow with the same warm end temperature difference. The booster in the simulation operated with a constant aftercooler temperature, so the heat added to the cold box increased in proportion to the extra flow in the packed plant. This accounted for most of the difference in refrigeration requirement, so a packed plant would probably have a lower economic booster aftercool temperature; it is more efficient to remove heat at this temperature than at the turbine temperature.

Comparison of Trayed and Packed Plants	Trayed Plant		Packed Plant	
Product information	Flow sm3/hr	Purity %O2	Flow sm3/hr	Purity %O2
Air Feed	183606	20.9560	194195	20.9560
Waste Air	900	20.9560	11489	20.9560
Gaseous Oxygen	38450	99.5001	38450	99.5001
Liquid Oxygen	0	99.6800	0	99.6800
Liquid Argon	700	1.8000	700	1.8000
Gaseous Argon	190	1.8000	190	1.8000
Warm Low Pressure Nitrogen	30000	0.0002	30000	0.0002
Warm Medium Pressure Nitrogen	2110	0.0002	2110	0.0002
Waste Nitrogen	111241	0.0001	111241	0.0001
Heat Exchangers	Pinch /K	UA / kcal/K	Pinch /K	UA / kcal/K
Warm Main Exchanger	4.098	1325779	4.862	1461037
Cold Main Exchanger	4.355	699955	5.277	329474
Gaseous Oxygen Product Heater	2.383	15609	2.374	15716
Poor Liquid Subcooler	2.207	222695	2.417	177980
Rich Liquid / Nitrogen Subcooler	2.1	101362	2.1	108102
Argon Condenser	1.138	797831	2.856	443741
Refrigeration System				
Air Compressor Outlet Pressure/ atm	6.297		5.52	
Lachmann Air Flow /sm3/hr	17500		17500	
Recycle (Waste) Air /sm3/hr	900		11489	
Total Turbine Flow /sm3/hr	18400		28989	
Reboiler-Condenser dT /K	1.5		1.5	
Heat Inleak/ kcal/hr	89803		93526	
Turbine/Booster Power /kW	371.7		448.8	
Relative Main Compressor Power	100		98.20	
Column System				
Theoretical Trays in High Pressure Column	35.8		31.9	
Theoretical Trays in Low Pressure Column	65.8		61.1	

Table 3-1 Comparison of simulation results for packed and trayed plants

Enthalpies based on air at 1atm, 288.5 K							
Heat balance around cold box of simulated plant with trays							
Stream	Flow into cold box	% of gas in feed to column	Temp-erature	Pressure	Enthalpy	Power out of cold box	% of power out of cold box
	Standard m3/hr		K	atm	kcal/sm3	kcal/hr	
Air to cold box	183606		288.5	5.992	-0.3546	65107	16.9
Booster inefficiency						-80705	-21.0
Turbine						319695	83.1
Heat leak						-89803	-23.3
Air to waste	-900		286	1.03	-0.7368	-663	-0.2
Liquid oxygen	0						
Gaseous Oxygen	-38450	99.921	286	1.383	-0.7746	-29783	-7.7
Liquid Nitrogen	0						
Gaseous Nitrogen	-32130	22.410	286	1.045	-0.7594	-24400	-6.3
Waste Nitrogen	-111241	77.590	286	1.03	-0.7363	-81907	
Liquid Argon	-700	41.1524	88.17	1.101	-108.27	-75793	-19.7
Gaseous Argon	-180	10.5820	286	1.03	-0.7363	-133	0.0
Total	5					1616	0.4
Heat balance around cold box of simulated plant with structured packing							
Stream	Flow into cold box	% of gas in feed to column	Temp-erature	Pressure	Enthalpy	Power out of cold box	% of power out of cold box
	Standard m3/hr		K	atm	kcal/sm3	kcal/hr	
Air to cold box	194195		288.5	5.215	-0.2966	57598	13.0
Booster inefficiency						-129295	-29.1
Turbine						386002	87.0
Heat leak						-93526	-21.1
Air to waste	-11489		286	1.03	-0.7368	-8465	-1.9
Liquid oxygen	0						
Gaseous Oxygen	-38450	99.921	286	1.129	-0.7724	-29699	-6.7
Liquid Nitrogen	0						
Gaseous Nitrogen	-32130	22.410	286	1.083	-0.7578	-24348	-5.5
Waste Nitrogen	-111241	77.590	286	1.03	-0.7363	-81907	
Liquid Argon	-700	41.1524	89.293	1.235	-107.7	-75394	-17.0
Gaseous Argon	-180	10.5820	286	1.03	-0.7363	-133	0.0
Total	5					834	0.2

Table 3-2 Comparison of heat and mass balances from simulation for packed and trayed plants

This suggests two improvements to plants which could improve their performance with packings. The first is to ensure that the boosted air is cooled before it enters the cold box and the second is to add power to the booster compressor so that its outlet pressure is the same as the trayed case. This will improve the refrigeration efficiency and reduce the net power consumption. Both these possibilities are investigated later. An alternative way of improving the

refrigeration efficiency still further would be to add another turbine. This would allow some of the heat to be removed more efficiently at a higher temperature, and reduce the temperature differences in the main exchanger. The cost of this would have to be balanced with any additional power saved. This possibility was not included in the present work because no information was available for the turbine cost.

Because the Lachmann air flow in the simulation was kept constant, the increased air flow in the packed plant was all sent to the waste stream. This means that the wasted air goes from almost zero, in the trayed plant to about 7% of the flow to the column (which is the same in each plant) in the packed plant. As a result, the increase in turbine flow increases the compressor power consumption more than if the Lachmann air flow in each plant were zero, or a constant proportion of the turbine air flow. So the power saving on the simulated plant is less than 2%, which is too low to be viable.

The reduced average pressure in the high and low pressure columns means that the relative volatilities of the components are greater. Consequently, in the simulation, where the flows and reflux ratios were the same in each plant, the packed columns needed fewer theoretical plates. Advantage may be taken of the increased relative volatilities to operate the column closer to minimum reflux by increasing the number of theoretical trays and processing more Lachmann air.

A consequence of the reduced thermodynamic efficiency of the cycle is that the heat exchanger surface area required is smaller because the temperature differences are larger. This allows a small capital saving, although we shall see later that the small change in heat exchanger cost is negligible in comparison to the large change in the column cost. As a result it is likely to be more economic to improve the refrigeration efficiency to take advantage of power savings which are worth more than the small capital saving.

In the example plant, the argon recovery is rather low, at only around 50%. The refrigeration needed in a plant with higher argon recovery would be greater because of the larger amount of liquid produced.

Another interesting point is that the argon pressure is higher when the columns are packed. This is because the bottom pressure of the argon column is similar with trays or packing in the low pressure column, but the pressure drop across it is much lower with trays. This means that the liquid argon temperature is higher and the temperature difference in the condenser can be much larger and the condenser can be made smaller. The disadvantage is that the average pressure in the argon column is increased and the relative volatility reduced. As a consequence, more theoretical trays would be needed. Solutions to this problem include using both trays and packing in the argon column (Victor et. al., 1991) and adding a pressure

reducing valve to the argon column feed and pumping (or gravity-feeding) the bottom liquid back into the low pressure column (Allam and Prentice, 1989).

The plant simulation showed a rather small advantage of using a structured packing rather than trays. This turned out to be because it was a rather unrealistic comparison. The Lachmann air flow was the same in each plant despite the difference in refrigeration requirement, whereas in practice, each plant would be optimised so that they had similar product recoveries. This can be accounted for by making the plants more comparable, by, in this case, assuming that no Lachmann air is processed and all the turbine air is sent to waste. The plant on which the analysis is performed is therefore not the same one as was simulated. It has been chosen so as not to put packing at an unrealistic disadvantage

These insights gained into the operation of an air separation plant by the simulation can now be used to produce a general, simplified design model for use in the economic analysis.

3.1.2 Description of analysis

We shall look first at the model of an air separation plant devised to allow calculation of the power consumption. We shall then consider how the economic information may be found, and lastly how these two sets of information may be combined to calculate the rate of return on the extra investment in the packed plant, which is used as a measure of the advantage of packing.

3.1.2.1 Plant design

In an ideal process for separating two ideal gases, a mixture with composition y of gas number one enters at ambient temperature T and pressure p and with molar flow F. Two streams emerge, still at temperature T and pressure p and with flows y.F and (1-y).F. Since the enthalpy of an ideal gas depends only on temperature, the (enthalpy x flow) of the stream in equals the (enthalpy x flow) of the streams out. No refrigeration needs to be provided, however, work W must be performed on the system for every mole flowing into it to compress the components isothermally from their partial pressures y.p and (1-y).p to their outlet pressure p. This is the work of separation needed to effect the increase in entropy from the inlet to the outlet streams. It is reversible, as it may theoretically be recovered by re-mixing the outlet streams, and is given by:

$$W = R\,T\,(\ln(y.p/p) + \ln((1-y).p/p)) = R\,T\,(\ln(y.(1-y)) = -T\,\Delta S,$$

If the gases are real, rather than ideal, there will be some change in enthalpy between the inlet and outlet. This is the change of enthalpy on mixing/separation

and it occurs because the gases interact with each other and because the enthalpies change with pressure and the partial pressures of the gases in the inlet and outlet are different. Extra work must then be performed by the system or heat transferred to it so that Q or W' is equal to the change in enthalpy, ΔH. This may be positive or negative, depending on the conditions. This work or heat transfer is also reversible, as it is obtained across a zero temperature difference and may again be recovered by re-mixing the separated components.

Such a separation process is still ideal because there are no losses due to the first or second-laws of thermodynamics; no unnecessary heat is added to the system and no work is converted into heat, or heat transferred, across a finite temperature difference.

In a real, cryogenic air separation plant, where the separation is performed by distillation, the mixture must first be cooled to cryogenic temperatures, then separated and re-heated to ambient temperature. This process involves both first- and second-law losses.

First-law losses occur because extra heat is added to the plant by inefficient machinery, when it leaks in through insulation and because the streams leaving the plant cannot reach as high a temperature as those leaving it, and so do not remove as much heat.

Second-law losses result from irreversibilities within the cooling, heating, refrigeration and distillation column (separating) systems. These are due to finite pressure drops in pipes and valves, irreversible mixing of streams and the transfer of heat across finite temperature differences. As a result more work must be performed on the plant to achieve the separation than in the reversible limit.

Work is performed on an air separation plant by the main air compressor. Because of the inefficiency of the compressor, some of this work is lost at this stage. The air is heated, so it must then be cooled back to ambient temperature by removing the extra heat with cooling water.

The air then enters the cold box, inside which any excess heat must be removed by making it perform work, because the temperature is too low to remove heat by exchange with a coolant.

In the simplest plants, no extra heat is added to the cold box because the Joule-Thompson effect is used to ensure that the compressed air entering the cold box is at a sufficiently high pressure to have the same enthalpy as the streams leaving it. This is thermodynamically inefficient, since the adiabatic expansion employed within the plant is highly irreversible; none of the extra work done by the main compressor to provide refrigeration by this means may be recovered from the plant.

In most plants, heat is removed almost reversibly from the cold box as work by near-isentropic expansion of compressed gas down to atmospheric pressure. These plants are much more efficient than those using the Joule-Thompson effect because

the compressor need not deliver such a high pressure and because some of the power supplied to it may be recovered by the turbine. However, a bigger air flow is often required to these plants, because if air is expanded it may not all be processed in the column system.

The work to be removed from the cold box of a plant may be calculated from a heat balance around it, that is from a consideration of the first-law of thermodynamics.

How much work must be supplied to the main compressor and how efficiently work is removed from the cold box will be determined by the second-law efficiency of the plant, which depends on its design. This will fix both the outlet pressure of the main compressor and the flow through it. The outlet pressure is found by a pressure balance around the plant, but equations for the flow of air required and the work to be performed by the refrigeration turbine must be solved simultaneously.

Pressure Balance.

The compressor outlet pressure is calculated, given the pressure drop in each part of the plant and the temperature difference in the reboiler-condenser. The gaseous nitrogen (product and waste) streams must leave the plant at a pressure just above that of the atmosphere, so the calculation proceeds back through the plant from the pressure limiting stream. Such a calculation is illustrated in table 3-3.

The pressure drops across the heat exchangers, pipes and valves are based on the simulated plant and are combined in the table over sections of the plant. The main difference between the pressure drops in different plants is due to the method used to remove water and carbon dioxide from the air. If reversing heat exchangers are used, the pressure drop is lower, but the waste flow necessary to regenerate them is higher than the alternative pre-purification absorption units (PPUs). The pressure drop across the purification device appears both just after the main compressor and just before the waste outlet. The pressure drop in the waste stream is more important in determining the plant power consumption, for the same reason as the low pressure column pressure drop is more important than that of the high pressure column. Because of this, blowers are sometimes used to drive the regeneration gas through the PPUs. This reduces the pressure drop in the waste stream and means that the main compressor pressure is lower.

To find the pressure drop across the distillation columns, the flows and behaviour of the internals must be known. The simulation assumes that the whole column operates at a constant fraction of flooding and that the pressure drop per tray is the same for each tray. If trays are used, they will be designed differently in each section to account for the different loadings, so that this will be the case. In a packed column, the less heavily loaded sections could be filled with a higher area,

more efficient, lower capacity packing so that this would again be the case. If the same packing is used throughout the column, the pressure drop across it could be very much smaller than the calculated one. This is because it falls very quickly as the vapour flow is reduced. So the pressure drop assumed in the case of a packed column should give a worst case estimate of the advantage of a packing.

Pressure Balance. Pressures in bar, Temperatures in Kelvin	RHE plant		PPU plant		Simulation	
	Trays	SP	Trays	SP	Trays	SP
Atmospheric Pressure	1.013	1.013	1.013	1.013	1.013	1.013
Pressure drop from top of low pressure column to atmosphere	0.280	0.280	0.580	0.580	0.204	0.242
Pressure drop across low pressure column	0.300	0.050	0.300	0.050	0.324	0.028
Pressure of liquid oxygen in reboiler	1.593	1.343	1.893	1.643	1.541	1.284
Temperature of liquid oxygen in reboiler	94.729	92.954	96.598	95.058	94.370	92.486
Temperature difference between condensing nitrogen and boiling oxygen	1.500	1.500	1.500	1.500	1.523	1.522
Temperature of condensing nitrogen	96.229	94.454	98.098	96.558	95.893	94.008
Pressure of condensing nitrogen	5.840	5.114	6.678	5.982	5.819	5.032
pressure drop across high pressure column	0.070	0.070	0.070	0.070	0.132	0.132
Pressure drop from main compressor outlet to bottom of high pressure column	0.120	0.120	0.420	0.420	0.430	0.430
Main compressor outlet pressure	6.030	5.304	7.168	6.472	6.380	5.593
Pressure ratio		0.880		0.903		0.877
Power ratio		0.929		0.948		0.929

Table 3-3 Pressure balance for plants with trays and structured packing. Typical values for Reversing Heat Exchanger and Pre Purification Unit plants and the values used in the simulated plant.

The boiling temperature of oxygen and condensing pressure of nitrogen (both assumed pure) are calculated with the Antoine equation and coefficients given by Sinnott (1989).

Mass and heat balance - turbine flow calculation.

It is assumed in the analysis that the trayed and packed plants must produce the same quantities of products at the same purities. The air flow to the column system is therefore taken to be the same in each case.

It is also assumed that the Lachmann air flow into the low pressure column is zero and that the number of theoretical plates is the same in each case. This enhances the advantage of a packed column over that seen in the simulation, but gives a smaller advantage than if a constant fraction of the turbine air were processed in the column system. A packed column with the same number of theoretical trays could process more Lachmann air than a trayed one. The optimum balance between the number of plates and Lachmann air flow could be found by performing the economic analysis with a more advanced design model, which would include the column calculations.

So any difference in the flow of air through the compressor in the two types of plant is due to the difference in flow through the refrigeration turbine. To establish this flow, a knowledge of the necessary refrigeration and the operation of the turbine is needed.

Heat must be removed as work by the turbine to make up for the heat gained by the streams inside the cold box. This heat gain is due to the heat leaking in through the insulation, the heat generated by inefficiencies in the booster compressor (which is assumed to be within the cold box) and because the streams entering the cold box carry more heat (have a larger enthalpy) than those leaving it. So the power which must be removed from the cold box by the turbine is given by:

$$P_{turb} = Q_{in} + P_{bi} + F_{in}\, H_{in} - \Sigma\, F_{out,j}\, H_{out,j},$$

that is the sum of the heat leaking in, the heat generated and the difference between the heat flowing in and out,

where

P_{turb} is the power generated by the turbine,
Q_{in} is the heat leaking into the plant per unit time,
P_{bi} is the heat flow generated by the booster inefficiency,
F_{in} is the air flow into the plant,
H_{in} is the enthalpy of the air entering the plant,
$F_{out,j}$ is the flow out of the plant of each stream, j, and
$H_{out,j}$ is the corresponding stream enthalpy,

The difference in enthalpy between the streams in and out of the cold box is caused by several factors. These are the difference in temperature between the

inlet and outlet streams, their difference in pressure, their difference in phase, and the enthalpy of mixing of the components to form air. It is useful to separate these factors to see their relative contributions to the refrigeration requirement. To do this, all the enthalpies are first written with respect to H_0, the enthalpy of air at the inlet temperature and one atmosphere,

$$P_{turb} = Q_{in} + P_{bi} + F_{in}(H_{in} - H_0) + \Sigma F_{out,j}(H_{out,j} - H_0),$$

Now, the enthalpy of stream j, $H_{out,j}$, may be written as $H_{Tout,j}+(H_{out,j}-H_{Tout,j})$, the sum of the enthalpy of the stream if it were at the main exchanger outlet temperature and atmospheric pressure and the difference in enthalpy between these conditions and the actual stream conditions.

Similarly, $H_{Tout,j}$ may be written as $H_{0,j}+(H_{Tout,j}-H_{0,j})$, where $H_{0,j}$ is the enthalpy at one atmosphere at the inlet air temperature, so that.

$$\Sigma F_{out,j}(H_{out,j} - H_0) = \Sigma F_{out,j}(H_{0,j}+(H_{Tout,j}-H_{0,j}) + (H_{out,j}-H_{Tout,j}) - H_0)$$

Because $F_{out,j} \triangleq y_j F_{in}$, where y_j is the mole fraction of component j in the feed,

$$\Sigma F_{out,j} = \Sigma F_{in}\, y_j = F_{in}\, \Sigma y_j = F_{in}.$$
$$\Sigma F_{out,j}\, H_{0,j} = \Sigma F_{in}\, y_j.H_{0,j} = F_{in}\, \Sigma y_j\, H_{0,j}$$
$$\text{and} \quad \Sigma F_{out,j}\, H_{Tout,j} = \Sigma F_{in}\, y_j\, H_{Tout,j} = F_{in}\, \Sigma y_j\, H_{Tout,j}$$

In addition, the enthalpy of air at the inlet temperature and one atmosphere, H_0, may be written as:

$$H_0 = \Sigma y_j\, H_{0,j} + \Delta H_{mix,0}$$

and the enthalpy of air at the main exchanger outlet temperature may be expressed as:

$$H_{Tout} = \Sigma y_j\, H_{Tout,j} + \Delta H_{mix,Tout}$$

where ΔH_{mix} is the change in enthalpy on mixing the individual components to form air, and is positive if heat is taken in on mixing.

These equations allow us to write the expression for the heat flow carried by the streams out of the plant as:

$$\Sigma F_{out,j}(H_{out,j}-H_0)=\Sigma F_{out,j}(H_{0,j}-H_0)+\Sigma F_{out,j}(H_{Tout,j}-H_{0,j})+\Sigma F_{out,j}(H_{out,j}-H_{Tout,j})$$
$$= F_{in}((H_{Tout} - H_0) - \Delta H_{mix,Tout}) + \Sigma F_{out,j}(H_{out,j}-H_{Tout,j})$$

We can see immediately the effect of the enthalpy of mixing on the refrigeration requirement. If the enthalpy of mixing is negative, i.e., heat is evolved on mixing (or absorbed on separation), the outflowing streams carry more heat and less refrigeration is needed.

The other terms may be re-expressed to show the effect of the temperature difference between the inflowing and outflowing streams and of their different pressures and phases.

Temperature difference at warm end of main exchanger

The difference between the enthalpy of air at one atmosphere at the inlet and outlet temperatures, $(H_{Tout} - H_0)$, may be written as:

$$(H_{Tout} - H_0) = c_p(T_{out} - T_{in})$$

where c_p is the average specific heat capacity of air between T_{out} and T_{in}.

Difference in pressure, phase and temperature

In the same way, the difference between the enthalpy of a stream at its actual conditions and at one atmosphere and the outlet temperature of the main exchanger, $(H_{out,j}-H_{Tout,j})$, may be written as:

$$(H_{out,j}-H_{Tout,j}) = c_{p,j}(T_{out,j} - T_{out}) - \Delta H_\phi + \alpha_j(p_{out,j} - p_0)$$

where

$c_{p,j}$ is the average specific heat capacity of the stream between $T_{out,j}$ and T_{out}.

$T_{out,j}$ is the actual temperature of the stream,

T_{out} is the temperature of the streams out of the main exchanger,

ΔH_ϕ is zero if the stream is gaseous or equal to the vaporisation enthalpy if it is liquid,

α_j is the average rate of change of enthalpy with pressure at constant temperature,

$p_{out,j}$ is the actual pressure of the stream,

and p_0 is atmospheric pressure.

Inlet air pressure; Joule-Thompson effect

Finally, to show the refrigeration achieved by the Joule-Thompson effect, the enthalpy of the inlet air, H_{in}, may be written as:

$$H_{in} = H_0 + \alpha(p_{in} - p_0)$$

where p_{in} is the pressure of air entering the cold box.

We may then substitute these expressions into the equation for the turbine power to get:

$$P_{turb} = Q_{in} + P_{bi} + F_{in}(\alpha(p_{in} - p_0) - (c_p(T_{out} - T_{in}) - \Delta H_{mix,Tout})) + \Sigma F_{out,j}(c_{p,j}(T_{out,j} - T_{out}) - \Delta H_{\phi} + \alpha_j(p_{out,j} - p_0)),$$

We must now calculate the heat added by the booster inefficiency and that leaking into the plant.

If the boosted air is not cooled, the heat added by the booster inefficiency, P_{bi} is given by:

$$P_{bi} = (1 - \eta_{b,it})\eta_{mg} P_{turb}$$

where

$\eta_{b,it}$ is the isothermal efficiency of the booster, and

η_{mg} is the combined efficiency of the generator and motor linking the turbine and booster.

Alternatively, if the boosted air is aftercooled so that its temperature is ΔT_b hotter than at the booster inlet, P_{bi} is given by:

$$P_{bi} = F c_p \Delta T_b$$

This is the expression used in the base case in the economic analysis.

The heat leaking into the cold box depends on its size and the thickness and type of insulation used. It may be economically optimised for a particular plant, however expressions given for heat inleak and cold box cost based on actual plants will reflect a general optimum. In this work, Latimer's (1967) expression for Q_{in} is used:

$$\frac{Q_{in}}{(\text{Btu/hr})} = 63{,}000 \left(\frac{F_{in}/(\text{std.cu.ft./hr.})}{1\,000\,000} \right)^{2/3}$$

or, in SI units,

$$\frac{Q_{in}}{(\text{kW})} = 18.48 \left(\frac{F_{in}/(\text{kmol/s})}{0.3327} \right)^{2/3}$$

Because packed plants have taller columns, the economic optimum heat inleak for a particular plant will be different from a trayed plant of the same capacity. In this case, the heat leaking into a packed plant with column height h_{pack} is assumed to be greater than that into a trayed plant by a factor h_{pack}/h_{tray}.

The overall heat balance then becomes:

$$P_{turb} = 18.48 \frac{h_{col}}{h_{tray}} \left(\frac{F_{in}}{0.3327} \right)^{2/3} + F\, c_p\, \Delta T_b$$
$$F_{in}(\alpha(p_{in} - p_0) - (c_p(T_{out} - T_{in}) - \Delta H_{mix,Tout})) +$$
$$\Sigma F_{out,j}(c_{pj}(T_{out,j} - T_{out}) - \Delta H_\phi + \alpha_j(p_{out,j} - p_0)),$$

Or, if all the booster inefficiency enters the cold box:

$$P_{turb}(1 - (1 - \eta_{b,it})\eta_{mg}) = 18.48 \frac{h_{col}}{h_{tray}} \left(\frac{F_{in}}{0.3327} \right)^{2/3} +$$
$$F_{in}(\alpha(p_{in} - p_0) - (c_p(T_{out} - T_{in}) - \Delta H_{mix,Tout})) +$$
$$\Sigma F_{out,j}(c_{pj}(T_{out,j} - T_{out}) - \Delta H_\phi + \alpha_j(p_{out,j} - p_0)),$$

with $F_{in} = F + F_{col}$, the turbine flow plus the flow to the column system (because zero Lachmann air flow is assumed).

Typical values of each term are given in table 3-4 which shows that the most important one is the main exchanger warm end temperature difference. The heat leak, booster inefficiency, Joule-Thompson and liquid terms are all important, but the gaseous product and enthalpy of mixing terms may be neglected.

Relative values of terms in refrigeration calculation	
Turbine Power	100
Air Pressure effect (Joule-Thompson)	-20.5
Booster inefficiency	25
Heat leak	28
Warm end temperature difference	43
Enthalpy of mixing	0
Liquid Products	24
Gaseous Products (pressure effect)	0.5
Total	100

Table 3-4 Comparison of relative sizes of terms in refrigeration calculation

So it is assumed in the economic analysis that all the streams leave the cold box at atmospheric pressure and the same temperature, except the liquid argon. Also, the enthalpy of the liquid argon is assumed to be the same as in the simulation (i.e. slightly lower in the packed plant).

Once the power to be generated by the turbine is known, the flow through it must be calculated by using an equation describing its behaviour. The calculation must be iterative because the refrigeration requirement depends on the turbine flow, which depends on the refrigeration requirement. To simplify the turbine

calculations, the gas in the turbine is assumed to behave ideally. The following expression gives the relationship between the power generated by and the flow through an isentropic turbine

$$P_{turb} = F\,Z\,R\,T_1 \frac{k}{k-1}\left(1-\left(\frac{p_2}{p_1}\right)^{\frac{k-1}{k}}\right)$$

where

P_{turb} is the work done by the turbine,
F is the molar flow of gas,
Z is the gas compressibility factor (=1 for an ideal gas),
R is the universal gas constant,
T_1 is the turbine inlet temperature,
k is the ratio of specific heat at constant pressure to that at constant volume,
p_2 is the turbine outlet pressure and
p_1 is the turbine inlet pressure.

Because the turbine is not isentropic, the isentropic efficiency, η_{ie}, is introduced so that:

$$P_{turb} = \eta_{ie}\,F\,Z\,R\,T_1 \frac{k}{k-1}\left(1-\left(\frac{p_2}{p_1}\right)^{\frac{k-1}{k}}\right)$$

In addition, the turbine outlet, rather than inlet, temperature is fixed. The inlet temperature is given by:

$$T_1 = T_2\left(\frac{p_1}{p_2}\right)^{\frac{k-1}{k}}$$

so

$$P_{turb} = \eta_{ie}\,F\,Z\,R\,T_2 \frac{k}{k-1}\left(\left(\frac{p_1}{p_2}\right)^{\frac{k-1}{k}}-1\right)$$

The turbine flow F may now be calculated by solving the following equation iteratively:

$$\eta_{ie}\,F\,Z\,R\,T_2 \frac{k}{k-1}\left(\left(\frac{p_1}{p_2}\right)^{\frac{k-1}{k}}-1\right)(1-(1-\eta_{b,it})\,\eta_{mg}) =$$
$$18.48\,\frac{h_{col}}{h_{tray}}\left(\frac{F+F_{col}}{0.3327}\right)^{2/3} +$$
$$(F+F_{col})(\,\alpha(p_{in}-p_0)-(c_p(T_{out}-T_{in})-\Delta H_{mix,Tout})) +$$
$$\Sigma\,F_{out,j}\,(c_{p,j}(T_{out,j}-T_{out})-\Delta H_{\phi}+\alpha_j\,(p_{out,j}-p_0)),$$

It is assumed in this work that packed and trayed plants have the same turbine outlet temperature.

This is the method used in the plant design model to calculate the refrigeration requirement and turbine flow. An example spreadsheet calculation is illustrated in lines 133 to 186 of the complete economic calculation in table 3-10.

3.1.2.2 Cost information

To complete the economic analysis, the difference between the capital and operating costs of packed and trayed plants must be calculated.

Operating cost

The only difference in operating cost is assumed to be due to the difference in power consumption. Other running costs, such as labour and cooling water are considered to be the same in each case. Any differences in these other costs will be very small in relation to the power cost saving, especially as the plant size increases and the power cost accounts for more and more of the operating cost.

The cost of power varies widely according to the plant location, from around £10/MWhr to £100/MWhr. The lowest cost power available in the UK is about £30/MWhr (Brown, 1992), so this value has been used for the base case. Higher power costs favour packed plants, so any packed plants built in the UK should show a greater return than the one calculated with this power cost.

The annual power cost saving is then the saving in power consumption multiplied by the power cost and the operational time of the plant per year.

Capital cost

The differences in capital cost are caused by the different sizes of equipment required in each case. The items accounting for most of the capital cost of an air separation plant are the main compressor, the booster compressor and expansion turbine, the heat exchangers, the pre-purification units (PPUs), the column system and the cold box. Table 3-5 shows the approximate proportion of the plant cost attributable to each item.

Of these, the columns, cold box, PPUs and booster compressor and expansion turbine will be larger, and therefore more expensive in a packed plant. The main compressor and heat exchangers will be smaller and cheaper, if the same cycle is used.

The main effect of the change from trays to packing is to increase the cost of the columns and cold box. The example design calculation in table 3-5b shows in line 41 that the height of a packed column is around twice that of a trayed one. The

increased cost of a packed column with its cold box may then be several times the cost of a trayed one. Even if the column and cold box cost is only around 10% of the plant cost, the increased cost of a packed plant would be of the order of 10%.

Small Air Separation Unit, Free on Board.		
	item cost/ £k	% of total
Main Compressor	350	35.0
Expansion Turbine	120	12.0
Heat Exchangers	50	5.0
Cold box	190	19.0
Column	70	7.0
Design	155	15.5
Other (PPUs, piping etc)	65	6.5
Total	1000	100.0
Large Plant, Built on Site		
	item cost/ £k	% of total
Main Compressor and		
Expansion Turbine	12000	40.0
Heat Exchangers	5000	16.7
Cold box	3000	10.0
Column	4000	13.3
Design	1500	5.0
Other (PPUs, piping etc)	4500	15.0
Total	30000	100.0

Table 3-5 Approximate costs of main pieces of equipment in air separation plant

The compressor may account for up to 50% of the plant cost, but if its size is reduced by 10%, the reduction in cost would only be around 5%. In practice, the compressor cost is unlikely to be much smaller in a packed plant, even if its power consumption is reduced by 10%; because of the standardisation of compressor components, both plants would probably use the same sized frame and so the costs would be similar.

The differences in the costs of the other plant components will be a small fraction of their value, and so will also be negligible compared with the difference in column and cold box cost. The combined effect of these other cost differences will also be negligible because some increase the cost and some reduce it.

The only capital costs which need to be considered in the analysis are therefore those of the column (with its internals) and cold box. The column shell and cold box costs were expressed as functions of the column size by fitting suitable equations to some cost estimates produced by BOC in 1988 for various sizes of packed and trayed columns and their associated cold boxes. The cost of trays was found in the same way, whilst that of packings, distributors and collectors was estimated from information from packing manufacturers together with a simple

analysis of the packing manufacturing process. Costs were all updated to mid 1992 using the Process Engineering composite index (Process Engineering, November 1992).

Column Shell Cost Equation							
Column shell cost = 0.38* height ^1.8* diameter ^ 0.9							
Column Height	Column Diameter	Column Shell Cost	Calculated Cost	% Deviation	Absolute % dev.	Deviation	Absolute deviation
m	m	£k	£k			£k	£k
20.4	1.04	130	90	-31.1	31.1	40	40
24	1.16	138	132	-4.0	4.0	6	6
39.8	1.14	239	324	35.6	35.6	-85	85
25.2	4.4	480	480	0.0	0.0	0	0
33.2	5.7	826	996	20.5	20.5	-170	170
53.4	5.04	2126	2097	-1.4	1.4	29	29
				mean	15.4	mean	55

Table 3-6 Column shell cost equation and comparison with data

Cold Box Cost Equation							
Cold Box Cost = 15.83* height ^ 0.85* diameter ^ 0.47							
Column Height	Column Diameter	Cold Box Cost	Calculated Cost	% Deviation	Absolute % dev.	Deviation	Absolute deviation
m	m	£k	£k			£k	£k
20.4	1.04	240	209	-12.8	12.8	31	31
24	1.16	257	253	-1.6	1.6	4	4
39.8	1.14	337	386	14.4	14.4	-49	49
25.2	4.4	500	493	-1.3	1.3	7	7
33.2	5.7	650	704	8.3	8.3	-54	54
53.4	5.04	995	995	0.0	0.0	0	0
				mean	6.4	mean	24

Table 3-7 Cold box cost equation and comparison with data

Tray Cost Equations								
Tray material cost = 148* diameter ^1.8								
Column Diameter	Tray Material Cost	Number of Trays	Material Cost per Tray	Calculated Cost	% Deviation	Absolute % dev.	Deviation	Absolute deviation
m			£	£			£	£
1.16	18800	95	198	193	-2.3	2.3	5	5
5.7	321800	95	3387	3395	0.2	0.2	-8	8
					mean	1.3	mean	6
Tray labour cost = 204 * diameter ^ 1.4								
Column Diameter	Tray Material Cost	Number of Trays	Fabrication Cost per Tray	Calculated Cost	% Deviation	Absolute % dev.	Deviation	Absolute deviation
m			£	£			£	£
1.16	23100	95	243	251	3.3	3.3	-8	8
5.7	229000	95	2411	2333	-3.2	3.2	78	78
					mean	3.3	mean	43

Table 3-8 Tray material and labour cost equations and comparison with data

The GRG2 generalised reduced gradient optimisation programme was used to fit equations to the cost data, and the data and expressions chosen are given in tables 3-6 to 3-8. The expressions used were between those which minimised the absolute deviation and the absolute percentage deviation. Figure 3-2 shows that a constant percentage error in the cost causes a bigger error in the rate of return for larger plants, whilst a fixed error in the cost causes a bigger error in the rate of return in smaller plants. The aim was therefore to ensure that the error in the rate of return was similar for all plant sizes. It is estimated to be around 4%.

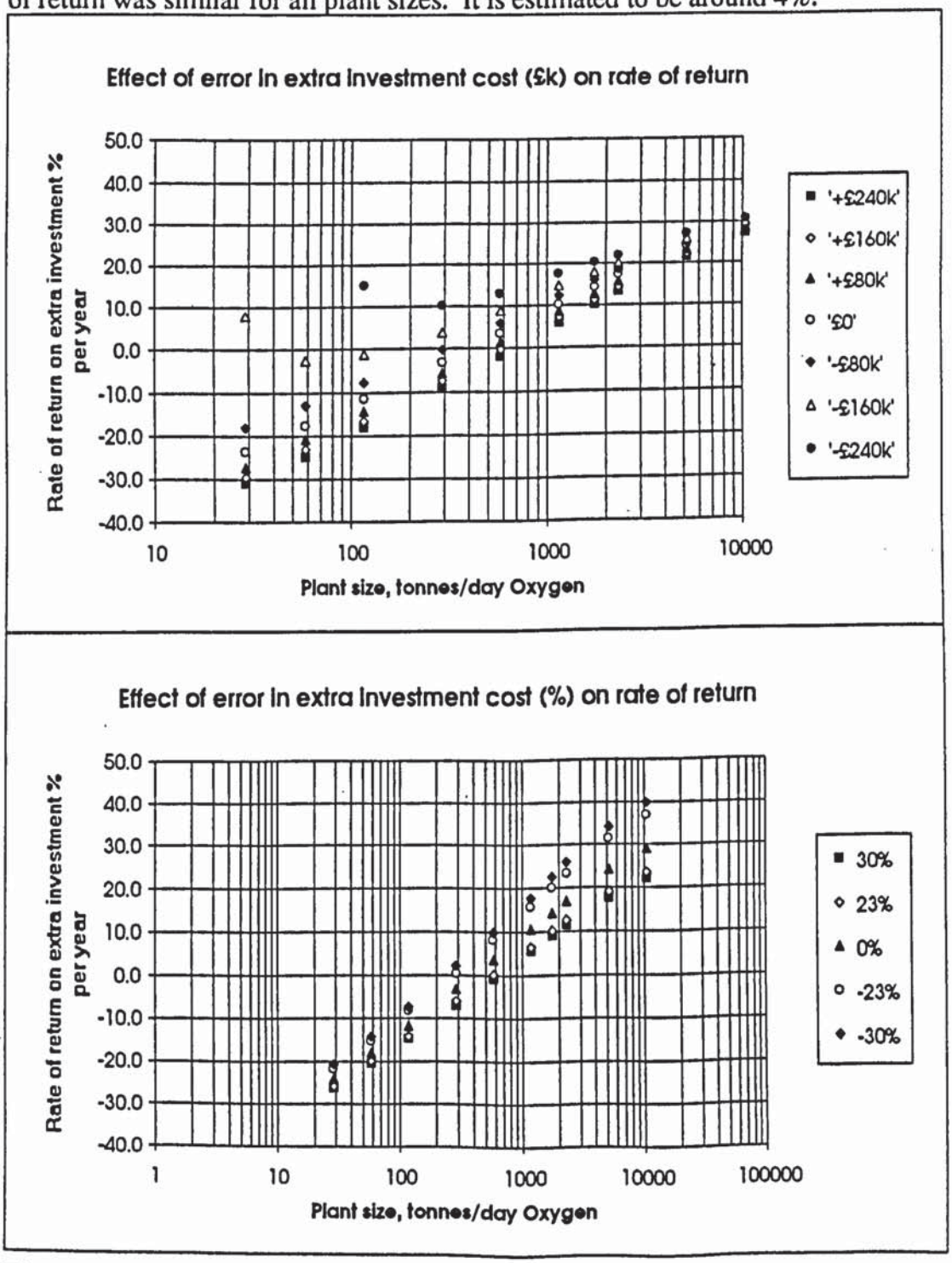

Figure 3-2 Comparison of effect of absolute and percentage error in investment cost on rate of return

The cost of the column shell is approximately proportional to the diameter (d) and the square of the height (h^2). Normally, the cost of a pressure vessel is proportional to its volume, i.e. to $h.d^2$, because the surface area is proportional to h.d and the thickness to d. This suggests that the thickness of an air separation column depends on its height, rather than its diameter. This makes sense because air separation columns operate at a sufficiently low pressure for hoop stresses (which depend on diameter) to be unimportant compared to the stress imposed by the weight of column, which, at a given diameter, depends on the height.

The analysis of cold box cost shows that it is proportional to the square root of diameter and the height. The cold box cost is usually on the basis of surface area, so this would be expected to depend on hd. That the power of d is about 0.5 is probably because there are economies of scale brought about by increasing diameter (for example in the pipework and instrumentation) which are not present with increasing height.

The cost of packed column internals is taken as proportional to diameter rather than its square, because economies of scale are assumed to apply in a similar way to the cold box.

The height and diameter of each type of column must be calculated to get its cost. This is achieved by assuming that both packed and tray columns have the same number of theoretical plates and the same vapour and liquid flows.

The column heights were calculated by assuming a height equivalent to a theoretical plate (tray spacing divided by efficiency in a tray column) and multiplying it by the number of theoretical plates, then adding any extra height required at the top and bottom of the columns or by feed trays, distributors or collectors.

The diameters were calculated for the most heavily loaded section of each column. In the case of the low pressure column, this is the section between the rich liquid liquid feed and the Lachmann air (if present) and rich liquid vapour feeds. A value was assumed for the maximum capacity factor for the trays or packing, and the column designed to operate at a fraction of this value.

For trays, Latimer's (1967) expression for the maximum capacity of sieve trays with 0.9 mm holes and 8% open area was used:

$$\frac{u_{max}}{\text{ft./sec.}} = 0.156 \sqrt{\left(\frac{\rho_l - \rho_g}{\rho_g}\right)\left(\frac{h_t}{4\text{ in.}}\right)}$$

where u_{max} is the superficial vapour velocity and h_t the tray spacing.

In SI units, this becomes:

$$\frac{u_{max}}{m/s} = 0.04755 \sqrt{\left(\frac{\rho_l - \rho_v}{\rho_v}\right)\left(\frac{h_t}{0.1016}\right)}$$

or, in terms of capacity factor, C_s,

$$C_{s,max} = u_{max} \sqrt{\frac{\rho_v}{\rho_l - \rho_v}} = 0.04755 \sqrt{\left(\frac{h_t}{0.1016}\right)}$$

A tray spacing of 4" or 0.1 m was used in this work, since it is the minimum normally used. This ensures that, particularly in large plants where the tray spacing is usually greater, the advantage due to the packing is a worst-case estimate.

In the case of packings, experimental data was used for $C_{s,max}$ and adjusted to account for differences in flow parameter, X, with the correlation of $C_{s,max}$ against X, given by Sulzer (1992), which is approximated to $C_{s,max} \propto X^{-0.38}$ for the range of flow parameters in an air separation plant.

The column diameter is then calculated from the total molar vapour flow in the column $V_{tot,mol}$, which is assumed to be a constant proportion of the flow to the column system and was determined from the plant simulation.

$$d = \frac{4}{\pi} \sqrt{\frac{(V_{tot,mol})\, M_r}{\phi\, (C_{s,max}) \sqrt{\rho_v\, (\rho_l - \rho_v)}}}$$

with ϕ equal to the fraction of maximum capacity at the design point.

3.1.2.3 Rate of return as a measure of the advantage of a packed plant

Because capital cost and running cost are expressed in different units (i.e. £ and £/year) and the value of money varies with time, some way of relating them must be established. The method used in this case is to calculate the interest rate which would be received over the plant lifetime on the extra capital invested in a packed plant, assuming the amount repaid each year is the cost of the power saved. This interest rate is the rate of return on the extra investment necessary in a packed plant. If a higher rate could be obtained by investing the money elsewhere at an equivalent risk, a packed plant should not be built instead of a trayed one. Whether this is the case will depend on the economic conditions over the plant lifetime, and particularly on the inflation rate.

The rate of return calculated is known as the discounted cash flow rate of return and is defined such that the net present value of the investment is zero. This means that if the inflation rate is equal to the rate of return, the capital will be repaid with a sum whose value in current money (its present value) is the same as the sum invested now.

An example of the meaning and calculation of the rate of return is given in table 3-9. This shows two equivalent calculation methods; a consideration of parallel debt and investment and a cash flow table over the lifetime of the plant, assumed to be 10 years. At the end of year -1 (i.e the beginning of year zero, one year before

the plant starts production), an extra capital sum of £5 000 000 is borrowed to cover the extra cost of the packed plant.

1. Parallel debt and investment							
Interest rate 21.1239							
End of year	Sum borrowed	Interest due	Value of debt	Income Invested	Interest received	Value of investment	Difference in value of investments and debt
-1	5000000	0	5000000	0	0	0	-5000000
0		1056195	6056195	0	0	0	-6056195
1		1279305	7335500	1500000	0	1500000	-5835500
2		1549544	8885044	1500000	316859	3316859	-5568186
3		1876868	10761913	1500000	700650	5517509	-5244404
4		2273336	13035249	1500000	1165513	8183022	-4852227
5		2753554	15788802	1500000	1728574	11411596	-4377207
6		3335212	19124014	1500000	2410575	15322170	-3801844
7		4039739	23163753	1500000	3236641	20058811	-3104942
8		4893089	28056842	1500000	4237204	25796015	-2260826
9		5926701	33983542	1500000	5449126	32745141	-1238401
10		7178651	41162194	1500000	6917053	41162194	0
2. Cumulative Cash Flow							
Interest rate 21.1239							
End of year	Sum borrowed	Interest due		Income	Net Income (cash flow)		Outstanding debt (cumulative cash flow)
-1	5000000	0		0	-5000000		-5000000
0		1056195		0	-1056195		-6056195
1		1279305		1500000	220695		-5835500
2		1232686		1500000	267314		-5568186
3		1176218		1500000	323782		-5244404
4		1107823		1500000	392177		-4852227
5		1024980		1500000	475020		-4377207
6		924637		1500000	575363		-3801844
7		803098		1500000	696902		-3104942
8		655885		1500000	844115		-2260826
9		477575		1500000	1022425		-1238401
10		261599		1500000	1238401		0

Table 3-9 Two methods of calculating the rate of return

The parallel investment method calculates the value of this investment at the end of the plant lifetime with an assumed interest rate. To cover the repayment of the capital with this accumulated interest, the annual power saving of £1 500 000 is invested at the end of each year, at the same rate. At the end of the tenth year the value of the capital investment and the power cost savings must be equivalent. The interest rate for which this is the case is found by iterative calculation.

The cash flow method assumes that the £1 500 000 power saving is received at the end of each year partly as a payment of interest on the outstanding capital and

partly as a repayment of capital. At the end of the plant's life, all the capital and interest due must be repaid, that is the cumulative cash flow must be zero. Again, the interest rate is found by trial, and is equivalent to the one found by considering parallel investments.

The rate of return is a useful measure of the advantage of one packed plant compared to another. Because it is rather sensitive to the timing of the initial investment, it is not quite such a good measure of the absolute advantage of a packed plant over a trayed one. It is however the best simple indicator of this advantage since it removes the rate of inflation from the calculations.

	A	B	C	D	E	F	G	H
1					Low Pressure column			Argon Column
2	Number of theoretical plates				60	0		50
3	HETP			m	0.2			=E3
4	Packing % flood			%	80			=E4
5	Packing pressure gradient			hPa/m	3			=E5
6	Packing maximum capacity			m/s	0.065			=E6
7	Distributor Height			m	2			=E7
8	Number of distributors				5			2
9								
10	Packing cost per unit volume			£/m^3	3940			=E10
11	Distributor cost per diameter			£/m	10000			=E11
12	Power cost			£/MWhr			30	
13								
14								
15		O2 production / tonnes/day			='QACD-1.XLS'!$D$3	='QACD-1.XLS'!$G$3	='QACD-1.XLS'!$J$3	='QACD-1.XLS'!$M$3
16	Rate of return on extra investment / %				='QACD-1.XLS'!$D$203	='QACD-1.XLS'!$G$203	='QACD-1.XLS'!$J$203	='QACD-1.XLS'!$M$203

Table 3-10a Input/Output part of spreadsheet calculation. Spreadsheet name QACDIO-1.XLS

	A	B	C	D
1	Air Separation Plant Design. Base Case. Fixed booster aftercool temperature			
2	Air flow into column system	kmol/s	18	18
3	Oxygen Production	t/day	=C2*0.21*31.999/1000*3600*24	=D2*0.21*31.999/1000*3600*24
4				
5	LP Column Design		trays	SP
6				
7	Relative Molecular Mass of Air	kg/kmol	28.8	28.8
8	Vapour Density in LP column	kg/m^3	6.6	6.6
9	Liquid density in LP column	kg/m^3	1650	1650
10	Reflux ratio in LPC, L/V		0.9	0.9
11	Number of theoretical plates		='QACDIO-1.XLS'!$E$2	=C11
12	HETP of packing	m		='QACDIO-1.XLS'!$E$3
13	Tray spacing	m	0.12	
14	Tray efficiency	%	80	
15	Percent flood	%	70	='QACDIO-1.XLS'!$E$4
16	Number of actual trays		=C11*100/C14	
17	Total pressure drop per actual tray	hPa	4	
18	Dynamic pressure drop per metre	hPa		='QACDIO-1.XLS'!$E$5
19	Total Reflux flow parameter, Xinf		=SQRT(C8/C9)	=SQRT(D8/D9)
20	Actual flow parameter, Xact		=C10*C19	=D10*D19
21	Capacity factor at flood, Cs,max	m/s	=0.0475*SQRT(C13/0.1016)	='QACDIO-1.XLS'!$E$6
22	F factor at flood, Fs,max	Pa^1/2	=C21*SQRT(C9-C8)	=D21*SQRT(D9-D8)
23	Vapour velocity at flood, Uv,max	m/s	=C21*SQRT((C9-C8)/C8)	=D21*SQRT((D9-D8)/D8)
24	Molar vapour flow at flood, Vmax	kmol/m^2/s	=C23*C8/C7	=D23*D8/D7
25	Design vapour velocity, Uv%fl	m/s	=C15/100*C23	=D15/100*D23
26	Design Vapour flow, V%fl	kmol/m^2/s	=C24*C15/100	=D24*D15/100

27	Total vapour molar flow, Vcol	kmol/s	=C2*0.788	=D2*0.788
28	Tray bubbling area, Abub	m^2	=C27/C26	
29	Column area, Acol	m^2	=C28*1.1	=D27/D26
30	Column diameter, Dcol	m	=SQRT(4/3.1415927*C29)	=SQRT(4/3.1415927*D29)
31				
32	Packed/trayed height, Hint	m	=C16*C13	=D11*D12
33				
34	Column static pressure drop	hPa	=C8*9.81*C41/100	=D8*9.81*D41/100
35	Column dynamic pressure drop	hPa	=C16*C17-C34	=D32*D18
36	Column total pressure drop	hPa	=C35+C34	=D35+D34
37				
38	Feed tray/Distributor height, Hdist	m	0.45	='QACDIO-1.XLS'!$E$7
39	Number of feed trays/distributors, Ndist		4	='QACDIO-1.XLS'!$E$8
40				
41	Low pressure column height, HLPC	m	=C32+C38*C39+4	=D32+D38*D39+4
42	High pressure column height, HHPC	m	=12	=12
43	Reboiler/condenser height, HRBC	m	2	2
44	Total column height, Hcol	m	=C42+C43+C41	=D42+D43+D41
45	********** ********** *****			
46	LP Column costing		Trays	SP
47	Cost escalation factor since mid 1988		=118/87	=118/87
48	Column Shell cost	£	=C47*380*C44^1.8*C30^0.9	=D47*380*D44^1.8*D30^0.9
49	Tray fabrication cost	£	=C47*C16*204*C30^1.4	
50	Tray Materiel cost	£	=C47*C16*148*C30^1.8	
51	Distributor/support cost per diameter	£/m		='QACDIO-1.XLS'!$E$11
52	Total Distributor/ Support cost	£		=D51*D39*D30
53	Packing cost per unit volume	£/m^3		='QACDIO-1.XLS'!$E$10

54	Total Packing cost	£		=D53*D29*D32
55				
56	Total column cost	£	=C48+C49+C50	=D54+D52+D48
57	Cold box cost	£	=C47*15830*C30^0.47*C44^0.85	=D47*15830*D30^0.47*D44^0.85
58	Total cost	£	=C57+C56	=D57+D56
59	********** ********** *****			
60	Argon Column Design		trays	SP
61				
62	Relative Molecular Mass in Ar column	kg/kmol	36	36
63	Vapour Density in Ar column	kg/m^3	6.7	6.7
64	Liquid density in Ar column	kg/m^3	1900	1900
65	Reflux ratio in ArC, L/V		0.975	0.975
66	Number of theoretical plates		='QACDIO-1.XLS'!$H$2	=C66
67	HETP of packing	m		='QACDIO-1.XLS'!$H$3
68	Tray spacing	m	0.12	
69	Tray efficiency	%	80	
70	Percent flood	%	70	='QACDIO-1.XLS'!$H$4
71	Number of actual trays		=C66*100/C69	
72	Dynamic+static pressure drop per actual tray	hPa	4	
73	Dynamic pressure drop per metre	hPa		='QACDIO-1.XLS'!$H$5
74	Total Reflux flow parameter, Xinf		=SQRT(C63/C64)	=SQRT(D63/D64)
75	Actual flow parameter, Xact		=C65*C74	=D65*D74
76	Capacity factor at flood, Cs,max	m/s	=0.0475*SQRT(C68/0.1016)	='QACDIO-1.XLS'!$H$6
77	F factor at flood, Fs,max	Pa^1/2	=C76*SQRT(C64-C63)	=D76*SQRT(D64-D63)
78	Vapour velocity at flood, Uv,max	m/s	=C76*SQRT((C64-C63)/C63)	=D76*SQRT((D64-D63)/D63)
79	Molar vapour flow at flood, Vmax	kmol/m^2/s	=C78*C63/C62	=D78*D63/D62
80	Design vapour velocity, Uv%fl	m/s	=C70/100*C78	=D70/100*D78
81	Design Vapour flow, V%fl	kmol/m^2/s	=C79*C70/100	=D79*D70/100

82	Total vapour molar flow, Vcol	kmol/s	=C2*0.17	=D2*0.17
83	Tray bubbling area, Abub	m^2	=C82/C81	
84	Column area, Acol	m^2	=C83*1.1	=D82/D81
85	Column diameter, Dcol	m	=SQRT(4/3.1415927*C84)	=SQRT(4/3.1415927*D84)
86				
87	Packed/trayed height, Hint	m	=C71*C68	=D66*D67
88				
89	Column static pressure drop	hPa	=C63*9.81*C96/100	=D63*9.81*D96/100
90	Column dynamic pressure drop	hPa	=C71*C72-C89	=D87*D73
91	Column total pressure drop	hPa	=C90+C89	=D90+D89
92				
93	Feed tray/Distributor height, Hdist	m	0.45	='QACDIO-1.XLS'!$H$7
94	Number of feed trays/distributors, Ndist		0	='QACDIO-1.XLS'!$H$8
95				
96	Argon column height HArC	m	=C87+C93*C94+4	=D87+D93*D94+4
97				
98	Condenser height, HACon	m	2	2
99	Total column height, Hcol	m	=C98+C96	=D98+D96
100				
101	Argon Column costing		Trays	SP
102	Cost escalation factor since mid 1988		=118/87	=118/87
103	Column Shell cost	£	=C102*380*C99^1.8*C85^0.9	=D102*380*D99^1.8*D85^0.9
104	Tray fabrication cost	£	=C102*C71*204*C85^1.4	
105	Tray Materiel cost	£	=C102*C71*148*C85^1.8	
106	Distributor/support cost per diameter	£/m		='QACDIO-1.XLS'!$H$11
107	Total Distributor/ Support cost	£		=D106*D94*D85
108	Packing cost per unit volume	£/m^3		='QACDIO-1.XLS'!$H$10
109	Total Packing cost	£		=D108*D84*D87
110				
111	Total column cost	£	=C103+C104+C105	=D109+D107+D103

112	Extra Cold box cost	£	=C102*1/2*15830*C85^0.47*C99^0.85	=D102*1/2*15830*D85^0.47*D99^0.85
113	Total cost	£	=C112+C111	=D112+D111
114	********** ********** *****			
115	Total LPC,HPC & ArC & cold box cost	£	=C113+C58	=D113+D58
116	********** ********** *****			
117	Atmospheric Pressure	bar	1.013	1.013
118	dP from LP column to atmosphere	bar	0.28	0.28
119	dP across LP column	bar	=C36/1000	=D36/1000
120	Pressure of boiling liquid oxygen	bar	=(C117+C118+C119)	=(D117+D118+D119)
121	Temperature of boiling liquid oxygen	K	=734.55/(15.4075-LN(C120*1000/1.332))+6.45	=734.55/(15.4075-LN(D120*1000/1.332))+6.45
122	dT across reboiler-condenser	K	1.5	1.5
123	Temperature of condensing nitrogen	K	=(C121+C122)	=(D122+D121)
124	Pressure of condensing nitrogen	bar	=EXP(14.9542-(588.72/(C123-6.6)))*1.332/1000	=EXP(14.9542-(588.72/(D123-6.6)))*1.332/1000
125	dP across HP column	bar	0.13	0.13
126	dP from compressor to HP column	bar	0.43	0.43
127	Compressor pressure	bar	=(C124+C125+C126)	=(D124+D125+D126)
128				
129	Power to compress air to column	kW	=1/0.8*8.3144*C157*C2*LN(C127/C117)	=1/0.8*8.3144*D157*D2*LN(D127/D117)
130	Relative Power to trayed column		=C129/C129	=D129/C129
131	Potential power saving of SP over trays	%	=(C130-C130)*100	=(C130-D130)*100
132				
133	Refrigeration calculation			
134	Enthalpy of mixing	kJ/kmol	0	0

135	Enthalpy of mixing effect	kW	=C158*C134	=D158*D134
136	Rate of change of enthalpy with pressure	kJ/kmol/bar	-6.49	-6.49
137	Pressure effect	kW	=C158*C136*(C161-1.013)	=D158*D136*(D161-1.013)
138	Warm end Temperature difference	K	2.5	2.5
139	Heat capacity of feed air	kJ/kmol/K	29.15	29.15
140	Delta T loss	kW	=C158*C138*C139	=D158*D138*D139
141	Heat inleak	kW	=18.48*(C158/0.3327)^(2/3)	=D44/C44*18.48*(D158/0.3327)^(2/3)
142	Boosted Air Temperature rise	K	5	5
143	Booster compressor inefficiency	kW	=C182*C139*C142	=D182*D139*D142
144	Argon gas - liquid enthalpy	kJ/kmol	12638	12687
145	Power removed by liquid	kW	=C144*(1-C65)*C82	=D144*(1-D65)*D82
146	Refrigeration required	kW	=C145+C143+C141+C140+C137+C135	=D145+D143+D141+D140+D137+D135
147				
148	For air boost cycle:			
149	Power to compress air to plant	kW	=C160+C177	=D160+D177
150	Relative Power to trayed column		=C149/C149	=D149/C149
151	Actual power saving of SP over trays	%	=(C150-C150)*100	=(C150-D150)*100
152				
153	Main Compressor (near isothermal)			
154	Motor efficiency		0.95	0.95
155	Isothermal efficiency		0.8	0.8
156	Inlet Pressure	bar	1.013	1.013
157	Inlet Temperature	K	300	300
158	Flow	kmol/s	=C2+C169	=D2+D169
159	Ratio of specific heats, k		1.4	1.4
160	Power consumption of motor	kW	=1/C155/C154*C158*8.3144*C157*LN(C161/C156)	=1/D155/D154*D158*8.3144*D157*LN(D161/D156)
161	Outlet Pressure	bar	=C127	=D127

162	Outlet Temperature after cooling	K	300	300
163	Relative Power consumption		=C160/C160	=D160/C160
164				
165	Expansion Turbine (near Isentropic)			
166	Isentropic efficiency		0.85	0.85
167	Inlet Pressure	bar	=C185	=D185
168	Inlet Temperature	K	=(C167/C172)^((C170-1)/C170)*C173	=(D167/D172)^((D170-1)/D170)*D173
169	Flow	kmol/s	=C171/(C166*(8.3144*C168)*C170/(C170-1)*((C172/C167)^((C170-1)/C170)-1))	=D171/(D166*(8.3144*D168)*D170/(D170-1)*((D172/D167)^((D170-1)/D170)-1))
170	Ratio of specific heats, k		1.4	1.4
171	Power Removed From Air	kW	=-C146	=-D146
172	Outlet Pressure	bar	=C117+C118	=D117+D118
173	Outlet Temperature (fixed)	K	100	100
174				
175	Air booster compressor (near isothermal)			
176	Power output of motor driven by Turbine	kW	=-C178*C171	=-D178*D171
177	Extra Power Supplied to motor	kW	=C184-C176	=(D184-D176)/D178
178	Motor efficiency		0.95	0.95
179	Isothermal efficiency		0.7	0.7
180	Inlet Pressure	bar	=C161	=D161
181	Inlet Temperature	K	300	300
182	Flow	kmol/s	=C169	=D169
183	Ratio of specific heats, k		1.4	1.4
184	Power output of motor	kW	=-C178*C171	=-D178*D171
185	Outlet Pressure	bar	=C180*EXP(C184/C182/8.3144/C181*C179)	=D180*EXP(D184/D182/8.3144/D181*D179)
186	Outlet Temperature after cooling	K	=C181+C142	=D181+D142
187				

188	********** ********** *****			
189	Power costs:			
190	Cost of electricity	£/MWhr	='QACDIO-1.XLS'!$G$12	=C190
191	Operating days per year		350	350
192	Operating hours/year		=C191*24	=D191*24
193	Plant Power consumption	MW	=C149/1000	=D149/1000
194	Annual Power cost	£	=C192*C193*C190	=D192*D193*D190
195	********** ********** *****			
196	Annual Power Saving	£		=C194-D194
197				
198	Tray total column and cold box cost	£	=C115	
199	SP total column and cold box cost	£		=D115
200				
201	Extra capital cost of SP over trays	£		=D199-C198
202				
203	Rate of return on extra investment	%		=100*RATE(10,D196,-D201*(1+D204/100),0,0,D196/D201*20)
204				=D203

Table 3-10b Complete economic calculation. Formulas displayed, spreadsheet name QACD-1.XLS

	A	B	C	D
1	Air Separation Plant Design. Base Case. Fixed booster aftercool temperature			
2	Air flow into column system	kmol/s	18	18
3	Oxygen Production	t/day	10450.62	10450.62
4				
5	LP Column Design		trays	SP
6				
7	Relative Molecular Mass of Air	kg/kmol	28.8	28.8

8	Vapour Density in LP column	kg/m^3	6.6	6.6
9	Liquid density in LP column	kg/m^3	1650	1650
10	Reflux ratio in LPC, L/V		0.9	0.9
11	Number of theoretical plates		60	60
12	HETP of packing	m		0.2
13	Tray spacing	m	0.12	
14	Tray efficiency	%	80	
15	Percent flood	%	70	80
16	Number of actual trays		75	
17	Total pressure drop per actual tray	hPa	4	
18	Dynamic pressure drop per metre	hPa		3
19	Total Reflux flow parameter, Xinf		0.063246	0.063246
20	Actual flow parameter, Xact		0.056921	0.056921
21	Capacity factor at flood, Cs,max	m/s	0.051622	0.065
22	F factor at flood, Fs,max	Pa^1/2	2.09271	2.635027
23	Vapour velocity at flood, Uv,max	m/s	0.814586	1.025683
24	Molar vapour flow at flood, Vmax	kmol/m^2/s	0.186676	0.235052
25	Design vapour velocity, Uv%fl	m/s	0.57021	0.820546
26	Design Vapour flow, V%fl	kmol/m^2/s	0.130673	0.188042
27	Total vapour molar flow, Vcol	kmol/s	14.184	14.184
28	Tray bubbling area, Abub	m^2	108.5456	
29	Column area, Acol	m^2	119.4001	75.43003
30	Column diameter, Dcol	m	12.32984	9.800025
31				
32	Packed/trayed height, Hint	m	9	12
33				
34	Column static pressure drop	hPa	9.582408	16.83396
35	Column dynamic pressure drop	hPa	290.4176	36
36	Column total pressure drop	hPa	300	52.83396
37				

38	Feed tray/Distributor height, Hdist	m	0.45	2
39	Number of feed trays/distributors, Ndist		4	5
40				
41	Low pressure column height, HLPC	m	14.8	26
42	High pressure column height, HHPC	m	12	12
43	Reboiler/condenser height, HRBC	m	2	2
44	Total column height, Hcol	m	28.8	40
45	********** ********** *****			
46	LP Column costing		Trays	SP
47	Cost escalation factor since mid 1988		1.356322	1.356322
48	Column Shell cost	£	2093701	3075805
49	Tray fabrication cost	£	698867.2	
50	Tray Materiel cost	£	1384871	
51	Distributor/support cost per diameter	£/m		10000
52	Total Distributor/ Support cost	£		490001.3
53	Packing cost per unit volume	£/m^3		3940
54	Total Packing cost	£		3566332
55				
56	Total column cost	£	4177438	7132138
57	Cold box cost	£	1216403	1443682
58	Total cost	£	5393841	8575820
59	********** ********** *****			
60	Argon Column Design		trays	SP
61				
62	Relative Molecular Mass in Ar column	kg/kmol	36	36
63	Vapour Density in Ar column	kg/m^3	6.7	6.7
64	Liquid density in Ar column	kg/m^3	1900	1900

65	Reflux ratio in ArC, L/V		0.975	0.975
66	Number of theoretical plates		50	50
67	HETP of packing	m		0.2
68	Tray spacing	m	0.12	
69	Tray efficiency	%	80	
70	Percent flood	%	70	80
71	Number of actual trays		62.5	
72	Dynamic+static pressure drop per actual tray	hPa	4	
73	Dynamic pressure drop per metre	hPa		3
74	Total Reflux flow parameter, Xinf		0.059383	0.059383
75	Actual flow parameter, Xact		0.057898	0.057898
76	Capacity factor at flood, Cs,max	m/s	0.051622	0.065
77	F factor at flood, Fs,max	Pa^1/2	2.246193	2.828284
78	Vapour velocity at flood, Uv,max	m/s	0.86778	1.092662
79	Molar vapour flow at flood, Vmax	kmol/m^2/s	0.161504	0.203356
80	Design vapour velocity, Uv%fl	m/s	0.607446	0.874129
81	Design Vapour flow, V%fl	kmol/m^2/s	0.113052	0.162685
82	Total vapour molar flow, Vcol	kmol/s	3.06	3.06
83	Tray bubbling area, Abub	m^2	27.06708	
84	Column area, Acol	m^2	29.77379	18.80934
85	Column diameter, Dcol	m	6.157042	4.89375
86				
87	Packed/trayed height, Hint	m	7.5	10
88				
89	Column static pressure drop	hPa	7.558605	11.83086
90	Column dynamic pressure drop	hPa	242.4414	30
91	Column total pressure drop	hPa	250	41.83086
92				
93	Feed tray/Distributor height, Hdist	m	0.45	2
94	Number of feed trays/distributors, Ndist		0	2

95				
96	Argon column height HArC	m	11.5	18
97				
98	Condenser height, HACon	m	2	2
99	Total column height, Hcol	m	13.5	20
100				
101	Argon Column costing		Trays	SP
102	Cost escalation factor since mid 1988		1.356322	1.356322
103	Column Shell cost	£	286537.9	472800.5
104	Tray fabrication cost	£	220289.5	
105	Tray Materiel cost	£	330654.4	
106	Distributor/support cost per diameter	£/m		10000
107	Total Distributor/ Support cost	£		97875
108	Packing cost per unit volume	£/m^3		3940
109	Total Packing cost	£		741087.8
110				
111	Total column cost	£	837481.8	1311763
112	Extra Cold box cost	£	230463.6	288948.7
113	Total cost	£	1067945	1600712
114	********** ********** *****			
115	Total LPC,HPC & ArC & cold box cost	£	6461786	10176532
116	********** ********** *****			
117	Atmospheric Pressure	bar	1.013	1.013
118	dP from LP column to atmosphere	bar	0.28	0.28
119	dP across LP column	bar	0.3	0.052834
120	Pressure of boiling liquid oxygen	bar	1.593	1.345834
121	Temperature of boiling liquid oxygen	K	94.72869	92.97542

122	dT across reboiler-condenser	K	1.5	1.5
123	Temperature of condensing nitrogen	K	96.22869	94.47542
124	Pressure of condensing nitrogen	bar	5.839786	5.122498
125	dP across HP column	bar	0.13	0.13
126	dP from compressor to HP column	bar	0.43	0.43
127	Compressor pressure	bar	6.399786	5.682498
128				
129	Power to compress air to column	kW	103452.8	96781.31
130	Relative Power to trayed column		1	0.935512
131	Potential power saving of SP over trays	%	0	6.448788
132				
133	Refrigeration calculation			
134	Enthalpy of mixing	kJ/kmol	0	0
135	Enthalpy of mixing effect	kW	0	0
136	Rate of change of enthalpy with pressure	kJ/kmol/bar	-6.49	-6.49
137	Pressure effect	kW	-664.081	-583.359
138	Warm end Temperature difference	K	2.5	2.5
139	Heat capacity of feed air	kJ/kmol/K	29.15	29.15
140	Delta T loss	kW	1384.285	1402.813
141	Heat inleak	kW	274.0089	383.9563
142	Boosted Air Temperature rise	K	5	5
143	Booster compressor inefficiency	kW	145.0701	182.1267
144	Argon gas - liquid enthalpy	kJ/kmol	12638	12687
145	Power removed by liquid	kW	966.807	970.5555
146	Refrigeration required	kW	2106.09	2356.092
147				
148	For air boost cycle:			

149	Power to compress air to plant	kW	114919.3	108947.4
150	Relative Power to trayed column		1	0.948034
151	Actual power saving of SP over trays	%	0	5.196631
152				
153	Main Compressor (near isothermal)			
154	Motor efficiency		0.95	0.95
155	Isothermal efficiency		0.8	0.8
156	Inlet Pressure	bar	1.013	1.013
157	Inlet Temperature	K	300	300
158	Flow	kmol/s	18.99534	19.24958
159	Ratio of specific heats, k		1.4	1.4
160	Power consumption of motor	kW	114919.3	108947.4
161	Outlet Pressure	bar	6.399786	5.682498
162	Outlet Temperature after cooling	K	300	300
163	Relative Power consumption		1	0.948034
164				
165	Expansion Turbine (near Isentropic)			
166	Isentropic efficiency		0.85	0.85
167	Inlet Pressure	bar	11.25026	9.394054
168	Inlet Temperature	K	185.544	176.2271
169	Flow	kmol/s	0.995335	1.249583
170	Ratio of specific heats, k		1.4	1.4
171	Power Removed From Air	kW	-2106.09	-2356.09
172	Outlet Pressure	bar	1.293	1.293
173	Outlet Temperature (fixed)	K	100	100
174				
175	Air booster compressor (near isothermal)			
176	Power output of motor driven by Turbine	kW	2000.785	2238.288
177	Extra Power Supplied to motor	kW	0	4.99E-08

178	Motor efficiency		0.95	0.95
179	Isothermal efficiency		0.7	0.7
180	Inlet Pressure	bar	6.399786	5.682498
181	Inlet Temperature	K	300	300
182	Flow	kmol/s	0.995335	1.249583
183	Ratio of specific heats, k		1.4	1.4
184	Power output of motor	kW	2000.785	2238.288
185	Outlet Pressure	bar	11.25026	9.394054
186	Outlet Temperature after cooling	K	305	305
187				
188	********** ********** *****			
189	Power costs:			
190	Cost of electricity	£/MWhr	30	30
191	Operating days per year		350	350
192	Operating hours/year		8400	8400
193	Plant Power consumption	MW	114.9193	108.9474
194	Annual Power cost	£	28959662	27454735
195	********** ********** *****			
196	Annual Power Saving	£		1504927
197				
198	Tray total column and cold box cost	£	6461786	
199	SP total column and cold box cost	£		10176532
200				
201	Extra capital cost of SP over trays	£		3714745
202				
203	Rate of return on extra investment	%		28.94571
204				28.94571

Table 3-10c Complete economic calculation for 10000t/d plant. Results displayed, spreadsheet name QACD-1.XLS

3.1.3 Results of analysis

In the analysis, the base case shown in the example calculation in table 3-10 was used. All the changes in variables were made around this. Because of the importance of the size of the plant in determining the rate of return, a range of plant

sizes from about 30 to 10000 tonnes per day of oxygen was examined for each change of variable. The complexity of the plant design means that a large number of variables affects the results of the economic analysis. These variables may be divided into three groups: Economic, packing and plant variables. The effects of changing the important variables in each of these groups will now be presented.

3.1.3.1 Effects of economic variables

The economic variables directly affecting the rate of return are the cost of power and the cost of the columns, cold box, trays and packing. Prevailing interest rates and taxes do not affect the rate of return, but must be accounted for when interpreting its significance.

Power cost

The power cost in the base case was £30 / MWhr, which is towards the lower limit. Figure 3-3 shows a plot of rate of return against plant size for different power costs. As the power cost increases, the minimum viable plant size is reduced. If power is very cheap (£10 per MWhr), it is unlikely that a packed plant would be worthwhile under the current analysis, since the return is only around 5%, even for a very large plant. But other factors, such as the feasibility of building a very large plant, may favour a packed plant. Very high power costs (£100 per MWhr) can lead to a very high rate of return (more than 50%) on large packed plants, although plants smaller than around 100 tonnes per day are still more economic with trays.

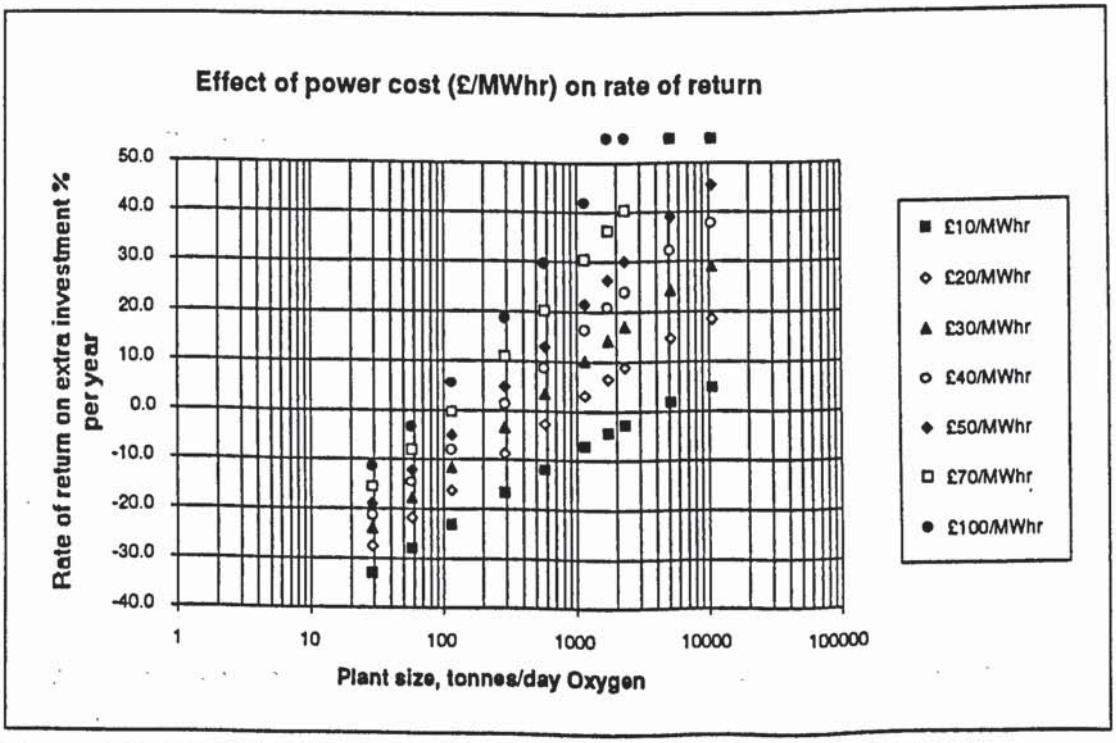

Figure 3-3 Effect of power cost on rate of return for different plant sizes

Material and labour costs - inflation

The material and labour costs are determined by the design of the equipment, but also by the current cost index in relation to that when the original estimates were prepared. Because the analysis depends only on the relative costs of power and capital equipment, varying the power cost is sufficient to show the effect of a difference in the balance between the two. For example, if the inflation rate is the same for power and construction costs, the rate of return will remain the same. If, however, the analysis is done for a future plant when power costs have increased more slowly than construction costs, the rate of return will be the same as assuming a suitably lower current power cost with the current construction costs.

Cost of capital (interest rates)

Interest rates do not enter the analysis directly, but must be considered in evaluating the results. They will set the lowest acceptable rate of return on the extra investment, and so will determine the smallest viable plant size. Figure 3-4 shows the minimum viable plant size for different acceptable rates of return for the base case.

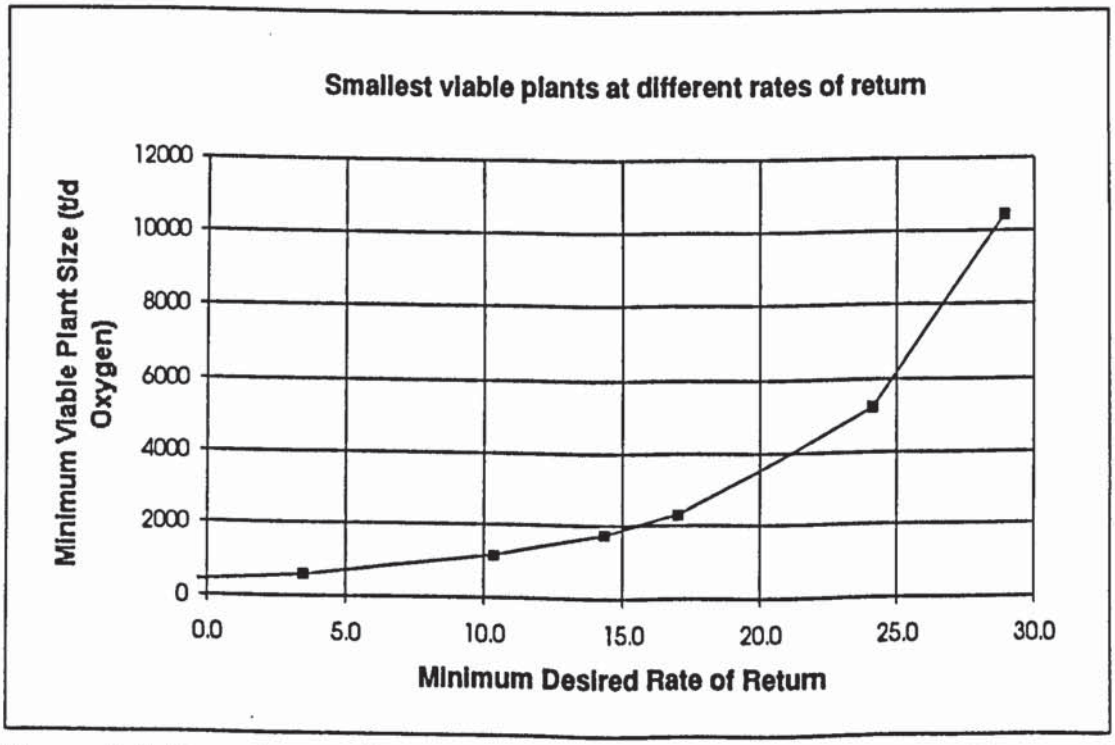

Figure 3-4 Dependence of smallest viable plant on minimum acceptable rate of return

3.1.3.2 Effects of packing variables

It is important when developing a new packing to know the effects of changing the different aspects of packing performance. The ones which can give the biggest increase in return can then be targetted for improvement. Each variable will now be

considered in turn. The percentage change in the variables which cause a 1% change in the rate of return are summarised in table 3-11

% change in base case value which increases rate of return by 1%				
Plant size, t/d Oxygen	10451	1742	290	29
Packing cost	-3.5	-6.6	-25.4	-169.0
Pressure gradient	-20.3	-25.3	-32.7	-30.6
Maximum capacity	2.0	2.8	4.5	8.2
HETP	-1.6	-2.0	-3.0	-3.7
Distributor cost	-23.8	-22.4	-33.3	-65.4
Distributor height	-5.8	-4.3	-4.6	-4.9
% change in base case value which has the same effect as a 1% increase in HETP				
Plant size, t/d Oxygen	10451	1742	290	29
Packing cost	2.3	3.3	8.6	46.3
Pressure gradient	13.1	12.7	11.1	8.4
Maximum capacity	-1.3	-1.4	-1.5	-2.2
HETP	1.0	1.0	1.0	1.0
Distributor cost	15.4	11.2	11.3	17.9
Distributor height	3.7	2.2	1.5	1.4

Table 3-11 Comparison of effects of each packing variable on rate of return

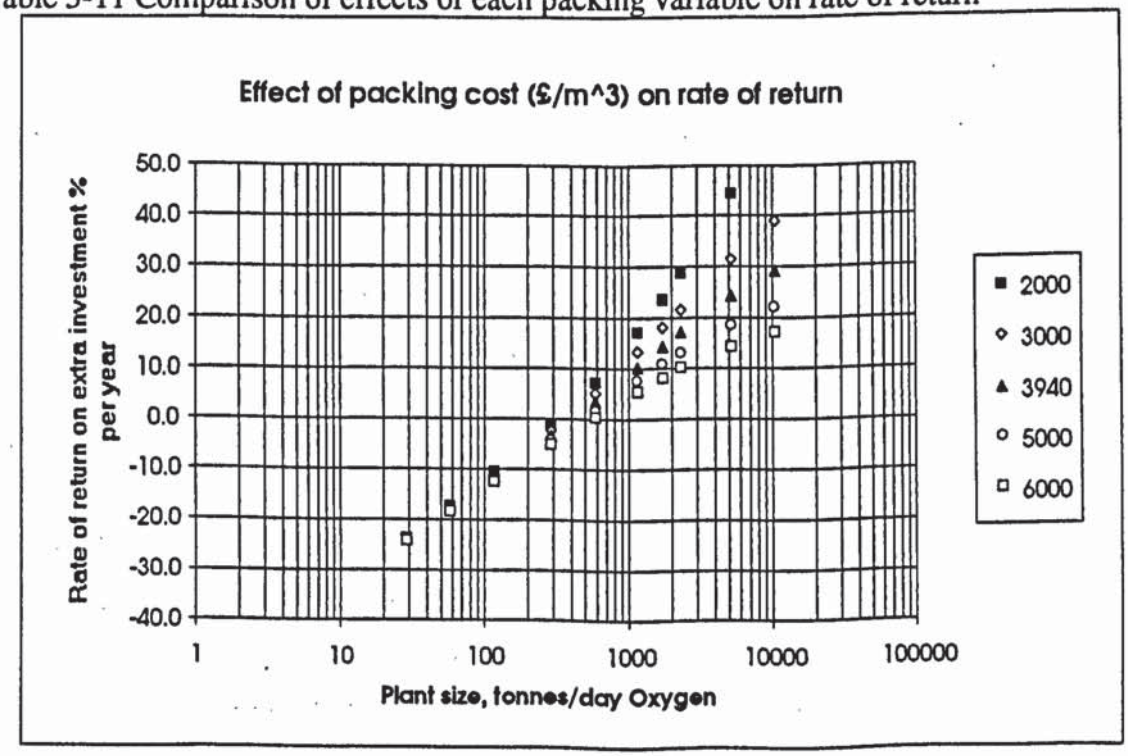

Figure 3-5 Effect of packing cost on rate of return for different plant sizes.

Cost of packing

Figure 3-5 shows the effect of the packing cost on the rate of return. If the plant is small, the column shell cost is much greater than the cost of the packing, so the rate of return is insensitive to the packing cost. In contrast, if the plant is very large, the packing cost dominates the shell cost and so a small change in it causes a large change in the rate of return. For example, to increase the rate of return on the base case by 1%, the packing cost would have to be reduced by about 170% for a 29 t/d plant (i.e. it is impossible), but only by 3.5% for a 10451 t/d plant.

Pressure gradient.

The rate of return at different pressure gradients is shown in figure 3-6. For all sizes of plant, the change in pressure gradient needed to achieve a 1% increase in the rate of return is between 20 and 30%. The larger plants are slightly more sensitive to changes in the pressure gradient because the power cost becomes more important.

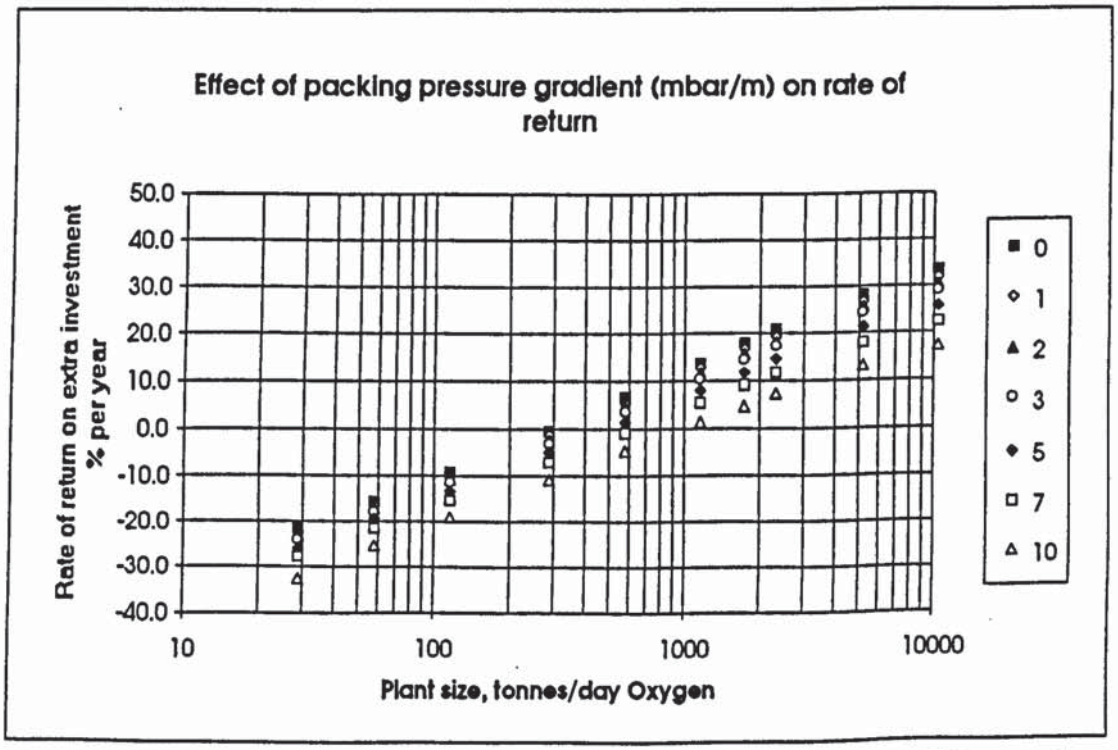

Figure 3-6 Effect of packing pressure gradient on rate of return for different plant sizes

Maximum capacity.

Figure 3-7 illustrates the change in the rate of return with the capacity of the packing. To increase the rate of return by 1%, the capacity needs to be increased by 2% in a very large (10451 t/d) plant, but 8% in a 29 t/d plant. This is because the capacity determines the diameter of the column shell and the volume of packing needed. The shell cost is relatively insensitive to the capacity, because the diameter

depends inversely on its square root. But the volume and therefore cost of the packing is inversely proportional to the capacity. So where the packing cost dominates, the rate of return is more sensitive to changes in the packing capacity.

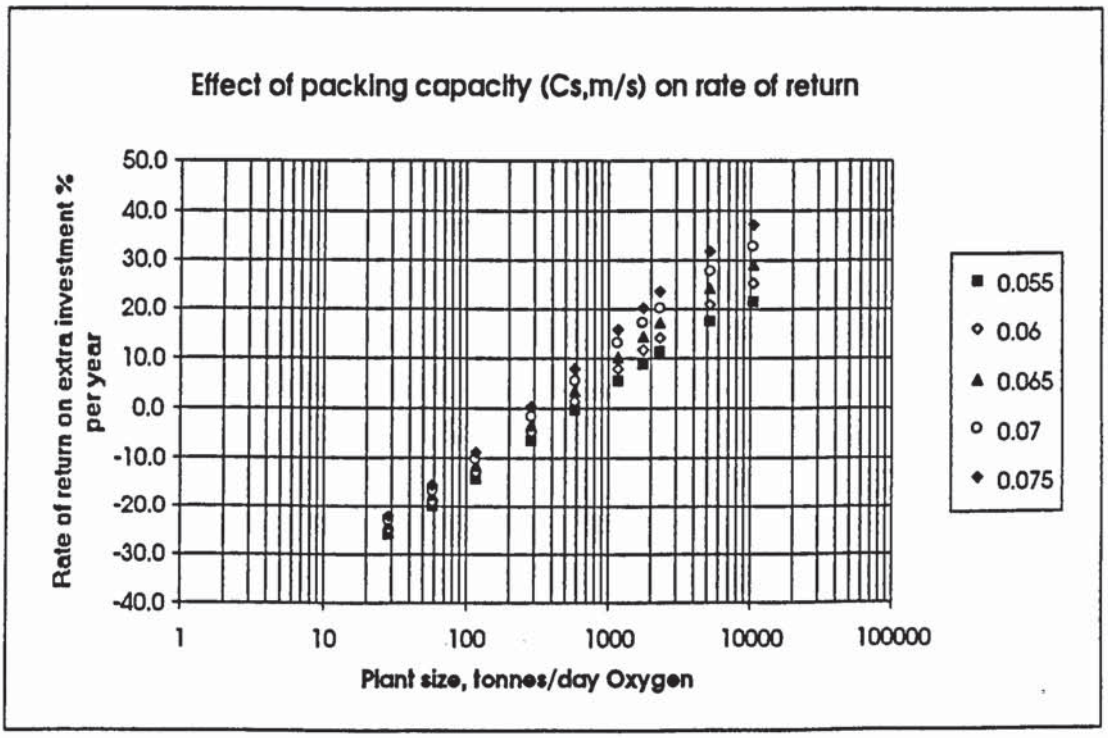

Figure 3-7 Effect of maximum capacity of packing on rate of return for different plant sizes

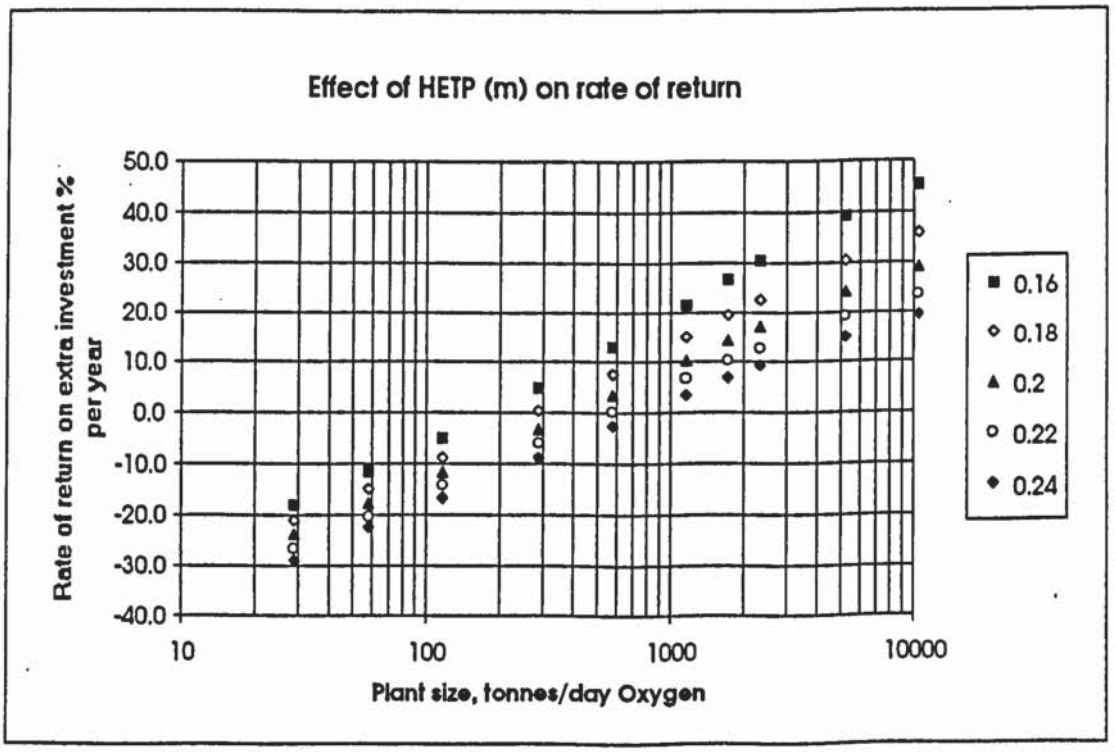

Figure 3-8 Effect of packing HETP on rate of return for different plant sizes

Mass transfer efficiency (HETP/NTSM)

The rate of return is extremely sensitive to the HETP of the packing (figure 3-8). A reduction of only 2-4% in HETP can increase the rate of return by 1%. The rate of return on larger plants is more sensitive to changes in HETP than that on smaller ones because of its effect on both the packing and column shell costs. In smaller plants, the effect on the packing cost is negligible in comparison to that on the shell cost.

Distributors

The cost and height of distributors have been included here because they are vital for the correct operation of the packing. It will be shown that the properties of the distributors can have a significant effect on the rate of return, and so improvements in distributors are as important as improvements in the packing.

Cost of distributors

The distributor cost is assumed to be proportional to the column diameter (diameter squared with economy of scale), so figure 3-9 presents the rate of return for different distributor costs per metre diameter. Like the packing cost, the distributor cost does not have much effect on the rate of return in smaller plants. However, the reduction in distributor cost necessary to increase the rate of return by 1% decreases from 65% for a 29 t/d plant to 24% for a 10451 t/d plant. The effect is not as pronounced as that of the packing cost in large plants, but could still be significant.

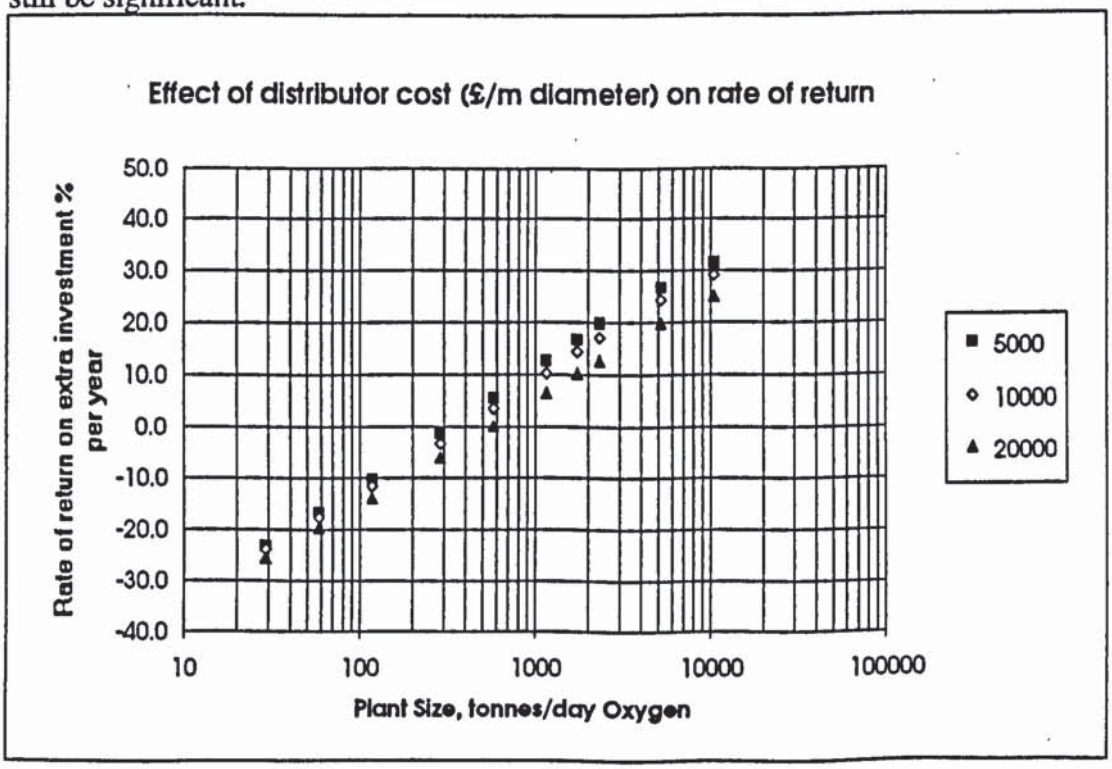

Figure 3-9 Effect of distributor cost on rate of return for different plant sizes

Height of distributors

Figure 3-10 shows that small changes in the distributor height have a similar effect on the rate of return for all plant sizes; a 5-6% reduction in distributor height can increase the rate of return by 1%. If, however, the distributor height can be significantly reduced in smaller plants, by around 75%, the rate of return may be increased by nearly 30%. This is because the column shell cost, which dominates the capital cost, is strongly dependent on the column height, which may be significantly reduced by using shallower distributors. As the packing cost becomes dominant, there is a smaller advantage to be gained by reducing the distributor height.

In practice, the distributors are likely to be deeper in larger diameter columns. If distributors must give the same variation in flow across the column diameter and are installed with the same angle of tolerance from the horizontal, and because the flow from a hole depends on the square root of the height of liquid above it, the distributor height will be proportional to the column diameter. Figure 3-11 shows that in this case, smaller plants become viable and larger plants do not give such a good return as when the distributor height is fixed.

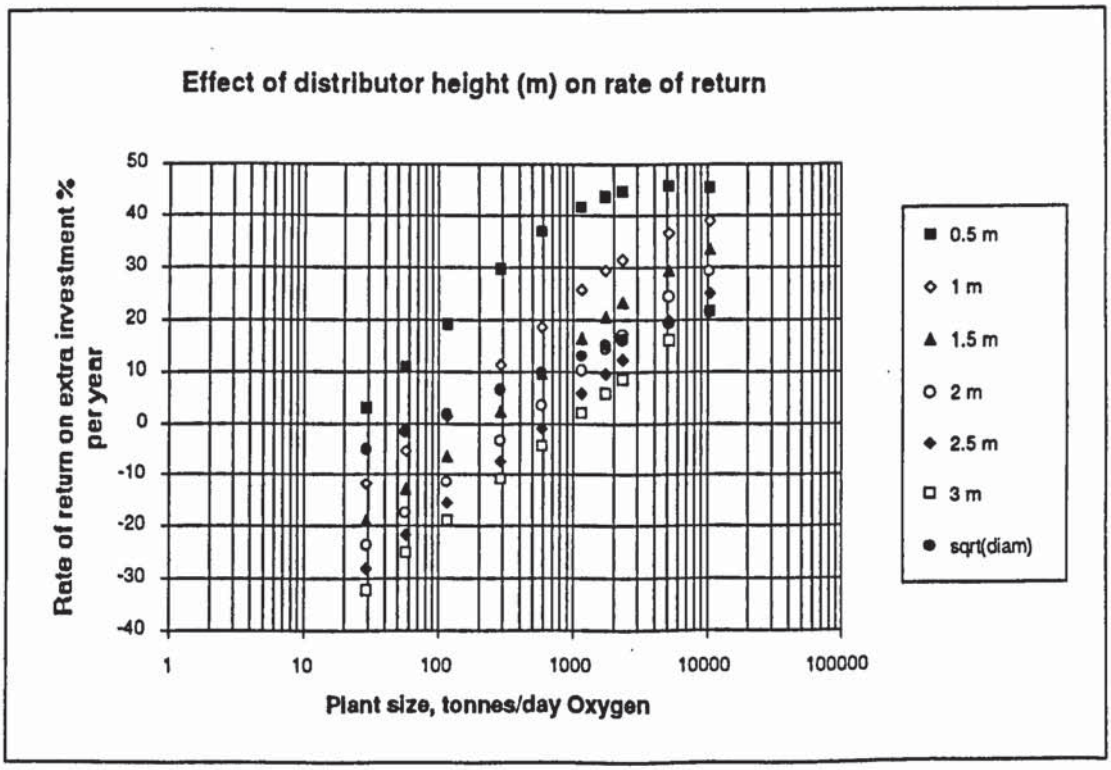

Figure 3-10 Effect of distributor height on rate of return for different plant sizes

Relative importance of packing variables

Table 3-11 shows the percentage change in each packing variable which would give the same change in the rate of return as a 1% reduction in HETP. It demonstrates that if the HETP can be reduced, even at the expense of increased pressure gradient or reduced capacity or increased cost, the rate of return should

be increased. It also shows that a reduction in distributor height is almost as important as a reduction in HETP, particularly in smaller plants, and it is likely to be worthwhile even if the distributor cost is increased significantly.

Plant size	t/d O2	10451	1742	290	29
Base case rate of return	%	28.9	14.3	-3.2	-24
Rate of change of rate of return with:					
Packing cost	%/(£/m³)	-0.0095	-0.0038	-0.001	-0.00015
Pressure gradient	%/(mbar/m)	-1.64	-1.32	-1.02	-1.09
Maximum capacity	%/(m/s)	775	560	340	190
HETP	%/m	-324	-250	-169	-136

Table 3-12 Rate of change of rate of return with packing variables about base cases with different plant sizes

For changes in the packing properties from the base case, the results may be linearised to provide a quick method of evaluating new packings. It is not so good for large changes from the base case, in which case the full analysis should be used. The linearisation provides an indication of the relative importance of each packing variable in determining the rate of return. Table 3-12 gives the rate of change of the rate of return with each packing variable.

Packing type

The packings available at present differ mainly in their specific surface area. As this is changed, the variables needed in the economic analysis all change together, not independently as assumed so far. Table 3-13 shows these variables for different types of packing, including the CY gauze packing.

Packing	Csmax	NTSM	HETP	Design HETP	Cost	Pressure gradient
	m/s	m^{-1}	m	m	£/m³	mbar/m
750Y	0.065	5.60	0.18	0.20	3940	3
500Y	0.070	4.20	0.24	0.26	2670	3
350Y	0.085	3.65	0.27	0.30	1910	3
250Y	0.100	2.60	0.38	0.42	1410	3
CY	0.065	8.50	0.12	0.13	11870	3
750/500 mix	0.070	4.90	0.21	0.23	3305	3
500/350 mix	0.085	3.95	0.25	0.28	2290	3
350/250 mix	0.100	3.10	0.32	0.36	1660	3

Table 3-13 Packing variables used in economic analysis

Figure 3-11 shows the rate of return for the different types of packing.

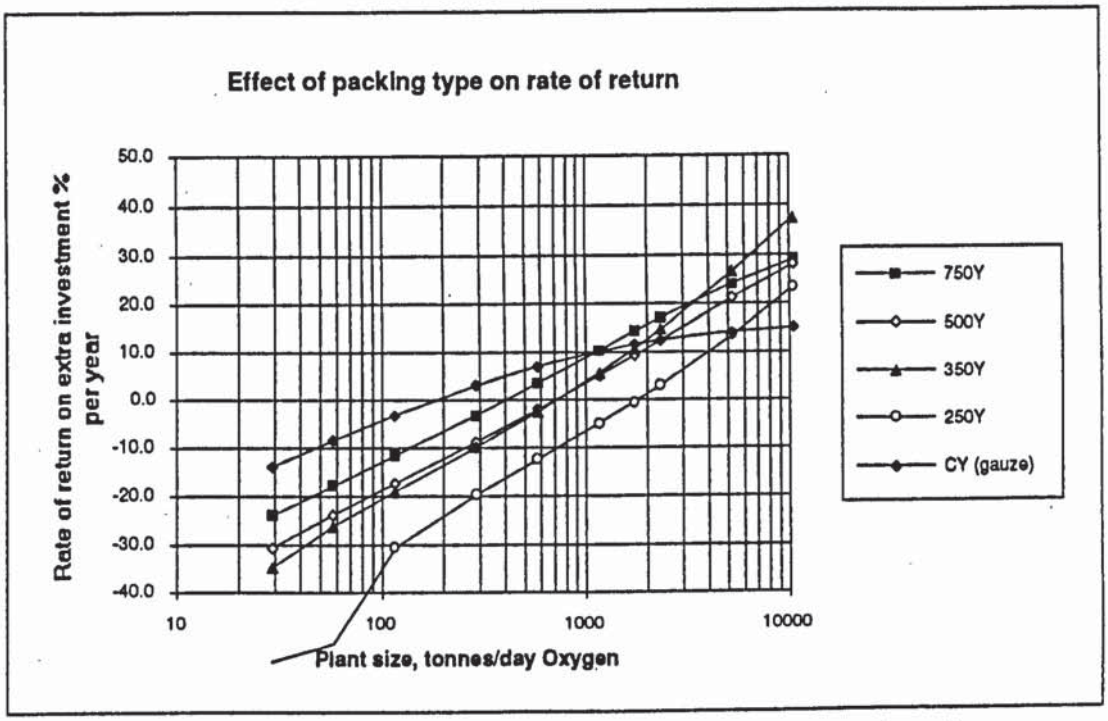

Figure 3-11 Effect of packing type on rate of return for different plant sizes

Of the currently available packings, the CY gauze gives the best return on plants up to around 1000t/d, the 750Y between 1000 and 4000t/d and the 350Y above 4000t/d. As the plant gets larger, the packing cost and capacity become more important compared to the HETP, so packings with smaller specific areas become more advantageous.

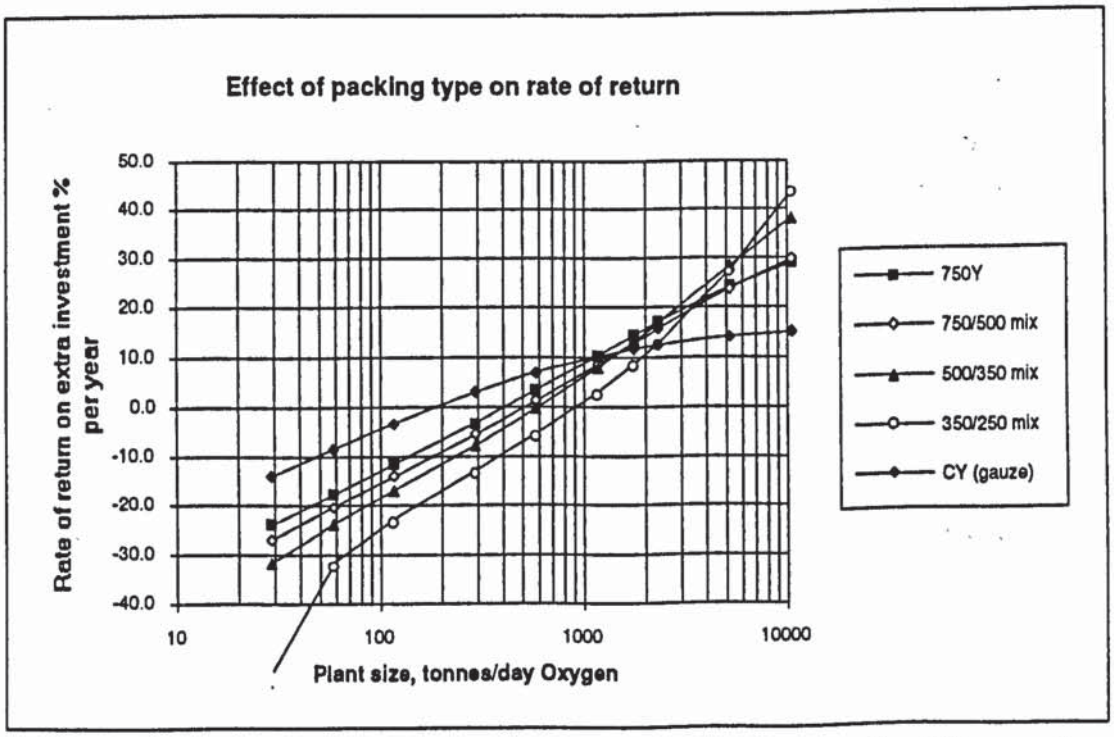

Figure 3-12 Effect of mixing packing types on rate of return for different plant sizes

Because some sections in the low pressure column are much more heavily loaded than others, it may be advantageous to use a lower area packing in these sections. We may allow for the effect of mixing packings by using the capacity of the lower area packing and taking an average efficiency. The results of such an analysis are presented in figure 3-12

So for a particular plant, the analysis allows us to find an optimum packing from those available which maximises the rate of return.

Design capacity

The packing variables also change in a dependent way if the design capacity (as a percentage of the maximum capacity) is altered. So for a particular plant and packing, there will be an optimum design capacity. Figure 3-13 shows that this optimum increases as the plant size increases, from around 80% to 90% of the flooding capacity. As the plant becomes larger, the capacity becomes more important because it determines the packed volume and total packing cost. In this case, the HETP is assumed to be the same up to 100% of maximum capacity. If it falls with higher loading, this should also be accounted for, and would reduce the optimum design capacity.

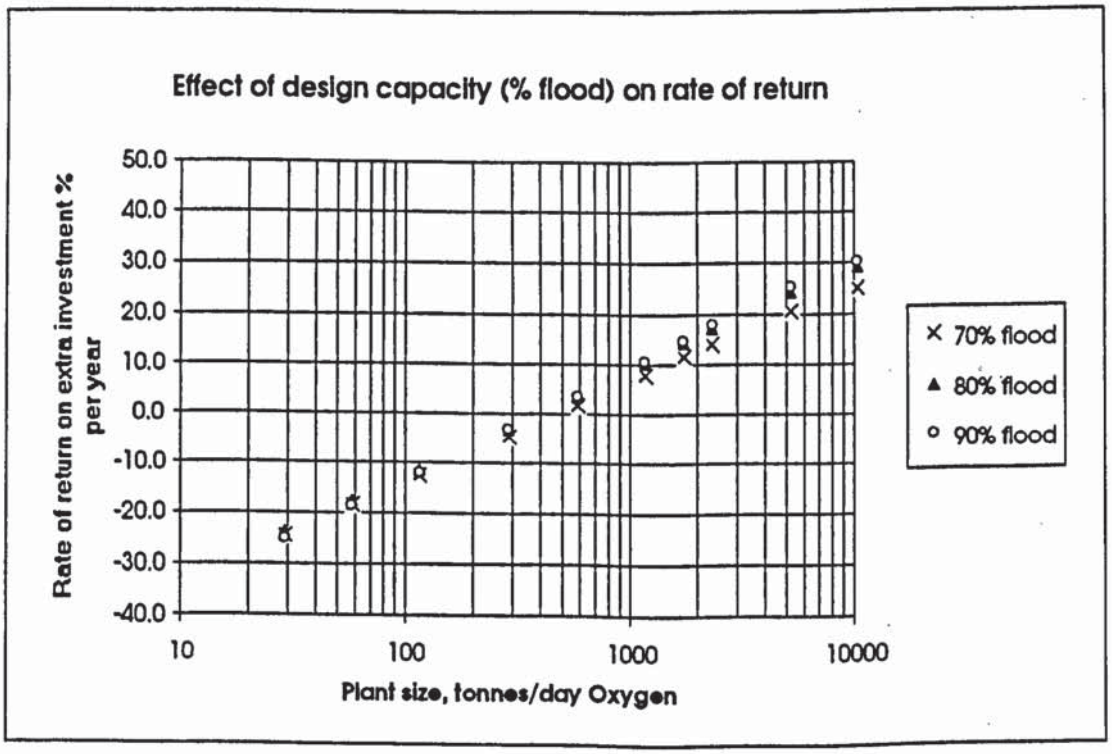

Figure 3-13 Effect of design capacity on rate of return for different plant sizes

3.1.3.3 Effects of plant variables

Plant size

The plant size is very important in determining the rate of return possible by using packing instead of trays. For this reason, all the results are presented to show the effect of the plant size. In general, the rate of return increases as the plant size increases. For very large plants, it reaches a limiting value and, depending on the particular circumstances, it may go through a maximum (for example figure 3-10, distributor height 0.5 m).

The economic analysis of packed plants shows that, below a certain size, they are uneconomic compared to trayed plants. This is because economies of scale are evident in the capital cost, C_{cap}, of a plant, but not in the power cost, C_{pow}. For example for a plant of output Q, $C_{cap} \propto Q^{0.6}$ but $C_{pow} \propto Q^{1}$. This means that over their lifetime, small plants consume power worth a fraction of their capital cost, whereas a large plant may consume power worth many times its capital cost. So for smaller plants, lower capital cost is more desirable than reduced power consumption, whereas the opposite is true of larger ones.

In small plants, the extra capital cost of a packed plant is due mainly to the extra column shell and cold box costs. This suggests that a very efficient packing, which could reduce the column size, may provide a saving even if its cost is high. The economic analysis shows that this is the case; if gauze packing is used, smaller plants become viable.

In large plants, the cost of the packing may be several times the column shell cost, so lower efficiency, higher capacity, cheaper packings are favoured. Again the economic analysis confirms this. Eventually, as the size increases, the extra capital cost becomes proportional to the packing volume. The rate of return on a packed plant then reaches a limiting value, as the extra capital cost and power cost saving increase at the same rate. This does ignore any reduction in the cost per unit volume of packing as the plant becomes large; whether there is any will depend on the packing market at the time.

Because the packing cost is dominant, a suitable method of evaluating packings for use in large plants is that used by Billet (1969) for vacuum distillation, namely the cost of packing per unit throughput per theoretical plate at a particular pressure gradient - the specific cost.

In addition to the limiting cases of small and large plants, the economic analysis reveals the interesting behaviour of intermediately sized plants. If the packing cost dominates at a relatively small plant size, the difference between the cost of packed and trayed columns may increase as Q^n where $n>1$. This could happen if the extra shell cost of a packed column is small (efficient packing or shallow distributors) or

if the packing is expensive. Because the power saved only increases as Q^1, the rate of return on the packed plant decreases. As a result there may be maximum return at an optimum plant size for a particular type of packing in a particular case.

Plant lifetime

The plant lifetime is important in determining the rate of return because it fixes the number of years over which the power saving is obtained. Figure 3-14 shows, however that as the plant lifetime becomes longer than about 10 years, there is a fairly small increase in the rate of return. This is because the power savings in the later years are worth little, as they are effectively discounted at the rate of return to get their present value. For a similar reason, the rate of return is also less sensitive to the plant lifetime as the plant size increases and the power saving is of the same order as the extra investment; most of the extra expenditure is repaid early on. Typical lifetimes for air separation plant are 10-15 years, so the base case assumes the lower limit of 10 years. Packed plants are unlikely to be the best option if the lifetime is likely to be less than 10 years.

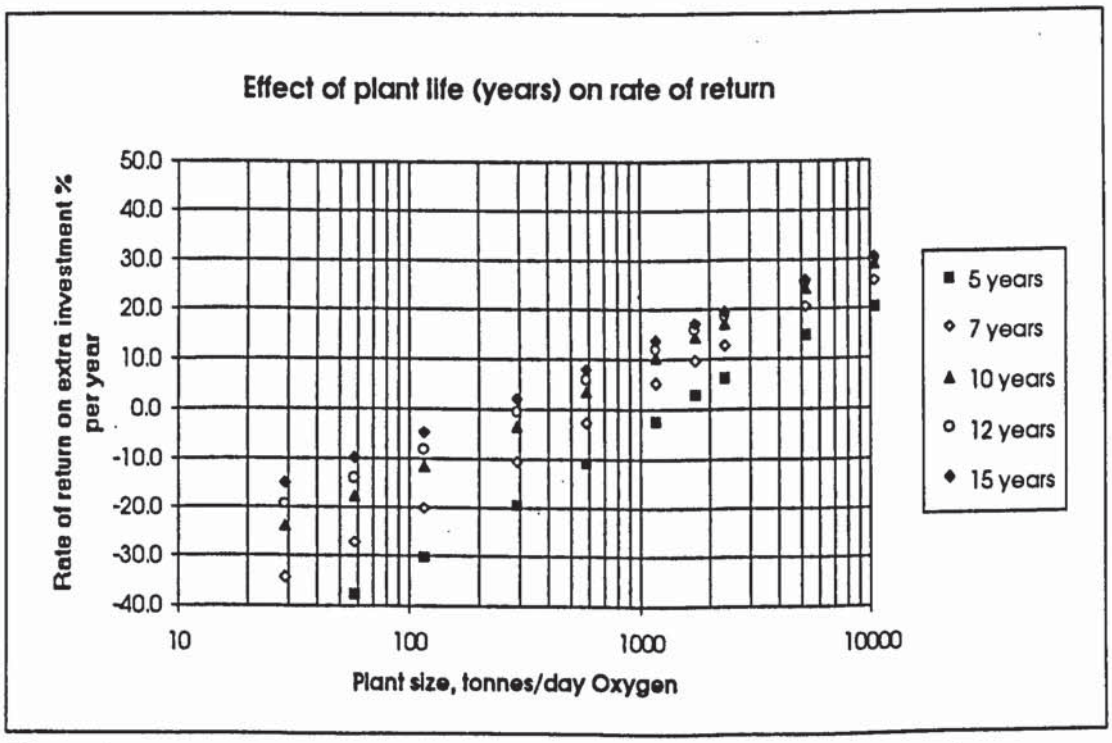

Figure 3-14 Effect of plant lifetime on rate of return for different plant sizes

Number of theoretical plates in columns (product purity)

Low pressure column

Figure 3-15 demonstrates that the rate of return improves as the number of theoretical plates in the low pressure column is increased. This is because of the reduced power penalty associated with extra theoretical plates if packing is used.

The increase in return per extra plate is smaller as the number of plates increases and as the plant size increases.

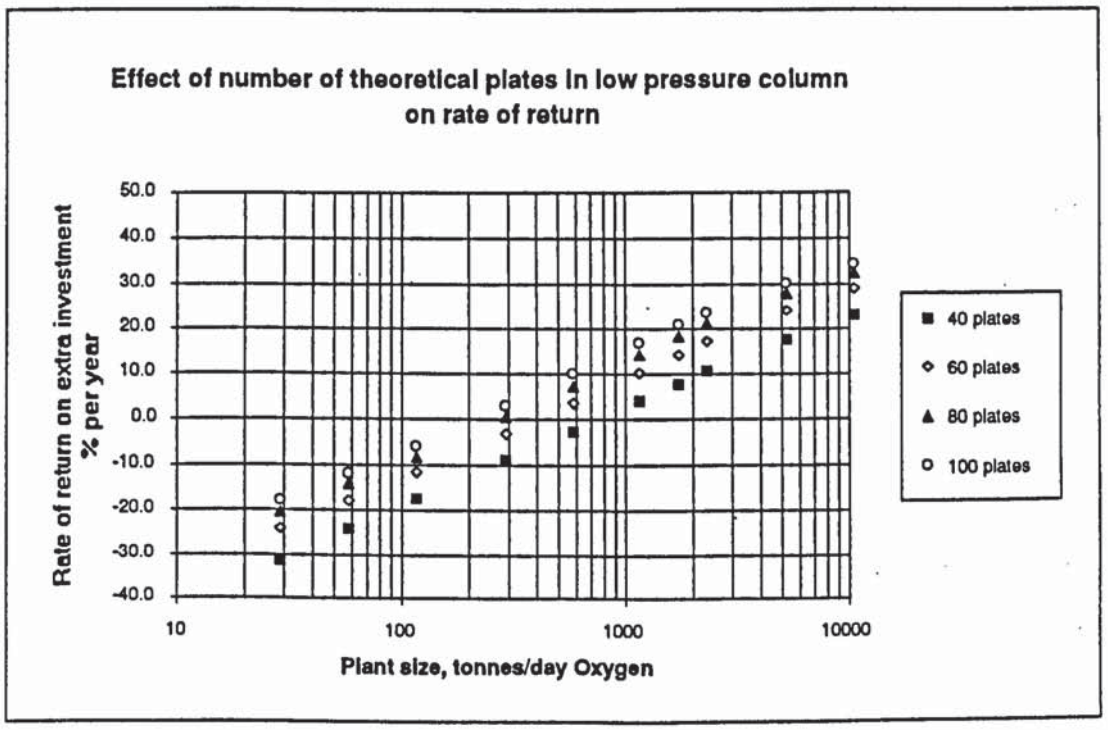

Figure 3-15 Effect of number of theoretical plates in the low pressure column on rate of return for different plant sizes

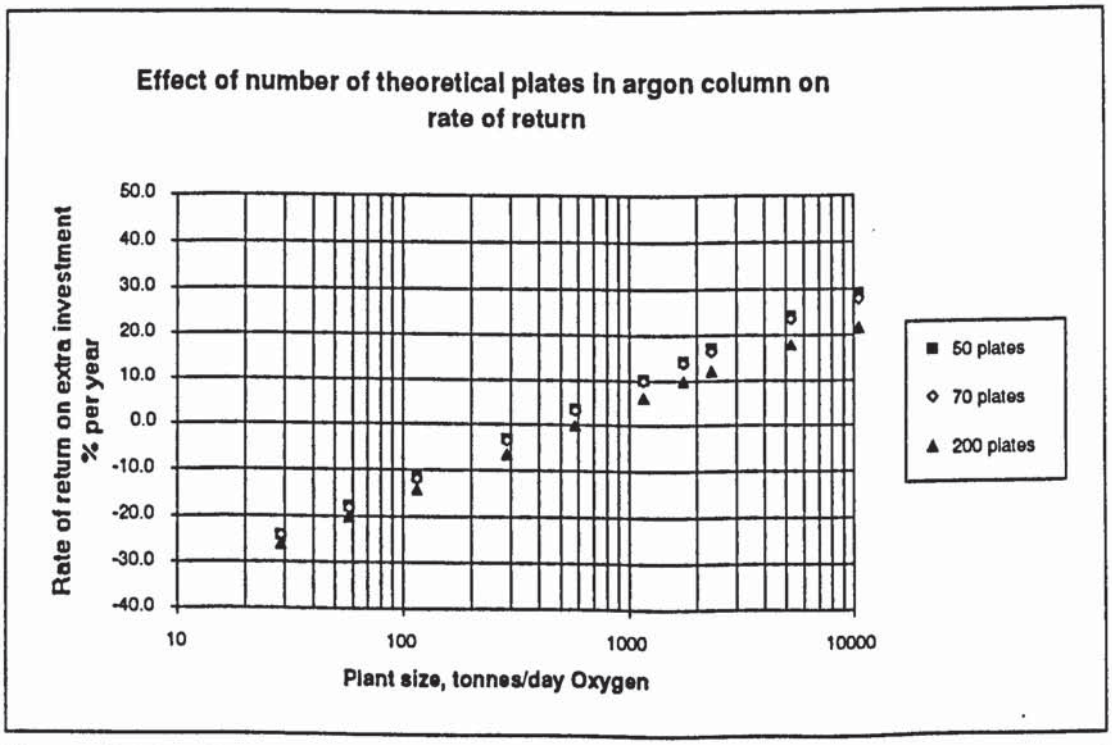

Figure 3-16 Effect of number of theoretical plates in argon column on rate of return for different plant sizes

Argon column

Increasing the number of theoretical plates in the argon column must reduce the rate of return because, under this analysis, no advantage is gained by doing so. Figure 3-16 shows this. But even if the number of theoretical plates in this column is increased to produce pure argon directly (for example to 200 as suggested by Rohde (1989) and Agrawal and Woodward (1991)), the effect on the rate of return is relatively small. In practice, the rate of return would probably be increased because the costs saved by not building and operating an argon purification unit could be offset against the extra cost of the argon column.

Number of distributors in the low pressure column

The number of distributors required in the low pressure column depends on the design of the plant, and whether some feeds are split or combined. It also depends on whether redistributors are added in deep packed beds. Figure 3-17 shows that the addition of an extra distributor reduces the rate of return by around 4%. This is because of the increased column shell cost. It is therefore likely to be desirable to avoid redistribution and to mix feeds, even at the expense of a worsening in packing HETP (due to poor distribution) or increased number of theoretical plates required (due to sub-optimal feed location) with a combined effect up to about 8%.

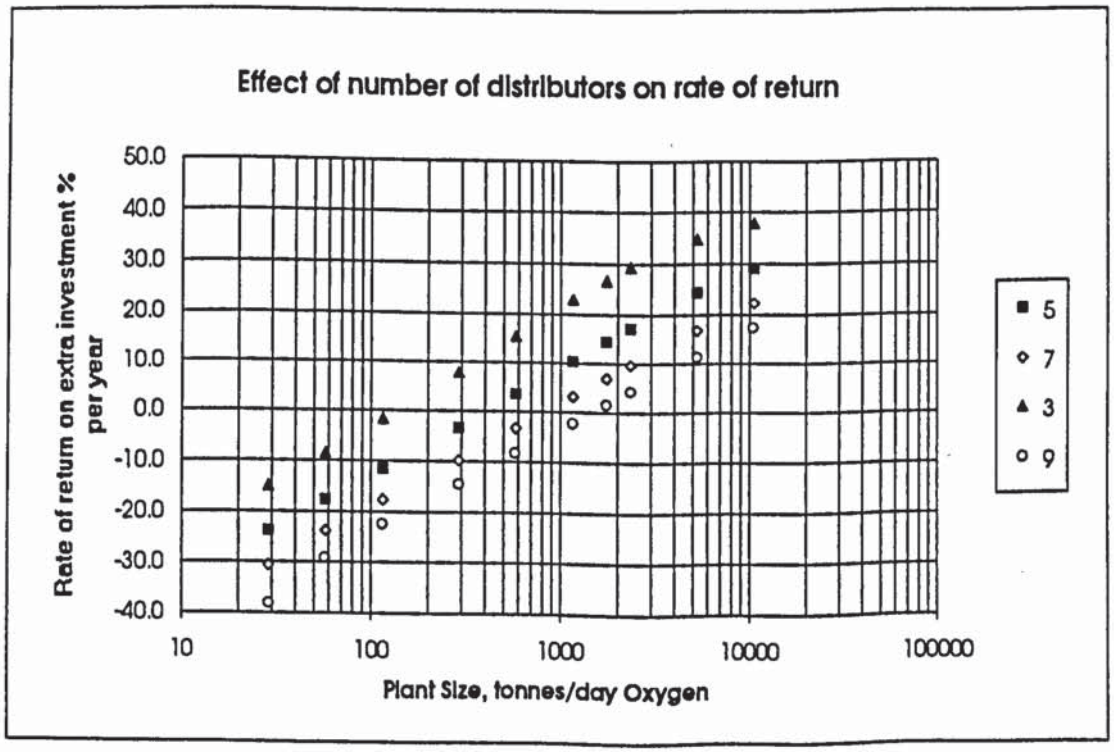

Figure 3-17 Effect of number of distributors on rate of return for different plant sizes

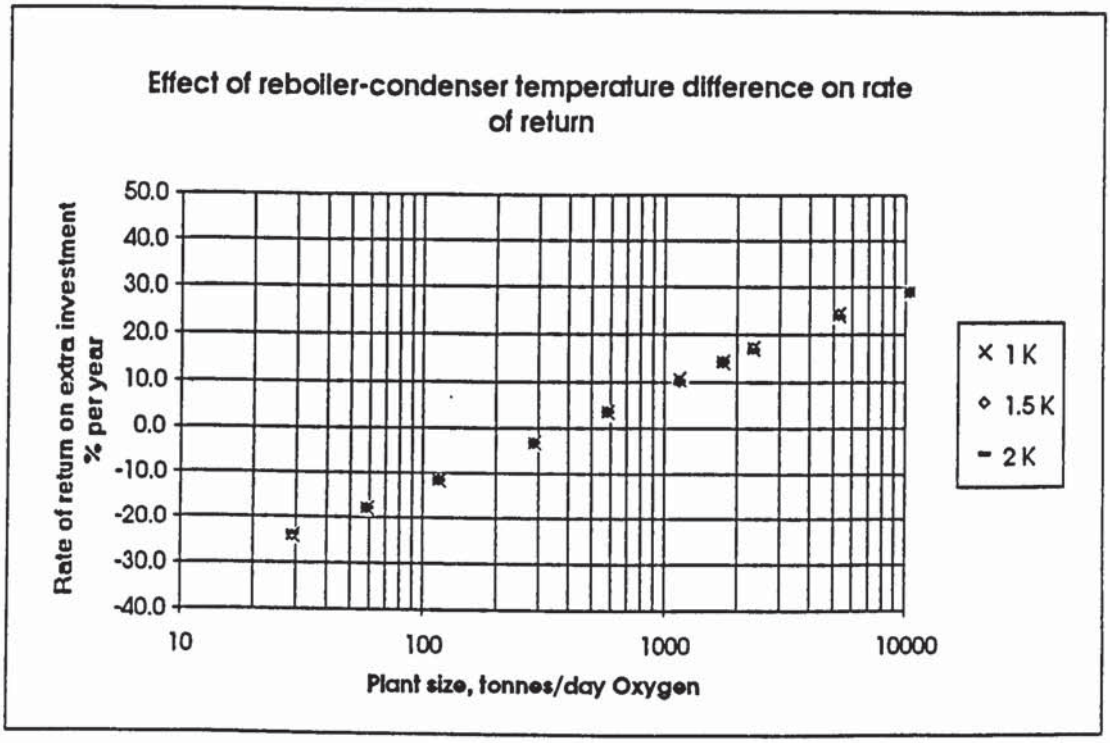

Figure 3-18 Effect of reboiler-condenser temperature difference on rate of return for different plant sizes

Reboiler-condenser temperature difference

Figure 3-18 shows that the reboiler-condenser temperature difference has little effect on the rate of return. A smaller temperature difference leads to a slightly higher return, but not enough to be significant. This is due to two opposing effects as the temperature difference increases. The reduction in high pressure column pressure for a given reduction in reboiler pressure is greater, but the actual pressure is higher, so that the percentage difference between trays and packings is almost the same.

Liquid production

If more liquid is produced by a plant, more refrigeration is needed to remove the heat which is not removed by the cold liquid. Because a packed plant has less efficient refrigeration, the rate of return is smaller if the liquid production is increased. However, figure 3-19 shows that a tripling of liquid production only reduces the rate of return by about 2%. If a large quantity of liquid were required, an integrated liquefier would be used, which could supply all the refrigeration with the same efficiency to a trayed or packed plant. This would increase the rate of return, but only by a small amount.

Boosted air temperature rise

If the temperature of the boosted air is raised when it enters the cold box, more refrigeration is needed to remove the excess heat. The rate of return is then lower

because the packed plant has less efficient refrigeration. A temperature rise of 10 K reduces the rate of return by around 2%, as shown in figure 3-20.

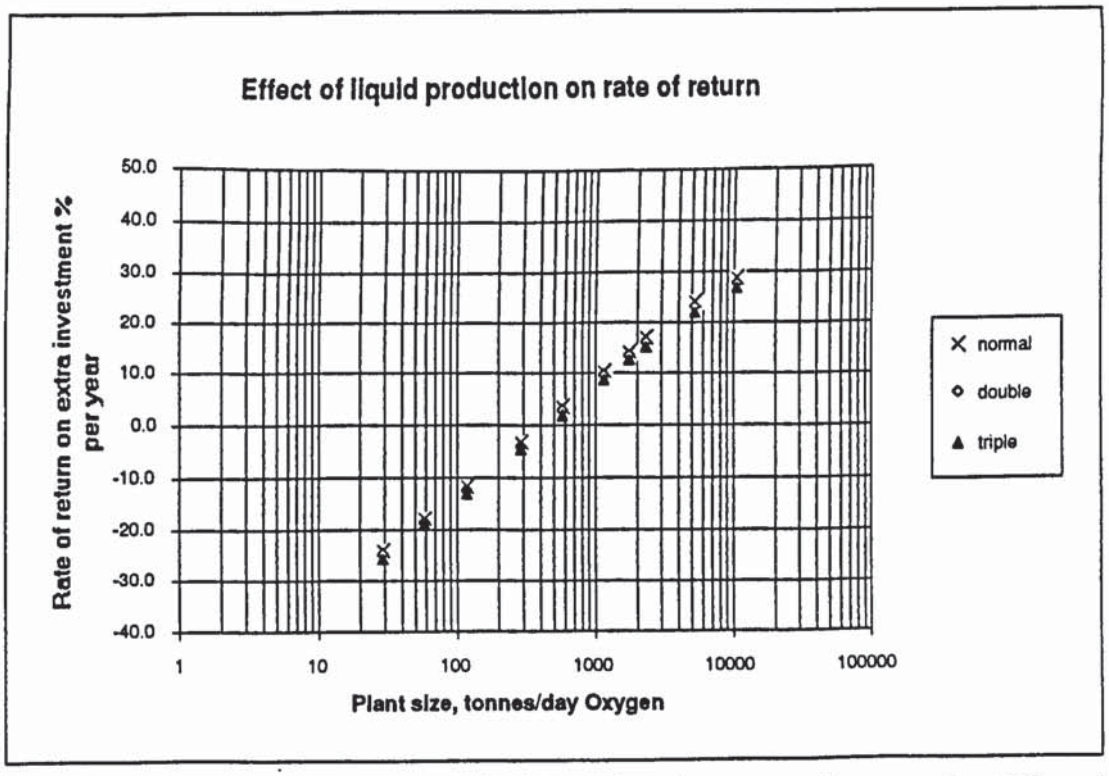

Figure 3-19 Effect of quantity of liquid produced on rate of return for different plant sizes

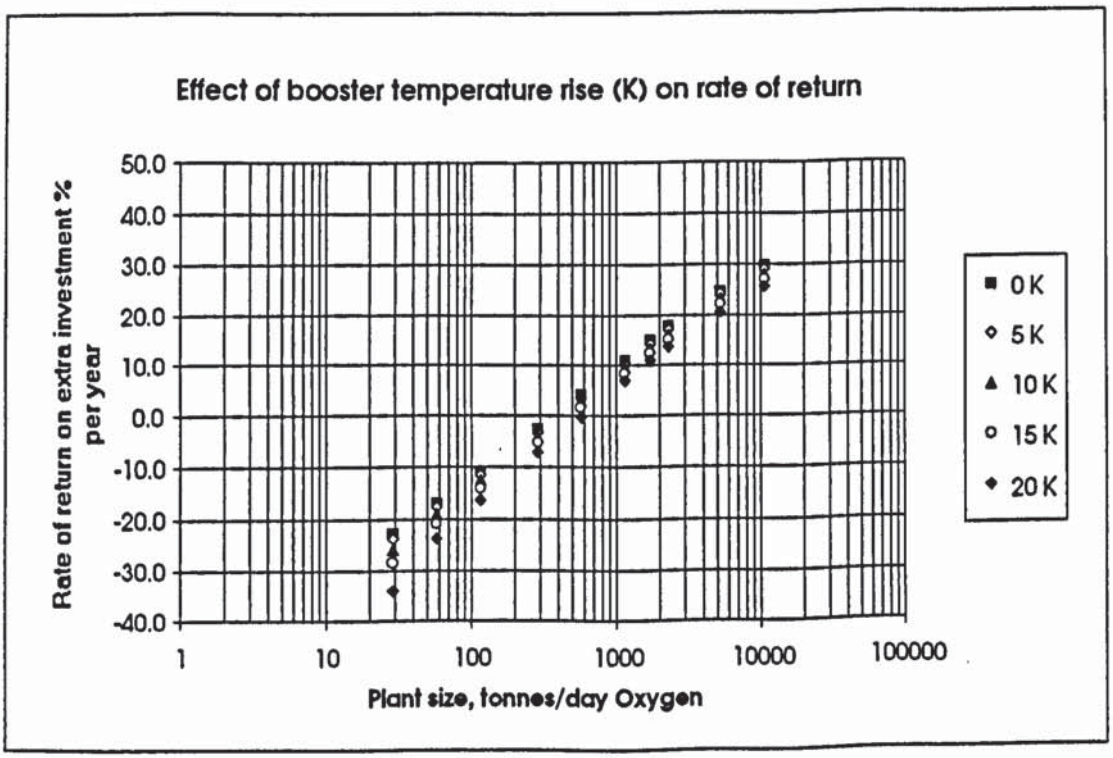

Figure 3-20 Effect of temperature rise over booster compressor on rate of return for different plant sizes

Method of air pre-purification

After being compressed, the air entering the plant must have carbon dioxide and water removed from it. This is commonly achieved by absorbing them in pre-purification units (PPUs) or by freezing them out in reversing heat exchangers (RHEs).

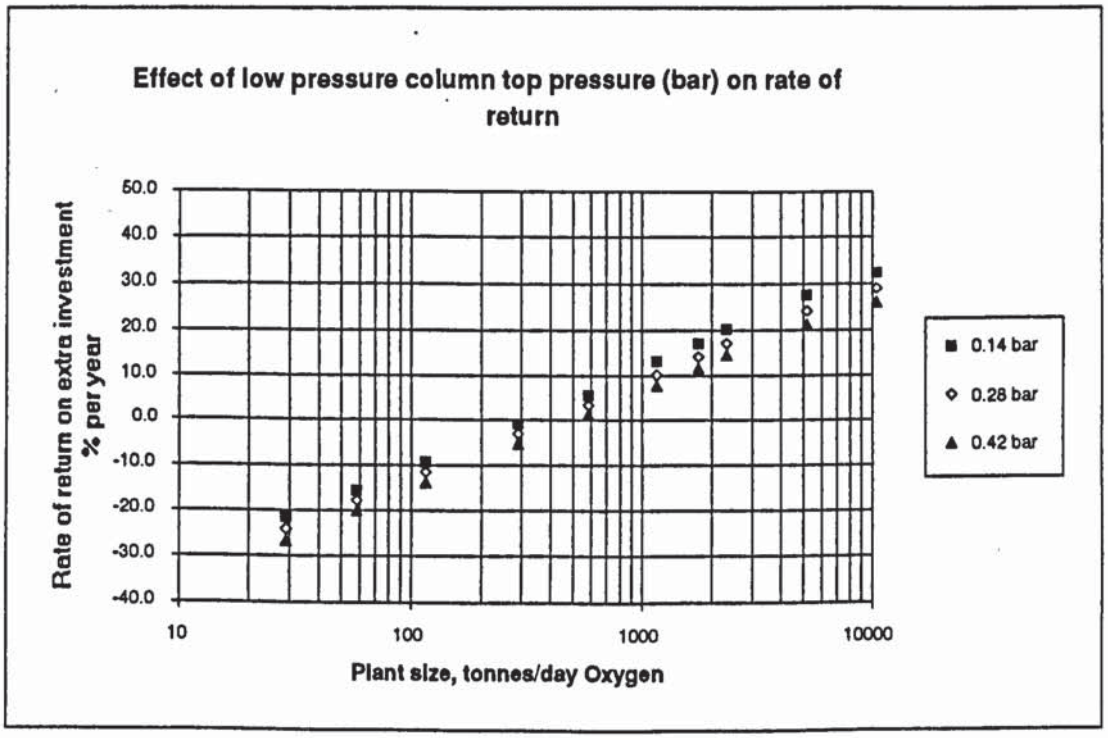

Figure 3-21 Effect of low pressure column top pressure on rate of return for different plant sizes

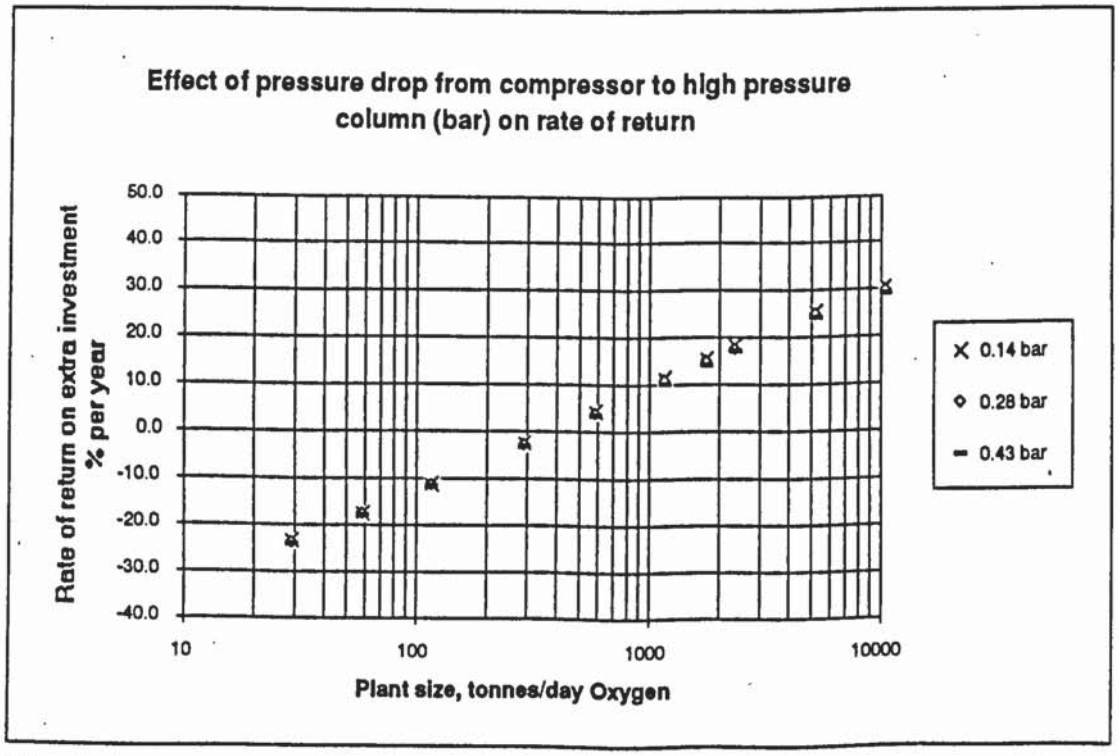

Figure 3-22 Effect of pressure drop from compressor to high pressure column on rate of return for different plant sizes

Waste nitrogen from the plant is used to regenerate the PPU or RHE. The pressure drop of both the incoming air and the waste nitrogen regeneration stream is higher if PPUs are used, unless blowers are used to compress the waste nitrogen for regeneration.

Figure 3-21 shows that the pressure at the top of the low pressure column, which is set by the required regeneration gas pressure, can affect the rate of return. The lower this pressure, the better, because the percentage reduction in the compressor pressure from trays to packings is larger when the pressure is lower. In the same way, the pressure drop from the compressor to the high pressure column affects the rate of return, but to a much smaller degree, as illustrated in figure 3-22. Reversing heat exchanger plants or ones with regeneration blowers should therefore show a greater return than standard PPU ones.

Column arrangement

Putting the columns side by side

In the base case, the low pressure column is mounted on top of the high pressure column with the argon column at the side. Because the column shell cost depends on the height to the 1.8 power, it should be possible to reduce the plant cost by putting all the columns next to each other and using pumps to circulate liquid where necessary. If the trayed plant has the arrangement in the base case, but the packed plant has the columns side by side, the rate of return is much increased, however for a fair comparison, the trayed plant should also have its columns next to each other. In this case, the rate of return is actually lower, except for the largest plant considered. Figure 3-23 shows this.

Whether or not Argon is produced

Figure 3-23 also shows that the rate of return is increased by around 5% if there is no argon column, because the argon column increases the capital cost without providing any benefit. In fact most plants require an argon column to allow sufficiently pure oxygen to be produced.

Packing the high pressure column.

If the high pressure column is packed, very little advantage is gained by the very small reduction in pressure drop, but the capital cost is greatly increased. This leads to a reduction in the rate of return of around 10% in a small plant or 15% in a large one (figure 3-23). If full advantage were to be taken of the wide operating range of packing, it may be necessary to pack the high pressure column. In this

case it is essential to improve the performance of the packing to make this type of plant viable.

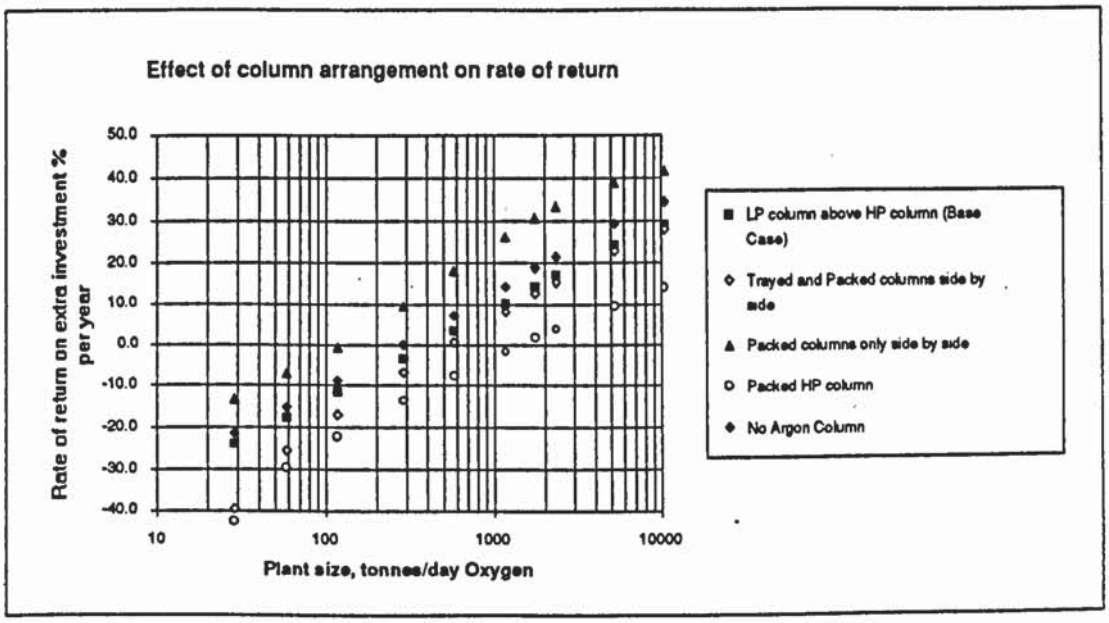

Figure 3-23 Effect of column arrangement on rate of return for different plant sizes

Cycle variations

Changes in the rate of return due to changes in the cycle occur mostly because of the difference in the quantity and efficiency of the refrigeration. Several different cases were examined and will now be presented.

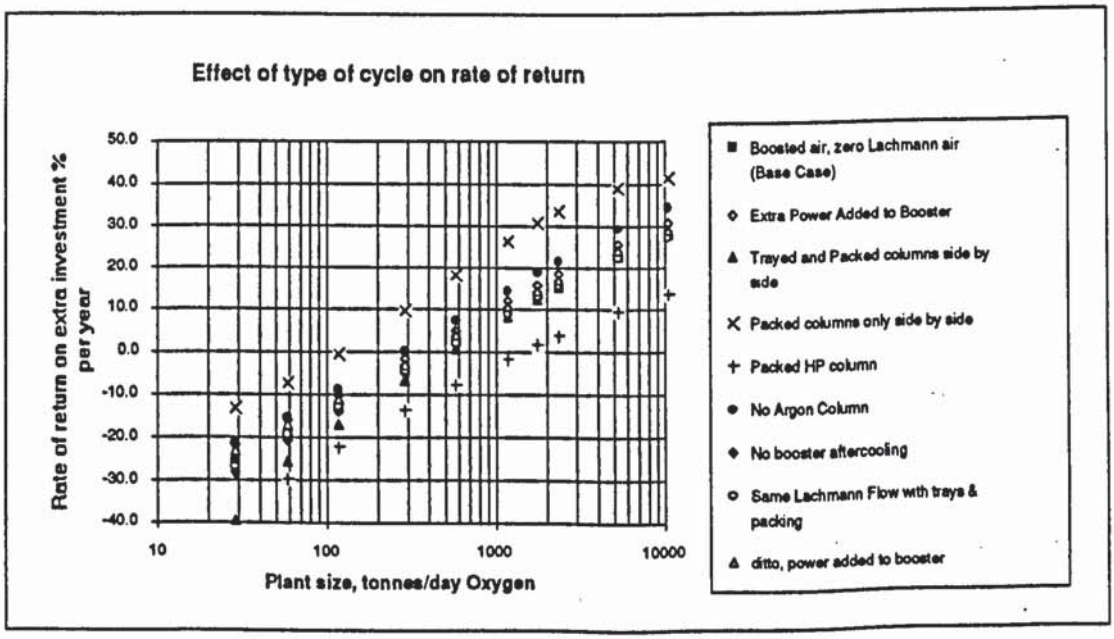

Figure 3-24 Effect of cycle variations on rate of return

Full Lachmann air flow in trayed plant, same flow in packed plant

The simulation assumed that nearly all the turbine exhaust air in the trayed plant was processed in the low pressure column. The extra flow required in the packed

plant was all sent to waste, so reducing the advantage of the packing. Figure 3-24 shows that the rate of return is slightly lower in this case than in the base case, but that the difference is rather small.

Power added to booster compressor

In the case of a packed plant, the reduced outlet pressure of the main compressor leads to a reduced temperature difference across the expansion turbine and reduced refrigeration efficiency. The refrigeration efficiency may be easily increased by adding enough power to the booster compressor to achieve the same pressure as in the trayed plant. The power saving provided by the reduced turbine flow is greater than the extra power consumed by the booster compressor. An increased rate of return of about 2% is possible, as illustrated in figure 3-24.

Booster aftercooling

It is important that as much excess heat as possible be removed from the plant at ambient temperature, so as to reduce the amount of refrigeration required from the turbine. If the boosted air is not cooled before it enters the cold box, the rate of return is reduced by about 1% over the base case in very large plants and 4% in very small ones.

No booster compressor

If a conventional cycle with no booster compressor is used, the rate of return on a packed plant is around 1% lower than if a booster is installed (figure 3-24). This is because the lower refrigeration efficiency of this type of cycle leads to a bigger deterioration in efficiency when the pressure is reduced by the use of packings.

3.1.4 Conclusions

Packing is more economically favourable than trays in plants above a certain size, depending on the rate of return required. If a rate of return of 5% is needed, the smallest viable plant is about 700 t/d oxygen with 750Y packing.

Different types of packing are better in different plants. In small plants, high cost, high efficiency packings are favoured, whereas in larger ones low cost, high capacity ones are better.

So, for a particular plant, an optimum packing and an optimum design point for this packing may be found.

The extra cost of making distributors shallower could be balanced with the resulting reduction in column shell cost to find an optimum distributor height for a particular plant.

It is likely to be economic to produce very pure argon directly from the argon column, provided there is a large enough market for it. In addition, high purity plants favour the use of packings.

Packing the high pressure column with current packings is unlikely to be economic unless it is necessary for some reason not taken into account, such as a requirement for increased turndown.

An advantage may be achieved in a packed or trayed plant by placing all the columns next to each other, rather than having the low pressure column above the high pressure column.

The rate of return may be improved by ensuring that the minimum possible refrigeration is needed and that it is achieved as efficiently as possible. In particular, the air boost cycle is advantageous, and it is necessary to remove heat added by the booster inefficiency as effectively as possible with cooling water. The refrigeration efficiency may be further improved with this cycle by supplying extra power to the booster to increase its outlet pressure. So in general, the more efficient the trayed plant, the higher the rate of return possible by changing to packing.

3.2 Economics of packing manufacture

Information is available from manufacturers on the 'budget cost' of packings with different specific surface areas and in different materials. But commercial packings are only available in blocks of a fixed depth. In addition, the different packings all have similar block heights, so if the effect of block height on packing cost is to be estimated, a method must be developed to do this. The actual cost of packing will depend on the volume purchased and on the competitiveness of the packing market, and may be around 50% of the budget price. So the analysis of the manufacturing process should also indicate the minimum possible cost of packing.

3.2.1 Analysis of the manufacturing process

The analysis is based on the very simple and labour intensive process used in Tianjin University Packing Factory in China, where labour costs are very low. In an automated process, the labour cost per hour would be very much greater but the labour time needed would be much less. In addition, the capital equipment cost and overheads would be much higher. An upper limit to the manufacturing cost may be obtained by using UK labour cost values with the Chinese production method, because automation would only be used to reduce manufacturing cost. The analysis shows, however that this approach leads to unrealistically high packing costs, especially when the surface area is high and the cost becomes dominated by the crimping time. A limited degreee of automation was therefore allowed for in

the analysis by balancing the extra press and tool cost against the reduced manufacturing time if several crimps were made with each press operation.

The packing manufacturing process operated at Tianjin University Packing Factory is described in more detail in chapter 2. It consists of six separate operations: Perforating the metal, giving it a surface treatment (corrugation in this case), crimping it, cutting it, arranging the sheets into blocks and assembling the sheets into blocks. This analysis also includes the step of installing the packing in the column, since the important cost in the analysis of the plant economics is the installed cost of the packing.

The labour costs of the process are calculated from the time taken for each operation. Other costs which are important are the press and tool costs, material costs and overheads. Overheads are included in the labour cost, whilst the other costs are estimated.

The packing geometry is described in chapter 2. In the analysis we shall consider blocks of packing of height h_b, width w_b and length l_b. The channel side dimension, s (see figure 2-8) is related to the crimp half-angle, ϕ and the specific area, a by:

$$a = \frac{2}{s \cos\phi \sin\phi} \qquad \text{or} \qquad s = \frac{2}{a \cos\phi \sin\phi}$$

Labour costs

Now, we will consider the time taken in each stage of the manufacturing process to make a unit volume of packing.

Perforation

The perforation time for a unit volume of packing, T_{perf} is the product of the perforation time per unit length of metal, t_{perf} and the metal length per unit volume of packing, l_m, so:

$$T_{perf} = t_{perf} l_m$$

with $l_m = \frac{a}{2 h_b}$ (a/2 because a includes both sides of metal)

In this case, t_{perf} is taken as 20 seconds per metre, independent of metal width (block height). In fact, if block height were reduced, this could probably be reduced, so that the area of metal perforated with one press action remained the same.

Surface treatment (corrugation)

Surface treatment is dealt with in the same way as perforation so that:

$$T_{st} = t_{st}\, l_m$$

The surface treatment time per metre is taken as 10 seconds. It is shorter than the perforation time because it is a continuous process, rather than a stepwise press operation.

Crimping

The crimping time per unit volume, T_{crimp}, is the product of the time per crimp, t_{crimp}, and the number of crimps per unit volume, N_{crimp}. The number of crimps per unit volume is given by the product of the number of crimps per unit metal length, n_{crimp} and the metal length per unit volume l_m, so that:

$$T_{crimp} = t_{crimp}\, N_{crimp} = t_{crimp}\, n_{crimp}\, l_m$$

with $n_{crimp} = \frac{1}{2s} = \frac{a \cos\phi \sin\phi}{4}$ (because one operation puts in two bends)

so $T_{crimp} = t_{crimp} \frac{a^2 \cos\phi \sin\phi}{8\, h_b}$

Because the crimping time depends on the square of the specific area, if this is large it tends to dominate the labour time and hence the cost (see table 3-14). The packing cost is therefore quite sensitive to the time for one crimp, t_{crimp}. The value used in the analysis is 1 second per crimp.

Cutting

The cutting time per unit volume, T_{cut}, is given by the time per cut, t_{cut}, times the number of sheets of metal per block n_{sheets}, times the number of blocks per unit volume, N_{blocks}:

$$T_{cut} = t_{cut}\, n_{sheets}\, N_{blocks} = t_{cut} \frac{w_b\, a \sin\phi}{2} \frac{1}{l_b\, h_b\, w_b} = t_{cut} \frac{a \sin\phi}{2\, l_b\, h_b}$$

The value of t_{cut} is taken as 10 seconds per cut, and includes the measuring time.

Arrangement into blocks

In the same way as the cutting, the time for arranging the sheets into blocks is given by the time per sheet (t_{arr}) times the number of sheets per unit volume, so that:

$$T_{arr} = t_{arr} \frac{a \sin \phi}{2 l_b h_b}$$

t_{arr} is assumed to be 2 seconds.

Fixing sheets to make blocks

The time taken per unit volume of packing to fix the sheets together, T_{fix}, is the product of the fixing time per block, t_{fix} and the number of blocks per unit volume, N_{block}:

$$T_{fix} = t_{fix} \frac{1}{l_b h_b w_b}$$

The time to fix the sheets together is taken to be 60 seconds per block.

Packing the column

In addition to the manufacturing process, we must also consider the time taken to pack the column with a unit volume of packing, T_{pack}. This is given by the product of the number of blocks per unit volume, N_{block}, and the time to put one block into the column, t_{pack}:

$$T_{pack} = t_{pack} \frac{1}{l_b h_b w_b}$$

The time taken to pack one block in the column is taken as 30 seconds.

Overall labour cost

The overall labour cost of a unit volume of packing, C_{lab}, is the hourly rate L multiplied by the labour time T_{tot} (in hours) to make it. In seconds, T_{tot} is given by:

$$T_{tot} = T_{perf} + T_{st} + T_{crimp} + T_{cut} + T_{arr} + T_{fix} + T_{pack}$$

$$= \frac{1}{l_b h_b w_b}\left(\frac{a l_b w_b}{2}(t_{perf}+t_{st}) + \frac{a^2 l_b w_b \cos\phi \sin\phi}{8} t_{crimp} + \frac{a w_b \sin\phi}{2}(t_{cut}+t_{arr}) + (t_{fix}+t_{pack})\right)$$

so:

$$\frac{C_{lab}}{£} = \frac{sec/hr}{3600}\ \frac{T_{tot}}{sec}\ \frac{L}{£/hr}$$

Material costs

The material cost, C_{mat}, is calculated by first calculating the volume of metal in a unit volume of packing, V_{metal}, and then multiplying this by the metal density, ρ_{metal}, and the cost per unit weight of metal c_{metal}. V_{metal} is given by:

$$V_{metal} = \frac{a}{2}\delta,$$

where δ is the thickness of metal in the packing.

So:

$$C_{mat} = \frac{a}{2}\delta\ \rho_{metal}\ c_{metal},$$

In this case the metal is assumed to be aluminium, with a density of 3000 kg/m^3 and a cost of £7 per kg. In the case of the gauze packing, the material cost is taken as five times that of the aluminium sheet.

Press and tool cost

The part of the volumetric cost of packing attributable to the machine and tool costs is calculated from their initial cost and lifetime and the yearly production volume. This is the most uncertain aspect of the cost, as it is difficult to estimate the component parts accurately, but table 3-14 shows that it is a relatively small part of the packing cost.

The tool cost is assumed to be dominated by that of the crimping tool:

$$C_{tool} = \frac{c_{tool}\ N_{crimp}}{n_{tool}} = \frac{c_{tool}\ a^2 \cos\phi \sin\phi}{8\ h_b\ n_{tool}}$$

where c_{tool} is the initial tool cost, n_{tool} is the tool lifetime in operations and N_{crimp} is the number of crimps per unit volume of packing.

The machine cost per unit volume of packing, C_{mach}, is given by:

$$C_{mach} = \frac{c_{mach}}{Q\ n_{mach}}$$

where Q is the volume of packing produced each year, n_{mach} the machine lifetime in years and c_{mach} the initial cost of the machines.

Overall manufacturing cost

The overall cost of manufacturing a unit volume of packing, C_{pack} is now given by:

$$C_{pack} = C_{lab} + C_{mat} + C_{tool} + C_{mach}$$

Selling price

The cost used for the packing in the economic evaluation includes a 30% markup on the manufacturing cost, to allow for the difference between the manufacturing cost and the selling price. Figure 3-11 showed that if the plant is large, a 25% reduction in packing cost can increase the rate of return by 10%, so it would be advantageous in this case to negotiate a reduction in the profit margin on the packing.

Semi-automation

The effect of performing several crimps in one press operation is to reduce the time per crimp, and hence the labour cost. It does however mean that a more powerful press and a more complex tool are required. The tool cost is assumed to be proportional to the number of crimps per operation and the increase in press cost is estimated by assuming that the cost depends on the number of crimps per operation to the 0.6 power, i.e. that economies of scale apply. The number of crimps per operation which minimises the manufacturing cost may then be calculated.

3.2.2 Results

An example calculation (for 750Y packing) is shown in table 3-14.

Results for several packings are presented in table 3-15. It is instructive to examine the breakdown of the costs for packings with different specific surfaces. The proportion of the manufacturing cost from each source is almost constant with differing specific areas. The material cost is about 50% of the minimised manufacturing cost for the standard packings, whilst it is about 85% for the gauze. For automated manufacturing processes, material costs are usually 50-80%, depending on the degree of automation, so the results of this analysis are reasonable. The press and tool costs are only around 13% of the manufacturing cost, whilst the labour cost is 37%.

Calculation of packing cost based on labour intensive manufacturing process with minimal automation							
area per unit volume	m^2m^3	750	750	750	750	750	750
crimp angle, phi	degree	45	45	45	45	45	45
cos phi		0.70711	0.70711	0.70711	0.70711	0.70711	0.70711
sin phi		0.70711	0.70711	0.70711	0.70711	0.70711	0.70711
channel side, S	m	0.00533	0.00533	0.00533	0.00533	0.00533	0.00533
block height	m	0.2	0.2	0.2	0.2	0.2	0.2
block width	m	0.3	0.3	0.3	0.3	0.3	0.3
block length	m	1	1	1	1	1	1
metal thickness	m	0.0002	0.0002	0.0002	0.0002	0.0002	0.0002
metal density	kg/m^3	3000	3000	3000	3000	3000	3000
metal cost per unit mass	£/kg	7	7	7	7	7	7
time for one crimping operation	s	1	1	1	1	1	1
time to perforate one metre of metal	s	20	20	20	20	20	20
time to suface treat one metre of metal	s	10	10	10	10	10	10
time to make one cut	s	10	10	10	10	10	10
time to arrange one sheet	s	2	2	2	2	2	2
time to fix sheets into a block	s	60	60	60	60	60	60
time to pack one block in column	s	30	30	30	30	30	30
time for crimping per m^3 packing	s/m^3	175781	87891	17578	7990	7324	6761
time for perforation per m^3 packing	s/m^3	37500	37500	37500	37500	37500	37500
time for surface treatment per m^3 packing	s/m^3	18750	18750	18750	18750	18750	18750
time for cutting per m^3 packing	s/m^3	13258	13258	13258	13258	13258	13258
time to arrange the sheets per m^3	s/m^3	2652	2652	2652	2652	2652	2652
time for fixing blocks per m^3	s/m^3	1000	1000	1000	1000	1000	1000
time to pack one m^3 in column	s/m^3	500	500	500	500	500	500
Total labour time	hr/m^3	69.3	44.9	25.3	22.7	22.5	22.3
Labour cost per hour	£/hr	50	50	50	50	50	50
Labour cost	$£/m^3$	3464	2244	1267	1134	1125	1117
Yearly production	m^3/yr	500	500	500	500	500	500
Press cost for one crimp per operation	£	50000	50000	50000	50000	50000	50000
Other Machine costs	£	150000	150000	150000	150000	150000	150000
Number of crimps per operation		1	2	10	22	24	26
Press cost	£	50000	75786	199054	319465	336587	353146
Machine Life in years	yr	4	4	4	4	4	4
Press cost per m^3 packing	$£/m^3$	100	113	175	235	243	252
Tool cost for one crimp per operation	£	5000	5000	5000	5000	5000	5000
Tool cost	£	5000	10000	50000	110000	120000	130000
Tool life in operations		1E+07	1E+07	1E+07	1E+07	1E+07	1E+07
Number of crimps per m^3	m^{-3}	175781	175781	175781	175781	175781	175781
Tool cost per unit volume	$£/m^3$	88	88	88	88	88	88
Metal cost / unit volume	$£/m^3$	1575	1575	1575	1575	1575	1575
Labour cost	$£/m^3$	3464	2244	1267	1134	1125	1117
Press cost per m^3 packing	$£/m^3$	100	113	175	235	243	252
Tool cost per unit volume	$£/m^3$	88	88	88	88	88	88
Metal cost / unit volume	$£/m^3$	1575	1575	1575	1575	1575	1575
Total manufacturing cost / unit volume	$£/m^3$	5227	4020	3105	3032	3031	3031
Selling price / unit volume	$£/m^3$	6796	5225	4036	3941	3940	3941

Table 3-14 Example calculation of packing manufacturing cost

3.2.3 Conclusions

This simple analysis of the packing manufacturing process gives reasonable values for the costs of packings and may be used to estimate the change in manufacturing cost on changing the dimensions of the packing blocks. It is useful because it allows the cost of new types of packing to be estimated so that they can be evaluated economically as well as technically.

Cost breakdown for different sizes of packing						
area per unit volume	m^2/m^3	250	350	500	750	750 gauze
Block height	m	0.2	0.2	0.2	0.2	0.2
Labour cost	£/m^3	400	542	766	1125	1125
Press cost per m^3 packing	£/m^3	148	175	197	243	243
Tool cost per unit volume	£/m^3	10	19	39	88	88
Metal cost / unit volume	£/m^3	525	735	1050	1575	7875
Total manufacturing cost / unit volume	£/m^3	1083	1470	2052	3031	9331
Selling price / unit volume	£/m^3	1408	1911	2668	3940	12130

Table 3-15 Calculated cost breakdown for different sized packings

3.3 Conclusions

We have seen that the use of structured packing in air separation has a number of effects on the plant design and operation. If the correct packing is chosen, it is economically better than using trays in most plants, except for small ones. The evaluation technique which has been developed may be used to assess the benefits of any new packing and allows us to target improvements in packing performance to those which will provide most benefit. The analysis of the packing manufacturing process will enable us to estimate the cost of a new packing, so that it may be evaluated economically.

Chapter 4 - Packing development

In chapter 2 we saw how structured packings have been developed so far and looked at some models and correlations which have been used to describe their operation. We also investigated some methods of enhancing heat and mass transfer. In this chapter, we shall make use of this knowledge to develop a new packing which is economically more attractive for air distillation.

To develop a new packing, it is first necessary to understand how packings work and what factors influence their performance. Because the packing is intended for use in air distillation, it is also important to know whether we can predict the performance for this system. So, we shall first look at published experimental results for different packings with different test systems (including air) and compare them with the predictions of some of the models. This should indicate how well we can predict changes in performance if the packing geometry or distillation system is changed.

The results of these investigations will then be used, together with the results of the economic analysis and the review of heat and mass transfer enhancement techniques, to devise some ideas for new packings. The manufacture of these new packings will be considered and estimates made of the manufacturing costs. Finally, the new packing chosen for manufacture will be described.

4.1 Effects on packing performance of changing the flows, distillation system and packing geometry

Our purpose is to develop a new packing which is particularly suited to air distillation. The economic analysis in chapter 3 identified that it should be as efficient as possible, even at the expense of a slightly increased pressure gradient or reduced capacity.

To estimate the changes in the performance of a packing if its geometry, the flow-rate through it or the distillation system is changed, we can use both correlations of experimental results and more fundamentally-based models. Because the range of available packing geometries is limited, the range of experimental correlations will also be limited. However, such experimental results allow the predictions of the models to be tested. If both methods agree, then the models can be used with a degree of confidence to predict the performance of new geometries.

Aspects of packing performance

The aspects of packing performance of interest are the efficiency, capacity and pressure gradient. The liquid hold-up is difficult to measure experimentally and not

of great practical importance, but it is important in most of the models because it influences the pressure gradient. Because of this, it will also be examined, however the pressure gradient and liquid hold-up will only be considered independently, that is in the region below loading. This is sufficient to compare the relative performance of different mixtures and geometries and avoids numerical solution of the more complex equations. Only the simpler expressions for calculating capacity and efficiency will be used, since these provide sufficient information for our purpose.

Point of comparison

If the distillation system or the packing geometry is changed, all the aspects of the performance change, including the capacity. A distillation column is normally designed to operate at a particular fraction of the maximum capacity, so that any change in the capacity leads to a change in the design velocity. Although we could compare the efficiency, pressure gradient and liquid hold-up at the same Reynolds number, vapour velocity or F-factor, it is more appropriate to compare them at the design point, that is at a particular fraction of the flooding velocity.

This means that we must first use a model or correlation to predict the flood point and then calculate the vapour and liquid velocities at the design point in terms of the variable of interest. It also means that it is important to know the dependence of the packing performance on the vapour and liquid flows in addition to the dependence on this variable.

We shall now look at some published experimental results for a range of packing geometries and distillation systems, and examine the predictions of some of the models. We shall consider only the channel-type packings, because there are no models of the other types and very little experimental data.

The problem when comparing the results of published packing tests is that different packings are tested on different scales with different test mixtures and at different pressures. This makes direct comparison of results almost impossible, and is the reason for testing standard packings alongside the new ones in this work. The most commonly-used test mixtures are chlorobenzene and ethylbenzene and cyclohexane and n-heptane, because they are suitable for use over a range of pressures, however a number of other mixtures have been used.

Throughput

The dependence of the pressure gradient and efficiency of a packing on the liquid and vapour flow through it are the most commonly presented data. These data are necessary to find the correct design point when the packing is used. Two types of packing will be considered here, sheet metal and gauze, because they show

different behaviours. The results examined are those presented by Spiegel and Meier (1987) and Sulzer Brothers Ltd. (1992).

Pressure gradient

All the pressure gradient results considered are at total reflux, since these give a good indication of the pressure drop in distillation close to minimum reflux, if the relative volatility is low. Some representative data, for Mellapak 500Y, are given in figure 4-1. In all cases, below about 60 % flood, the presence of liquid has little influence on the pressure gradient. In this region, it is proportional to the vapour velocity at very low flows and to its square at higher flows. This is consistent with a transition from laminar to turbulent flow, which takes place at a different fraction of the maximum capacity in different packings and at different pressures. Some data do not show the laminar regime, because the flows do not go low enough. Most of the models use an experimentally-determined friction factor to calculate the pressure gradient below loading, and so can show good agreement with the data.

Above the loading point at 60-80% of maximum capacity, the pressure gradient increases sharply as the liquid and vapour flows interact. This behaviour may be approximated as a dependence on the sixth power of vapour velocity until flooding is reached and the pressure gradient increases even more sharply. The models show varying degrees of success in this region. The closest fit is given by Spiegel and Meier (1987 and 1992), but this is achieved by fitting a curve to the results. The pressure gradients in gauze and sheet metal packings behave in the same way as the throughput is changed.

Liquid hold-up

Only a few experimental measurements of liquid hold-up in structured packings have been published, and these are for air and water with fixed liquid flow rates rather than for distillation. What data there are show that the hold-up below loading is constant, and at loading it increases rapidly. For simplicity, we shall only consider the case below loading. Figure 4-2 shows the dependence of the liquid hold-up on liquid superficial velocity below loading for several different area packings, as presented by Bravo et al. (1992) and Spiegel and Meier (1992). This shows that the hold-up in these packings at the higher liquid flows may be approximated by:

$$h_l = 0.00133\ u_{ls}^{0.6}\ a^{1.17}$$

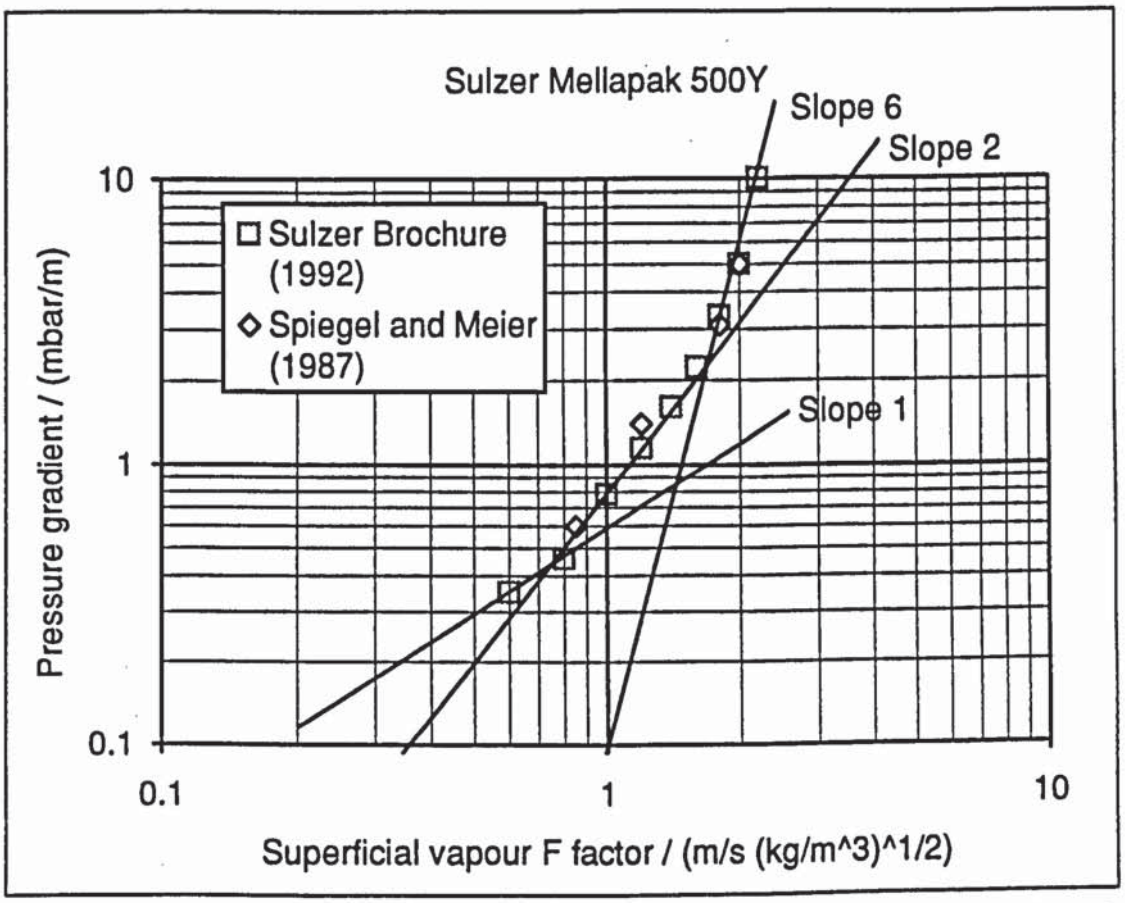

Figure 4-1 Example of dependence of pressure gradient on vapour flow (F-factor) at total reflux for Sulzer Mellapak 500Y.

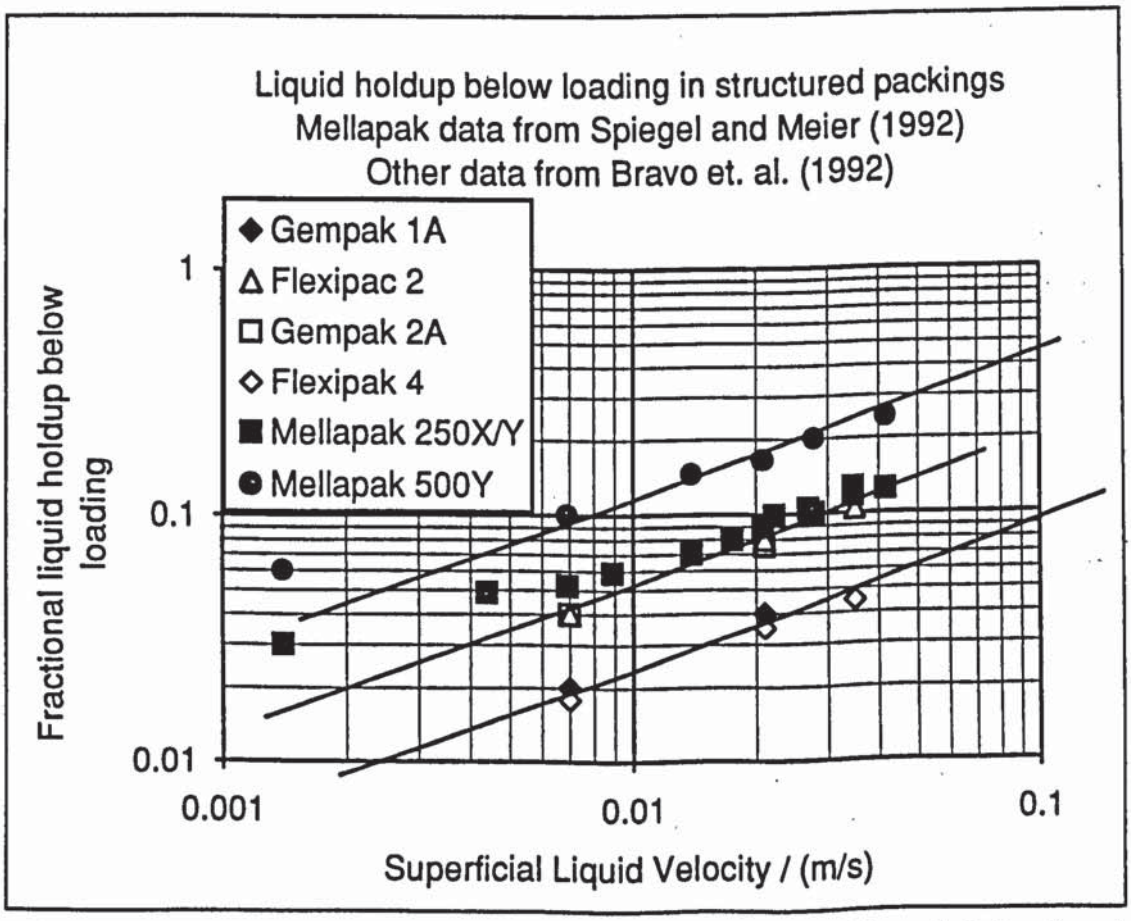

Figure 4-2 Liquid hold-up below loading (Bravo et al., 1992 and Spiegel and Meier, 1992)

For a laminar film, the models give $h_l \propto u_{ls}^{1/3}$ whilst for a turbulent film we have $h_l \propto u_{ls}^{2/3}$. The models of Bravo et al. (1992) and Billet and Schultes (1992), which include an empirical wetted area term, assume a laminar film so that $h_l \propto a_w^{2/3} u_{ls}^{1/3}$ and give $h_l \propto u_{ls}^{0.5}$ and $h_l \propto u_{ls}^{0.66}$ respectively. The dependence is therefore closer to the experimental one in those models which are based more on actual results.

Efficiency

The efficiency of sheet metal packings is almost independent of liquid and vapour loads, as illustrated in figure 4-3 for Mellapak 500Y. The HETP is proportional to the 0 to 0.1 power of vapour velocity, except near flooding where it undergoes a rapid increase as the flooding velocity is reached. Some data show an increase in efficiency near the loading point of around 10% over the average value (see for example the data of Spiegel and Meier (1987) in figure 4-3). This increase could be due to mass transfer enhancement as the phases begin to interact, or could be an effect of small column diameters, where it is more pronounced.

The models (most of which are based on experimental data) show a scatter of around 30% around the experimental data, probably because they were each developed with results under different conditions. The dependence on throughput varies, but is weak in all cases.

In gauze packings, the efficiency depends much more strongly on throughput than in sheet metal ones. This is normally attributed to the better wetting in gauze packings increasing the interfacial area at low flows. The HETP of the BX packing, and the CY packing at low pressures is proportional to the 0.45 power of vapour velocity. At atmospheric pressure, the efficiency of the CY packing depends less strongly on vapour velocity; the HETP is proportional to its 0.2 power. The results for the CY packing are reasonably well predicted by the model of Zogg, which was developed from them.

Separate phase resistances to mass transfer

No experimental values of the liquid and vapour phase resistances have been published. Predictions of the models for each are shown in figures 4-4 and 4-5. These differ widely depending on the model, especially in the liquid; the predicted transfer unit height may differ by nearly two orders of magnitude.

The liquid phase resistance generally increases with throughput, but this increase is smaller in those models based on results for sheet metal packings. The resistance actually decreases slowly with increasing throughput in some cases.

The vapour phase resistance increases with throughput in those models where total wetting is assumed. However, if wetting is accounted for, it decreases.

So, the liquid phase resistance becomes more important as the throughput is increased.

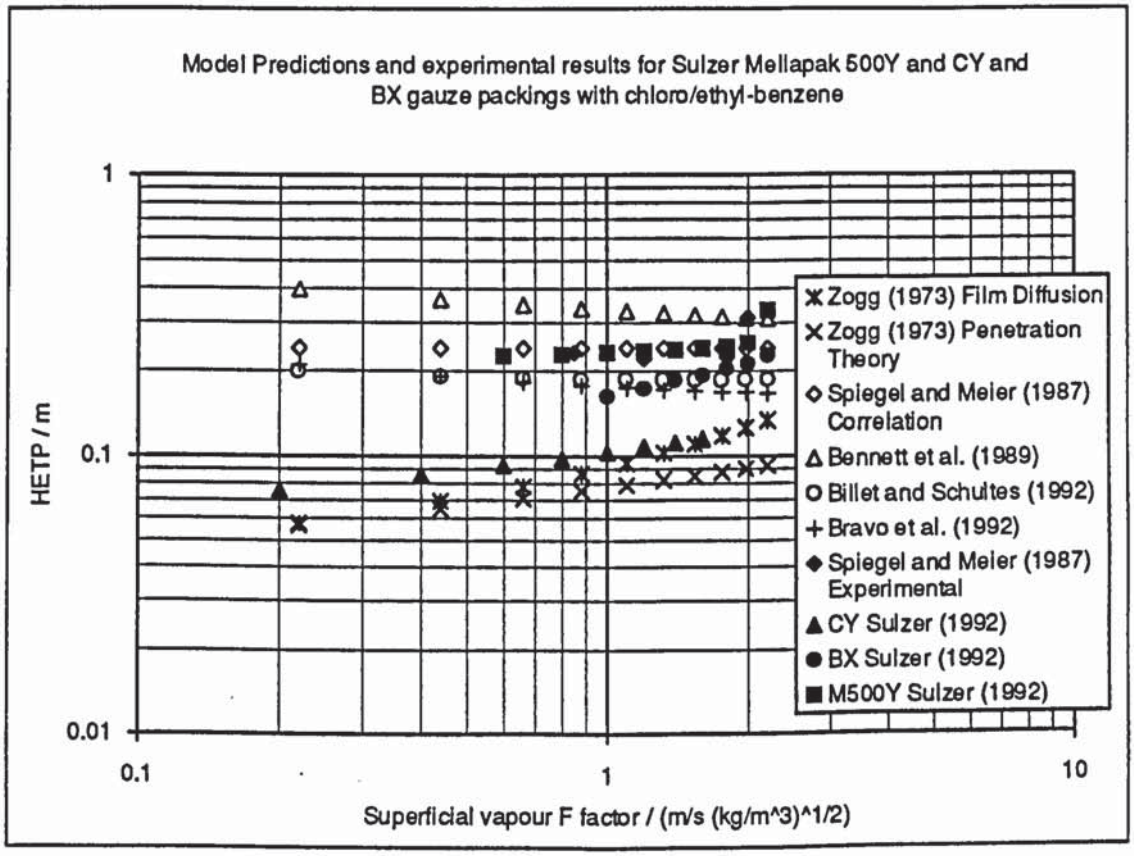

Figure 4-3 Experimental and predicted dependence of HETP on vapour flow (F-factor) at total reflux for Sulzer Mellapak 500Y and CY and BX gauze packings. Chlorobenzene/ethylbenzene test mixture at 960 mbar.

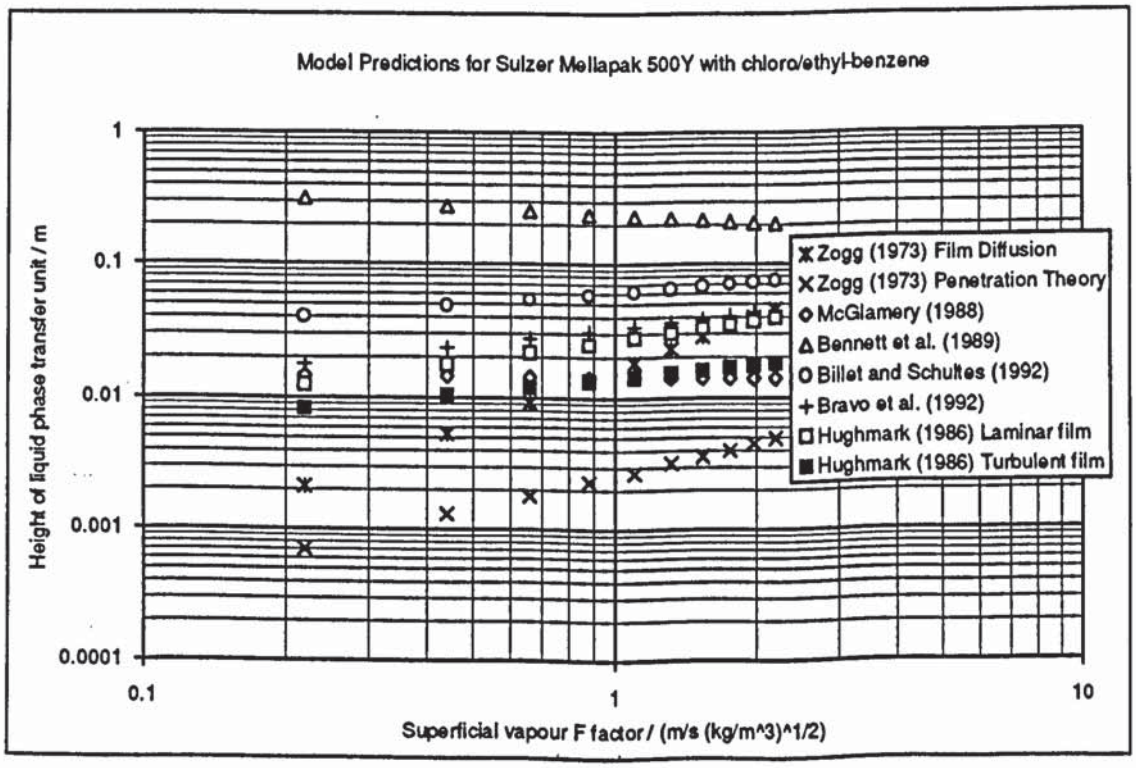

Figure 4-4 Comparison of model predictions of height of liquid phase transfer unit for chlorobenzene/ethylbenzene at 1 bar

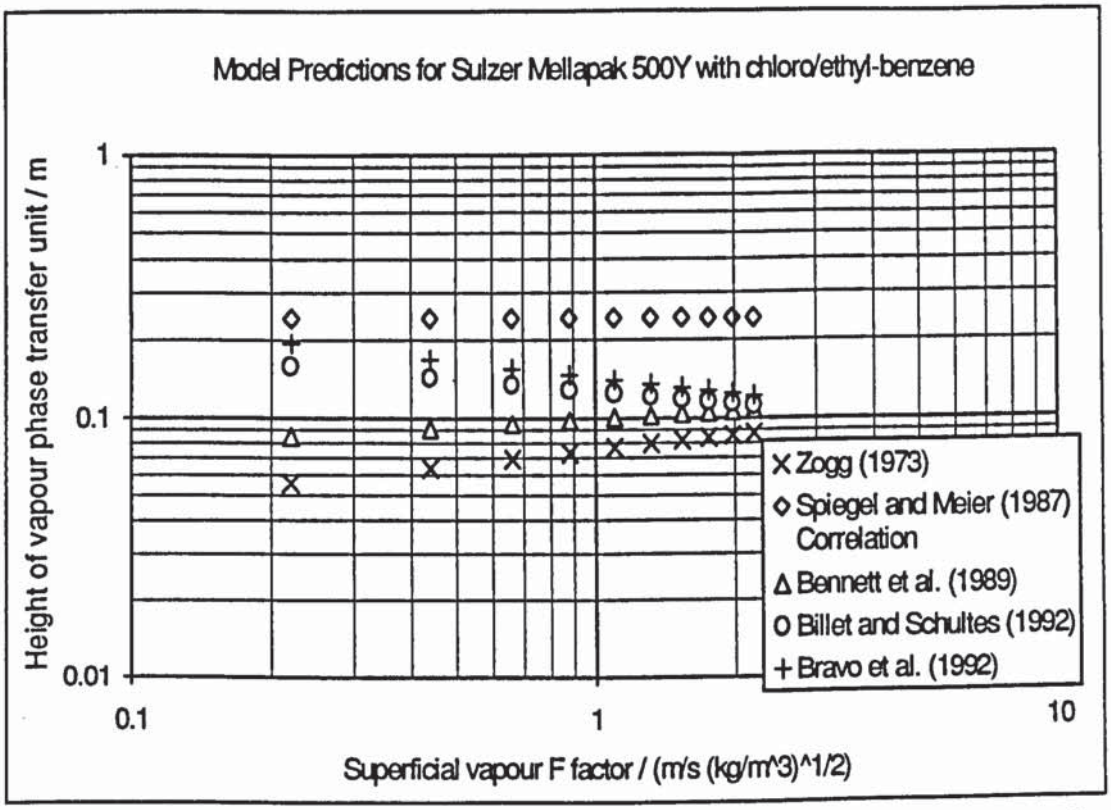

Figure 4-5 Comparison of model predictions of height of vapour phase transfer unit for chlorobenzene/ethylbenzene at 1 bar

Distillation system and operating pressure

Because the performance of a packing depends on the physical properties of the distillation system, it will change if the system or pressure is changed. It would be useful to predict the changes in performance of a packing for a new system or at a new pressure from results with a different system or pressure. Unfortunately, it is difficult to separate the effects due to a particular property on the packing performance, because all the properties normally change together. In addition, the relevant physical properties, particularly diffusion coefficients may be poorly known. However, Porter and Jenkins (1979) found that the physical properties of distillation systems correlated well with the total reflux flow parameter, that is the square root of the ratio of vapour density to liquid density. This means that we may be able to correlate the packing performance, which depends on these properties, against total reflux flow parameter so as to predict changes with pressure or system. Indeed, the capacity is already usually correlated against the flow parameter.

We shall now consider correlations against total reflux flow parameter of the results presented by Fair and Bravo (1987), Spiegel and Meier (1987 and 1992), Norton (1988), Sulzer (1992), and Bravo et al. (1992).

Capacity

Table 4-1 gives approximate expressions for the graphical results presented by each of the authors. As the flow parameter is increased, the capacity falls; the liquid and vapour are more similar and the liquid film occupies more of the packing. It appears that if the flow parameter is greater than about 0.1, the capacity falls more rapidly with increasing flow parameter (Fair and Bravo, 1987). This is due to an increased interaction between the vapour and the thicker, less viscous liquid film. Figure 4-6 illustrates the predictions of the different correlations. Spiegel and Meier's (1987) results under predict the others by about 10%, but the rest agree to within about 5%. Spiegel and Meier do in fact say that flooding occurs at a 10% higher flow than their definition of maximum capacity (10 mbar/m).

Author	Expression for capacity factor
Billet (1986) presented by Fair and Bravo (1987)	for X<0.08: $c_{gs,fl} = 0.345\ X^{-0.165}\ d^{0.40}$ for X>0.08: $c_{gs,fl} = 0.168\ X^{-0.450}\ d^{0.40}$
Spiegel and Meier (1987)	for X < 0.1: $c_{gs,fl} = 0.309\ X^{-0.30}\ d^{0.49}$
Sulzer (1992) brochure	for X < 0.1: $c_{gs,fl} = 0.374\ X^{-0.3}\ d^{0.4}\ (\sin\theta)^{1.4}$
Modified Alekseev et al. (1972) expression for structured packings.	$c_{gs,fl} = 0.460\ \varepsilon\ (\sin\theta)^{1.373}\ g^{0.373}\ X^{-0.180}\ d^{0.246} \left(\frac{\sigma}{\rho_l - \rho_g}\right)^{0.127} \left(\frac{\rho_l}{\rho_l - \rho_g}\right)^{0.090} \left(\frac{1+\mu}{\mu_w}\right)^{0.148}$

Table 4-1 Correlations of capacity factor against flow parameter.

Hold-up & Pressure gradient

Extensive data on the pressure gradient at total reflux are available, and some of these data are plotted in figure 4-7. As the total reflux flow parameter increases, the pressure gradient at the design point falls, due mainly to the reduced vapour velocity. The large scatter in the results is due to the difficulty in locating the flooding velocity and the rapid change in pressure gradient with throughput.

The system-dependent parts of the friction factor equation for dry pressure gradient give:

$$\left(\frac{dp}{dz}\right)_{dry} \propto \phi\ \rho_v\ u_{gs}^2$$

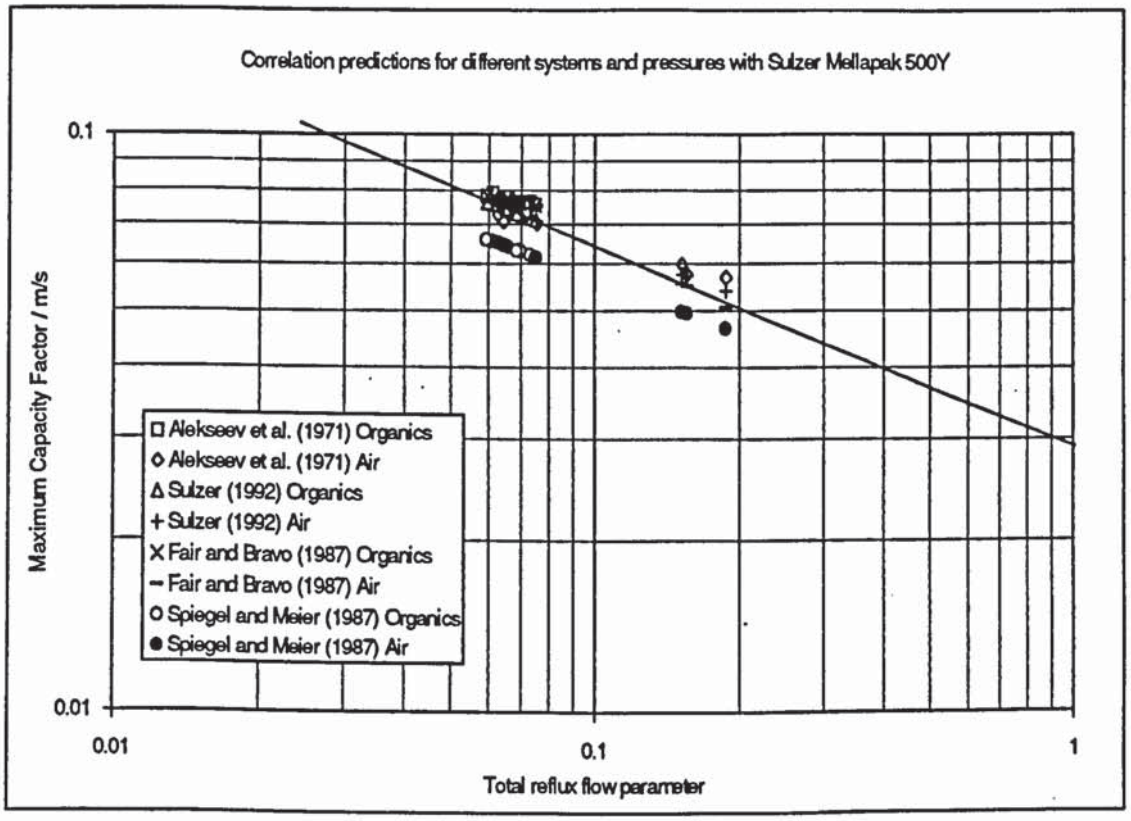

Figure 4-6 Comparison of flooding correlations for different distillation systems

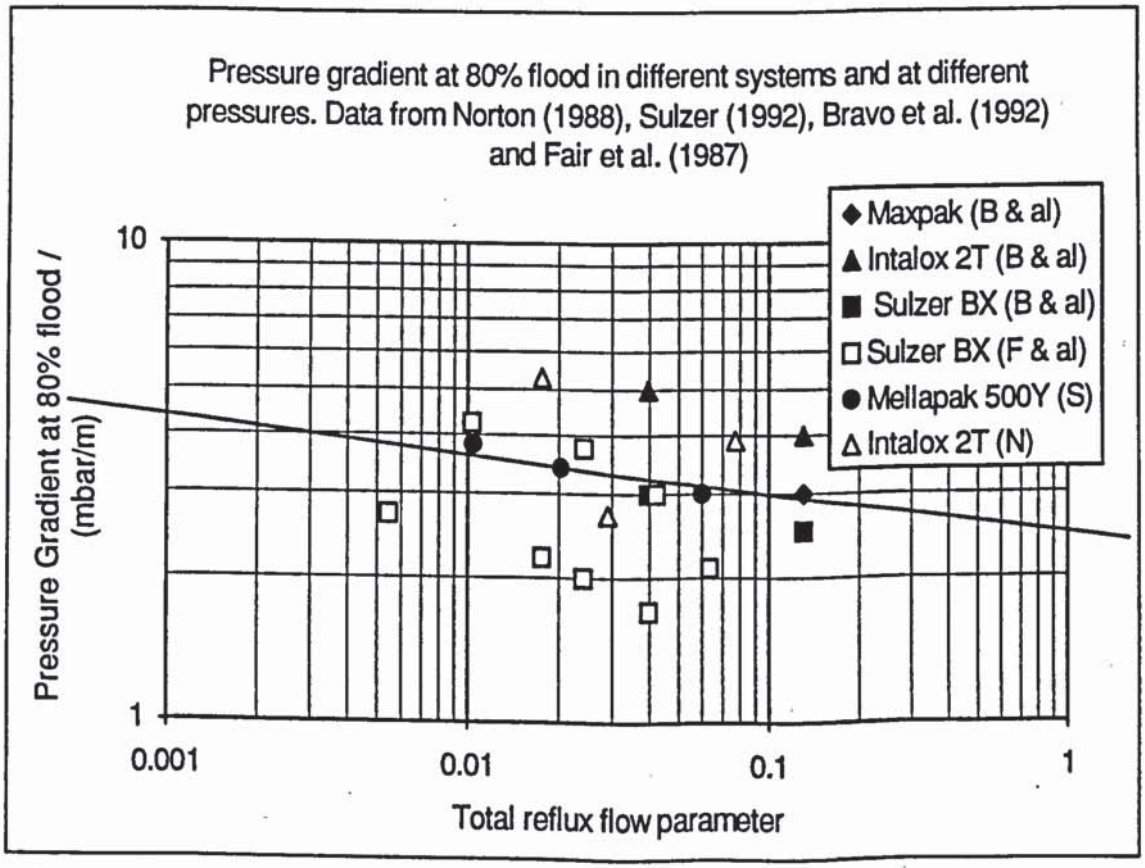

Figure 4-7 Pressure gradient at 80% flood for different systems and operating pressures

Now $u_{gs} \propto c_{s,fl} X_{\infty}^{-1}$, and $c_{s,fl} \propto X_{\infty}^{-0.3}$ so that

$$\left(\frac{dp}{dz}\right)_{dry} \propto \phi\, \rho_v\, X_{tt}^{-2.6} \propto \phi\, \rho_l\, X_{tt}^{-0.6}$$

Since ρ_l varies relatively slowly with X_{tt}, the dry pressure gradient at a particular fraction of flooding should be reduced as the density ratio increases, provided that the friction factor remains the same.

In fact, the dependence is approximately on $X_{tt}^{-0.1}$ rather than $X_{tt}^{-0.6}$. This is because, in a wetted packing, the friction factor will change with the properties of the system as the degree of interaction between the two phases changes. In this case it appears to increase as $X_{tt}^{0.5}$.

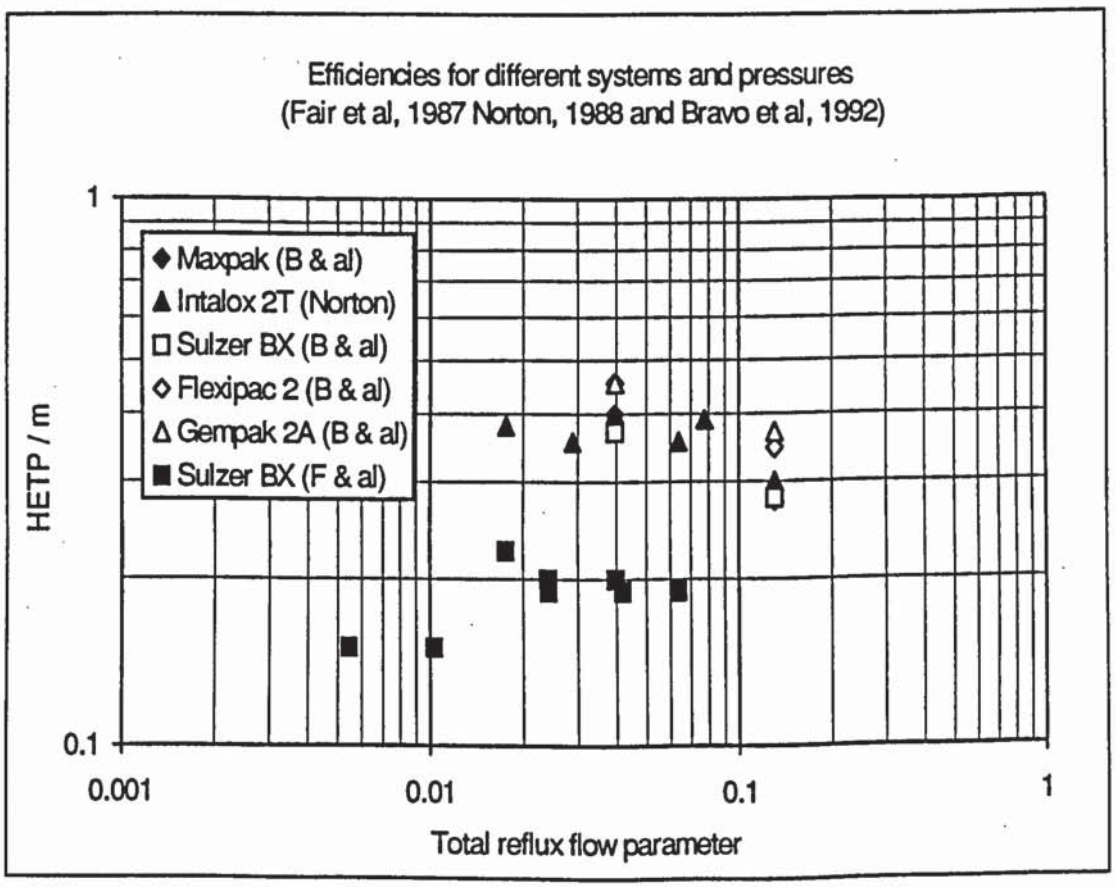

Figure 4-8 Efficiency at 80% flood for different systems and operating pressures

Efficiency

The efficiency is probably the most important parameter to estimate if the system or pressure is changed, since it determines whether the products may be produced at the required purity. Some results (Bravo et al, 1992; Norton, 1988 and Fair et al, 1987) are presented in figure 4-8. This shows that, for the results from a particular source, the efficiency tends to increase very slightly as the total reflux flow parameter increases, although at very low pressures, where the liquid load is very low, the efficiency may be much higher than expected. There is considerable scatter in the results, which is to be expected as data were obtained

under different conditions and the physical properties do not correlate perfectly against the flow parameter.

The predicted HETP for oxygen, nitrogen and argon at two pressures is plotted against total reflux flow parameter in figure 4-9. This shows that, as the pressure changes, the HETP is predicted to be proportional to the 0 to -0.5 power of total reflux flow parameter, depending on the model. Because different models predict different dependences of efficiency on pressure, it is difficult to predict with certainty the effect on the packing efficiency of changing the system pressure.

Figure 4-10 shows that the different models also predict differing HETPs for the same systems. Moreover, whilst some models predict that the efficiency will increase from one system to another, others predict that it will be reduced. Even if we do not consider the model of Bennett et al. (1989), the variation between models for a particular system is greater than the variation in efficiency predicted by a particular model from system to system. Althogh figure 4-8 showed that the efficiency seemed to correlate reasonably well with X, it is still difficult to predict with any degree of accuracy the efficiency of an untested system.

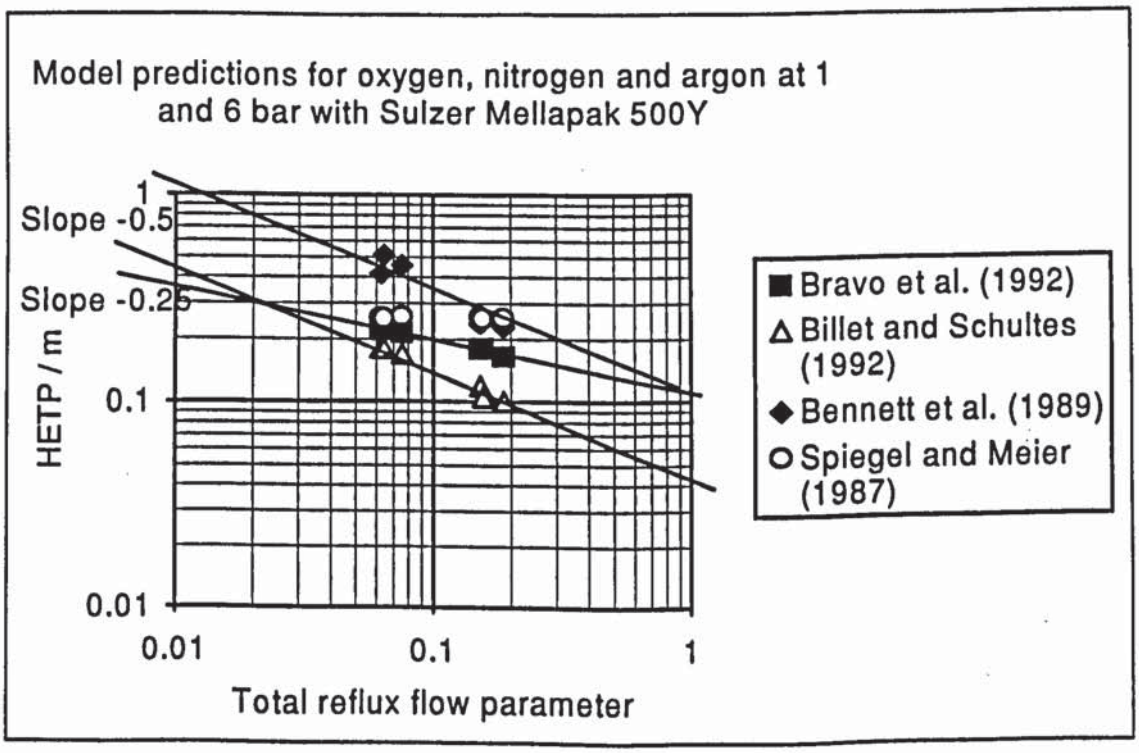

Figure 4-9 Model predictions for HETP for air at 1 bar and 6 bar plotted against total reflux flow parameter for 500Y packing

Packing performance in air separation

There are no data available in the open literature on the performance of commercially available structured packings with the oxygen-nitrogen-argon system. So this work on models to predict the performance of packings with different distillation systems was intended to allow us to estimate the performance

of a particular packing in air distillation. But the large differences between the different prediction methods give an indication that such an estimate would not be very accurate. The predictions for air distillation at 1 bar and 6 bar are presented in figures 4-9 and 4-10 along with the predictions for some organic test mixtures.

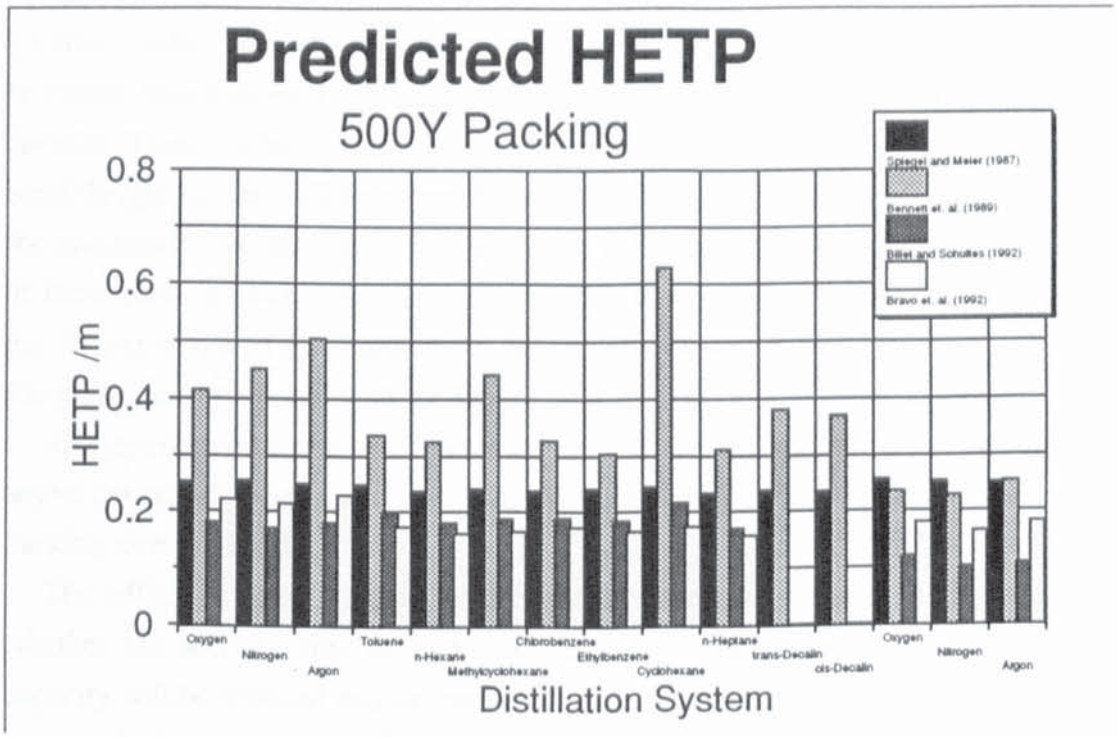

Figure 4-10 Model predictions of HETP for different system components for 500Y packing

The models of Spiegel and Meier (1987) and Billet and Schultes (1992) predict a similar HETP for air as in organic systems, whereas the others calculate it to be higher. The predictions of higher HETP are mainly due to the lower diffusivity in the air system because of the very low temperatures, particularly in the liquid; the liquid Schmidt number is about twice that of the organic systems. Most of the models predict a reduced HETP at higher pressure for the air system; the liquid phase resistance is reduced by the higher liquid diffusivity, the vapour phase resistance is reduced because the Reynolds number is increased as the density increases and the interfacial area is increased because the wetting gets better as the surface tension is reduced.

Packing Geometry

Packings which are available commercially all have a similar geometry; they have been optimised for most general applications within the chemical industry. We have, however, seen that the economics of distillation columns are different in air separation than in other applications because of the requirement to minimise the pressure drop and column surface area. As a consequence, we should expect that

a simple change in packing geometry could improve the economic viability of structured packing in air distillation. To predict the effects of such a change, we must first examine the existing geometries in more detail.

Spiegel and Meier (1987) published test results for four different sizes of Mellapak with the chlorobenzene / ethylbenzene mixture at several pressures. In addition, Sulzer give representative results for all types of Mellapak in their 1992 brochure, based on tests with chlorobenzene / ethylbenzene and cis-decalin / trans-decalin. These packings range in specific area from 125 to 750 m^2/m^3, all have a block height of about 200 mm and have channel angles of 45 and 60 degrees from the horizontal. Sulzer (1992) also present a correlation for the maximum capacity of these packings based on tests with air and water. Because these results cover the widest range of packings under similar conditions, it is these which will be correlated and compared with the model predictions.

The geometrical variables of potential interest are: the specific area; the channel angle; the channel shape, surface texture and crimp angle; the void fraction; and the packing element height.

The effect of void fraction is difficult to ascertain, because it depends on whether the specific area or hydraulic diameter is maintained. In general, the capacity will be reduced and the pressure gradient increased as the void fraction is increased. Anyway, the void fraction is of little importance in structured packings since it is usually greater than 0.95.

No experimental data exist on the effect of packing block height on packing performance and none of the models predicts any effect. It could be expected to alter the performance, particularly the pressure gradient, because the vapour would have to change direction more often in a given height. However, due to the lack of data, we shall not consider this further.

Neither are we able to study the influence of the channel shape, surface texture or crimp angle; no data exists which allows a comparison under similar circumstances.

We will now consider the dependence of the experimental capacity, pressure gradient and efficiency on the specific area and channel angle.

Capacity

Figure 4-10 is a logarithmic plot of capacity factor at flooding against specific area for the two channel angles. This shows that the capacity may be approximated by

$$c_{s,max} = 1.43 (\sin \theta)^{1.4} a^{-0.4}$$

The capacity is therefore reduced as the channels are made more horizontal or their diameter is reduced (specific area increased).

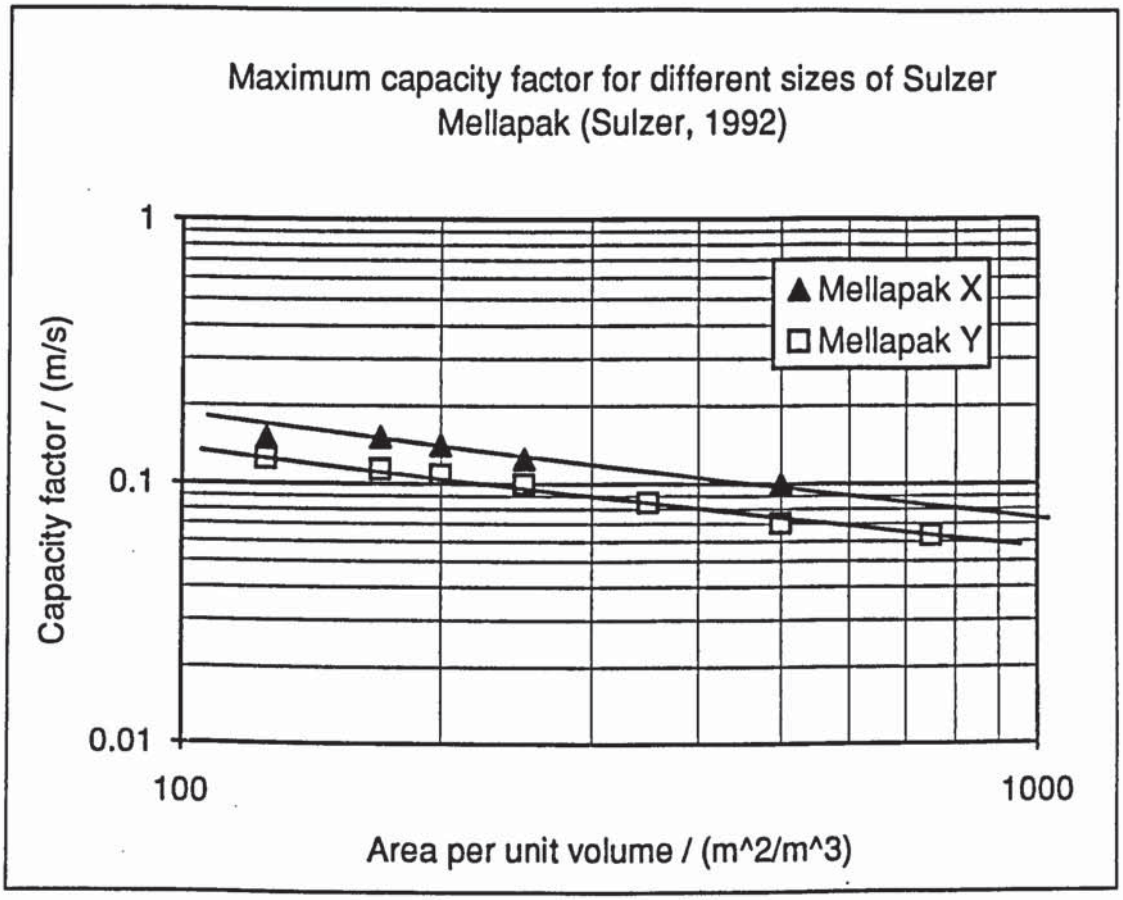

Figure 4-10 Logarithmic plot of maximum capacity factor at X=0.07 against specific area for Mellapak (Data from Sulzer, 1992)

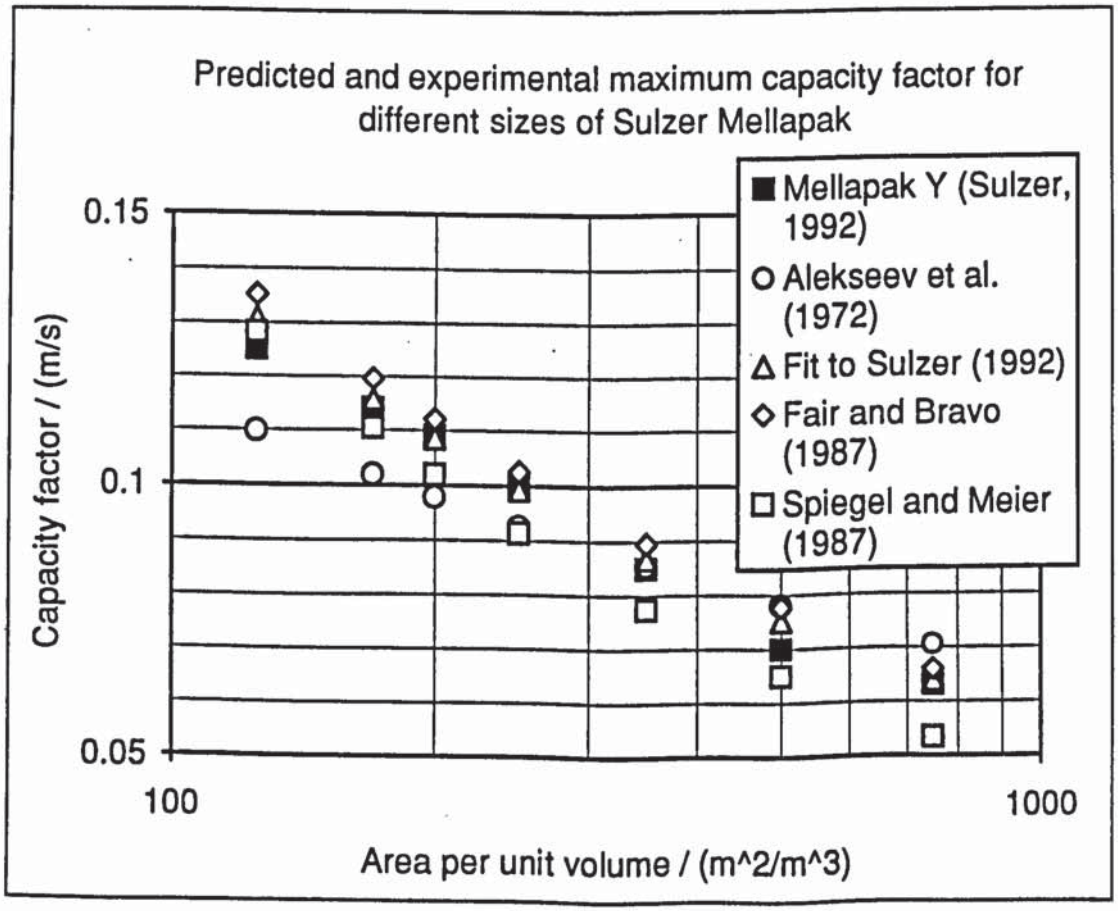

Figure 4-11 Comparison of flooding correlations for different specific areas

Figure 4-11 shows the predictions of the different flooding correlations for different packing areas. The modified expression of Alekseev et al. (1972), which was best for wetted wall columns, shows the worst agreement; the predicted dependence of capacity on area is lower than the results show. The other expressions show good agreement with the data except for that of Spiegel and Meier (1987), which tends to under predict the capacity of higher area packings. This could be because hydraulic flooding occurs at a higher pressure gradient in these packings and so a constant pressure gradient definition of flooding will under predict the capacity.

The only flooding model to allow the channel angle to be accounted for is that of Alekseev et al. (1972) after it has been modified for structured packings. This gives $c_{s,fl} \propto (\sin \theta)^{1.373}$, which is in good agreement with the empirical data.

Pressure gradient

In figure 4-12, the pressure gradient at a constant fraction of flooding is plotted logarithmically against specific area. This shows that the design pressure gradient for Mellapak may be approximated as:

$$\frac{dp}{dz} = 0.631\ a^{0.2}$$

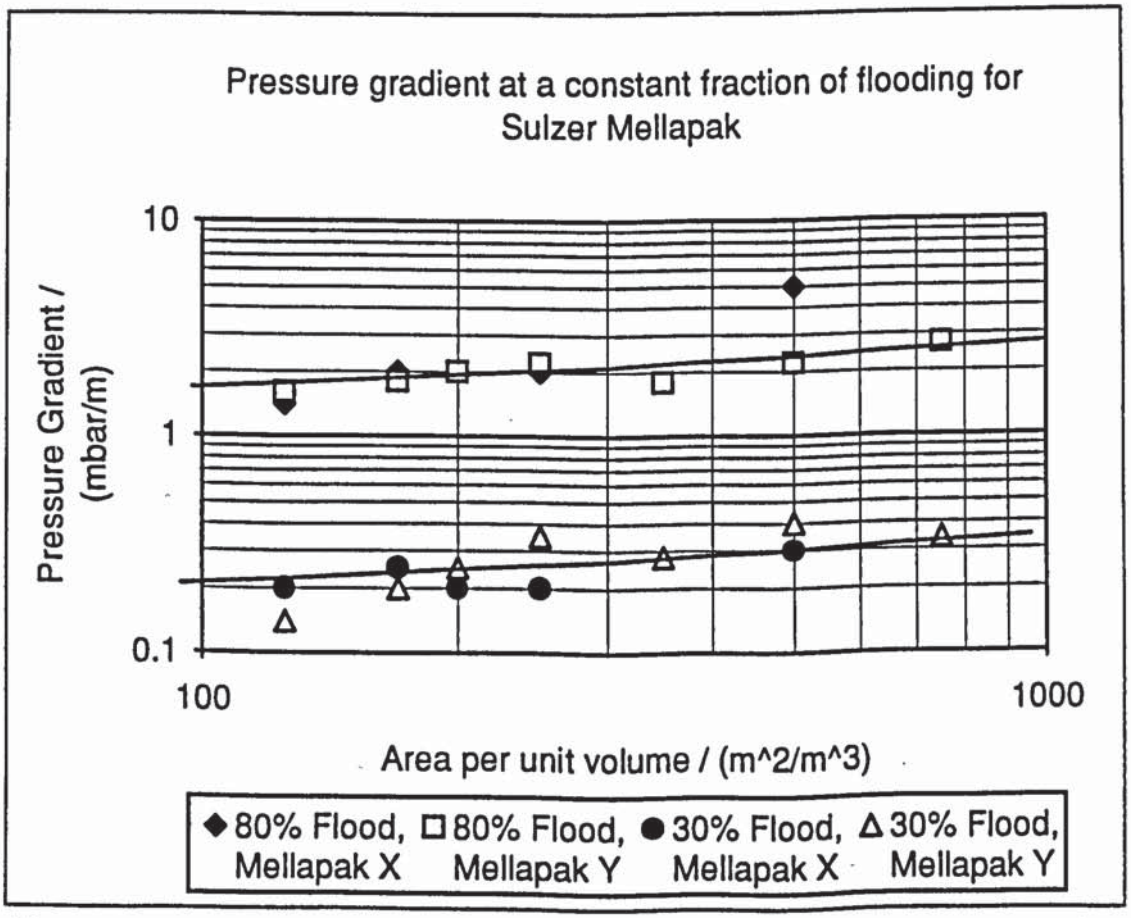

Figure 4-12 Logarithmic plot of pressure gradient at 80% flood against specific area for Mellapak. (Data from Sulzer, 1992)

This applies to all the packings except the 500X, which has an unexpectedly high pressure gradient. There is a considerable amount of scatter on these results because the rapid variation of pressure gradient with vapour velocity around the design point means that errors in the design velocity are amplified in the pressure gradient. The pressure gradient at the design point does not appear to depend on the channel angle.

The general theoretical expression for pressure gradient in a dry packed bed (or an irrigated one below loading) is:

$$\frac{dp}{dz} = 4\,\phi_{local}\,\frac{\rho_g\,u_{gs}^2}{(\sin\theta)^3\,d}$$

where ϕ_{local} is a local friction factor which (with a given mixture) depends only on channel shape and surface texture.

At a constant fraction of the design velocity, this gives a dependence on the geometric variables of:

$$\frac{dp}{dz} \propto \phi_{local}\,\frac{u_{gs}^2}{(\sin\theta)^3\,d} \propto \phi_{local}\,(\sin\theta)^{-0.2}\,d^{-0.2} \propto \phi_{local}\,(\sin\theta)^{-0.2}\,a^{0.2}$$

This suggests that, in Mellapak, the friction factor does not depend on specific area and it increases slightly as the channels are made more vertical (as $(\sin\theta)^{0.20}$).

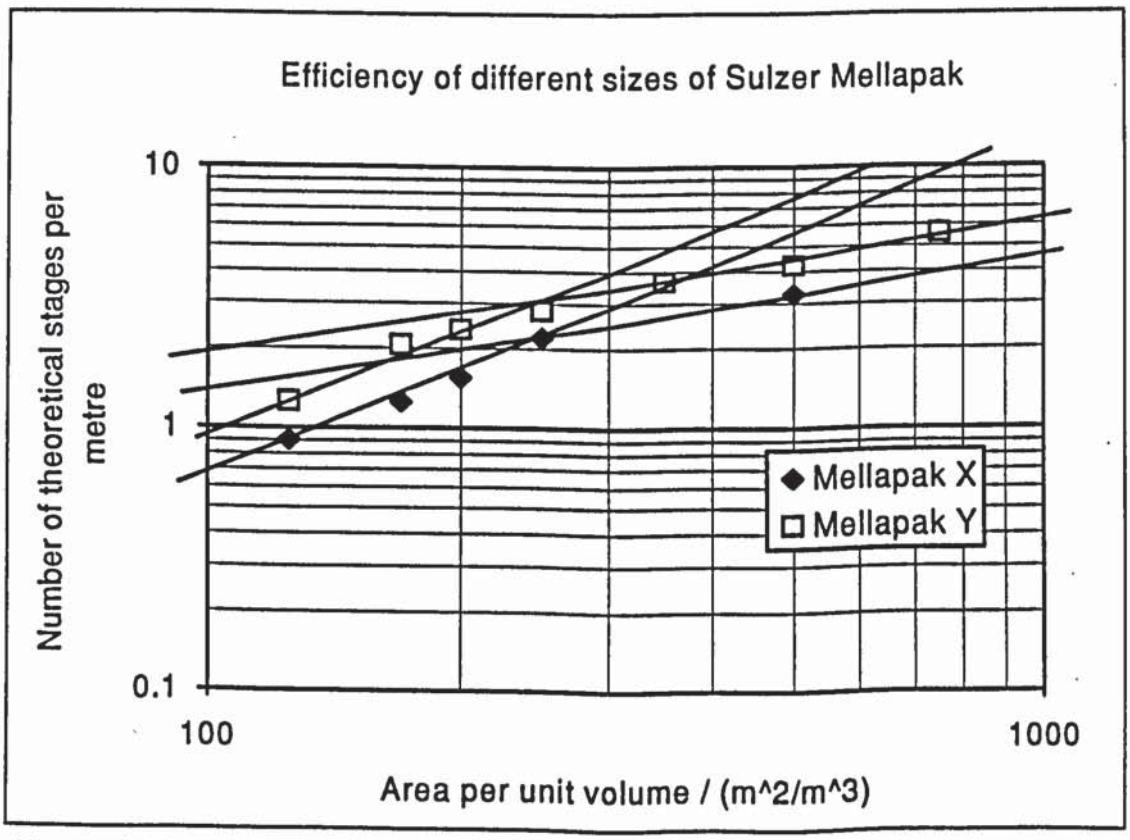

Figure 4-13. Logarithmic plot of number of theoretical stages per metre against specific area for Mellapak. (Data from Sulzer, 1992)

Efficiency

Like the pressure gradient, the efficiency (NTSM) is plotted logarithmically against area at a constant fraction of the maximum capacity (figure 4-13).

This gives the approximations:

$NTSM = 0.00133 (\sin \theta)^{-1.65} a^{1.3}$ if $a < 250$ m^2/m^3 or

$NTSM = 0.110 (\sin \theta)^{-1.65} a^{0.5}$ if $a > 250$ m^2/m^3

Or, written in terms of HETP:

$HETP = 752 (\sin \theta)^{1.65} a^{-1.3}$ if $a < 250$ m^2/m^3 or

$HETP = 9.09 (\sin \theta)^{1.65} a^{-0.5}$ if $a > 250$ m^2/m^3

The efficiency of the packing increases as the specific area is increased and as sin θ becomes smaller, that is, as the channels are made more horizontal. When the specific area is greater, the efficiency increases more slowly with area. There are two reasons for this. It becomes increasingly difficult to wet the larger surface, and the liquid film resistance becomes more dominant as the vapour phase resistance decreases in the smaller channels.

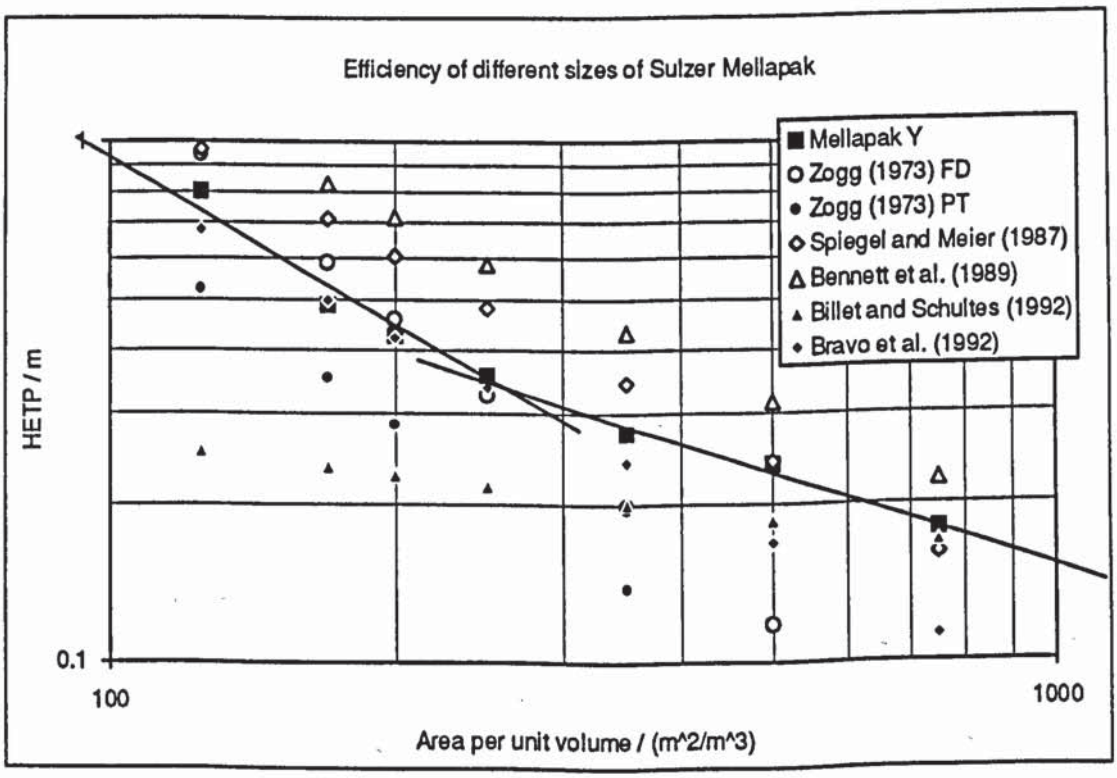

Figure 4-14 Experimental and predicted efficiency of Mellapak Y with different specific areas.

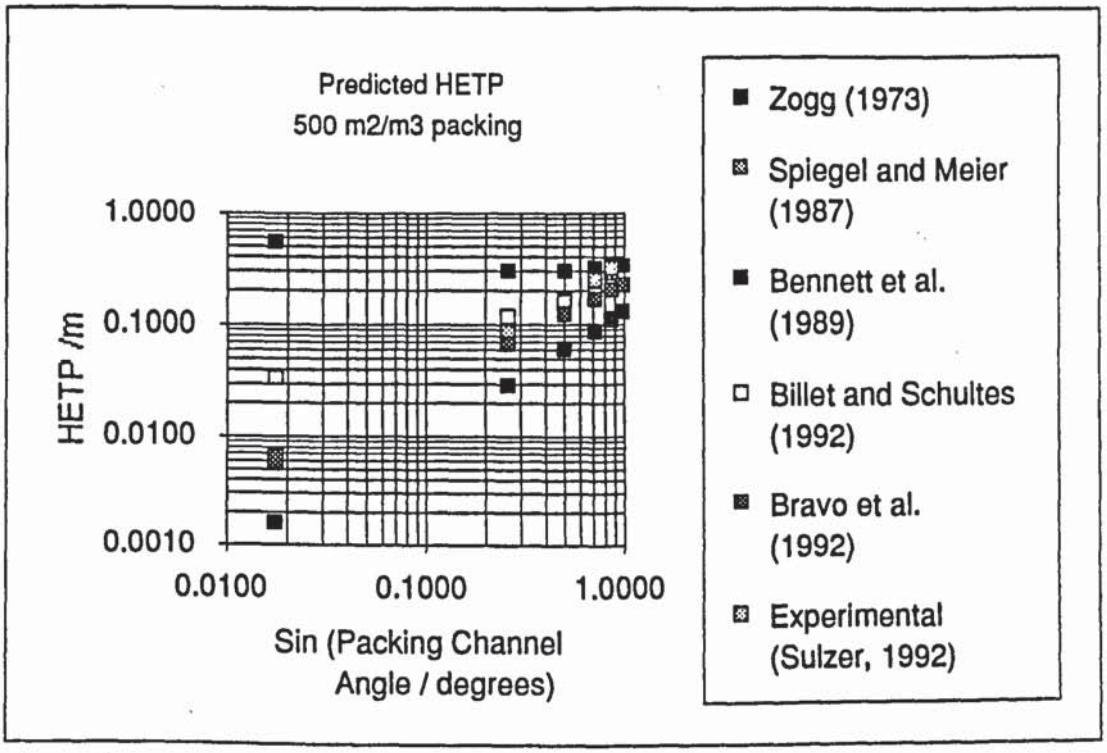

Figure 4-15 Experimental and predicted dependence of HETP on channel angle.

The empirical dependence of HETP on specific area (on $a^{-1.3}$ or $d^{1.3}$) agrees approximately with the models in low area packings with larger hydraulic diameters (figure 4-14). The reduction in the strength of the dependence in high area packings to $a^{-0.5}$ or $d^{0.5}$ is not accounted for by these models. It could be explained if the liquid phase resistance became dominant and depended weakly on area, however most of the models for H_L have a dependence on d^n where $n>0.5$. Another possibility is that the wetting becomes worse as the area is increased, but this ought to be accounted for in those models which take wetting into account.

Figure 4-15 shows that all the models except for that of Bennett et al. (1989) give similar dependences of efficiency on channel angle to the experimental one. In the model of Bennett et al. (1989) the liquid phase resistance is important and the dependences of vapour and liquid resistance on channel angle cancel.

Conclusions

We have seen that a number of different models and correlations have been used to describe and predict the performance of conventional structured packings, with varying degrees of success. Changes in distillation system are difficult to allow for because of the number of physical properties which influence the results and the uncertainty in their value. The pressure gradient and liquid hold-up in a wetted packing and the flooding velocity are difficult to predict because of the difficulty in describing the complex two-phase flow, however they may be well correlated for a particular type of packing. Efficiency may be measured, but separating vapour and liquid phase resistances is difficult and there is much uncertainty in the model

predictions, particularly for the liquid phase. We can make use of the predictions of the models and correlations for different test mixtures and packing geometries, but must do so with caution as the accuracy of the results is limited.

4.2 Improvements to packings for air separation use

The economic work has shown there is usually an optimum packing for a particular application. The current range of packings is limited in that only two channel angles are available in a limited number of specific areas. It is likely that the optimum packing will in many cases be outside the range available, even if the basic shape is the same. As a result, a relatively simple change in the geometry could produce a more economic packing.

The economic evaluation of packings in air separation shows the relative importance of the different aspects of the performance and the cost of the packing. It is clear from the results in tables 3-11 and 3-12 that the mass transfer efficiency affects the rate of return most strongly; a certain percentage change in the HETP has more impact than the same percentage change in any of the other variables. The rate of return is also quite sensitive to the packing capacity and the distributor height, whilst it is less dependent on the pressure gradient and packing and distributor costs.

We will now consider what changes could be made to the existing shape to increase the economic advantage. We shall then identify changes to the packing shape which could further enhance the benefit. Finally we shall look at changes in the materials and manufacturing process to reduce the packing cost.

4.2.1 Changes to packing geometry

Changing the existing packings to reduce the HETP will inevitably lead to an reduction in capacity. Nevertheless, two changes will be explored; increasing the specific area and reducing the channel inclination angle.

Increasing surface area per unit volume

To find the effect on the efficiency of increasing the specific area, we shall use the empirical correlation derived from figure 4-13, because it gives the most pessimistic prediction of HETP. For a 45 degree channel angle, the predicted HETP at 1000 m^2/m^3 is 0.162 m compared with 0.187 m (about 13% less) at 750 m^2/m^3. The pressure gradient is not significantly changed, but the drawback is that the maximum capacity factor (at X=0.07) is reduced from 0.062 m/s to 0.056 m/s (about 10%), and the cost increased from about £4000 to £5330 per m^3 (30%).

Plant size	t/d O2	10451	1742	290	29
Base case rate of return	%	28.9	14.3	-3.2	-24
Rate of change of rate of return with:					
Packing cost	%/(£/m^3)	-0.0095	-0.0038	-0.001	-0.00015
Pressure gradient	%/(mbar/m)	-1.64	-1.32	-1.02	-1.09
Maximum capacity	%/(m/s)	775	560	340	190
HETP	%/m	-323	-250	-168	-136
Test case values:	Base case				
Packing cost	4000	5333	5333	5333	5333
Pressure gradient	3	3	3	3	3
capacity	0.065	0.059	0.059	0.059	0.059
HETP	0.2	0.173	0.173	0.173	0.173
Difference in rate of return from base case due to:					
Packing cost		-12.6	-5.1	-1.3	-0.20
Pressure gradient		0	0	0	0
Maximum capacity		-4.65	-3.36	-2.04	-1.14
HETP		8.74	6.75	4.56	3.68
Total		-8.54	-1.71	1.18	2.34

Table 4-2 Estimated effect on rate of return of increasing specific area to 1000 m^2/m^3.

In table 4-2 these results (modified to allow a design margin and to account for the actual flow parameter) are used with the linearised dependence of the rate of return on these variables to estimate the change in rate of return for several plant sizes. This table shows a slight increase in rate of return in small plants, but a reduction in larger ones as the packing cost becomes important. This indicates that there is a relatively small amount to be gained by further increasing the specific area of current packings.

Reducing channel angle with horizontal

In this case we shall assume that the HETP is proportional to sin θ, as predicted by most of the models for vapour phase resistance. This will give the most pessimistic results. If we replaced the 750Y packing with one with channels at 30 degrees to the horizontal, we predict a reduction in HETP from 0.187 m to 0.132 m (30%). Again, we find that the pressure gradient is not significantly changed but that the maximum capacity factor is reduced from 0.062 to 0.038 (39%), however the cost remains the same in this case. Putting these changes into the linearised expression for rate of return near the base case (table 4-3, we find that it is slightly increased for all plant sizes. The increase is larger for smaller plants, as in the case of increased area. The table indicates that making the channels more horizontal is better than increasing the specific area, because it does not increase the packing cost.

Plant size	t/d O2	10451	1742	290	29
Base case rate of return	%	28.9	14.3	-3.2	-24
Rate of change of rate of return with:					
Packing cost	%/(£/m^3)	-0.0095	-0.0038	-0.001	-0.00015
Pressure gradient	%/(mbar/m)	-1.64	-1.32	-1.02	-1.09
Maximum capacity	%/(m/s)	775	560	340	190
HETP	%/m	-323	-250	-169	-136
Test case values:	Base case				
Packing cost	4000	4000	4000	4000	4000
Pressure gradient	3	3	3	3	3
capacity	0.065	0.04	0.04	0.04	0.04
HETP	0.2	0.14	0.14	0.14	0.14
Difference in rate of return from base case due to:					
Packing cost		0	0	0	0
Pressure gradient		0	0	0	0
Maximum capacity		-19.4	-14	-8.5	-4.75
HETP		19.4	15	10.1	8.2
Total		0	1.0	1.6	3.4

Table 4-3 Estimated effect on rate of return of reducing channel angle with horizontal to 30 degrees

Plant size	t/d O2	10451	1742	290	29
Base case rate of return	%	28.9	14.3	-3.2	-24
Rate of change of rate of return with:					
Packing cost	%/(£/m^3)	-0.0095	-0.0038	-0.001	-0.00015
Pressure gradient	%/(mbar/m)	-1.64	-1.32	-1.02	-1.09
Maximum capacity	%/(m/s)	775	560	340	190
HETP	%/m	-324	-250	-169	-136
Test case values:	Base case				
Packing cost	4000	4000	4000	4000	4000
Pressure gradient	3	6	6	6	6
capacity	0.065	0.065	0.065	0.065	0.065
HETP	0.2	0.17	0.17	0.17	0.17
Difference in rate of return from base case due to:					
Packing cost		0	0	0	0
Pressure gradient		-4.92	-3.96	-3.06	-3.27
Maximum capacity		0	0	0	0
HETP		9.71	7.5	5.06	4.09
Total		4.79	3.54	2.00	0.82

Table 4-4 Estimated effect on rate of return on changing channel shape to reduce HETP by 15% and double pressure gradient.

Changes to packing shape

Changes in the packing shape should be designed to increase the efficiency without significantly reducing the capacity at a particular specific area. This will

almost certainly lead to an increased pressure gradient, but, as we found in the economic analysis, this is relatively unimportant. It might also lead to a reduction in capacity, depending on the nature of the modification. Table 4-4 illustrates that if the HETP could be reduced by 15% at the expense of doubling the pressure gradient but without changing the capacity or packing cost, then the rate of return may be increased, particularly for large plants. Indeed, for large plants in which packings are most likely to be used, this would prove more advantageous than either of the previously considered improvements.

So far, as we have seen in chapter 2, packing development has been concentrated on reducing the liquid phase resistance to mass transfer. However, most of the models predict a very much lower resistance in the liquid phase than in the vapour. This is common in distillation, as opposed to absorption, where the liquid phase resistance is often dominant. It suggests that there is potential for reducing the vapour phase resistance by modifying the packing shape.

The liquid phase resistance must still be taken into account, however, because it becomes more important as the distillation pressure (flow parameter) or specific area of the packing increase or if the vapour phase resistance is reduced. So the liquid spreading and mixing characteristics of any new shape should therefore be at least as good as in current packings.

In the folded surface type of packing, both the vapour and liquid are directed along the channels. Both phases can mix at the points where the channels cross, so we would expect an enhancement in mass transfer over plain tubes. In grid-type packings such as Rombopak, the liquid is directed over a surface, whilst the vapour is not directed, but is well mixed around the packing.

The advantage of the folded surface is that it maintains control of the liquid film at high flows, whereas the efficiency of the grid type packings tends to fall at high flows and higher operating pressures where the surface is not sufficient to hold all the liquid. The grid type packings should, however, have a lower vapour phase resistance, as the vapour should be more turbulent.

The survey of mass transfer augmentation techniques identified several ways of increasing the mass transfer in both phases. The best regime for both phases is the turbulent or transition one. This is normally achieved in the vapour, but if the packing surface were smooth, the liquid flow would be laminar. This is why most packings have a roughened surface - it renders the liquid film partly turbulent and reduces the liquid phase resistance. Mixing across the liquid film is beneficial in the same way as turbulence and is promoted by the presence of holes in the sheet as well as by the surface texture and breaks in the surface, for example at block boundaries. Because we are interested in mass transfer from the liquid film to the vapour rather than to the wall, it is the interface which should be disturbed as opposed to the liquid adjacent to the wall. This means that, although mass transfer

to liquids may be increased by small scale roughness in the boundary layer, large scale roughness is needed on the packing surface to achieve roughness in the interfacial boundary layer. In his experiments, McGlamery (1988) tested a number of surfaces which are used in structured packings and concluded that the one with the lowest liquid film resistance was the fluted surface used in Sulzer's Mellapak. Since this surface was already produced at the Tianjin University Packing Factory, it was decided that this should be used in the new packing. If time permitted, alternatives could be investigated.

In the vapour, large scale roughness or disturbance of the main flow would be needed to reduce the mass transfer resistance. This fits the requirement for the liquid phase of disturbing the interface, as large scale protrusions into the vapour flow would project through the interface. This suggests that the packing should have tabs pressed out of the surface into the channels to create turbulence in the vapour phase and mixing and interfacial turbulence in the liquid. These tabs could be twisted to promote swirl flow in the vapour and further reduce its mass transfer resistance. Some prototype packings with such tabs were made from cardboard and are illustrated in figure 4-16.

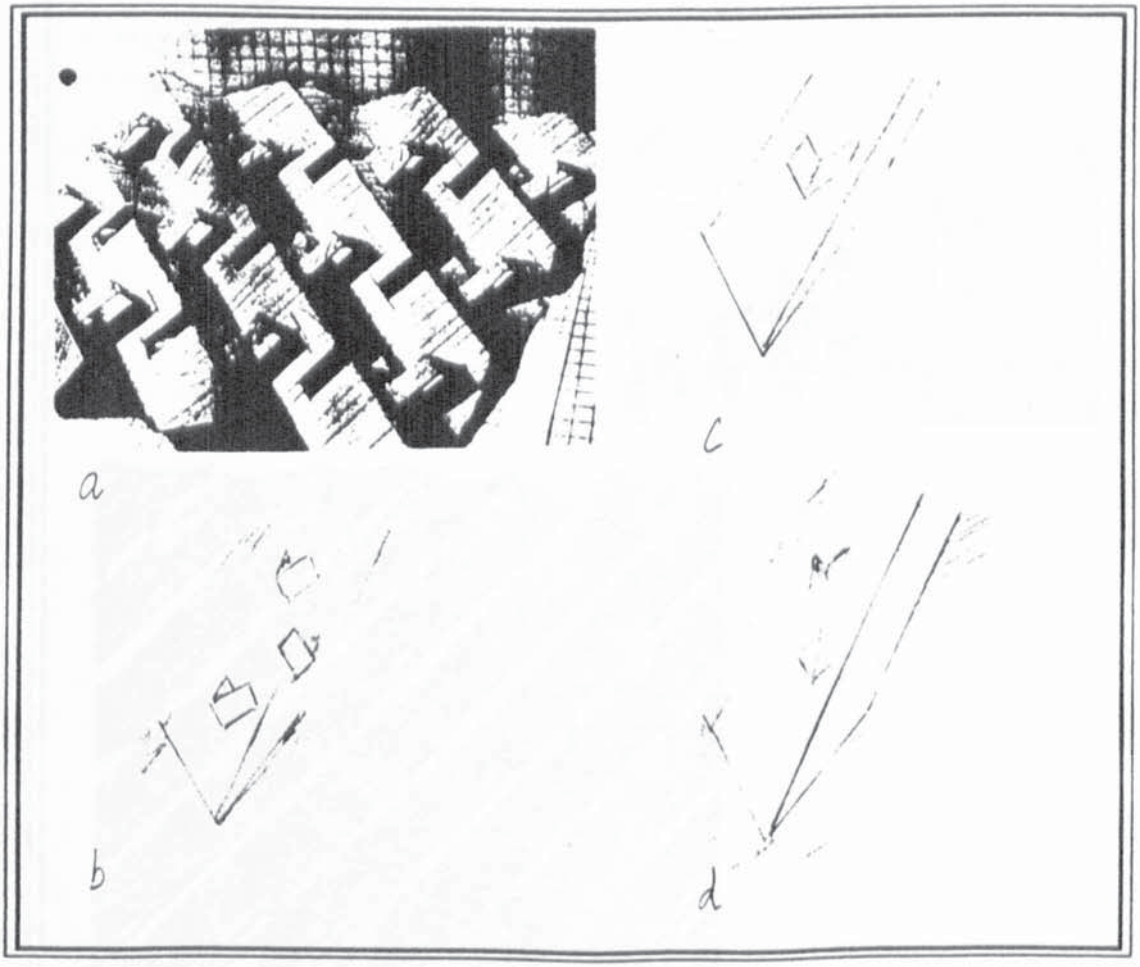

Figure 4-16 Prototype packings with tabs to disturb the vapour flow

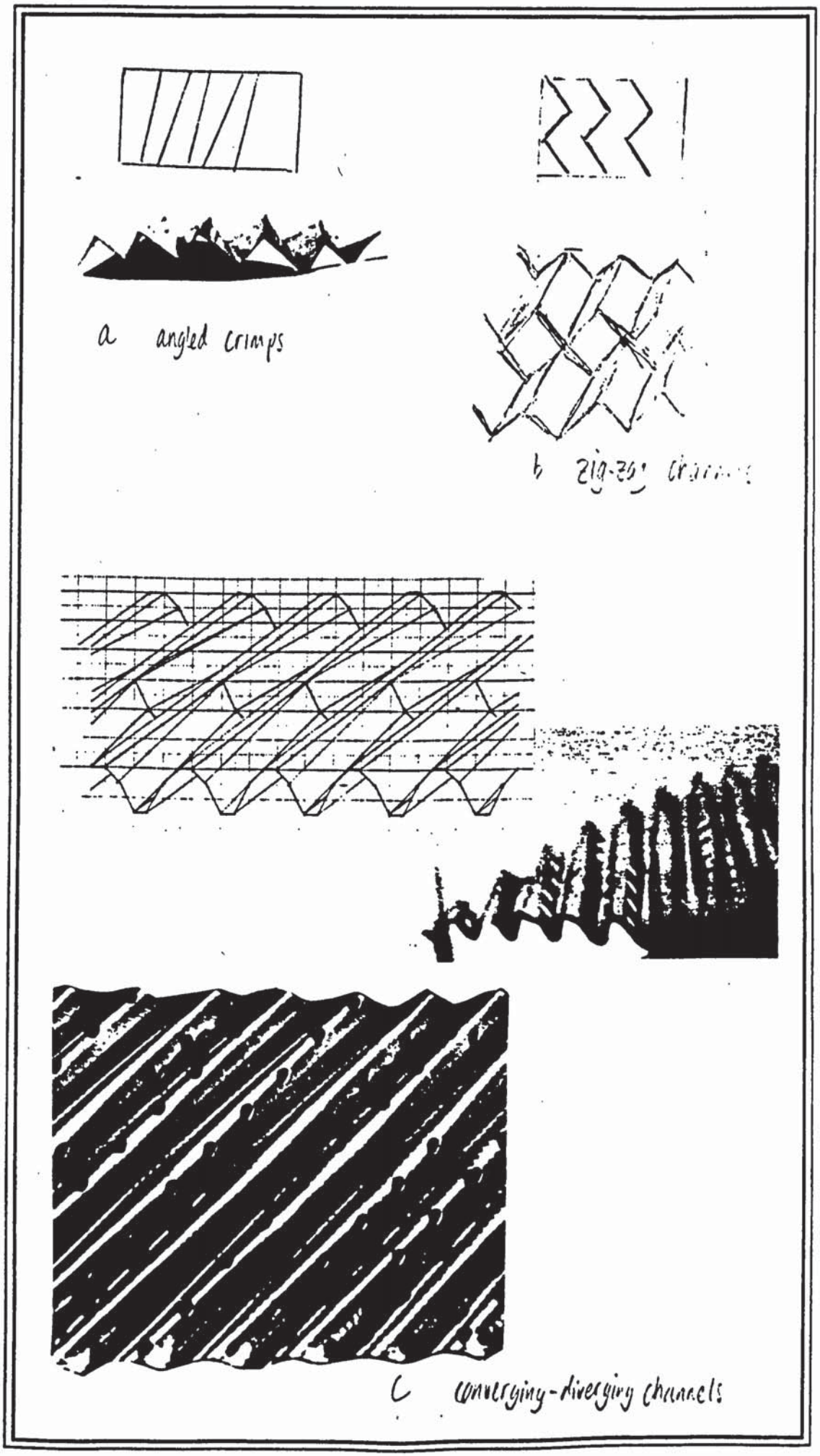

Figure 4-17 Prototype packings with new channel shapes

An alternative way to disturb the main vapour flow would be to change the shape of the channels, for example so that they followed a zigzag course or so that their cross section varied. Cardboard prototypes were also made of these ideas, and these are illustrated in figure 4-17. Only the packing with the variable cross section channels was chosen for manufacture and testing, and the reasons for this are discussed later.

4.2.2 Changes in materials and manufacturing process - cost reduction

The economic analysis of the manufacturing process identified that the minimum cost occurs where the material cost is about half the total manufacturing cost. The remainder of the cost is due to the labour, machine and tool costs. In the labour intensive process which was considered, the labour costs are considerably more than the tool costs. This suggests two obvious ways to cut the cost of packing; to cut the material cost or to automate the process.

Material cost

Some progress has already been made by packing manufacturers towards cutting material costs. The original Mellapak and Tianjin university packings were made from 0.2 mm thick metal - the minimum possible for the packing to be rigid enough. Embossing the surface, rather than corrugating it has allowed this to be reduced to 0.1 mm.

Alternative ways of reducing the metal content whilst maintaining the surface area would be to use expanded metal or to use even thinner metal reinforced by, for example, folding it over at the edges or by modifying the packing shape to increase rigidity.

Manufacturing cost

The most labour intensive parts of the packing manufacture are the initial stages which produce the crimped sheets. If these could be automated so that supervision of the machines could be reduced, the labour time could be significantly reduced.

Alternatively, the cost could be reduced by devising a completely different, continuous production method. Examples of such processes include roll-forming and roller pressing. A preliminary investigation of these processes led to the conclusion that they were unsuitable for small scale production of a prototype packing. As a result, these cost reduction techniques have not been explored in detail here as they would be more appropriately carried out as part of a development programme of a particular packing. It is impracticable to develop a

new production process to manufacture only enough packing to perform initial tests.

4.3 Choice of shape for easy and economic manufacture

To test any of the new packing shapes, the new packing needed to be manufactured in sufficient quantity. This meant that the shape should be suitable for small scale, low cost manufacture as well as being economic to manufacture on a large scale. Most of the proposed shapes could be made with the existing manufacturing process with little modification.

Discussions with the staff of Tianjin University packing factory, who were to make the new packing revealed that some of the shapes were unsuitable. Four main problems were identified: any stretching of the sheet must be the same all along the sheet, so that it does not tend to curve; the sheets should not need accurate alignment between layers; there should be no sharp changes of the direction of pressing which could cause creasing; and any tabs pushed out into the channels should be avoided as they would considerably increase the complexity of the tool which would need a means of stripping the pressed sheet from itself. The first problem was evident in the shape in figure 4-17a, the second in the design in figure 4-16a, the third in the design in figure 4-17b and the fourth in the designs in figure 4-16.

The accurate alignment of sheets necessary in the second example would mean that the cuts would have to be accurately located. Instead of one cut for each sheet, two cuts would have to be made, with a small waste piece in between, so as to achieve the accurate alignment. This would increase the manufacturing time by around 15% and the total cost by around 8%.

The increased complexity of the tool in the fourth case would lead to a more expensive manufacturing process, and an extra stage or stages may need to be added. The packing cost would be increased by at least 2%, assuming a doubling of the tool cost, but probably by as much as 6% if the crimping must be done in two operations instead of one.

As a result of these discussions, the shape in figure 4-17c was chosen. It has alternately converging and diverging channels which may be made with a very similar tool to the standard one. Provided the angles are not too severe it may be made without creasing or curving of the sheet, and the channels may be aligned in any position with the adjacent sheets. It is described in more detail in the following section, together with its manufacture.

4.4 Description, manufacture and modification of the new packing

The new packing was that illustrated in figure 4-17c. It is a crimped sheet packing, like most of the commercially available ones, because they are relatively easy to manufacture. The new feature is that the channels become narrower and wider again along their length. This converging-diverging shape should promote turbulence and mixing in both phases and help liquid spreading.

The crimping tool would be slightly more complex to produce than one for a packing with straight channels, but would not be so complex as the shapes requiring tabs to be pushed out. These would have needed either another stage in the manufacturing process or a much more complex tool incorporating punches and a stripping plate.

After deciding on the shape, the exact dimensions had to be fixed. The variables to be defined are the ratio of the largest to the smallest channel cross-sectional area, the block height, the number of converging and diverging sections in a block, the angle of the channels with the horizontal and the specific surface area. These were dictated mainly by the ease of manufacture of the prototype packing. The ratio of largest to smallest cross-sectional area was fixed at about 1.3, so as not to reduce the capacity of the packing too much. The number of converging and diverging sections in a block was minimised to make the crimping tool more straightforward. One convergence or divergence per block was used in the 500Y packing and two in the 350Y. The block height was smaller than usual so that there would be a significant angle of convergence or divergence; the blocks of 350Y had a height of 100 mm, while those of 500Y had a height of 50 mm. This led to average divergence angles of 1.5 degrees in the 350Y and 1.2 degrees in the 500Y. The surface areas per unit volume were chosen to compare with Sulzer Mellapak 500YW and the standard Tianjin University packings of 350 and 500 m^2/m^3. Unfortunately, the difference in the shapes made it difficult to match the surface areas exactly, and these varied by up to 15%. All the packings were of the Y type, that is the channels were at 45 degrees to the horizontal, because of their higher efficiency than the X type.

The new crimping tool and packing were manufactured at the Tianjin University Packing Factory, using the same process as that described in chapter 2. The only differences were the differently-shaped crimping tool and the use of a grinder rather than the guillotine to cut the sheets. The guillotine could not be used because of the changing cross section.

All the packings manufactured for this work are listed in table 4-4. After manufacture in Tianjin, they were shipped to Aston University for the tests.

Packing type	Material	Surface treatment	Block Height / mm	Measured specific area / m^2/m^3	Measured element diameter / mm
Tianjin Mellapak 500Y	Stainless steel sheet	Fluted and perforated	100	440	310
Tianjin Mellapak 350Y	Stainless steel sheet	Fluted and perforated	100	302	313
New 500Y	Stainless steel sheet	Fluted and perforated	50	478	316
New 350Y	Stainless steel sheet	Fluted and perforated	100	345	314
New gauze 500Y	Stainless steel gauze	Perforated	50	495	316
New Gauze 350Y	Stainless steel gauze	Perforated	100	327	316
New 350Y, Tianjin University surface	Stainless steel sheet	Embossed and perforated	100	350	318

Table 4-5 Packings manufactured for tests.

Because of the labour intensive manufacturing method, quality control proved difficult. The packing elements supplied had several non-uniformities, and it was not clear which ones would affect their performance. These problems were as follows:

Perforation

The perforations were punched in groups. Each group was inconsistently placed with respect to the previous one. This is likely to have little effect on the efficiency because of the randomness of the deviation.

Crimping

The angle of the crimps with the axis of the sheet was not consistent, with deviations of about 2 degrees. This again is unlikely to alter the efficiency

significantly. Another minor problem was the occasional folding of the sheet as it was being crimped.

Cutting

The sheets were cut with a grinder to avoid having to make a specially shaped guillotine. Bandsawing the sheets would have been difficult because they are so thin. As a result there were large burrs on the edge of the sheets and the cut angle was variable. It was unclear to what extent the burrs caused or prevented wall flow of liquid or by-passing of vapour round the elements. Experimental results with the new wall-wiping bands appear to demonstrate that the burrs are unimportant.

Assembly into elements

Because of the variations in the cutting of the sheets, when they were assembled into blocks, the dimensions were variable and some would not fit the column. There were also problems with the method of holding the sheets together. The gauze bands into which the sheets were forced sometimes came off as the packing was installed in the column. They were not stiff enough to keep the blocks central in the column and experiments showed that they were also ineffective at taking liquid from the wall back into the packing, causing an impairment of efficiency.

Development of new wall wiping bands

So the only significant manufacturing problems were the incorrect size of the elements and the poor wall-wiping bands. Some effort was made to improve the method of assembly into blocks, and the blocks were dismantled and reassembled at Aston with some sheets removed and with a new type of wall-wiping band.

The Tianjin University packings had an average diameter of about 310 mm, whilst the column inside diameter was 316 mm. However, their diameter varied, and some types would not fit the column The commercial packings from Norton and Sulzer, on the other hand, were each considerably smaller than the column in diameter, with average diameters of 303 and 305 mm.

Each manufacturer used a different method of holding the packing sheets together and of attempting to prevent wall flow.

Norton's packing had the sheets spot welded together and two, 0.2 mm thick by 50 mm deep soft stainless steel sheet bands round each 265 mm deep element, with 25 mm by 25 mm tabs bent down to touch the walls. The Sulzer packing elements were held together by one 10 mm wide stainless steel band fastened with a crimp fastener. Each 204 mm deep element also had two 50 mm stiff stainless steel gauze bands around, with 15 mm deep by 15 mm wide tabs bent down to touch the

column walls. All the Tianjin University packings were bound into elements by forcing the sheets into two soft stainless steel gauze bands which varied in width from 20 to 50 mm according to the type of packing. The bands were prepared by spot welding the ends of gauze strips together to form a band of the required diameter. After the elements had been assembled, the top band had 10 mm deep cuts made at 30 mm intervals, and the tabs created were bent down to touch the column walls.

The wall-wiping arrangements of the Tianjin University and Sulzer packings appear at first sight very similar, however there are two significant differences. Firstly, the gauze used by Sulzer has a special weave pattern and is made from stiffer wire. This makes it more effective at preventing liquid flowing through the mesh and removing liquid from the wall by ensuring a firm contact. Secondly, Sulzer's separate binding band ensures a consistent element diameter, which, combined with the spring effect of the stiffer tabs, means that the sheets never touch the walls. In contrast to this, The Tianjin University binding method means that some elements are loosely and some tightly bound and that the elements may not be properly centred. This increases the possibility of sheets touching, and so putting flow onto, the walls.

The new binding must therefore hold the sheets tightly together and press firmly against the walls so as to ensure that the elements are centred and that any liquid is removed from the walls. There seemed to be no particular advantage in using gauze, indeed it would be less stiff, more difficult to fasten and would be more difficult and expensive to obtain than metal sheet. The best choice, then would be hard or half-hard (rather than soft) stainless steel with a thickness similar to or slightly bigger than the Norton wall wipers. The dimensions of the Norton bands seemed reasonable, and so were copied. One new wall-wiper was installed on each 100 mm deep element, so that the number of wall wipers per metre would be comparable with the Sulzer and Norton packings.

The packing chosen for rebinding was the new 350Y, since it was only necessary to remove one sheet from each element, and not to cut the sheets down, to reduce the diameter to 305 mm. This diameter was considered a maximum desirable diameter to avoid contact of the packing sheets with the wall. The actual metal used for the wall wipers was 0.25 mm thick half-hard brass as it was cheaper and easier to get than stainless steel. Before the elements were rebound, one 1 m long by 50 mm wide strip of brass was prepared for each element and 25 mm cuts made every 25 mm. To rebind an element, it was dismantled, a central sheet removed and the sheets rearranged loosely inside a 300 mm Jubilee clip. The brass strip was placed around the element, inside the Jubilee clip, and the clip tightened. When the element was held together tightly enough, two 3 mm holes were drilled on the overlap of the ends of the brass strip and the strip fastened with pop rivets .

The tabs were then bent down so that the packing was ready to be installed in the column.

4.5 Conclusions

In this chapter we have looked at some experimental results and model predictions of the performance of folded surface type packings with a range of geometries, distillation systems and flow rates. Although there are significant differences between the predictions of the different correlations, we have been able to use the understanding obtained from this work to confirm that packings will perform similarly in the distillation of air to that of organic mixtures. There may however be a slight reduction in efficiency due to the reduced diffusivities at cryogenic temperatures. We have also used it, together with the economic work in chapter 3 and the review of heat and mass transfer enhancement in chapter 2 to propose some improvements to packings for use in air separation, particularly by considering how to reduce the vapour phase resistance to mass transfer. One of these packings was then chosen by considering how easy the new shapes would be to manufacture. Finally the new packing and its manufacture have been described, together with its subsequent modification to prevent wall-flow.

Chapter 5 - Apparatus Design and Construction

5.1 Aim of experiments

The experimental work was planned to compare existing packings and newly developed packings under the same conditions to see which would be most suitable for use in air separation. A secondary aim was to gather information about each packing under a variety of operating conditions so as to get a better understanding of the operation of the packings and the reasons for their different performances.

To satisfy these aims, the packings should ideally be tested under large scale cryogenic distillation at the pressures of industrial importance, namely 1 to 2 bar and 5 to 7 bar. This was impracticable because of the additional costs and difficulties of building and operating a cryogenic test rig. It seemed better to compare the packings on a near industrial scale, albeit with a hydrocarbon system and at atmospheric pressure, than to operate a very small cryogenic unit. Consequently, the packings would first be tested under total reflux at atmospheric pressure with the commonly-used test system of chlorobenzene and ethylbenzene.

If time permitted, the packings would then be tested at partial reflux with chlorobenzene and ethylbenzene and at total and partial reflux with the test systems n-hexane / toluene to simulate nitrogen / oxygen and methylcyclohexane / toluene to simulate argon / oxygen. Time limitations have however led to all the results being with the one test system and most of those being at total reflux.

5.2 Design and description of apparatus

Because the present work is concerned with evaluating packings for use on an industrial scale, we decided to use the largest practicable size of column. The maximum size was limited mainly by the steam and cooling water available in the department, but also by cost and time considerations. It was also decided to build a rig capable of operating at partial as well as total reflux, to enable more extensive tests to be conducted than the normal ones at total reflux. This led to the development of the flowsheet in figure 5-1.

5.2.1 Main components

A nominal one-foot diameter stainless steel distillation column, complete with thermosyphon reboiler and condenser were available from the department stores. Preliminary calculations (appendix 1) showed that to flood the highest capacity packing available, Sulzer Mellapak 125Y at partial reflux, would require about 80% of the department's steam boiler output of 1000 lb/hr (454 kg/hr). This indicates that a larger diameter distillation column would need more heating and

cooling than could practicably be supplied. As a result, it was decided to erect the existing column with its condenser and reboiler.

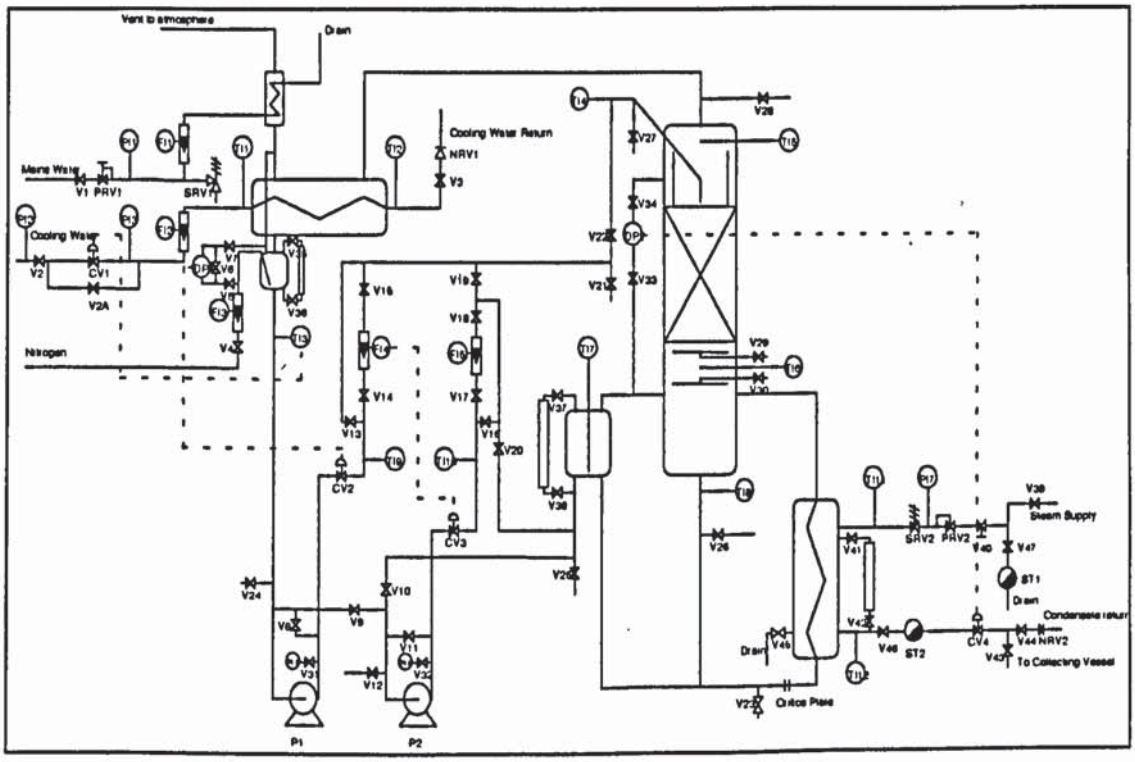

Figure 5-1 Test rig flowsheet

Distillation column

The column is illustrated in figure 5-2. It was designed by J E Mack and Associates and was constructed by Aston Services Ltd from 12" nominal bore schedule 5S 316 stainless steel tubing. There are four sections connected by flanged joints. Nozzles were provided at intervals to allow withdrawal of samples, and two windows were included in an intermediate section and one in the bottom one. The column was originally designed for four sieve trays, 18 inches apart, so there was potentially 54 inches or 1.37 metres of packed height. The packing support plate could not, however, be placed as low as the bottom tray because the nozzle through which samples could be withdrawn was too high. Moreover, the top of the packed bed had to be below the level of the top windows, to allow observation of the distributor performance. These limitations meant that the available packed height was only about 0.7 m or about 3 theoretical plates with Mellapak 500Y. This was considered too small to eliminate end effects, and, for the chlorobenzene / ethylbenzene test mixture the separation would be so small that the error in composition analysis would be significant. An additional column section was therefore designed at Aston University and built by Poseidon Alloys Ltd and T Bullows and Sons. This extended the packed height to about 2 metres or 9 theoretical plates with Mellapak 500Y.

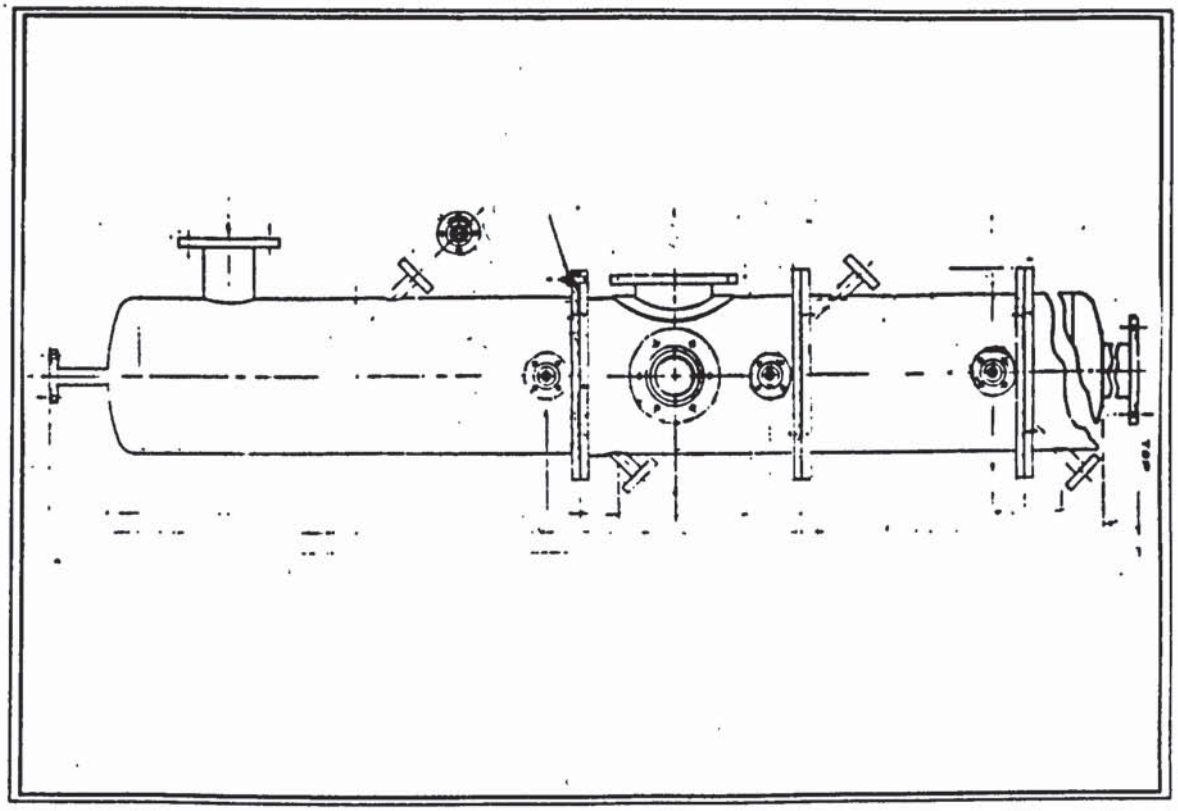

Figure 5-2 Distillation column

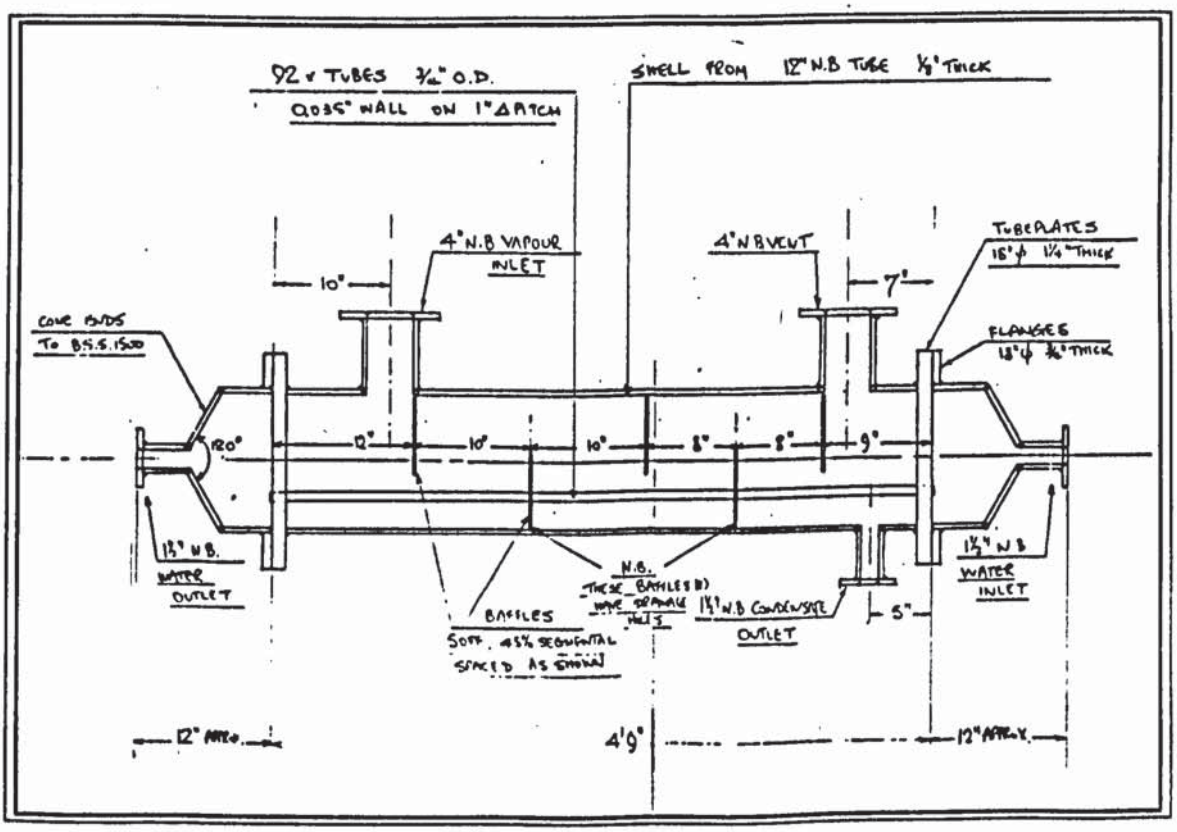

Figure 5-3 Condenser

This section was designed to take 3 more trays, if the column should ever be used for sieve trays, and so was 1.37 m long. Nozzles were included in the same positions as in the other column sections so that, if necessary, samples could be taken from or temperatures measured in the centre of the bed. The working temperature of the column is 0 - 200 °C and the working pressure 0 to 44.7 psia (3

bar). The specified test pressure is 54 psig, although it was hydraulically tested to 60 psig before erection.

Condenser and reflux tank

The condenser was a shell and tube device designed by Dr J K Maund of Aston University. It was also manufactured by Aston Services Ltd and is illustrated in figure 5-3. The shell and tubes were from 316 stainless steel and the ends were conical (to BS 1500) and of mild steel. Its specified working temperature was 0 to 120 °C and its working pressure was 0 to 30 psig. Although these values are lower than the maximum temperature and pressure of operation, it was deemed safe to operate for two reasons. Firstly, the maximum cooling water temperature would be about 60 °C, so that temperatures of more than 120 °C would be very localised. Secondly, a safety factor of 10 had been applied to the design pressure, so that operating at 50 psi still gives a safety factor better than 5. There are 92 19 mm diameter tubes in the condenser which are 1.38 m long, giving a total surface area of 7.6 m^2

The condenser was designed to be mounted below the level of the top of the column, so the reflux had to be pumped. This arrangement had the advantages that the column height could easily be changed and that the condenser need not be mounted so high up. It did have the serious disadvantage of increasing the complexity of operation by requiring a reflux tank with a level controller, but this was considered to be outweighed by avoiding the difficulties associated with mounting the condenser near the roof of the laboratory. The reflux tank was from 8 inch nominal bore tube, was 11 inches high and made from 316 stainless steel. It was designed by Dr J D Jenkins of Aston University.

Reboiler

The reboiler was a vertical thermosyphon shell and tube device, with steam in the shell side. It is illustrated in Figure 5-4. It was sized by Dr J D Jenkins of Aston University and mechanical design was by J E Mack and Associates. Construction was again by Aston Services Ltd. The tube plates are from 321 stainless steel, whilst the rest is in 316 stainless steel. Its 8" nominal bore shell contains 42 19 mm tubes with a length of 1.55 m and has a surface area of 3.9 m^2. The design temperature is 200 °C whilst the design pressure is 30 psig on the process side and 225 psig on the steam side. It was pressure tested to approximately 150 psig before use.

The operation of the boiler with water as the process fluid is described in more detail by Vetencourt (1978) and Merican (1977). It is mounted below the bottom of the column .

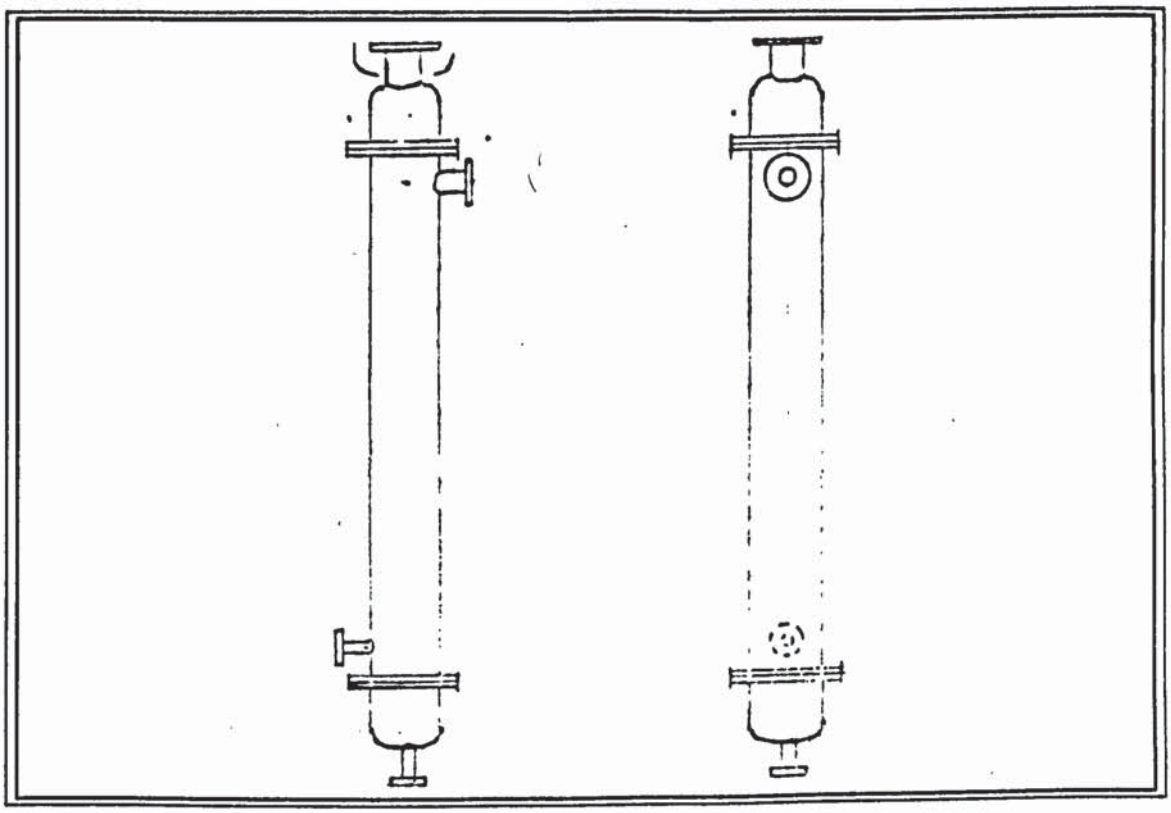

Figure 5-4 Reboiler

Bottom tank

An unusual feature of the arrangement was the low liquid hold-up in the bottom of the column. This was advantageous in that the time to reach steady state would be reduced, but meant that a tank had to be included in parallel with the bottom of the column. This doubles the surface area of liquid so as to reduce the variation in level as the column is started up and liquid is distributed around the rest of the system and to damp the fluctuations in level caused by variations in flow in the thermosyphon loop. This tank was designed by Dr J D Jenkins of Aston University. It is of 12 inch nominal bore tube and is 12 inches high.

5.2.2 Error Analysis

Method

Before the detailed design of the apparatus was undertaken, an analysis of the effect of errors in the various measurements was undertaken. This was to ensure that all the results would be as accurate as possible and that their error would be acceptable in all the proposed experiments. The analysis also allows the instruments to be specified to have the minimum acceptable accuracy (to keep

costs down). Moreover, given the instruments to be used and the system to be distilled, the optimum packed height may then be found.

The analysis follows the approach of Sealey (1970), who considers the effect on the separation of each theoretical plate due to the following measurement errors and errors in the system properties. Measurement errors are assumed to be random and system property errors systematic.

Operating line location and terminal composition

Errors in the composition measurements will bring about an error in the number of steps between the top and bottom compositions. At partial reflux, they will also cause an error in the location of the operating line, which will lead to an additional error in the number of theoretical plates. Such measurement errors will be both random and systematic. Random errors will occur in the sampling and analysis, whilst systematic errors will arise if the calibration of the analysis is in error. However, this analysis assumes that all the measurement error is random. It is just as important that the samples obtained should represent the true compositions in the column as it is that the analysis should be accurate.

Operating line gradient

At total reflux, errors in the measured flows do not lead to an error in the calculated efficiency. At partial reflux, however, errors in the feed and reflux flows generate an error in the internal reflux ratio, or operating line gradient. Errors occur in the flows for four reasons: They may be unstable, the scale on the flow meter may only be read to a certain accuracy, the calibration of the flow meter may be in error or the volumetric properties of the fluid may be uncertain. The first two will cause random errors and the last two systematic ones.

Equilibrium line

The accuracy of the equilibrium data will affect the calculated efficiency at both partial and total reflux. It is a systematic error, although, since it is different in different composition ranges, it could vary from one result to another.

Other errors

In his paper, Sealey (1970) did not account for end effects. These could be important in the packed column because of the difficulties of sampling at each end of the bed, the subcooled reflux and the difference in packing behaviour at different flows. Consequently, they were included in this analysis.

In the closed system employed in this work, the mixture composition is fixed. This, together with the hold-up at the top and bottom of the column, determines

the top and bottom compositions for a given number of theoretical plates. The mixture composition and hold-up distribution will therefore also affect the accuracy of the results. For example, if the mixture is of such a composition that a pinch is caused, this will result in a very much larger error than with no pinch.

A computer programme was written in TURBO PASCAL to perform the analysis; it is listed in appendix 3.

The programme performs the analysis for fixed numbers of theoretical plates. A top or bottom composition is guessed, depending on whether the internal reflux ratio is less or greater than one. The other composition is then calculated and tested against the mass balance, and the initial guess modified until this is satisfied. Finally, the errors are calculated for each plate and combined to give the total error.

The estimated measurement errors which are used as input to the programme will now be considered.

Accuracy of composition analysis.

The accuracy of the composition measurements is limited by how accurately the instrument could be read and how accurately standard samples could be made up. The instrument reads the time period value to six figures. The full range of compositions from 0 to 1 covered a range of about 0.300000 to 0.390000, that is about 1 part in 10^5. Readings were consistent to at least 1 part in 10^4. Standard samples with a minimum of 1 g of one type of liquid were made up by weight on 4 place scales. This gives an accuracy of 1 part in 10^4, although with evaporation losses, this is estimated to be reduced to about 5 in 10^4. The use of a quadratic curve fit to the calibration points may further reduce the accuracy of the analysis to a minimum of about 0.001 in mole fraction. Over most of the range, the accuracy is around 0.0005, and, if necessary, could be increased by further calibration.

Accuracy of sampling.

It is most important that the samples obtained should represent the average composition of the fluid at the sample point. If the samples are taken from pipes, this is relatively easy, provided that the sample lines and valves are purged and fresh liquid is taken from the pipe. Samples from the column are more difficult, however. Liquid and vapour samplers were installed, but liquid samples were relied upon, as it was judged easier to obtain a well-mixed liquid sample. The liquid sampling device is shown in figure 5-12, and mixes liquid from the whole column cross section except for the walls. For the purposes of the error analysis, the samples are assumed to be perfect, with any imperfection accounted for in the assumed end effect.

End effects

These are due to a variety of factors such as poor distribution of liquid in the top layer of packing, subcooling of the reflux and incomplete mixing of samples. The maximum error is assumed to be half a theoretical plate.

Accuracy of Vapour Liquid Equilibrium data.

The chlorobenzene / ethylbenzene system has been well documented, and Onken and Arlt (1990) recommend the use of a constant relative volatility at atmospheric pressure. This is assumed to give a maximum deviation in the equilibrium vapour composition of about 0.001. This is similar to the accuracy of measurement of the terminal compositions.

Accuracy of flow meters.

The rotameters are estimated to be accurate to about 2% in total, of which 0.5% is assumed to be a systematic error due to the inaccuracies in the density prediction and 1.5% is random measurement error. This may be optimistic, because the flow is not that stable, but if enough readings are taken, this level of accuracy should be achievable.

Results of the analysis

The results of a typical error analysis are illustrated in figures 5-5 and 5-6. Figure 5-5 shows a plot of the total error in the efficiency as a percentage of the total number of theoretical plates for different numbers of theoretical plates and reflux ratios. There is an optimum number of plates in each case which is smaller, the further the reflux ratio is from 1. The error at this optimum increases as the reflux ratio becomes further from 1.

Figure 5-6 shows the individual components of the error as percentages of the number of theoretical plates at total reflux and at a reflux ratio of 1.2, and with different numbers of plates. It shows that at total reflux, where the operating and equilibrium lines are almost parallel so that the separation per plate is fairly constant, the errors are more or less constant over a large number of plates. At partial reflux, however, the size of the errors increases rapidly as the number of plates is increased because the operating and equilibrium lines pinch together and the separation per plate is reduced. The errors are then a significant part of the separation of each plate, and are cumulative over the number of plates.

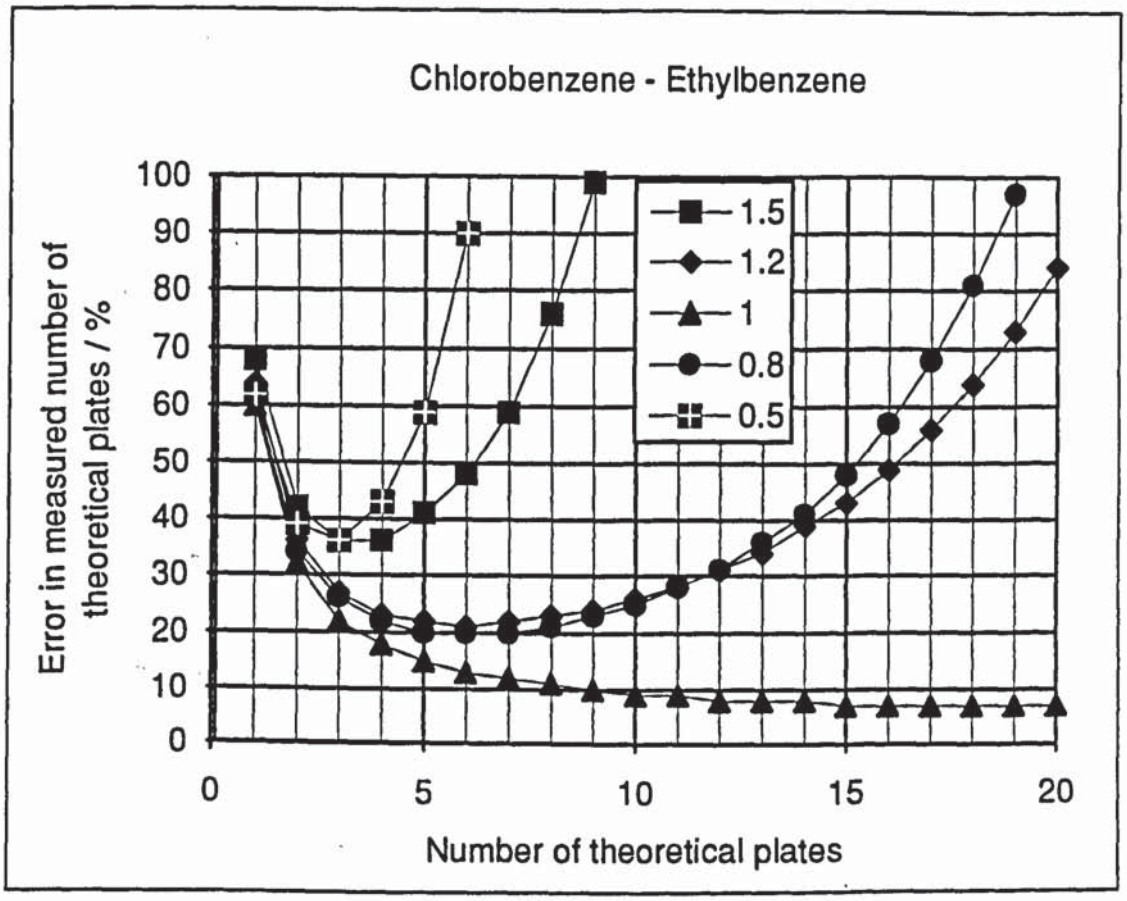

Figure 5-5 Calculated error in measured efficiency of packing for different numbers of theoretical plates and reflux ratios; chlorobenzene-ethylbenzene system.

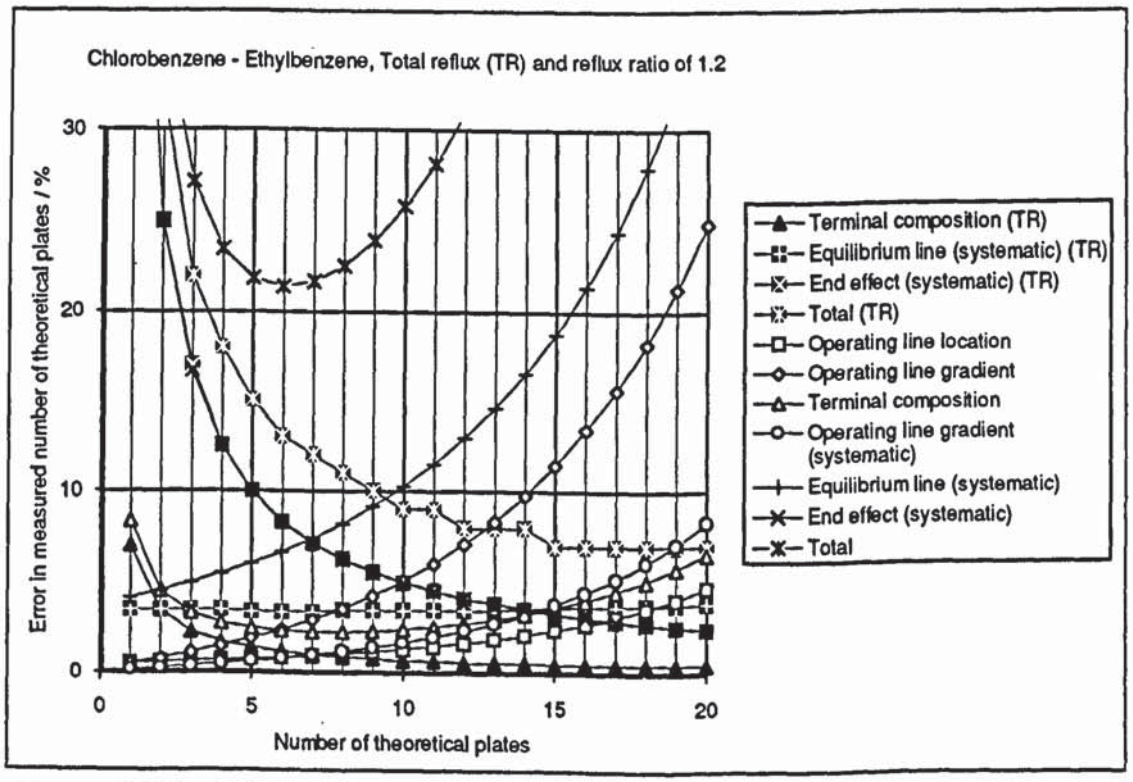

Figure 5-6 Breakdown of calculated error in measured efficiency.

The error in the equilibrium line is a significant part of the error in each case. End effects are more important when the number of plates is small. The error due to the composition analysis is very small at total reflux in comparison with the

equilibrium and end effects, which are around 4%. Because the equilibrium error is systematic, this should mean that total reflux results are repeatable to between about 1% and 5%, depending on the random nature of any end effects. At finite reflux, the errors due to the composition and flow measurements are about 4% and those due to equilibrium and end effects about 7% each. Consequently, results at partial reflux should be repeatable to between 8% and 15%, depending again on the randomness of the end effects.

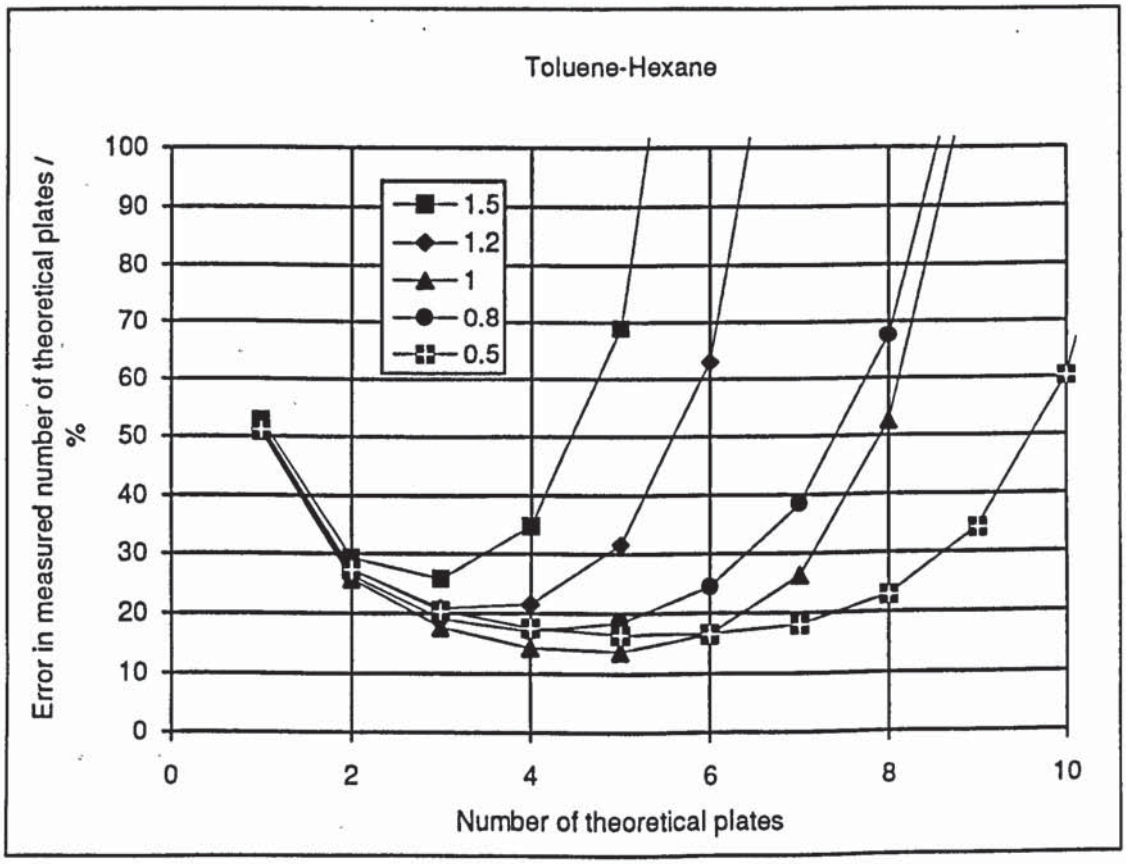

Figure 5-7 Calculated error in measured efficiency of packing for different numbers of theoretical plates and reflux ratios; toluene-hexane system.

Figure 5-7 shows a similar plot to figure 5-5, but for the toluene/hexane system. In this case, the separation is much easier than with chlorobenzene and ethylbenzene and the errors at total reflux increase more rapidly as the number of plates increases. This is because of the reduced separation per plate as the operating and equilibrium lines pinch together at the ends of the column. When operating at partial reflux, the increase in the error is less with this system, because the equilibrium and operating lines become more parallel, and the separation per plate becomes more constant than at total reflux. End effects are also more important with this system because of the smaller optimal number of plates.

An investigation of the effect of changing the mixture composition and the errors in each of the measurements was carried out. It showed that the mixture composition should be chosen so as to avoid a pinch in the column, if the errors are

to be minimised. Increasing the errors reduces the optimal number of plates and increases the minimum error. Also, if one error has a very much smaller effect on the total error than all the others at the optimum number of plates, then little may be gained by reducing it further. It is better to reduce the dominant errors.

The error due to uncertainty in the equilibrium curve appears to be the dominant one for both systems. Given this error, it is not worth measuring the terminal concentrations much more accurately than this. Similarly, measuring the flows to a much higher degree of accuracy would not be worthwhile to increase the overall accuracy unless the equilibrium error were also reduced. Increasing the accuracy of the flow and terminal composition measurements should, however, improve the repeatability of the results by reducing the random error; the equilibrium error is a systematic one.

Conclusions

The results show that, given the assumed equilibrium error of 0.001 in mole fraction, errors up to around 0.001 in mole fraction of the end compositions and 2% in flow are acceptable. These errors should give results which are repeatable to about 1% at total reflux (excluding end effects) or about 6% at a reflux ratio of 1.2, provided that the number of theoretical plates is close to the optimum.

At partial reflux, it is particularly important to be able to vary the packed height so that the number of theoretical plates can be close to the optimum.

5.2.3. Safety Analysis

In a piece of apparatus of the proposed size, it is extremely important that it be designed to be safe to build and operate and to minimise the possibility of a catastrophic failure during operation. The major hazards present are the toxicity of the materials and the flammability of the vapour, which has the potential to escape in large quantities, should the cooling system fail. Other hazards are also present, and all are considered individually in the next sections and summarised in table 5-1. The University is covered by the Health and Safety at Work Act (1974), the Highly Flammable Liquids and Liquefied Petroleum Gases Regulations (1972) and the Control of Substances Hazardous to Health regulations (1988), so these must all be complied with. The Factories Act (1961) does not apply.

Flammability hazards

The substances which were to be distilled were classed as flammable or highly flammable. Chlorobenzene had the highest flash point at 24 °C and n-hexane the lowest at -23 °C. This meant that precautions had to be taken against the build up of explosive atmospheres and against the presence of possible sources of ignition.

Hazard	Source or type of Hazard	Way to avoid hazard
Ignition sources	Electrical equipment	Flameproof or intrinsically safe
	Burners	None allowed in Lab.
	Hot surfaces	All below lowest autoignition temperature
	Static Electric Discharges	Proper earthing Care over clothing
	Mechanical Sparks	Remove unnecessary equipment
	Sunlight	Windows too small
	Cigarettes	No Smoking
Explosive Atmosphere	Vapour cloud	Backup condenser backup windows
	Vent to atmosphere	Secondary condenser Flame arrester
Raised pressure	Nitrogen supply	Strap cylinder Care with regulator
	Air supply	Minimise pressure check equipment shut-off valve
	Water supply	Shut-off valve Pressure test condensers
	Steam	Shut-off valve Relief valve
	Pumped process fluids	Shut-off valves Pump emergency stop
	Heated Vapour	Secondary condenser Backup windows
	Glass equipment	Screen and reinforce where possible Provide isolation where possible
High temperatures	Boiler surfaces	Insulate
	Steam and Condensate Piping	Insulate
Electricity	Shock	Proper earthing
	Ignition (see above)	Use explosion proof equipment
Corrosive materials	Solvents	Specify resistant sealing materials
	Water	Minimise use of mild steel.
Toxic materials	Inhalation	Minimise possibility Mask for dealing with spills
	Ingestion	Wash hands after handling
	Skin absorption	Wear rubber gloves
Dusts		Keep swept clean
Biological		Treat cooling water
Mechanical	Lifting	Use suitable lifting tackle
	Tripping and falling	Safety rail, minimise obstructions
	Dropping	Minimise number of tools Wear hard hat Don't allow anyone underneath
	Noise	Minimise sources, Insulate Wear ear protectors
Personnel	Cleaners	Not admitted Supervise if admitted
	Maintenance staff	Supervise Notify of dangers
	Visitors	Supervise Provide with eye and ear protection

Table 5-1 Summary of hazards and precautions necessary to avoid them

Such ignition sources may be sparks or excessive temperatures. Sparks may come from electrical apparatus, discharges of static electricity or metal objects striking each other and excessive temperatures may be generated by some electrical apparatus.

Electrical equipment

British Standard 5345 governs the use of electrical apparatus in areas where flammable materials are present. Such an area is known as a 'Hazardous area' and is classified as being in one of three zones. Zone 0 is an area in which an explosive atmosphere is continuously present, or present for long periods. In Zone 1, an explosive atmosphere is likely to occur in normal operation and Zone 2 is where an explosive atmosphere is not likely to occur in normal operation, and if it does occur, it will exist only for a short time. Areas where there is no flammable material are known as 'non-hazardous' rather than 'safe'.

This standard also specifies methods of protection of electrical apparatus so that it may be used in hazardous areas. Nine methods are listed, but only two are of interest in this work. These are flameproofing, or Ex 'd' protection and intrinsic safety, or Ex 'i' protection.

Flameproof equipment is capable of withstanding an internal explosion without communicating it to the external explosive atmosphere. This means that any joints or openings in the casing must be so small that flames cannot propagate along them.

Intrinsically safe equipment, on the other hand, restricts the amount of electrical energy in a piece of apparatus to below the level that could cause ignition. This requires that if the apparatus is connected to any other equipment outside the hazardous area, it must have protection against excessive energy reaching it from this equipment. Electrical barriers are normally installed which would short circuit any excessive current or voltage to earth.

Certain types of protection are limited to certain zones, for example only some intrinsically safe equipment may be used in zone 0, and it must be designated Ex ia. If it is Ex ib, it is suitable only for zone 1. Flameproof equipment may only be used in zones 1 and 2.

BS 5345 also classifies equipment by the maximum possible surface temperature. Class T1 has a maximum temperature of 450 °C, T2 of 300 °C, T3 of 200 °C and so on to T6 at 85 °C. Of the intended distillation mixtures, the lowest autoignition temperature is that of n-hexane, at 260 °C, so that classes T3 and above are suitable. All the equipment used was in fact class T4 or higher.

The Chemical Engineering building was already equipped with a laboratory in which all the electrical equipment was flameproof. This laboratory also had a flameproof air supply and extraction system. The distillation column was therefore

erected in this laboratory. Most of the laboratory was classified as zone 2, because the extraction system meant that any vapour could be dispersed quickly. The area under the fume hood near the door was classified as zone 1, because solvents were transferred to and from drums in this area, and explosive atmospheres were likely to occur in view of their low flash points. Inside the apparatus was classified as zone 0, to be on the safe side, although zone 1 would probably have been adequate because it is not operated continuously. All the electrical equipment within the column, namely the differential pressure transducers and temperature probes were therefore intrinsically safe, Ex ia.

Electrostatic hazards.

The control of undesirable static electricity is covered by British Standard 5958. This covers both general principles and particular examples.

Objects may acquire static electric charge by one of three methods. The most important is the contact electrification of non-conductors. As they make contact at the same potential, a small amount of charge is transferred from one to the other. If they are then separated, the charge is not completely transferred back, and a potential difference arises between them. Contact electrification is increased by rubbing the objects together. Insulated conductors in an electric field may acquire a potential by induction if they are moved around in the field. Such a conductor which has been earthed in one part of the field may be capable of a discharge in another part where it has a different potential. The final source of electrification is by charge transfer when charged objects touch. Examples of this are charged sprays settling on an object or a stream of ions hitting it.

BS 5958 states that significant electrostatic charge will build up on an object only if the resistance to earth is greater than 10^6 ohms.

The hazard posed by static electricity is the sudden release of energy in a discharge. Such discharges may take several forms, but the most important is the spark, which is capable of releasing enough energy to ignite a flammable material.

As a liquid flows through a pipe, contact electrification occurs. If it is discharged from the pipe and its conductivity is low, it carries charge with it. If its conductivity is high, any charge is conducted back to the pipe through the liquid. Electrification of liquids may also take place if a jet hits an obstruction or generates a spray or mist. The pumping of liquid into or out of drums or tanks is therefore a potentially hazardous procedure and care must be taken to minimise the risk of discharges. BS 5948 recommends that precautions be taken with any liquid where the conductivity is less than 50 pS/m (for example toluene). These precautions are that the drum should be earthed, the velocity in the line should be less than 1 m/s and any splashing should be avoided by having the liquid entry at the bottom of the tank.

Gases and vapours do not in themselves pose a hazard, however they may carry charged mists or powders. Such a hazard could exist if the condenser failed and a mist were discharged through the vent pipe. This is therefore earthed and a flame arrester fitted at the end.

High resistivity solids, either in powder or block form, are also a potential hazard. This work does not involve the use of powders, but the sealing materials used in valves and the glassware could present a hazard by blocking the earthing of the conducting apparatus. Where necessary, earthing wires have been provided to bypass such equipment.

Static electricity may also build up on people, if they are insulated from earth. Clothes made from high resistivity materials should therefore be avoided, and clothes should not be put on or taken off in the hazardous area. Adequate earthing should take place through contact with the earthed platform structure.

Mechanically generated sparks

Sparks may also be caused by objects striking each other. The most likely cause of this is if things are dropped. The likelihood of a flammable mixture being present is small, but falling objects are dangerous for other reasons, so things such as tools should be handled carefully and not left on the platform during operation unless they are necessary.

Toxicity hazards

The materials used are covered by the control of substances hazardous to health (COSHH) regulations. The COSHH assessment is given in table 5-2.

COSHH Assessment: Distillation in 1 foot diameter column Aim: to measure efficiency of various packings in continuous binary distillation Hazardous processes: Steam at high pressure, Cooling water at high pressure, Vapour present in column Information Sources: Fisons catalogue, BDH health and safety information sheets Assessor: Paul Higginbotham Supervisor: Prof. K E Porter				
Substance or product	Ethylbenzene (Mutagen)	Chlorobenzene (Carcinogen and Mutagen)	Toluene	n-Hexane (Mutagen)
Risk Phrases	Highly flammable Harmful by inhalation	Flammable Harmful by inhalation	Highly flammable Harmful by inhalation	Highly flammable Harmful by inhalation Danger of serious damage to health by prolonged exposure
Can you use a less hazardous substance?	No	No	No	No

Safety Phrases	Keep away from ignition sources Avoid contact with skin and eyes Do not empty into drains	Avoid contact with skin and eyes	Keep away from ignition sources Avoid contact with eyes Do not empty into drains Take precautions against static discharges	Keep container well ventilated Keep away from ignition sources Avoid contact with skin and eyes Do not empty into drains Use only in well-ventilated areas
Control measures to be used	Ventilate lab when rig in use - door open and extractor fan on Fume hood on when pouring Use Flameproof lab. Earth all containers Use drip trays			
Personal protection required	Goggles or face shield Nitrile gloves Gas mask			
In-compatibilities	Oxidising agents	Oxidising agents	Oxidising agents Boron trifluoride diNitrogen tetroxide Uranium hexafluoride Nitric acid	Oxidising agents
Flammability code	Highly Flammable	Flammable	Highly Flammable	Highly Flammable
Quantity	50 dm^3 max.	50 dm^3 max.	75 dm^3 max.	50 dm^3 max.
Storage details	In 25 dm^3 drums in solvent stores	In 25 dm^3 drums in solvent stores	In 25 dm^3 drums in solvent stores	In 25 dm^3 drums in solvent stores
Disposal method code	6 Incinerate 7 Waste solvent drum	5 Allow to evaporate in safe open area 6 Incinerate 8 Waste drum for halogenated hydrocarbons	5 Allow to evaporate in safe open area 6 Incinerate 7 Waste solvent drum	5 Allow to evaporate in safe open area 6 Incinerate 7 Waste solvent drum
First aid in case of accident	Standard: Skin: wash and remove contaminated clothing Eyes: Wash Inhalation: remove from vapour Ingestion: give 250 ml water Call Doctor if necessary			
Action in case of spillage	Shut off ignition sources Evacuate area Wear breathing apparatus and protective clothing Absorb using absorbant in lab. Wash spillage site		Shut off ignition sources Wear face shield, gloves and rubber boots Absorb Ventilate area	
Action in case of personal contamination	Remove contaminated clothing Wash with lots of cold water Call doctor if necessary			
Type of fire extinguisher used	F: alcohol or polymer foam P: powder C: carbon dioxide H: Halons / BCF		F: alcohol or polymer foam P: powder C: carbon dioxide H: Halons / BCF NOT W: do not use water	

Table 5-2 COSHH assessment for distillation experiments

The aim during the design of the apparatus was to minimise contact with the solvents or their vapours. Pouring was avoided by using drums with taps connected to a hose which fed liquid under gravity to the feed pump. Liquid could then be pumped into the column with minimal contact with the operator.

The concentration within the laboratory was measured with Draeger tubes if it was suspected that the level was too high. The chlorobenzene/ethylbenzene mixture smells strongly at levels well below the exposure limit, so that if it can be kept below this level, it should be safe. Two masks with filters suitable for organic vapours were provided for use in clearing up spills.

Mechanical hazards

A number of mechanical hazards are present. During construction and reconfiguring of the apparatus, heavy parts had to be lifted. A lifting tackle was used for this purpose. Safety rails were provided on all levels and round ladders to minimise the risk of falling. Hard hats were always worn when working in the laboratory because of the risk of falling tools from higher levels. The pumps are the source of two mechanical hazards; they are noisy and contain rotating parts. Ear defenders or ear plugs were worn for protection against the noise and guards were fitted over the shaft and couplings. Glassware in the rig is also potentially hazardous because of the risk of breaking it. Valves were provided where possible to isolate glass parts if they should be broken. This was not possible with the secondary condenser or the windows in the column. The secondary condenser is not normally necessary and if it should become so, the rig should be shut down. The risk of a leak from it is therefore minimal. The windows in the column were reinforced with a polycarbonate layer separated by a small air gap. This provided protection against breaking from the outside, and would contain the vapour whilst the rig was shut down if the windows break inside. They also provide thermal insulation.

Pressure hazards

Almost all the apparatus operates above atmospheric pressure, so there is the possibility of leaking fluids and a potential danger from failure of vessels, pipes or instruments. Pressurised gases are very much more dangerous than liquids because of the large amount of compression energy stored in them.

Temperature hazards

The equipment gets very hot during operation, and touching the metal directly could cause burns. Other possible dangers are from leaking hot fluids, particularly

vapours including steam. The easiest way to minimise this hazard is to use thermal insulation wherever possible and to shut down immediately if any leak develops. The temperatures present in the apparatus are well below the autoignition temperatures of the solvents, so the risk of ignition due to high temperatures is very slight.

'What if?' analysis

As well as the consideration of all the hazards associated with the rig, it is important to consider the consequences of various failures and the actions to be taken if they occur. In this case, this took the form of a 'what if?' type analysis, in which all the possible failures were listed and their individual and combined effects noted. To do this completely, it is necessary to have the complete flow sheet for the apparatus, which may then have to be changed in the light of the results. Table 5-3 shows the final 'What if' analysis, and the following section describes specific modifications to the design made for safety.

Failure of:	consequences	precautions	action	dangerous combinations and precautions
Services:				
Air	Loss of control, reflux pump may run dry	Controller alarm	Shut down	
Nitrogen	Loss of level control, reflux pump may run dry	Controller alarm	Shut down	
Mains Water	Loss of secondary condenser	none	Shut down	
Cooling Water	Loss of cooling, vapour cloud release	Secondary condenser and vent pipe to atmosphere	Shut down immediately	Steam valve sticks open. Second valve in other lab. Vent pipe leaks or condenser fails
Steam	Loss of heating: not hazardous	none	Shut down	
Electricity	Loss of pumping and control, liquid build up in reflux tank and condenser	Enough hold-up at top to contain all liquid	Shut down	
Ventilation system	Potential build up of toxic and flammable vapour	Two level ventilation system, extract and emergency extract fans	Shut down	Leak. Shut down if ventilation fails to avoid leak developing
Equipment:				

Pumps	Build up of liquid in reflux tank and condenser	Enough hold-up at top to contain all liquid	Shut down	
Seals, joints or drain or sample valves	leak of liquid or vapour	Keep checking for leak, emergency pump stop buttons, absorbant for major leaks	Shut down immediately, isolate leak, ventilate lab, use absorbant	Ventilation failure.
Control Valves	loss of control, reflux pump may run dry	none	Shut down	
Instruments and control system	loss of information and control, reflux pump may run dry	none	Shut down	
Glassware	Rapid leak of liquid or vapour	isolation valves, safety screens, emergency pump stop buttons, absorbant for major leaks	Shut down immediately, isolate leak, ventilate lab, use absorbant	Ventilation failure, cooling water failure.
Pipes and hoses	leak of liquid or vapour	Clip hoses, check joints for leaks, emergency pump stop buttons, absorbant for major leaks	Shut down immediately, isolate leaks, ventilate lab, use absorbant	Ventilation failure, cooling water failure.
Explosion proofing or earthing	Potential ignition source	Reminder to earth drums on each drum	Shut down immediately	Flammable mixture present
Steam pressure regulation	Heat transfer rate is too high	Safety relief valve is provided	Shut down	

Table 5-3 What if? analysis

Emergency plans

Because of the potential for a large release of flammable vapour, a plan was made for emergency action. This is given in appendix 7. Two alarms could be used, depending on the seriousness of the incident. If help was needed, a remote controlled siren could be used to summon aid. If evacuation of the building was necessary, the fire alarm located immediately outside the laboratory could be used. Non-conducting foam fire extinguishers were provided for use on all types of minor fire.

Storage and waste disposal

When they were not in use inside the rig, the solvents were kept in the University solvent stores, in 25 dm^3 drums. For day-to-day operation they were left inside the rig, and the ventilation inside the laboratory was kept on permanently. The eventual waste disposal problem was considered before purchasing the solvents. They should be disposed of through a contractor, preferably by controlled incineration. Care should be taken when changing distillation systems not to contaminate non-chlorinated systems with chlorinated solvents, as these are more costly to dispose of.

5.2.4 Support and access structure

The support structure was designed to be as compact as possible at ground level to fit into a limited space in the laboratory. It is illustrated in figure 5-8. The main support frame holds the base of the distillation column and the top of the reboiler. The distillation column is free to expand upwards whilst the boiler expands downwards. The condenser is supported at a higher level, and is on a cradle which is mounted on springs to allow it to move as the column expands and contracts.

Two levels of access platform were provided. The first level coincided with the bottom of the distillation column and the top of the reboiler, and is about 2.4 m above ground level. A 1 m wide gallery with a wire grid floor is provided all the way round the equipment and is surrounded by a safety rail. Ladders allow access at either end, next to the fire exit or the main exit. This level is used for most of the column operation.

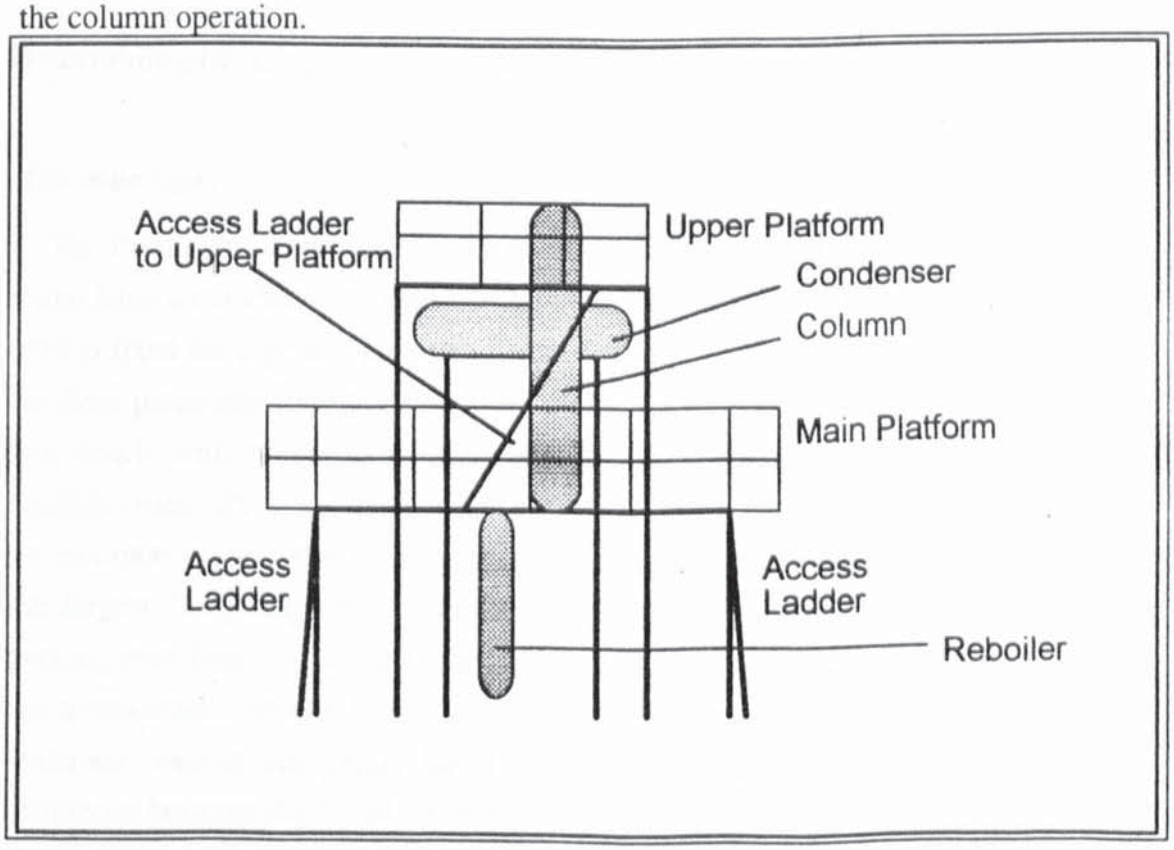

Figure 5-8 Column support and access structure.

The second floor level is 2.4 m above the first so that it is above the condenser and below the top of the column. Access is via a ladder from the first floor level. This level is used when the column is being packed or unpacked. It has a solid wooden floor, to minimise the danger of dropping tools, nuts or bolts. A bracket for the lifting gear is located near the roof and accessible from this floor.

The support frame and platforms were constructed mainly from 50 mm box section steel, 3 mm or 5 mm thick. Because of their 4.8 m length, the support legs for the upper platform were from 100 mm x 5 mm thick box section.

5.2.5 Process flows and equipment

The apparatus was designed in two stages. The preliminary design was to produce the flowsheet and establish that sufficient steam and cooling water were available. The more detailed design gave more detailed information such as control valve sizes and pipe diameters. Detailed calculations are given in appendix 1. The preliminary calculations were carried out on the basis that the rig should be capable of operating at flooding with Mellapak 125Y. This is the lowest area (and therefore highest capacity) packing which was ever likely to be tested, although because air separation plant favours high area packings, the present work was not concerned with packings with such a small area. Later detailed calculations showed that with the chlorobenzene - ethylbenzene mixture, the heating rate was limited by the steam pressure so the lowest area packing which could be used was 250Y.

Determining the range of flows in the column

Maximum flows

The maximum vapour and liquid flows through a packed column are normally found from a correlation of capacity factor against flow parameter. As the density ratio is fixed for a given system and is very similar for all the systems considered, the flow parameter depends mainly on the reflux ratio. The capacity factor only falls slowly with increasing flow parameter, so that the maximum vapour flow is possible when L/V has a minimum value and the maximum liquid flow when it has its maximum value. The smallest practicable reflux ratio was taken to be 0.5, and the largest 1.5 giving flow parameters of 0.03 and 0.10. The highest capacity packing ever likely to be used is a 125Y. At these flow parameters, this packing has a maximum capacity factors of 0.14 m/s and 0.10 m/s which correspond to maximum vapour and liquid flows of about 0.6 kg/s. The feed flow is the difference between the liquid and vapour flows, so the maximum feed flow is about 0.2 kg/s at a reflux ratio of 1.5. The highest capacity packing used in this work

was Norton's IMSP 1T, so the maximum practical flows were those needed to flood this packing at total reflux.

Minimum flows

The minimum flows in the column were determined by the 10:1 turndown of the distributor and the maximum flows. This time the minimum vapour flow is at the maximum L/V, and the minimum liquid flow at the minimum L/V.

The minimum feed flow is essentially zero, if the reflux ratio is very close to 1. It is limited practically by the ability to measure it.

Examples of the vapour, liquid and feed flows for different packings and reflux ratios of 0.5, 1 and 1.5 are given in appendix 1.

These flows give the range of flows to be handled by the reflux and feed systems and flow meters.

Distributor specification

If the rig operates at partial reflux, the feed flow is the difference between the liquid and vapour flows. If the column is in rectifying mode, L/V is less than 1, and the feed is pumped from the top of the column to the bottom. The flow to the distributor is therefore less than at total reflux. If it operates as a stripping section, the feed is pumped from the bottom to the top, and the distributor must handle the maximum reflux flow. Because packings with a range of areas were to be tested, the distributor was designed to operate only at total reflux with the lowest area packing (Norton IMSP 1T) so as to operate at the lowest possible flows with the highest area packing.

Several types of liquid distributor are available. Liquid either flows through holes or slots or over weirs. Distributors with holes are less susceptible to installation errors as the change in head to produce the same change in flow is larger than in ones with slots or weirs. The widest range of a single stage distributor is about 3:1, which would not be suitable for the range of packings and flows to be examined. The desired turndown was about 10:1, and so a three stage distributor was chosen. This was a Sulzer UNIHEX type, and was designed for flows of 3 to 30 dm^3 / min (see appendix 1).

Pumps

Two pumps were required; one to pump the reflux back into the column and one to pump the feed if the column operated at partial reflux. They had to be capable of handling the maximum flows given in appendix 1. The pressure delivered at these flows had to be sufficient to allow the liquid to be pumped back

to the top of the column and to overcome pressure drop in the pipes and through the control valves.

They were mounted at ground level to provide sufficient net positive suction head to prevent boiling if they were to pump saturated reflux.

Flameproof pumps are expensive, and so it was desirable to use pumps which were available from the department stores or from an unused rig. Two stainless steel Beresford B30-A6 pumps were found with flameproof motors. One was unused, but needed a new end cover, as the existing one was cracked. The other was borrowed from a flameproof liquid-liquid extraction rig. These pumps are capable of delivering the maximum required reflux flow of 41 dm^3/min at a head of around 2 bar, which is more than adequate. They were provided with bypasses to allow adjustment of the head pressure when operating at lower flows.

Valves

Control valves

Several pneumatic control valves were available from the department stores. Preliminary tests using water with the pumps which were to be used indicated that four of these would be suitable (appendix 1).

Pump bypass valves

These had to allow a continuous adjustment of the pump bypass flow, and so 1/2" stainless steel globe valves with PTFE seals were used. These were purchased from Valvestock Ltd.

Shut off valves

Most of the valves in the design were simple on-off valves, needed to change the configuration of the rig, to isolate glassware in an emergency or to fill and drain the rig. 3/4" BSP Stainless steel ball valves with PTFE seals were chosen for this duty and were obtained from Alco Valves Ltd.

Sample valves

1/4" Stainless steel ball valves, also supplied by Alco Valves Ltd. were used to control the withdrawal of samples

Process piping

The process piping was all from 316 stainless steel so as to be resistant to most possible process fluids. The pipework was designed so that the velocity in

unpumped lines would be a maximum of 1 m s^{-1} and in pumped lines would be no more than 3 m s^{-1}. This led to the use of two sizes of pipe; 1" BSP standard for the unpumped lines and 3/4" outside diameter for the pumped lines. Joints were made mainly with compression fittings, although some were welded and some made with BSP threaded fittings. The piping layout was planned in advance and the pipes bent by the suppliers to the required shape.

Seals

To avoid leaks, it was important to use sealing materials which are resistant to hot solvents. Viton rubber and PTFE were used for all the process seals. The main column flanges were sealed with Viton rubber O-rings. All the valves had PTFE seals and PTFE gaskets were used in the connections to the flow meters. PTFE ferrules in compression fittings were used for connection to the level glasses and to seal the temperature probe entries.

Secondary condenser

This was a 4" QVF glass condenser. It was installed in the vent duct immediately above the main condenser, to reduce the flow of any vapour escaping if the main cooling water should fail. It also serves the purpose during normal operation of reducing evaporation losses from the column.

5.2.6 Services

Cooling water

The cooling water circuit in the chemical engineering building is illustrated in figure 9. Water from a tank on the roof of the building (approximately 15 m above the laboratory) is pumped into the main 75 mm cooling water supply pipe. A bypass valve in the main pilot plant allows some of this water into the cooling water return pipe. Water returns through this pipe to a cooling tower on the roof, mounted above the storage tank and draining into it. The cooling tower relies on natural air circulation to cool the water. Evaporation or leakage losses are made up from mains water and a small quantity of disinfectant is fed into the system at a controlled rate.

Apparatus which requires cooling water is fed from the cooling water supply pipes and feeds the used water into the return line; it is in parallel with the main bypass valve. To allow sufficient flow through the apparatus, the pressure drop across it and its associated piping must be small; the pressure of water leaving the apparatus must be sufficient for its return to the roof.

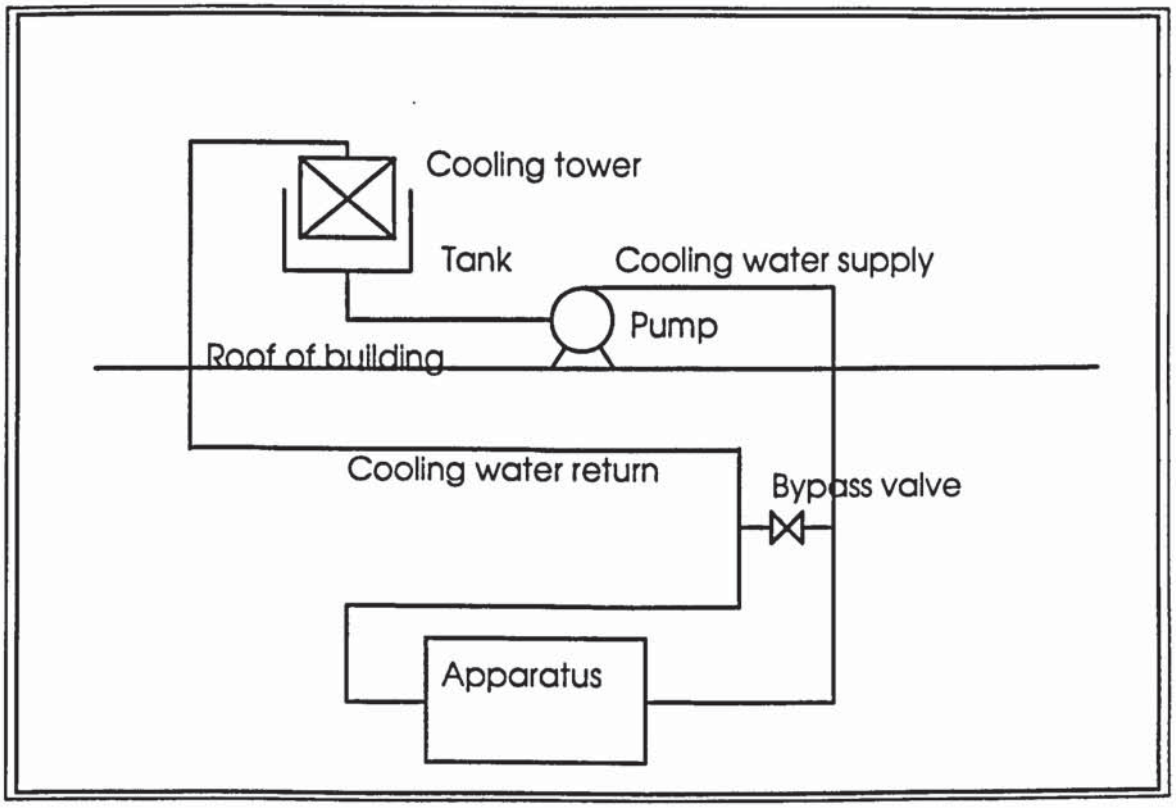

Figure 5-9 Department cooling water circuit

The flow of cooling water needed when the rig operates at its maximum capacity, that is with 125Y packing at a reflux ratio of 1/2, was calculated to be around 150 dm^3/min with a temperature rise of 20 K.

It was impossible to obtain the required flow of cooling water from the existing 1" piping in the flameproof lab. Extra 2.5" pipes were therefore installed from the 2.5" ring main in the adjacent main pilot plant. This piping was in copper, with brass compression joints. Cooling water entered the condenser through a 25 mm reinforced PVC hose, to allow movement of the condenser as the column expands and contracts. This was attached to a short length of 28 mm copper piping, on which were mounted a further shut off valve, the control valve and bypass valve, the flow meter and two pressure gauges, one to measure the supply pressure and one for the condenser inlet pressure. After leaving the condenser, the cooling water passed through a further section of PVC hose, a 28 mm copper pipe section containing a shut-off valve and non-return valve and finally back into the 2.5" copper piping.

Steam

Steam is used by the rig to provide heat to the column reboiler by condensation.

The steam system in the Chemical Engineering building is illustrated in figure 5-10. The boiler is capable of providing a maximum of 1000 lb/hr (454 kg/hr) steam at 120 psig (9.2 bar abs), but there is a pressure regulator on the supply pipe which limits the steam supply pressure to 80 psig (6.5 bar abs). In addition to the original

steam pipes, there is an additional 3" (75 mm) pipe which runs the length of the main pilot plant and supplies the 2.4 m (8') diameter air/water simulator. Because the steam pipe in the flameproof laboratory was only 1" (25 mm) diameter, the 3" (75 mm) pipe was extended through the wall from the main pilot plant. This was to ensure that enough steam was available at the required pressure.

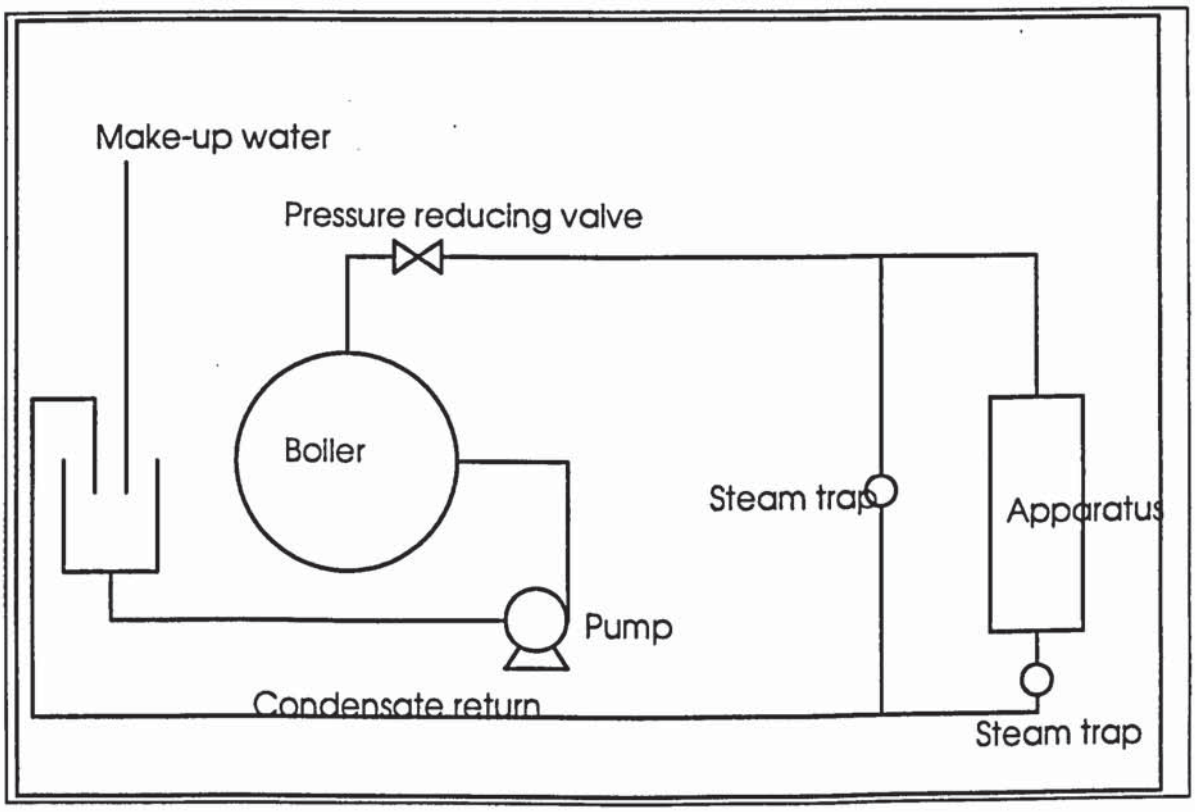

Figure 5-10 Department steam system

Any steam condensate from a piece of apparatus returns to a tank at atmospheric pressure and is pumped back into the boiler for re-use. A separate $1^1/_4$" condensate return line also existed in the main pilot plant, and this too was extended into the flameproof lab.

The boiler was attached to the steam supply via a 65 mm mild steel pipe. To separate water from the steam before it enters this pipe, the pipe was taken horizontally from a vertical section of the steam main. Water is carried down the vertical section and is drained from the bottom through a valve and steam trap.

Steam passes from the main through a 65 mm shut-off valve, a 40 mm strainer, a 40 mm IMI Bailey Burkitt Ltd type 470 pressure-reducing valve and a 50 mm pressure relief valve. Finally, it enters the boiler through a 50 mm pipe and a flanged joint.

Condensate leaves the boiler along a 20 mm mild steel pipe. It passes through a shut-off valve, a strainer, a Spirax FT 550 ball float steam trap, a non-return valve and the condensate control valve. It may then be directed to the condensate return system or to a drum for collection and weighing.

Earlier work on the reboiler used in this rig (Vetencourt, 1978 and Merican, 1977) gave the heat transferred when boiling water with different temperature driving forces. This indicates that to flood 250Y packing at a reflux ratio of 1/2 would require a heat flow of about 170 kW, which would need a temperature difference of about 28 K. This would lead to a maximum steam temperature of 165 °C, when boiling ethylbenzene, and a pressure of 6.8 bar, or 85 psig. This is in principle possible with the current arrangement, but the pressure reducing valve at the boiler would need resetting. The maximum currently practicable pressure of 70 psig (157 °C) was sufficient to flood the Norton IMSP 1T packing.

Compressed air

Compressed air is used to drive the pneumatic control valves and to purge the column. It is supplied from the main compressor via a tank and the department piping system. At the rig, two condensation separators and pressure regulators are provided. One is for the supply to the digital to pneumatic converters and the other for the manual control system supply The pressure is normally set to 3 bar gauge. The air supply to the control valves may be switched between the digitally controlled one or one with manual control of the pressure.

Mains water

Mains water is used in the secondary condenser in case the cooling water system fails, and because its glass construction means that it must be operated at atmospheric pressure. A pressure regulator and relief valve are provided to protect the condenser against excessive pressure, and a rotameter measures the water flow.

Electricity

The control equipment needs a standard 240 V mains supply, which was installed in the room adjacent to the flameproof lab. The pumps were supplied from a three-phase 415 V supply via flameproof cabling.

Nitrogen

Nitrogen is supplied to the rig from a cylinder in the adjacent lab. through 3/8" copper piping. The pressure is normally set to 0.5 bar gauge during operation of the rig. It is used to purge the lines to the column pressure-drop manometer and reflux tank level sensor. A connection is provided to allow purging of the column with nitrogen rather than air for highly flammable mixtures.

5.2.7 Instrumentation and Control

The instrumentation and control system serves four purposes. It enables the rig to achieve stable operation quickly, maintains this stable operation, confirms that it is stable and provides the measurements necessary to find the performance of the packing.

The ultimate aim of the experiments is to find the efficiency and pressure gradient in the packing at different flows through it. The flows are measured with flow meters and confirmed by heat balance. Temperatures and pressures at various points are needed to allow these calculations to be made. The pressure drop across the column is measured directly.

Flow meters

Four flows were measured: those of the cooling water, steam, reflux and feed. The flow meters had to be as accurate as possible, but also cheap. Turbine flow meters and Coriolis mass flow meters, with accuracies better than 0.5% were considered, but were too expensive. Rotameters were available and were estimated to give flow readings accurate to about 2% after calibration, and so these were used to measure the reflux and feed flows. Their major disadvantage was that they would need to be read manually. They were series 2102 devices from KDG Flow meters. A size 24 tube was used for the feed flow meter and size 35 for the reflux flow meter. Their maximum temperature is specified as 100 °C and the maximum pressures for liquid flows are 8.5 bar for the 24 and 7.0 bar for the 35. Initially stainless steel floats were used, but these were later replaced by korannite ones to make full use of the scale. The curve-fits to the calibration data are given in appendix 6.

The pressure limit of a rotameter large enough to measure the cooling water flow was below the pressure of the cooling water, so a high pressure variable area flow meter was used to measure this flow. This is similar to a rotameter, but is more compact because the force on the float is counterbalanced with a spring rather than by the weight of the float. It was supplied by ICC Ltd and was type IC.EFW.1002. Its quoted accuracy and repeatability are 5% and 1% of full scale and its pressure limit is 10 bar.

The most accurate method of determining the steam flow was considered to be that of collecting and weighing the condensate from the boiler over a period of about 10 minutes. The main errors in the flow measured by this process are due to errors in the scales used and to evaporation from the tank caused by flashing the condensate. The accuracy is estimated to be 2-3%.

Thermometer number	Stream	Reason for measurement	Length of probe / mm	Length of lead / m	Calibration equation. Actual temperature =
T1	Cooling water in	Condenser heat balance	150	6	$\frac{T_m-0.124}{1.002}$
T2	Cooling water out	Condenser heat balance	150	6	$\frac{T_m-0.343}{0.994}$
T3	Reflux tank	Condenser heat balance	300	6	$\frac{T_m-0.271}{0.998}$
T4	Reflux into distributor	Reflux subcooling	200	8	$\frac{T_m-0.349}{0.996}$
T5	Vapour above packing	Composition estimate and stability check	300	8	$\frac{T_m-0.211}{0.999}$
T6	Vapour under packing	Composition estimate and stability check	300	4	$\frac{T_m-0.236}{0.998}$
T7	Bottom tank	Stability check, Feed subcool if rectifying.	650	3	$\frac{T_m-0.276}{0.998}$
T8	Column bottom liquid	Composition estimate and stability check	150	3	$\frac{T_m-0.386}{0.995}$
T9	Reflux rotameter	Mixture density	200	4	$\frac{T_m-0.186}{0.998}$
T10	Feed rotameter	Mixture density	200	4	$\frac{T_m-0.076}{1.002}$
T11	Steam into boiler	Boiler heat balance	150	3	$\frac{T_m-0.410}{0.990}$
T12	Condensate out of boiler	Boiler heat balance	100	4	$\frac{T_m-0.253}{0.998}$

Table 5-4 Details of temperature probes

Temperature measurement

Temperatures at a number of points are required to allow the calculation of the physical properties at those points. The temperatures measured are listed in table 5-4, together with the reason for the measurement and details of the probes used.

The temperatures were to be logged by computer, to avoid time consuming manual recording during operation of the rig. Platinum resistance thermometer probes were chosen rather than thermocouples because of their better stability; they would only require a single calibration. Because they were to be calibrated, class B sensors were chosen, as they are cheaper than class A, which conform more closely to the standard specification. All were sheathed in 6 mm diameter stainless steel pockets and were obtained from A J Thermosensors Ltd. They were installed in the rig through bored-through compression fittings with PTFE ferrules, to allow adjustment of their position. The thermometers were calibrated by Gor and Wan (1992) to an accuracy of 0.1 K, which was limited by the logging equipment. This is quite good enough for this work.

Pressure measurement

Actual

The most important pressure measurement was that of the steam pressure, as a check against the temperature measurement. The other pressures measured were the pump outlet pressures, the cooling water supply and return pressures and the mains water pressure into the secondary condenser. These measurements were mainly to provide extra information if any problems are encountered. All the pressures were measured with standard bourdon gauges. The pump pressure gauges were in stainless steel, whilst all the others were brass. The gauges measuring the pressure of hot streams were mounted at the end of a length of tube to allow the fluid to cool before reaching the gauge.

Differential

Two differential pressure measurements were made: The pressure drop across the column and the pressure of liquid in the reflux tank. The pressure drop across the column is one of the most important measurements; it is used both to control the heat input to the column and to characterise the packing, and has to be as accurate as possible.

An intrinsically safe type 200 differential pressure transducer was purchased from PSM Ltd for this measurement and was factory-calibrated to provide a 4-20 mA signal over the range 0-60 mbar. This transducer can be adjusted if necessary to measure up to 100 mbar differential pressure. The quoted maximum error of this device is 0.5%. Its maximum temperature is 85 °C, so it was mounted with a length of tube between it and the column. The 4-20 mA transmitter is mounted in the laboratory and the signal is passed to the control room through a Zener barrier, where it is converted to a 0-5 V signal by passing it through a standard 250 Ω resistor.

A water manometer was also installed to measure the pressure drop across the column as a check on the instrument value. The lines to this manometer were purged with nitrogen to stop vapour condensing in them. After initial problems with vapour condensing in the lines to the transducer were solved, agreement between the two measurements was very good.

The pressure of liquid in the reflux tank was a measure of its level and was used to control the reflux flow. Consequently, accuracy in this measurement was unimportant, although stability during a run was desirable. An intrinsically safe, type TF7 differential pressure transducer, manufactured by Tekflo Ltd. was available from a dismantled rig in the flameproof laboratory, but its range was only 0 to 2.5 mbar. Because accuracy was not critical for this measurement, a 'potential

divider' arrangement was used to divide the actual pressure drop across the tank before measuring it. This is illustrated in figure 5-11. It is rather difficult to adjust, and should be left alone as much as possible. It contains its own Zener barriers and provides a 0 to 10 V output directly to the computer.

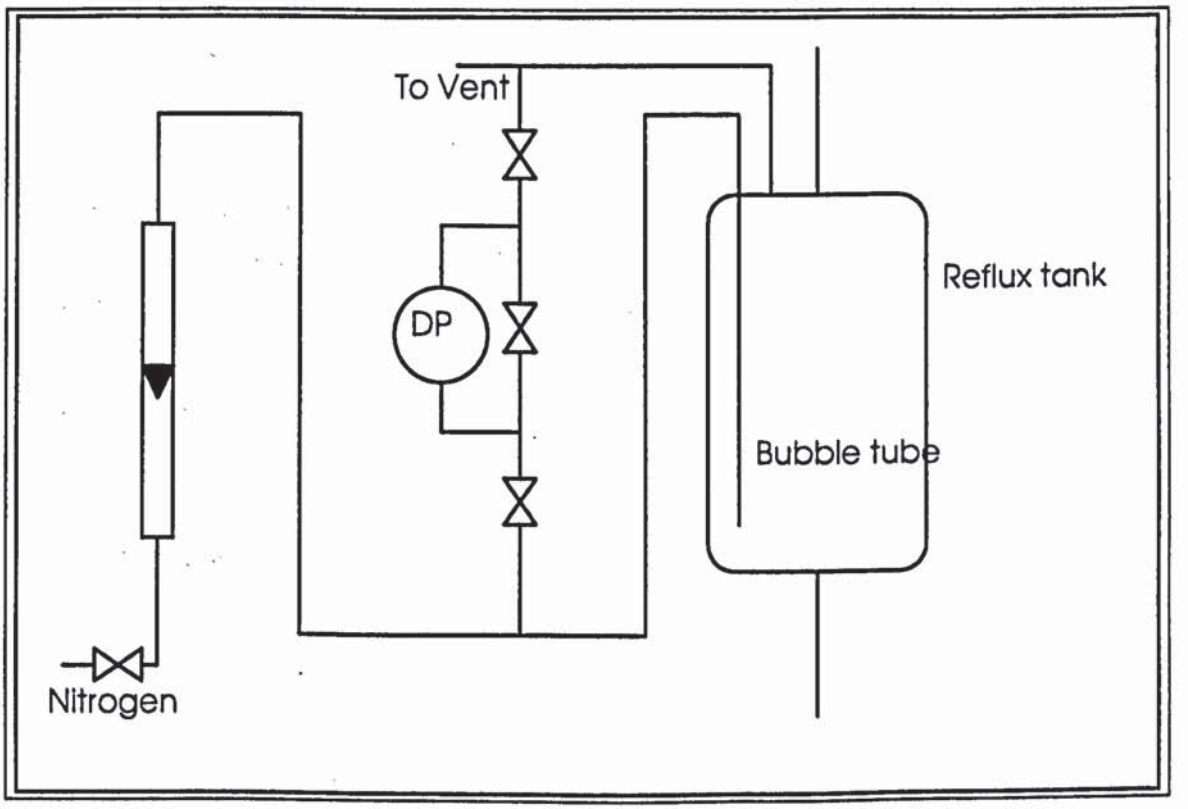

Figure 5-11 Reflux tank level sensor arrangement

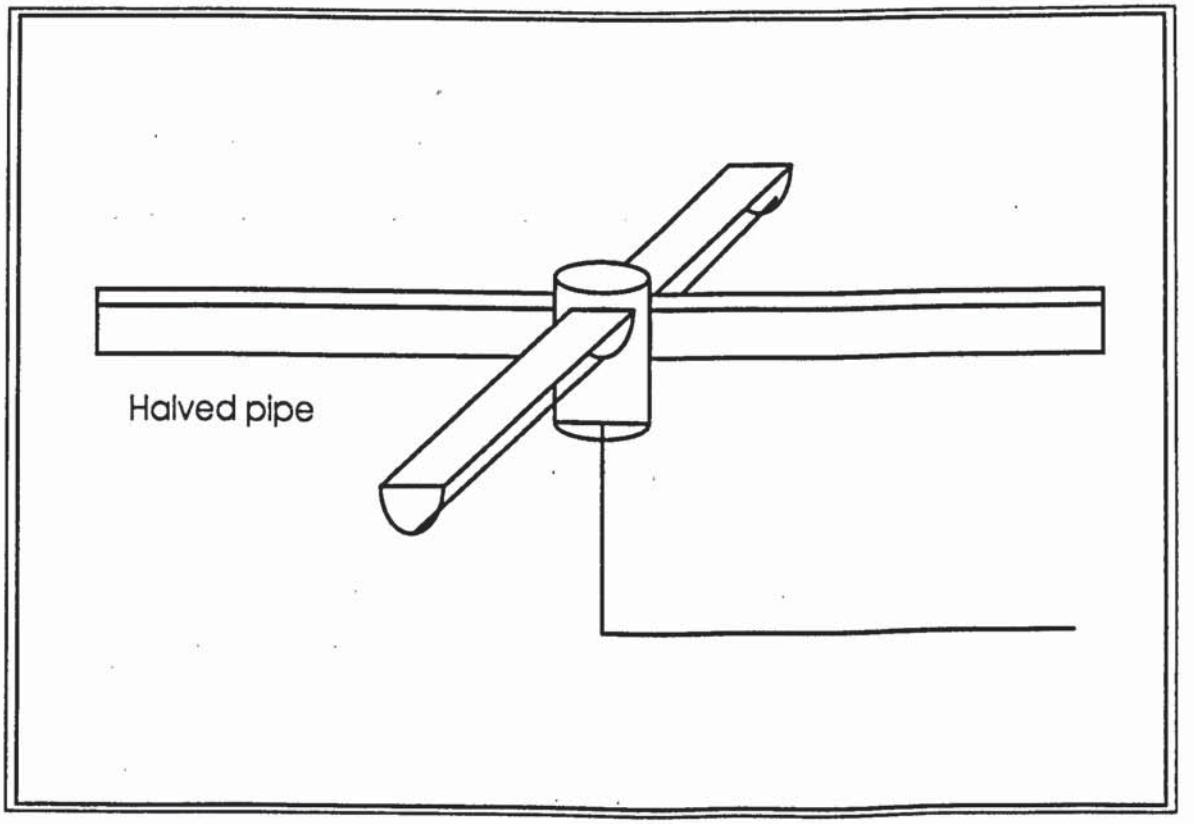

Figure 5-12 Liquid sampler

Sampling

On-line composition analysis would have been possible, but it would have been prohibitively expensive to achieve the same degree of accuracy as the laboratory method used. Sampling was through 1/8" stainless steel tubes and 1/4" stainless steel ball valves. All the samples were taken directly from the process piping except the vapour at the top and bottom of the column and the liquid from under the packing. The vapour was removed through a sampling device containing knitted wire to avoid withdrawal of liquid, and was condensed in the tube when it left the column. The liquid from the bottom of the packing was collected in a cross-shaped sampler made from halved tubing and illustrated in figure 5-12. Samples were collected in 7 ml glass vials, as described in the operating procedure. Because of the difficulty of ensuring that the vapour samples were free of liquid, these samples were not relied upon, and used only as an approximate check on the other samples.

Control valves

Four pneumatically actuated control valves were taken from the department stores. These are described in more detail by Gor and Wan (1992). They are summarised in table 5-5

These valves are supplied with compressed air through 3/8" copper pipes. They have slightly smaller discharge coefficients than those calculated, but because of the high pump capacity and the use of a bypass on the cooling water valve, they were acceptable. They did not have positioners, and so suffer from the problem of hysteresis; the same air pressure produces a different flow depending on whether the valve is opening or closing.

Valve	CV1	CV2	CV3	CV4
Plug	1/2"	3/8" Micro Form	1/4" Micro Flute	1/4" Micro Flute
Characteristic	Linear	Equal percentage	Equal percentage	Equal percentage
Manufacturer	Introl	Fisher Controls	Fisher Controls	Fisher Controls
Body Connection	1/2" BSP	1" BSP	1" BSP	1" BSP
Spring range	0 - 15 psi	3 - 14 psi	3 - 14 psi	3 - 14 psi
Trim Material	316 Stainless Steel	316 Stainless Steel	316 Stainless Steel	316 Stainless Steel
Body Material	Mild Steel	316 Stainless Steel	316 Stainless Steel	316 Stainless Steel
Fully open Discharge Coefficient (US gallons per minute per sqrt(psi))		0.4	0.2	0.2

Table 5-5 Summary of control valves

Control loops

It would be possible to operate a distillation column at total reflux with no control, provided that the condenser were mounted above the column so that the reflux flowed back into the column under gravity. The steam flow would be fixed by setting the position of its supply valve or the condensate return valve. This would determine the flow in the column. The condenser flow would be fixed and the cooling water outlet temperature would float.

The arrangement of this apparatus differs from this in two respects. The condenser is mounted below the top of the column and the rig may be operated at partial reflux, either as a rectifying section, with a bottom feed or as a stripping section, with a top feed. Because of the necessity of pumping the feed and the reflux, control of their flows is necessary so that a constant level is maintained in the reflux drum and the pumps do not run dry.

In addition to this necessary control, it was decided to control the rate of heat input to allow rapid attainment of the required value and to reduce the susceptibility to disturbances such as fluctuations in steam pressure.

A further control loop was incorporated into the design to allow control of the cooling water flow. This could be used to control either the cooling water temperature out of the condenser or the reflux temperature of systems with lower boiling points. It was not used in the experiments described here because the reflux was subcooled to such a great extent.

Cooling water- reflux temperature

This loop was incorporated to allow some degree of control of the reflux temperature. Because the cooling water temperature is so much lower than the boiling point of the chlorobenzene- ethylbenzene mixture, a large amount of subcooling was inevitable with this system. As a result, this loop was not used in the experiments described here. Had the toluene- n-hexane system been used, this control loop would have been more useful. The existence of the loop should also make it easy to add a reflux heater in the future; it could be used to control the heat input to such a heater. A proportional-integral control algorithm is used, although in all the experiments, the set point temperature was set to zero to allow the maximum cooling water flow.

Reflux tank level - reflux flow

This control loop is important to ensure that the reflux pump does not run dry. It is also important to ensure a steady flow of reflux into the column. A continuous level measurement was therefore necessary rather than two level

switches. The method chosen was to measure the pressure of liquid in the tank, because an intrinsically safe transducer was available.

A proportional-integral control algorithm was used, to avoid the excessive disturbance that a derivative element would introduce if the signal were noisy. To find suitable values of the constants for the control algorithm, a model of the tank and control system was constructed. The disturbance input to the model d(t) is the difference between the actual flow into the tank and the initial steady state flow with no disturbance. The output from the model y(t) is the difference between the actual height in the tank and the desired set point. The system then has the transfer function G_{load} so that Y(s), the Laplace transform of y(t) is related to D(s) by:

$$Y(s) = G_{load}\, D(s)$$

G_{load} is a combination of the disturbance, process and controller transfer functions, G_d, G_p and G_c (Stephanopoulos, 1984):

$$G_{load} = \frac{G_d}{1 + G_p G_c}$$

In this case, $G_d = G_p = 1/As$, where A is the tank area, 0.037 m^2. For the proportional-integral controller chosen, G_c is given by:

$$G_c = K_c\left(1 + \frac{1}{\tau_i s}\right)$$

where K_c is the proportional gain and τ_i is the integral time constant.

G_{load} is then given by the general expression for a second order system:

$$G_{load} = \frac{K_p s}{\tau^2 s^2 + 2\zeta\tau s + 1}$$

with the process gain, K_p, system time constant τ and damping factor ζ given by:

$$K_p = \frac{\tau_i}{K_p}$$

$$\tau = \sqrt{\frac{A\,\tau_i}{K_c}}$$

and $\zeta = \frac{1}{2}\sqrt{\frac{K_c \tau_i}{A}}$.

It was decided to aim for a critically damped response, to give the maximum speed of response without causing oscillations in the reflux flow. This occurs when $\zeta = 1$, so that K_c and τ are given by:

$$K_c = \frac{4A}{\tau_i}$$

$$\text{and } \tau = \frac{\tau_i}{2}$$

With a sampling interval, T, of one second, Stephanopoulos (1984) states that the system should be stable if $\tau > 5T$, so that τ_i should be bigger than 10 s. A number of values of K_c and τ_i were tried (Gor and Wan, 1992), and the values of 0.0037 m^2/s and 40 s were found to give a good response. If the gain were much higher, problems were caused by noise on the measurement. If it were lower, the response was too slow. To implement the controller, these were converted into units which gave the height as a percentage of the full tank depth of 0.2 m and sent a control value to give a percentage of the maximum flow of 30 dm^3/min or 0.0005 m^3/s. As a result, the gain value actually used had units of s^{-1} and is converted from the calculated value by multiplying by 0.2 / 0.0005 to give a value of 1.6 s^{-1}.

Further operating experience indicated that under some circumstances it was better to operate with a smaller gain of 0.8 s^{-1}, so that the system was under damped.

Reflux ratio - feed flow

Two alternatives were available for the feed flow control; either to set it to a constant value, or to control the reflux ratio, that is the ratio of feed to reflux flows. If the column operates in rectifying mode, some of the reflux is taken as the feed and introduced to the bottom of the column. So if a constant feed flow were specified that were too high, the reflux tank could be emptied and the reflux pump could run dry. To avoid this, the feed rate was controlled to be a constant proportion of the reflux rate. This is a form of feedforward control. The reflux rate was estimated from the reflux control valve position and the set point for the feed flow calculated from this. The feed flow was controlled with a proportional-integral control algorithm; derivative control was not used because of the noisy signal. The controller constants were found by experiment, and are given in table 5-7. It was found that a slow response was desirable, so that the feed rate was not disturbed unnecessarily by short term fluctuations in the reflux flow.

Column pressure drop - heat input (steam condensate flow)

Although it is not strictly necessary to control the heat input to the boiler, it was decided to do so for two reasons: It allows a steady value to be reached more quickly and the operation of the column is less susceptible to small disturbances, such as a fluctuating steam pressure.

The heat input could be controlled in several ways. The most obvious is to adjust the steam flow into it to give the required heating rate. This has a fast response time, and would require a larger control valve than controlling the condensate flow. This alternative relies on condensate building up in the boiler and reducing the heat transfer area until the rate of condensation of steam is equal to the condensate flow from the boiler. It has a much slower response time, making control easier, and so was chosen for this apparatus.

The easiest variable to measure to get the heating rate is the pressure drop in the column, which is directly related to the vapour flow. The only disadvantage is that there is some delay between the control action and the measured response, because the change in heat input must cause a change in vapour flow, which must then propagate up the column before being translated to a changed pressure drop. This time lag must be accounted for when choosing the controller constants. It also makes derivative control unsuitable, so a proportional-integral algorithm was used.

Because of the non-linear relationship between pressure drop and vapour flow (especially at higher flows), the proportional gain must also be varied with the set point. This is partly accounted for by dividing the specified gain value by the square root of the set point to give a smaller gain where the pressure drop is higher and varies more rapidly with changing heat input.

The dead time in this control loop makes finding the controller constants more difficult than in the other cases. They were initially found by using the process reaction curve method of Cohen and Coon, described by Stephanopoulos (1984) and then modified by experiment.

After a step change in condensate flow, the pressure drop across the column changes from its initial value and reaches a new one, even with no control. The process reaction curve is in this case a plot of the change in pressure drop against time.

It may be approximated as a dead time, t_d, over which the pressure drop does not change, and an exponential approach to the new value, whose time period τ is given by the slope at the point of inflexion of the actual curve. The static gain, K, is also used, which is the ratio of the steady state pressure drop to the condensate flow (measured as control valve position). The best values of the proportional gain and integral time constant for the controller are then given by:

$$K_c = \frac{1}{K}\frac{\tau}{t_d}\left(0.9 + \frac{t_d}{3\tau}\right)$$

and

$$\tau_i = t_d \frac{30 + 6t_d/\tau}{9 + 20t_d/\tau}$$

Values of K, τ and t_d were estimated at pressure drops of 10 and 2 mbar (assuming that pressure drop is proportional to the square of the heat load), for a 10% change in pressure drop and K_c and τ_i calculated. These values are given in table 5-6.

Pressure drop	mbar	2	10
Change in pressure drop	mbar	0.2	1
Static gain	mbar / (% open)	0.06	0.13
Dead time	s	67	30
Time constant	s	270	120
Calculated K_c	(% open) / mbar	61	28
Calculated τ_i	s	147	66

Table 5-6 Initial controller constants for heat input control loop.

The experimental values of K_c*(set point)$^{1/2}$ and τ_i are given in table 5-7. It was found to be better to use a smaller time constant and larger gain than the calculated values, to reduce the size of the fluctuations in pressure drop at the expense of a less steady condensate flow.

Implementation of control loops

The control loops are implemented with the velocity form of the discrete proportional-integral-derivative (PID) control algorithm (see for example Stephanopoulos, 1984), although in all the experiments the derivative time constants were set to zero. The equation for this is:

$$\Delta c_n = K_c\left(1 + \frac{T}{\tau_i} + \frac{\tau_d}{T}\right)\varepsilon_n - K_c\left(1 + \frac{2\tau_d}{T}\right)\varepsilon_{n-1} + K_c\frac{\tau_d}{T}\varepsilon_{n-2}$$

where K_c is the proportional gain,
T is the length of the sampling interval (1 second in this case),
τ_i is the integral time constant,
τ_d is the derivative time constant,

Δc_n is the change in the control output in the nth sampling period and

ε_n is the error in the nth sampling interval (the difference between the desired and actual value of the measured variable).

This algorithm has the advantages that it does not need an initial value of the control output signal and it can recover quickly if integral windup occurs and the control valve becomes saturated because of a persistent error.

Details of the four control loops are given in table 5-7:

Controlled variable	Measured variable	Proportional Gain	Integral Time Constant / s	Derivative Time Constant
Control valve 1 position (cooling water flow)	Reflux tank temperature / C	6	40	0
Control valve 2 position (reflux flow)	Reflux tank level / %	0.8-1.6	40	0
Control valve 3 position (feed flow)	Control valve 2 position (and reflux ratio) / %	-0.3	40	0
Control valve 4 position (steam condensate flow)	Column Pressure drop / mbar	-200/sqrt(set point in mbar)	60	0

Table 5-7 Details of the control loops

Computer and interfacing

The computer used to control the rig and to log data from it was an Opus Technology PCIII, which is compatible with an IBM XT. It had to receive information from the rig about the temperatures, column pressure drop and reflux tank level. It also had to control the four pneumatic control valves.

Inputs from column

Because of the flammable materials to be distilled, the devices in the laboratory sending information to computer had to be isolated from it. This was achieved with Zener barriers, which would short-circuit any excessive voltage trying to enter the laboratory.

Serial inputs from temperature sensors

Because of the number of temperature sensors, individual barriers for each sensor would be expensive, and the signals would still have to be interpreted by the computer. As a result, an MTL 831/836 multiplexed barrier unit was used, which was supplied by Measurement Technology Ltd. This unit consists of an MTL 831

transmitter, mounted in the laboratory, which converts the measured voltages into temperature values. These are then sent to an MTL 836 receiver in the control room, along two wires, so that only two barriers are needed. The receiver translates the temperatures into RS-232 format for transmission to the computer. The computer was already equipped with an RS-232 serial port so that this approach avoided any extra interfaces.

Analogue inputs from differential pressure transducers

The signals from the differential pressure transducers were both in the form of voltage signals, which had to be read by the computer. This required an analogue to digital converter, to convert these voltages into numbers which could be read by the computer. A PC27 16 channel, 12 bit analogue to digital converter was purchased for this purpose from Amplicon Liveline Ltd. It could read voltages from 0 to 4 V and convert them into numbers between 0 and 4095, a resolution of about 1 mV. The signal from the level transducer was reduced from 0-10 to 0-4 V with a simple potential divider. The 1-5 V signal from the pressure drop transducer was fed directly to the converter, so as not to impair its accuracy. This resulted in a reduction in the maximum measurable pressure drop from 60 to 45 mbar. Any pressure drops over 45 mbar were measured on the water manometer.

Output to column - Digital to pneumatic conversion

Two options were available for transmitting the control signal from the computer to the control valves. Either an electrical signal could be sent to a flameproof, electrically actuated valve, or the electrical signal from the computer could be translated into an air pressure and sent to a pneumatically actuated valve. The first option would provide more precise control, however pneumatically actuated control valves were available in the department, together with digital to pneumatic converters, and so these were used. It was still necessary to provide a digital signal from the computer, and so a PC14AT 48 line programmable input/output board was purchase from Amplicon Liveline Ltd to do this. It also contained three 16 bit counter/timers which could be used to provide a timing signal to interrupt the computer every second to execute the control programme. One of the six 8-bit output ports was used to send the control signal to each valve, leaving two spare. These digital signals (numbers between 0 and 255) were converted to 4-20 mA current signals in a digital to analogue converter unit made in the department. The current signals from this unit were converted to air pressures by type 100X current to pneumatic converters, manufactured by John Watson and Smith Ltd. These were not intrinsically safe, and so were mounted in

the control room, close to the computer and the pneumatic signals piped through the wall to the valves in the laboratory.

Control and data logging software

The control and data logging software had to provide reliable control of the rig and record sufficient information to establish that the operation was stable and to allow all the aspects of the packing's performance to be calculated. In addition, it was also designed to provide estimates of the packing performance during operation and to allow the controller constants and set points to be changed.

Control

The control part of the programme runs independently of the rest of the programme. It is executed every half second and controls two of the control loops each half second, so that the sampling interval for each loop is one second. It is interrupt driven, and the interrupt signal is generated by the timer on the analogue to digital converter board, which reads the reflux tank level and column pressure drop. The reflux tank level is read on one interrupt and the column pressure drop on the next. The control signal is read and the change in control valve position calculated as described earlier. Because the control valves exhibit considerable hysteresis, a correction is applied to the calculated output value which depends on whether the valve is opening or closing.

Data logging

The data logging programme must read and record information and allow information to be entered.

The temperature information is requested and read through the computer's serial port. The nature of this port means that each byte received must be read before the next one arrives and bytes cannot be transmitted until the previous one has left. An interrupt driven programme is therefore used to send data to and read it from the serial port.

This programme takes commands from an output buffer and passes received information to the rest of the programme through an input buffer. It can either send commands and receive data only when requested, or it can request and read temperature data continuously.

The interrupts are generated by the computer's system timer, the interrupt with the highest priority; the rate is changed from the usual 18.2 Hz to 518 Hz. This rate is more than double the rate of reception of bytes with the baud rate (number of bits per second) set to 2400, so there is no chance of missing one. Each byte is transmitted with a parity bit and a stop bit so that with a baud rate of 2400, 240

bytes are received per second. Every time an interrupt is received, the programme checks whether information is ready to be sent or received and takes the appropriate action.

The rest of the data logging programme runs continuously. A central 'core' loop is executed as frequently as possible from within all parts of the programme, to update the information displayed on the screen. The variables containing the input data are automatically updated by the interrupt routines, so this programme is only concerned with displaying results and allowing information to be entered, such as flow readings or new controller parameters. The programme operates from a menu system, which lets the operator choose whether to enter data or display additional information, such as a heat balance. This programme is described in more detail in appendix 4.

5.3 Commissioning

Considerable effort was necessary to commission the system. This work consisted of pressure testing the main components, testing the pipework for leaks, calibrating the temperature probes and flow meters, setting the controller constants, measuring the control valve characteristics and developing the operating procedure. Gor and Wan (1992) assisted in this work.

5.3.1 Pressure testing and leak testing

Pressure testing

The reboiler, condenser and distillation column all had to be hydraulically tested before they were erected. For the reboiler, this was a legal requirement, and the test was witnessed by a representative of the University's insurance company. The tests were carried out by assembling all the equipment and blanking all the openings. Each item was filled with water and pressure applied with a high pressure hand pump. The test pressure was maintained for about 20 minutes and the apparatus observed for leaks. All the items were found to be free from leaks except for the newly manufactured column section, which had to be returned to the fabricators for re-welding.

Leak testing

The pipework was tested for leaks by applying the highest possible static pressure, by filling the rig with water. The pipes carrying pumped fluid were tested as far as possible to the maximum pump pressure. Most of the problems were with screwed joints, which were sealed with PTFE tape.

5.3.2 Calibrations

The temperature sensors, flow meters and column pressure drop transducer all needed to be calibrated. Calibration of the temperature sensors and flow meters was undertaken by Gor and Wan (1992) and is described in detail by them. The temperature calibrations were given in table 5-4. The flow meter calibration equations are given in appendix 6. The column pressure drop transducer was factory-calibrated, and so it was necessary only to ensure that the analogue input board read the correct voltage corresponding to the current signal from the transducer. This was achieved by adjusting the range setting on the board with the aid of a digital multimeter.

The temperature probes were calibrated against a standard probe by placing them all in a water bath up to 50 °C and an oil bath from 50 to 160 °C. About 30 readings were taken at each temperature and the average taken, to reduce the random error. The deviation was plotted against the standard temperature and found to be linear.

The flow meters were calibrated with water by measuring the volume collected in a given time, for a series of scale readings. The resulting calibration graphs were close to the standard curves supplied for water. Originally, stainless steel floats were used in the rotameters, but only a small range of the scale was used. Consequently, they were replaced by korannite ones to increase the accuracy of the readings. The flow meters were then re-calibrated.

5.3.3 Control loops

The proportional gain and integral time constant for each loop were set initially as described earlier. They were adjusted by experiment to give an acceptable response, which had to be fast enough to cope with any changes in operation without becoming unstable. Too high a gain would cause oscillations, whilst too high an integral time constant would give too slow a response. The constants used were given in table 5-7. We saw that the non-linear relationship between column pressure gradient and vapour flow meant that the constants for this loop depend on the set point.

Whilst setting up the controllers, it proved necessary to apply a correction for hysteresis in the control valves, so as to improve the stability of the flows and the accuracy of the flow measurements. The control valve characteristics were therefore measured. These were approximated by equations which are used by the control programme to determine the valve position for a required flow (see appendix 4).

5.3.4 Preliminary experiments

The rig was tested as extensively as possible with water as the process fluid. All the instruments and the control system could be checked in this way and any remaining leaks found. Experiments were also carried out to establish that the vent pipe was big enough and that the secondary condenser would be effective in reducing the discharge of vapour if the cooling water failed.

The heat balance was tested at this stage, and whilst the balance over the boiler agreed with the measured reflux flow to within a few percent, the condenser heat balance overestimated the heat removed by as much as 20%. Despite extensive investigations of the cooling water flow meter and temperature probes, the source of this discrepancy was not found. Because the other readings agreed so well, the cooling water heat balance was subsequently ignored.

After the experiments with water, the rig was drained and cleaned with methylated spirit, to dissolve any remaining water. It was again drained and finally purged with compressed air for several days to evaporate any remaining solvent, before being filled with the chlorobenzene- ethylbenzene test mixture.

The column was packed initially with Mellapak 500YW, so that its operation could be verified against Sulzer's published data for this packing and test mixture. These first tests agreed closely with the published results and confirmed that the column operated correctly.

5.4 Conclusions

The 317 mm inside diameter distillation column test rig, complete with support and access structure was successfully designed, built in a flameproof laboratory. and commissioned. The accuracy of the measurements and safety during construction and operation were considered during the design process. An extensive instrumentation and control system was designed and installed to allow easy, safe and stable operation by a single operator. It is capable of operating at total and partial reflux with a packed height up to 2 m.

Chapter 6 - Experimental packing tests

The primary purpose of the experimental work was to compare the performance of packing with the new shape with that of a standard shape under distillation, and so to establish whether it would be better for air distillation. This could be achieved satisfactorily with tests at total reflux and with a standard test system. All the packings for these tests were supplied by Tianjin University Packing Factory.

Before these tests were carried out, the rig was to be tested with Sulzer's Mellapak 500YW and the standard test system of chlorobenzene and ethylbenzene to ensure that published results could be repeated.

Partial reflux tests were also planned in the hope of obtaining some information about the relative resistances in the vapour and liquid phases in each shape and with different types of surface.

A further aim of the work was to test all the packings, and additionally Norton's IMSP 1T under a range of conditions which should be similar to those in air distillation; the test system of toluene and n-hexane was chosen for this work, and runs were planned both at total and partial reflux.

As a result of a failure of some of the packings to perform as anticipated under distillation, a second piece of apparatus was constructed to measure the flow down the walls in a packed column section.

Packings tested

Several different types of packing were supplied by Tianjin University packing factory. These were manufactured in both the standard and new shapes with a standard fluted surface and in two nominal specific areas. Their standard packings were very similar to Sulzer's Mellapak.

The new packing was also made in gauze and with a surface developed at Tianjin University, to allow investigation of surface type.

To reduce the complexity and cost of the prototype tool, the new 350Y packing was made in 100 mm high blocks (half the normal size) and the new 500Y in 50 mm blocks. The standard packings were supplied with a 100 mm block height so as to be comparable.

Because the shapes of the new and standard packings were so different, the metal relaxed to different degrees after pressing. The curved new shape relaxed more and so the specific area of the new packing was higher than that of the standard packing with the same nominal area. This must be remembered when comparing the performance of the packings. The dimensions of the packings were given in table 4-5.

6.1 Distillation Tests

Choice of test mixture

Three possible test mixtures were identified. The first was chlorobenzene and ethylbenzene, because it is well documented (Onken and Arlt, 1990) and because it was used by Sulzer in tests whose results have been published (Spiegel and Meier, 1987). This would allow direct comparison of the results from the Mellapak packing and the published results.

The second was toluene and n-hexane. This was chosen to match the density ratios and vapour-liquid equilibrium of oxygen and nitrogen as closely as possible. Density ratio was used as a comparison because Porter and Jenkins (1979) succeeded in correlating all the physical properties of distillation systems against this parameter, so that systems with similar density ratios have similar properties in distillation.

The final potential mixture was methylcyclohexane and toluene to match argon and oxygen.

Table 6-1 shows some physical properties of each of these systems. It shows a reasonable match between the properties of the cryogenic and hydrocarbon systems, although the cryogenic systems are less viscous, have lower surface tensions and lower diffusivities on account of their much lower temperature.

Property	Units	Oxygen	Nitrogen	Argon	Toluene
Pressure	bar	1	1	1	1
Relative molecular mass	kg /kmol	31.9990	28.01	39.95	92.14
Boiling point	K	90.1800	77.35	87.29	383.80
Saturated vapour density	kg/m^3	4.4800	4.62	5.78	2.91
Saturated liquid density	kg/m^3	1136.00	807.10	1393.00	778.00
Saturated vapour viscosity	micro Pa s	6.8500	5.41	7.43	9.00
Saturated liquid viscosity	micro Pa s	195.800	163.00	261.00	251.00
Saturated vapour kinematic viscosity	micro m^2/s	1.5290	1.17	1.29	3.09
Saturated liquid kinematic viscosity	micro m^2/s	0.1724	0.20	0.19	0.32
Saturated liquid surface tension	mN/m	13.1900	8.85	14.50	18.00
Total reflux flow parameter		0.0628	0.0757	0.0644	0.0612
Critical temperature	K	154.8000	126.30	150.90	594.00
Critical pressure	MPa	5.0900	3.40	4.90	4.05
Critical density	kg/m^3	405.000	304.00	536.00	290.00
Vaporisation Enthalpy	kJ/kg	212.300	197.60	160.00	359.00
Saturated vapour thermal conductivity	mW/K m	8.5000	7.54	6.09	11.10
Saturated liquid thermal conductivity	mW /K m	148.000	136.70	123.20	113.00
Saturated vapour heat capacity (Cp)	kJ/kg K	0.9600	1.12	0.55	1.13

Saturated liquid heat capacity (Cp)	kJ/kg K	1.6300	2.06	1.08	1.81
Saturated vapour self-diffusivity	m^2/s	$2.56*10^{-6}$	$1.92*10^{-6}$	$2.17*10^{-6}$	$5.28*10^{-6}$
Saturated liquid self-diffusivity	m^2/s	$1.92*10^{-9}$	$1.86*10^{-9}$	$1.40*10^{-9}$	$6.18*10^{-9}$
Vapour Schmidt number		0.5970	0.61	0.59	0.59
Liquid Schmidt number		89.8056	108.31	134.03	52.25
Property	Units	n-Hexane	Chloro-benzene	Ethyl-benzene	Methyl-cyclo-hexane
Pressure	bar	1	1	1	1
Relative molecular mass	kg /kmol	86.18	112.56	106.17	98.19
Boiling point	K	341.90	404.90	409.30	374.10
Saturated vapour density	kg/m3	3.30	3.43	3.26	3.34
Saturated liquid density	kg/m3	613.00	970.00	751.00	697.11
Saturated vapour viscosity	microPa s	7.30	10.00	9.00	8.50
Saturated liquid viscosity	microPa s	202.20	287.00	230.00	300.00
Saturated vapour kinematic viscosity	micro m2/s	2.21	2.92	2.76	2.54
Saturated liquid kinematic viscosity	micro m2/s	0.33	0.30	0.31	0.43
Saturated liquid surface tension	mN/m	13.33	20.50	16.60	15.20
Total reflux flow parameter		0.0734	0.0595	0.0659	0.0692
Critical temperature	K	507.40	632.40	617.10	572.20
Critical pressure	MPa	3.03	4.52	3.61	3.47
Critical density	kg/m3	232.80	365.00	284.00	267.00
Vaporisation Enthalpy	kJ/kg	332.60	324.00	341.60	321.00
Saturated vapour thermal conductivity	mW/K m	16.70		16.90	
Saturated liquid thermal conductivity	mW/K m	100.40	108.00	99.00	
Saturated vapour heat capacity (Cp)	kJ/kg K	1.91	1.14	1.67	
Saturated liquid heat capacity (Cp)	kJ/kg K	2.39		1.98	
Saturated vapour self-diffusivity	m2/s	$4.07*10^{-6}$	$5.31*10^{-6}$	$4.92*10^{-6}$	$4.53*10^{-6}$
Saturated liquid self-diffusivity	m2/s	$6.46*10^{-9}$	$5.80*10^{-9}$	$7.02*10^{-9}$	$4.91*10^{-9}$
Vapour Schmidt number		0.54	0.55	0.56	0.56
Liquid Schmidt number		51.04	51.02	43.60	87.68

Table 6-1 Comparison of physical properties of test components and the components of air

Experiments with the first two mixtures were planned and they were both purchased, but there was insufficient time to use the second. It was judged more important to test more packings than to look at fewer in more detail.

We will consider first the methods of packing and operating the column and of processing the experimentally obtained data. We will then go on to examine the results for the different types of packing.

6.1.1 Experimental procedure

Packing the column

The packings manufactured by Sulzer and Norton were supplied de-greased. All the Tianjin university packings were very greasy and so were all de-greased before use by washing them in a tank of trichloroethane.

Inside the column, the packing is supported on a grid which is clamped against the column walls with bolts (figure 4-1). This must be installed perfectly level, once the vapour and liquid samplers under the packing have been installed. Normally it does not need to be disturbed when the packing is changed.

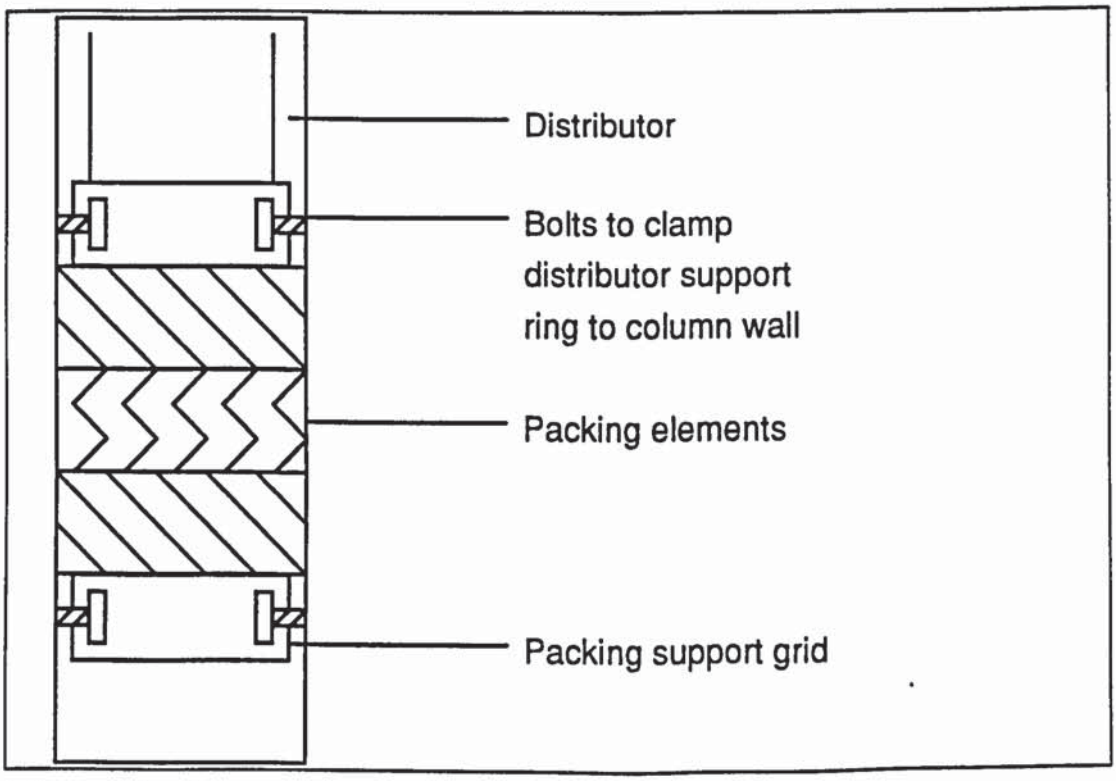

Figure 6-1. Arrangement of packing in column

To pack the column, it is opened at the top, and the top section removed. The wall wipers on the elements are bent down to ensure good contact with the walls and the elements are pushed down the column, one by one with a specially constructed plunger. Care must be taken to ensure that the alignment of elements is correct and does not change as they are pushed down the column. They are usually packed so that each element is perpendicular to the one below.

When the last element has been put in place, the distributor is placed on top and clamped against the column walls in the same way as the support grid (figure 6-1). Great care is necessary to ensure that it is horizontal. Finally the top section of column is replaced and bolted in place.

To unpack the column, it is first purged with nitrogen or compressed air for several hours. The top section is then removed and a lifting bracket bolted to the top flange. Next, the bottom flange is undone and the packed section raised with lifting gear until the elements can be pushed out of the bottom and removed one by one.

Column operation.

The operating procedure for the distillation column rig (including the method of filling and draining it) was developed at the design and commissioning stages and modified during actual operation. It was designed to ensure consistent, safe operation and accurate results. Appendix 7 contains the detailed procedure. Assuming the column is already filled, the procedure is summarised briefly as follows. First the computer is switched on and the input file (appendix 5) is prepared. The control equipment is then switched on, the control programme started and the time noted. Next the cooling water is switched on and then the steam. Any condensate in the boiler is drained until steam leaves the drain valve, to remove any air from the system. The steam flow is restricted with the main valve until liquid appears in the reflux tank (about 5-10 minutes). At this stage, the reflux pump is started and the steam valve fully opened so that the computer control may operate. It is best to start with a high flow (pressure drop set point) so that the rig warms up quickly, and then to reduce the flow to the one required. When the rig has been operating stably for around 15 minutes at high flows to 90 minutes at very low flows, the samples may be taken. Flow and other readings should be taken periodically to check the stability of operation. To shut down the rig, the steam valve is closed. When the reflux tank is emptied, the reflux pump is switched off. Finally, when the cooling water leaving the condenser is the same temperature as that entering it, the cooling water may be switched off and the control programme stopped. The .LOG file should then be copied immediately to floppy disc.

Sampling and composition analysis.

The samples were collected in 7 ml glass vials. Each vial was filled twice and emptied into a waste bottle before the third sample was kept. This ensured that the remains of any old mixture in the line or in the vial are removed. All the waste mixture was kept for re-use in the column.

When the run was finished, the samples were analysed with a Paar Scientific digital density meter. The detailed analysis procedure is given in appendix 7 and the calibration for this instrument in appendix 6. 2 ml samples were injected into the sampling cell with a syringe and the time period of the cell oscillations read

from the instrument. After the reading was taken, the samples were withdrawn back into the syringe and put into a waste bottle, again for re-use in the column. The time period was converted to a composition by use of the calibration equation.

6.1.2 Recording and processing experimental data

As much as possible of the experimental data was logged by the computer. This included all the temperatures and the column pressure drop, so that only the sample compositions, steam and atmospheric pressures and the flow rates needed to be recorded manually. The pressure drop across the packing was usually noted as a check on the value read by the computer. The data recorded by hand was entered on a data sheet, an example of which is given in appendix 7. A data file was then prepared (with the suffix .DPI) to give this data to the data processing programme. Appendix 5 contains an example of this file with more detailed information about its contents. This appendix also contains an example of the .LOG file which is produced by the computer and is also used by the data processing programme.

The data processing programme CEDPKOR2.PAS is listed and described in appendix 6. This produces an output file (suffixed .OUT) which gives time averaged values of the measured variables, a heat balance, the flows and physical properties at the top and bottom of the column and the measured packing efficiency. The most important of these are the flow rate, expressed as the F factor, the efficiency, expressed as HETP or NTSM and the pressure gradient in the packing in mbar/m. The heat balance around the rig is also given as a check on the measured flows. An example output file is given in appendix 5.

The programme calculates the values based on time-averaged results over a chosen interval, and gives the standard deviations of the measurements as well as their values for this period. This gives an indication of how stably the rig was operating, and how accurate the results are likely to be.

6.1.3 Total reflux results

The experiments at total reflux provide an accurate comparison of the different packings. Random errors in the measurements have a small effect on the total error, whilst systematic errors will be substantially the same for each packing. The tests should therefore be able to differentiate packings whose performance differs by only a few percent.

Estimated reliability of results

We saw in the error analysis that the results at total reflux are expected to be highly repeatable. This was confirmed by repeating some points. An error in the

flow could cause an apparently larger error in the efficiency if the efficiency changes quickly with flow and the measured flow does not correspond to the actual one.

Stability of operation

The stability of the operation of the column could be estimated by examining the standard deviations of the measured variables. The standard deviation in the reflux control valve position was normally less than 1% of fully open. This indicates that the flow should be stable to a similar degree of accuracy. The steam condensate flow is less stable, usually around 5%, however the pressure gradient is normally very stable, with a standard deviation of about 1-2% of its value. The vapour temperatures at the top and bottom of the column always have a standard deviation of 0.1 C, the resolution of the displayed temperatures.

Heat balance

An analysis of the heat loss calculated from the reflux and steam flows as a percentage of the total heat input shows that the mean value is about 6%, with a standard deviation of about 2%. The scatter is likely to be due to random errors in the steam and reflux flow measurements, whilst the mean value could be due to genuine heat loss, or to systematic errors in the calculation, or, more likely to a mixture of the two.

The cooling water heat balance was very variable and for this reason was not used in the analysis of the results.

Standard test

The experimental results for the Mellapak 500YW are plotted along with published results for Mellapak 500Y (Spiegel and Meier, 1987) in figures 6-2 and 6-3. The results of this work show a slightly higher efficiency and slightly lower capacity than those found by Spiegel and Meier. But given the slight differences in the packing surface and operating pressure and the smaller column diameter, the agreement was considered good. So the test rig could be used with confidence to compare the other packings with each other and with this standard.

Wall flow and new wall wipers

The first tests carried out were of the new 500, the new 350 and the Tianjin 350. The measured efficiency of these packings is given in figures 6-4. This graph shows that, in contrast to the standard Sulzer Mellapak, the efficiency of these packings falls significantly as the flow (F factor) is reduced.

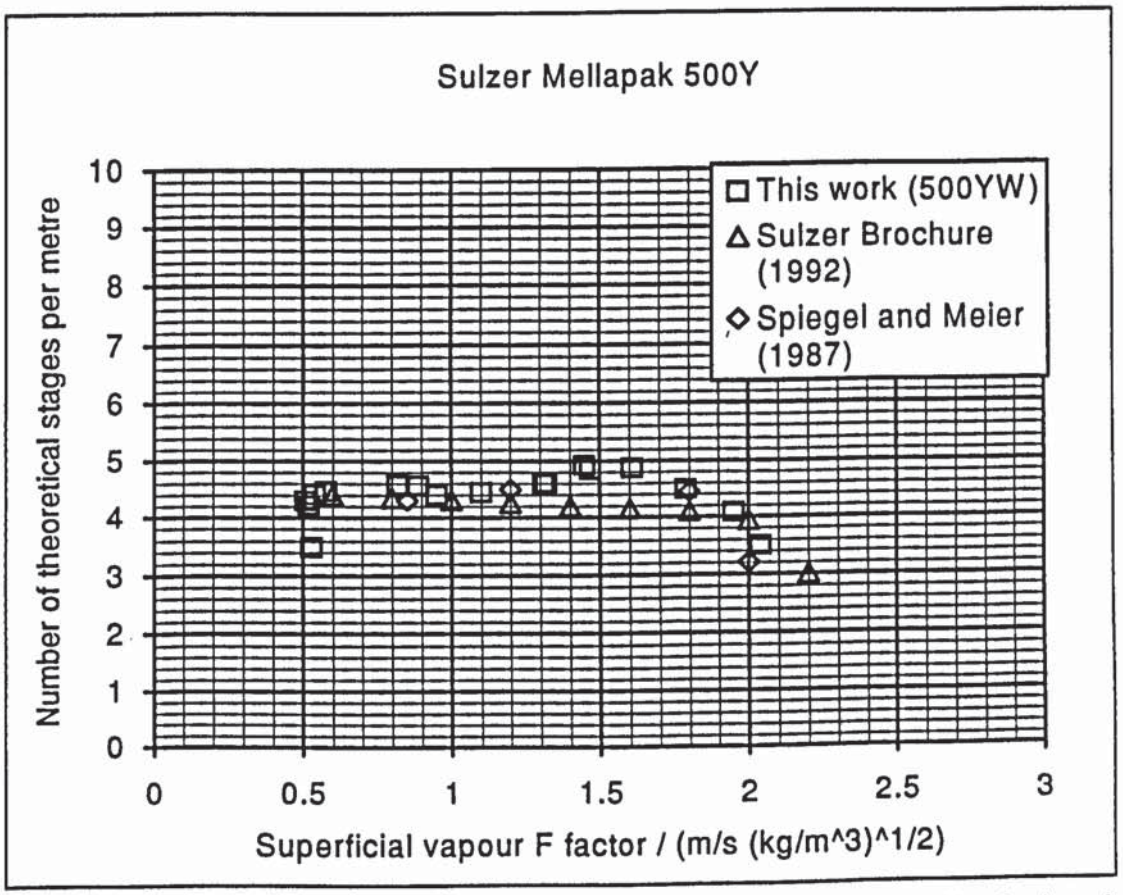

Figure 6-2 Comparison of published efficiency of Mellapak 500Y (960 mbar) and experimental efficiency of Mellapak 500YW (1000 mbar)

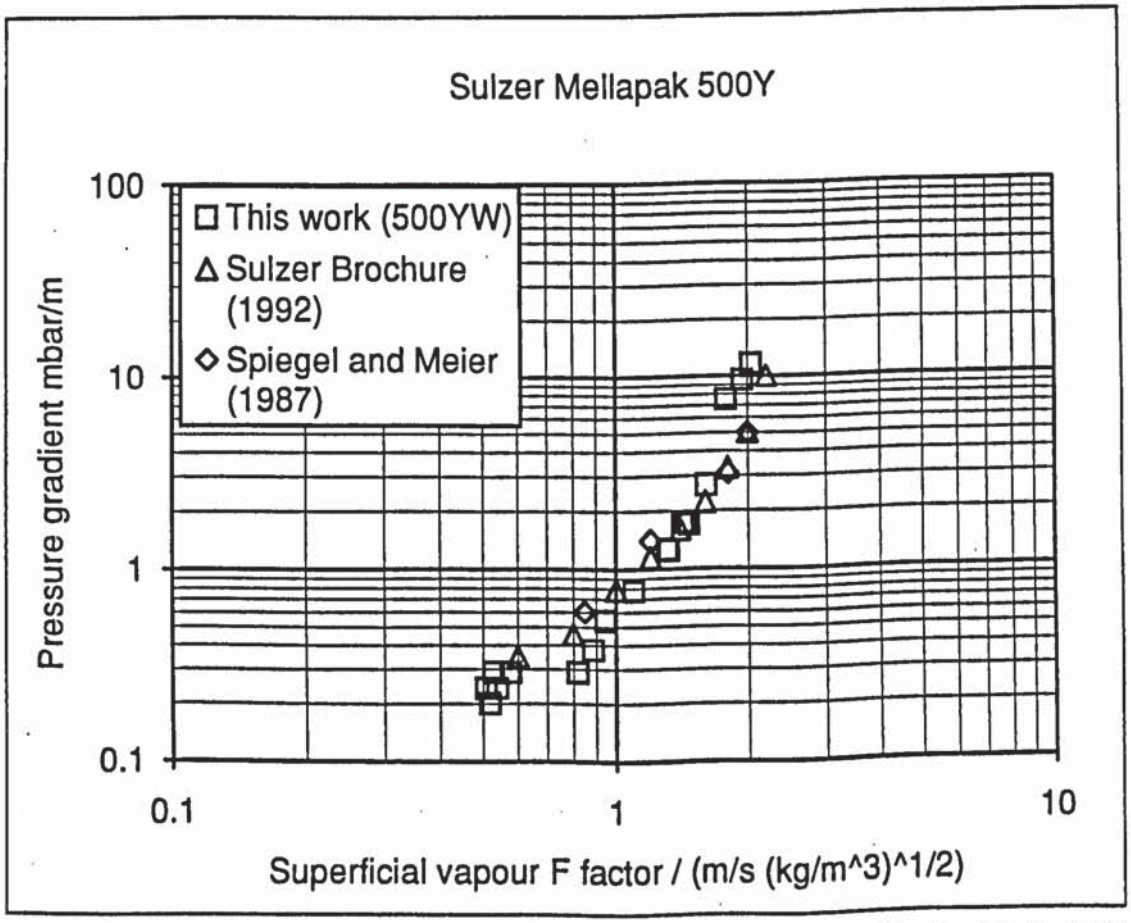

Figure 6-3 Comparison of published pressure gradient of Mellapak 500Y (960 mbar) and experimental pressure gradient of Mellapak 500YW (1000 mbar)

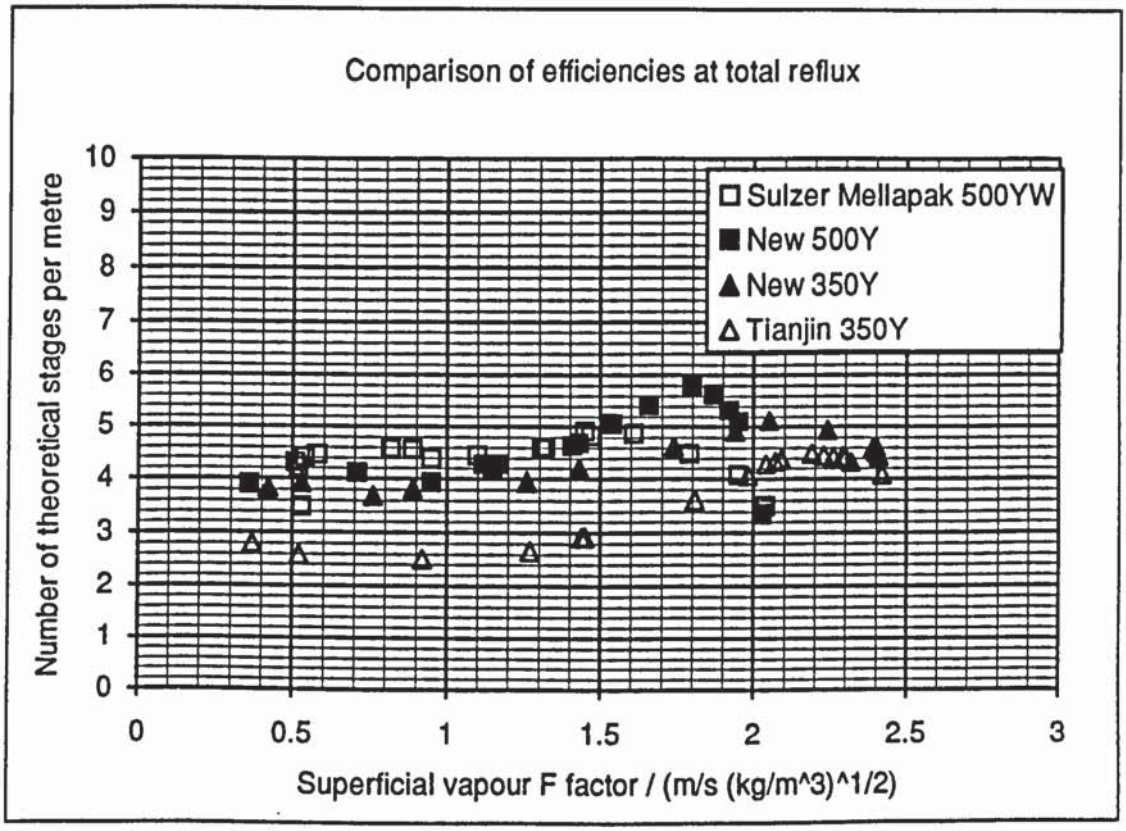

Figure 6-4 Measured efficiencies of packings at total reflux

These results were not expected, particularly in the case of the Tianjin 350 packing, since this is so similar to Mellapak. Observations through the window below the packed bed during operation at low flows showed that most of the liquid was flowing down the column walls, and not through the packing. In the case of the Mellapak, liquid fell evenly from the whole of the bed. At the higher flows, above the loading point of the packing, the increased vapour flow appears to distribute the liquid more evenly and prevent wall flow. Evidence of this is provided by visual observation through the window and by the dramatic increase in efficiency above loading.

One of the advantages of using a structured packing in air separation is the wide range of operation possible, so a reduction in efficiency at low flows is undesirable. Although the effect of wall flow should be reduced as the column diameter is increased, discussions with Professor Yuan revealed that wall flow of up to 30 % had been observed in a 1 m diameter column packed with Tianjin University packing. So wall flow could still be significant at the column diameters likely in a small-scale industrial plant.

Wall-flow has long been known to reduce the efficiency of packings, especially in small columns, and is eliminated in most structured packings by careful design of the wall-wiping bands. For example, Billet and Mackowiak (1988) reported an improvement in performance of Ralu-Pak 250YC of about 20% with sealing bands

over that without. So the performance of the packing at low flows ought to be considerably improved if the wall flow could be eliminated.

After tests with water in a section of column to measure the wall flow (described later), a new type of wall-wiping band was developed which eliminated the wall flow. When this was fitted to the new 350Y packing and the distillation tests repeated, a significant improvement in efficiency of about 25% was observed at low flows. This is illustrated in figure 6-5, which also shows that there is a considerable improvement towards flooding, but that the peak efficiency (excluding near flooding) is about the same. These results are different from those reported by Billet and Mackowiak (1988), in that the peak performance is not increased in the present case, although the size of the improvement at low flows is similar. The capacity was reduced by about 1% by the addition of wall wipers but the pressure gradient at a particular fraction of flooding was not changed (figure 6-6). Given the estimated errors, the reduction in capacity is insignificant.

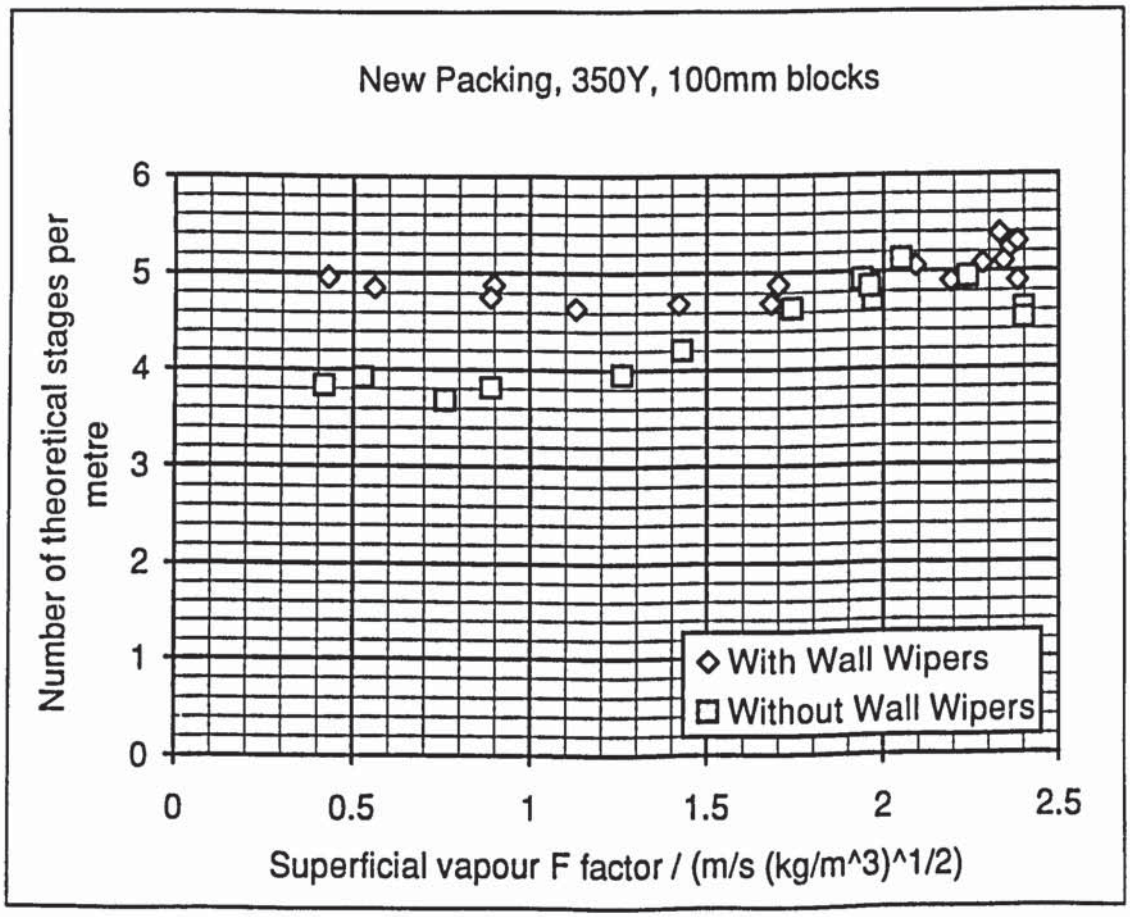

Figure 6-5. Comparison of efficiency of new 350Y packing with and without wall-wipers.

The results show that, with wall wipers, the new 350Y packing is more efficient than the Sulzer Mellapak 500YW over the whole range of F-factors and has a higher capacity. At the same F factor, it has a comparable pressure gradient, although the pressure gradient at a particular fraction of flooding is higher.

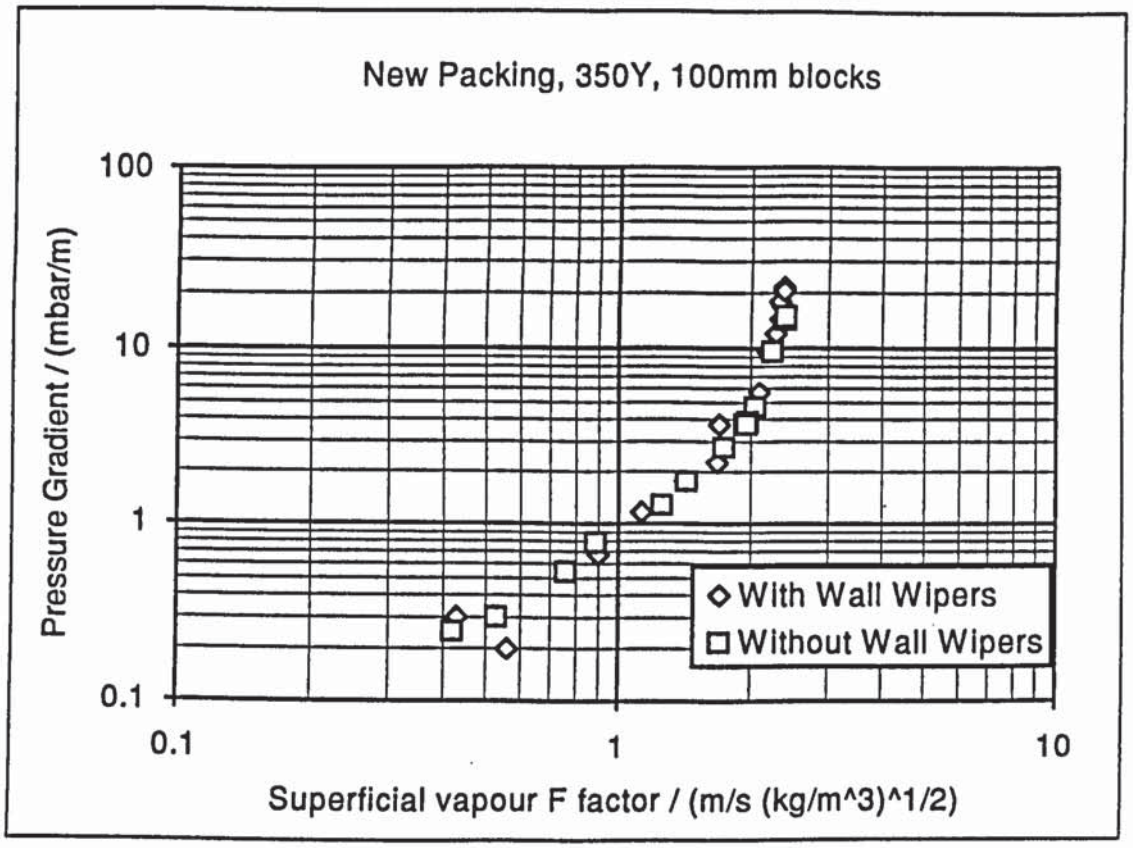

Figure 6-6. Comparison of pressure gradient in new 350Y packing with and without wall-wipers

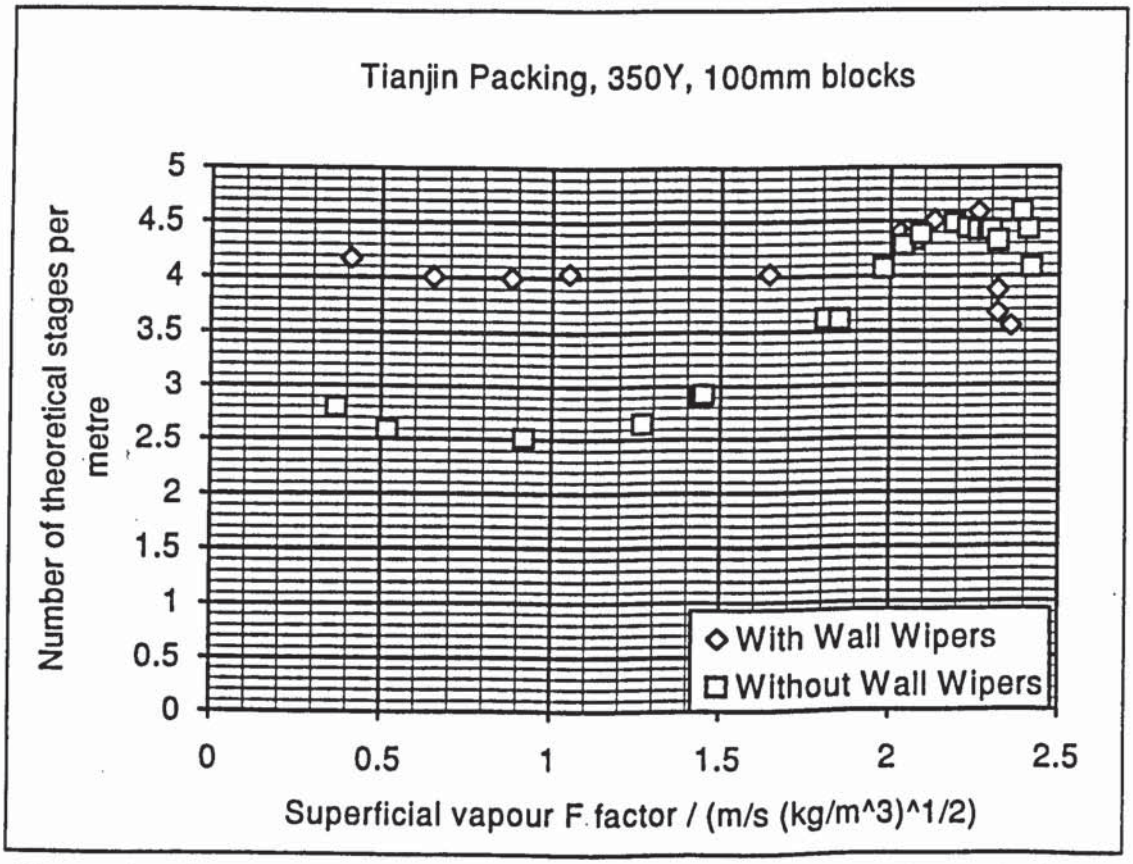

Figure 6-7. Comparison of efficiency of Tianjin 350Y packing with and without wall-wipers. (Data for packing with wall wipers is from Zhang and Robertshaw, 1992)

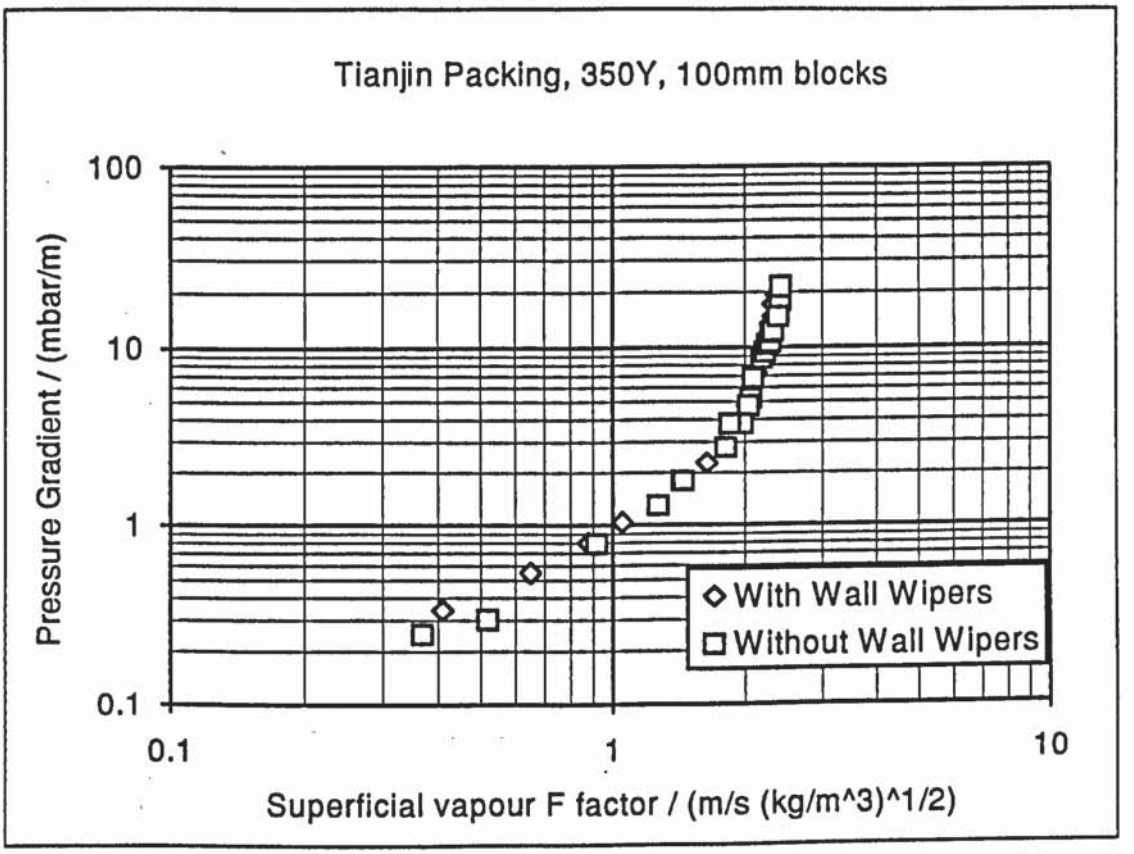

Figure 6-8. Comparison of pressure gradient in Tianjin 350Y packing with and without wall-wipers. (Data for packing with wall wipers is from Zhang and Robertshaw, 1992)

Tests by Zhang and Robertshaw (1992) on the Tianjin 350Y packing with the new wall wipers confirmed that the peak efficiency is not changed, and that the efficiency at low flows is considerably improved. The efficiency of this packing with and without wall-wipers is plotted in figure 6-7. The pressure gradient is given in figure 6-8, which confirms that the capacity and pressure gradient are not significantly altered.

Comparison of Packings

Our aim in conducting the experiments was to establish whether the new channel shape leads to a better packing for air distillation than the conventional one. The main comparison was therefore intended to be between packings which were the same except for the shape.

Unfortunately, because of the manufacturing difficulties, the packings differ in block height, specific area (even if they have the same nominal area) and quality of wall-wiping bands as well as in shape. This makes comparison difficult, but not impossible.

The efficiencies of the new 500Y, new 350Y, Tianjin 350Y and Mellapak 500YW are plotted against superficial vapour F factor in figure 6-9. This graph shows that the packings with the new shape have a higher peak efficiency than

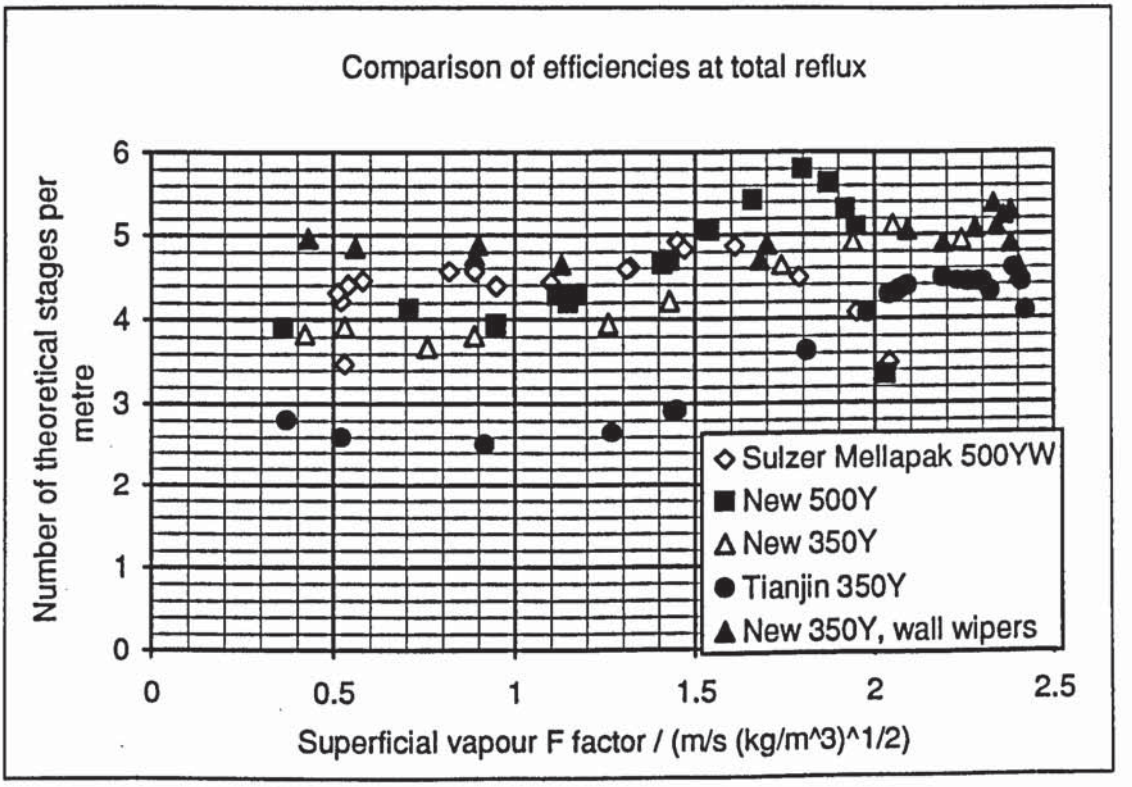

Figure 6-9. Measured efficiencies of packings at total reflux

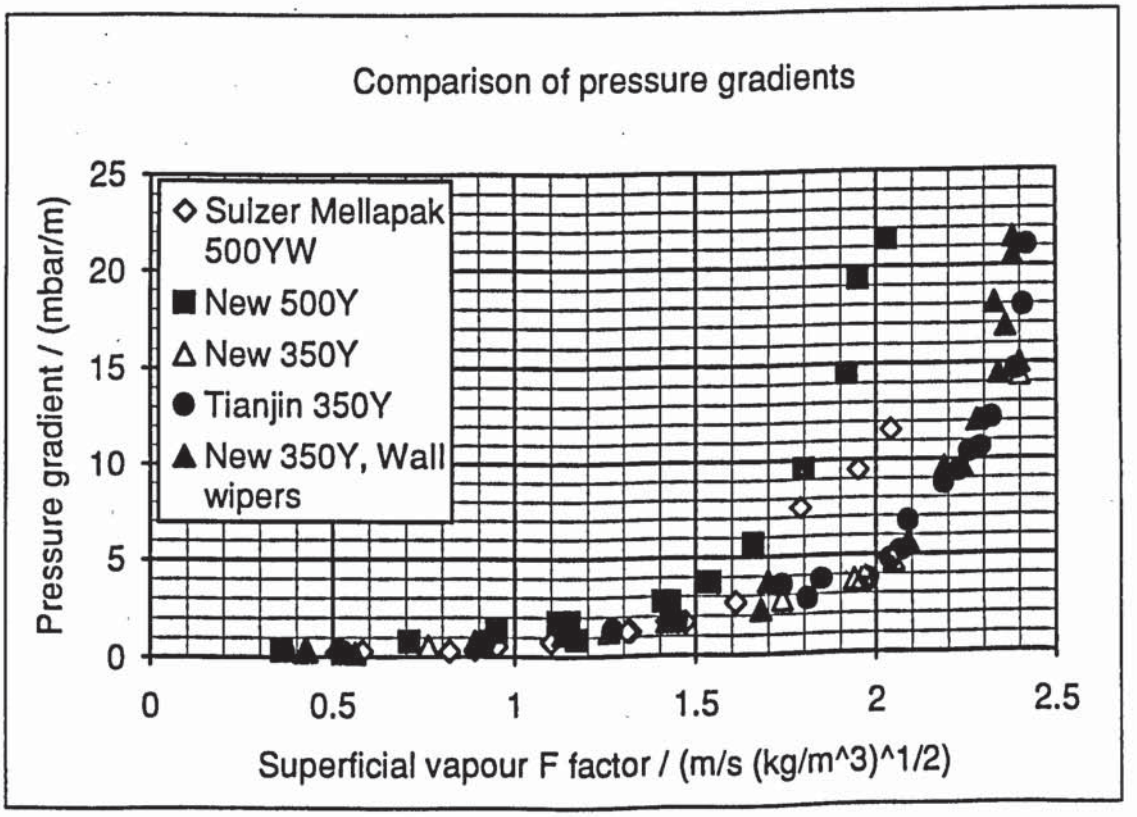

Figure 6-10. Measured pressure gradients in packings at total reflux.

those with the old shape and the same nominal specific surface area. The new 350Y with wall-wipers is as efficient as the Mellapak 500YW and has a higher capacity because of its lower surface area per unit volume. This means that less packing is required per theoretical plate (because of the higher capacity) and that

the packing that is needed uses less metal (because of the lower area). The new packing, is, therefore an improvement on the Mellapak 500YW.

Figure 6-10 is a plot of pressure gradient against F factor. It shows that the packings with comparable specific areas have similar capacities, but that the packings with shorter blocks have a higher pressure gradient at a particular F factor and also at flooding.

The results of the tests with and without wall-wipers showed that the peak efficiency is unaffected by the presence of wall-wipers. This allows us to eliminate the effect of wall flow by comparing the peak efficiencies of the different packings. The design (minimum) efficiency is about 9% less than the peak once wall flow is eliminated, and it is this value which is used for comparison.

The most important variable to make allowance for is the specific area. The simple models predict that the HETP is inversely proportional to specific area, and the more complex ones predict a similar dependence. However, in chapter 4 we saw that the actual dependence at high areas is less than this, and so it is better to use these actual results than the models for the correction. To compare the different packings, we can plot the results for these packings over the results for different sizes of Mellapak in figure 4-13. If we assume that the efficiency depends on area in the same way in all the packings, this will allow us to predict the efficiency of one packing at the specific area of another, and so compare them fairly. We can do the same for pressure gradient and capacity to obtain a complete comparison. Once the effect of area has been allowed for, we can determine the differences made by the packing shape and the block height.

Correction for differing specific area.

Figure 6-11 is a plot against specific area of the design efficiencies (9% less than the peak) of the packings tested, superimposed on the results from Sulzer's (1992) brochure. Experimental efficiencies of the new 500Y and 350Y packings, together with those of the standard shaped Mellapak 500YW and Tianjin University 350Y are shown. The result of a test on the same rig by Zhang and Robertshaw (1992) of Norton's IMSP 1T is also given.

This graph shows that the efficiency of the Mellapak 500YW is about 12% higher than expected from the published values for Mellapak Y, after taking into account that its specific area is only 422 m^2/m^3. This could be due partly to the difference in scale of the tests and partly to the improved surface texture of Mellapak 500YW. Once the results from the Norton IMSP 1T and Tianjin 350Y have been corrected for specific area differences, both these packings show an efficiency about 8% higher than the Sulzer Mellapak 500YW. The new 500Y performs very similarly, with a 9% higher efficiency than the Mellapak 500YW,

whilst the new 350Y shows a dramatically better 15% higher efficiency, or 7% better than the Tianjin 350Y.

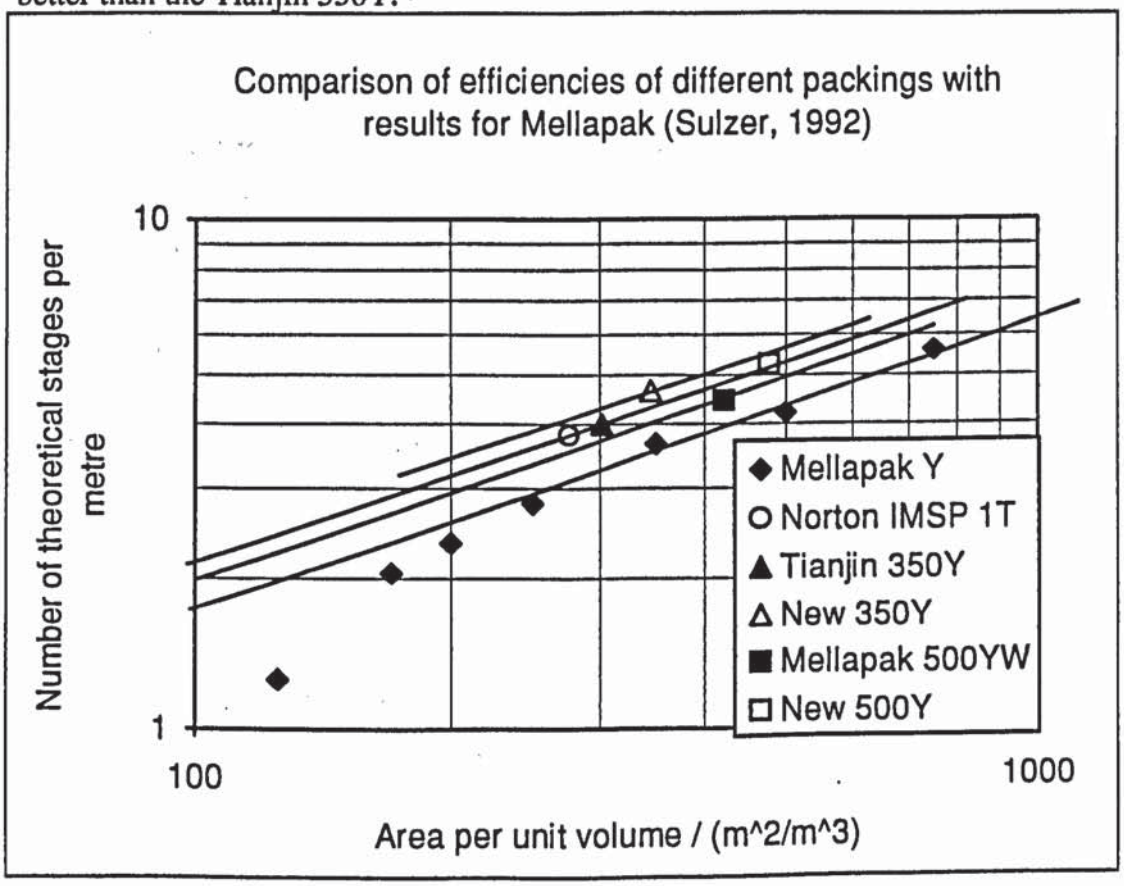

Figure 6-11. Plot of efficiency against specific area for packings tested and for Mellapak. (Data from Sulzer, 1992)

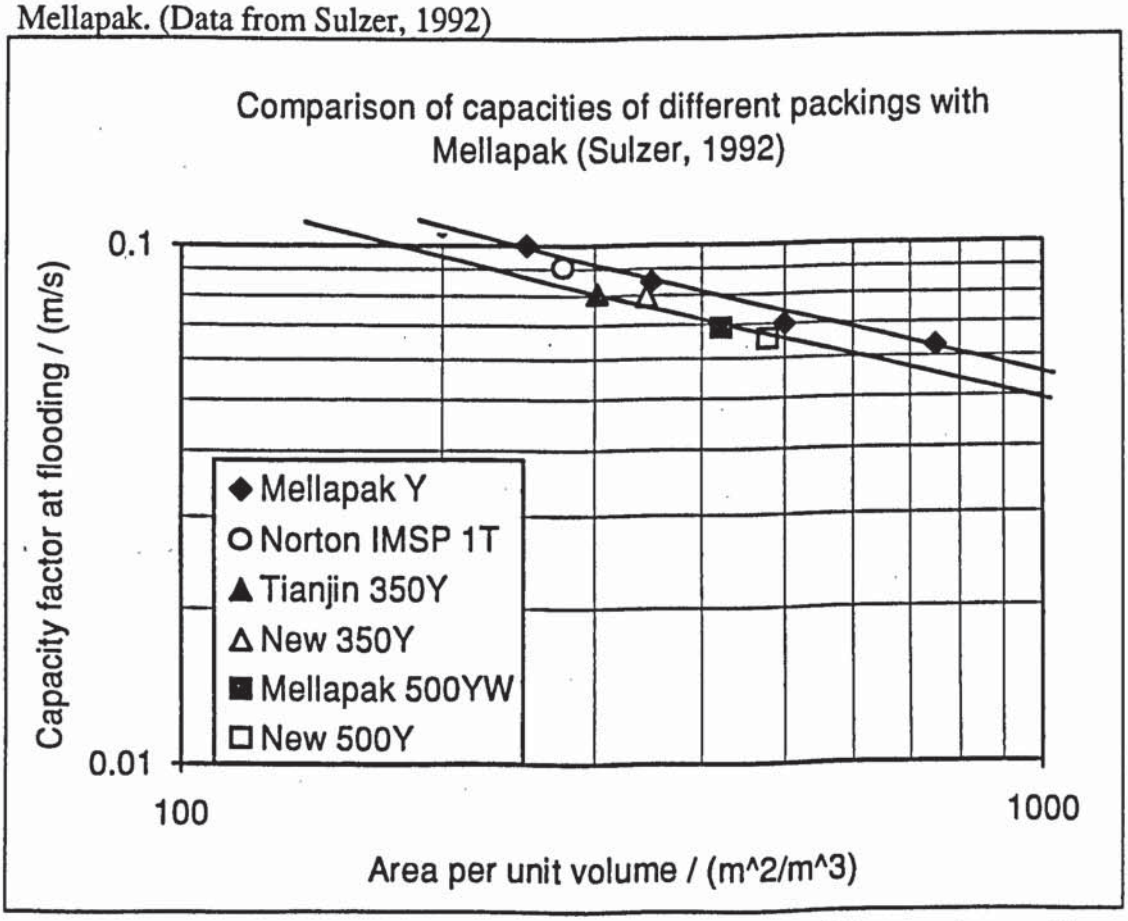

Figure 6-12. Plot of maximum capacity factor against specific area for packings tested and for Mellapak (Data from Sulzer, 1992)

Figure 6-12 shows how the measured capacities of the different packings compare with those of different sizes of Mellapak. This shows that the Mellapak 500YW, New 500Y and Tianjin 350Y all have capacities about 13% lower than the corresponding Mellapak types. This could be due to a systematic error in the flow measurements or to the difference between the packings. The new 350Y packing has a 3% higher capacity for its area than the Tianjin 350Y, which suggests that the new shape in this form actually increases the capacity. In the new 500Y, the shape appears to have no effect. The Norton IMSP 1T has an even bigger capacity for its area; it is about 7% greater than expected from the other packings tested.

The pressure gradients at 80% flood in the packings tested are plotted against specific area in figure 6-13. These show that the Mellapak 500YW has a higher pressure gradient at 80% flood than the Mellapak Y. This is most likely to be due to the definition of flooding used. In this work, hydraulic flooding is used, which occurs at a higher vapour flow than the capacity defined by Sulzer, where the pressure gradient is 12 mbar/m. The Tianjin 350Y and new 350Y both show a higher pressure gradient than the Mellapak 500YW. The new 500Y packing has a still higher pressure gradient, and the Norton IMSP 1T has the highest.

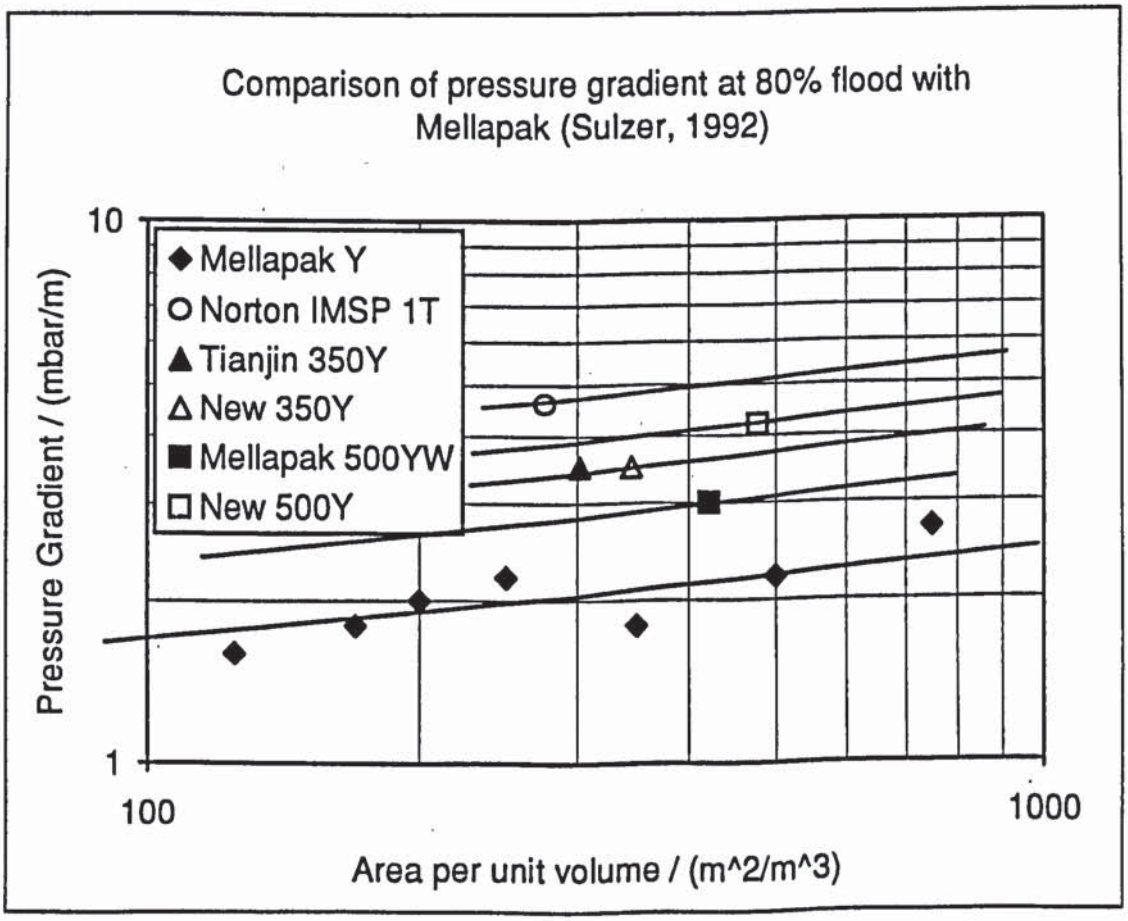

Figure 6-13. Plot of pressure gradient at 80% flood against specific area for packings tested and for Mellapak. (Data from Sulzer, 1992)

These results for pressure gradient should be treated with caution, as the standard results for Mellapak show a considerable amount of scatter (as we saw in chapter 4). The size of the deviation from the best-fit line is similar to the size of the difference between packings, and so any differences may not be significant.

Effect of block height on packing performance

The improved efficiency of the Tianjin 350Y over the Mellapak 500YW was unexpected, as these are essentially the same packing. If anything, the Tianjin 350Y would have been expected to have a lower efficiency, because it has the older fluted surface texture. Since the only other difference is the block height, it must be the lower block height which causes the increase in efficiency. This is likely to be due to increased mass transfer at the leading edge of the blocks because of entrance effects. This is contrary to the results reported by Gaise and Kottke (1989) for a catalyst packing with vapour only flow. In this the mass transfer was enhanced by no more at the entrance to the block than it was at the points where the channels crossed.

A similar entrance effect could be expected in Norton's IMSP 1T packing, since the channel peaks switch to troughs and vice-versa twice in each block. This leads to a height between entrance effects of about 90mm, which is similar to the Tianjin University 350Y packing. In fact, the same enhancement of efficiency is observed.

The new 500Y packing, with even shorter (50mm) blocks could be expected to show an even greater enhancement of efficiency. But even with the new shape, the enhancement of efficiency is only 9% over the Mellapak 500YW. More tests need to be done to establish more conclusively the effect of block height on packing efficiency.

The entrance effect in a pipe depends on the ratio of its length to its diameter. Because packings tend to be made in a variety of specific areas, but all with the same block height, the length to diameter ratio will increase as the specific area increases. This means that any enhancement of efficiency at low areas may not be present in higher area packings, which would explain why the rate of increase of efficiency with area falls as the area increases.

The capacity of the packings appears to be unchanged by the block height. This is unsurprising, since, even if flooding occurs at block boundaries, increasing their number will not change the flooding velocity.

The pressure gradient results appear to show that the as the block height is reduced, the pressure gradient at 80% flood is increased. This is illustrated in figure 6-14, which shows the pressure gradients of the packings at 80% flood, corrected to assume all the packings have a specific area of 400 m^2/m^3. These are plotted against the number of block boundaries per metre. We might expect this to give a linear relationship, as a certain amount of pressure is lost at each boundary.

This appears to be true, with each boundary accounting for about 0.075 mbar pressure drop at 80% flood. This pressure loss is of the order of one velocity head per boundary - $\rho u^2 \sim 4 * 1^2$ Pa = 0.04 mbar.

The Norton packing shows a higher pressure gradient than expected from its area or block height. This is because its different shape leads to a more gradual increase in pressure gradient with throughput in the loading region.

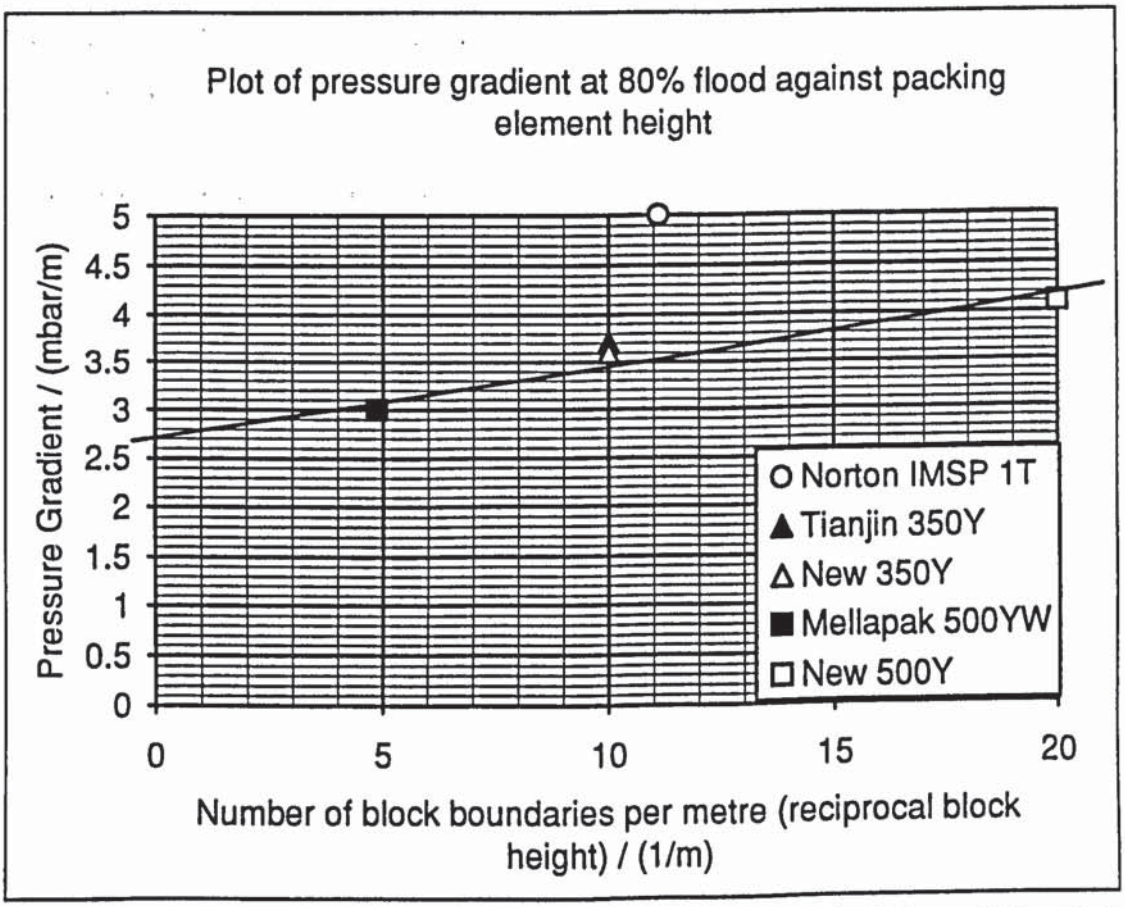

Figure 6-14. Plot of pressure gradient at 80% flood normalised for a 400 m^2/m^3 specific area against number of element boundaries per metre for the packings tested.

Effect of shape on packing performance

The new 350Y packing shows an efficiency which is about 7% higher than that expected if it had the same actual area as the Tianjin 350Y. Since the only difference between these packings (apart from the area) is the shape, we may conclude that the new shape increases the efficiency. In contrast, the new 500Y shows almost no improvement over the Tianjin 350Y (when corrected for the different areas), even though it also has shorter blocks. This could be because of the slightly smaller convergence angle or because a single divergence or convergence in one block provides a smaller advantage than both in the same block. This could only be confirmed by tests with a better match of specific areas.

Surprisingly, the capacity does not appear to be reduced by the new shape, and it may even be increased in the new 350Y packing, which has both convergence and divergence in a block.

The pressure gradients in the new shaped packings are not significantly different from those in the conventionally-shaped ones; the block height appears to have a much bigger impact on pressure gradient than the shape.

These results suggest that the angle of divergence and convergence could be increased, since in its present form the new shape does not disturb the flow sufficiently to alter the capacity or pressure gradient.

Understanding of packing operation

One of the objectives of this work was to improve our understanding of how packings operate. Unfortunately, time did not allow such extensive tests as were planned, however we can still gain some insight from the results obtained, particularly into which areas are still poorly understood and merit further investigation.

Pressure gradient

A logarithmic graph of pressure gradient against F factor for each type of packing tested is presented in figure 6-15. The results of Robertshaw and Zhang (1992) for Norton IMSP 1T are also given.

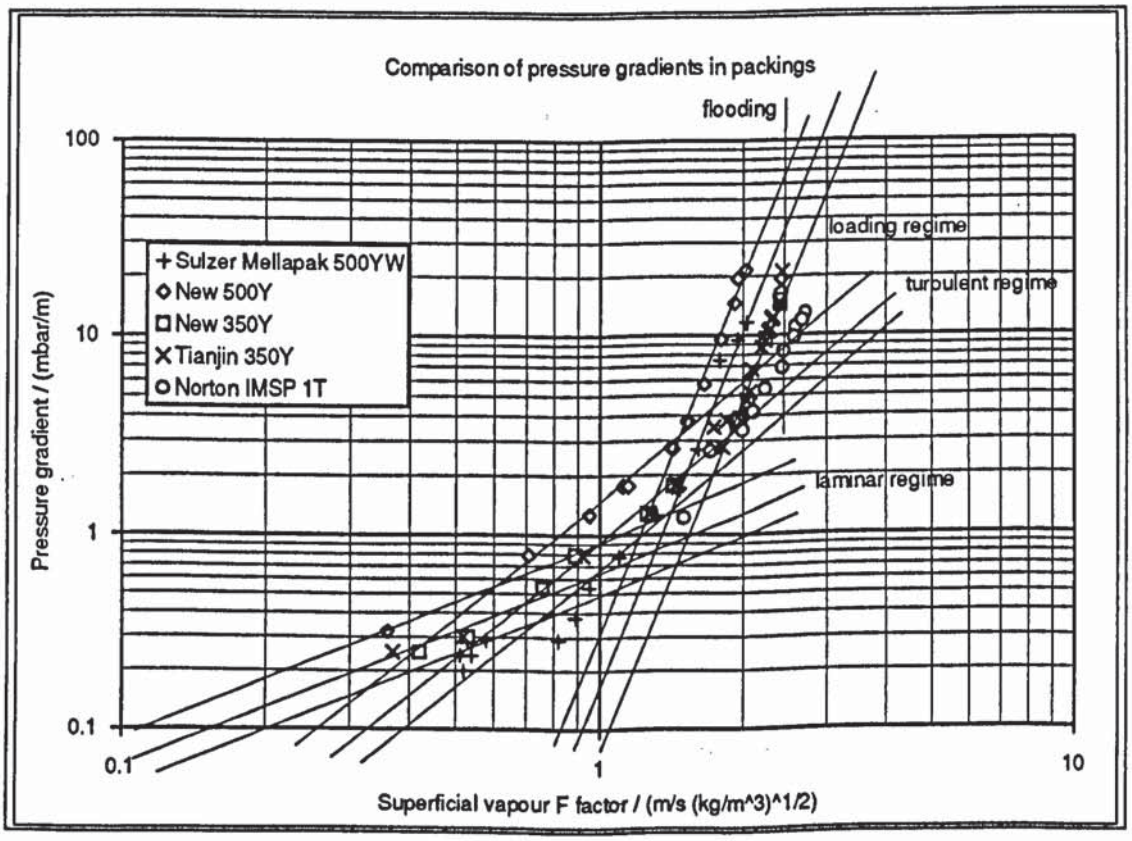

Figure 6-15. Pressure gradients in packings, logarithmic scale

These plots identify the four regimes of operation of the packings: The laminar regime, where pressure gradient (dp/dz) is proportional to vapour velocity (u), the turbulent regime, where $dp/dz \propto u^2$, the loading regime where the vapour and liquid flows interact and $dp/dz \propto u^6$, and flooding where dp/dz increases very rapidly with u. In the Norton packing, the pressure gradient appears to increase less rapidly than u^6 and so the capacity is higher than would otherwise be the case. The pressure gradient at a particular fraction of flooding is also higher.

The transition from the laminar to turbulent regimes occurs at low F factors, and so the laminar regime is unimportant for most operations. Not enough data have been gathered to establish the criterion for the transition.

The velocity at the transition from turbulence to loading depends on the specific area, and, for a particular shape of packing, is a constant fraction of the velocity at flooding. The transition velocities are similar in the new 500Y and Mellapak 500YW and so do not appear to depend on block height, although the pressure gradient at the transition does. If the blocks are smaller, so that the vapour must change direction more often, the pressure gradient is higher. We would also expect that there is an additional pressure drop associated with the entrance region of a block where the boundary layer is not fully established and momentum transfer to the walls is greater.

The new packing shape did not appear to increase the pressure gradient significantly. It is probably not severe enough to create the extra turbulence it was designed for.

These results suggest that the pressure gradient in a structured packing may be considered to be made up of three components: The skin friction, the pressure drop due to changes in direction of the channels and the pressure drop caused by entrance effects. The regimes appear to be defined only by the skin drag term, because the transitions are independent of block height.

Bravo et al. (1992) assumed that pressure gradient was independent of packing type, although they acknowledged that this did not allow accurate modelling of Norton's packings, which are different from most of the others. Their work allows useful predictions of pressure drops in existing packings, but only because they are all so similar. The new approach would allow the effects of changing the design of packing to be taken into account to a greater extent than at present, but finding the size of each contribution would not be straightforward.

Capacity

The capacity of trays and packings is normally measured with different flows of air and water and presented as a plot of capacity factor against flow parameter (see chapter 4). There was insufficient time available for such tests on the packings in this work, and so the capacity could only be established for a single value of the

flow parameter. This is adequate for an initial comparison of different packing types, but it would be desirable to test all the packings at different flow parameters to see whether the capacity changed in the same way for all types of packing.

Packing	Capacity factor at hydraulic flood (X = 0.065)
Sulzer Mellapak 500YW	0.069
New 500Y	0.066
Tianjin 350Y	0.081
New 350Y	0.080
Norton IMSP 1T	0.091

Table 6-2. Measured capacity factors at flooding.

The measured capacities of the packings are listed in table 6-2. The maximum capacities given are those at hydraulic flood, where liquid was held up on the top of the packing. A constant pressure gradient definition was unsuitable because the pressure gradient at hydraulic flood depended on block height.

The hydraulic flood point is the most useful definition for understanding packing operation; it gives the absolute maximum flows, and the pressure drop gives valuable information about the flooding process (Bravo et al. (1992)).

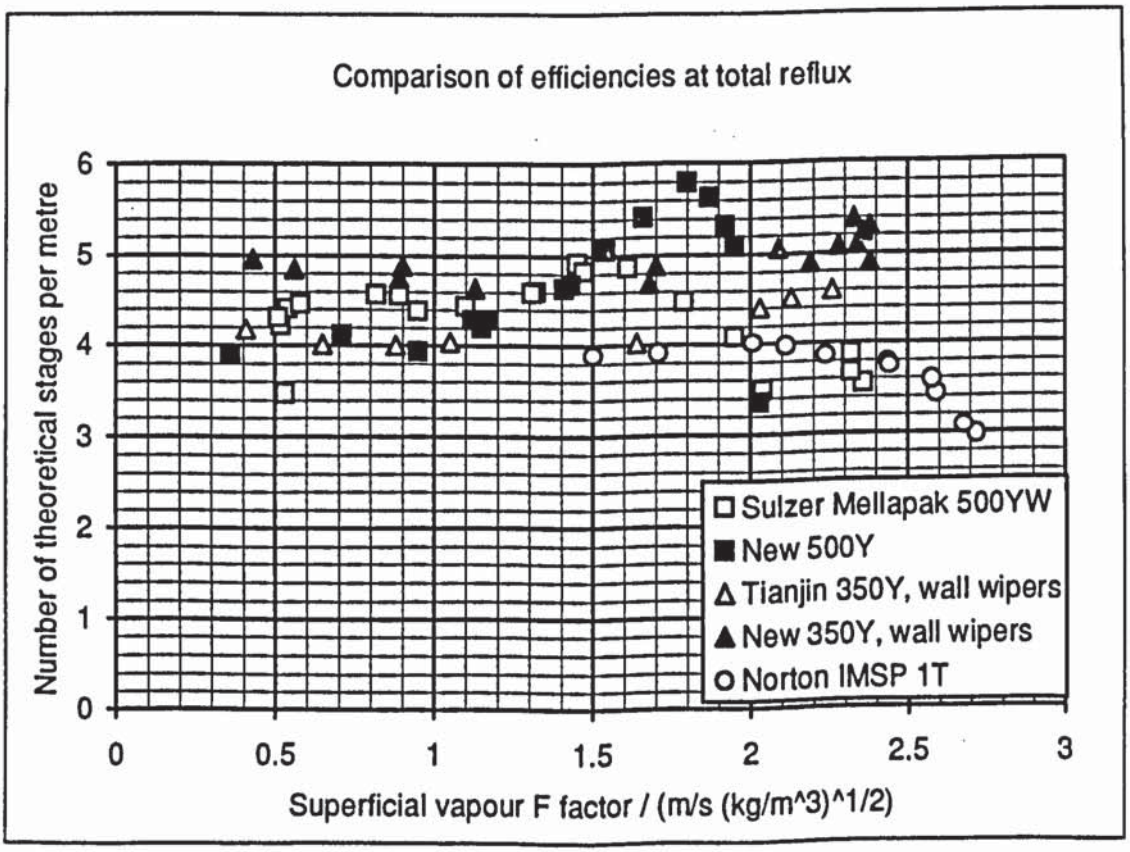

Figure 6-16. Measured efficiencies of packings at total reflux

Efficiency

The efficiency of each type of packing is plotted against F factor in figure 6-16. All the packings show a peak in efficiency as they approach flooding.

The higher area packings are in general more efficient. However, the new 350Y packing is more efficient than the Mellapak 500YW and the Tianjin 350Y packing is more efficient than the published results for Mellapak 350Y. This suggests an improved efficiency due to the shorter block height, which was not anticipated.

The nature of the flow regime appeared to determine the behaviour of the efficiency, although in a particular regime, different packings behaved in differing ways.

At low F factors, the efficiency of the lower area packings decreased with increasing velocity, although not as strongly as the models based on wetted-wall column correlations predict. The higher area packings showed a fall in efficiency as the F factor was reduced below about 0.6. This is likely to be because the distributor was operating below its lower limit. If the specific surface is high, the packings are more susceptible to maldistribution because the liquid must be distributed over a larger area and the cross-mixing per theoretical plate is reduced.

In the turbulent regime, the efficiency is almost independent of velocity. It decreases slightly with increasing velocity, then increases slightly towards loading. The packings in which wall-flow was observed behaved differently; in these, the efficiency increased continually up to loading. This indicates that the wall-flow is reduced as the vapour flow increases, so, even below loading, the vapour flow can influence that of the liquid. This agrees with the findings of Olujic et al. (1992) that gas flow will smooth a maldistributed liquid flow in a small column, however they found that this was not the case in a larger column.

As the velocity is increased further, into the loading regime, the efficiency of each of the packings reaches a local maximum. If wall-flow was absent, this was around 9% above the lowest value of efficiency. This effect appears to be due to the enhanced cross-mixing in the relatively small column; Meier et al. (1979) show that the peak is not present in results from a 1 m diameter column, but it is in those from a 0.27 m one.

There were notable differences in the behaviour of the efficiency of the different packings at flooding. The Sulzer Mellapak 500YW, the new 350Y and 500Y showed a sharp decrease in efficiency from the maximum. In contrast, the efficiency of the Tianjin 350Y and the new 350Y with new wall-wipers had an even higher peak at hydraulic flood and was only reduced when large quantities of entrainment were present above the packing. It was thought that the reduction in efficiency could be due to vapour following lower resistance paths round the packing blocks, but this is not supported by the occurrence of the effect in the new 500Y, which was a very tight fit in the column. Various Russian authors (e.g.

Kafarov, 1969) have reported similar large increases in efficiency near flooding for random packings, whereas most results from manufacturers show a decrease (Sulzer (1992), Norton (1991)). The effect is interesting, but is of little practical significance because the pressure gradient is too high and the efficiency too sensitive to throughput for operation in this region. Like the peak in efficiency at loading, it could be an effect which is only present in small columns.

Models of structured packing efficiency usually predict that the efficiency depends more strongly on vapour velocity than is measured. This is often accounted for by assuming that the interaction between vapour and liquid increases the effective area available for mass transfer as the velocity increases. None of the models is sophisticated enough to allow prediction of the peak in efficiency. The development of rate-based models which take into account liquid and vapour spreading and mixing might eventually make this possible.

6.1.4 Partial reflux results

The partial reflux tests were carried out for two reasons: To attempt to separate the vapour and liquid phase resistances to mass transfer and to see whether the efficiency changes significantly at partial reflux. Time limitations meant that a very limited number of partial reflux runs was possible, and not all the packings were tested under these conditions. Because of the magnitude of the potential measurement errors, the quantity of data is not really sufficient to draw definite conclusions. Nevertheless, the results will be presented with provisional conclusions, as a basis for further work which may be undertaken. Future work at partial reflux could also investigate the effect of reflux ratio on the capacity of the packing.

Efficiency and pressure gradient

The efficiency and pressure gradient of the partial reflux runs are plotted over the results of the total reflux runs for each packing in figures 6-17 to 6-20. This shows, as expected, that the pressure drop with $L/V < 1$ is less than that at the same vapour rate at total reflux. Similarly, the pressure drop at $L/V > 1$ is greater than at total reflux. The efficiency seems to be unchanged at partial reflux; any deviations are within the error limits. Although the efficiency of Mellapak 500Y at partial reflux agrees with the total reflux value within the expected error limit, the disagreement is larger than with the other packings. This could be because stainless steel rotameter floats were used, which reduced the accuracy of the flow measurement, or it may be a significant effect which is worth further investigation. Only further work would establish this.

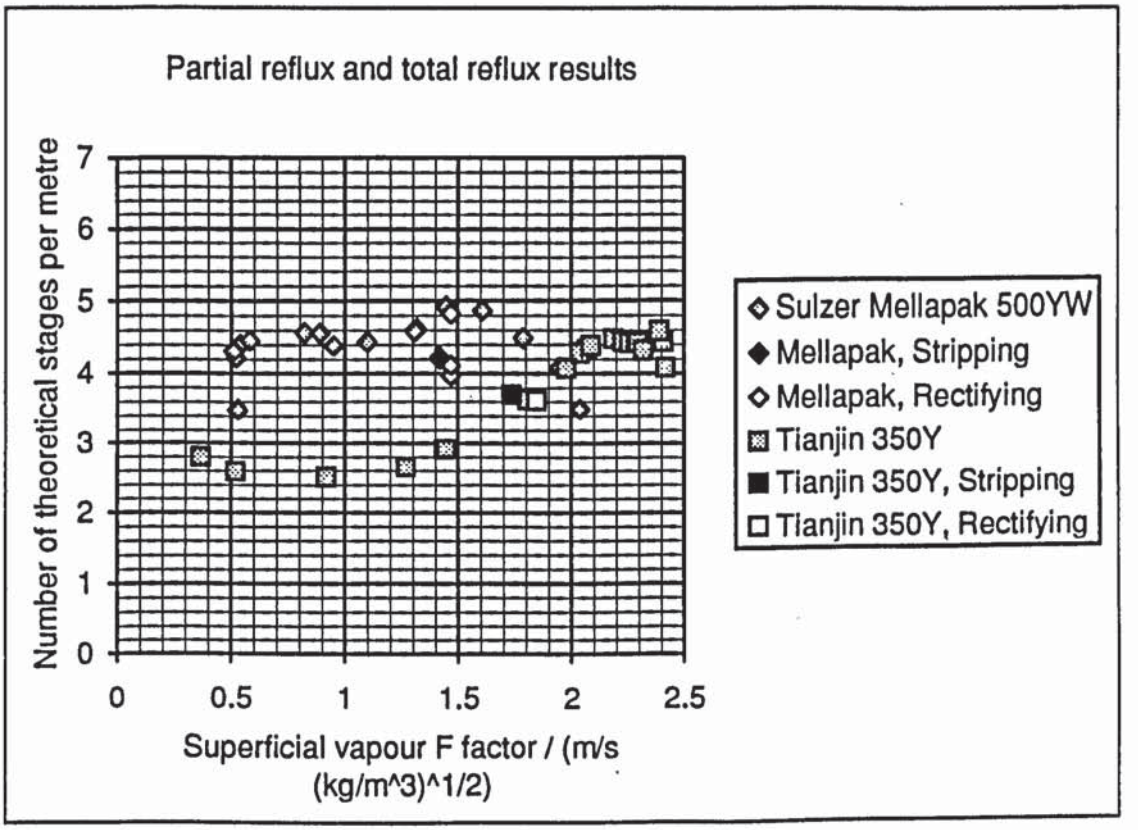

Figure 6-17. Efficiencies of conventionally-shaped packings at partial and total reflux

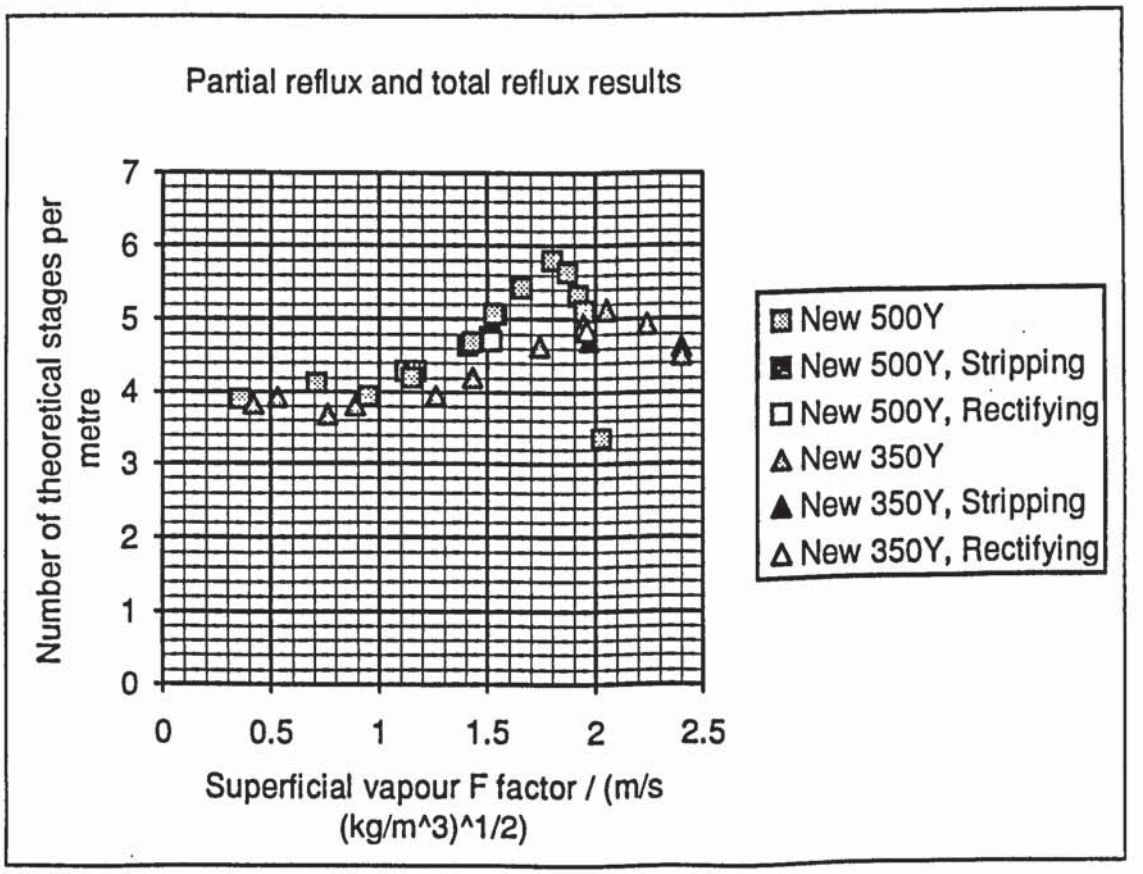

Figure 6-18. Efficiencies of packings with new shape at partial and total reflux

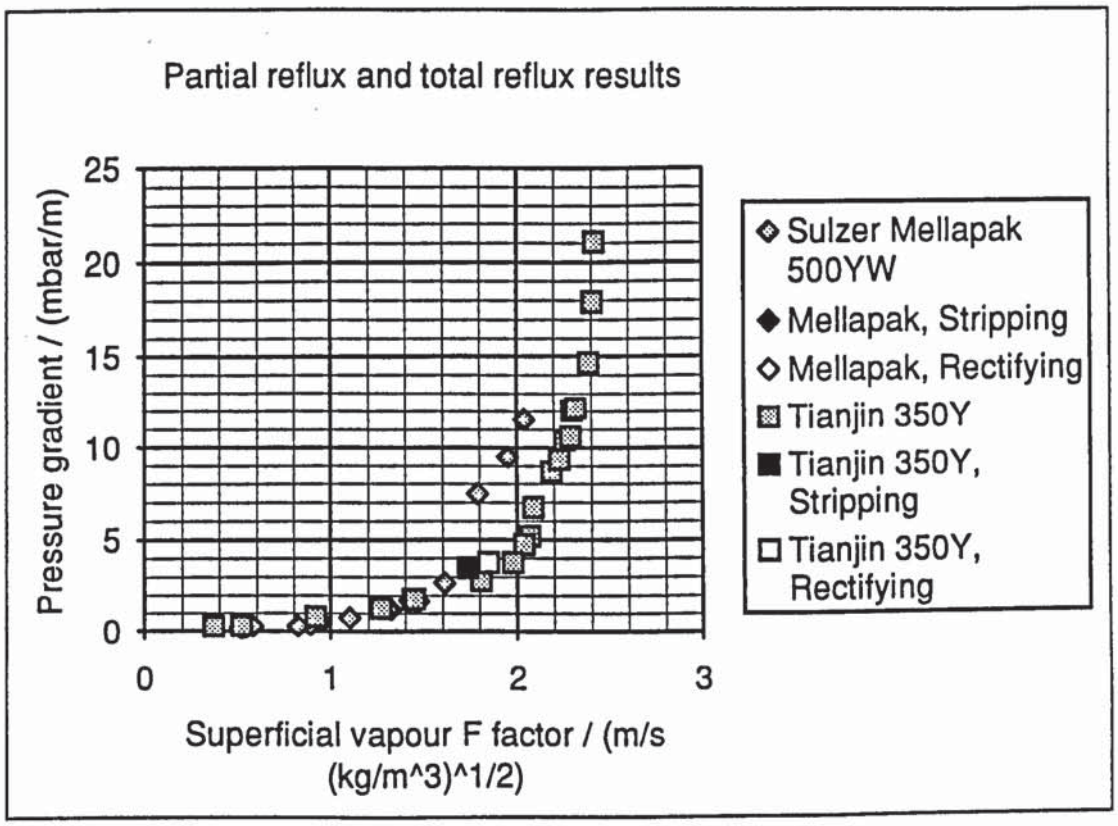

Figure 6-19. Pressure gradients in conventionally-shaped packings at partial and total reflux

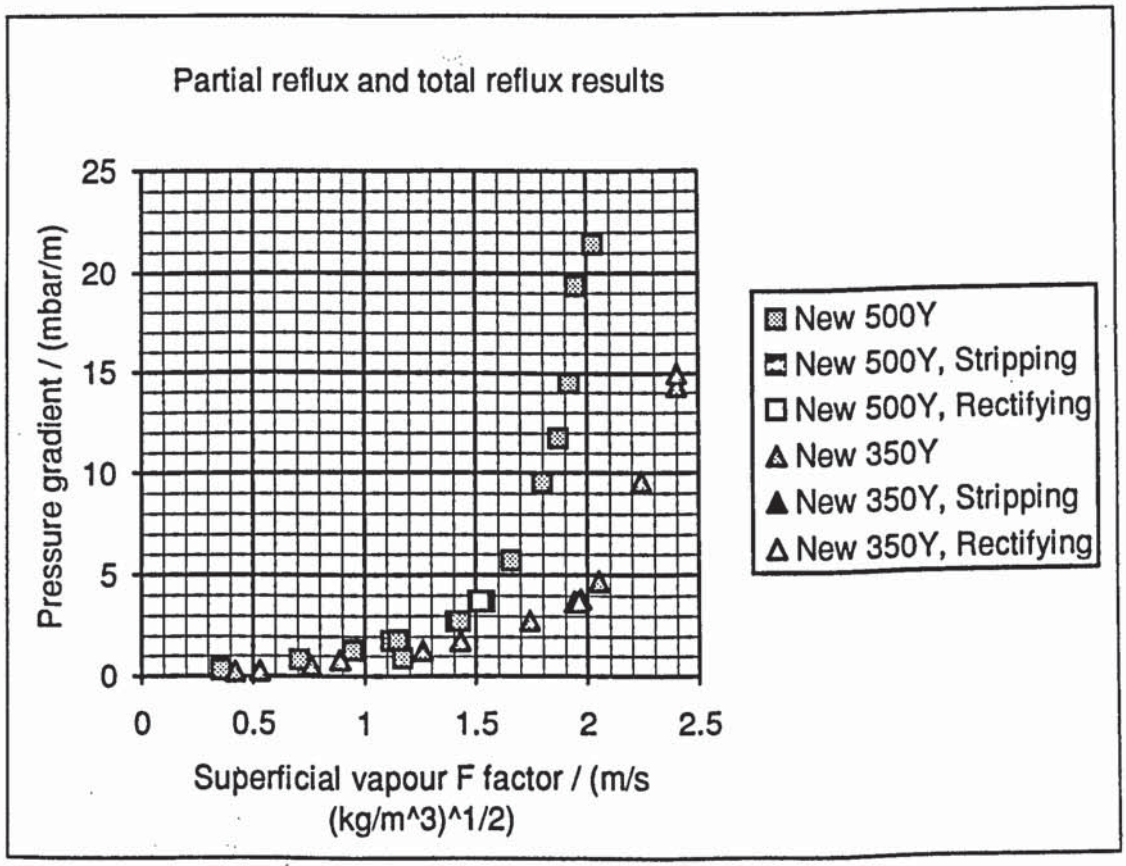

Figure 6-20. Pressure gradients in packings with new shape at partial and total reflux

Vapour and liquid phase resistances

To separate the vapour and liquid phase resistances, we make use of the equation:

$$H_{ov} = H_v + \lambda H_l$$

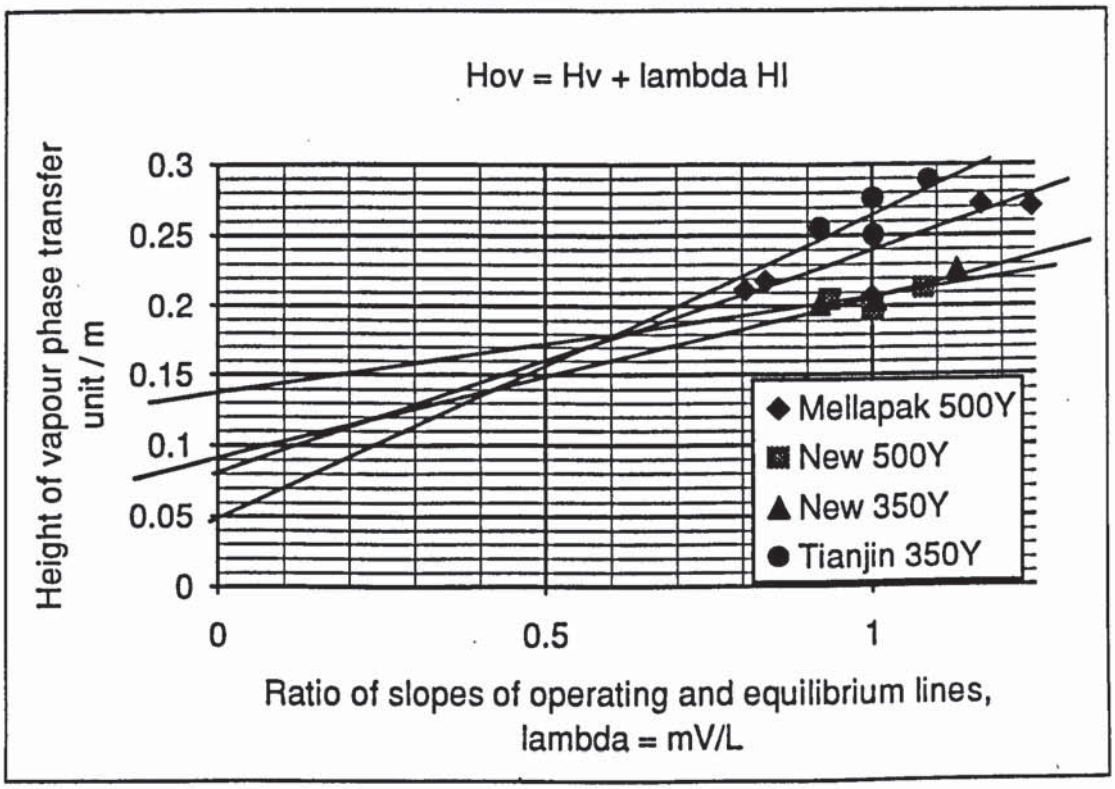

Figure 6-21. Plot to establish resistance in gas and liquid phases in distillation. Intercept gives H_v and gradient gives H_l

If we assume that H_v and H_l are constant, because we vary the flows by only a small amount, then a plot of H_{ov} against λ has intercept H_v and gradient H_l. Such plots are given in figure 6-21 for each packing which was tested at partial reflux. These seem to demonstrate that under the conditions in the rig, the liquid and vapour phase resistances are similar. In the standard shaped packings, the vapour phase resistance accounts for 20% to 30% of the total, whereas in those with the new shape, it is 50 to 70%. So the modification to the packing shape appears to have increased the vapour phase resistance and reduced the liquid phase resistance, the opposite effect to that anticipated.

However, it may be that the difference is insignificant, given the size of the errors. Nevertheless, the effect would be worth further investigation.

It is interesting to compare these results with the models of packing performance (chapter 4). Most predict that the vapour phase resistance accounts for 70 to 80 % of the total, as it appears to in the new shaped packings, but in contrast to the results for the standard packings. The model of Bennett et al.

(1989), however, predicts that the proportion of the resistance in the vapour phase is about 30%, as it seems to be in the standard packings. But this model does significantly over-predict the HETP's of these packings.

6.2 Wall-flow measurements

Earlier in this chapter, we saw that, in the first tests, the distillation performance of the packings manufactured in Tianjin was impaired at low flows because of liquid flowing down the column walls. In order to confirm this effect and then eliminate it, an experiment was designed to measure the proportion of liquid flowing down the walls of a test section of column with packed heights up to 1.2 m. Since the main significance of wall flow is below the loading point, where vapour and liquid do not interact, the experiments were done using liquid only. The liquid chosen was water, even though its wetting properties are different from the hydrocarbon and cryogenic systems, because it is so much easier and safer to use. It is unlikely that the results would be significantly different for other liquids as the packing and column were thoroughly wetted before each set of measurements, and the wall flows measured were steady.

6.2.1 Description of Apparatus and Procedure

The apparatus is illustrated in figure 6-22. Packing was supported in a 1.4 m long section of 12 inch nominal bore schedule 10S pipe, identical to the distillation column. Water was supplied at between 2 and 20 litres per minute through a 24S rotameter to measure the total flow rate into a seven point distributor on top of the packed bed. At the bottom of the bed, a polypropylene funnel with a diameter 10 mm smaller than the inside diameter of the column was held centrally inside the column below the support plate by three bolts. This collected any water flowing out of the packing, while letting any flow down the walls go directly to the drip tray under the column and to the drain. The central flow from the funnel was measured by collecting water in a 5 litre beaker for a suitable time and recording the volume collected. The total flow was obtained from the rotameter calibration chart. Each flow was accurate to about 1%, so the proportion of wall flow was calculated to about 2%.

6.2.2 Results

The results are presented in figures 6-23 and 6-24. It is clear from these results that there is considerably more wall flow from the packings from Tianjin University than from the Norton and Sulzer Packings. The wall flow also builds up very quickly, achieving over 90% of the infinite depth value after only 0.6 m in the case of the new 350Y packing. This packing has less wall flow than the old Tianjin

University 350Y packing. This is expected, as its distillation efficiency at lower flows is reduced from the peak value by a smaller proportion. A more surprising result is that the new 500Y packing has a much smaller proportion of wall flow than the new 350Y although the reduction in efficiency at low flows is comparable. The worst packing was the Tianjin University 500Y with over 70% of liquid flowing down the walls, whilst the best of the Tianjin University packings were the gauze ones. Unfortunately there was no time to test any of these under distillation. The fraction of flow on the walls did not change very much with total flow although it tended either to increase or decrease at low flows, depending on the packing, in an unpredictable manner.

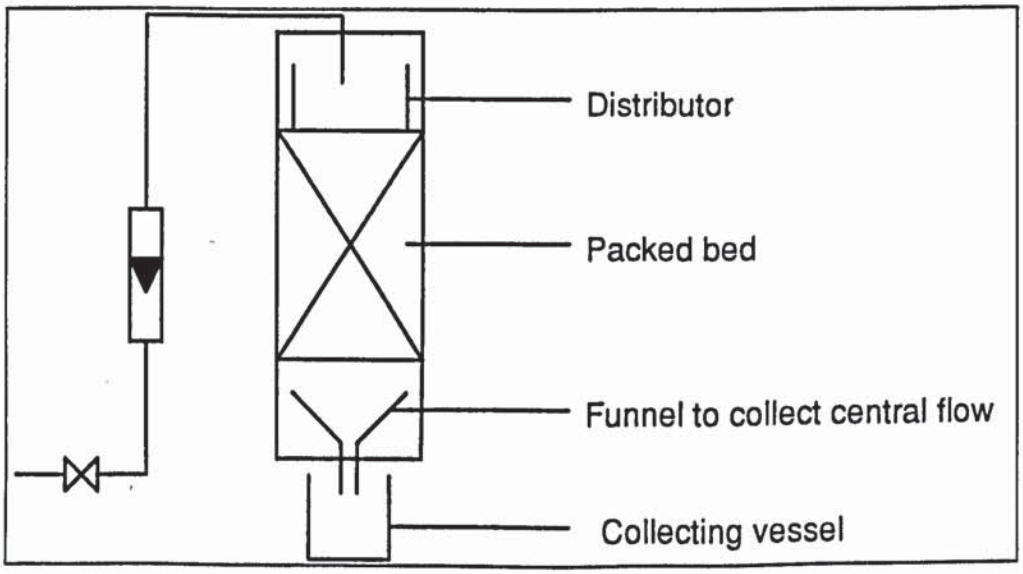

Figure 6-22. Wall flow measuring apparatus

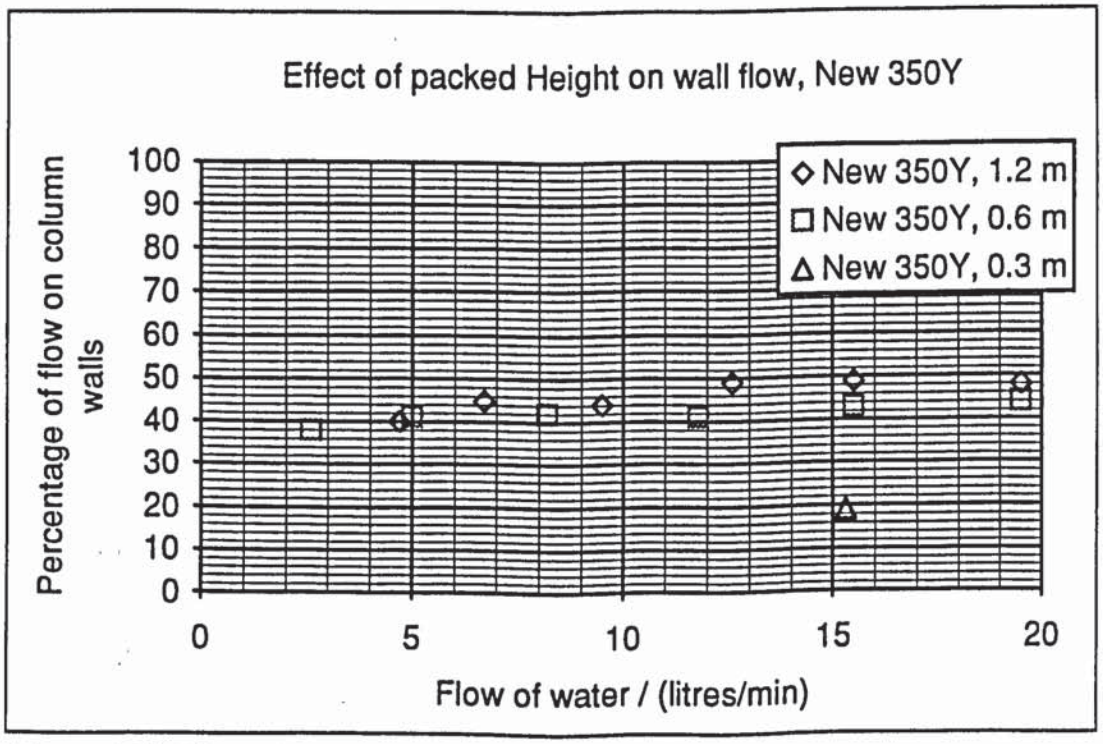

Figure 6-23 Effect of packed height on measured wall flow

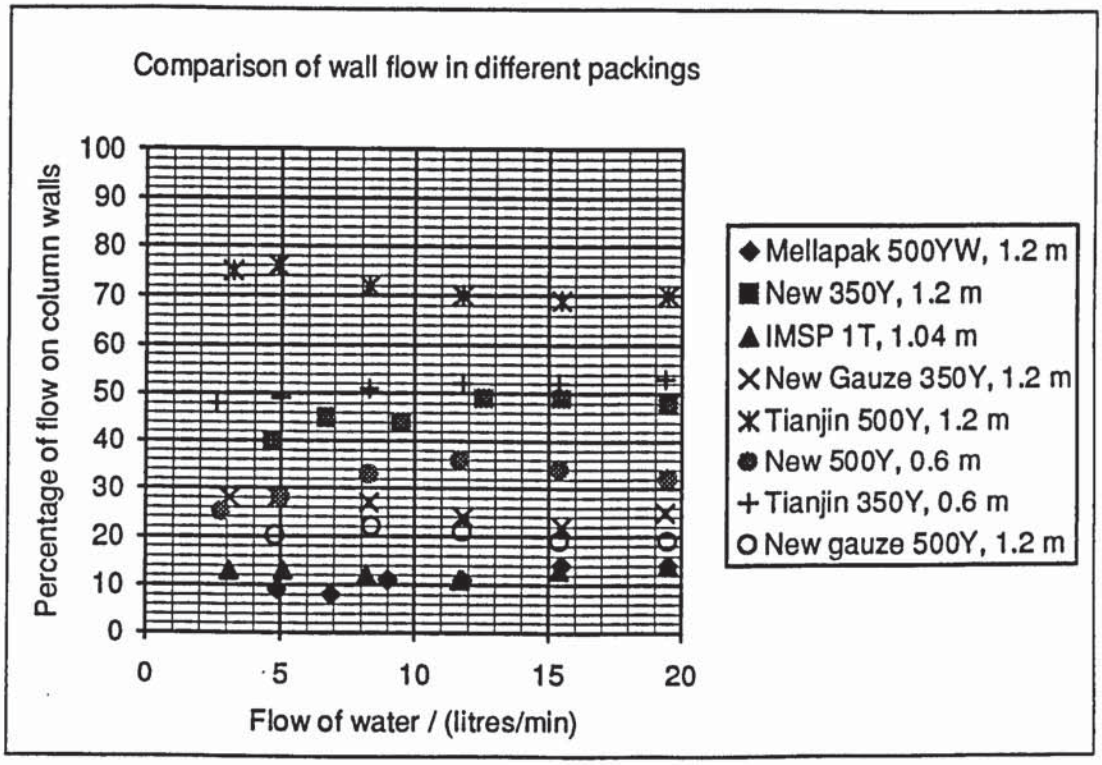

Figure 6-24 Measured wall flow in different packings

The distillation performance of the packings with the wall flows measured could be predicted with a simple model for liquid maldistribution such as the zone-stage model of Zuiderweg et al. (1981). The wall flow will, however, vary with installation and with column diameter, and in any case, because it reduces the packing's efficiency, the most important task is to eliminate it rather than to predict its effect.

Because of this, the new method of binding the packing sheets together into elements (described in chapter 4) was devised to stop the wall flow. The new 350 packing elements were all reassembled with one fewer sheet (to leave more clearance round the blocks) and with the new wall-wiping bands and retested in the wall-flow column. No measurable wall flow was found over the whole range of flows used - a much better result than anticipated. When the distillation tests were repeated with this packing, the efficiency at low flows was increased, as we saw earlier, and so it is recommended that the new wall wiping bands should be used in all future packings.

6.3 Conclusions

The tests on the Sulzer Mellapak confirmed the published data, and verified that the test rig operated as it should, and that the test procedure was satisfactory.

The packings manufactured for this work all showed considerable wall-flow, and it was necessary to modify the design to prevent this. A very efficient wall wiper was developed.

Manufacturing difficulties also meant that packings with the same nominal specific areas actually had different actual specific areas. Nevertheless, comparison was possible by plotting the capacities and peak efficiencies against specific area.

The packings with shorter blocks appear to show an efficiency about 8% higher than the Mellapak with 200 mm blocks. The new shape with a converging section and a diverging section in one block and a convergence/divergence angle of 1.5 degrees is about 7% more efficient than the standard one, once the different surface areas are accounted for, and has a slightly higher capacity. However, the new shape with a single convergence or divergence in a block and an angle of 1.2 degrees appears to be no better than the standard one.

A limited number of partial reflux distillation results did not provide sufficient data to reliably separate the vapour and liquid phase resistances.

Chapter 7 - Discussion

This work has covered three areas: A method has been developed to investigate the economics of changing the column internals from trays to structured packings in an air separation plant; a new structured packing has been developed and a distillation test rig has been designed, built and commissioned and used to test the new packing and compare it with existing ones. We shall now discuss the achievements in each of these areas and the implications of the results for the use in air distillation of the packings tested.

7.1 Economics of air separation processes

Bennett et al. (1989) had already established that, because of their low pressure drop, structured packings could provide a power saving over trays, and so reduce running costs. But because of the unique features of air separation columns - in particular their very closely-spaced trays - it was generally known that structured packings would increase their capital cost. This contrasts with normal distillation columns, where structured packings can lead to smaller columns and a reduction in capital cost (Robinson, 1991). However, no quantitative work has yet been published on the economic balance between power and capital cost.

A method was therefore developed (chapter 3) which allows the extra capital cost due to the use of packing to be balanced with the running cost saved.

The detailed simulation of an air separation plant revealed that changing from trays to structured packing affects the power consumption in two ways. The column system is made more efficient, but the refrigeration and heat exchange system becomes less efficient because of the reduced air supply pressure. The cycle must therefore be carefully chosen to maximise the power saving due to structured packing. From the results of this simulation, a simple model of an air separation plant was constructed to calculate the power consumption with trays and packings and the column sizes. Other running costs did not need to be considered, since these would be the same in each case.

An analysis of the capital costs of the major items of equipment showed that changing to packing would significantly affect only the column and cold box costs. The cost of the other items - heat exchangers, pre-purification units and machines - would be slightly changed, but would have less impact on the capital cost difference between trays and packing. Cost models were therefore established for the columns and their internals and the cold box.

The power and capital cost obtained were then used to calculate the rate of return on the extra investment in a packed plant. The analysis was therefore

relative, and needed to consider only the differences between packed and trayed plants.

This economic analysis showed that there are many variables which affect the capital and running cost of a plant. By quantifying the balance between these variables in a particular case, it allows us to decide whether or not it is advantageous to choose a high capital cost, low running cost packed plant.

The variables may be divided into three groups: plant and market variables, economic variables and packing variables. We shall now discuss the dependence of the economic balance on the variables in each group.

Plant and Market variables

These are considered together because many of the plant variables are set by market demand, for example what size the plant should be, what product purities are required, or how much liquid is to be produced. The most significant of these variables was found to be the plant size, however a number of process changes were also investigated.

Plant size.

The economic analysis has shown that packings provide a greater advantage over trays in larger plants. This is because economies of scale are evident in the capital cost of a plant, but not in its power cost. So, over their lifetime, small plants consume power worth a fraction of their capital cost, whereas a large plant may consume power worth many times its capital cost. In smaller plants, lower capital cost is more desirable than reduced power consumption, whereas the opposite is true of larger ones.

It is interesting to compare this finding with that of Brennan (1992), who compared different air separation methods. He found the economic process depends on plant capacity. Membrane separation is cheapest up to about 20 tonnes per day of oxygen and pressure swing adsorption from 20 to about 100 t/d. Above 100 t/d, cryogenic distillation is favoured. This change in economic separation process is because of the same changing balance between capital and operating costs; distillation is more thermodynamically efficient, and so consumes less power, but cryogenic plant is more expensive.

The largest distillation plants built to date produce around 2200 t/d oxygen. At this size, closely-spaced trays become increasingly difficult to install correctly; the column diameter is around 6 m, and small errors in levelness are critical. So packings may make building larger plants easier. The comparison between trayed and packed plants over 2200 t/d does not take into account the cost due to the

increased difficulty of installing trays, and so probably underestimates the advantage of a packed plant.

In small plants, the extra capital cost of a packed plant is due mainly to the extra column shell and cold box costs, so that highly efficient, high cost packings are favoured. In large plants, the cost of the packing may be several times the column shell cost, so lower efficiency, higher capacity, cheaper packings are better.

Eventually, as the size increases, the extra capital cost becomes proportional to the packing volume. The rate of return on a packed plant then reaches a limiting value, as the extra capital cost and power cost saving increase at the same rate. This does ignore any reduction in the cost per unit volume of packing as the plant becomes large; whether there is any will depend on the packing market at the time.

Because the packing cost is dominant, a suitable method of evaluating packings for use in large plants is that used by Billet (1969) for vacuum distillation, namely the cost of packing per unit throughput per theoretical plate at a particular pressure gradient, or specific cost.

In addition to the limiting cases of small and large plants, the economic analysis reveals the interesting behaviour of intermediately sized plants. If the packing cost dominates at a relatively small plant size, there may be maximum return at an optimum plant size for a particular type of packing in a particular case.

Product mix, purities and demand fluctuations

If purer products are to be produced, more theoretical plates are required. The use of a structured packing means that less extra pressure drop is introduced by these extra plates, so the rate of return increases with the tray count.

A plant which produces argon has an additional argon side column, at least part of which must be packed. Addition of such a column does not reduce the power consumption, but does increase the capital cost. Because a packed argon column has a higher capital cost than a trayed one, the rate of return is lower than that of a plant with no argon column.

In fact, if pure oxygen or nitrogen is to be produced, an argon column is essential, so that argon does not contaminate these products. This means that the comparison between plants with and without argon production is rather unrealistic. Structured packing is still likely to be viable in plants with an argon column, because higher purity products favour packings.

Structured packing also makes possible the addition of many extra theoretical plates in the argon column. This would allow production of pure, rather than crude, argon directly from the argon column. As a result the capital and running costs of an argon purification unit would be saved. The increase capital cost of the argon column could be set against this saving. This work has not investigated this possibility because a considerable amount of argon is used in the crude form. The

size of the market for pure argon would also have to be considered, especially if the proposed plant were large.

The reduced refrigeration efficiency of a packed plant means that if more liquid is produced, the power saving over the comparable trayed plant is less. The rate of return is therefore lower. If a large quantity of liquid is required and is produced by an external liquefier or an additional liquefaction cycle, the packed plant would show a greater return. In general, the less refrigeration needed in the separation cycle of a packed plant, the better the return.

Packed plants have the advantages both of faster response time, because of lower liquid hold-up in the column and of a wider range of operating capacity. They are therefore able to adjust more easily to both long and short term variations in demand. However, if the plant were to operate below design capacity for a significant period, the power cost saving and hence the rate of return would be reduced.

To take full advantage of the wide range of operation it may be necessary to pack the high pressure column as well as the low pressure and argon columns. This would also reduce the rate of return because of the increased capital cost and small additional power saving.

To allow for these effects in the economic analysis, some value should be placed on being able to adjust easily to demand, for example reduced storage costs.

Other plant variables.

Other plant variables which were considered are the plant lifetime, the low pressure column top pressure (set by the air purification method), the reboiler-condenser temperature difference, the arrangement of the columns and the choice of cycle (refrigeration method).

As the plant lifetime increases, power saving becomes more important relative to capital cost. This means that if the plant lifetime is significantly shorter than the 10 years assumed, packing is unlikely to be economic.

The pressure at the top of the low pressure column needs to be just high enough to enable withdrawal of the nitrogen product. If the air is purified in an adsorption unit, the nitrogen pressure needed to regenerate the adsorbers is the limiting factor; the low pressure column top pressure is higher unless blowers are used for the regeneration. The results show that the lower this pressure, the bigger the rate of return possible by using structured packing. If this pressure is lower, the percentage reduction in the high pressure column pressure from trays to packing is greater and the compressor power saving is bigger.

For a similar reason, reducing the temperature difference between the oxygen and nitrogen in the reboiler-condenser increases the rate of return, but the effect is less significant.

If the columns are placed side by side, so as to reduce the cold box height, the rate of return on a packed plant is reduced, because the proportionate increase in cold box height is greater. Packing the high pressure and argon columns also reduces the rate of return because it provides little power saving but increases the cost.

An important finding of the work is that the cycle should be carefully chosen to optimise the advantage of packing. The more efficient the refrigeration method is, the smaller the deterioration in efficiency in changing to a packed plant. This is illustrated by the difference between the air boost and simple air expansion cycles. Changing to packing has less impact on the air boost cycle, because the percentage increase in flow is lower.

The analysis led to the conclusion that the refrigeration efficiency of the air boost cycle may be maintained in the change to a packed plant by adding power to the booster to maintain its pressure. The extra power added is less than the power saved, and the rate of return on the change to packing is increased.

Economic conditions

As economic conditions change, the relative costs of power and construction materials will change, as will taxes and interest rates. The first two variables will affect the rate of return in a particular plant, whereas the second two will determine what the acceptable rate of return is.

A higher power cost increases the cost saving associated with a particular power saving, and so will increase the rate of return on a packed plant and make smaller packed plants viable. In assessing the viability of a packed plant, an average power price over the whole plant lifetime should be considered.

The cost of capital does not directly affect the economic analysis, but it will determine the lowest rate of return required. So the level of interest rates will affect the minimum feasible packed plant size.

Taxes are not accounted for in the economic model. Like interest rates, the level of tax will affect the rate of return necessary structured packings to be worthwhile.

The construction costs in the model are for to mid 1992. Any future use of the model would have to ensure that up-to-date values were used. Higher capital costs will favour trays and increase the size of the smallest viable packed plant

Packing variables

The economic analysis allows the effect on the rate of return of a change in a particular packing variable to be established, if all the other variables are held constant. This may then be compared with the change in the other variables

required to effect the same change in the rate of return. In this way, the relative advantage of changing one packing variable rather than another has been determined. The balance between the variables is different according to the plant size; the pressure gradient and capacity are more important in larger plants, whereas the efficiency, distributor height and packing cost are more important in smaller plants.

Efficiency.

Improving the efficiency of the packing increases the rate of return by reducing the extra capital cost. It reduces the packed height, which decreases both the extra column shell cost and the packed volume. A particular change in packing efficiency has a greater effect on the rate of return if the plant is smaller and the shell cost is dominant. This is because the shell cost depends on the height squared, whereas the packing volume and hence cost are directly proportional to height.

Capacity.

An increase in packing capacity increases the rate of return. It reduces the column diameter and packed volume, and so the extra capital cost is less. Because the column shell cost is only weakly dependent on diameter, and the packed volume depends on its square, the effect of a change in packing capacity is greater if the plant is larger and the packing cost is dominant. This is the opposite effect to that of efficiency in which case the column shell cost depends more strongly on height than the packed volume does.

Pressure gradient.

The pressure gradient affects the power saving possible with a packed plant. A high pressure gradient means a larger pressure drop across the low pressure column and a smaller power saving. However, because the change in pressure drop from trays to structured packing is so great, most of the saving is achieved with this change. Even a packing with double the pressure gradient of existing packings does not show a drastic reduction in the rate of return. The reduction in the rate of return caused by an increased pressure gradient is greater as the plant size increases and power costs become more important.

Cost.

The cost of the packing becomes more important as the plant size increases. In large plants it dominates the column shell cost and can have a significant impact on the rate of return. However, in smaller plants, it is of little significance; in a 30 t/d

plant, the packing cost would have to increase by about 170% to reduce the rate of return by 1%.

Distributor height.

Reducing the height of column required for distributors increases the rate of return by reducing the column shell cost. It also leads to the packing cost dominating the shell cost at a smaller plant size, and can mean a large rate of return at around this plant size. Effort would be well spent on developing shallow distributors, particularly for small plants. The rate of return on a packed plant could then be quite large.

Distributor cost

The cost of distributors is the variable to which the rate of return is least sensitive. This reinforces the conclusion that shallower distributors should be developed, even if they cost more.

Actual packings.

Changing between actual packings will of course change several variables together. The economic analysis allow us to choose the optimum packing for a particular plant from those available by taking these changes into account.

In smaller plants we find that the higher the specific area, the better the rate of return. This is because, whilst the pressure gradient at the design point is about the same, the efficiency increases approximately in proportion to the square root of specific area ($a^{0.5}$), whereas the capacity is only reduced in proportion to $a^{-0.4}$. This means that the column volume per unit throughput, and therefore shell cost is reduced as $a^{-0.1}$. The packing cost per unit volume, however, depends on a^{1}, so the cost of packing per unit throughput increases with specific area as $a^{0.9}$. Larger plants therefore favour lower area packings.

When developing a new packing, any improvement made in one aspect of packing performance is likely to be at the expense of another. The economic analysis allows us to conclude that the most desirable trade-off is to increase efficiency (and so reduce capital expenditure) at the expense of increased pressure gradient, reduced capacity and slightly reduced power saving. This would increase the benefit of packing particularly in plants up to about 2000 t/d where it is currently not so favourable.

7.2 Packing development and manufacture

To develop a new packing it was first necessary to understand how existing packings perform and how they have been modelled. With this knowledge, and the results of the economic analysis, a number of ways of improving packings for air distillation were proposed. The packing which was eventually chosen was the one which would be easy and cheap to manufacture, both as a prototype and in commercial quantities.

7.2.1 Development of new packing

We shall now consider, with reference to correlations of packing performance, the modifications to packing design which were proposed.

Correlation and modelling of packing performance

A number of experimental test results have already been published over a range of throughputs for structured packings with different specific areas and channel angles. This allowed a satisfactory correlation of the efficiency, pressure gradient and capacity of these packings against area and channel angle. The predictions of the different models differed in their agreement with these results. Even the more empirically based models did not show complete agreement. None of the models allows the effects of changing the packing element height to be accounted for, and all the published test results have been for packings with similar block heights.

Predictions of the models for different distillation mixtures did not show good agreement with the experimental results. An equally good estimate of efficiency could be made by assuming it to be constant or correlating it with total reflux flow parameter. Some models predicted an efficiency up to 30% lower in air distillation than in distillation of organics, but others predicted a similar value.

Packing modifications considered.

By making existing packings with a higher specific surface, the efficiency may be increased, but the capacity will be reduced and the cost increased. Nevertheless, a slight advantage could be gained in smaller air separation plants. Similarly, if the channels were made more horizontal, the efficiency could be increased, but the capacity would be drastically reduced and the pressure gradient increased. This would provide a small advantage in all plant sizes. However a bigger advantage could be achieved by intensifying the mass transfer process to improve the efficiency at the expense of some increase in pressure gradient, but with less increase in cost or reduction in capacity.

Almost all the models of packing performance predicted that the liquid phase resistance accounts for less than 30% of the total mass transfer resistance. Even

so, most packing development so far has concentrated on reducing this resistance, rather than the larger vapour phase resistance.

So the modifications which were considered to existing packings were aimed mainly at reducing the vapour phase resistance to mass transfer. Nevertheless, the fluted surface texture was chosen to give the lowest liquid phase resistance. In addition, any modification to reduce the vapour phase resistance would probably have a similar effect on that in the liquid.

The review of mass transfer enhancement revealed that the best way to increase mass transfer in the vapour phase was to disturb the main flow in the packing. Two approaches were possible; to completely break and re-form the boundary layer by providing tabs protruding into the channels or to promote boundary layer separation and turbulence by introducing changes in direction or cross-section of the channels. Both these methods have been successfully employed to increase heat transfer in plate-fin heat exchangers.

Changes chosen for economic manufacture.

The design of packing chosen for testing was the easiest one to manufacture, whilst still having the potential to improve mass transfer. It had channels which converged on one side of the sheet and diverged on the other. Tabs would have made stripping the sheet from the press more difficult and sharp changes in channel direction would have introduced problems of metal creasing. The angle of convergence or divergence was small to simplify tool design. With a fixed ratio of maximum to minimum channel cross section and a fixed block height, the convergence angle is set by the number of convergences and divergences in the block. For easy tool-making this number should be small. It was also for this reason that shorter than standard blocks were used.

7.2.2 Manufacture of new packing

We have seen that the shape of packing to be made was chosen as one that could easily be made manually with a minimum of re-tooling at the Tianjin University packing factory.

Quality control.

Because of the labour intensive manufacturing method, quality control proved difficult. The packing elements supplied had several non-uniformities, and it was not clear which ones would affect their performance.

The only significant manufacturing problems proved to be the incorrect size of the elements and the poor wall-wiping bands. Some effort was made to improve the method of assembly into blocks, and a new type of wall-wiping band was

developed and tested in an experiment to measure wall-flow. The new packing was reassembled with the new wall-wiping band and tested under distillation.

Wall wipers.

The improved wall-wipers were based on Norton's design, but were fastened with rivets and were also used to hold the sheets together. An additional improvement was the use of half-hard metal so that the wipers were stiff and pressed hard against the column walls. This prevented liquid leaking past and made sure that the blocks were held centrally in the column. Experiments with water showed that wall flow, which had been around 50% of the total flow, was completely eliminated. Distillation tests also showed an improvement of about 20% in the performance at low flows.

Packing cost.

The economic analysis of the packing manufacturing process provided some insights into the balance between labour and material costs. A labour-intensive process is favoured if labour costs are low, such as in China. But because the crimping time increases as the square of the specific area, high labour costs favour an increased level of mechanisation. In particular several crimps should be made at the same time, requiring a larger press and more complex tool. An optimisation shows that the minimum manufacturing cost increases approximately linearly with specific area. In addition, the manufacturing cost depends on block height; smaller blocks are more expensive to make. The minimised cost is increased by about 40% for a halving of the block height.

A critical variable which determines the material cost of a packing is the thickness of metal sheet used. The packings from Tianjin were made from 0.2 mm sheet, whereas the other packings were from 0.1 mm sheet. It appears that if more rigidity is given to the sheets by the surface treatment, thinner sheet may be used. Further investigation of potential material costs reductions could be worthwhile, for example expanded metal could be used instead of sheet.

The economic analysis of the manufacturing process allowed sensible estimates of packing cost to be made for input to the main economic evaluation of the air separation plant.

7.3 Experimental tests and comparison of packings

The test rig built was on the largest scale possible, given the capacities of the department's steam boiler and cooling water system. It was designed to operate at both total and partial reflux and with different distillation systems. In the design, potential errors in the measurements were analysed, so as to minimise their effect.

An analysis of potential hazards was also carried out and a number of precautions taken, particularly the location of the rig in a flameproof lab and the use of explosion proof electrical equipment. An instrumentation and control system was developed for the test rig so that it could be easily and safely operated by one person. An IBM-compatible personal computer was used to log data and effect control. A programme was written for this in TURBO PASCAL.

The rig was pressure-tested before use and successfully commissioned, first using water as the process fluid, then using the chlorobenzene - ethylbenzene test mixture with Sulzer Mellapak 500YW packing.

7.3.1 Total reflux Distillation Results

The standard test of Sulzer's Mellapak 500YW produced results very similar to those published for Mellapak 500Y. A slight reduction in capacity and increased efficiency were apparent, but not considered significant because of the difference in the scale of the test rig, the operating pressure and the packing surface.

The test results of the Tianjin university packings all exhibited a rapid fall in efficiency as the flow was reduced. This was discovered to be due to liquid flowing down the column walls. After experiments with water to measure the wall flow in different packings, and the replacement of the wall-wiping bands with a new design, the efficiency at low flows was greatly improved.

Because of manufacturing difficulties, the packings with the new shape did not have exactly the same specific area as the standard ones. It was therefore necessary to account for these differences by using correlations of capacity and efficiency with specific area.

After accounting for the different specific areas in this way, the Tianjin 350Y packing, with blocks half as high as the Mellapak 500YW, was found to be about 8% more efficient with the same capacity. No previous work has been published to suggest that changing the block height has such an effect, so the result was surprising.

The new 350Y shows a further improvement in efficiency over the Tianjin 350Y due to the new shape of about 7%, and a small increase in capacity of about 3%. In contrast, the new 500Y shows about the same efficiency and capacity as expected from the Tianjin 350Y, despite its even shorter blocks. The lack of advantage due to the new shape is probably because of the reduced angle of convergence and divergence in this packing and the fact that it has only a single convergence or divergence in a block.

Those packings with shorter blocks were found to have higher pressure gradients at the design throughput because of the more frequent changes in direction and resultant pressure loss of the vapour.

7.3.2 Partial reflux distillation results

Only a limited number of partial reflux tests were undertaken, because of a shortage of time. These had two aims; to confirm that the performance of structured packings does not depend on reflux ratio and to attempt to separate the vapour and liquid phase resistances to mass transfer.

The efficiency was not significantly affected by reflux ratio, as was found by Meier et al. (1979).

The separation of resistances is not reliable enough to draw firm conclusions, because so few tests were performed and because of the large uncertainty in the measured efficiency. However, the results so far suggest that the liquid film resistance to mass transfer is more important than the models predicted, accounting for as much as 80% of the resistance. It is normally assumed to be much less in distillation and Spiegel and Meier (1987) had ignored it completely in modelling packing efficiency. In addition, the new shape appears to reduce the liquid phase resistance, but increase that in the vapour.

These unexpected results could be due to the errors in the measurements, but could also arise if the transfer unit heights change rapidly with flow; to separate the resistances, they were assumed to be constant as the reflux ratio changed. Further experiments would be worthwhile to establish whether the liquid phase resistance really is so important.

7.3.3 Wall-flow experiments

It is well known that poor distribution of liquid in random or structured packing has a detrimental effect on efficiency. Flow of liquid down the column walls is particularly undesirable because it by-passes the region inside the packing where the separation takes place. Such a flow was seen in the distillation tests on the original packings from Tianjin University, and reduced the efficiency by up to 50%.

For a particular packing and column size, liquid flow builds up on the walls until the rate of accumulation equals the rate at which liquid re-enters the packing. The experiments with water were designed to show how quickly the wall-flow builds up and what fraction of the total flow is down the column walls. The apparatus was also used to see whether potential improvements to the wall-wipers on the packings worked as intended.

The results showed that the equilibrium wall-flow fraction is attained very quickly - after only about 3 elements. In addition, without adequate wall-wipers, very small differences in the assembly of the blocks can have a large effect on the wall fraction - the Tianjin 500Y and 350Y did not differ noticeably, but their wall-flow fractions were about 70% and 50%.

The commercial packings showed relatively low wall-flows, as expected - less than 10%. Gauze packings generally allowed less wall-flow than sheet metal ones, but they were not tested under distillation to establish the differences in efficiency. The new wall wiping bands eliminated all the wall-flow.

These experiments emphasise the importance of careful manufacture and good quality control of structured packings, especially when they are intended for small columns. They should enable the Tianjin University packing factory to modify the assembly of their blocks of packing where efficiency is particularly important.

In addition, they demonstrate that, although structured packings can provide a large advantage over trays, their performance depends critically on the quality of their manufacture and installation. There is a considerable amount of technology in this area with which an air separation company would have to become familiar if it were to manufacture and install its own packings. The cost of the development work necessary would have to be balanced with the savings possible by manufacturing packings rather than buying them from a specialist company.

7.4 Implications of results for air separation processes

7.4.1 Application of experimental results to air separation

The tests conducted in this work have been with a single system and mainly at total reflux. In an air separation plant, internal reflux ratios vary between about 0.5 and 1.5, and the system may be effectively oxygen/nitrogen or oxygen/argon. Many tests on different packings show that the efficiency changes with the system used, and, as we saw in chapter 4, models to predict these changes are unreliable. Their accuracy is normally only of the order of the variation between systems, mainly because of large uncertainties in physical properties, particularly in the diffusion coefficients.

To design a distillation column for a particular system, it is usually necessary to test the packing with that system or to allow a safety factor on the HETP of at least 10-20%. Bennett et al. (1989) claim that the HETP of the oxygen/argon system is comparable with that of organic systems, but that of oxygen/nitrogen is higher. Further tests would be desirable before designing an air separation plant with a structured packing, but these are best done by the industry itself. The economic analysis has assumed a 10% higher HETP than for the chlorobenzene/ethylbenzene system, but this may be optimistic. This test system is rather well-behaved compared to other ones. Comparative performances of packings are likely to be the same with different systems, but before investing heavily in a new packing, a company should test it in air distillation.

Changes in capacity with physical properties are usually represented on a plot of capacity factor, C_s against flow parameter, X. The behaviour of these curves is generally similar for different packings (Kister, 1992) and so a calculation of packing capacity for air distillation should be relatively easy and reliable.

The pressure gradient at a proportion of the flooding capacity is similar for a wide variety of systems, and so could also be accurately estimated.

7.4.2 Comparison of the economic advantages of the packings tested in air distillation

To re-run the economic analysis of an air separation plant with the performance of packings other than Mellapak, the costs of the packings are required in addition to their performance data. The best method of estimating the cost of packings was to use the economic analysis of the manufacturing process with the specific area and the block height of the packings. This assumes that all the packings use the same thickness of metal. The tool costs for the new packings and the Norton packing were assumed to be higher because of the more complex shape. Estimates of the costs of the packings tested are given in table 7-1.

Cost breakdown for different sizes of packing and different block heights							
area per unit volume	m^2/m^3	M 500YW	IMSP 1T	T350	T500	N350	N500
block height	m	0.2	0.27	0.1	0.1	0.1	0.05
Labour cost	£/m^3	649	410	915	1311	1050	2045
Press cost per m3 packing	£/m^3	186	162	186	217	197	235
Tool cost per unit volume	£/m^3	28	42	29	61	76	152
Metal cost / unit volume	£/m^3	886	733	634	924	733	733
Total manufacturing cost / unit volume	£/m^3	1749	1347	1763	2512	2056	3165
Selling price / unit volume	£/m^3	2274	1751	2293	3266	2672	4114

Table 7-1 Manufacturing costs for packings tested

The other variables used in the economic comparison are the values listed in table 7-2. The measured values of pressure gradient and efficiency are used together with a 10% higher HETP. An imaginary new 350Y packing is also compared which has the standard block height and so is 8% less efficient than the one tested, but is also cheaper.

The results of the economic analysis in the base case plant with the different packings are plotted for different plant sizes in figure 7-1. The rate of return with Mellapak 750Y (the base case) is also given for comparison.

Packing type	Packing cost / £/m^3	Maximum capacity factor / m/s	Design HETP / m	Design pressure gradient / mbar/m
Mellapak 500YW	2274	0.069	0.247	3
Norton IMSP 1T	1751	0.091	0.289	4.6
Tianjin 350Y	2293	0.081	0.275	3.5
New 350Y	2672	0.080	0.237	3.5
New 500Y	4114	0.066	0.210	4.2
New 350Y with 0.2 m blocks (imaginary)	1935	0.080	0.257	3

Table 7-2 Packing variables used as input for economic comparison

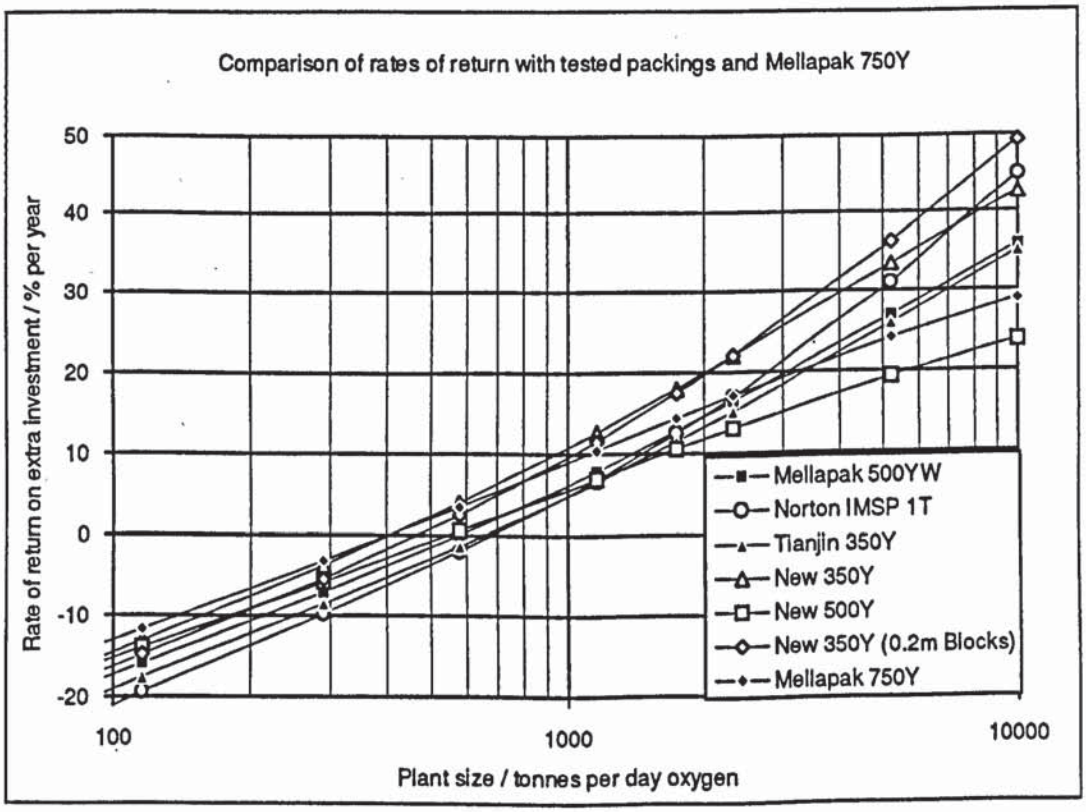

Figure 7-1 Comparison of economics of tested packings in air separation

New Shape.

The results show that even in its current form, the new 350Y packing is more economic than Mellapak 750Y over the whole range of plants where it is economic to use a sheet metal packing. If a rate of return of 5% is required, the smallest viable size of packed plant is reduced from 700 to 650 t/d oxygen, whilst in a 2000 t/d plant, the new 350Y packing increases the rate of return from 16% to 20%. This economic advantage is brought about mainly by the significantly lower cost (£2672 /m^3 rather than £3940 /m^3) and increased capacity (0.080 m/s cf. 0.063m/s) compared with Mellapak 750Y. In this case the lower efficiency and slightly increased pressure gradient are not enough to outweigh the other advantages.

The new 500Y packing is the least economic packing in plants where packings are viable. This is mainly due to the very high cost of the very short blocks (this packing is more expensive than Mellapak 750Y) and to the higher pressure gradient and HETP and only slightly higher capacity than Mellapak 750Y.

Block height

Using shorter blocks without changing the packing shape is not economic compared with using the higher area packing with the same cost. The Tianjin 350Y is less advantageous than the Mellapak 500YW over the whole range of plant sizes, despite its higher capacity. This is because, whilst its cost is similar, its efficiency is lower. The increased capacity is not sufficient to outweigh the disadvantage of reduced efficiency, even in very large plants.

Because shorter blocks do not appear to be advantageous, it is interesting here to consider the effect of making the new 350Y with 0.2 m high blocks, so that its efficiency and cost are both reduced. In this case, in plants up to about 2200 t/d oxygen, the shorter blocks appear to be better, however above this, the cost reduction outweighs the reduced efficiency if larger blocks are used.

Sulzer Mellapak 500YW

The Mellapak 500YW is less advantageous than Mellapak 750Y in plants up to about 2300 t/d. It is therefore better than the Mellapak 500Y based on Sulzer's (1992) results, because of its lower surface area ($422 m^2/m^3$) and consequent lower cost. Above 2300 t/d it is also more economic than the Tianjin 350Y and the new 500Y.

Norton IMSP 1T

The Norton IMSP 1T, with the relatively low specific area of 276 m^2/m^3, is the highest area packing currently available from Norton. In this analysis, it has been assumed to be significantly cheaper than the other packings would be with a similar area because of its deeper blocks. This assumption is not based on prices from the manufacturers and so the results should be treated with caution. With this assumption, the IMSP 1T is better than all except the new 350Y packing in plants larger than 2500 t/d. However, it is only more advantageous than the new packing in extremely large plants, bigger than about 7500 t/d. Even in these plants it is worse than the new 350Y packing if it were made with taller blocks.

Conclusions

The new 350Y packing in its present form, with short blocks is the most economic packing out of those investigated for use in air separation. If it were to

be made with taller blocks, it would be even better in very large plants producing more than 2200 t/d oxygen. The new 500Y packing has no advantage, mainly because of its high manufacturing cost.

The use of a lower area packing with short blocks instead of the higher area packing with taller blocks and a similar cost and efficiency appears to give no advantage. However replacing a packing of the same specific area with one with shorter blocks can provide an advantage in smaller plants.

To be economic in sizes of air separation plant which are currently built, a higher area version of Norton's IMSP 1T would need to be developed.

Sulzer's YW series packings appear to be more economic in air separation than the Y series, because of their slightly increased efficiency.

7.5 Conclusion

The economic analysis has shown that, despite their high capital cost, structured packings can provide an economic advantage over trays in air distillation, especially in large and very large plants. In particular plants, particular sizes of packings are favoured.

The detailed analysis of the economic balance allowed the development of a new packing to be targeted towards improving the efficiency, which has the biggest impact on the size of the advantage. To increase the efficiency, changes in the channel shape were proposed with the aim of reducing the vapour phase resistance to mass transfer. The new packing was made in cooperation with the Tianjin University packing factory.

The new distillation column test rig was successfully designed, built and commissioned, and used to test the new packing along with several standard ones. The results showed that wall flow has a detrimental effect on the efficiency and should be eliminated. Because of other manufacturing difficulties, the packings could not be compared directly. However, a method was devised to allow for differences in the specific area. This showed that, unexpectedly, shorter blocks enhanced the efficiency by about 8% and the new shape with the larger angle of convergence/divergence and with both convergence and divergence in one block further enhanced it by about 7%. The new shape with a single convergence or divergence in a block and a smaller convergence/divergence angle appeared to show no advantage.

The packings as tested were compared, using the economic analysis, with each other and with the base case with Mellapak 750Y. This demonstrated that the best packing for use in air distillation is the new 350Y, which lowers the minimum viable plant size and increases the rate of return on a particular plant.

Chapter 8 - Conclusions

1. It has been confirmed that the replacement of trays with structured packing in the low pressure column of an air separation plant reduces power consumption and running cost but increases the capital cost of the plant. But unless the cycle is modified, the full power saving is not achieved because the refrigeration is less efficient when the compressor pressure is lower.

2. The rate of return on the extra investment in a packed column increases with plant size, may go through a maximum and eventually reaches a limiting value. So in a particular situation, there is a minimum viable packed plant size, and there may be an optimum and maximum economic size. For example, if 750Y packing is used and a minimum return of 5% is required, the smallest viable plant is 700 t/d oxygen.

3. An overall saving can be achieved if presently available structured packings are used in air separation plant. In different plants, different packings will give the greatest rate of return, so the saving may be maximised for a particular plant by careful choice of packing. For example, in plants up to 1200 t/d, CY gauze packing is best, from 1200 to 3500 t/d 750Y is best and above 3500 t/d, 350Y is best.

4. An economic analysis of the packing manufacturing process was also carried out both to provide costs for existing packings and to allow prediction of the cost of potential new packings. It shows that in standard packings, manufacturing and material costs each account for about half the total cost, that the cost is approximately proportional to specific area and that if the block height is halved, the cost is increased by about 40%.

5. The economic analysis indicates that the most important aspect of a packing to improve is the efficiency, even at the expense of slightly increased cost or pressure gradient or reduced capacity. It is also important to reduce the height of the liquid distributors required at the top of the packed bed.

6. The predictions of a number of models were compared with published experimental results for changes in the packing geometry, throughput and distillation system. These were found not to be sufficiently reliable to make predictions for new types of packings. But correlations of experimental results were used to predict the effect of simple changes to the packing geometry.

7. New shapes of packing were considered, with reference to heat and mass transfer intensification techniques and the cost and ease of their manufacture. The aim was to reduce the vapour-phase mass transfer resistance. Consultations with the staff of the Tianjin University packing factory about the ease of making the new shapes on their existing production line led to the choice of a packing shape similar to existing ones, but whose channels changed in cross-section.

8. Two types of new packing were manufactured. One had a single divergence or convergence in one block, with an angle of 1.2 degrees. This had a nominal specific surface of 500 m^2/m^3 and a block height of 50 mm. The other had both a convergence and a divergence, with a 1.5 degree angle, in one block. It had a nominal specific surface of 350 m^2/m^3 and a block height of 100 mm. Normal corrugated sheet packings with block heights of 100 mm and nominal specific areas of 500 and 350 m^2/m^3 were also supplied by the Tianjin University packing factory for comparison.

9. All the packings originally supplied from Tianjin University were of variable diameter and some were a tight fit in the column. They had a much reduced efficiency at low F factors and most of the liquid was seen to flow down the column walls. Experiments with water only showed that up to 70% of the flow was down the walls, whereas the Sulzer and Norton packings showed at most 10% wall flow. So slight variations in the assembly of the blocks have a significant effect on the wall flow and efficiency.

10. The new 350Y packing was rebuilt with an improved wall-wiping band, made from half-hard brass strip. This eliminated the wall flow and improved its distillation performance by 20% at low flows.

11. The general form of the pressure gradient versus F factor results is the same in each case, but the magnitude of the pressure gradient depends on block height, which sets the number of times the vapour must change direction in a given height.

12. The efficiency results all showed a maximum close to flooding with a reduction in efficiency at lower F factors. The behaviour close to flooding and at low flows differed between packings.

13. A limited number of runs at partial reflux show that the packing efficiency is more or less the same as at total reflux.

14. The new 350Y packing has an efficiency about 7% better than expected from the Tianjin 350Y (which has the same short blocks) and a 3% higher capacity.

It is more efficient than the Mellapak 500YW and has a higher capacity, although it is about 18% more expensive to make. It is more economic in air separation even than Mellapak 750Y, and reduces the minimum viable plant size (with a 5% rate of return) from 700 t/d to 650 t/d.

15. The Tianjin 350Y packing, with blocks half the height of the Sulzer Mellapak packings, has a peak efficiency about 8% higher than expected from its specific area. Its capacity is the same as the Mellapak 500YW after accounting for the different areas. But its cost is 40% higher than if it had 0.2 m blocks. So an easy way to improve packing efficiency is to use shorter blocks. This can provide an advantage in air distillation over the corresponding packing with taller blocks if the plant is small and the extra cost is justified by the increased efficiency.

16. The new 500Y, which has shorter blocks and a smaller divergence angle does not show a significant improvement over that expected from the short blocks and is much more expensive to make. So it is never the most economic packing in air separation.

Chapter 9 - Recommendations for further work

This work has been concerned with defining the problems and making a start on the solutions in three main areas. These are understanding the advantages and disadvantages of using structured packing in air separation plant, understanding how structured packings work and using these insights to develop a new structured packing especially suited to air separation. There still remains a considerable amount of work which could be done in each of these areas.

9.1 Structured packing in air separation

The current economic analysis has provided valuable insights into the advantages and disadvantages of replacing trays with structured packing in an air separation plant. There are however a number of possibilities not considered, such as those of producing very pure argon directly from the argon column or changing the cycle to improve the refrigeration efficiency, for example by adding an extra turbine. Further work could be done to take these process modifications into account, and could be linked to detailed simulation of potential cycles.

9.2 Understanding structured packings

9.2.1 Experimental work

The distillation rig could be used to obtain experimental data about the performance of packings under different conditions. In particular the effects of liquid distribution, reflux ratio, mixture composition (i.e. different composition ranges) and distillation system on the efficiency, pressure gradient and capacity should be investigated. The column could also be modified to measure temperature and composition profiles in the packing and to investigate the effect of reflux condition (e.g. subcooled or saturated). Possible modifications to the rig are as follows:

Modifications to the distillation column.

To make the column easier to operate over a wide range of boil-up rates, a valve should be put into the reboiler circulation loop rather than the fixed size orifice plates. This would allow the constriction to be altered during operation and would avoid having to drain the column to change the range of possible boil-up rates.

A filter should be added somewhere in the column system, since, with extraction fans sucking air and dust into the laboratory it is very difficult to avoid getting grit

into the column. The grit can cause problems by blocking the sample valves and polluting the mixture.

A reflux heater could be added to the reflux line, preferably close to the top of the column, so that the reflux need not be subcooled, as at present. Control of this heater would be relatively easy, as it could be based on the reflux temperature - cooling water flow control loop, which is not used at the moment.

To measure temperature and composition profiles, more resistance thermometers and samplers could be introduced to the packed bed through the existing regularly spaced nozzles.

For more accurate measurements of efficiency at partial reflux, a better flow control and metering system should be used, although this would be expensive. More accurate control valves, probably electrically driven ones, should be used together with coriolis mass flow meters or turbine flow meters. Both these types of flow meter would allow the flows to be logged by the computer, and would therefore make operation easier.

9.2.2 Theoretical work.

The experimental results obtained from the rig should be used to test and develop further the theories of structured packing operation and performance. Because of the well-defined geometry of a structured packing, this work could include numerical solutions to the flow and mass transfer equations.

This increased theoretical understanding would make easier the development of new packing shapes by making possible a prediction of their performance without having to test them.

9.3 Further development of structured packings.

The results of the tests on the new packings demonstrate that the new shape provides a small advantage. Further tests would be worthwhile on a modification of the shape with a larger angle of divergence, which would be expected to further increase this advantage. These tests should if possible compare the new packing with the standard shaped packing of an identical specific area.

The packing block height appears to have quite a large effect on efficiency. This effect should be confirmed and examined in more detail, as it would provide a simple way of reducing the column size. The new shape should also be tested with deeper blocks, since it may show a larger improvement over comparable existing packings as the block height is increased.

Other changes in the arrangement of blocks in the column and of sheets into blocks could be considered. Examples of these are to put spacers between blocks or to arrange the packing sheets at an angle rather than vertically.

An investigation of some of the other possible new shapes of packing would also be worthwhile, such as ones with corrugated channels or tabs pushed out into the channels. Other materials of construction, such as expanded metal to reduce cost and gauze to increase efficiency should also be tried out.

As well as investigating the packings themselves, the liquid and vapour distribution system should be studied, in order to minimise the height of column occupied by distributors. The scale of the present rig is rather on the small side for this, however one of the Aston air/water simulators would provide a good starting point for this work.

Chapter 10 - Notation and conversion factors

10.1 Symbols

A	General constant	
	Column cross sectional area	m^2
a	Surface area of packing per unit bed volume	$m^2\ m^{-3}$
	General constant	
a_i	Interfacial area per unit volume of packing	$m^2\ m^{-3}$
B	General constant	
	Distillation column bottoms molar flow	$kmol\ s^{-1}$
b	General constant	
C	General constant	
	Concentration	$kmol\ m^{-3}$
C'	Dimensionless Constant	
C_{cap}	Capital cost of air separation plant	£
C_E	Constant correction to penetration time in Bravo and Fair packing model	
C_{lab}	Labour cost per unit volume of packing	$£\ m^{-3}$
C_{mach}	Press (machine) cost per unit volume of packing	$£\ m^{-3}$
C_{mat}	Material cost per unit volume of packing	$£\ m^{-3}$
C_{pack}	Manufactured cost per unit volume of packing	$£\ m^{-3}$
C_{pow}	Total power cost over air separation plant lifetime	£
C_s	Superficial capacity factor	$m\ s^{-1}$
C_{tool}	Cost of press tool per unit volume of packing produced	$£\ m^{-3}$
c	Concentration	$kmol\ m^{-3}$
	Wave velocity	$m\ s^{-1}$
	General constant	
c_{mach}	Initial cost of press (machine)	£
c_{metal}	Cost per unit mass of metal from which packing is made	$£\ kg^{-1}$
c_p	Specific heat capacity at constant pressure	$kJ\ kg^{-1}\ K^{-1}$ or $kJ\ kmol^{-1}\ K^{-1}$
$c_{p,j}$	Average molar heat capacity of stream j	$kJ\ kmol^{-1}\ K^{-1}$
c_s	Superficial capacity factor	$m\ s^{-1}$
$c_{s,fl}$, $c_{s,max}$	Superficial capacity factor at flooding	$m\ s^{-1}$

c_{tool}	Initial cost of press tool	£
c_v	Specific heat capacity at constant volume	kJ kg^{-1} K^{-1} or kJ kmol^{-1} K^{-1}
D	Mass Diffusivity	m^2 s^{-1}
	Distillate molar flow	kmol s^{-1}
D_E	Mass Diffusivity	m^2 s^{-1}
D_r	Radial spreading coefficient = D_r / u_z	m^2 s^{-1}
D_z	Axial spreading coefficient = D_z / u_z	m^2 s^{-1}
D_r	Radial dispersion coefficient	m^2 s^{-1}
D_z	Axial dispersion coefficient	m^2 s^{-1}
d	Diameter, hydraulic diameter or characteristic dimension	m
	General constant	
d_h, d_{hyd}	Hydraulic diameter	m
d_p	Characteristic particle diameter in packed bed	m
E_{mv}	Murphree vapour efficiency of distillation stage	
e	Height of wall roughness elements	m
F	Molar feed flow	kmol s^{-1}
	Molar flow	kmol s^{-1}
	Molar flow through turbine	kmol s^{-1}
	Flow through cooling water flow meter	dm^3 min^{-1}
	Molar feed flow	
F_{col}	Molar air flow into column system	kmol s^{-1}
F_{CW}	Cooling water flow	kmol s^{-1} or kg s^{-1}
F_{in}	Molar air flow into plant	kmol s^{-1}
F_m	Flow read from cooling water flow meter (centre of marker)	dm^3 min^{-1}
	Molar Feed flow measured by rotameter	kmol s^{-1}
$F_{out,j}$	Molar flow of stream j out of plant	kmol s^{-1}
F_s	Superficial F-factor = $u_s \rho_v^{1/2}$	m s^{-1} (kg m^{-3})
F_{se}	Surface enhancement correction factor in Bravo and Fair packing model	
F_T	Theoretical maximum rotameter capacity	dm^3 min^{-1}
Fo	Fourier number = $D_r z / R^2$	
Fr	Froude Number = $u^2 / g d$	
f	Fanning friction factor = 2 ϕ	

	General function	
	Fugacity	
	Fraction of theoretical maximum flow through rotameter	
G	Molar gas or vapour flow	kmol s^{-1}
g	Acceleration due to gravity	9.81 m s^{-2}
H	Henry's law constant	Pa
	Enthalpy	kJ $kmol^{-1}$
	HETP	m
H_0	Enthalpy of air at inlet temperature and 1 atmosphere	kJ $kmol^{-1}$
$H_{0,j}$	Enthalpy of stream j at inlet temperature and 1 atmosphere	kJ $kmol^{-1}$
H_{in}	Enthalpy of air into plant	kJ $kmol^{-1}$
$H_{out,j}$	Enthalpy of stream j out of plant	kJ $kmol^{-1}$
H_{OL}	Height of overall liquid phase transfer unit	m
H_{OV}	Height of overall vapour phase transfer unit	m
H_L	Height of liquid phase transfer unit	m
H_{stm}	Steam enthalpy	kJ $kmol^{-1}$ or kJ kg^{-1}
H_{Tout}	Enthalpy of air at main exchanger outlet temperature	kJ $kmol^{-1}$
H_{tw}	Height of transfer unit assuming total wetting of surface	m
H_V	Height of vapour phase transfer unit	m
H_{wat}	Water enthalpy	kJ $kmol^{-1}$ or kJ kg^{-1}
h	Heat transfer coefficient	W m^{-2} K^{-1}
	Height	m
h_b	Height of block of packing	m
h_{col}	Height of column	m
h_l	Liquid hold-up	m^3/m^3
h_{pack}	Height of packed column	m
h_{tray}	Height of trayed column	m
h_t	Tray spacing	m
I	Parameter in rotameter calibration representing fluid properties	
i	Component subscript	

J	Mass flux with respect to frame with no net molar flow	kmol m^{-2}
j	Stream subscript	
K	Dimensionless Kozeny-Carman constant with Reynolds number based on hydraulic diameter	approx 20
	General constant	
K'	Dimensionless Kozeny-Carman constant with Reynolds number based on characteristic particle diameter	approx 40
	General constant	
K"	General constant	
K_1	Rotameter constant, depends on tube size	s $cm^{-1/2}$
K_2	Rotameter constant, depends on tube size	$cm^{-3/2}$ dm^3 min^{-1}
K_i	Equilibrium constant of component i = y_i / x_i	
K_F	Dimensionless film number = $\rho \sigma / g \mu^4$	
K_x	Overall mass transfer coefficient in liquid phase units	kmol s^{-1} m^{-2}
K_y	Overall mass transfer coefficient in vapour phase units	kmol s^{-1} m^{-2}
k	Thermal conductivity	W m^{-1} K^{-1}
	Mass transfer coefficient	kmol m^{-2} s^{-1} $kmol^{-1}$ m^3 = m s^{-1}
	Dimensionless loss coefficient = $8 \phi L / d$	
	Ratio of specific heat capacity at constant pressure to that at constant volume	
k_L, k_l	Mass transfer coefficient in the liquid phase	m s^{-1}
k_L^*	Dimensionless mass transfer coefficient in the liquid phase = Sh / N_T	
k_{l+}	Alternative dimensionless mass transfer coefficient	
k_x	Mass transfer coefficient in the liquid phase	m s^{-1}
k_y, k_g	Mass transfer coefficient in the vapour phase	m s^{-1}
L	Length	m
	Molar liquid flow rate	kmol s^{-1}
	Liquid mass flow	kg s^{-1}
	Liquid volume flow	m^3 s^{-1}
	Labour rate (including overheads)	£ hr^{-1}

l	Channel length within packed bed	m
l	Prandtl mixing length	m
l_b	length of block of packing	m
l_m	length of metal per unit volume of packing	$m\ m^{-3}$
M_r	Relative molecular mass	
m	Slope of equilibrium line (local or average)	
	general constant	
N	Mass flux with respect to fixed frame	$kmol\ m^{-2}$
	Dimensionless transfer coefficient = $\xi\ d / \delta$ (δ is general diffusivity)	
N_{blocks}	Number of packing blocks per unit volume	m^{-3}
N_{crimp}	Number of crimps per unit packing volume	m^{-3}
N_{OL}	Number of overall liquid phase transfer units	
N_{OV}	Number of overall vapour phase transfer units	
N_L	Number of liquid phase transfer units	
N_T`	Dimensionless Nusselt film thickness parameter = $\delta\ (g \sin\theta / \nu^2)^{1/3}$ (δ is film thickness)	
N_V	Number of vapour phase transfer units	
Nu	Nusselt number = $h\ d / k$	
n	General exponent	
n_{crimp}	Number of crimps per unit metal length	m^{-1}
n_{mach}	Press (machine) lifetime	years
n_{sheets}	Number of sheets per block of packing	
n_{tool}	Press tool lifetime in operations	
P	Total pressure of system	$Pa = N\ m^{-2}$
	Power	W
P_{turb}	Turbine power	W
P_{bi}	Power due to booster inefficiency	W
Pe	Peclet number = $u\ d / \alpha$	
	Packed bed Peclet number = $u\ d_h / \varepsilon\ D$	
Pe_{mass}	Mass Peclet number = $u\ d / D$	
Pr	Prandtl number = ν / α	
p	Pressure	$Pa = N\ m^{-2} = kg\ m^{-1}\ s^{-2}$
	Pressure at point in packed bed	$Pa = N\ m^{-2} = kg\ m^{-1}\ s^{-2}$

p_0	Atmospheric pressure	101325 N m^{-2}
p_1	Turbine inlet pressure	N m^{-2}
p_2	Turbine outlet pressure	N m^{-2}
p_i	Partial pressure of component i	N m^{-2}
$p_{out,j}$	Actual outlet pressure of stream j	N m^{-2}
Q	Heat flow	W m^{-2}
	Volumetric liquid flow	m^3 s^{-1}
	Heat transferred	J
	Volume of packing produced per year	m^3 yr^{-1}
	Air separation plant output	t day^{-1} of product (O_2, N_2, Ar)
Q_{in}	Heat leaking into plant per unit time	W
	Heat supplied to boiler per unit time	kW
Q_{loss}	Heat leaking through insulation	kW
Q_{out}	Heat removed from condenser per unit time	kW
q	Feed condition; number of moles of liquid formed on feed plate per mole of feed	
R	Column radius	m
	Resistance to mass transfer	s m^{-1}
R	Universal gas constant	8.3144 kJ $kmol^{-1}$ K^{-1}
R_{int}	Internal reflux ratio = L / V	
R_{ext}	External reflux ratio = L / D	
Re	Reynolds number = u d / ν	
r	Radial coordinate	m
r_x	Resistance to mass transfer in liquid phase	s m^{-1}
r_y	Resistance to mass transfer in vapour phase	s m^{-1}
S	Surface area of packed bed per unit solid volume	m^2 m^{-3}
	Column cross sectional area	
	Entropy	kJ $kmol^{-1}$ K^{-1}
	Packing channel side dimension	m
	Rotameter scale reading	cm
Sc	Schmidt number = ν / D	
Sh	Sherwood number = k d / D	
s	Spacing of roughness elements on wall	m
	Packing channel side dimension	m

T	Temperature	K or °C
T_1	Turbine inlet temperature	K
T_2	Turbine outlet temperature	K
T_{arr}	Time to arrange packing sheets into blocks per unit volume	$s\ m^{-2}$
T_b	Boiling temperature of distillation mixture	
T_{crimp}	Crimping time per unit volume of packing	$s\ m^{-3}$
T_{cut}	Cutting time per unit volume of packing	$s\ m^{-3}$
T_f	Subcooled feed temperature	K or °C
T_{fic}	Time to fix sheets into blocks per unit volume of packing	$s\ m^{-3}$
T_{in}	Temperature of air into main exchanger	K
T_{out}	Temperature of streams out of main exchanger	K
$T_{out,j}$	Actual outlet temperature of stream j	K
T_{pack}	Time to pack the column with a unit volume of packing	$s\ m^{-3}$
T_{perf}	Perforation time per unit volume of packing	$s\ m^{-3}$
T_r	Subcooled reflux temperature	K or °C
T_{sat}	Saturation temperature	K or °C
T_{st}	Surface treatment time per unit volume of packing	$s\ m^{-3}$
T_{tot}	Total labour time per unit volume of packing	$s\ m^{-3}$
t	Time	s
	Corrugated sheet thickness - vertical distance from peak to trough	m
t_{arr}	Time to arrange packing sheets into one block	s
t_c	Penetration theory contact time	s
t_{crimp}	Time per crimp	$s\ m^{-3}$
t_{cut}	Time per cut	$s\ m^{-3}$
t_{fix}	Time to fix packing sheets into one block	s
t_{pack}	Time to pack the column with one block of packing	$s\ m^{-3}$
t_{perf}	Perforation time per unit length of metal	$s\ m^{-3}$

t_{st}	Surface treatment time per unit length of metal	$s\ m^{-3}$
u	Velocity (in x direction)	$m\ s^{-1}$
u_+	Dimensionless velocity (in x direction) $= u / v_{*wall}$	
u_{av}	Average velocity	$m\ s^{-1}$
u_{bed}	Local velocity within packed bed	$m\ s^{-1}$
u_{fl}	Velocity at flooding	$m\ s^{-1}$
u_l	Liquid velocity	$m\ s^{-1}$
u_l^*	Dimensionless liquid velocity	$m\ s^{-1}$
u_{max}	Maximum velocity	$m\ s^{-1}$
u_s, u_{sup}	Superficial velocity (empty bed, fluid fills bed)	$m\ s^{-1}$
u_v, u_g	Gas or vapour velocity	$m\ s^{-1}$
u_v^*, u_g^*	Dimensionless gas or vapour velocity	$m\ s^{-1}$
V	Molar Gas or Vapour flow	$kmol\ s^{-1}$
V_{add}	Molar vapour flow condensed by subcooled feed at top of column	$kmol\ s^{-1}$
V_m	Measured molar vapour flow through reflux rotameter	$kmol\ s^{-1}$
V_{metal}	Volume of metal per unit volume of packing	$m^3\ m^{-3}$
$V_{tot,mol}$	Total molar vapour flow in column	$kmol\ s^{-1}$
v	Velocity	$m\ s^{-1}$
v_*	Friction velocity - characteristic turbulence fluctuation velocity	$m\ s^{-1}$
W	Work performed	$kJ\ kmol^{-1}$
w_b	Width of block of packing	m
X	Flow parameter $= L / V\ (\rho_v/\rho_l)^{1/2}$	
X_∞	Total reflux flow parameter $= (\rho_v/\rho_l)^{1/2}$	
x	Coordinate dimension	m
	Mole fraction in liquid phase	
	Contact length in penetration theory	m
x^*	Equilibrium mole fraction in liquid phase	
x_D	Mole fraction of more volatile component in distillate	
x_B	Mole fraction of more volatile component in bottoms	
y	Coordinate dimension	m
	Mole fraction in vapour phase	

y^*	Equilibrium mole fraction in vapour phase	
y_+	Dimensionless distance from wall = $y\, v_{*_{wall}} / \nu$	
Z	Gas compressibility factor	
z	Coordinate dimension (along the packed bed axis)	m
	Packed height	m
	Contact length in Zogg model	m
α	Thermal diffusivity = $k/\rho\, c_p$	$m^2\, s^{-1}$
	General constant	
	Relative volatility	
	Rate of change of enthalpy with pressure	
α_E	Eddy thermal diffusivity = $k/\rho\, c_p$	$m^2\, s^{-1}$
α_j	Rate of change of enthalpy with pressure of stream j	
Γ	Peripheral mass flow of liquid	$kg\, s^{-1}\, m^{-1}$
γ	Activity coefficient	
	Wetting angle of liquid on solid surface	degrees or radians
ΔH_{mix}	Enthalpy of mixing of air	$kJ\, kmol^{-1}$
ΔH_{vap}	Enthalpy of vaporisation of distillation mixture	$kJ\, kmol^{-1}$
ΔH_{ϕ}	Enthalpy of vaporisation of air	$kJ\, kmol^{-1}$
Δp	Pressure drop across distillation column	$N\, m^{-2}$ or mbar
$\Delta p_{dynamic}$	Dynamic pressure drop across distillation column	$N\, m^{-2}$ or mbar
Δp_{static}	Static pressure drop across distillation column	$N\, m^{-2}$ or mbar
ΔT_b	Temperature rise across booster and aftercooler	K
δ	Liquid film thickness	m
	Metal sheet thickness	m
δ_+	Dimensionless film thickness	
δ_{film}	Mass transfer film thickness	m
δ_{damp}	Thickness of film in which turbulent eddies are damped at a surface	m
ε	Void fraction	$m^3\, m^{-3}$
η	Efficiency	
$\eta_{b,it}$	Isothermal booster compressor efficiency	
η_{ie}	Isentropic turbine efficiency	

η_{mg}	Combined efficiency of motor and generator	
Θ	Angle of liquid flow with horizontal in Zogg model	degrees or radians
θ	Angle of liquid flow with horizontal	degrees or radians
θ	Angle of packing channels with horizontal	degrees or radians
κ	Von Karman scale factor - universal constant for turbulent flows	approx. 0.4
λ	Resistance coefficient = 8 ϕ	
	Wavelength	m
	Ratio of slopes of equilibrium and operating lines = m V / L	
	Corrugation wavelength in packing	m
μ	Coefficient of viscosity	N s m^{-2} = kg m^{-1} s^{-1}
	Chemical potential	kJ $kmol^{-1}$
	Mass of metal per unit volume of packing	kg m^{-3}
μ_E	Eddy viscosity	N s m^{-2} = kg m^{-1} s^{-1}
μ_g, μ_v	Gas or vapour viscosity	N s m^{-2} = kg m^{-1} s^{-1}
μ_l	Liquid viscosity	N s m^{-2} = kg m^{-1} s^{-1}
μ_w	Viscosity of water	0.001 N s m^{-2}
ν	Momentum diffusivity or kinematic viscosity = μ/ρ	m^2 s^{-1}
	Kinematic viscosity of rotameter fluid	Stoke (10^{-4} m^2 s^{-1})
ν_g ν_v	Kinematic viscosity of gas or vapour	m^2 s^{-1}
ν_l	Kinematic viscosity of liquid	m^2 s^{-1}
ν_E	Eddy kinematic viscosity = μ_E/ρ	m^2 s^{-1}
ξ	General transfer coefficient	m s^{-1}
	Dimensionless contact length in Zogg model = z/δ	
π	constant	3.1415927
ρ	Mass density	kg m^{-3}
	Density of rotameter fluid	g cm^{-3}

ρ_g, ρ_v	Gas or vapour mass density	kg m^{-3}
ρ_l	Liquid mass density	kg m^{-3}
ρ_{metal}	Mass density of metal from which packing is made	kg m^{-3}
σ	Surface tension	N m^{-1} = kg s^{-1}
	Density of rotameter float	g cm^{-3}
τ	Shear stress or momentum flux	N m^{-2} = (kg m s^{-1}) m^{-2} s^{-1}
	Time period	s
	Density meter time period reading	s
ϕ	Dimensionless friction factor = 2 d (dp/dz) / (8 ρ u^2)	
	Fraction of maximum capacity at packed column design point	
	Packing channel crimp half-angle	degrees
	Steam dryness fraction	
ϕ_{bed}	Local friction factor within packed bed	
Ψ	General flux	[property] m^{-2} s^{-1}
ψ	General property	[property] m^{-3}
ω	Mass of rotameter float	g

10.2 S I Multipliers used

S I multiplier	Name	Multiplier
M	Mega	1 000 000
k	kilo	1 000
h	hecto	100
-	-	1
d	deci	0.1
c	centi	0.01
m	milli	0.001
μ	micro	0.000 000 1
n	nano	0.000 000 000 1
p	pico	0.000 000 000 000 1

10.3 Conversion factors

Length	1	in (inch)	equals	0.0254	m
	1	ft (foot)	equals	0.3048	m
Mass	1	lb (pound)	equals	0.454	kg
Time	1	min (minute)	equals	60	s
	1	hr (hour)	equals	3600	s
	1	day	equals	86400	s
	1	yr (year)	equals	$3.1536\ 10^7$	s
Pressure	1	bar	equals	100	kPa
	1	atmosphere	equals	101.325	kPa
	1	psi (lb in^{-2})	equals	6.803	kPa
Kinematic viscosity	1	Stoke	equals	0.0001	$m^2\ s^{-1}$
Viscosity	1	Poise	equals	0.1	Pa s

10.4 Abbreviations

AOD argon oxygen decarburisation - steelmaking process
APU argon purification unit
ASP Air separation plant
BSP British standard pipe (fitting sizes)
COSHH Control of substances hazardous to health (regulations)
FRI Fractionation research incorporated - distillation research consortium
HETP Height equivalent to a theoretical plate - measure of packing efficiency
HTU Height of a transfer unit
HPC High pressure column
LPC Low pressure column
PL Poor liquid - Nitrogen from top of HPC
PPU Pre-purification unit - adsorption unit to remove water and carbon dioxide from air before it enters the cold box
PTFE PolyTetraFluoroEthene - Corrosion resistant plastic
RHE Reversing heat exchanger
RL Rich liquid - from bottom of HPC

Chapter 11 - References

Alekseev, V. P., Poberezkin, A. E. and Gerassimov, P. V. (1972) 'Determination of flooding rates in regular packings' Heat transfer - Soviet research 4 (6) pp159-163 in English translation

Alekseev, V. P., Poberezkin, A. E. and Gerassimov, P. V. (1973) 'Packed columns for air rectification: advantages of regular shaped packings' International Institute of Refrigeration Commission A3, Brighton.

Ali, Q. H. (1984) 'Gas distribution in shallow, large diameter packed beds' PhD Thesis, Department of Chemical Engineering, University of Aston in Birmingham, Birmingham, UK.

Allam, R. J. and Prentice, A. L. (1989) 'Control method to maximise argon recovery from cryogenic air separation units' European Patent Office Publication number 0 341 512 A1.

Agrawal, R. and Woodward, D. W. (1991) 'Production of oxygen-lean argon from air' US patent number 4 994 098.

Baker, T., Chilton, T. H. and Vernon, H. C. (1935) Trans. AIChE. 31 p295

Bauermann, H. D. and Benhamou, W. (1983) 'Amenagements internes pour la distillation sous vide' Informations Chimie no. 209 pp 93-96

Bejan, A. (1982) 'Entropy Generation Through Heat and Fluid Flow' John Wiley and Sons, New York ISBN 0-471-09438-2

Bemer, G. G. and Kalis, G. A. J. (1978) 'A new method to predict hold-up and pressure drop in packed columns' Transactions of the Institution of Chemical Engineers, 56 pp200-204

Bennett, D. L., Ludwig, K. A., Witmer, G. S. and Woods, C. M. (1989) 'Separating argon/oxygen mixtures using a structured packing' US patent no. 4 836 836

Bennett, D. L., Ludwig, K. A., Patrylak,A. J. and Zabrensky, J. S. (1989a) 'Suitable distillation packing for the cryogenic separation of air' European patent application number 88120824.3, European Patent Office Publication Number EP 0 320 885 A2

Billet, R. (1969) 'Optimisation and comparison of mass transfer columns' Institution of Chemical Engineers Symposium Series no. 32 pp 4:42-4:63

Billet, R. (1987) 'Modelling of fluid-dynamics in packed columns' Institution of Chemical Engineers Symposium Series no. 104 pp A170-A182

Billet, R. and Mackowiak, J. (1988) 'Application of modern packings in thermal separation processes' Chem. Eng. Technol. 11 pp213-227

Billet, R. and Mackowiak, J. (1985) 'Hochwirksame metallische Packung fuer Gas- und Dampf Fluessigkeits-Systems' Chemie Ingenieur Technik 57 (11) pp976-978

Billet, R. and Schultes, M. (1987) 'Determination of liquid hold-up in gas-liquid two-phase countercurrent mass transfer columns' Institution of Chemical Engineers Symposium Series no. 104 pp A159-A170

Billet, R. and Schultes, M. (1992) 'Determination of liquid hold-up in gas-liquid two phase countercurrent mass transfer columns' Institution of Chemical Engineers Symposium Series no. 128 pp B129-B136

Bird, R. B., Stewart, W. E. and Lightfoot, E. N. (1960) 'Transport Phenomena' John Wiley and Sons, New York, ISBN 0-471-07395-4.

Bliss, H. and Dodge, B. F. (1949) 'Oxygen manufacture - part I' Chemical Engineering Progress 45 (1) pp51-64

Bosquain, M., Darchis, F. and Lehman, J-Y. (1989) 'Heat and material exchange device and manufacturing process' International patent application WO 89/10527

Bravo, J. L., Rocha, J A. and Fair, J. R. (1985) 'Mass transfer in gauze packings' Hydrocarbon processing 64 (1) pp 91-95

Bravo, J. L., Rocha, J. A. and Fair, J. R. (1986) 'Pressure drop in structured packings' Hydrocarbon processing 65 (3) pp 45-49

Bravo, J. L., Rocha, J. A. and Fair, J. R. (1992) 'A comprehensive model for the performance of columns containing structured packing' Institution of Chemical Engineers Symposium Series no. 128 pp A439-A458

Brennan, D. J. (1992) 'Evaluating scale economies in process plants' Trans IChemE, Vol 70, Part A, September 1992, pp516-526.

Brodkey, R. S. and Herschey, H. C. (1988) 'Transport Phenomena - A Unified Approach' McGraw-Hill Book Company, New York ISBN 0-07-007963-3

Brown, S. (1992) 'Coal, too heavy a price?' Process Engineering, 73 (11) November 1992 pp33-34

Buehlmann, U. (1983) 'Rombopak, ein neuer geordneter Packungskoerper fuer Stoffaustauchkolonnen' Chemie Inginieur Tecknik 55 (5) pp379-

Buehlmann, U. (1987) 'Performance of ROMBOPAK structured column packing in distillation' Institution of Chemical Engineers Symposium Series no. 104 pp A115-A127

Buchanan (1969) 'Pressure gradient and liquid holdup in irrigated packed towers' Industrial and Engineering Chemistry Fundamentals 8 (3) pp502-511

Chang, H. N. and Park, J. K. (1986) 'Effect of Turbulence Promoters on Mass Transfer' from Cheremisinoff, N. P. (Editor) 'Handbook of heat and mass transfer, Volume 2: Mass transfer and reactor design' Gulf Publishing Company, Houston, ISBN 0-87201-412-6.

Chen, G. K. and Acerra, M. (1987) 'Structured tower packing' European patent application number 87117655.8, European Patent Office publication number 0 270 050 A2

Chen, G. K., Kitterman, L. and Shieh, J. (1983) 'High efficiency packing for product separation' Chemical Engineering Progress, September, pp46-49

Coulson, J. M. and Richardson, J. F. (1989) 'Chemical Engineering, Volume 2' Pergamon, Oxford and New York, ISBN 0-08-022919-0.

Das, R. N. (1969) 'Packed Column Distillation at Reduced Pressures' PhD Thesis, Department of Chemical Engineering, University of Birmingham, Birmingham, UK.

Davies, J. T. (1972) 'Turbulence Phenomena' Academic Press, London and New York, 1972, ISBN 0-12-206070-9.

Dudukovic, A. P. and Koncar-Djurdjevic, S. K. (1979) 'The effect of the array of disks on mass transfer rates to the tube walls' American Institute of Chemical Engineers Journal 25 (5) pp 895-899

Dukeler, A. E. and Bergelin, O. P. (1952) Chemical Engineering Progress 48 pp557-

Dutkai, E. and Ruckenstein, E. (1970) Chemical Engineering Science 25 pp483-

Ellis, S. R. M., Hands, C. H. G. and Parry, D. W. (1969) 'Fractional Distillation in Four-inch Diameter and Eight-inch Diameter Columns Operated at Low Column-top Pressure and Low Pressure Gradient' Institution of Chemical Engineers Symposium Series no. 32 pp 4:25-4:30

Ergun, S. (1952) 'Fluid Flow Through Packed Columns' Chemical Engineering Progress 48 (2) pp 89-94.

Faigle, H. (1972) 'Packing for a cooling tower' US Patent 3 652 066

Fair J. R. and Bravo, J. L. (1987) 'Prediction of mass transfer efficiencies and pressure drop for structured tower packings in vapour/liquid service' Institution of Chemical Engineers Symposium Series no. 104 pp A183-A201

Foust, A. S., Wenzel, L. A., Clump, C. W., Maus, L and Anderson, L B (1980) 'Principles of Unit Operations' second edition, John Wiley and Sons, New York, ISBN 0-471-26897-8

Gaiser, G. and Kottke, V. (1989) 'Waerme- und Stoffuebergang in Katalysatoren mit regelmaessiger Formgebung' Chemie Ingenieur Technik 61 (9) pp729-731

Gilliland, E. R. and Sherwood, T. K. (1934) 'Diffusion of vapours into air streams' Industrial and Engineering Chemistry 26 (5) pp 516 - 523

Gor, A. and Wan, P. (1992) 'Commissioning a binary distillation column' Final year industrial project, Chemical engineering department, Aston University, Birmingham, UK.

Grossman, G. (1986) 'Heat and Mass Transfer in Film Absorption' from Cheremisinoff, N P (Editor) 'Handbook of Heat and Mass Transfer, Volume 2: Mass Transfer and Reactor Design' Gulf Publishing Company, Houston, ISBN 0-87201-412-6.

Hayter, A. J. (1952) Industrial Chemist, 28 pp59-64.

Henstock, W. H. and Hanratty, T. J. (1976) A. I. Ch. E. J. 22 pp990-

Hoek, P. J. (1983) 'Large and small scale maldistribution in a packed column' PhD Thesis, Delft University of Technology, Netherlands.

Hoek, P. J., Zuiderweg, F. J. and Wesselingh, J. A. (1986) Chem. Eng. Res. Des. pp431-

Holmberg, R. and Strindehag, O. 'Contact body for cooling towers' US patent 3 963 810

Hoppe, K. and Keller, J. (1980) 'Erfahrung aus dem industriellen Einsatz der Perform-Grid-Packung in der chemischen und erdoelverarbeiteneden Industrie' Chem. Techn. 32 (7) pp334-338

Hoppe, K. and Kunze, R. (1985) 'Chemieanlagen und Pruefmaschinen aus der DDR' Chem. Anlagen Verfahren 18 (5) pp273-275

Hsia, M. A. (1987) 'Tower Packing Element' US patent 4 670 196

Huber, M. (1985) 'X-Shaped packing layers and method of making' US patent 4 497 752

Huber, M (1980) 'Packing element of foil-like material for an exchange column' US patent 4 186 159

Huber, M. and Hiltbrunner, R. (1966) 'Fuellkoerperrektifizierkolonnen mit maldistribution' Chemical Engineereing Science 21 (7) pp819-832

Hughmark, G. (1980) 'Mass transfer and flooding in wetted-wall and packed columns' Industrial and Engineering Chemistry Fundamentals 19 pp385-389

Hughmark, G. (1986) 'Packed column efficiency fundamentals' Industrial Engineering Chemistry Fundamentals 25 (3) pp405-409

Ioan, S., Mircea, M., Mircea, M. and Vilcea, R. (1986a) 'Ordered Packing for Isotope Separation Columns' Romanian Patent number 90566

Ioan, S., Mircea, M., Mircea, M. and Vilcea, R. (1986b) 'Ordered Packing for Isotope Separation Columns' Romanian Patent number 90567

Isalski, W. H. (1989) 'Separation of Gases' Oxford University Press, 1989. ISBN 0-19-854811-7.

Jaeger (1988) 'Metal Max-Pak' Product Bulletin 500, Jaeger Products Inc, Spring, USA

Kaminskii, V. A. and Giorgadse, N. A. (1971) 'The simulation of hydrodynamic processes in the separation of isotopes in packed columns' Atomnaya Energiya 30 (1) pp48-49

Kaminskii, V. A. and Giorgadse, N. A. (1973) Isotopenpraxis 9 (1) pp 1-

Kister, H. Z. and Gill, D. R. (1992) 'Flooding and pressure drop prediction for structured packings' Institution of Chemical Engineers Symposium Series no. 104 pp A109-A123

Kouri, R. J. and Sohlo, J. J. (1987) 'Liquid and gas flow patterns in random and structured packings' Institution of Chemical Engineers Symposium Series no. 104 pp B193-B211

Kraybill, P. R. (1953) PhD Dissertation, University of Michigan, USA

Kuehni (1992) '9M, 4M, The new types of Rombopak' Kuehni Ltd, Allschwil, Switzerland

Kunesh, J. G. (1987) 'Recent developments in packed columns' Canadian Journal of Chemical Engineering 65 pp 907-913

Latimer, R. E. (1967) 'Distillation of Air' Chemical Engineering Progress 63 (2) February 1967 pp35-59

Lockett, M. J. and Victor, R. A. (1989)'Structured column packing with liquid holdup' European patent application number 89104721.9, European Patent office publication number 0 337 150 A1

Martsenyuk, A. S. (1987a) 'Regular packing for heat-mass exchange apparatus' USSR patent SU 1311767 A1

Martsenyuk, A. S. (1987b) 'Regular packing for heat-mass exchange apparatus having mixed flow of dispersed phase' USSR patent SU 1327939 A1

Martsenyuk, A. S. and Guseynov, R. N. (1987a) 'Regular packing for heat-mass exchange apparatus' USSR patent SU 1318269 A1

McGlamery, G. G. (1988) 'Liquid film transport characteristics of textured metal surfaces' PhD thesis, University of Texas at Austin, Texas, USA.

McQuillan, K. W. and Whalley, P. B. (1985) 'A comparison between flooding correlations and experimental flooding data for gas-liquid flow in vertical circular tubes' Chemical Engineering Science 40 (8) pp1425-1440

Meier, W. (1981) 'Packing element for an exchange column' US patent number 4 296 050

Meier, W. (1984) 'Packing for an exchange column' US patent number 4 455 339

Meier, W., Hunkeler, R. and Stoecker, D. (1979) 'Performance of the new regular tower packing 'Mellapak'.' Institution of Chemical Engineers Symposium Series no. 56 pp 3.3/1 - 3.3/17

Meier, W., Stoecker, W. D. and Weinstein, B. (1977) Chemical Engineering Progress 73 (11) pp71-

Merican, J. (1977) 'The effect of the submergence in a vertical thermosyphon reboiler - a preliminary study' MSc Thesis, Aston University, Birmingham, UK.

MTL (1990) 'MTL 836/837 multiplexer receicer units - system protocol' Measurement Technology Ltd, Luton, UK. Publication INM830A-1

Mullin, J. W. (1957) 'The effect of maldistribution on the performance of a packed column' Industrial Chemist 33 pp 408-

Narayanan, C. M. and Bhattacharyya, B. C. (1988) 'Some studies on heat transfer in diverging-converging geometries' Industrial and Engineering Chemistry Research 27 pp 149-153.

Nishimura, T., Kajimoto, Y. and Kawamura, Y. (1986) 'Mass transfer enhancement in channels with a wavy wall' Journal of Chemical Engineering of Japan 19 (2) pp 142-144

Norton (1988) 'Intalox High-Performance Structured Packing' Bulletin IS-1 Norton Chemical Process Products, Akron, USA

Nutter (1987) 'Montz High-Efficiency Structured Packings' Bulletin B-1, Nutter Engineering Ltd, Tulsa, USA

Olujic, Z., Stoter, F. and de Graauw, J. (1992) 'Measurement of large scale gas and liquid maldistribution in structured packings' Institution of Chemical Engineers Symposium Series no. 128 pp B151-B157

Onken, U. and Arlt, W. (1990) 'Recommended test mixtures for distillation columns' The Institution of Chemical Engineers, Rugby, UK. ISBN 0 85295 248 1

Plegat, A. E. (1969) 'Method of manufacturing a heat exchanger' US patent 3 422 777

Pluess, R. (1985) 'Zig-zag profile packing and method of making' US patent 4 497 751

Portalski, S. (1963) Chem. Eng. Sci. 18 pp787-

Porter, K. E. (1968) 'Liquid flow in packed columns - 1: The rivulet model' Trans. I. Chem. E. 46 pT69

Porter, K. E. and Jenkins, J. D. (1979) 'The interrelationship between industrial practice and academic research in distillation and absorption' Institution of Chemical Engineers Symposium Series no. 56 pp 5.1/1-

Porter, K. E. and Templeman, J. J. (1968) 'Liquid flow in packed columns - 3: Wall flow' Trans. I. Chem. E. 46 ppT86-

Process Engineering (1992) ' PREDICT Indices' PE 73 (11) p21

Ramadhyani, S. (1986) 'Numerical prediction of flow and heat transfer in corrugated ducts' in Shah, R. K. and Pearson, J. T. (Ed.s) 'Advances in Heat Exchanger Design' HTD-vol. 66 American Society of Mechnical Engineers, New York pp.37-43.

Regehr, U. (1975) 'Contact body for the transfer of heat and/or substances' US Patent number 3 887 664

Reid, R. C., Prausnitz, J. M. and Poling, B. E. (1987) 'The Properties of Gases and Liquids' Fourth Edition, McGraw-Hill Book Company, New York ISBN 0-07-051799-1

Robinson, K. (1991) 'Trays or packings - which to choose?' The Chemical Engineer no. 499, 27 June 1991, pp23-26.

Rogers, G. F. C. and Mayhew, Y. R. (1980) 'Thermodynamic and transport properties of fluids' Basil Blackwell, Oxford, UK. ISBN 0 631 12891 3

Rohde, W. and Corduan, H. (1989) 'Verfahren und Vorrichtung zur Luftzerlegung' European Patent Office Publication number 0 377 117 A1.

Ruhemann, M. (1949) 'The Separation of Gases' second edition, Oxford University Press, London.

Rushton, J. H. (1946) Summary Technical Report of division 11, National Defense Research Committee, Volume 1, Office of Scientific Research and Development, Washington, pp 139-191.

Rushton, J. H. and Stevenson, E. P. (1947) 'Developments in oxygen production' Transactions of the American Institute of Chemical Engineers 43 (2) pp 61-68

Schofield, R. C. (1950) Chemical Engineering Progress 46 (8) p 405

Seah, A. M. (1986) 'Structured "WV" packing elements' European patent application number 86307365.6, European Patent Office publication number 0 218 417 A1

Sealey, C. J. (1970) 'The optimal design of a laboratory distillation column for efficiency studies at finite reflux' Chemical Engineering Science 25 pp 561-668

Shi, M. G. and Mersmann, A. (1985) 'Effective interfacial area in packed columns' German Chemical Engineering 8 pp 87-96

Sinnott, R. K. (1989) 'Volume 6 - Design' from Coulson, J. M. and Richardson, J. F. (series eds.) 'Chemical Engineering' Pergamon, Oxford and New York 1989 ISBN 0-08-022970-0.

Souza Mendes, P. and Sparrow, E. M. (1984) 'Periodically converging-diverging tubes and their turbulent heat transfer, pressure drop, fluid flow and enhancement characteristics' Journal of Heat Transfer 106 pp 55-63

Spiegel, L. and Meier, W. (1987) 'Correlations of the performance characteristics of the various Mellapak types' Institution of Chemical Engineers Symposium Series no. 104 pp A203-A215

Spiegel, L. and Meier, W. (1992) 'A Generalised Pressure Drop Model for Structured Packings' Institution of Chemical Engineers Symposium Series no. 128 pp B85-B94

Stackhouse, D. W. (1987) 'Gas/Liquid contact apparatus' US patent number 4 670 197

Stedman, D. F. (1937) 'Improved packed fractionating columns' Canadian Journal of Research, section B, 15 (10), pp383-400.

Stein, W. A. (1992) 'A new equation for heat and mass transfer in pipe flow' International Chemical Engineering 32 (3) pp431-448

Stephan, K. and Hildwein, H. 'Recommended data of selected compounds and binary mixtures' Dechema Chemistry Data Series vol IV, parts 1+2 DECHEMA, Germany.

Stephanopoulos, G. (1984) 'Chemical Process Control: an introduction to theory and practice' Prentice Hall inc., Englewood Ciffs, USA. ISBN 0-13-128596-3

Stichlmair, J., Bravo, J. L. and Fair, J. R. (1989) 'General model for prediction of pressure drop and capacity of countercurrent gas/liquid packed columns' Gas Separation and Purification, 3 (3) pp 19-28.

Stikkelman, R. M. and Wesselingh, J. A. (1987) 'Liquid and gas flow patterns in packed columns' Institution of Chemical Engineers Symposium Series no. 104 pp B155-B164.

Stoter, F., Olujic, Z. and de Graauw, J. (1992) 'Modelling of hydraulic and separation performance of large diameter columns containing structured packing' Institution of Chemical Engineers Symposium Series no. 128 pp A201-A210

Streiff, F. (1985) 'Corrugated sheet packing and method of making' US patent 4 497 753

Suess, P. (1992) 'Analysis of gas entries of packed columns for two phase flow' Institution of Chemical Engineers Symposium Series no. 128 pp A369-A383

Sulzer Brothers (1966) 'Improvements relating to Liquid/Vapour Material Exchange Columns' UK patent number 1 020 190

Sulzer Brothers Ltd (1992) 'Separation Columns for Distillation and Absorption' Brochure, Sulzer Brothers Ltd, Product Division Chemtech Separation Columns, Wintertur, Switzerland

Thorogood, R. M., Bennett, D. L., Dawson, B. K., Prentice, A. L. and Allam, R. J. (1989) 'Air separation process using packed columns for oxygen and argon recovery' European patent application number 89304114.5, European Patent Office publication number EP 0 341 854 A1

Treybal, R. E. (1980) 'Mass-Transfer Operations' McGraw-Hill Book Company, New York ISBN 0-07-065176-0

Ukhanev, V. P., Rilo, R. P., Zalkind, G. R., Zhilin, A. G., Ovchinnikov, A. I., Taran, Y. A., Molchanov, V. I. (1985) 'Regular packing for heat and mass transfer apparatus' USSR Patent SU 1168278 A

Vetencourt, R. A. (1978) 'Submergence effects in a vertical thermosyphon reboiler' MSc Thesis, Aston University, Birmingham, UK.

Victor, R. A. and Lockett, M. J. (1989) 'Double column air separation apparatus and process with hybrid upper column' European patent application number 89102253.5, European Patent Office publication number 0 328 112 A2

Victor, R. A., Lockett, M. J. and Dray, J. R. (1991) 'Cryogenic air separation system with hybrid argon column' US Patent number 5 019 144

Vlastimil, B. (1989) 'Ordered column packing for diffusion processes' Czechoslovakia Patent 263904.

Watson, H. E. (1949) Industrial Chemist, 25 pp503-506.

Weedman, J. A. and Dodge, B. F. (1947) 'Rectification of liquid air in a packed column' Industrial and Engineering Chemistry, 39 (6) pp732-744.

Westhaver, J. W. (1942) 'Theory of open-tube distillation columns' Industrial and Engineering Chemistry 34 (1) pp126-130

Yih, S. M. (1986) 'Modeling Heat and Mass Transport in Falling Liquid Films' from Cheremisinoff, N. P. (Editor) 'Handbook of heat and mass transfer, Volume 2: Mass transfer and reactor design' Gulf Publishing Company, Houston, ISBN 0-87201-412-6.

Yih, S. M. and Chen, C. H. (1982) Proceedings of 7th International Heat Transfer Conference volume 3 pp125-

Zel'venskiy, Ya. D., Fetisov, Ye. I. and Kovalenko, A. Ye. (1978) 'Rectification of argon in columns with regular coiled packing' Scientific Research Institute for Technical and Economic Studies (NIITEKhIM), USSR.

Zhang, Z., Wang, S. Y. and Yu G. C. (1988) 'Study on liquid phase mixing in packed columns' Journal of Chemical Industry and Engineering (China) 3 (2) pp294-310 of English translation.

Zhang, Z., Wang, S. Y. and Yu G. C. (1990) 'A new mathematical model for packed columns' Tianjin University, Tianjin 300072, P R China

Zogg, M. (1973) 'Stoffaustauch in der Sulzer Gewebepackung' Chemie Ingenieur Technik 45 (2) pp 67-

Zuiderweg, F. J., Hoek, P. J. and Lahm, L. (1987) 'The effect of liquid distribution and redistribution on the separating efficiency of packed columns' Institution of Chemical Engineers Symposium Series no. 104 pp A217-A231

Zuiderweg, F. J., Hoek, P. (1987) 'The effect of small scale liquid maldistribution ("natural flow") on the separating efficiency of random packings' Institution of Chemical Engineers Symposium Series no. 104 pp B247-B253

Zuiderweg, F. J., Kunesh, J. C. and Ring, D. W. (1981) AIChE Meeting, Pittisburg, PA. August 1981

Zukauskas, A. (1989) (and Karni, J. (English Edition Editor)) 'High-Performance Single-Phase Heat Exchangers' Hemisphere Publishing Corporation, New York ISBN 0-89116-975-X.

Chapter 12 - Appendices

Appendix 1 - Test rig design calculations

Preliminary design

The preliminary design was to establish the maximum steam and cooling water flows required by the rig. The approximate maximum flow of vapour in the column was calculated from Sulzer's correlation for the capacity of different sizes of Mellapak against flow parameter. The use of Mellapak 125Y packing with a minimum reflux ratio of 0.5 was assumed, to give the highest possible vapour load. The capacity factor at flooding was 0.14 m/s for all the possible components. From this capacity factor, the cross-sectional area of the column and the densities of each component, the vapour flows were calculated as follows:

$$V_{mass} = \rho_v u_{vs} A = A C_s \sqrt{\rho_v (\rho_l - \rho_v)}$$

where A is the column cross sectional area = 0.0783 m^2.

and $C_s = u_{vs} \sqrt{\frac{\rho_v}{\rho_l - \rho_v}}$

From the vaporisation enthalpies of the components, the boiler and condenser duties corresponding to the vapour flows were calculated:

$$Q_{in} = Q_{out} = V_{mass} \Delta h_{vap}$$

where Δh_{vap} is the vaporisation enthalpy per unit mass

The steam flow was calculated from the boiler duty by using the same equation assuming total condensation of dry steam at a pressure of 5.5 bar, whose vaporisation enthalpy is 2100 kJ/kg.

The cooling water flow was calculated by assuming a maximum allowable temperature rise over the condenser of 20 K.

$$F_{cw} = \frac{Q_{out}}{c_p \Delta T}$$

where c_p is the specific heat capacity of water, 4.2 kJ/(kg K)

These calculations are summarised in table A1-1

Component		n-Hexane	Toluene	Chloro-benzene	Ethyl-benzene
Saturated vapour density	kg / m^3	3.30	2.91	3.43	3.26
Saturated liquid density	kg / m^3	613	778	970	751
Density Ratio	-	0.00538	0.00374	0.00354	0.00434
Total reflux flow parameter $(\rho_v/\rho_l)^{1/2}$	-	0.0734	0.0612	0.0595	0.0659
Flow parameter if L/V=0.5	-	0.0367	0.0306	0.0297	0.0329
Flow parameter if L/V=1.5	-	0.1101	0.0917	0.0892	0.0988
Boiling point	°C	68.7	110.6	131.8	136.2
Capacity factor for M125Y at flooding, L/V=0.5	m s^{-1}	0.14	0.14	0.14	0.14
Vapour mass flow	kg/s	0.496	0.525	0.636	0.546
Vaporisation enthalpy at 1 bar	kJ/kg	333	359	324	337
Boiler or condenser duty	kW	165	188	206	184
Steam flow	kg/s	0.079	0.090	0.098	0.088
	kg/hr	283	323	353	315
Cooling water flow for 20 K temperature rise	kg/s	1.96	2.24	2.45	2.19
	dm^3/min	118	135	147	131

Table A1-1 Preliminary calculations of maximum steam and cooling water flows

The results show that a maximum steam flow of about 0.1 kg/s or 6 kg/min is required. The boiler can provide 0.12 kg/s, so the only limitations are the steam piping and the quantity of steam used in the rest of the building.

A maximum cooling water flow of about 2.5 kg/s (150 dm^3/min) is required with a 20 K temperature rise. This is well within the capability of the cooling water system pump, so again, the only limitation is the frictional pressure drop in the pipes and across the condenser.

Detailed design calculations

Range of flows for different packing sizes

To be able to specify the pipework, flowmeters and distributor, the range of operating flows needs to be established. This will depend on the sizes of packing which may be used and the required turndown in the tests. The maximum capacity

factors and corresponding maximum heat loads for the different packings at different reflux ratios are listed in table A1-2

Reflux ratio	0.5		1		1.5	
Flow Parameter	0.032		0.065		0.098	
	$C_{s\,max}$	Q / kW	$C_{s\,max}$	Q / kW	$C_{s\,max}$	Q / kW
Mellapak 125Y	0.138	206	0.116	171	0.100	147
Mellapak 250Y	0.110	162	0.093	137	0.080	118
Mellapak 350Y	0.094	138	0.079	116	0.068	100
Mellapak 500Y	0.077	113	0.065	96	0.056	82
Mellapak 750Y	0.069	102	0.059	87	0.050	74

Table A1-2 Maximum capacity factors (m/s) and corresponding maximum heat loads (kW) for different packings at different reflux ratios.

Reflux ratio = 0.5	n-Hexane			Toluene			Chloro-benzene			Ethyl-benzene		
Flow / dm³/min	V	L	F	V	L	F	V	L	F	V	L	F
Mellapak 125Y	49	24	24	41	20	20	39	20	20	44	22	22
Mellapak 250Y	38	19	19	32	16	16	31	15	15	34	17	17
Mellapak 350Y	32	16	16	27	13	13	26	13	13	29	14	14
Mellapak 500Y	27	13	13	22	11	11	22	11	11	24	12	12
Mellapak 750Y	24	12	12	20	10	10	19	9	9	22	11	11
Reflux ratio = 1.0	n-Hexane			Toluene			Chloro-benzene			Ethyl-benzene		
Flow / dm³/min	V	L	F	V	L	F	V	L	F	V	L	F
Mellapak 125Y	41	41	0	34	34	0	33	33	0	37	37	0
Mellapak 250Y	33	33	0	27	27	0	26	26	0	30	30	0
Mellapak 350Y	28	28	0	23	23	0	22	22	0	25	25	0
Mellapak 500Y	23	23	0	19	19	0	18	18	0	21	21	0
Mellapak 750Y	21	21	0	17	17	0	17	17	0	19	19	0
Reflux ratio = 1.5	n-Hexane			Toluene			Chloro-benzene			Ethyl-benzene		
Flow / dm³/min	V	L	F	V	L	F	V	L	F	V	L	F
Mellapak 125Y	35	56	17	29	43	14	28	42	14	31	46	15
Mellapak 250Y	28	42	14	23	34	11	22	33	11	25	37	12
Mellapak 350Y	24	36	12	20	30	10	19	28	9	17	25	8
Mellapak 500Y	20	30	10	16	24	8	16	24	8	14	21	7
Mellapak 750Y	18	27	9	15	22	7	14	21	7	13	19	6

Table A1-3 Vapour liquid and feed flows at flooding for different components and packing sizes.

Table A1-3 gives the calculated maximum flows for each component at different reflux ratios. The flows of vapour, liquid and the feed flows are given in dm^3/min of liquid.

Boiler capacity calculations

Vetencourt (1978) tested the boiler which was to be used in this work with water. He achieved a maximum heating rate of 710000 btu/hr boiling water at 1 bar with a temperature difference of 69 °F or 38 °C. This corresponds to a rate of (710000 btu/hr / (0.9478 btu/kJ * 3600 s/hr)) = 208 kW. The boiler is therefore capable of providing the maximum heating rate required.

However, if ethylbenzene is to be boiled at a temperature of 136 °C, this means that the steam temperature required is 174 °C corresponding to a pressure of 8.8 bara or 115 psig. The practical maximum steam pressure is 75 psig or 6.1 bara, which corresponds to a temperature of 159 °C. This allows a temperature difference of 23 °C (41 °F), leading to a heating rate of about 420000 btu/hr or 123 kW. This is well short of the 200 kW needed to flood Mellapak 125Y at a reflux ratio of 0.5, but is almost sufficient to flood 250Y at total reflux, and should allow operation with 350Y at a wide range of reflux ratios.

Since the lowest area packing to be tested was the Norton IMSP 1T, with an area of 276 m^2/m^3, this presented no problem.

Distributor specification

The distributor needed to allow the packings to be tested over as wide a range of flows as possible. Sulzer's three level distributors are able to provide a turndown of 10:1 relatively easily, so this was the specified turndown. The maximum flow desired in the tests was that needed to flood the 276m^2/m^3 packing at total reflux, with the toluene / n-hexane mixture. This corresponded to a maximum distributor flow of about 30 dm^3/min. A minimum flow of 3 dm^3/min would then be possible, allowing the highest area packing to be tested (500Y) to be operated down to about 17% of its maximum capacity, to an F factor of about 0.35.

Pipe sizes

Two criteria were used to determine the process side pipe sizes; the velocity in unpumped lines should not exceed 1.5 m/s and that in pumped ones should not exceed 3 m/s. For simplicity, only two pipe sizes were to be used, so that the maximum necessary flows in each type of line would set the size.

The maximum unpumped flow required was 49 dm³/min flow from the condenser when operating Mellapak 125Y at a reflux ratio of 0.5. This gives a pipe diameter of:

$$d = \sqrt{\frac{4\ (\text{volume flow})}{\pi\ (\text{velocity})}} = 26\text{mm}$$

Some 1" (25 mm) BSP standard stainless steel piping was available from the depertment stores, together with a number of compression fittings. It had previously been used in the boiler tests (Vetencourt, 1978) so this was considered suitable and used.

The maximum pumped flow needed was 41 dm³/min - the reflux flow for Mellapak 125Y at total reflux. With a maximum velocity of 3m/s, this gives a diameter of 17 mm. 0.75" (19 mm) outside diameter stainless steel pipe was therefore used, and joints were made with compression fittings.

Flowmeter sizing.

The flowmeters had to be capable of accurate measurement over as wide a range of flows as possible. Three flowmeters were used, to measure the cooling water, reflux and feed flows. These had to be able to measure the maximum flows possible, but without compromising the accuracy in the limited flow range of the tests. After considering turbine flowmeters, because of their good accuracy, rotameters were eventually specified, because they were much cheaper and were held in the department stores.

The maximum reflux flow to be measured is 41 dm³/min if Mellapak 125Y is used, but only 28 dm³/min with 350Y. The minimum required flow is 3 dm³/min, the lower limit of the distributor. A type 35 rotameter tube is capable of measuring up to 50 dm³/min water with a stainless steel float and 22.5 with a korannite one. This corresponds to flows of hexane of 64 and 29 dm³/min The range of a rotameter is around 1:10, so a type 35 rotameter with a korannite float was used for measuring the reflux flow. This tube could also be used if lower area packings were to be tested; only the float would need to be changed.

The maximum feed flow 24 dm³/min if Mellapak 125Y is operated at a reflux ratio of 0.5, but only 16 dm³/min with 350Y. The minimum required flow is as close to zero as possible, so that reflux ratios very close to 1 may be used. A type 24 rotameter tube can measure up to 20 dm³/min water with a stainless steel float and 9.6 with a korannite one. These water flows correspond of 26 and 12 dm³/min of hexane. So a type 24 rotameter with a korannite float was used to measure the feed flow. Again, this tube could still be used, but with a stainless steel float, if lower area packings were to be tested.

The final flowmeter to be specified was for the cooling water. This had to be operated at up to 4 bar gauge so that a rotameter was unsuitable. Instead, a spring-loaded variable area flowmeter was used. This had a range of 5-100 dm^3/min, since the version with a range up to 150 dm^3/min had a higher pressure drop at 100dm^3/min and would restrict the flow too much. It was considered practicable to operate the condenser with a 30 K temperature rise if it should be necessary to test low area packings, so reducing the maximum flow to 100 dm^3/min.

Control valve and pump check

Preliminary tests of the spare Beresford B30-A6 pump with water gave the characteristic in figure A1-1. This illustrates that it is capable of providing the maximum necessary reflux flow of 41 dm^3/min (M125Y at total reflux) with a head pressure of about 2 bar.

Figure A1-1 Measured characteristic of Beresford B30-A6 pump

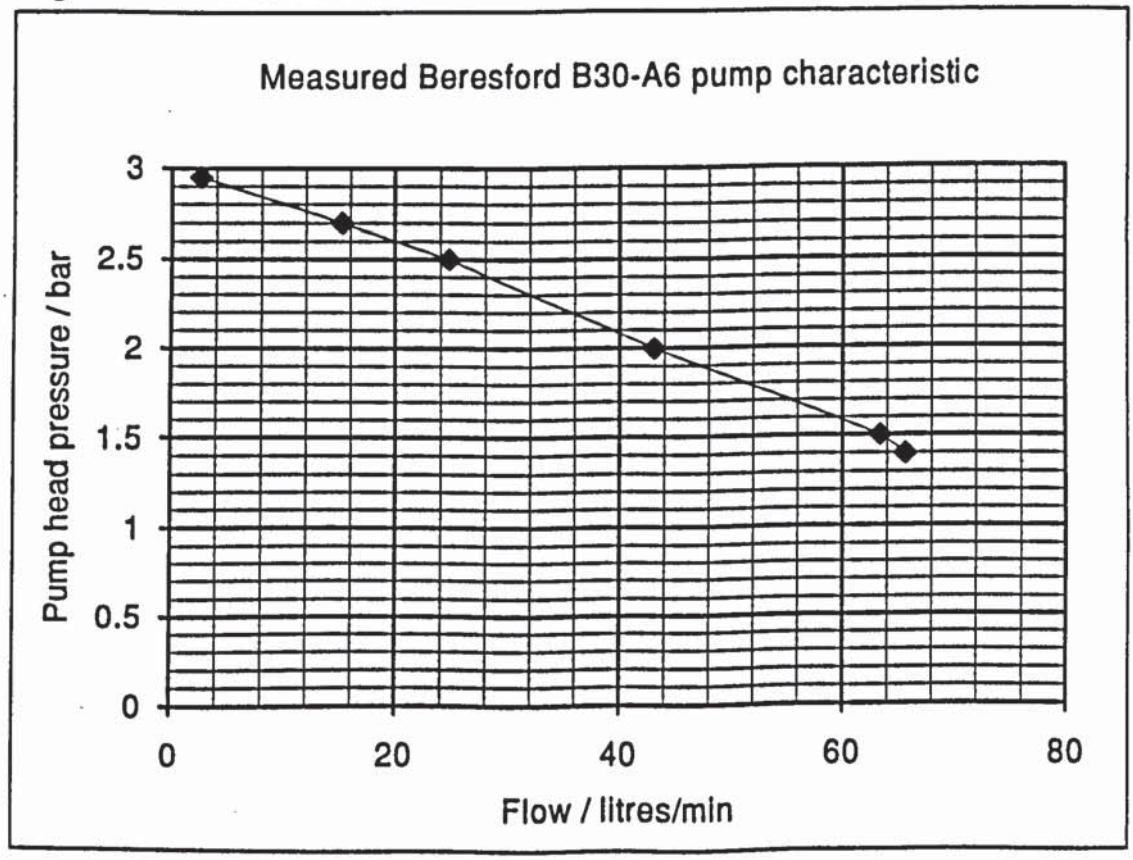

Six control valves were available from the department stores. Two were of carbon steel and made by Introl of Halifax and had 1/2" BSP connections. Because they were made of carbon steel, they would only be suitable for controlling the cooling water or steam condensate flows. Tests with water (figure A1-2) showed that if a pressure drop of 1 bar was allowable, then the cooling water flow would only be about 50 dm^3/min, so a bypass for the control valve would be necessary and the flow could not be controlled down to zero. These valves closed on air failure, and so the bypass would also be necessary for safety reasons, so that the cooling water would not accidentally be cut off. The maximum steam condensate flow required was about 6 dm^3/min, so the other Introl valve would be much too big for this.

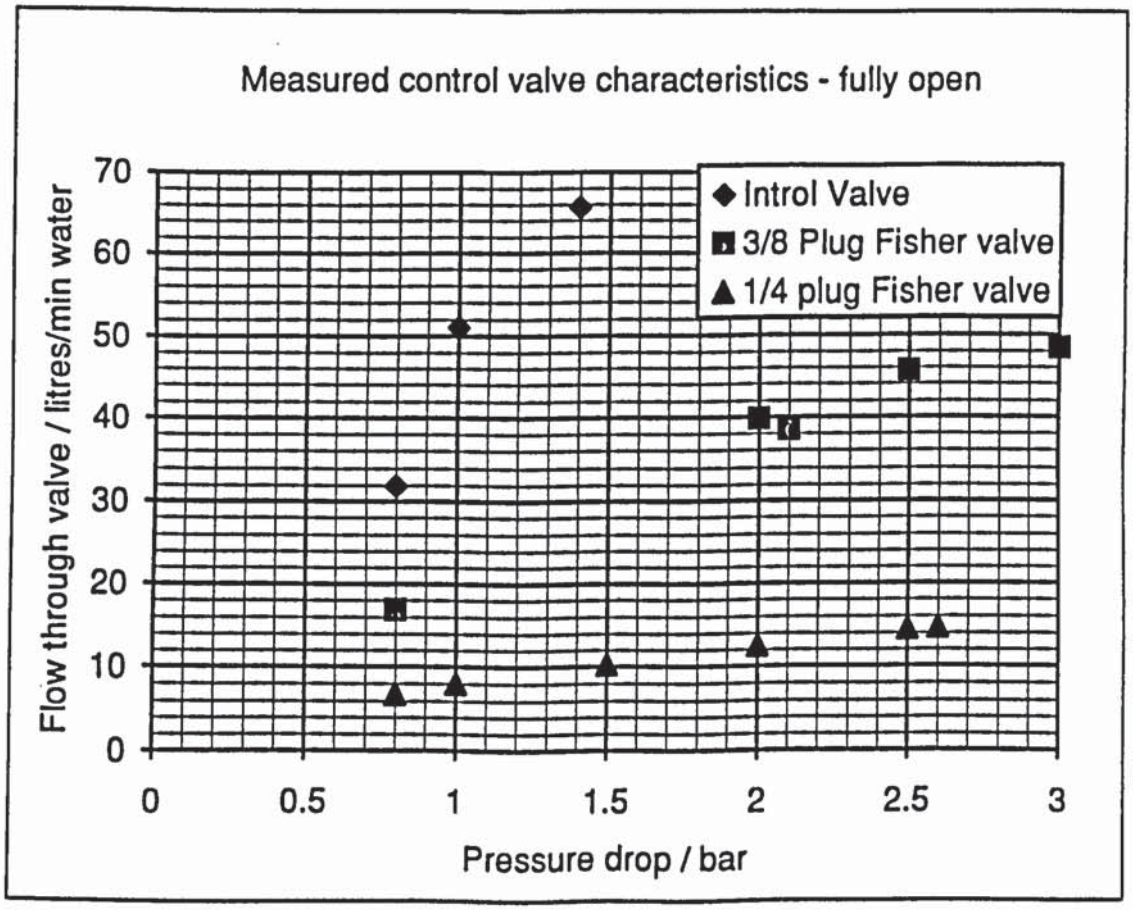

Figure A1-2 Measured characteristics of fully-open control valves

The other valves were of stainless steel and made by Fisher, and would be suitable for controlling the process side flows. All had 1" BSP connections. Three had a 1/4" plug and the other a 3/8" plug. The measured flows through these valves are also given in figure A1-2.

The 3/8" valve is capable of supplying the necessary reflux flow of around 40 dm^3/min with a pressure drop of 2 bar, which is about equal to the pump delivery pressure. It is therefore just large enough for controlling the reflux flow, although if the pressure drops in the pipes and flowmeter are significant, it may be necessary to run the feed and reflux pumps in parallel to achieve the maximum flow with low area packings.

The 1/4" valves were well suited to control of the steam condensate, with a flow of 6 dm^3/min at a pressure drop of about 0.7 bar. They would also be suitable controlling the feed flow, although to obtain the maximum required 24 dm^3/min flow, a pressure drop of about 4 bar would be needed, which the pump could not provide. So to use one of these valves would mean that higher area packings could not be operated at reflux ratios so far from 1 as planned. Nevertheless, for the planned tests, the valve would be quite adequate, and was therefore used.

Cooling water piping

The main cooling water supply and return pipes would have to supply up to 150 dm^3/min cooling water with negligible pressure loss. Based on the assumption that the velocity should not exceed 1 m/s, this leads to a required diameter of 54 mm. The current 1" (25 mm) diameter pipes would therefore be inadequate and extra piping had to be installed. For this, 2.5" pipes (64 mm) pipes were chosen.

Steam piping

As with the cooling water, the supply pressure drop should be negligible. In the case of the steam, this is so that the maximum possible pressure may be obtained in the reboiler at the maximum flow of 0.1 kg/s. With a steam density of about 3 kg/m^3 at 6 bar, this corresponds to a volume flow of 0.033 m^3/s. To obtain a low pressure drop, the steam velocity should not exceed about 15 m/s, so that the pipe diameter should be greater than 53 mm. The existing 1.25" (32 mm) piping was therefore too small. Because a 3" (75mm) secondary steam main was available just through the wall in the main pilot plant, it was decided to extend this into the flameproof laboratory.

Appendix 2 - Notes on TURBO PASCAL programmes

Borland's Turbo Pascal (Borland, 1987) was chosen as the programming language for this work because it allowed easy access to the input and output facilities on the IBM-compatible PC. It was also possible to write the interrupt routines in this language rather than in the lower level assembly language. The programmes were originally written in version 4.0 and later run under version 5.5 to take advantage of the faster compiler. None of the advanced features of the version 5.5 language (such as object oriented programming) was used. For explanations of any unfamiliar terms and more details of this language, the Borland Turbo Pascal User Manual is recommended (Borland, 1987). For details of the MS-DOS operating system, the 'MS-DOS User Manual' should be consulted.

Turbo Pascal programmes can be run either from the 'Integrated Development Environment' (IDE), or compiled and then run from MS-DOS. The IDE is an editor, which may be used to edit any file (for example data files) as well as programme files which are given the extension '.PAS'.

A Pascal programme may contain functions and subroutines, which must be defined before the actual programme. It may also use functions and subroutines which are defined in programme 'units'. The programmes presented here make extensive use of such units, to break down the programme into more manageable sections. The programme units are contained in files with the extension '.PAS', just like the main programme. Before the main programme can be run, these units must be compiled into 'Turbo Pascal Unit' files with the extension '.TPU'. When the main programme is compiled from the IDE, the compiler automatically compiles the units and then 'builds' the run file (extension '.EXE') from the main programme file and from the '.TPU' unit files.

Appendix 3 - Error analysis programmes

These programmes calculate the errors from different sources in the measured number of theoretical plates at different reflux ratios and with different numbers of theoretical plates.

In the input file, the following parameters must be given: The ratio of the holdup at the bottom of the to the total, the mixture composition, the absolute error in the measured compositions, the absolute error in the vapour liquid equilibrium composition data, the random percentage error in the measured flows, the systematic percentage error in the measured flows, the error in the number of theoretical plates due to end effects, the maximum number of theoretical plates for which the analysis must be done, the ratio of the vaporisation enthalpy of the less volatile component to that of the more volatile one and finally, for the chlorobenzene - ethylbenzene mixture, the relative volatility.

Two output files are generated. One (suffix .OUT) contains the detailed calculation results, with the compositions on each plate. The other (.ERR) contains a summary of the errors for each number of plates at each reflux ratio.

ERRCE.PAS

The input file for this programme is ERRCE.IN and the output files generated are ERRCE.OUT and ERRCE.ERR

ERRTH.PAS

The input file for this programme is ERRTH.IN and the output files are ERRTH.OUT and ERRTH.ERR.

CVLEN55.PAS

This unit is used by the error analysis programmes to provide vapour liquid equilibrium data.

Appendix 4 - Control and data logging programme

The programme which is used to control the rig and record data from it is presented here. It is stored on the hard disc of the control computer. The programme is divided into a number of units (see appendix 2). These contain subroutines which may be called from the main programme and from other units. Each one is presented with a brief description of its function.

The parts of the programme which perform the control and which read the temperature information run alongside the part which displays and records the data. They are 'Interrupt driven'. This means that at predetermined intervals, a so-called 'interrupt' occurs and the computer stops running the main programme to do the next part of the control or to read the next piece of temperature information.

CKOR.PAS

This is the main control programme for use when the rotameters contain korannite floats. It executes the startup procedures and then operates the main menu system. If a command is selected, the appropriate subroutine is called.

CCORE2.PAS

This is the programme unit which contains the startup procedures which begin the control programme and the core routines which update the information displayed on the screen and save the data to disc at predetermined intervals.

CMENU1.PAS

This unit provides the menu system for the control programme.

CFLOWKOR.PAS

This unit estimates flows from control valve positions and allows measured flows to be entered. The flows can then be used in the heat balance and packing performance estimate.

CCOMPNS.PAS

This unit estimates compositions from temperatures and allows measured compositions to be entered. The estimates are not very accurate because of the poor NRTL equilibrium data, however they give some idea of the performance of the packing.

CHEATBAL.PAS

This unit displays an approximate heat balance while the rig is running.

CPACKPKO.PAS

This unit is used by the control programme to estimate the performance of the packing during a run. It is not particularly accurate and should not be relied upon to give useable results.

CGLOBALS.PAS

This unit contains the definitions of the 'global' variables, that is those shared by all the parts of the control programme.

CUTILS.PAS

This unit contains a variety of 'utility' procedures and functions for the control programme.

CSERIAL.PAS

This unit is used to set up and carry out the procedures for communicating with the MTL analogue multiplexer unit. The communications are serial, that is binary digits are sent one after the other at regular intervals. The control programme must be interrupted frequently enough to read each digit as it is transmitted. This unit contains the interrupt service routine (ISR) to read and write data to the device. It also contains the routines necessary to start and stop the ISR. When the .LOG file is being written to disc, the serial ISR must be stopped, so that the writing is not interrupted.

CMTL.PAS

This unit contains procedures to send commands to the MTL 836 analogue multiplexer which is used to read the measured temperatures. For details of these commands, the manual for this device (MTL, 1990) should be consulted.

CCONTROL.PAS

This is the part of the programme which performs the control actions. It does this within an 'Interrupt service routine' (ISR). Procedures to start and stop the ISR are also included. The ISR is executed every half-second, when the computer receives an 'interrupt' signal from its internal timer. It is independent of the rest of the program, and runs wherever that program may be in its execution. The control loops are implemented with the velocity form of the discrete proportional-integral-derivative (PID) control algorithm (see chapter 5).

CRECORDS.PAS

This unit performs no function at present. If extra data is to be recorded during a run, the code to do this may be added to this unit.

CVALVES.PAS

This unit contains functions which estimate the flow through the control valves at a particular percentage open for different systems.

CROTAKOR.PAS

This unit contains functions and procedures which are used to convert the rotameter scale readings into flow values (with korannite floats). It is also used by the data processing programme. It contains numerical curve fits to the calibration data obtained with water and to the standard calibration graph for water, and converts these to give actual flows of the test mixture. The method is described in appendix 6.

CVLENRTL.PAS

This unit calculates the vapour liquid equilibrium for toluene and hexane or chlorobenzene and ethylbenzene, using the Margules or Non-Random Two Liquid equations. Two variables must be given from: composition in vapour, compostion in liquid, temperature and pressure, whilst one is returned.

CCEPROPS.PAS

This unit calculates various physical properties of mixtures of chlorobenzene and ethylbenzene. Equations used for the physical properties and their references are given in appendix 6.

CHEAT.PAS

This unit contains routines used in calculating the heat balance. They are mostly to give the properties of water and steam. Expressions for the properties and their sources are given in appendix 6.

CNTP.PAS

This unit calculates the number of theoretical stages, given the mixture, the terminal compositions and operating pressure.

Appendix 5 - Example Data Files

Data is transferred from one programme to another in data files. A plan of the data files required and produced by each programme is given in figure A5-1. Example data files are given here for the run CW3T12AA.

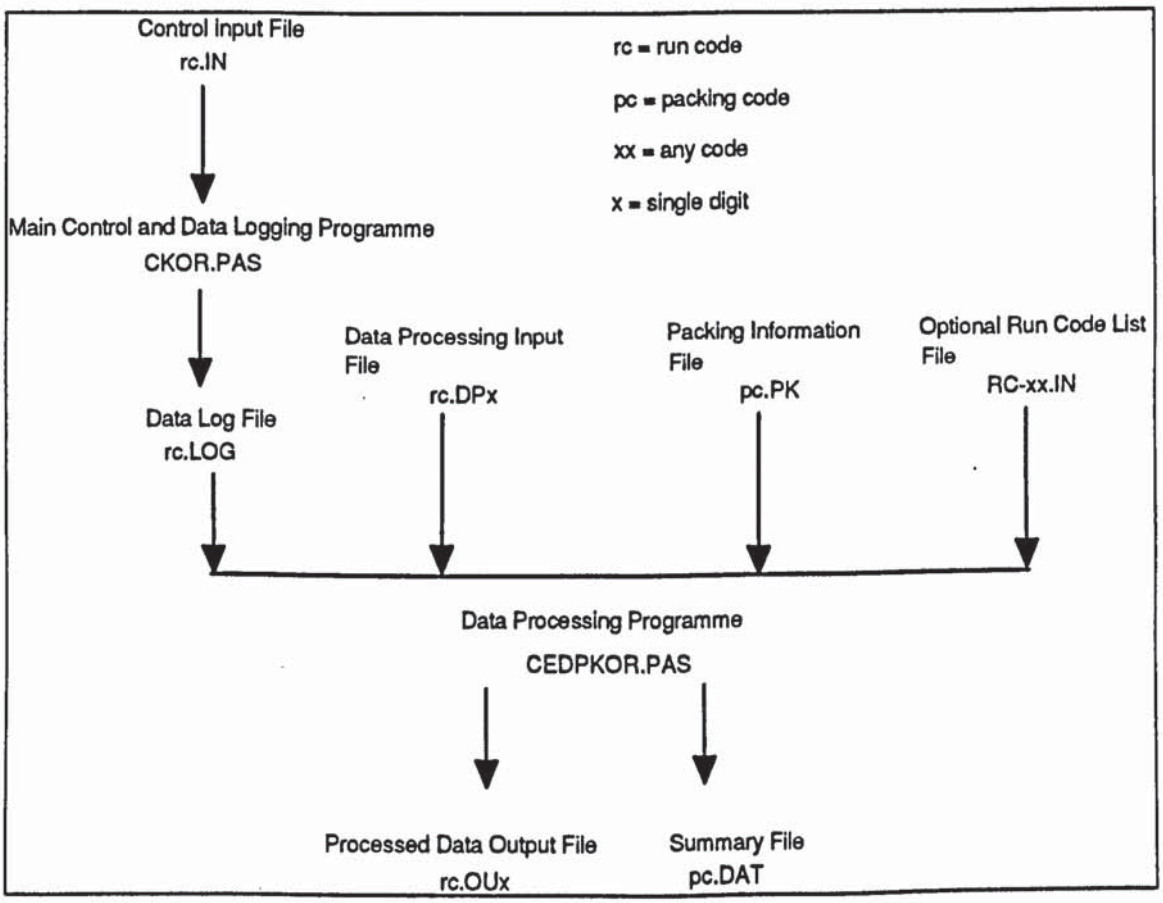

Figure A5-1 Plan of files required and produced by each programme

CW3T12AA.IN

This file is needed by the control and data logging programme. It contains information about the packing and rig setup, the run code and the required control parameters. Before a run, a file with the run code name and the suffix .IN should be created in this format, normally by editing an existing file within the Turbo Pascal editor.

```
Run Code (used as output file name)                                *cW3t12AA
Atmospheric pressure /bar                                          *1.005
Height of Packing /m                                               *2.044
Type of Packing                                                    *TN350Y wall wipers
Configuration; Total Reflux, Stripping or Rectifying               *T
System; Water, Hexane/Toluene or Chloro/Ethyl-benzene              *CE
Cooling water flow /(dm3/min): with CV1 closed                     *44
                               with CV1 open                       *74
Initial Steam pressure /psia                                       *74.5
Superheated; True or False                                         *F
Dryness fraction or degrees C of superheat                         *1
Steam Condensate flow/(kg/min): with CV4 closed                    *0
                                with CV4 open                      *-1
Approximate desired reflux ratio                                   *1.0
Control parameters:  Cooling water flow / Reflux temp: Kc          *6
                                                       Ti/sec      *40
                                                       Td/sec      *0
                                                 set point/deg C   *0
                     Reflux flow / Reflux tank level : Kc          *0.8
                                                       Ti/sec      *40
                                                       Td/sec      *0
                                                 set point/% full  *30
                 reflux ratio / feed valve position : Kc           *-0.3
                                                       Ti/sec      *40
                                                       Td/sec      *0
                                 initial set point / % open        *0
          Steam condensate flow / Column Pressure drop: Kc         *-200
{units of     sec}                                     Ti/sec      *60
                                                       Td/sec      *0
                                                 set point/mBar    *40
Skip setup of multiplexer inputs?                                  *Yes
```

CW3T12AA.LOG

This is the log file which is produced by the control programme and contains all the data recorded by the programme. It is produced automatically and is needed by the data processing programme to calculate average values over the period of the run. The start of this file is a repeat of the data read from the .IN file. The rest of the file gives the temperatures, column pressure drop and control valve positions approximately every 20 seconds during the run. Only the first part of this file is illustrated, because it is so long; approximately one hour's data is given.

```
Run Code (used as output file name)                                *cW3t12AA
Atmospheric pressure /bar                                          * 1.0050000000E+00
Height of Packing /m                                               * 2.0440000000E+00
Type of Packing                                                    *TN350Y wall wipers
Configuration; Total Reflux, Stripping or Rectifying               *T
System; Water, Hexane/Toluene or Chloro/Ethyl-benzene              *CE
Cooling water flow /(dm3/min): with CV1 closed                     * 4.4000000000E+01
                               with CV1 open                       * 7.4000000000E+01
Initial Steam pressure /psia                                       * 6.1429310345E+00
Superheated; True or False                                         *F
Dryness fraction or degrees C of superheat                         * 1.0000000000E+00
Steam Condensate flow/(kg/min): with CV4 closed                    * 0.0000000000E+00
                                with CV4 open                      *-1.0000000000E+00
Approximate desired reflux ratio                                   * 1.0000000000E+00
Control parameters:  Cooling water flow / Reflux temp: Kc          * 6.0000000000E+00
                                                       Ti/sec      * 4.0000000000E+01
                                                       Td/sec      * 0.0000000000E+00
                                                  set point/deg C  * 0.0000000000E+00
                     Reflux flow / Reflux tank level : Kc          * 8.0000000000E-01
                                                       Ti/sec      * 4.0000000000E+01
                                                       Td/sec      * 0.0000000000E+00
                                                  set point/% full * 3.0000000000E+01
                  reflux ratio / feed valve position : Kc          *-3.0000000000E-01
                                                       Ti/sec      * 4.0000000000E+01
                                                       Td/sec      * 0.0000000000E+00
                                 initial set point / % open        * 0.0000000000E+00
          Steam condensate flow / Column Pressure drop: Kc         *-2.0000000000E+02
(units of     sec)                                     Ti/sec      * 6.0000000000E+01
                                                       Td/sec      * 0.0000000000E+00
                                                  set point/mBar   * 4.0000000000E+01
Skip setup of multiplexer inputs?                                  *Yes
      1099
      4 100.00  24.14  30.00   0.00   0.00 100.00  40.00  -0.01
  11.9  11.7  12.2  14.5  13.4  12.4  12.7  12.1  12.2  12.2  11.6  11.5
     21 100.00  13.94 30.00   0.00   0.00 100.00  40.00  -0.03
  12.9  12.7  13.3  15.7  14.5  13.5  13.8  13.2  13.2  13.3  12.6  12.4
     40 100.00   2.54  30.00  0.00   0.00 100.00  40.00  -0.01
  13.0  12.8  13.4  15.8  14.6  13.6  13.9  13.2  13.4  13.4  12.7  12.5
     60 100.00   0.00  30.00   0.00   0.00 100.00  40.00   0.03
  13.0  12.8  13.3  15.9  14.6  13.6  13.9  13.2  13.4  13.4  12.7  12.5
     80 100.00   0.00  30.00   0.00   0.00 100.00  40.00  -0.01
  13.0  12.8  13.4  16.0  14.7  13.6  13.9  13.3  13.5  13.4  12.8  12.5
    101 100.00   0.00  30.00   0.00   0.00 100.00  40.00   0.04
  13.1  12.8  13.4  16.0  14.7  13.6  13.9  13.4  13.5  13.4  12.8  12.4
```

```
  120 100.00   0.00  30.00   0.00   0.00 100.00  40.00   0.00
13.1  12.8  13.4  16.0  14.7  13.6  13.9  13.3  13.3  13.4  12.7  12.5
  140 100.00   0.00  30.00   0.00   0.00 100.00  40.00  -0.03
13.1  12.8  13.4  16.1  14.7  13.6  13.9  13.3  13.3  13.4  12.8  12.4
  160 100.00   0.00  30.00   0.00   0.00 100.00  40.00  -0.03
13.1  12.8  13.4  16.1  14.7  13.6  13.9  13.3  13.4  13.4  12.8  12.4
  181 100.00   0.00  30.00   0.00   0.00 100.00  40.00   0.01
13.0  12.8  13.3  16.0  14.6  13.6  13.9  13.3  13.3  13.4  12.8  12.4
  201 100.00   0.00  30.00   0.00   0.00 100.00  40.00  -0.04
13.0  12.8  13.3  16.0  14.6  13.5  13.9  13.2  13.4  13.4  12.7  12.4
  220 100.00   0.00  30.00   0.00   0.00 100.00  40.00  -0.01
13.1  12.8  13.2  15.9  14.5  13.5  13.8  13.1  13.2  13.4  12.8  12.4
  240 100.00   0.00  30.00   0.00   0.00 100.00  40.00   0.01
13.1  12.8  13.4  16.1  14.7  13.7  13.9  13.3  13.3  13.4  12.8  12.4
  260 100.00   0.00  30.00   0.00   0.00 100.00  40.00  -0.01
13.0  12.8  13.4  16.0  14.6  13.6  13.9  13.3  13.3  13.4  12.7  12.4
  281 100.00   0.00  30.00   0.00   0.00 100.00  40.00  -0.03
13.1  12.8  13.4  16.1  14.7  13.7  13.9  13.3  13.4  13.4  12.8  12.4
  300 100.00   0.00  30.00   0.00   0.00 100.00  40.00   0.00
13.0  12.8  13.4  16.0  14.6  13.7  13.9  13.4  13.3  13.4  12.7  12.4
  320 100.00   0.00  30.00   0.00   0.00 100.00  40.00  -0.01
13.0  12.8  13.2  15.9  14.6  13.6  13.7  13.3  13.2  13.4  12.8  12.4
  340 100.00   0.00  30.00   0.00   0.00 100.00  40.00   0.00
13.1  12.8  13.4  16.1  14.7  13.7  13.9  13.3  13.4  13.4  12.8  12.4
  361 100.00   0.00  30.00   0.00   0.00 100.00  40.00  -0.03
13.1  12.8  13.4  16.1  14.8  13.7  13.9  13.4  13.3  13.4  12.8  12.3
  380 100.00   0.00  30.00   0.00   0.00 100.00  40.00   0.01
13.0  12.8  13.2  15.9  14.5  13.4  13.7  13.1  13.2  13.4  12.7  12.2
  400 100.00   0.00  30.00   0.00   0.00 100.00  40.00  -0.03
13.0  12.8  13.2  15.8  14.6  13.6  13.7  13.3  13.1  13.4  12.8  12.2
  421 100.00   0.00  30.00   0.00   0.00 100.00  40.00   0.03
13.0  12.8  13.4  16.0  14.6  13.6  13.9  13.3  13.3  13.4  12.7  12.2
  440 100.00   0.00  30.00   0.00   0.00 100.00  40.00  -0.03
13.1  12.8  13.3  15.9  14.6  13.6  13.8  13.2  13.2  13.3  12.6  12.1
  461 100.00   0.00  30.00   0.00   0.00 100.00  40.00  -0.03
13.1  12.8  13.4  16.1  14.7  13.6  13.9  13.3  13.3  13.4  12.8  12.3
  481 100.00   0.00  30.00   0.00   0.00 100.00  40.00  -0.01
13.1  12.8  13.4  16.1  14.8  13.6  13.8  13.5  13.3  13.4  12.8  12.3
  500 100.00   0.00  30.00   0.00   0.00 100.00  40.00  -0.06
13.1  12.8  13.3  16.0  14.7  13.5  13.6  13.3  13.2  13.4  12.8  12.3
  520 100.00   0.00  30.00   0.00   0.00 100.00  40.00   0.00
13.1  12.8  13.4  16.2  14.7  13.7  13.8  13.4  13.3  13.4  12.8  12.3
  540 100.00   0.00  30.00   0.00   0.00 100.00  40.00  -0.06
13.0  12.8  13.2  16.0  14.4  13.5  13.7  13.3  13.1  13.4  12.7  12.2
  561 100.00   0.00  30.00   0.00   0.00 100.00  40.00   0.03
13.0  12.8  13.4  16.1  14.6  13.6  13.9  13.4  13.3  13.4  12.8  12.2
  580 100.00   0.00  30.00   0.00   0.00 100.00  40.00  -0.06
13.1  12.8  13.4  16.2  14.8  13.6  13.9  13.4  13.3  13.3  12.6  12.1
  600 100.00   0.00  30.00   0.00   0.00 100.00  40.00   0.01
13.1  12.8  13.4  16.2  14.8  13.7  13.9  13.5  13.3  13.4  12.8  12.3
  620 100.00   0.00  30.00   0.00   0.00 100.00  40.00   0.03
13.1  12.8  13.3  16.1  14.5  13.5  13.8  13.3  13.2  13.4  12.8  12.3
  640 100.00   0.00  30.00   0.00   0.00 100.00  40.00  -0.04
13.1  12.8  13.4  16.2  14.8  13.7  13.9  13.4  13.3  13.4  12.8  12.3
  661 100.00   0.00  30.00   0.00   0.00 100.00  40.00  -0.01
12.9  12.7  13.3  16.1  14.5  13.5  13.8  13.2  13.2  13.3  12.6  12.1
  680 100.00   0.00  30.00   0.00   0.00 100.00  40.00  -0.04
13.1  12.8  13.4  16.2  14.7  13.7  13.9  13.3  13.3  13.4  12.8  12.2
```

```
  700 100.00   0.00  30.00   0.00   0.00 100.00  40.00  -0.07
13.1  12.8  13.4  16.2  14.7  13.6  13.9  13.3  13.3  13.4  12.8  12.3
  721 100.00   0.00  30.00   0.00   0.00 100.00  40.00  -0.01
13.0  12.8  13.4  16.2  14.7  13.7  13.9  13.3  13.3  13.4  12.7  12.2
  740 100.00   0.00  30.00   0.00   0.00 100.00  40.00   0.00
13.1  12.8  13.4  16.2  14.7  13.6  13.9  13.3  13.3  13.4  12.8  12.2
  760 100.00   0.00  30.00   0.00   0.00 100.00  40.00  -0.06
13.1  12.8  13.4  16.2  14.8  13.6  13.9  13.3  13.3  13.4  12.8  12.1
  780 100.00   0.00  30.00   0.00   0.00 100.00  40.00  -0.04
13.1  12.8  13.3  16.1  14.6  13.5  13.8  13.2  13.2  13.4  12.8  12.1
  800 100.00   0.00  30.00   0.00   0.00 100.00  40.00  -0.04
12.9  12.7  13.3  16.1  14.5  13.5  13.8  13.2  13.2  13.3  12.6  12.0
  821 100.00   0.00  30.00   0.00   0.00 100.00  40.00  -0.03
12.9  12.7  13.3  16.1  14.6  13.6  13.8  13.3  13.2  13.3  12.7  12.0
  840 100.00   0.00  30.00   0.00   0.00 100.00  40.00  -0.04
13.0  12.7  13.4  16.2  14.8  13.8  13.9  13.3  13.3  13.4  12.8  12.1
  860 100.00   0.00  30.00   0.00   0.00 100.00  40.00  -0.03
13.1  12.8  13.3  16.1  14.5  13.5  13.8  13.1  13.2  13.4  12.8  12.1
  881 100.00   0.00  30.00   0.00   0.00 100.00  40.00  -0.01
13.1  12.8  13.4  16.2  14.7  13.7  13.9  13.3  13.3  13.3  12.6  11.9
  900 100.00   0.00  30.00   0.00   0.00 100.00  40.00  -0.01
12.9  12.7  13.3  16.1  14.6  13.7  13.8  13.3  13.3  13.4  12.7  12.0
  920 100.00   0.00  30.00   0.00   0.00 100.00  40.00  -0.04
13.0  12.8  13.4  16.1  14.7  13.6  13.9  13.3  13.3  13.4  12.7  12.0
  941 100.00   0.00  30.00   0.00   0.00 100.00  40.00  -0.03
13.1  12.8  13.4  16.2  14.7  13.7  13.9  13.3  13.3  13.4  12.7  12.1
  960 100.00   0.00  30.00   0.00   0.00 100.00  40.00  -0.04
13.1  12.8  13.4  16.2  14.7  13.8  13.9  13.3  13.3  13.3  12.7  12.1
  981 100.00   0.00  30.00   0.00   0.00 100.00  40.00  -0.03
13.1  12.8  13.3  16.1  14.6  13.6  13.8  13.2  13.2  13.4  12.8  12.1
 1000 100.00   0.00  30.00   0.00   0.00 100.00  40.00  -0.03
13.1  12.8  13.3  16.1  14.5  13.6  13.8  13.1  13.2  13.2  12.5  11.9
 1020 100.00   0.00  30.00   0.00   0.00 100.00  40.00  -0.03
13.0  12.8  13.4  16.2  14.6  13.6  13.9  13.3  13.3  13.4  12.6  12.1
 1040 100.00   0.00  30.00   0.00   0.00 100.00  40.00  -0.03
13.1  12.8  13.4  16.3  14.7  13.6  13.9  13.3  13.3  13.4  12.7  12.0
 1060 100.00   0.00  30.00   0.00   0.00 100.00  40.00   0.01
13.1  12.8  13.4  16.4  14.7  13.6  13.9  13.3  13.3  13.4  12.8  12.1
 1081 100.00   0.00  30.00   0.00   0.00 100.00  40.00   0.03
13.1  12.8  13.4  16.4  14.7  13.6  13.9  13.3  13.3  13.3  12.6  12.0
 1100 100.00   0.00  30.00   0.00   0.00 100.00  40.00  -0.03
13.0  12.8  13.4  16.3  14.7  13.6  13.9  13.2  13.3  13.3  79.8  12.9
 1120 100.00   0.00  30.00   0.00   0.00 100.00  40.00  -0.06
13.1  12.8  13.4  16.4  14.7  13.7  13.9  13.5  13.3  13.1 140.7  22.4
 1141 100.00   0.00  30.00   0.00   0.00 100.00  40.00  -0.04
13.0  12.7  13.4  16.4  14.7  13.8  13.9  13.5  13.3  13.3 152.3  20.9
 1160 100.00   0.00  30.00   0.00   0.00 100.00  40.00   0.16
13.0  12.8  13.4  16.3  14.6  42.8  13.9  13.5  13.3  13.3 152.6  22.8
 1180 100.00   0.00  30.00   0.00   0.00  84.42  40.00   3.82
13.0  12.8  13.4  16.3  14.7 103.6  13.9  46.9  13.3  13.2 152.7  24.0
 1200 100.00   0.00  30.00   0.00   0.00 100.00  40.00   5.07
13.0  12.8  13.3  16.3  14.6 121.5  13.7  97.2  13.1  13.2 151.6  22.5
 1221 100.00   0.00  30.00   0.00   0.00  98.22  40.00   9.44
13.0  12.8  13.4  16.3  14.8 127.5  28.2 114.9  13.3  13.2 149.5  22.2
 1241 100.00   0.00  30.00   0.00   0.00  72.69  40.00  13.58
13.0  12.8  13.4  16.3  14.6 131.3  66.1 125.6  13.3  13.2 151.9  25.2
 1261 100.00   0.00  30.00   0.00   0.00  83.25  40.00   4.09
12.9  12.7  13.3  16.2  14.6 133.7  90.5 132.0  13.1  13.1 149.7  65.6
```

```
 1281 100.00   0.00  30.00   0.00   0.00 100.00  40.00  -0.67
13.0  12.8  13.4  16.3  14.6 133.9  91.1 132.9  13.3  13.3 142.8  69.9
 1301 100.00   0.00  30.00   0.00   0.00 100.00  40.00   1.16
13.1  12.8  13.3  16.2  14.5 133.9  91.0 132.7  13.2  13.3 142.0  87.6
 1320 100.00   0.00  30.00   0.00   0.00  77.50  40.00   2.62
13.0  12.8  13.5  16.4  14.7 134.0  93.2 132.8  13.3  13.3 143.3 100.1
 1340 100.00   0.00  30.00   0.00   0.00 100.00  40.00   2.92
13.1  12.8  13.4  16.4  14.8 134.0  94.7 133.0  13.2  13.1 143.8 101.9
 1361 100.00   0.00  30.00   0.00   0.00 100.00  40.00   5.74
13.1  12.8  13.4  16.4  14.7 134.2  96.9 133.2  13.3  13.3 144.3 102.3
 1381 100.00   0.00  30.00   0.00   0.00 100.00  40.00   4.47
13.0  12.8  13.3  16.2  14.7 134.0  98.1 133.2  13.1  13.2 144.4 101.8
 1401 100.00   0.00  30.00   0.00   0.00  74.27  40.00   4.42
13.1  12.8  13.3  16.2  14.7 134.0  99.2 133.4  13.2  13.3 144.7 102.5
 1420 100.00   0.00  30.00   0.00   0.00 100.00  40.00   3.69
13.1  12.8  13.4  16.4  14.8 134.4 100.6 133.7  13.3  13.3 144.8 102.6
 1440 100.00   0.00  30.00   0.00   0.00 100.00  40.00   3.00
13.0  12.8  13.3  16.3  14.6 134.3 101.8 133.6  13.1  13.2 144.9 102.8
 1460 100.00   0.00  30.00   0.00   0.00  53.01  40.00   6.96
13.1  12.8  13.4  16.4  14.8 134.4 102.9 133.7  13.3  13.3 145.2 103.5
 1480 100.00   0.00  30.00   0.00   0.00 100.00  40.00   4.64
13.0  12.8  13.4  16.3  14.6 134.3 103.9 133.6  13.2  13.2 145.1 104.1
 1500 100.00   0.00  30.00   0.00   0.00 100.00  40.00   5.80
13.0  12.7  13.4  16.3  14.7 134.2 104.4 133.6  13.3  13.2 145.2 105.0
 1520 100.00   0.00  30.00   0.00   0.00 100.00  40.00   6.42
13.0  12.8  13.4  16.4  14.8 134.3 105.8 133.8  13.2  13.2 145.3 105.8
 1540 100.00   0.00  30.00   0.00   0.00 100.00  40.00   5.27
13.0  12.8  13.4  16.4  14.8 134.3 106.4 133.8  13.3  13.2 145.3 106.5
 1560 100.00   0.00  30.00   0.00   0.00 100.00  40.00   6.24
13.0  12.8  13.4  16.4  14.8 134.3 107.1 133.8  13.3  13.2 145.5 107.4
 1581 100.00   0.00  30.00   0.00   0.00 100.00  40.00   6.83
13.1  12.8  13.4  16.5  14.8 134.4 107.5 134.0  13.3  13.3 145.5 108.4
 1600 100.00   0.00  30.00   0.00   0.00 100.00  40.00   8.79
13.0  12.8  13.5  16.5  14.8 134.3 107.6 133.8  13.2  13.2 145.4 109.0
 1621 100.00   0.00  30.00   0.00   0.00 100.00  40.00   7.43
13.1  12.9  13.5  16.5  14.8 134.4 108.3 133.9  13.3  13.3 145.5 109.9
 1640 100.00   0.00  30.00   0.00   0.00 100.00  40.00   6.40
13.2  12.8  13.5  16.5  14.8 134.4 108.9 134.1  13.3  13.3 145.5 110.7
 1660 100.00   0.00  30.00   1.42   0.00 100.00  40.00   8.00
13.1  12.8  13.4  16.5  14.8 134.3 109.1 134.0  13.3  13.2 145.4 111.0
 1680 100.00   0.00  30.00   0.00   0.00 100.00  40.00   5.04
13.1  12.8  13.5  16.5  14.8 134.4 109.8 134.0  13.3  13.3 145.7 111.6
 1701 100.00   0.00  30.00   0.00   0.00 100.00  40.00   6.97
13.1  12.8  13.3  16.3  14.6 134.2 109.7 133.8  13.1  13.2 145.6 112.2
 1720 100.00   0.00  30.00   0.00   0.00 100.00  40.00   8.15
13.0  12.9  13.5  16.5  14.8 134.5 110.1 134.0  13.3  13.1 145.4 112.4
 1740 100.00   0.00  30.00   0.00   0.00  41.91  40.00   8.69
13.1  12.7  13.6  16.5  15.2 134.6 110.6 134.1  13.3  13.3 145.7 113.2
 1760 100.00   0.00  30.00   0.00   0.00 100.00  40.00   6.55
13.1  12.8  13.5  16.5  15.7 134.5 110.8 134.1  13.3  13.3 145.7 113.7
 1780 100.00   0.00  30.00   0.00   0.00 100.00  40.00   5.58
13.1  12.8  13.5  16.5  16.9 134.6 111.1 134.1  13.3  13.3 145.7 114.2
 1801 100.00   0.00  30.00   0.00   0.00  44.25  40.00   7.75
13.0  12.9  13.5  16.5  72.3 134.5 110.8 133.9  13.3  13.2 145.7 114.7
 1821 100.00   0.00  30.00   0.00   0.00 100.00  40.00   7.08
13.2  13.0  13.4  16.4 125.3 134.4 111.4 133.9  13.2  13.3 145.9 114.9
 1840 100.00   0.00  30.00   0.00   0.00 100.00  40.00   6.86
13.1  12.8  13.6  16.5 131.5 134.6 111.8 134.1  13.3  13.3 145.9 115.1
```

```
 1860 100.00   0.00  30.00   0.00   0.00 100.00  40.00   5.93
13.0  12.7  13.4  16.4 131.2 134.3 111.5 133.8  13.2  13.1 145.6 115.2
 1880 100.00   0.00  30.00   0.00   0.00 100.00  40.00   5.96
13.0  12.8  13.5  16.5 131.5 134.5 111.7 134.0  13.3  13.2 145.8 115.6
 1900 100.00   0.00  30.00   0.00   0.00 100.00  40.00   5.48
13.1  12.9  13.6  16.5 132.4 134.6 112.4 134.1  13.3  13.3 145.9 116.0
 1920 100.00   0.00  30.00   0.00   0.00 100.00  40.00   6.29
13.2  13.0  13.4  16.3 132.8 134.3 112.4 133.8  13.1  13.2 145.9 115.9
 1941 100.00   0.00  30.00   0.00   0.00  67.88  40.00   5.11
13.1  12.9  13.3  16.3 132.9 134.3 112.2 133.8  13.1  13.2 146.0 116.0
 1960 100.00   0.00  30.00   0.00   0.00 100.00  40.00   4.22
13.1  13.4  13.7  16.5 133.4 134.6 113.0 134.1  13.5  13.3 146.1 116.2
 1980 100.00   0.00  30.00   0.00   0.00  75.25  40.00  13.22
13.0  14.4  14.2  16.5 133.4 134.6 113.2 134.0  13.5  13.2 150.6 119.1
 2000 100.00   0.00  30.00   0.00   0.00 100.00  40.00   9.71
13.2  17.5  14.8  16.5 133.9 135.1 115.7 134.7  13.6  13.3 154.5 122.0
 2020 100.00  21.13  30.00  31.65   0.00 100.00  40.00   6.59
13.1  20.0  15.0  16.5 134.1 135.1 117.8 134.8  13.6  13.4 154.5 122.1
 2041 100.00  48.09  30.00  55.48   0.00 100.00  40.00   3.90
12.9  22.2  33.6  16.3 133.4 134.8 119.3 134.4  18.0  13.1 154.2 120.6
 2061 100.00  78.01  30.00  74.90   0.00 100.00  40.00   5.44
13.0  24.4  49.7  20.0 133.0 134.9 119.4 134.6  30.7  13.3 154.3 125.2
 2081 100.00  76.48  30.00  56.31   0.00 100.00  40.00   7.34
13.2  25.6  61.4  30.7 133.0 135.3 120.3 134.9  41.1  13.4 154.4 129.7
 2100 100.00  70.24  30.00  39.90   0.00 100.00  40.00  10.77
13.0  25.2  68.8  41.2 133.0 135.2 123.4 134.8  52.2  13.4 154.1 138.2
 2121 100.00  52.19  30.00  18.51   0.00  87.27  40.00  16.69
13.0  25.2  73.1  53.0 133.1 135.2 128.0 134.9  62.3  13.3 154.0 142.3
 2141 100.00  43.37  30.00  15.58   0.00 100.00  40.00  21.58
13.2  25.6  76.1  61.1 133.3 135.7 129.0 135.2  68.3  13.4 153.9 145.2
 2160 100.00  44.74  30.00  22.93   0.00 100.00  40.00  23.05
13.1  26.5  78.2  64.3 133.2 135.6 128.8 135.3  70.9  13.3 153.7 145.7
 2181 100.00  59.35  30.00  41.49   0.00 100.00  40.00  21.35
13.2  28.1  80.8  67.6 133.5 135.8 127.9 135.5  74.2  13.4 153.6 145.6
 2201 100.00  73.01  30.00  48.03   0.00 100.00  40.00  20.09
13.1  29.4  83.0  71.4 133.3 135.7 126.4 135.4  77.7  13.3 153.4 145.3
 2220 100.00  86.62  30.00  54.43   0.00  97.45  40.00  21.88
13.4  30.7  85.1  76.1 133.5 135.9 126.5 135.6  81.0  13.4 153.6 145.0
 2240 100.00  91.17  30.00  50.70   0.00  99.16  40.00  25.77
13.3  31.3  86.5  80.3 133.5 136.0 125.9 135.7  84.0  13.4 153.4 145.4
 2260 100.00  83.07  30.00  35.53   0.00  93.06  40.00  29.32
13.4  31.7  87.9  83.3 133.4 136.3 126.0 136.0  86.2  13.4 153.4 145.4
 2281 100.00  78.97  30.00  29.79   0.00 100.00  40.00  31.47
13.3  32.3  88.6  85.2 133.3 136.4 126.1 136.0  87.7  13.4 153.2 145.3
 2300 100.00  75.62  30.00  26.79   0.00 100.00  40.00  31.96
13.3  33.0  89.2  86.6 133.5 136.4 126.0 136.2  88.9  13.4 153.2 145.8
 2320 100.00  75.38  30.00  27.11   0.00 100.00  40.00  31.79
13.6  33.6  89.9  87.9 133.6 136.5 126.0 136.3  90.0  13.4 153.3 146.1
 2341 100.00  79.04  30.00  31.67   0.00 100.00  40.00  32.07
13.6  34.4  90.4  88.9 133.6 136.5 126.0 136.3  90.7  13.4 153.4 146.1
 2360 100.00  78.96  30.00  30.67   0.00 100.00  40.00  31.75
13.6  35.6  90.8  89.6 133.6 136.5 126.0 136.3  91.4  13.6 153.4 146.4
 2380 100.00  82.41  30.00  33.24   0.00 100.00  40.00  31.74
13.7  36.2  91.2  90.3 133.6 136.6 126.0 136.3  91.9  13.5 153.5 146.4
 2400 100.00  83.09  30.00  31.79   0.00  99.42  40.00  32.31
13.7  36.3  91.6  91.0 133.6 136.6 126.0 136.4  92.3  13.6 153.5 146.6
 2420 100.00  87.54  30.00  36.39   0.00 100.00  40.00  33.01
13.7  36.7  92.1  91.3 133.5 136.5 125.9 136.4  92.7  13.6 153.4 146.6
```

```
 2441 100.00  85.57  30.00  32.94   0.00 100.00  40.00  33.92
13.9  37.6  92.8  91.9 133.6 136.6 126.0 136.5  93.3  13.6 153.5 147.1
 2460 100.00  80.39  30.00  26.64   0.00 100.00  40.00  34.27
13.8  37.9  93.0  92.4 133.4 136.5 125.9 136.3  93.7  13.5 153.3 146.9
 2480 100.00  82.01  30.00  28.52   0.00  98.03  40.00  34.95
13.9  37.7  93.4  92.8 133.6 136.8 126.0 136.7  94.3  13.6 153.5 147.0
 2500 100.00  81.11  30.00  27.91   0.00  92.59  40.00  36.15
13.8  37.9  93.5  93.1 133.3 136.6 125.8 136.5  94.5  13.5 153.2 147.2
 2520 100.00  83.05  30.00  30.55   0.00 100.00  40.00  36.89
14.0  38.0  93.9  93.5 133.3 136.9 126.1 136.6  94.9  13.5 153.3 147.4
 2540 100.00  79.60  30.00  26.11   0.00 100.00  40.00  37.23
14.1  38.2  94.1  94.0 133.4 137.0 126.1 136.7  95.4  13.6 153.5 147.7
 2561 100.00  82.38  30.00  29.57   0.00  97.86  40.00  37.57
14.2  38.4  94.2  94.2 133.3 136.9 126.1 136.7  95.5  13.7 153.5 147.7
 2580 100.00  90.75  30.00  39.00   0.00 100.00  40.00  37.58
14.2  38.7  94.4  94.5 133.5 137.2 126.2 136.9  95.7  13.8 153.7 147.8
 2600 100.00  85.85  30.00  32.55   0.00 100.00  40.00  37.86
14.2  38.5  94.2  94.5 133.2 137.0 126.0 136.6  95.7  13.7 153.4 147.6
 2620 100.00  81.65  30.00  27.72   0.00  97.30  40.00  38.23
14.4  38.8  94.5  94.8 133.4 137.1 126.1 136.8  96.0  13.7 153.5 147.9
 2640 100.00  85.31  30.00  32.87   0.00  98.94  40.00  38.49
14.3  39.2  94.5  94.7 133.2 137.1 126.0 136.7  95.9  13.7 153.5 147.9
 2661 100.00  83.56  30.00  29.62   0.00  98.22  40.00  38.56
14.6  39.3  94.8  95.0 133.4 137.4 126.2 137.0  96.3  13.8 153.7 148.2
 2682 100.00  81.29  30.00  28.40   0.00 100.00  40.00  38.78
14.5  39.1  94.8  95.1 133.2 137.2 126.1 136.9  96.3  13.8 153.5 148.1
 2701 100.00  82.71  30.00  29.89   0.00  98.17  40.00  38.20
14.6  39.2  94.8  95.1 133.3 137.1 126.1 136.8  96.5  13.7 153.5 148.0
 2720 100.00  82.29  30.00  28.99   0.00 100.00  40.00  38.12
14.6  39.6  94.9  95.2 133.3 137.1 126.0 136.8  96.4  13.8 153.4 148.1
 2740 100.00  81.22  30.00  27.69   0.00  99.75  40.00  38.07
14.7  40.0  94.9  95.4 133.2 137.0 126.0 136.8  96.6  13.8 153.4 148.1
 2760 100.00  82.31  30.00  28.74   0.00 100.00  40.00  38.07
14.8  40.3  95.2  95.5 133.4 137.1 126.1 136.9  96.7  13.9 153.5 148.4
 2780 100.00  82.20  30.00  28.96   0.00 100.00  40.00  37.64
14.9  40.0  95.3  95.7 133.4 137.2 126.1 137.0  96.9  14.0 153.7 148.3
 2800 100.00  82.07  30.00  28.28   0.00 100.00  40.00  37.52
15.0  40.1  95.4  95.7 133.4 137.3 126.0 136.9  96.9  13.9 153.6 148.4
 2820 100.00  82.22  30.00  28.64   0.00 100.00  40.00  36.66
15.1  40.1  95.5  95.9 133.4 137.2 126.0 137.0  97.1  14.0 153.5 148.9
 2840 100.00  83.94  30.00  30.38   0.00  99.83  40.00  36.81
15.0  40.0  95.5  95.8 133.4 137.1 125.9 136.8  97.0  14.1 153.4 148.9
 2860 100.00  84.62  30.00  29.55   0.00  92.49  40.00  37.52
15.1  40.4  95.5  95.9 133.3 137.0 125.8 136.8  97.1  14.0 153.3 149.2
 2880 100.00  83.74  30.00  28.96   0.00 100.00  40.00  37.88
15.3  40.1  95.8  96.1 133.4 137.4 126.0 136.9  97.3  14.1 153.5 149.4
 2900 100.00  82.54  30.00  26.91   0.00  98.52  40.00  37.54
15.3  40.7  95.8  96.2 133.5 137.2 126.0 137.0  97.4  14.1 153.5 149.6
 2921 100.00  81.80  30.00  27.94   0.00 100.00  40.00  37.52
15.2  40.4  95.7  96.1 133.2 137.0 125.8 136.8  97.3  14.1 153.4 149.5
 2940 100.00  79.15  30.00  24.76   0.00 100.00  40.00  37.47
15.4  40.9  95.9  96.2 133.3 137.1 125.9 136.9  97.5  14.1 153.5 149.4
 2960 100.00  86.64  30.00  33.97   0.00 100.00  40.00  37.48
15.5  40.8  96.0  96.3 133.4 137.2 125.9 136.9  97.5  14.2 153.4 149.5
 2980 100.00  84.54  30.00  31.97   0.00 100.00  40.00  37.47
15.6  40.8  96.0  96.4 133.2 137.2 125.8 136.8  97.6  14.2 153.3 149.4
 3000 100.00  80.81  30.00  27.45   0.00  99.39  40.00  37.05
15.6  41.1  96.0  96.4 133.2 137.0 125.8 136.8  97.6  14.1 153.4 149.4
```

```
 3021 100.00  81.92  30.00  28.52   0.00 100.00  40.00  37.32
15.8  41.1  96.0  96.4 133.3 137.0 125.8 136.8  97.6  14.1 153.4 149.4
 3040 100.00  85.67  30.00  33.87   0.00  99.65  40.00  37.14
15.9  41.3  96.1  96.5 133.4 137.1 125.9 136.9  97.7  14.2 153.6 149.7
 3060 100.00  82.39  30.00  28.18   0.00 100.00  40.00  37.55
16.1  41.2  96.0  96.5 133.3 137.1 125.8 136.9  97.6  14.5 153.7 149.6
 3081 100.00  83.43  30.00  29.69   0.00  98.87  40.00  37.89
16.3  41.4  96.0  96.6 133.4 137.4 125.9 137.0  97.8  14.5 153.7 149.8
 3102 100.00  80.59  30.00  26.62   0.00  94.33  40.00  38.40
16.1  41.7  96.0  96.6 133.5 137.3 126.0 137.0  97.8  14.4 153.6 149.7
 3120 100.00  86.58  30.00  35.02   0.00 100.00  40.00  38.02
16.1  41.7  95.8  96.4 133.3 137.1 125.8 136.8  97.6  14.3 153.4 149.4
 3140 100.00  79.44  30.00  26.67   0.00 100.00  40.00  38.14
16.3  41.6  95.8  96.4 133.3 137.1 125.8 136.8  97.6  14.3 153.4 149.5
 3160 100.00  87.87  30.00  35.34   0.00 100.00  40.00  37.88
16.4  41.8  95.9  96.5 133.5 137.2 125.9 136.9  97.7  14.4 153.5 149.4
 3180 100.00  87.76  30.00  33.55   0.00  99.95  40.00  38.27
16.4  41.6  96.0  96.6 133.3 137.1 125.8 136.8  97.6  14.5 153.4 149.2
 3200 100.00  90.46  30.00  36.80   0.00  97.80  40.00  38.58
16.5  42.1  96.1  96.6 133.3 137.2 125.9 136.9  97.7  14.6 153.5 149.1
 3220 100.00  93.08  30.00  39.88   0.00 100.00  40.00  38.45
16.6  42.0  96.0  96.6 133.3 137.3 125.8 136.8  97.6  14.5 153.4 149.0
 3240 100.00  82.46  30.00  26.15   0.00  99.81  40.00  38.81
16.8  41.8  96.2  96.7 133.5 137.4 125.9 136.9  97.9  14.6 153.5 149.1
 3260 100.00  92.06  30.00  39.22   0.00 100.00  40.00  38.59
17.0  41.9  96.5  96.8 133.5 137.4 126.0 137.0  98.0  14.6 153.7 149.2
 3281 100.00  82.60  30.00  27.52   0.00  99.51  40.00  38.26
17.0  42.4  96.4  96.9 133.4 137.2 125.9 136.9  98.1  14.6 153.5 149.3
 3300 100.00  79.97  30.00  25.71   0.00  98.97  40.00  37.73
17.1  42.3  96.5  96.9 133.6 137.4 126.0 137.0  98.2  14.8 153.7 149.6
 3320 100.00  81.87  30.00  29.30   0.00 100.00  40.00  36.62
17.0  42.0  96.3  96.8 133.3 137.0 125.6 136.8  98.1  14.7 153.4 149.2
 3340 100.00  80.83  30.00  28.13   0.00 100.00  40.00  35.97
17.2  42.4  96.4  97.0 133.5 137.0 125.8 136.9  98.2  14.7 153.4 149.5
 3360 100.00  92.27  30.00  40.63   0.00 100.00  40.00  36.34
17.4  42.4  96.5  97.1 133.6 137.2 125.8 137.0  98.3  14.8 153.5 149.4
 3381 100.00  78.85  30.00  25.05   0.00 100.00  40.00  36.86
17.4  43.1  96.6  97.0 133.5 137.1 125.8 136.9  98.2  14.8 153.5 149.5
 3401 100.00  81.50  30.00  32.28   0.00 100.00  40.00  36.63
17.4  42.7  96.7  97.1 133.6 137.4 125.8 137.0  98.3  15.0 153.7 149.6
 3420 100.00  82.78  30.00  32.87   0.00 100.00  40.00  35.63
17.6  42.8  96.7  97.1 133.6 137.2 125.8 137.0  98.5  15.0 153.7 149.4
 3441 100.00  82.42  30.00  29.35   0.00  99.97  40.00  36.53
17.6  43.2  96.7  97.3 133.6 137.2 125.8 136.9  98.5  15.0 153.7 149.4
 3461 100.00  83.77  30.00  31.28   0.00  93.18  40.00  37.27
17.7  43.0  96.6  97.2 133.5 137.1 125.8 136.9  98.4  14.9 153.6 149.5
 3480 100.00  82.65  30.00  29.13   0.00 100.00  40.00  36.95
17.8  43.0  96.7  97.3 133.6 137.3 125.8 137.0  98.3  15.0 153.7 149.6
 3500 100.00  81.40  30.00  26.42   0.00 100.00  40.00  36.98
17.9  43.2  96.6  97.2 133.5 137.2 125.8 136.9  98.4  14.9 153.5 149.4
 3521 100.00  84.42  30.00  32.41   0.00  99.03  40.00  36.98
17.9  43.0  96.5  97.1 133.4 137.2 125.7 136.8  98.3  15.0 153.5 149.4
 3540 100.00  82.62  30.00  27.30   0.00 100.00  40.00  36.72
18.1  43.0  96.6  97.2 133.5 137.2 125.7 136.9  98.4  15.1 153.5 149.5
 3560 100.00  83.41  30.00  28.99   0.00 100.00  40.00  37.08
18.1  43.6  96.9  97.3 133.6 137.4 125.8 137.0  98.5  15.1 153.7 149.6
 3580 100.00  83.80  30.00  30.48   0.00 100.00  40.00  37.23
18.2  43.3  96.8  97.2 133.5 137.2 125.7 136.9  98.4  15.1 153.5 149.5
```

```
 3600 100.00  87.09  30.00  38.19   0.00  92.80  40.00  37.83
18.4  43.9  96.9  97.4 133.6 137.4 125.8 137.0  98.7  15.1 153.7 149.6
 3620 100.00  83.45  30.00  28.60   0.00  98.26  40.00  38.02
18.5  44.0  96.8  97.4 133.5 137.2 125.7 137.0  98.5  15.1 153.7 149.5
 3640 100.00  84.55  30.00  31.18   0.00  98.02  40.00  37.98
18.7  44.2  96.7  97.3 133.4 137.2 125.7 137.0  98.6  15.1 153.7 149.3
 3660 100.00  86.25  30.00  35.19   0.00  98.27  40.00  38.33
18.7  44.2  96.9  97.4 133.5 137.2 125.7 137.0  98.6  15.2 153.7 149.1
 3680 100.00  85.33  30.00  32.38   0.00 100.00  40.00  37.73
18.9  44.0  96.8  97.4 133.5 137.2 125.7 137.0  98.6  15.2 153.7 149.1
```

CW3T12AA.DP4

This is an example of the input file for the data processing programme. These files have the suffix .DPI. If more than one pressure drop setting has been done under the same run code, one of these files is needed for each one. The I in the suffix is then replaced by a digit 1 to 0. The .DPI files must be created manually to give the data processing programme the information which was recorded by hand, namely the average flows and compositions during the run. The times at the beginning of the file are the number of seconds from the time the control programme was started, so it is important to record this time. The data is normally averaged over a period of about 20 minutes (1200 seconds) before the samples were taken.

```
10200                    {seconds to beginning of average}
11400                    {seconds to end of average}
14.6                     {reflux rotameter scale reading}
0.0                      {feed rotameter scale reading}
72.0                     {cooling water rotameter reading}
2.334                    {steam flow in kg/min}
0.5                      {column pressure drop with no flow}
0.387396                 {reflux (at pump) sample}
-2                       {-2 indicates use this compn for NTP}
-1                       {Top Vapour}
-1                       {reflux into distributor}
-1                       {bottom vapour}
0.381287
-2                       {liquid under packing}
0.380945                 {liquid from column bottom}
-1                       {use for ntp calculation}
-1                       {bottom tank}
```

W350.PK

This file is an example of the packing information file needed by the data processing programme. The values in it are measured ones, rather than the nominal ones given by the packing vendors. It should be constructed manually in this format with the Turbo Pascal editor.

```
45          {packing angle with horizontal, degrees}
0.969       {void fraction}
345         {area per unit volume, m2/m3}
2.044       {packed height, m}
0.101       {element height, m}
```

RC-CW3.IN

This file is used if more than one run is to be processed by the data processing programme. It must begin with the prefix RC- and have the suffix .IN and it contains a list of the run codes to be processed. If the input file name ends in .DPI, then just the run code is given, but if it ends in .DPx, where x is a single digit, then the suffix -x is added to the run code. It must be constructed manually, normally from within the Turbo Pascal Editor.

```
cw3t09aa-1
cw3t09aa-2
cw3t09aa-3
cw3t09aa-4
cw3t12aa-1
cw3t12aa-2
cw3t12aa-3
cw3t12aa-4
cw3t12aa-5
cw3t13aa-1
cw3t13aa-2
cw3t13aa-3
cw3t13aa-4
cw3t13aa-5
cw3t16aa-1
cw3t16aa-2•
```

CW3T12AA.OU4

This file is produced by the data processing programme. For each .DPx file, a corresponding .OUx file is produced. It gives the flows, compositions, temperatures and pressure drop, together with the efficiency of the packing, the heat balance over the rig and various dimensionless groups for the run.

```
Run Code                                cw3t12aa
Rotameter scale readings: Reflux     14.600 cm Feed      0.000 cm
Cooling water flow reading  72.000 dm3/min, Corrected flow  69.546 dm3/min
Steam flow                          2.334 kg/min
Column pressure drop,zero flow      0.500 mBar, dp cell reading   1099
Density meter time period readings:
Reflux at pump              0.387396
Average time period    0.387396 Composition          0.7197
Liquid under Packing        0.381287
Average time period    0.381287 Composition          0.4517
Liquid from column bottom   0.380945
Average time period    0.380945 Composition          0.4361
Average of      60 points from   10200 seconds to   11400 seconds from start
                              Average                 min     max     stdev
Control valve 1 (cooling water) 100.00 percent open 100.00 100.00    0.00
Control valve 2 (reflux)         60.53 percent open  58.05  63.00    0.95
Reflux tank level set point      30.00 percent       30.00  30.00    0.00
Reflux tank level                30.28 percent       28.01  34.19    1.59
Control valve 3 (feed)            0.00 percent open   0.00   0.00    0.00
Control valve 4 (condensate)     33.60 percent open  26.33  39.77    3.24
Column pressure drop set point    5.00 mBar           5.00   5.00    0.00
Average column pressure drop      5.01 mBar           4.89   5.17    0.06
Corrected column pressure drop    4.60 mBar
Column pressure gradient    2.25 mBar/m
 T1  Cooling water in             31.6 Degrees C      31.4   31.8     0.1
 T2  Cooling water out            50.8 Degrees C      50.4   51.4     0.2
 T3  Reflux drum                 102.2 Degrees C     101.6  102.5     0.2
 T4  Reflux - distributor        102.9 Degrees C     102.4  103.2     0.2
 T5  Vapour - column top         133.2 Degrees C     133.1  133.4     0.1
 T6  Vapour - column base        135.3 Degrees C     135.1  135.5     0.1
 T7  Bottom tank                 119.3 Degrees C     118.8  119.8     0.3
 T8  Bottom of column            135.0 Degrees C     134.8  135.3     0.1
 T9  Reflux rotameter            104.4 Degrees C     104.0  104.8     0.2
 T10 Feed rotameter               18.9 Degrees C      18.8   19.2     0.1
 T11 Steam in                    154.6 Degrees C     154.4  154.9     0.1
 T12 Steam condensate out        131.3 Degrees C     130.5  132.3     0.4
 Steam 154.6  C  63.49 psig= 5.383 bar a Sat. press  63.49 psig= 5.383 bar a
 Saturated - dryness fraction:  1.000 Enthalpy in   2752.11 kJ/kg
 Condensate temperature  131.3 C
 Assuming Steam Condensate at Bottom Column Temperature   135.0 C
 Enthalpy out   567.76 kJ/kg  Steam Flow   2.33 kg/min  Heat in    84.97 kW
 Cooling Water Tin 31.6 C Tout 50.8 C Hin  132.41 kJ/kg, Hout 212.62 kJ/kg
 Flow   69.78 dm3/min=   69.44 kg/min  Heat removed    92.83 kW
 Heat loss   -7.86 kW=  -9.25 %heat in
Heat carried by vapour flow at top    79.8674 kW, loss=   6.01%
>> Top column properties
Relative molecular mass, Mr   110.8
Vapour Density  3.411 kg/m3, Viscosity 0.00972 cP, Diffusivity 5.131E-06 m2/s
```

```
Liquid Density  910.6 kg/m3, Viscosity 0.26132 cP, Diffusivity 6.209E-09 m2/s
** Bottom column properties
Relative molecular mass, Mr   109.1
Vapour Density  3.438 kg/m3, Viscosity 0.00937 cP, Diffusivity 5.176E-06 m2/s
Liquid Density  849.1 kg/m3, Viscosity 0.24835 cP, Diffusivity 6.717E-09 m2/s
** Reflux flow  13.849 dm3/min =   0.001965 kmol/sec
     Corrected for subcooling   0.002202 kmol/sec
Feed flow      0.000 dm3/min =   0.000000 kmol/sec
>> Flows at top of column, based on rotameter readings
Vapour flow  0.002202 kmol/s  0.2439 kg/s  0.0281 kmol/m2s    3.11 kg/m2s
Superficial velocity     0.91 m/s, actual velocity     1.33 m/s
F factor   1.684 m/s*sqrt(kg/m3), Cs 0.05590 m/s
Liquid flow  0.002202 kmol/s  0.2439 kg/s  0.0281 kmol/m2s    3.11 kg/m2s
Peripheral flow  7.07E-04 kg/m/s, velocity  0.0285 m/s
>> Dimensionless groups at top of column, based on rotameter readings
Vapour Reynolds Numbers: superficial   3708.0 effective   5527.7
Vapour Schmidt Number   0.5556
Vapour Sherwood Number /kv ie (deq/Dv)      2259.5 s/m or     73385.1 s m2/kmol
Liquid effective Reynolds Number:        138.0
Estimated kv (Bravo et al)  1.9417072857E-02
Estimated kl  1.9128431553E-03
** Flows at bottom of column, based on rotameter readings
Vapour flow  0.002202 kmol/s  0.2401 kg/s  0.0281 kmol/m2s    3.06 kg/m2s
Superficial velocity     0.89 m/s, actual velocity     1.30 m/s
F factor   1.651 m/s*sqrt(kg/m3), Cs 0.05678 m/s
Liquid flow  0.002202 kmol/s  0.2401 kg/s  0.0281 kmol/m2s    3.06 kg/m2s
Peripheral flow  6.96E-04 kg/m/s, velocity  0.0294 m/s
** Dimensionless groups at bottom of column, based on rotameter readings
Vapour Reynolds Numbers: superficial   3787.2 effective   5652.2
Vapour Schmidt Number   0.5266
Vapour Sherwood Number /kv ie (deq/Dv)      2239.9 s/m or     71047.0 s m2/kmol
Liquid effective Reynolds Number:        142.9
Estimated kv (Bravo et al)  1.9590255863E-02
Estimated kl  2.0444098535E-03
Reflux ratio                          1.0000
** Flows at top of column, based on heat input
Vapour flow  0.002355 kmol/s  0.2609 kg/s  0.0300 kmol/m2s    3.33 kg/m2s
Superficial velocity     0.98 m/s, actual velocity     1.42 m/s
F factor   1.801 m/s*sqrt(kg/m3), Cs 0.05980 m/s
Liquid flow  0.002355 kmol/s  0.2609 kg/s  0.0300 kmol/m2s    3.33 kg/m2s
Peripheral flow  7.56E-04 kg/m/s, velocity  0.0298 m/s
** Dimensionless groups at top of column, based on rotameter readings
Vapour Reynolds Numbers: superficial   3966.4 effective   5910.1
Vapour Schmidt Number   0.5556
Vapour Sherwood Number /kv ie (deq/Dv)      2259.5 s/m or     73385.1 s m2/kmol
Liquid effective Reynolds Number:        147.6
Estimated kv (Bravo et al)  2.0484420977E-02
Estimated kl  1.9783606707E-03
** Flows at bottom of column, based on heat input
Vapour flow  0.002355 kmol/s  0.2568 kg/s  0.0300 kmol/m2s    3.27 kg/m2s
Superficial velocity     0.95 m/s, actual velocity     1.39 m/s
F factor   1.766 m/s*sqrt(kg/m3), Cs 0.06073 m/s
Liquid flow  0.002355 kmol/s  0.2568 kg/s  0.0300 kmol/m2s    3.27 kg/m2s
Peripheral flow  7.44E-04 kg/m/s, velocity  0.0307 m/s
** Dimensionless groups at bottom of column, based on heat input
Vapour Reynolds Numbers: superficial   4051.1 effective   6043.1
Vapour Schmidt Number   0.5266
Vapour Sherwood Number /kv ie (deq/Dv)      2239.9 s/m or     71047.0 s m2/kmol
```

```
Liquid effective Reynolds Number:        152.9
Estimated kv (Bravo et al)  2.0666709273E-02
Estimated kl  2.1144337097E-03
Reflux ratio                          1.0000
** Compositions: under packing 0.4517 Column bottom 0.4361 Column top 0.7197
>> With alpha=1.126, Reflux Ratio from Rotameter flows:
** To bottom of column sample
NTP  10.11, NTP per m (NTSM)  4.95 HETP= 0.2021m ,From Hov HETP= 0.2019m
Overall vapour phase transfer units: Number, NTUov 10.22 Height, Hov 0.1999m
Overall liquid phase transfer units: Number, NTUol 10.03 Height, Hol 0.2039m
Average slope of equilibrium line, m      0.9806 lambda = mV/L     0.9806
Kv*a     0.1404 kmol/m3/s Kl*a     0.1377 kmol/m3/s
>> To sample under packing
NTP   9.58, NTP per m (NTSM)  4.69 HETP= 0.2133m ,From Hov HETP= 0.2131m
Overall vapour phase transfer units: Number, NTUov  9.69 Height, Hov 0.2108m
Overall liquid phase transfer units: Number, NTUol  9.49 Height, Hol 0.2154m
Average slope of equilibrium line, m      0.9788 lambda = mV/L     0.9788
Kv*a     0.1331 kmol/m3/s Kl*a     0.1303 kmol/m3/s
Number of extra plates from packing to column bottom  0.53
```

W350.DAT

This summary file is produced by the data processing programme if several runs are processed together. It contains the following summary information for each run: F factor, column pressure drop, standard deviation in pressure drop, pressure gradient, standard deviation in pressure gradient,.number of theoretical plates, number of theoretical plates per metre, HETP, pressure drop per theoretical plate.

```
cw3t09aa 2.34 29.55 0.58 14.46 0.28 10.43 5.10 0.196  2.83
cw3t09aa 1.70  7.61 0.36  3.73 0.18  9.98 4.88 0.205  0.76
cw3t09aa 0.90  1.36 0.24  0.67 0.12  9.98 4.88 0.205  0.14
cw3t09aa 2.36 34.51 0.74 16.88 0.36 10.71 5.24 0.191  3.22
cw3t12aa 2.33 36.94 0.72 18.07 0.35 11.00 5.38 0.186  3.36
cw3t12aa 2.19 19.61 0.23  9.59 0.11 10.02 4.90 0.204  1.96
cw3t12aa 2.09 11.55 0.19  5.65 0.09 10.34 5.06 0.198  1.12
cw3t12aa 1.68  4.60 0.06  2.25 0.03  9.58 4.69 0.213  0.48
cw3t12aa 0.56  0.40 0.04  0.20 0.02  9.91 4.85 0.206  0.04
cw3t13aa 2.28 24.59 0.19 12.03 0.09 10.38 5.08 0.197  2.37
cw3t13aa 1.42  3.59 0.05  1.76 0.02  9.58 4.69 0.213  0.38
cw3t13aa 0.89  1.60 0.04  0.78 0.02  9.70 4.75 0.211  0.16
cw3t13aa 1.13  2.38 0.04  1.17 0.02  9.47 4.64 0.216  0.25
cw3t13aa 0.43  0.61 0.03  0.30 0.02 10.14 4.96 0.202  0.06
cw3t16aa 2.47 43.91 0.02 21.48 0.01 10.02 4.90 0.204  4.38
cw3t16aa 2.38 41.98 0.86 20.54 0.42 10.83 5.30 0.189  3.88
```

Appendix 6 - Data Processing Programme and Calculation Procedures

Calculations

The calculations performed by the data processing programme are given below:

Composition

The compositions are derived from the density meter time periods by a curve fitted to experimental calibration data. They are estimated to be accurate to 0.001 in mole fraction or better. The equation used is:

$$x = -56.94097 + 255.4925\,\tau - 275.3015\,\tau^2$$

This equation is only for the chlorobenzene/ethylbenzene system in cell 1 of the density meter at 25 degrees C and on the 1k range setting. The value of τ is read directly from the meter.

Physical properties

Various physical properties of the distillation mixture, water and steam are all needed to calculate the desired results. The methods used to obtain these properties are given in tables A6-1 to A6-4.

Steam Data			
Property	units	Source	Expression
Vapour Pressure	bar	Sinnott (1989)	$1.332\ 10^{-3} \exp\left(18.3036 - \frac{3816.44}{(T/K - 46.13)}\right)$
Saturation Temperature	degrees C	Sinnott (1989)	$46.13 - 273.15 + \frac{3816.44}{18.3036 - \ln(p/(1.332\ 10^{-3}))}$
Heat Capacity	kJ / kg K	Reid, Prausnitz and Poling (1987)	$\frac{1}{18.015}(32.243 + 1.924\ 10^{-3}\,T + 1.055\ 10^{-5}\,T^2 - 3.596\ 10^{-9}\,T^3)$
Saturated Enthalpy	kJ / kg	Rogers and Mayhew (1980) & curve fit	$H_{wat,sat} + \phi\,\Delta H_{van}$ $\Delta H_{van} = 2470.6 - 1.6679\,T - 4.7117\ 10^{-3}\,T^2$ $95\ C < T < 165\ C$
Superheated Enthalpy	kJ / kg		$H_{stm,sat} + \int_{Tsat}^{T} c_{p,stm}\,dT$
Water Data			
Property	units	Source	Expression
Density	kg / dm^3	curve fit to data of Rogers and Mayhew (1980)	$0.99995 + 2.0129\ 10^{-5}\,T - 5.9910\ 10^{-6}\,T^2 + 1.6445\ 10^{-8}\,T^3$ $0\ C < T < 100\ C$
Heat Capacity	kJ / kg K	curve fit to data of Rogers and Mayhew (1980)	$4.1167 + 1.6590\ 10^{-3}\,T - 1.4738\ 10^{-5}\,T^2 + 8.4182\ 10^{-8}\,T^3$
Cooling water enthalpy at 1 bar	kJ / kg	curve fit to data of Rogers and Mayhew (1980)	$0.075959 + 4.2093\,T - 1.2142\ 10^{-3}\,T^2 + 2.5151\ 10^{-5}\,T^3 - 2.5336\ 10^{-7}\,T^4 + 1.4023\ 10^{-9}\,T^5$ $0\ C < T < 100\ C$

Saturated Enthalpy	kJ / kg	curve fit to data of Rogers and Mayhew (1980)	$6.6284 + 4.0295\ T + 9.3573\ 10^{-4}\ T^2$ 95 C < T < 165 C
Steam condensate Enthalpy	kJ / kg		$H_{wat,sat} - \int_{T}^{Tsat} c_{p,wat}\ dT$

Table A6-1 Physical property methods for water and steam

Chlorobenzene Data			
Vapour			
Property	units	Source	Expression
Saturated Density	kg / m^3	curve fit to data of Stphan and Hildwein	$-179.56 + 1.5379\ T - 4.4643\ 10^{-3}\ T^2 + 4.4017\ 10^{-6}\ T^3$ 390 K < T < 430 K
Vaporisation enthalpy at 1 bar	kJ / kg	Onken and Arlt (1990)	324
Viscosity	cP	Reid, Prausnitz and Poling (1987)	Corresponding States method See reference or programme for details
Diffusivity	m^2 / s	Reid, Prausnitz and Poling (1987)	Fuller et. al. method See reference or programme for details
Liquid			
Property	units	Source	Expression
Density	kg / m^3	Reid, Prausnitz and Poling (1987)	Hankinson - Brobst - Thompson method See reference or programme for details
Heat Capacity	kJ / kg K	Onken and Arlt (1990)	$1.21834 + 6.2086\ 10^{-3}\ T - 6.3518\ 10^{-5}\ T^2$
Enthalpy	kJ / kg		$\int^{T} c_p\ dT$
Viscosity	cP	Reid, Prausnitz and Poling (1987)	Yaws et. al. correlation: $\exp(-4.573 + 1196 / T + 1.370\ 10^{-3}\ T - 1.378\ 10^{-6}\ T^2)$
Infinite dilution diffusivity	m^2 / s	Reid, Prausnitz and Poling (1987)	Hayduk and Minhas Correlation with Parachor from group contributions. See reference or programme for details

Table A6-2 Physical property methods for chlorobenzene

Ethylbenzene Data			
Vapour			
Property	units	Source	Expression
Saturated Density	kg / m^3	curve fit to data of Stphan and Hildwein	$-161.51 + 1.3796\ T - 3.9917\ 10^{-3}\ T^2 + 3.9203\ 10^{-6}\ T^3$ 390 K < T < 430 K
Vaporisation enthalpy at 1 bar	kJ / kg	Onken and Arlt (1990)	337
Viscosity	cP	Reid, Prausnitz and Poling (1987)	Corresponding States method See reference or programme for details
Diffusivity	m^2 / s	Reid, Prausnitz and Poling (1987)	Fuller et. al. method See reference or programme for details
Liquid			
Property	units	Source	Expression
Density	kg / m^3	Reid, Prausnitz and Poling (1987)	Hankinson - Brobst - Thompson method See reference or programme for details

Heat Capacity	kJ / kg K	Onken and Arlt (1990)	$1.67523 + 3.0488\ 10^{-3}\ T - 3.3350\ 10^{-7}\ T^2$
Enthalpy	kJ / kg		$\int^T c_p\ dT$
Viscosity	cP	Reid, Prausnitz and Poling (1987)	Yaws et. al. correlation: $\exp(-6.106 + 1353 / T + 5.112\ 10^{-3}\ T - 4.552\ 10^{-6}\ T^2)$
Infinite dilution diffusivity	m^2 / s	Reid, Prausnitz and Poling (1987)	Hayduk and Minhas Correlation with Parachor from group contributions. See reference or programme for details

Table A6-3 Physical property methods for ethylbenzene

Chlorobenzene / ethylbenzene mixture data. Mole fraction x of chlorobenzene			
Vapour			
Property	units	Source	Expression
Saturated Density	kg / m^3	Combination of pure component densities	$\frac{M_{r,mix}}{\rho_{mix}} = \frac{x\ M_{r,clb}}{\rho_{clb}} + \frac{(1 - x)\ M_{r,etb}}{\rho_{etb}}$
Vaporisation enthalpy at 1 bar	kJ / kg	Onken and Arlt (1990)	$x\ M_{r,clb}\ 324 + (1 - x)\ M_{r,etb}\ 337$
Viscosity	cP	Reid, Prausnitz and Poling (1987)	Corresponding States method with Lucas mixing rules See reference or programme for details
Diffusivity	m^2 / s	Reid, Prausnitz and Poling (1987)	Fuller et. al. method See reference or programme for details
Liquid			
Property	units	Source	Expression
Density	kg / m^3	Reid, Prausnitz and Poling (1987)	Hankinson - Brobst - Thompson method See reference or programme for details
Heat Capacity	kJ / kmol K	Onken and Arlt (1990)	$x\ M_{r,clb}\ (1.21834 + 6.2086\ 10^{-3}\ T - 6.3518\ 10^{-5}\ T^2) + (1 - x)\ M_{r,etb}\ (1.67523 + 3.0488\ 10^{-3}\ T - 3.3350\ 10^{-7}\ T^2)$
Enthalpy	kJ / kmol		$\int^T c_{p,mix}\ dT$
Viscosity	cP	Reid, Prausnitz and Poling (1987)	Grunberg - Nissan method See reference or programme for details
Diffusivity	m^2 / s	Reid, Prausnitz and Poling (1987)	Vignes relation, assuming thermodynamic correction factor, alpha, is equal to one. See reference or programme for details

Table A6-4 Physical property methods for mixtures of chlorobezene and ethylbenzene

Column pressure drop and pressure gradient

The total pressure drop measured across the column is output by the data logging programme in mbar. The pressure drop of interest when looking at the performance of a packing is the dynamic pressure drop, that is the pressure drop caused by the momentum transfer from the flow. The measured pressure drop includes the static pressure drop, caused by the difference between the weight of the vapour and that of air; the pressure drop is set to zero when the column is full of air. The static part must be subtracted from the measured pressure drop to get the dynamic part:

$$\Delta p_{total} = \Delta p_{static} + \Delta p_{dynamic}$$

so that

$$\Delta p_{dynamic} = \Delta p_{total} - (\rho_{vapour} - \rho_{air})\, g\, h$$

where h is the height of the top connection to the transducer above the bottom one.

The dynamic pressure gradient is calculated by assuming that all the pressure drop occurs across the packing and dividing the dynamic pressure drop by the packed height.

Flows

Feed and reflux rotameter flows

The procedure for calculating the flow of the test mixture from the calibration data for water is described in the booklet 'Calibration data for metric series rotameters' and is presented here:

For a particular rotameter tube, the parameters I and F_T are calculated. I is used to represent changes in fluid viscosity and density and F_T gives the theoretical maximum capacity of the flowmeter. Curves are plotted on a graph of I against scale reading for different values of f, the fraction of the theoretical maximum capacity. For a particular fluid, I and F_T are calculated and the scale reading read at different f values. In this way, a calibration graph can be plotted. The programme assumes that the ratio of the measured flow to the theoretical flow at a particular scale reading is the same with water and the distillation mixture. The equations used are as follows:

$$I = \lg\left(10^4\, K_1\, \nu \sqrt{\frac{\sigma\, \rho}{\omega\, (\sigma - \rho)}} \right)$$

$$F_T = K_2 \sqrt{\frac{\omega\, (\sigma - \rho)}{\sigma\, \rho}}$$

Where K_1 and K_2 are constants for a particular tube size,
ν is the kinematic viscosity of the fluid in stokes,
ω is the weight of the float in grammes,
σ is the density of the float in g/cm^3 and
ρ is the density of the fluid in g/cm^3.

In the programme, curve fits to the graphical data were used, so that:

$$f = a + b\, S + c\, S^2$$

Where the coefficients a, b and c depend on I as follows:

$$a = a_1 + a_2\, I + a_3\, I^2$$

$$b = b_1 + b_2 I + b_3 I^2 + b_4 I^3$$
$$c = c_1 + c_2 I + c_3 I^2 + c_4 I^3$$

The experimental calibration data was represented by a quadratic of the form:

$$S = a_{exp} + b_{exp} f_{exp} + c_{exp} f_{exp}^2$$

The constants and coefficients are given in table A6-5 for the two rotameters used.

	Feed Rotameter Type R24	Reflux Rotameter Type R35
float material	korannite	korannite
K_1	0.865	1.50
K_2	2.314	3.330
ω	26.55	79.72
σ	2.53	2.53
a_1	0.11114	0.10265
a_2	0.01514	0.021043
a_3	-0.02537	-0.023225
b_1	0.030568	0.027184
b_2	-0.014965	0.00051150
b_3	0.023858	0.00020000
b_4	-0.012542	0
c_1	0.00020354	0.00027926
c_2	0.00033189	-0.000057645
c_3	-0.00054441	0.000032292
c_4	0.00027552	0
a_{exp}	-0.15258	-0.011016
b_{exp}	4.3303	1.4759
c_{exp}	-3.1751	-2.8529

Table A6-5 Coefficients and constants for rotameter calibrations

Cooling water rotameter flow

This was calibrated with water and the following correction applied to the flow read from the centre of the marker. The results showed considerable scatter and it is still only estimated to be accurate to about 5%, as the float had a tendency to stick.

$$F = 2.10 + 0.937 F_m$$

Steam flow

The average steam flow was measured over about 10 minutes. The condensate was diverted into a drum, placed on scales which read in pounds. The weight at the beginning and end of the chosen time period was noted and the flow calculated. It was converted into kg/min for input to the data processing programme. Losses due to flashing of the condensate were minimised by partly filling the drum with cold water and submerging the condensate outlet in this.

The accuracy of this procedure was limited by the accuracy of the scales, the stability of the steam flow and the losses due to flashing the condensate. Timing errors were insignificant. The total error is estimated to be 2-3%.

Flows in the column

To calculate the actual flows in the column, allowance had to be made for the reflux being subcooled. To do this, it was assumed that the reflux was brought to its boiling point by totally condensing part of the vapour at the top of the column. This is assumed to happen on the distributor and not in the packing, so that the performance of the packing is unaffected.

If the column operates under total reflux or as a rectifying section, the molar flow of vapour in the column is then:

$$V = V_m \left(1 + \frac{1}{\Delta H_{vap}} \int_{Tr}^{Tsat} c_{p,liq} dT \right)$$

Where V_m is the measured molar flow through the reflux rotameter,
T_r is the subcooled reflux temperature in K,
ΔH_{vap} is the vaporisation enthalpy of the mixture in kJ/kmol and
$c_{p,liq}$ is the heat capacity of the reflux liquid in kJ/kmol K

If the column operates as a stripping section, then there is a feed at the top, which may also be subcooled. This will cause an additional condensation, given by:

$$V_{add} = F_m \left(1 + \frac{1}{\Delta H_{vap}} \int_{Tf}^{Tsat} c_{p,liq} dT \right)$$

Where F_m is the measured molar flow through the feed rotameter,
T_f is the subcooled feed temperature in K,
ΔH_{vap} is the vaporisation enthalpy of the mixture in kJ/kmol and
$c_{p,liq}$ is the heat capacity of the feed liquid in kJ/kmol K

The liquid flow in the column is given by mass balance.

For total reflux: $L = V$

For rectification: $L = V - F$

For stripping: $L = V + F$

The total molar flows in the column were converted to superficial velocities as follows:

$$u_{vs} = \frac{V M_r}{\rho_v A} \text{ and}$$

$$u_{ls} = \frac{L M_r}{\rho_l A}$$

Where V and L are molar flows,
M_r is the mixture relative molecular mass
A is the column cross sectional area and
ρ_v and ρ_l are the densities of the vapour and liquid, which are assumed to be saturated.

The vapour superficial F factor is given by:

$$F_s = u_{vs}\sqrt{\rho_v}$$

and the capacity factor by:

$$C_s = u_{vs}\sqrt{\frac{\rho_v}{\rho_l - \rho_v}}$$

The peripheral liquid velocity, Γ, is given by:

$$\Gamma = \frac{L M_r}{a}$$

Where a is the packing area per unit volume (which is the same as the perimeter per unit area).

Heat balance

The heat balances around the condenser, the reboiler and the column are straightforward:

Condenser

$$Q_{out} = F_{CW}\,(\,H_{wat}(T_{out}) - H_{wat}(T_{in})) = V_m\left(\Delta H_{vap} + \int_{Tr}^{Tsat} c_{p,liq}\,dT\right)$$

Where Q_{out} is the heat removed from the condenser per unit time (kW)
F_{CW} is the cooling water flow,
T_{in} and T_{out} are the cooling water inlet and outlet temperatures,
$H_{wat}(T)$ is the enthalpy of water at temperature T
T_r is the temperature in the reflux drum
and the other synbols are defined earlier.

The heat flows calculated from each side of this equation were calculated and the percentage difference evaluated.

Boiler

$$Q_{in} = F_{cond}\left(\phi\,\Delta H_{vap,wat}(T_{sat}) + \int_{Tcond}^{Tsat} c_{p,wat}\,dT\right) = V\,\Delta H_{vap} + F\int_{Tf}^{Tb} c_{p,liq}\,dT$$

Where Q_{in} is the heat supplied to the boiler per unit time (kW)

F_{cond} is the steam condensate flow (which is the same as the steam flow)

ϕ is the dryness fraction of the steam (normally assumed to be 1)

$\Delta H_{vap,wat}(T_{sat})$ is the vaporisation enthalpy of water at the steam temperature and pressure,

T_{cond} is the temperature of the condensate out of the boiler, or the liquid temperature at the bottom of the column, whichever is higher,

T_{sat} is the temperature of saturated steam,

F is the bottom feed flow and is zero unless the column operates as a rectifying column,

T_f is the temperature of the feed,

T_b is the boiling temperature of the distillation mixture

and the other quantities are defined above.

The Vapour flow at the bottom of the column was calculated from this heat balance and compared with that calculated at the top from the rotameter flow.

Column

The heat loss through the insulation is given by the difference between the heat input at the boiler and the heat removed by the condenser

$$Q_{loss} = Q_{in} - Q_{out}$$

Dimensionless groups

These were calculated to indicate the likely flow regime within the packed bed and to allow easy comparison of the experimental data to the predictions of the various models.

Reynolds number

Three Reynolds numbers were evaluated for each run; the liquid Reynolds number and the superficial and effective vapour Reynolds numbers.

$$Re_{liq} = \frac{4\,\Gamma}{\mu_l}$$

$$Re_{vap} = \frac{\rho_v\, u_{vs}\, d}{\mu_v} = \frac{\rho_v\, u_{vs}\, 4}{a\,\mu_v}$$

$$Re_{vap,eff} = \frac{\rho_v\, u_{vs}\, 4\,\varepsilon}{a \sin\theta\,\mu_v}$$

Where d is the hydraulic diameter of the packing,

ε is the void fraction of the packing and

θ is the angle of the packing channels with the horizontal.

Schmidt number

The vapour schmidt number was calculated as:

$$Sc_v = \frac{\mu_v}{\rho_v D_v}$$

Packing efficiency

To calculate the efficiency of the packing, we need the vapour-liquid equilibrium relation for the distillation system. The data processing programme can use either a constant relative volatility, as recommended by Onken and Arlt (1990) or the non-random two liquid (NRTL) model recommended by Stephan and Hildwein. The former method was used to obtain all the data presented, because the latter method is based on experimental data from a notoriously unreliable type of still.

The calculations also allow for a correction if the components have widely differing molar enthalpies of vaporisation, by using a corrected relative molecular mass for the mole fraction calculations.

Number of theoretical plates and HETP

The number of theoretical plates is calculated by stepping between the operating and equilibrium lines, as in a McCabe-Thiele diagram, and counting the number of steps. The operating line equation is:

$$y = R\,x + (1 - R)\,x_{end}$$

or

$$x = 1/R\,(y + (R - 1)\,x_{end})$$

Where (x,y) is the operating line

R is the internal reflux ratio, L/V and

x_{end} is the top composition for $R < 1$ (rectifying) or the bottom composition for $R > 1$ (stripping) or either if $R = 1$.

The equilibrium line equation is:

$$y^* = \frac{x^* \alpha}{1 + (\alpha - 1)\,x^*}$$

or

$$x^* = \frac{y^*}{y^* + \alpha\,(1 - y^*)}$$

Where (x^*,y^*) is the equilibrium line and

α is the relative volatility

The algorithm used may be found in the programme unit DPNTP.PAS.

The HETP is then found by dividing the packed by the height number of theoretical plates.

Number and height of transfer units

If the transfer unit height is assumed to be constant over the packed section, the number of overall transfer units is given by:

Vapour: $$N_{ov} = \int_{y_1}^{y_2} \frac{1}{y^* - y} dy$$

Liquid $$N_{ol} = \int_{x_1}^{x_2} \frac{1}{x^* - x} dx$$

Where x_1, x_2, y_1 and y_2 are the compositions in the liquid and vapour at the top and bottom of the column.

These expressions are evaluated by numerical integration (using Simpson's rule) over fifty points.

The average value of m, the slope of the equilibrium line, is then given by :

$$m = \frac{L N_{ol}}{V N_{ov}}$$

Finally, the heights of the transfer units are found by dividing the packed height by the number of transfer units.

Mass transfer coefficients

The volumetric overall mass transfer coefficients were calculated by dividing the molar flow per unit column cross section by the transfer unit heights. To get the actual overall mass transfer coefficients, these must be be further divided by the area of the vapour-liquid interface.

Data processing programme and associated units

These programmes are installed on the hard disc of the computer in the directory C:\DISTCOL\DATAPROC. The input data files must be in the following directories

Log file	C:\DISTCOL\RIGDATA\LOGFILES*.LOG
Data Processing Input file	C:\DISTCOL\RIGDATA\DPIFILES*.DPI
Packing information file	C:\DISTCOL\RIGDATA\DPIFILES\PKFILES*.PK
Run code files	C:\DISTCOL\RIGDATA\DPIFILES\RCFILES\RC-*.IN

In addition, the directories C:\DISTCOL\RIGDATA\OUTFILES and C:\DISTCOL\RIGDATA\SUMFILES must exist for the programme to store the output and summary output files in.

CEDPKOR2.PAS

This is the main data processing programme for the chlorobenzene/ethylbenzene system and korannite rotameter floats. It requires three input files: the log file from the data logging programme (*.LOG), a data processing input file with the suffix .DPI or .DPx (x=0..9) and a packing information file with the suffix .PK. In addition, if more than one run is to be processed, a run code file may be used. This lists the code for each run and must begin with 'RC-' and end in '.IN'. An output file is produced by the programme for every run processed and a summary file is produced for each group of runs processed and is given the same name as the packing information file, but with the suffix .SUM.

DPGLOBAL.PAS

This unit contains the definitions of the 'global' variables, that is those shared by all the parts of the data processing programme.

DPIN.PAS

This unit reads data from the .LOG file and calculates the averages for use by the main programme.

DPOUT.PAS

This unit is used to write the processed data to the output file.

CCEPROP2.PAS

This unit calculates various physical properties of mixtures of chlorobenzene and ethylbenzene. Equations used for the physical properties and their references are given in tables A6-1 to A6-4.

Is is derived from the units CCEPROPS.PAS and CROTAKOR.PAS used by the control programme.

CHEAT.PAS, CROTAKOR.PAS, CUTILS.PAS, CVLENRTL.PAS

These units are the same as the ones used by the control programme and are described in appendix 4.

DPNTU.PAS

This unit contains functions to calculate the number of overall vapour and liquid phase transfer units from the experimental data. The number of transfer units is calculated by numerical integration of the equations by Simpson's rule.

DPNTP.PAS

This unit calculates the number of theoretical plates from the experimental data by stepping between operating and equilibrium lines. It allows for correction of the data if the molar latent heats are significantly different by using a ficticious molar mass.

Appendix 7 - Operating and emergency procedures for the test rig and procedure for sample analysis

1 Draining

1. Prop open door and switch on extractor fan and fume hood fan.

2. Open all process valves except drain and sample valves.

To drain the column and boiler:

3. Attach hose securely to boiler drain valve V23.

4. Earth drum under fume hood, make sure its tap is closed and put the free end of the hose into the top hole, making sure it will not come out easily.

5. Open the valve until the drum is as full as required, then close it.

6. If liquid is left, transfer the earth wire and hose to a new drum, and repeat the above procedure until the boiler is completely empty.

7. Make sure the hose is drained (into a bottle or beaker), then remove it.

To drain the feed and reflux piping and pumps:

8. Attach a hose securely to the filling valve V12 on the inlet to pump P2.

9. Drain the remaining liquid into earthed drums in the same way as before.

10. Collect liquid from all sample valves and the pump drain valves in a beaker or bottle and add it to the drums.

11. If the liquid is not volatile, undo the seal of the valve at the bottom of the reflux tank level glass and drain the liquid into a beaker.

Purging

12. Purge all vapour from column with compressed air or nitrogen, depending on the flammability of the mixture.

13. Remove top column section with care - if vapour is still present in column, replace it and continue purging.

2 Filling

1. Prop open door and switch on main extractor fan and fume hood fan.

2. Ensure steam supply valve V40 and condensate return valve V44 are closed and the boiler is cold.

3. Check that there is no unwanted fluid in the column - especially in the tank level glasses and distributor. If there is, follow draining instructions.

4. If the liquid to be loaded is extremely flammable, fill the column with nitrogen via the boiler drain valve V23.

5. Ensure that all sample and drain valves are closed.

6. Close feed pump (P2) inlet valves to prevent back flow of liquid to drum.

7. Set path from P2 through feed rotameter (FI5) to bottom tank; Close V19 and V16 and open V18,V19 and V20.

8. Attach a hose securely to the feed valve V12 and ensure that it is dry.

9. Put drum of liquid to be loaded on the metal cabinet under the fume hood, remove the lid to allow air into the drum as it drains and attach the earth clip to the top thread.

10. Attach the hose to the tap on the drum with a jubilee clip.

11. Open feed valve V12 and the tap on the drum. If no liquid is already in the column, open valve V10 - bottom tank to pump inlet - until as much liquid as possible has flowed into column, then close it again.

12. Close feed control valve CV3 and start feed pump P2.

13. Open CV3 to give desired flow. Estimate quantity loaded by flow*time, by visual inspection, by weight loss or by using a dipstick in the drum.

14. When the drum is empty or the required amount of liquid has been loaded, close the tap on the drum, detach the hose from the drum and hold up the end until all the remaining liquid flows into the column. Then close the feed valve V12.

15. Switch off the pump P2.

16. If necessary, repeat with further drums until all the required liquid is loaded.

3 Operating

1. Decide on mixture to be distilled and required steam pressure.

2. Decide on approximate mixture composition and mode of operation (Total reflux, stripping (top feed) or rectifying (bottom feed)).

3. Make sure extract fan is on and all sample and drain valves are closed.

4. If necessary, fill column (see Filling instructions).

5. Set the reflux and feed paths according to the mode of operation.

6. Make sure that the regulator control on the nitrogen cylinder is fully unscrewed and open the cylinder valve. Check that the pressure in the cylinder is sufficient to last the length of the run and if it is, set the regulator to 0.5 bar.

7. Read atmospheric pressure by one of the following methods:

Read mercury barometer in 4th floor analytical lab. and correct for temperature of mercury and elevation of 4th floor above the rig. Convert mmHg to bar

Read digital barometer in lab. 209 and correct for elevation above the rig.

8. Read the aneroid barometer in the flameproof lab. and then read off the actual pressure in bar from the calibration graph.

9. Switch on all the electronics (MTL multiplexer, Column pressure drop transducer, Reflux tank level sensor, Control valve interface and Computer.).

10. Make sure all control valves are set to computer control.

11. Prepare input file for control programme in directory c:\distcol\rigdata\infiles (see control programme documentation). Edit it with the Turbo Pascal 5.5 editor TP55.

12. Change the directory to c:\distcol\cont, load the control programme CKOR.PAS and run it from the editor by ALT-R R.

13. Note the start time of the programme clock on the run sheet.

14. Switch on the water to the secondary condenser.

15. Check the cooling water is switched on and sufficient flow is available.

16. Prepare a new run sheet and record the cooling water flow and column pressure drop manometer reading, checking that they are reasonable.

17. Close the condensate return valve V44 and fully open the steam shut-off valve V40.

18. Drain the steam side of the reboiler through the vent valve V45 until steam comes out, then shut it.

19. Restrict the steam pressure by partially closing the steam shut-off valve V40 to limit the rate of vapour production and avoid entrainment of mixture with air leaving column.

20. When the liquid level in the reflux tank starts to rise, switch on the reflux pump P1 and if necessary the feed pump P2.

21. Open the condensate return valve, V44 and fully open the steam shut-off valve V40.

22. Ensure that the set point for the column pressure drop is correct and wait for the column to reach thermal steady state.

23. While column is operating, keep checking for leaks and broken glass; check windows, sight glasses, secondary condenser, rotameters, pump seals and hoses on condenser.

24. Also check the reflux tank level and that cooling water outlet temperature is below 60 degrees C.

25. Allow a time of roughly 3*volume of liquid in column/reflux flow before taking samples.

26. While waiting to take samples, record the cooling water, reflux and feed flows and the column pressure drop manometer reading at least every 5 minutes.

27. Also, measure the steam flow as follows: Put some cold water into the steam collection tank on the scales and divert the condensate flow into the tank for a timed period of about 10 minutes. To divert the flow, open the condensate drain valve, V43 and close the condensate return valve V44. Record the weight of condensate collected.

28. Repeat the condensate rate measurement while samples are being taken.

29. To take samples, fill the sample vial twice from the sample valve and drain it into a bottle for later re-use. Then fill the vial again, seal it and record its number, the time the sample was taken and the sample point on the sample record sheet.

30. Samples normally taken are from the reflux into pump P1, the bottom of the column and the liquid under the packing.

31. To close down, switch off the steam supply valve V40 and condensate return valve V44.

32. Switch off the feed pump P2 and when the reflux tank is empty, switch off the reflux pump P1.

33. Usually leave the cooling water on while mixture is in the column. If it is to be turned off, wait until the cooling water leaving the condenser is the same temperature as that entering.

34. Choose Exit from the control programme menu to re-enter the Turbo Pascal editor.

35. Quit the Turbo Pascal editor with ALT-F Q, and enter XTREE PRO by typing XTPRO.

36. Copy the log file from directory c:\distcol\rigdata\logfiles to a floppy disk and also the input file from c:\distcol\rigdata\infiles.

37. Leave XTREE PRO and type PARK to park the hard disk.

38. Switch off the computer and the instruments.

39. Switch off the nitrogen supply by reducing the regulator pressure to zero and then closing the cylinder valve.

4. Emergency Shutdown Procedure

1. If liquid is being pumped out of a leak or level control has failed, switch off pumps and open feed pump inlet valves V9 and V10 to drain the reflux tank into the bottom of the column.

2. Isolate the leak if possible.

3. Shut off the steam supply - close steam valve V40 and condensate return valve V44.

4. If possible, increase cooling water flow on main and secondary condensers to maximum.

5. If a large quantity of liquid has leaked out, cover it in absorbent.

6. If vapour escapes into the lab. or from the vent in large quantity or solvent enters the drain or there is a fire or other danger of fire, sound the fire alarm.

7. Call help as appropriate.

5 Procedure for sample analysis with density meter

1. Switch on density meter, set period select to 1K, sample cell to number 1 and water bath to 25.0 degrees Celsius and wait until a stable empty cell reading has been reached.

2. Fill 2ml syringe from sample vial through PVC tube until 1.9ml fluid is in syringe. Then suck fluid in tube into syringe and remove tube.

3. Put syringe into syringe holder and screw down to expel all air from the syringe.

4. Fit filter to syringe, and fit syringe with filter to density meter inlet tube.

5. Screw down syringe holder to transfer liquid into cell.

6. When a stable period value is displayed, record it.

7. Remove syringe from holder and slowly withdraw sample back into syringe by gently pulling plunger.

8. Remove syringe from tube and switch on air pump to clean cell.

9. Transfer waste solvent from syringe into jar for re-use or disposal.

10. Remove filter from syringe, fill syringe with air and re-fit filter. Blow out any remaining liquid into the waste jar.

11. Dismantle the syringe and leave in fume cupboard with filter for solvent to evaporate.

12. Wait until original empty cell period value is reached before inserting next sample with a clean syringe and filter.

Appendix 8 - List of equipment suppliers

A J Thermosensors Ltd
Martlets Way
Goring by Sea
Worthing
West Sussex
BN12 4EG
(0903) 502471

Alco Valves Ltd

Amplicon Liveline Ltd
Centenary Industrial Estate
Brighton
BN2 4AW
(0273) 570220

M. Barnwell Services Ltd
Reginald Road
Smethwick

Beresford Pumps Ltd
Carlton Road
Foleshill
Coventry
CV6 7FL
(0203) 638484

Binney and Son Ltd.
12 Louisa Street
Edward Street
Birmingham
B1 2RP
021 236 0521

T Bullows and Sons
Deepdale Lane
Lower Gornal
Dudley
West Midlands
DY3 2AF
(0384) 257441

J Cullen Thermals Ltd
202 Deykin Avenue
Witton
Birmingham
B6 7BH

021 327 5260

R W Dunlop
Central Heating Engineer
17 Oakland Road
Moseley
Birmingham
B13 9DN
021 449 6089

Eurogrid Ltd
Halesfield 19
Telford
Shropshire
TF7 4QT
(0952) 581988

Fisher Controls

Fisons Ltd

ICC (flow)

I M I Bailey Burkitt
Balme Road
Cleckheaton
West Yorkshire
BD19 4EY
(0274) 875771

Introl

John Watson and Smith Ltd
Melville Place
Leeds
LS6 2EU
(0532) 457587

KDG Mobrey
(0293) 525151

Measurement Technology Ltd
Power Court
Luton
LU1 3JJ
(0582) 450042

Norton Chemical Process Products
King Street, Fenton

Stoke-on-Trent
ST4 2LT
(0782) 744561

Parker Hannifin plc
Instrumentation Connectors Division
Riverside Road
Pottington Industrial Estate
Barnstaple
Devon
EX31 1NP
(0271) 73349

Philip Corns Ltd
Claybrook Drive
Washford
Reddich
B98 0DT
(0527) 510555

Platon Flowbits Ltd
Platon Park
Viables
Basingstoke
Hampshire
RG22 4PS
(0256) 460122

Poseidon Alloys Ltd
Progress Works
Cross Street North
Wolverhampton
West Midlands
WV1 1PP
(0902) 870404

PSM - Pressure Sensors (Marketing) Ltd
Unit 4, Fairview Industrial Estate
Holland Road
Oxted
Surrey
RH8 9BD
(0883) 717266

H V Skan Ltd
425-433 Stratford Road
Shirley
Solihull
West Midlands

B90 4AE
(021) 733 3003

S A Equipment Ltd
6 Sunny Place
Sunny Gardens Road
London
NW4 1RS
(071) 203 6866

Spirax Sarco Ltd
Cheltenham
GL63 8ER

Sulzer Brothers Ltd
PO Box CH-8401
Winterthur
Switzerland
010 41 52 262 11 22

Sulzer UK Ltd
Farnborough
Hants
GU14 7LP
(0252) 544311

Tekflo Ltd
Albany Road
Granby Industrial Estate
Weymouth
Dorset
DT4 9TH
72237

Tianjin University Packing Factory
Tianjin 300072
P. R. China
010 86 22 380847

Valvestock Ltd

V T Plastics

Waverley Components and Products Ltd
33 Caxton Way
Holywell Industrial Estate
Watford
Herts
WD1 8TG